



HEINRICH HEINE
UNIVERSITÄT DÜSSELDORF

**APOBEC3 DNA deaminases: A mechanistic study of
A3A, A3C, and A3G action on retroviruses and
counteraction by viral proteins**

Ananda Ayyappan Jaguva Vasudevan

(from Madurai, India)

A dissertation

submitted in partial fulfillment of the requirements of the
degree of

Doctor of Philosophy

To the Faculty of Mathematics and Natural Sciences

at the Heinrich-Heine-University

Düsseldorf

2017

From the **Clinic for Gastroenterology, Hepatology, and Infectiology**,
Medical faculty, at the Heinrich-Heine-University Düsseldorf

Published with the approval of the Faculty of Mathematics and Natural
Sciences, at the Heinrich-Heine-University Düsseldorf

Supervisor : Prof. Dr. Carsten Münk

Co-supervisor : Prof. Dr. Dieter Willbold

Date of the oral examination: November 23, 2017

**“தெய்வத்தான் ஆகா தெனினும் முயற்சிதன்
மெய்வருத்தக் கூலி தரும்”**

Couplet: 619, Thirukkural by Thiruvalluvar

**“Though fate-divine should make your labour vain;
Effort its labour's sure reward will gain”**

(translated by
Rev. Dr. G. U. Pope, Rev W. H. Drew, Rev. John Lazarus and Mr F. W. Ellis)

Contents

Introduction	1
Scientific publications	24
Strategic findings of this thesis	25
References	26
Chapter I	42
Chapter II	59
Chapter III	89
Chapter IV	118
Chapter V	162
Chapter VI	175
Chapter VII	191
Chapter VIII	215
Chapter IX	233
Chapter X	241
Chapter XI	276
Summary	297
Summary in German (Zusammenfassung)	299
Acknowledgements	301
Biographical Sketch	303
Declaration	305

Introduction

Eukaryotes developed the defense system referred to as immune system to guard them against invading pathogens such as bacteria, protozoan parasites, and viruses. The immune system encompasses non-specific physical barriers and cellular responses as well as pathogen-specific immune responses to a single microbial type (of species) (Charles A Janeway, 2001). Noteworthy, CRISPR-Cas-based adaptive and heritable immunity was discovered recently in prokaryotes (Garneau et al., 2010, Bhaya et al., 2011, Koonin and Krupovic, 2015).

The so-called innate (non-adaptive) immune system builds the front-line defense against pathogen attack. The intrinsic immune mechanisms act immediately after an infectious agent enters the host but do not generate lasting protective immunity. The innate system is an evolutionarily older defense strategy and is the dominant immune system found in fungi, insects, plants, and in primitive multicellular organisms. The complement cascade system derived from hepatocytes and leukocytes such as natural killer cells, eosinophils, mast cells, basophils, and phagocytic cells (including macrophages, neutrophils, and dendritic cells) is an essential part of the innate immune system (Charles A Janeway, 2001). In contrast, acquired immunity (specific) are driven by the responses of lymphocytes (B and T cells) after the exposure of a particular pathogen. Acquired immunity creates immunological memory (memory B cells and memory T cells) after an initial response to a specific pathogen, leading to an enhanced response to subsequent encounters with that same pathogen, which is the basis of vaccination. The system is highly adaptable because of somatic hypermutation (a process of accelerated somatic mutations), and V(D)J class switch recombination (an irreversible genetic recombination of antigen receptor gene segments). This mechanism facilitates a small number of genes to produce a large number of distinct antigen receptors, which are then exclusively expressed on each individual lymphocyte. Lymphocytes, NK cells (O'Sullivan et al., 2015), antigen presenting cells, antibodies and various cytokines are the components of the adaptive immune system.

The immune system may be unsuccessful to neutralize a pathogen which as a result causing deleterious health issues, consequently, may lead to death. Viruses such as Human

Immunodeficiency Virus (HIV) are a classic example of invading the human immune system, replicate, damage the immunity and ultimately causing Acquired Immunodeficiency Syndrome (AIDS). Human immunodeficiency virus type-1 (HIV-1) belongs to the family of *Retroviridae* and genus *Lentivirus*. The disease of AIDS was observed for the first time in 1981 (Gottlieb et al., 1981) in the United States. In 1983, research groups led by Robert Gallo and Luc Montagnier independently declared that a novel retrovirus infection leads to the disease (Gallo et al., 1983, Barre-Sinoussi et al., 1983), and the term HIV was coined in 1986 (Coffin et al., 1986).

HIV-1 infection causes a dramatic reduction in CD4+ T cells (T helper cells, cell count below 200 cells/ μ l blood (Opportunistic Infections Project Team of the Collaboration of Observational et al., 2012)). Primate lentiviruses such as HIV, simian immunodeficiency virus (SIV) use the cell receptors CD4 and a chemokine co-receptor to enter the host cells. Macrophages and T helper cells are the target cells for HIV-1. As the infection progresses to the AIDS phase (2-10 years post infection), the severely damaged human immune system cannot prevent the infections normally controlled or neutralized. In addition the incidence of tumors increases during the decay of the immune system. It is chiefly believed that the HIV strains (HIV-1 and HIV-2) originated and evolved from the strains of SIVs (SIV_{cpz} in chimpanzees and SIV_{smm} in sooty mangabeys) and likely transmitted to humans through the blood contact with primates during hunting activities in Africa (for a review see, (Sharp and Hahn, 2011). HIV is primarily transmitted via human to human sexual contact, or by using contaminated syringes and blood transfusions.

AIDS continues to be a major global health issue with estimated deaths of more than 25 million over last three decades. According to the latest survey carried out by World Health Organization (<http://www.who.int/gho/hiv/en/>) in 2015, there were 36.7 million people approximately living with HIV with 2.1 million new infections. It was estimated about 1.1 million AIDS-related deaths in 2015, significantly lower than the 2.3 million in 2005. Sub-Saharan African population (25.5 million) contributed 69.5% of the total infected people. As a result of research done over 30 years, valuable information about the HIV replication cycle in humans and the mechanisms it adapts to escape from innate restriction factors was identified. Administration of highly effective antiretroviral drugs (cART-combination antiretroviral therapy) can stop the virus replication and the destruction of the immune

system will be stopped, the damaged immune system can recover and the infected individual might have a regular life expectancy. However, we do not have a cure for or a vaccine against this epidemic.

A topic in the field of HIV research is the understanding of human lentiviral restriction factors. Like other viruses, HIV-1 relies on various host cellular factors (dependency factors) for infection. These affirmative factors are facilitating the entry, reverse transcription and the integration of the viral genome into the host genome. In contrary, there are regulatory factors in the host that inhibit the spreading of HIV at different stages of the virus life cycle. Deep understanding of host restriction factor-virus interaction at a molecular level may help for the development of promising new antiretroviral therapeutics and preventive measures. This dissertation emphasizes on the molecular understanding of the action of APOBEC3A (A3A), A3C and A3G on retroviruses and studied the following host-viral interaction: HIV-1 Vif with human A3C and A3G; murine leukemia virus glycosylated gag (glycogag) with human A3A and mouse A3; foamy virus Bet with human A3G. Also, the knowledge was further extended to understand the restriction of retroelements (LINE-1 element) by A3C and the role of APOBEC4 were explored. An outline of background knowledge and basic facts about retroviruses, retroelements, foamy viruses, human APOBEC3 family proteins are narrated below.

Retroviruses and retrotransposons

Retroviruses and retroelements are found in mammals, plants and some insects. Their replication is essentially dependent on host cellular machinery. Mobilization of retroelements in genomes and infection of retroviruses are known to cause deleterious effects in the host. This section discusses the structure, genome organization and pathogenesis of some retroviruses and retroelements.

Retroviruses

Retroviruses belong to the family of enveloped RNA viruses, *Retroviridae* (Murphy et al 1995) possess two copies of single-stranded RNA (+ strand) which are often termed as

'pseudodiploid' as only one integrated copy of the viral DNA is detected after infection with single virion (*Principle of virology, second edition*). The basic genome organization of simple retrovirus is shown in Figure 2A. The genome is composed of *gag* (group specific antigen), *pol* (polymerase) and *env* (envelope) genes flanked by LTRs (Long terminal repeats). The genetic message stored in the RNA genome is reverse transcribed into double-stranded cDNA by viral reverse transcriptase (RT). The *retro* synthesized DNA is then transported into the nucleus and incorporated into the host genome at random location by the enzyme viral integrase (IN). Thus irreversibly integrated viral DNA, referred as a provirus, can survive for the lifetime of the infected cell. The host cell aids the expression of viral genes with the help of host cellular machinery, thus produces viral proteins and RNA genome to make new copies of the virus.

Evolution of Retroviruses

The genetic closeness or the distance among retrovirus families based on the sequence of viruses is shown in a phylogenetic tree (Kenyon and Lever, 2011) (Fig. 1). Immunodeficiency viruses such as HIV-1 and its subtypes, SIV, and FIV collectively fall into lentivirus genus. Studies concerned with lentiviruses (exogenous retroviruses) are of particularly interesting because some cause AIDS, while others seem not to harm their hosts. Intriguingly, the presence of endogenous lentiviruses such as leporid retroviruses like RELIK in rabbits and prosimian immunodeficiency virus (PSIV) in Lemurs of Madagascar was discovered recently (Goldstone et al., 2010, Katzourakis et al., 2007, Keckesova et al., 2009, Gifford et al., 2008, Gilbert et al., 2009). It suggests that lentiviruses are more widespread than thought before, can be incorporated into the host germline, and are ancient, existing prior to 12 million years (van der Loo et al., 2009, de Matos et al., 2011).

Humans, like other mammals, possess retroviruses that exist in two forms: as normal genetic elements in the chromosomes (endogenous retroviruses) and as horizontally transmitted infectious viruses which can be spread among human (HIV and human T cell leukemia virus, HTLV) (Cloyd, 1996). As the viruses are constantly facing the pressure from the immunity of the host, they co-evolve continuously to counter-adapt from the host restriction machinery (Arnaud et al., 2007). Host-virus co-evolution aged deep time (many million years), the

“arms race” between lentivirus and its host is ongoing (Gifford, 2012, Daugherty and Malik, 2012).

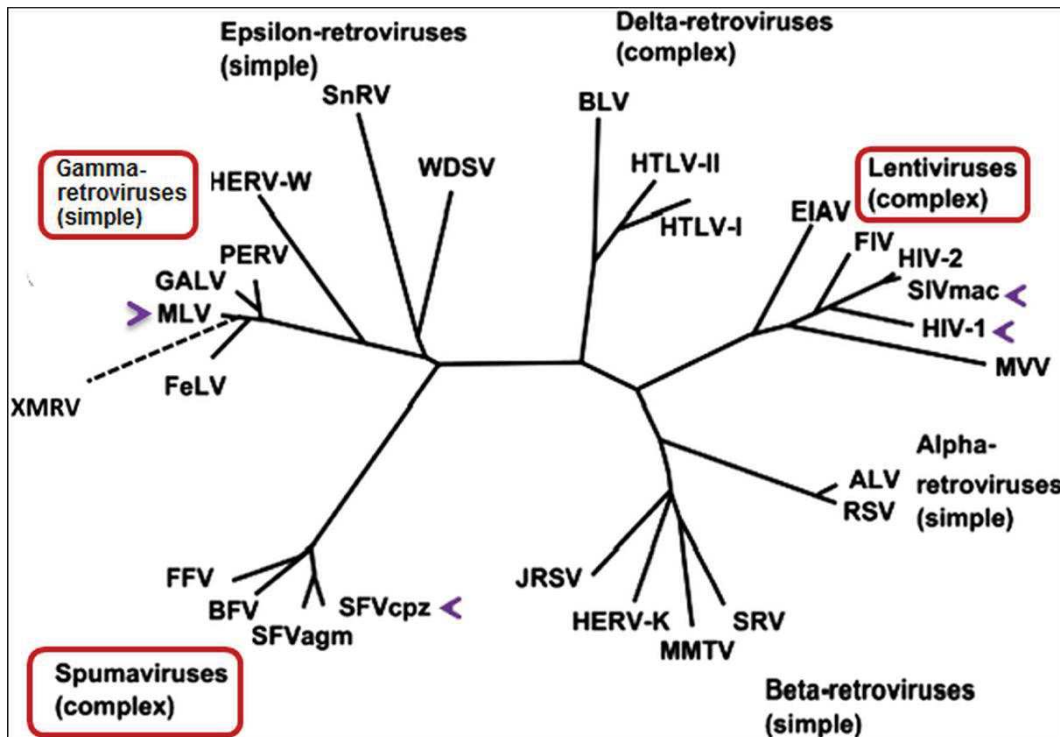


Figure 1: Phylogenetic tree of retrovirus families. Unrooted phylogenetic tree of retrovirus families according to its relatedness in their genetic sequence. Virus models used in this thesis are highlighted with a box and arrow. (Figure was adapted from (Kenyon and Lever, 2011) with permission from Oxford University press).

Human immunodeficiency virus type 1 (HIV-1)

The basic genetic organization of a retrovirus is given in Fig. 2A. Mature spherical HIV-1 virions are about 145 nm in diameter (Briggs et al., 2003). The genetic and the structural components of HIV-1 are shown in Figs. 2B and 2C. HIV-1 consists of two single-stranded RNA with the size of 9.7 kb. In addition to the basic retroviral genes *gag*, *pol* and *env*, HIV-1 genome contains genes for accessory proteins as shown in Fig. 2B (it possesses nine ORFs that encode 15 proteins). A detailed functional report of HIV-1 proteins are listed in (Swanson and Malim, 2008). Regulatory proteins Tat (transactivator of transcription) and Rev (regulator of expression of virion proteins) play crucial roles in virus replication (Dayton et al., 1986, Fisher et al., 1986, Pollard and Malim, 1998), in particular Tat upregulates the expression of all viral genes (Jeang et al., 1999), Rev on the other hand mainly enhances Gag,

Pol and Env protein expression while down regulating the Rev and Tat expression (Felber et al., 1990). Accessory proteins such as Vif and Vpu are counteracting cellular restriction factors (Neil et al., 2008, Yu et al., 2003). Together with Vpr and Nef these auxiliary proteins strongly inhibit the barrier to escape from adaptive and innate immunity of the host (Li et al., 2005, Malim and Emerman, 2008, Yan and Chen, 2012, Li and De Clercq, 2016).

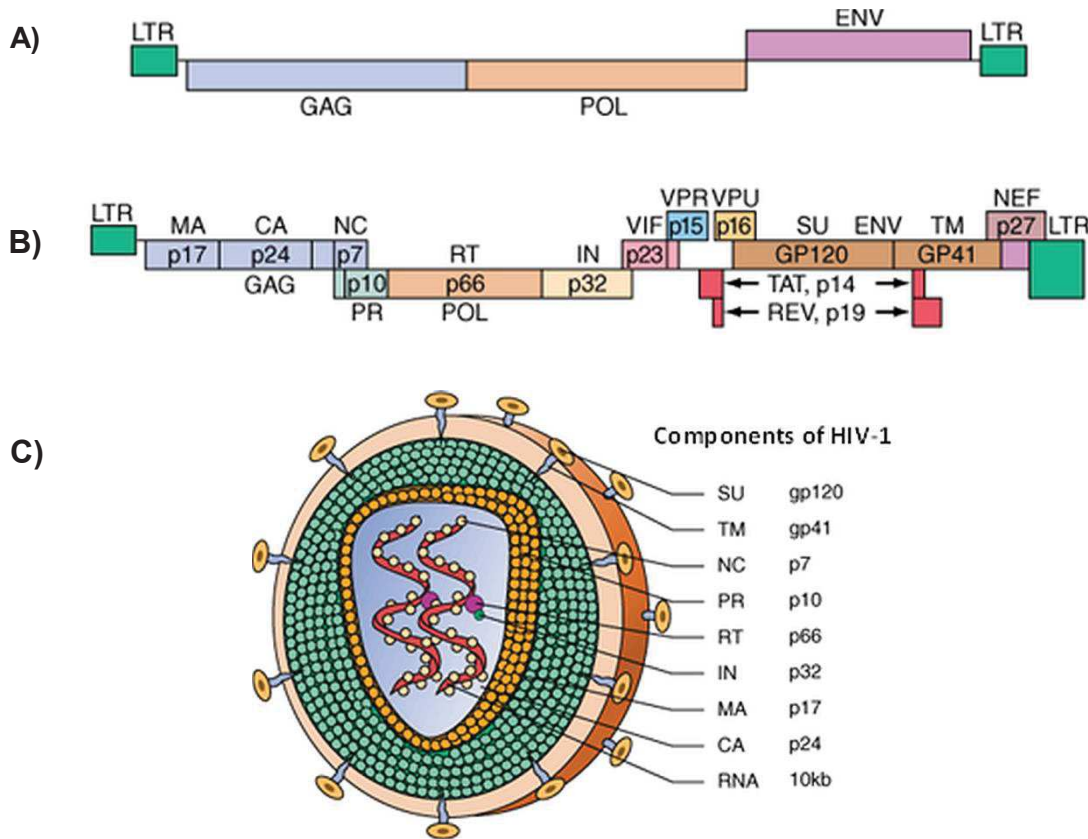


Figure 2: Retroviral genomes and HIV-1 particle: A): Portrayal of a simple retrovirus genome organization. Flanking LTRs are shown in green (terminals), genes *gag*, *pol* and *env* are represented in three different colors. B) & C): Schematic illustration of the genomic and structural organization of HIV: A) retroviral genomes are typically made up of three structural genes namely, *gag*, *pol* and *env*. The *gag* region codes matrix (MA), capsid (CA) and nucleocapsid (NC) proteins. The *pol* gene in HIV makes protease (PR) and reverse transcriptase (RT) and integrase (IN). The *env* gene encodes a surface protein (SU) and a small transmembrane anchoring protein (TM). In addition, HIV has six accessory genes such as *tat*, *rev*, *vif*, *net*, *vpr* and *vpu* for various regulatory functions during infection. LTR, long terminal repeats in both ends. B) The spherical structure of the virus is conferred by its membrane that contains surface protein gp120 and transmembrane protein gp41 (proteins involved in the entry of virus into the human cells by binding to their receptors). Two copies of the viral RNA (pseudodiploid) are coated with nucleocapsid (p7). Viral protease (p10) functions to cleave the polyproteins (*gag*, *pol*, and *env*). Reverse transcriptase (p66) and integrase (p32) forms complex machinery to incorporate proviral DNA into the host genome. The matrix proteins (p17) cover the viral core. The capsid proteins (p24) build the core shell.

(Figure was adapted from Harrison's Principles of Internal Medicine 17th Edition with permission from the McGraw-Hill Companies).

HIV-1 replication cycle

In order to formulate a therapeutic or preventive measure against HIV infection, one has to look closely at the mode of HIV-1 infection and replication in the host (Fig.3). The replication cycle of HIV starts as soon as it enters the blood stream (reviewed in (Stevenson, 2003)). It infects CD4⁺ target cells either as a free virus particle or transmitted by dendritic cells via the virological synapse. Binding of HIV surface protein gp120 to CD4 receptor triggers conformational changes in the protein complex allowing a domain of gp120 to interact with the chemokine receptor CCR5 or CXCR4 (Clapham and McKnight, 2002). This, in turn, permits gp41 to penetrate the cell membrane, resulting in the fusion of viral membrane (Sierra et al., 2005). Only the viral core enters the cytoplasm and undergoes uncoating to release the RNA and viral enzymes, and reverse transcription initiated by binding of cellular tRNAs and viral RT (Harrich and Hooker, 2002). Viral ssRNA reverse-transcribed to dsDNA and the viral cDNA imported to the nucleus. With the catalytic activity of IN, the cDNA gets integrated into the chromosomal DNA at the random locus generating a transcriptionally active provirus (Van Maele and Debyser, 2005). Cellular transcription factors initiate transcription of the integrated provirus by interacting with the viral promoter in the 5' LTR region. Newly translated viral polyproteins assemble with viral genomic RNAs at the cytoplasmic membrane and together with cellular proteins such as APOBEC3G, nascent particles are formed and bud out of the infected cell.

Viral escape strategies to evade human cellular restriction factors

The biology of HIV-1 depends on specific interactions with cellular proteins that support its infection in human cells. The role of the dependency factors (such as the CD4 receptor used for cell entry or the interaction of host Cyclophilin A is required for capsid uncoating) contrasts the function of cellular antiviral proteins called restriction factors. At each step in the course of HIV-1 infection in human cells, the virus is subjected to encounter diverse intrinsic cellular antiviral restriction factors (for detailed reviews, see (Jia et al., 2015,

Goubau et al., 2013, Yan and Chen, 2012, Harris et al., 2012)). Most prominent examples of HIV-1 restriction factors are APOBEC3G, TRIM5 α , Tetherin and SAMHD1 (Malim and Bieniasz, 2012, Schaller et al., 2012). Very recently, the list is further extended with the discoveries of SLFN11, MxB (GTPase), and SERINC5 (counteracted by Nef) proteins (Haller, 2013, Li et al., 2012, Liu et al., 2013, Razzak, 2012, Goujon et al., 2013, Kane et al., 2013, Sood et al., 2017, Rosa et al., 2015, Usami et al., 2015, Fricke et al., 2014). It appears that the key role of some HIV's accessory proteins is the counteraction of cellular restriction factors, eg: HIV proteins Vif and Vpx trigger the degradation of A3 proteins and SAMHD1, respectively (illustrated in Figure 3 and 5). The SLX4 protein complex was identified as cellular factors for Vpr-mediated G2/M cell cycle arrest and HIV-1 escape mechanism from immune sensing. Vpr induced premature activation of the SLX4 complex was achieved by direct interaction of Vpr with SLX4 and following events causing replication stress (Laguette et al., 2014).

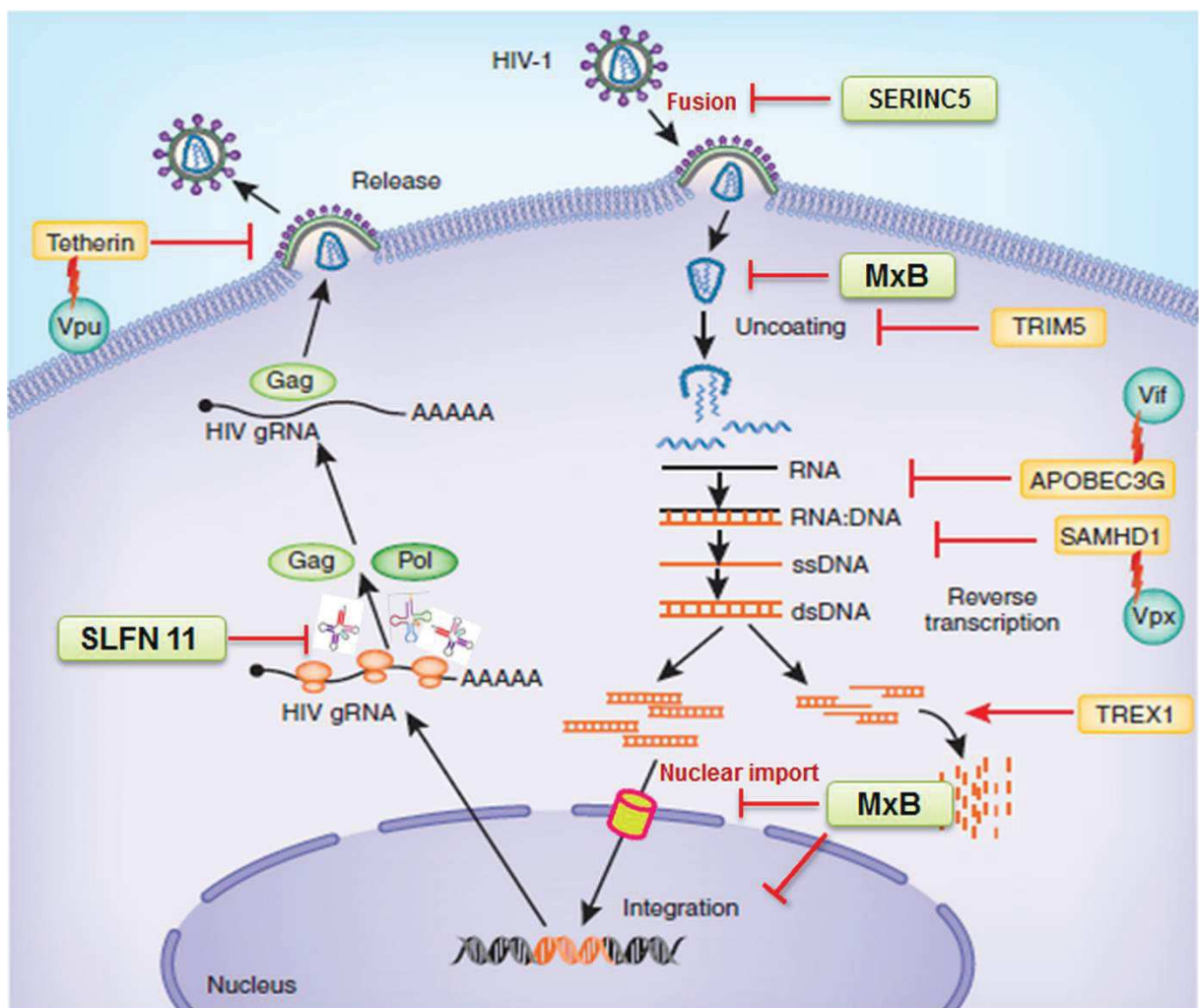


Figure 3: Intrinsic antiviral factors against HIV1. Host restriction factors such as SERINC5, MxB, TRIM5, APOBEC3G, tetherin, SAMHD1, SLFN11 target multiple steps that occur in virus life cycle. HIV-1 has evolved strategies to counteract these antiviral factors, through accessory proteins such as Vif, Vpu and Vpx or other unknown mechanisms. gRNA, genomic RNA; ssDNA, single-stranded DNA; dsDNA, double-stranded DNA (Figure was adapted from (Yan and Chen, 2012) with permission from Nature publishing group)

For lentiviruses, it has been proposed that the virus (HIV-1) benefits from a partially active APOBEC3 by exploiting this particular cellular mechanism of innate immunity to enhance viral diversity (Kim et al., 2010, Münk et al., 2012a, Sadler et al., 2010, Wood et al., 2009). This dissertation mainly focuses on the antiviral activity of APOBEC3 (A3) family proteins - the IFN induced, post-entry inhibitor of HIV 1 infection. As a theme, this thesis studied A3s activity against HIV-1, SIV, Murine leukemia virus (MLV), prototype foamy virus (PFV) and retroelements. The following section elucidates the known facts and the antiviral role of A3 family enzymes.

APOBEC3 family enzymes

Apolipoprotein B mRNA editing enzyme, catalytic polypeptide-like (APOBEC3, A3) genes are found only in placental mammals, but might be evolutionary, as old as the origin of mammals (LaRue et al., 2009, Münk et al., 2012b, Münk et al., 2008). APOBEC3G (A3G) was recognized as an HIV restriction factor in the search to understand the lack of replication of HIV-1 variants lacking *vif* gene expression (HIV-1 Δ *vif*) in certain cells such as peripheral blood mononuclear cells (Sheehy et al., 2002); discovered as a DNA deaminase (Harris et al., 2002) and as a member of putative RNA editing family by genome sequencing (Jarmuz et al., 2002). A3G belongs to the family of APOBECs that include in humans AID, APOBEC1, APOBEC2, APOBEC4, APOBEC5 and seven A3s (A3A, A3B, A3C, A3D, A3F, A3G, and A3H). All seven human A3 proteins are single-strand DNA (ssDNA) cytidine deaminases known to inhibit diverse retroviruses, retroelements, RNA and DNA viruses (Arias et al., 2012, Chiu and Greene, 2009, Sheehy and Erthal, 2012, Holmes et al., 2007, Cullen, 2006, Chiu and Greene, 2008) and can be induced by interferons (Peng et al., 2007, Peng et al., 2006, Tanaka et al., 2006, Berger et al., 2010, Mohanram et al., 2013). Cytidine deamination of single-stranded DNA (ssDNA) was shown to be the principle activity of A3 proteins (Yu et al., 2004a, Suspene

et al., 2004, Harris and Dudley, 2015, Browne et al., 2009), several biochemical and biophysical properties such as DNA and RNA binding and oligomerization features, deamination activity, three-dimensional structures, inter and intramolecular interaction were studied in detail in recent years (Strebel and Khan, 2008, Belanger et al., 2013, Hache et al., 2005, Huthoff et al., 2009, Iwatani et al., 2006, McDougall et al., 2011, Salter et al., 2009, Salter et al., 2016, Marino et al., 2016), they are collectively elaborated in chapter I, of this thesis (Vasudevan et al., 2013).

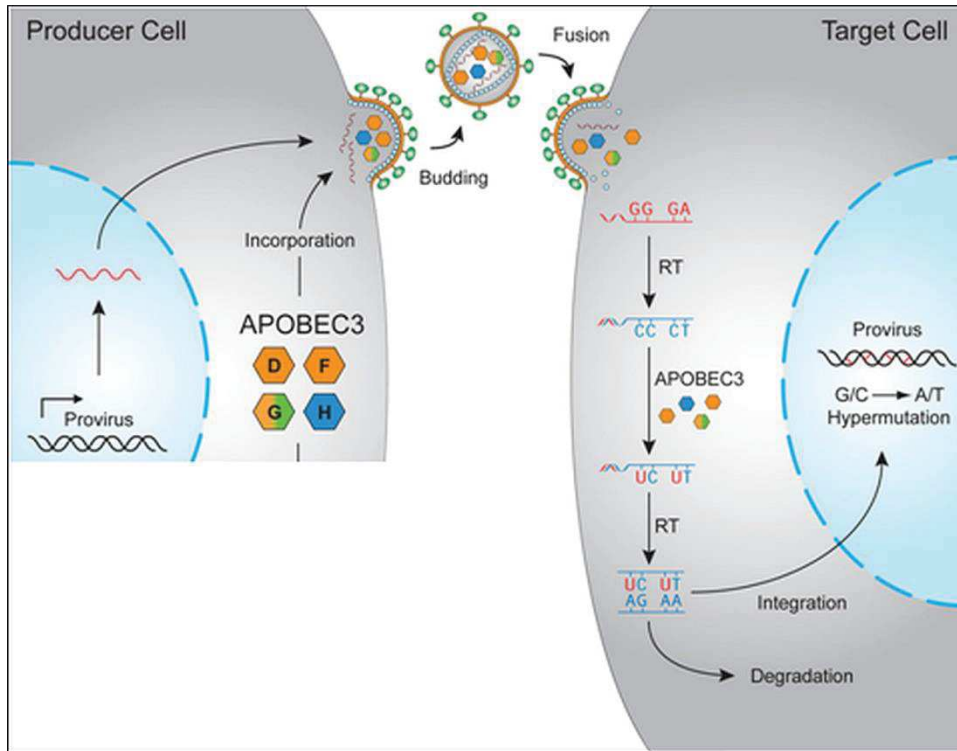


Figure 4: HIV restriction by APOBEC3 proteins. APOBEC3 proteins can be encapsidated into HIV virions and result in the deamination of cytidines to uridines in viral cDNA upon initiation of reverse transcription (RT) in target cells. Uracil templates adenine upon second-strand synthesis, resulting in a G to A hypermutation. These viral cDNAs are subsequently degraded (still controversial in the field) or integrated (although many are rendered non-functional). (Figure was adapted from (Harris et al., 2012) with permission from ASBMB).

Depending on the experimental conditions, infectivity of HIV-1 Δ vif particles can be reduced by human A3G up to 1000-fold by accumulative mechanisms (Hultquist and Harris, 2009, Malim and Bieniasz, 2012). Under laboratory settings, the Vif protein of HIV-1 counteracts efficiently, but not completely A3D, A3F, A3G and A3H (Hultquist and Harris, 2009). In HIV-1 Δ vif infected cells, A3G binds to the viral nucleocapsid protein and gets incorporated into the budding virus particle (Fig. 4) (Malim and Bieniasz, 2012). In the next round of infection,

after cell entry, the viral (+) strand RNA is reverse transcribed into (-) strand DNA that is the template for the (+) strand DNA synthesis, generating a complete, double-stranded DNA. The particle-delivered A3G can inhibit HIV-1 through multiple mechanisms early in the infection cycle, and viral genomes isolated in the first hours post infection contain many G-to-A mutations also called hypermutations (Harris et al., 2003, Mangeat et al., 2003, Mariani et al., 2003, Zhang et al., 2003). A3s deaminate cytidines in the single-stranded viral (-) strand DNA, mutating them to uracils. As a consequence, the viral coding (+) strand shows G-to-A changes (Fig. 4). The A3-induced editing of the viral genome can cause missense or nonsense mutations in the viral genes and can damage the viral regulatory elements. In addition, A3G interferes with multiple steps of reverse transcription (Bishop et al., 2008, Guo et al., 2006, Guo et al., 2007, Langlois and Neuberger, 2008, Li et al., 2007, Mbisa et al., 2010, Wang et al., 2012, Mbisa et al., 2007, Iwatani et al., 2007, Münk et al., 2012a) and A3G and A3F can directly interact with the viral integrase and negatively affect the integration efficiency of HIV-1 Δ vif (Luo et al., 2007, Mbisa et al., 2010). The HIV-1 genomes with hypermutations that accomplish to get integrated as a provirus may be defective, depending on whether mutations occurred in the promoter regions or the *tat* gene. Conversely, HIV virus evolution may benefit by sub-lethal mutation of host APOBEC3s (Dapp et al., 2013, Jaszczur et al., 2013, Münk et al., 2012a, Bourara et al., 2007).

A3 acts as carcinogen

Many important aspects of the biology of A3 proteins are not resolved, and it is still unknown how A3s distinguish self from non-self ssDNA. Evidence inferred that A3B impairs genome stability by inducing base substitutions in genomic DNA in human cells (Shinohara et al., 2012). Enforced overexpression of A3A causes DNA damage (double strand breaks-DSB) and mutation that consequently trigger cell cycle arrest (Landry et al., 2011, Stenglein et al., 2010, Suspene et al., 2011, Shee et al., 2013, Caval et al., 2013). Recent data support a role of human A3 proteins, especially for A3B, to act oncogenic and cause C-to-T mutations in breast cancer tissue (Burns et al., 2013a, Nowarski and Kotler, 2013, Taylor et al., 2013, Nik-Zainal et al., 2012a). Somatic mutations from 21 breast cancer genomes reported recently, they found a fascinating phenomenon of localized hypermutation, termed “kataegis” was observed (Nik-Zainal et al., 2012a, Nik-Zainal et al., 2012b, Taylor et al., 2013). Evidence for A3B mutagenesis pattern in multiple distinct cancers were recently reported (Burns et al.,

2013b, Roberts et al., 2013). Thus the A3 family proteins can act as “double-edged sword”: to protect the host from viral pathogens, and conversely can affect self-genome integrity, in consequence, causing detrimental diseases. A short review on A3’s involvement in cancers is given in chapter VI.

Viral infectivity factor (Vif): A protein that determines species specificity and engages in intracellular duel with A3 proteins

The Vif protein of HIV-1 is required for the virus replication in A3G expressing cells (Gabuzda et al., 1992, Strebel et al., 1987, von Schwedler et al., 1993, Yu et al., 2003, Yu et al., 2004b). Vif binding to A3G will induce polyubiquitination and degradation of A3G by the cellular proteasome machinery. The A3-Vif interaction is thought to be an important species specificity determinant for HIVs and the related SIVs: A3 proteins that do not interact with Vif are not counteracted (Mariani et al., 2003). The Vif protein governs species specificity: For example, the Vif proteins of HIV-1 and chimpanzee SIV (SIVcpz) can induce the degradation of human (h) A3G, enabling these viruses to infect humans. Conversely, hA3G is resistant to the activity of SIVagm Vif, and humans are resistant to infection by this virus. In addition, agmA3G is resistant to HIV-1 Vif, although it is susceptible to SIVagm Vif (Mariani et al., 2003, Bogerd et al., 2004, Mangeat et al., 2004, Zhang et al., 2008).

To achieve polyubiquitination and subsequent degradation of A3G, Vif acts as an A3G substrate receptor molecule by mimicking the SOCS-box component of a cellular E3 ubiquitin ligase in the Vif-Cullin 5-Elongin B/C ubiquitin ligase complex (Bergeron et al., 2010, Kobayashi et al., 2005, Liu et al., 2005, Marin et al., 2003, Mehle et al., 2004, Stanley et al., 2008, Wolfe et al., 2010, Yang et al., 2001, Yu et al., 2004b, Wissing et al., 2010, Jager et al., 2012b). The SOCS-box in Vif (residues 144–173), which consists of the BC-box and the Cullin-box, is required for multimerization. The BC-box recruits EloC and the Cullin-box interacts with Cul5 (Mehle et al., 2004, Yang et al., 2001, Yu et al., 2004b, Donahue et al., 2008, Stanley et al., 2008, Wolfe et al., 2010).

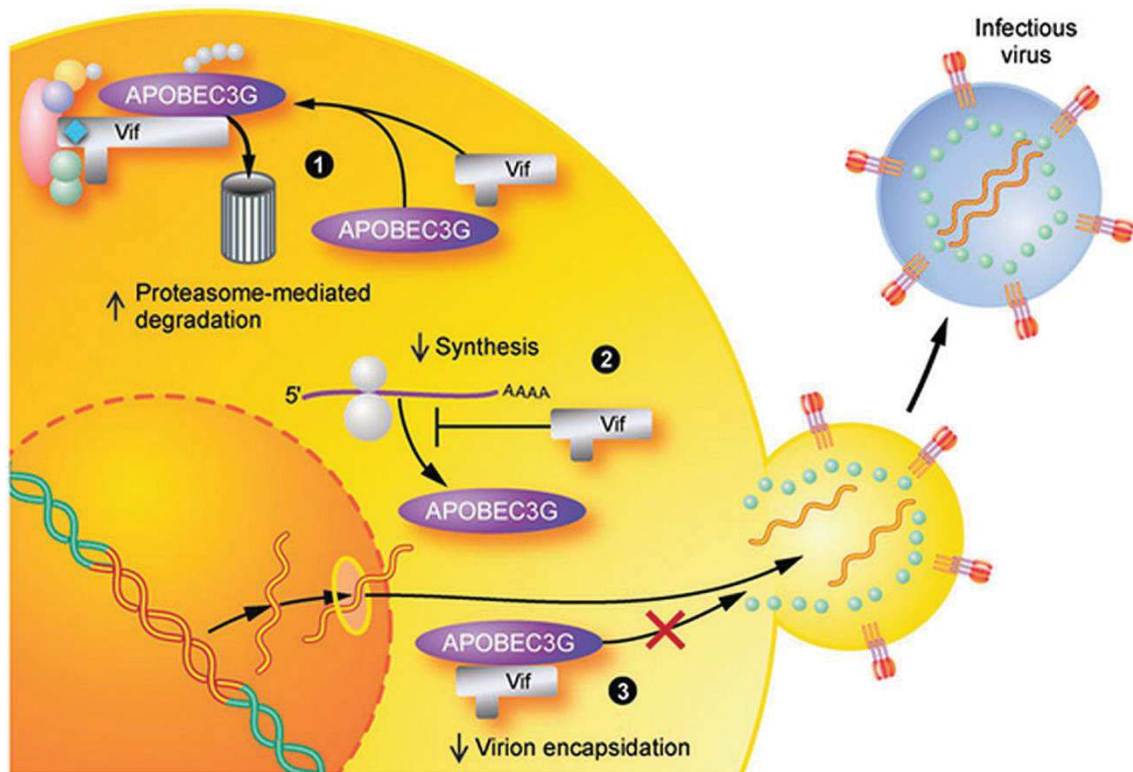


Figure 5: The interplay of Vif and APOBEC3G: Vif diminishes the intracellular pool of A3s impairing virion encapsidation

(1) Vif defeats the antiviral activity of hA3 principally by both binding to hA3 and recruiting an E3 ligase complex that mediates polyubiquitylation (Ubn) of hA3. Vif connects the cellular E3 ubiquitin ligase with A3 which initiates the polyubiquitination of the A3 proteins by 26S proteasomes. (2) Vif also partially impairs the translation of hA3 mRNA and thus reduces the cellular protein pool. (3) These dual effects of Vif effectively deplete hA3 in the virus-producing cells; thus, hA3 is not available for incorporation into virions budding from these cells. Other auxiliary functions of Vif have been proposed, including the physical exclusion of hA3G from virion encapsidation in the absence of degradation, perhaps owing to sequestration of hA3G away from the sites of viral assembly/budding. (Figure was adapted from (Chiu and Greene, 2008) with permission from Annual Reviews)

The binding of Cul5 to Vif is also mediated by the zinc-binding HCCH-box (residues 108–139) and the T(Q/D/E)x5ADx2 (I/L) motif (residues 96–107) (Wolfe et al., 2010, Yu et al., 2004b, Dang et al., 2010b, Luo et al., 2005, Mehle et al., 2006, Xiao et al., 2006, Xiao et al., 2007). Vif additionally hijacks the transcription cofactor CBF- β (Core binding factor β) to form this active protein complex to degrade A3G and promote HIV-1 infection (Fig. 5) (Jager et al., 2012b, Salter et al., 2012, Zhang et al., 2012, Matsui et al., 2014, Guo et al., 2014). There is little knowledge about the regulation of Vif; it is not associated with kinases (Jager et al., 2012a) and here as a part of this thesis, it was reported that Vif is not a phosphoprotein, and serine/threonine phosphorylation of A3G or Vif is not required for Vif mediated A3

degradation and viral infectivity (Kopietz et al., 2012) (in contrary to (Shirakawa et al., 2008, Yang et al., 1996)). Several A3-Vif interaction motifs have recently been described in Vif such as for A3G the G-box (residues 40-44) together with the WxSLVK motif (residues 21-26), the FG-box (residues 55-72), the LGxGxxlxW motif (residues 81-89) and the T(Q/D/E)_xAD_x₂(I/L) motif (Dang et al., 2010a, Dang et al., 2010b, Dang et al., 2009, He et al., 2008, Pery et al., 2009, Russell and Pathak, 2007). Vif mutants that have a defect in binding to A3G, or Cullin 5, or Elongin C are unable to counteract the antiviral activity of A3G by degradation. Besides depleting A3G, Vif exploits alternative pathways to block packaging of A3G. In experimental systems that lack Vif dependent A3G degradation, the presence of Vif, still protected HIV-1 particles from A3G, suggesting that binding of Vif to A3G can be sufficient (Kao et al., 2007, Kao et al., 2004, Opi et al., 2007). Thus, it is possible that Vif induces structural changes in A3G that prevent packaging and/or inhibit the enzymatic function of A3G (Dang et al., 2009, He et al., 2008, Pery et al., 2009). In addition, Vif may specifically also inhibit the translation of A3G mRNA by 30% - 50% and packaging of A3G into nascent virions (Fig. 5) (Kao et al., 2003, Stopak et al., 2003).

There are a few reports that describe the activity of Vif on the cell cycle (DeHart et al., 2008, Izumi et al., 2010, Sakai et al., 2006, Wang et al., 2007) suggesting that Vif has a role in pathogenesis, in addition to its function of A3 counteraction. By expressing Vif, lentiviruses can induce the degradation of APOBEC3 proteins, thereby overcoming these intrinsic restriction factors. How viruses such as EIAV, MLV, HTLV, or foamy viruses (which do not carry *vif* genes) resist inhibition by APOBEC proteins is an interesting issue.

Vif is a 23 kDa basic protein (192 amino acids), which is expressed late during the HIV-1 infection. Vif was found to interact with RNA and to short single- and double-stranded DNA (Bernacchi et al., 2007, Dettenhofer et al., 2000, Henriët et al., 2005, Henriët et al., 2007, Khan et al., 2001, Zhang et al., 2000). The disordered region of Vif protein, which contains Cullin box was not observed in the crystal structure (Stanley et al., 2008). Results from molecular modeling and mass spectrometry analysis also suggested that the C-terminal domain (CTD) of Vif may be intrinsically unstructured which may gain its structure upon binding the co-factors or during self-assembly (Auclair et al., 2007, Balaji et al., 2006, Barraud et al., 2008). High resolution molecular structural determination of Vif by X-ray crystallography or NMR has been precluded by an inability to produce soluble full-length Vif protein (Barraud et al., 2008, Gallerano et al., 2011, Marcsisin and Engen, 2010, Marcsisin et

al., 2011), recently it was reported that co-expression of human CBF β in *E. coli* greatly increased the solubility of full-length Vif (Zhou et al., 2012).

The first complex structure containing HIV-1 Vif-CBFB-CUL5-ELOB-ELOC was solved recently. Vif structure contains two distinct regions namely α -domain and α/β domain. CBFB binds to the larger α/β domain (similar to RUNX1 binding) and ELOC/CUL5 interacted cooperatively with small α -domain of Vif (Guo et al., 2014).

Retroelements

Retrotransposons or retroelements are the mobile genetic elements, ubiquitously present in many eukaryotic genomes, and might mediate the genome evolution (Baltimore, 1985). Human genome sequencing demonstrated that about half of the genome comprised of transposon or its remnants. Retrotransposons contribute about 42% of the genome whereas DNA transposons account merely 2-3% (Lander et al., 2001, Venter et al., 2001, Li et al., 2001). Very recently, it was proposed that induced pluripotent stem (iPS) cells of human and non-human primate (NHP) revealed differences in the regulation of L1 by APOBEC3B and PIWIL2 gene expression, suggesting that L1 retrotransposons are differently active during primate development. Differences in L1 mobility may have differentially shaped the genomes of humans and NHPs and could have continuing adaptive significance (Marchetto et al., 2013).

Genetic organisation and L1 replication cycle

Retrotransposons are classified into two sub-categories on the basis of the presence or absence of long terminal repeat (LTR) regions. The Long Interspersed Elements type 1 (LINE-1 or shortly, L1) retrotransposons are a group of proliferating, autonomous, non-LTR elements that represent a major evolutionary force acting on the structure and composition of eukaryotic genomes (and diseases) (Beck et al., 2010, Goodier and Kazazian, 2008, Huang et al., 2010, Iskow et al., 2010, Kazazian et al., 1988). Approximately 21.1% of our chromosomal DNA consists of L1 sequences (about 520,000 copies) (Lander et al., 2001, Lindblad-Toh et al., 2005, Schumann et al., 2010). But only 80-100 L1s are functional and retrotransposition competent in the average genome (Brouha et al., 2003). Unlike SINEs

(short interspersed repeat elements) which lack internal RT, L1 RNA consists of two open reading frames that encode functional ORF1p and ORF2p proteins, respectively (Figure 6A). ORF1p is an RNA binding protein that has nucleic acid chaperone activity *in vitro* (Kolosha and Martin, 1997, Martin and Bushman, 2001, Kolosha and Martin, 2003, Khazina and Weichenrieder, 2009) and ORF2p has endonuclease (Feng et al., 1996) and reverse transcriptase activities (Dombroski et al., 1994, Mathias et al., 1991). Like other retroviruses and retrotransposons, L1 elements replicate via an RNA intermediate using a ‘copy-and-paste’ mechanism. Strikingly, for retroviruses and LTR retrotransposons, reverse transcription takes place in the cytoplasm (Goodier and Kazazian, 2008). In contrast, for non-LTR retrotransposons reverse transcription occurs in the nucleus and is directly coupled to genomic integration by target-primed reverse transcription (TPRT) (Cost et al., 2002, Luan et al., 1993).

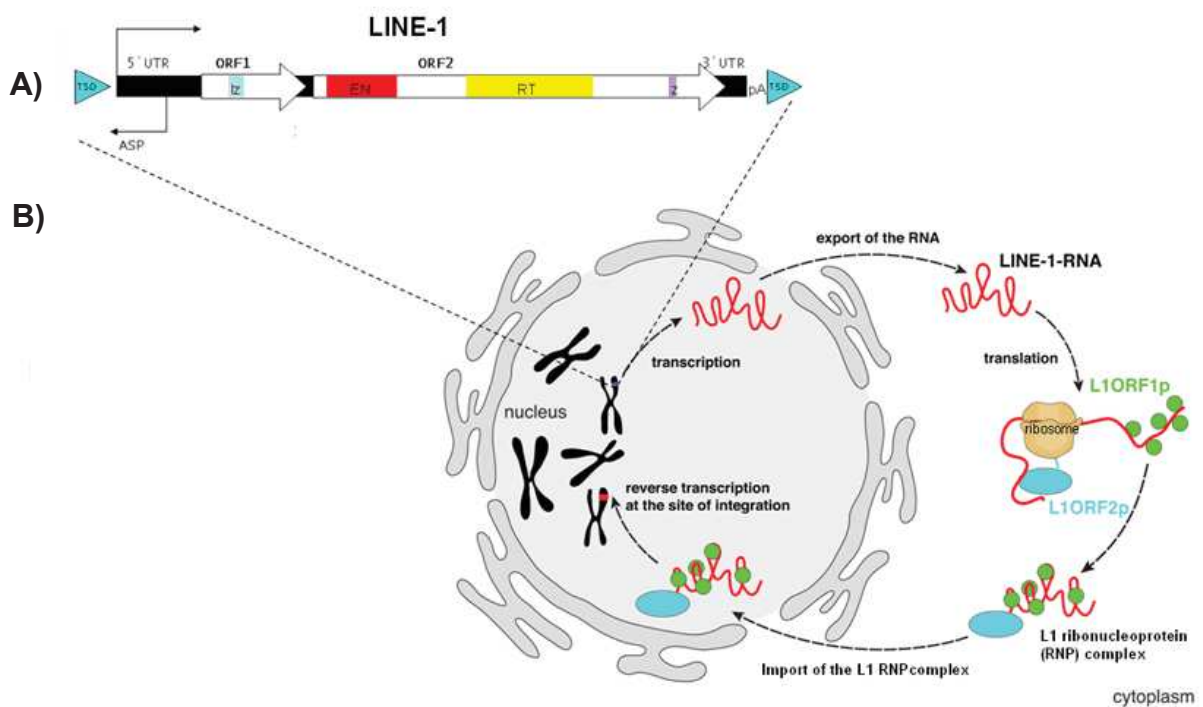


Figure 6: Genetic organisation of L1 and its retrotransposition cycle. A) A functional L1 element is 6 kb long that includes a 5'-untranslated (UTR) region, consisting of an internal promoter, two open reading frames (ORFs) separated by a 63 nucleotide intron and a 3' UTR terminating in a poly (A) tail (Dombroski et al., 1991). B) Reverse transcribed L1 mRNA (red) exported to the cytoplasm, produce ORF1p and ORFp2 proteins with host machinery and forms RNP complex. This complex is then imported back to the nucleus for the site primed reverse transcription by its ORF2 and integrate into the host chromosome (**Figure courtesy:** Dr. Elena Khazina and Prof. Oliver Weichenrieder)

After transcription, L1 mRNA is exported to the cytoplasm for the synthesis of L1 proteins: ORF1p, ORF2p. The products subsequently bind their own mRNA and form ribonucleoprotein (RNP) complexes (Hohjoh and Singer, 1996, Kulpa and Moran, 2005) which will gain access to the nucleus where it is reverse transcribed into cDNA more likely via TPRT by its RT enzyme (Cost et al., 2002, Feng et al., 1996) and integrated into the genome (Fig. 6B) (Zingler et al., 2005).

Effects of retrotransposition

Mobilization of L1 elements and other transposons can be detrimental to the human genome. L1 retrotransposon activity can cause diseases by insertional mutagenesis, recombination, providing enzymatic activities for other non-long terminal repeat (non-LTR) retrotransposons, and perhaps by transcriptional over-activation and epigenetic effects (such as methylation changes in DNA) (Goodier and Kazazian, 2008, Solyom and Kazazian, 2012). Genetic disorders such as haemophilia (Kazazian et al., 1988), cystic fibrosis, muscular dystrophy, neurofibromatosis, breast and colon cancer, altogether 96 diseases up to date, were shown to be the consequences of genomic instabilities caused by L1, Alu and SVA elements (Hancks and Kazazian, 2012). Recent reports propose that the endonuclease activity of L1 may facilitate genome instability and chromosomal breaks (Gasior et al., 2006, Lin et al., 2009).

In order to limit such lethal effects of retrotransposition, host cells have adopted different strategies to control the propagation of transposons. Mechanisms such as DNA methylation (Bourc'his and Bestor, 2004, Yu et al., 2001), small RNA (siRNA) mediated regulation (Aravin et al., 2007, Malone and Hannon, 2009, Yang and Kazazian, 2006), DNA repair factors (Gasior et al., 2008, Suzuki et al., 2009), and restriction by TREX1 DNA exonuclease (Stetson et al., 2008) and recently the member of APOBEC3 cytidine deaminase family (Muckenfuss et al., 2006, Kinomoto et al., 2007) (for an in-depth review, see (Levin and Moran, 2011)). Here the effect of APOBEC3C on LINE elements and their mechanism of action of retrotransposition was investigated, which is included in the thesis chapter X (Horn et al., 2014).

Foamy Viruses

In addition to retroviruses HIV or SIV, peculiar retroviruses such as the foamy virus (Fig. 1) were reported to be prevalent in African monkey species. The following section describes its origin, molecular features, infectivity cycle and foamy virus Bet protein.

Historical perspective

The first description of foamy virus (FV) was reported in 1954 (Enders and Peebles, 1954). It was found as a contaminant with an atypical cytopathic effect (CPE) with the formation of multinucleated and vacuolated giant cells in primary kidney cell cultures from Old World monkeys of the *Macacaceae* family. The name foamy virus or spumavirus was derived from the foam-like appearance of syncytia in the infected monolayer cell cultures. Foamy viruses were classified as retroviruses after the detection of FV RT enzyme. The first isolate of the “foamy viral agent” was in 1955 (Rustigian et al., 1955). In 1971, a viral agent with FV-like characteristics was isolated and identified from lymphoblastoid cells from a Kenyan patient suffering from nasopharyngeal carcinoma (NPC) (Achong et al., 1971). At the time it was called SFVcpz (hu) because of its origin and its marked similarity to the Simian Foamy Virus found in chimpanzees. The origin of SFVcpz (hu) was debated until 1994, when SFVcpz was cloned and sequenced (Herchenroder et al., 1994). The 86 to 95% amino acid identity between SFVcpz and SFVcpz (hu) suggested that SFVcpz (hu) is likely a variant of SFVcpz and not a unique isolate (Herchenroder et al., 1994). Sequence comparisons between the original SFVcpz (hu) isolate and SFV from four distinct subspecies of chimpanzee demonstrate that SFVcpz (hu) is most closely related to FV from *Pan troglodytes schweinfurthii*, whose natural habitat includes Kenya. Since the original human foamy virus (HFV) isolate came from a person who might have had contact with *P. troglodytes schweinfurthii* in Kenya, the virus was probably acquired as a zoonotic infection (transmission from animals to human) (Meiering and Linial, 2001) (for a detailed review on Foamy Virus Epidemiology and Infection, see (Meiering and Linial, 2001, Gessain et al., 2013)). HFV has now been renamed as the Prototype foamy virus (PFV) although it is much of debate, whether the “real” origin of the virus isolates spread through *in vivo* cross-species transmission from chimpanzee or if it is originated from a cell culture contamination

(Gessain et al., 2013). Notably, most monkeys which are infected by foamy viruses carry also an SIV infection.

Host-Virus co-speciation and evolution

FV genomes display a high evolutionary conservation among all the species infected and FV genetic variability within one infected animal is very low overtime (<1% variation) (Schweizer et al., 1999). The phylogenetic analysis of SFV polymerase and mitochondrial cytochrome oxidase subunit II (COII) from African and Asian monkeys and apes provide very similar branching order and divergence times among the two trees, supporting the co-speciation. Molecular clock calibrations revealed an extremely low rate of SFV evolution, 1.7×10^{-8} base substitutions per site per year, making FV the slowest-evolving virus documented so far (observed that the substitution rates for the host and SFV genes were very similar). These results revealed highly congruent relationships, indicating virus-host co-evolution for at least 30–40 million years, making them the oldest known vertebrate viruses (Switzer et al., 2005, Holmes, 2008). This ancient relationship may be responsible for the non-pathogenic phenotype of SFV. The various SFVs do not seem to cause any recognizable disease in their natural hosts, despite they are highly cytopathic in tissue culture (Linial, 2000, Meiering and Linial, 2001, Murray and Linial, 2006, Gessain et al., 2013). There are reports of recombination events between several circulating FV strains as well as deletions and mutations have been reported in wild-living chimpanzees, in spite of their global genetic stability (Liu et al., 2008).

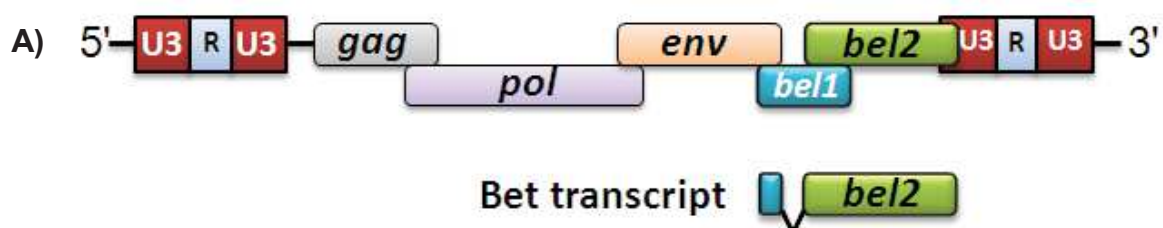
When retroviruses get access to gametocytes, the resulting endogenous form of the virus can be passaged in the germline along with the host cell genome and is no longer transmitted as an exogenous virus (Holmes, 2011, Katzourakis and Gifford, 2010). The recent discoveries of endogenous foamy viruses in the Madagascar aye-aye (*Daubentonia madagascariensis*, a strepsirrhine primate/a primitive prosimian), a Chinese bat and the two- and three-toed sloth from South America (*Choloepus hoffmanni*), of foamy virus-like insertions within the genome of a “living fossil,” the *Coelacanth* (*Latimeria chalumnae*) that provides the details of FV-host coevolution represents an age of over 400 million years ago (MYA) (so the oldest known virus-host relationship), most recently from platyfish

(*Xiphophorus maculatus*) and cod species (Han and Worobey, 2012a, Han and Worobey, 2012b, Katzourakis et al., 2009, Scharl et al., 2013, Wu et al., 2012). These finding of novel endogenous and exogenous FVs not only extend the age of FVs, but the finding in non-mammalian vertebrate phyla, supports the concept of the great evolutionary success of this retroviral subfamily (Rethwilm and Bodem, 2013).

SFVs are highly prevalent in captive primate populations, with infection rates ranging from 70% to 100% in adult animals (Gessain et al., 2013, Meiering and Linial, 2001, Murray and Linial, 2006). People like hunters, poachers, zookeepers, temple workers and villagers who are occupationally exposed to non-human primates (NHP) can become infected with SFV (Switzer et al., 2004, Wolfe et al., 2004, Gessain et al., 2013, Schweizer et al., 1995, Jones-Engel et al., 2008) (documented in review (Gessain et al., 2013)). Such transmission in personnel from zoos or primate centres was also recently demonstrated in Gabon and in China (Huang et al., 2012, Mouinga-Ondeme et al., 2012, Mouinga-Ondeme et al., 2010), recent study also confirmed the mode of cross-species transmission in hunters in Gabon is as a result of severe bites (saliva) from gorillas (Mouinga-Ondeme et al., 2012).

Molecular biology of FV

Foamy viruses, also known to be as *syncytial* or *spumaretroviruses* represent an unusual branch of the retrovirus family tree (Meiering and Linial, 2001). They have complex genomes like HIV or HTLV [ranging from 10.5 kbp (Feline FV (Bodem et al., 1998)) to 13kbp (SFV, chimpanzee strain (Herchenroder et al., 1994))] that encode Tas (or bel-1) (a nuclear transcriptional transactivator) and Bet (an auxiliary protein), in addition to Gag, Pol and Env, and their replication strategies differ from those of other retroviruses (Figure 8) (Linial, 1999); genome is flanked by LTRs.



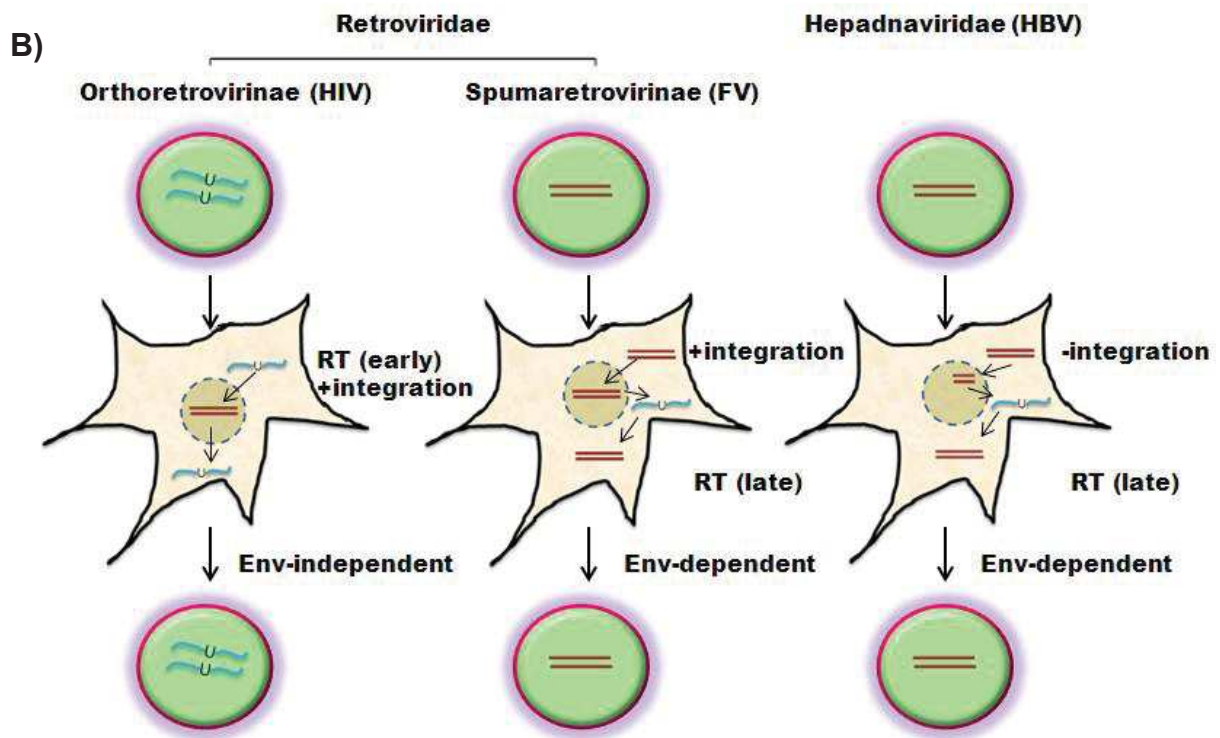


Figure 8: Genome organization of FV and replication strategies of viruses using RT. A) Similar to HIV-1, FV possesses *gag*, *pol*, and *env* genes. The regulatory and accessory *bel1* and *bel2* genes are localized between *env* and the 3'LTR. The Bet protein is a product of a spliced transcript and consists of Bel1 and Bel2 parts (self-made figure modified from (Lukic et al., 2013)). B) Replication cycle: Orthoretroviruses (RNA genome in the virion) such as HIV replicated through dsDNA intermediate and require integration of viral genome into host genome for propagation, hepadnaviruses (ds DNA in the virion) in contrary, doesn't integrate their genome but require RNA intermediate (late RT) for its replication. FVs are bridging these pathways, as they integrate their genome (DNA) into host (like orthoretroviruses), they undergo late reverse transcription (like hepadnaviruses), in the virus particles the genomes are mostly made of DNA. Moreover, the release of FV depends on their related glycoprotein (Lindemann and Goepfert, 2003) as in hepadnaviruses, while budding of orthoretroviral particles is Env-independent. RT, reverse transcriptase, RNA and DNA molecules are denoted by blue lines with U and brown lines respectively. Arrows in the figure guide the path of the viral replication event. (self-made figure adapted from (Rethwilm and Bodem, 2013))

Foamy viruses can retrotranspose within a single cell and, even when viral particles are released, reverse transcription occurs mainly in producer cells such that extracellular virions contain double-stranded DNA (Yu et al., 1999). Regulation of FV genome expression, multiplicing at the internal promoter and nuclear export strategies are reviewed in (Rethwilm, 2010). Very recently, reviews on foamy virus molecular virology, tropism, zoonotic transmission (Kehl et al., 2013), unique nature of foamy virus gag proteins (Mullers,

2013), FV budding and release (Hutter et al., 2013), host interaction and intracellular trafficking (Berka et al., 2013), RNA-protein interaction during the FV replication (Rethwilm, 2013), and evolution of FV (Rethwilm and Bodem, 2013) were appeared, implying that the focus of researchers are being attracted towards the understanding of FV biology. FV are promising candidates for the development of potential retroviral vectors for gene delivery and vaccination (Lindemann and Rethwilm, 2011, Rethwilm, 2007, Trobridge, 2009, Schwantes et al., 2003, Erlwein and McClure, 2010), due to their non-pathogenicity in any species. In addition, FV may serve as a model for developing antiretroviral drugs for HIV-1 as three-dimensional structure of FV integrase was the first solved retroviral integrase protein by X-ray crystallography (Hare et al., 2010, Krishnan et al., 2010, Maertens et al., 2010, Valkov et al., 2009). Recently, with crystallography and cryo-electron microscopy techniques, structures of the intasomes from β -retrovirus mouse mammary tumor virus (Ballandras-Colas et al., 2016), α -retrovirus Rous sarcoma virus (Yin et al., 2016), lentivirus maedi-visna virus (Ballandras-Colas et al., 2017), and HIV-1 (mutated IN) (Passos et al., 2017) were solved (Engelman and Cherepanov, 2017).

FV auxiliary protein Bet

FVs are the only member of *Spumaretrovirinae* and possess a complex genome that encodes the accessory protein Bet (Fig. 8B). While Bet is found in vast amounts in the cytoplasm of infected cells (Cullen, 1992) its exact function is not well understood (Linial, 1999). Studies in past years provided debatable results. PFV Bet has been suggested to be involved in resistance to viral superinfection (Bock et al., 1998).

Bet protein from feline foamy virus (FFV) was shown to inhibit cytidine deamination of the viral genome and in particular, hinders the antiretroviral activity of the feline APOBEC3 (fe3) without triggering their proteolytic degradation (Lochelt et al., 2005, Chareza et al., 2012, Münk et al., 2008). The Bet protein domain involved in A3 counteraction was just identified (Lukic et al., 2013). A mechanism for FFV Bet activity has not been identified, but an interaction of FFV Bet and feline A3s was demonstrated to be vital (Chareza et al., 2012). For the PFV system, controversial data regarding the function of Bet as an A3G antagonist have been reported (Russell et al., 2005, Delebecque et al., 2006). Russell *et al.* (36) demonstrated that human A3G and A3F proteins inhibit PFV due to a specific Gag-A3 interaction and

induce guanine to adenine mutations in viral reverse transcripts. They also presented binding of PFV Bet to human A3F and A3G, but not to murine A3 (mA3). PFV Bet could rescue the infectivity of PFV Δbet and Vif-deficient HIV-1 in the presence of A3G (Russell et al., 2005). In contrast, Delebecque *et al.* found that PFV can be effectively restricted by A3G, independent of Bet; they demonstrated human A3G, A3F (but not A3C), and A3G from chimpanzee and African green monkey and mA3 were potentially restricted FV replication in cell culture irrespective of Bet; FV Bet did not rescue the HIV-1 Δvif defect in presence of hA3G (Delebecque et al., 2006). Like the Bet activity of FFV, the mechanism of PFV Bet's inhibition of the antiviral activity of A3G has not been resolved. This conclusion, however, leaves open the question of how foamy viruses persist in their native, APOBEC3-expressing hosts.

Strikingly, it was reported recently that PFV Bet inhibits antiviral activity of human A3C using PFV and Lentiviral based reporter vector system. Bet binding to A3C failed to induce degradation of A3C but instead, it inhibited the crucial dimerization of A3C (Perkovic et al., 2009). Here, the thesis aimed to address whether PFV Bet can protect PFV and lentiviruses against the antiviral activity of human A3G and attempted to understand the fate of A3G bound Bet in human cell line (Jaguva Vasudevan et al., 2013), presented in chapter V. In addition to cellular A3 factors, tetherin was also reported to inhibit the release of PFV and FFV (Dietrich et al., 2011, Xu et al., 2011).

Scientific publications

This thesis is based on the following papers:

1. Jaguva Vasudevan, A. A., Smits, S. H., Hoppner, A., Häussinger, D., Koenig, B. W., and Münk, C. (2013) Structural features of antiviral DNA cytidine deaminases. *Biol Chem* **394**, 1357-1370
2. Jaguva Vasudevan, A. A., Hofmann, H., Willbold, D., Häussinger, D., Koenig, B. W., and Münk, C. (2017) Enhancing the Catalytic Deamination Activity of APOBEC3C Is Insufficient to Inhibit Vif-Deficient HIV-1. *J Mol Biol* **429**, 1171-1191
3. Jaguva Vasudevan, A. A., Zhang, Z., Häussinger, D., and Münk, C. A Naturally Occurring APOBEC3C from Sooty Mangabey Potently Inhibits Human Immunodeficiency Virus Replication. Manuscript under preparation
4. Jaguva Vasudevan, A. A., Krikoni, A., Franken, A., Marino, D., König, R., Schumann, G. G., Häussinger, D., and Münk, C. Glycosylated gag protects murine leukemia virus from producer cell-derived but not from target cell APOBEC3A. Manuscript under preparation
5. Jaguva Vasudevan, A. A., Perkovic, M., Bulliard, Y., Cichutek, K., Trono, D., Häussinger, D., and Münk, C. (2013) Prototype foamy virus Bet impairs the dimerization and cytosolic solubility of human APOBEC3G. *J Virol* **87**, 9030-9040
6. Jaguva Vasudevan, A. A., Göring, W., Häussinger, D., and Münk, C. Detection of APOBEC3 proteins and catalytic activity in urothelial carcinoma. (Accepted for a book chapter on "Urothelial Carcinoma", to be published in the lab protocol series, *Methods in Molecular Biology*, by Springer (2017) in press (Chief editor: W. A. Schulz)
7. Marino, D., Perkovic, M., Hain, A., Jaguva Vasudevan, A. A., Hofmann, H., Hanschmann, K. M., Muhlebach, M. D., Schumann, G. G., König, R., Cichutek, K., Häussinger, D., and Münk, C. (2016) APOBEC4 Enhances the Replication of HIV-1. *PLoS One* **11**, e0155422

Additional Publications

8. Zhang, Z., Gu, Q., Jaguva Vasudevan, A. A., Jeyaraj, M., Schmidt, S., Zielonka, J., Perkovic, M., Heckel, J. O., Cichutek, K., Häussinger, D., Smits, S. H., and Münk, C. (2016) Vif Proteins from Diverse Human Immunodeficiency Virus/Simian Immunodeficiency Virus Lineages Have Distinct Binding Sites in A3C. *J Virol* **90**, 10193-10208
9. Kopietz, F., Jaguva Vasudevan, A. A., Kramer, M., Muckenfuss, H., Sanzenbacher, R., Cichutek, K., Flory, E., and Münk, C. (2012) Interaction of human immunodeficiency virus type 1 Vif with APOBEC3G is not dependent on serine/threonine phosphorylation status. *J Gen Virol* **93**, 2425-2430
10. Horn, A. V., Klawitter, S., Held, U., Berger, A., Vasudevan, A. A., Bock, A., Hofmann, H., Hanschmann, K. M., Troschmeier, J. H., Flory, E., Jabulowsky, R. A., Han, J. S., Lower, J., Lower, R., Münk, C., and Schumann, G. G. (2014) Human LINE-1 restriction by APOBEC3C is deaminase independent and mediated by an ORF1p interaction that affects LINE reverse transcriptase activity. *Nucleic Acids Res* **42**, 396-416
11. Widera, M., Hillebrand, F., Erkelenz, S., Vasudevan, A. A., Münk, C., and Schaal, H. (2014) A functional conserved intronic G run in HIV-1 intron 3 is critical to counteract APOBEC3G-mediated host restriction. *Retrovirology* **11**, 72

* equally contributed to the work

Strategic findings of this thesis

- A point mutation in A3C (S61 to P61), boost the catalytic activity and enhances the antiviral activity of A3C
- A3C prefers 5'-TTCA motif in single-stranded DNA (ssDNA) substrate as a hotspot for cytidine deamination
- A3C.S61P hypermutates the viral genomes of SIV Δ vif and MLV but not of HIV-1 Δ vif, indicating an unknown escape mechanism of HIV-1
- A3C from a primate, sooty mangabey (smmA3C) potently restricts the replication of HIV-1 in a deamination-dependent manner (reportedly, it resist Vif-mediated degradation)
- Replacing the N-terminal region of hA3C with that of smmA3C drastically enhances hA3C's antiviral activity against HIV-1 Δ vif
- Enzymatically active, producer cell and target cell A3A restrict MLV
- Glycosylated Gag (glycogag) of MLV inhibits the encapsidation of A3A, and to a lesser extent of murine A3; but target cell A3A was not affected by glycogag
- Foamy virus Bet binds to A3G and prevents its encapsidation into virus, without inducing its degradation but by impairing its cytosolic solubility
- The Bet - A3G interaction is independent of RNA, presumably a direct binding, this does not affect the catalytic activity of A3G
- The catalytic activity of A3C is not required for inhibiting L1 retrotransposition, but the self-association of A3C appears crucial for interacting with L1 ORF1p proteins, thereby inhibiting RT activity of L1
- Unlike A3s, APOBEC4 did not exhibit ssDNA cytidine deamination, weakly interacted ssDNA, enhanced the production of HIV-1

References

- ACHONG, B. G., MANSELL, P. W., EPSTEIN, M. A. & CLIFFORD, P. 1971. An unusual virus in cultures from a human nasopharyngeal carcinoma. *J Natl Cancer Inst*, 46, 299-307.
- ARAVIN, A. A., SACHIDANANDAM, R., GIRARD, A., FEJES-TOTH, K. & HANNON, G. J. 2007. Developmentally regulated piRNA clusters implicate MILI in transposon control. *Science*, 316, 744-7.
- ARIAS, J. F., KOYAMA, T., KINOMOTO, M. & TOKUNAGA, K. 2012. Retroelements versus APOBEC3 family members: No great escape from the magnificent seven. *Front Microbiol*, 3, 275.
- ARNAUD, F., CAPORALE, M., VARELA, M., BIEK, R., CHESSA, B., ALBERTI, A., GOLDBER, M., MURA, M., ZHANG, Y. P., YU, L., PEREIRA, F., DEMARTINI, J. C., LEYMASTER, K., SPENCER, T. E. & PALMARINI, M. 2007. A paradigm for virus-host coevolution: sequential counter-adaptations between endogenous and exogenous retroviruses. *PLoS Pathog*, 3, e170.
- AUCLAIR, J. R., GREEN, K. M., SHANDILYA, S., EVANS, J. E., SOMASUNDARAN, M. & SCHIFFER, C. A. 2007. Mass spectrometry analysis of HIV-1 Vif reveals an increase in ordered structure upon oligomerization in regions necessary for viral infectivity. *Proteins*, 69, 270-84.
- BALAJI, S., KALPANA, R. & SHAPSHAK, P. 2006. Paradigm development: comparative and predictive 3D modeling of HIV-1 Virion Infectivity Factor (Vif). *Bioinformatics*, 1, 290-309.
- BALLANDRAS-COLAS, A., BROWN, M., COOK, N. J., DEWDNEY, T. G., DEMELER, B., CHEREPANOV, P., LYUMKIS, D. & ENGELMAN, A. N. 2016. Cryo-EM reveals a novel octameric integrase structure for betaretroviral intasome function. *Nature*, 530, 358-61.
- BALLANDRAS-COLAS, A., MASKELL, D. P., SERRAO, E., LOCKE, J., SWUEC, P., JONSSON, S. R., KOTECHA, A., COOK, N. J., PYE, V. E., TAYLOR, I. A., ANDRESDOTTIR, V., ENGELMAN, A. N., COSTA, A. & CHEREPANOV, P. 2017. A supramolecular assembly mediates lentiviral DNA integration. *Science*, 355, 93-95.
- BALTIMORE, D. 1985. Retroviruses and retrotransposons: the role of reverse transcription in shaping the eukaryotic genome. *Cell*, 40, 481-2.
- BARRAUD, P., PAILLART, J. C., MARQUET, R. & TISNE, C. 2008. Advances in the structural understanding of Vif proteins. *Curr HIV Res*, 6, 91-9.
- BARRE-SINOUSSE, F., CHERMANN, J. C., REY, F., NUGEYRE, M. T., CHAMARET, S., GRUEST, J., DAUGUET, C., AXLER-BLIN, C., VEZINET-BRUN, F., ROUZIOUX, C., ROZENBAUM, W. & MONTAGNIER, L. 1983. Isolation of a T-lymphotropic retrovirus from a patient at risk for acquired immune deficiency syndrome (AIDS). *Science*, 220, 868-71.
- BECK, C. R., COLLIER, P., MACFARLANE, C., MALIG, M., KIDD, J. M., EICHLER, E. E., BADGE, R. M. & MORAN, J. V. 2010. LINE-1 retrotransposition activity in human genomes. *Cell*, 141, 1159-70.
- BELANGER, K., SAVOIE, M., ROSALES GERPE, M. C., COUTURE, J. F. & LANGLOIS, M. A. 2013. Binding of RNA by APOBEC3G controls deamination-independent restriction of retroviruses. *Nucleic Acids Res*, 41, 7438-52.
- BERGER, A., MÜNK, C., SCHWEIZER, M., CICHUTEK, K., SCHULE, S. & FLORY, E. 2010. Interaction of Vpx and apolipoprotein B mRNA-editing catalytic polypeptide 3 family member A (APOBEC3A) correlates with efficient lentivirus infection of monocytes. *J Biol Chem*, 285, 12248-54.
- BERGERON, J. R., HUTHOFF, H., VESELKOV, D. A., BEAVIL, R. L., SIMPSON, P. J., MATTHEWS, S. J., MALIM, M. H. & SANDERSON, M. R. 2010. The SOCS-box of HIV-1 Vif interacts with ElonginBC by induced-folding to recruit its Cul5-containing ubiquitin ligase complex. *PLoS Pathog*, 6, e1000925.
- BERKA, U., HAMANN, M. V. & LINDEMANN, D. 2013. Early events in foamy virus-host interaction and intracellular trafficking. *Viruses*, 5, 1055-74.
- BERNACCHI, S., HENRIET, S., DUMAS, P., PAILLART, J. C. & MARQUET, R. 2007. RNA and DNA binding properties of HIV-1 Vif protein: a fluorescence study. *J Biol Chem*, 282, 26361-8.

- BHAYA, D., DAVISON, M. & BARRANGOU, R. 2011. CRISPR-Cas systems in bacteria and archaea: versatile small RNAs for adaptive defense and regulation. *Annu Rev Genet*, 45, 273-97.
- BISHOP, K. N., VERMA, M., KIM, E. Y., WOLINSKY, S. M. & MALIM, M. H. 2008. APOBEC3G inhibits elongation of HIV-1 reverse transcripts. *PLoS Pathog*, 4, e1000231.
- BOCK, M., HEINKELEIN, M., LINDEMANN, D. & RETHWILM, A. 1998. Cells expressing the human foamy virus (HFV) accessory Bet protein are resistant to productive HFV superinfection. *Virology*, 250, 194-204.
- BODEM, J., LOCHELT, M., DELIUS, H. & FLUGEL, R. M. 1998. Detection of subgenomic cDNAs and mapping of feline foamy virus mRNAs reveals complex patterns of transcription. *Virology*, 244, 417-26.
- BOGERD, H. P., DOEHLE, B. P., WIEGAND, H. L. & CULLEN, B. R. 2004. A single amino acid difference in the host APOBEC3G protein controls the primate species specificity of HIV type 1 virion infectivity factor. *Proc Natl Acad Sci U S A*, 101, 3770-4.
- BOURARA, K., LIEGLER, T. J. & GRANT, R. M. 2007. Target cell APOBEC3C can induce limited G-to-A mutation in HIV-1. *PLoS Pathog*, 3, 1477-85.
- BOURC'HIS, D. & BESTOR, T. H. 2004. Meiotic catastrophe and retrotransposon reactivation in male germ cells lacking Dnmt3L. *Nature*, 431, 96-9.
- BRIGGS, J. A., WILK, T., WELKER, R., KRAUSSLICH, H. G. & FULLER, S. D. 2003. Structural organization of authentic, mature HIV-1 virions and cores. *EMBO J*, 22, 1707-15.
- BROUHA, B., SCHUSTAK, J., BADGE, R. M., LUTZ-PRIGGE, S., FARLEY, A. H., MORAN, J. V. & KAZAZIAN, H. H., JR. 2003. Hot L1s account for the bulk of retrotransposition in the human population. *Proc Natl Acad Sci U S A*, 100, 5280-5.
- BROWNE, E. P., ALLERS, C. & LANDAU, N. R. 2009. Restriction of HIV-1 by APOBEC3G is cytidine deaminase-dependent. *Virology*, 387, 313-21.
- BURNS, M. B., LACKEY, L., CARPENTER, M. A., RATHORE, A., LAND, A. M., LEONARD, B., REFSLAND, E. W., KOTANDENIYA, D., TRETYAKOVA, N., NIKAS, J. B., YEE, D., TEMIZ, N. A., DONOHUE, D. E., MCDUGLE, R. M., BROWN, W. L., LAW, E. K. & HARRIS, R. S. 2013a. APOBEC3B is an enzymatic source of mutation in breast cancer. *Nature*, 494, 366-70.
- BURNS, M. B., TEMIZ, N. A. & HARRIS, R. S. 2013b. Evidence for APOBEC3B mutagenesis in multiple human cancers. *Nat Genet*, 45, 977-83.
- CAVAL, V., SUSPENE, R., VARTANIAN, J. P. & WAIN-HOBSON, S. 2013. Orthologous Mammalian APOBEC3A Cytidine Deaminases Hypermutate Nuclear DNA. *Mol Biol Evol*.
- CHAREZA, S., SLAVKOVIC LUKIC, D., LIU, Y., RATHE, A. M., MÜNK, C., ZABOGLI, E., PISTELLO, M. & LOCHELT, M. 2012. Molecular and functional interactions of cat APOBEC3 and feline foamy and immunodeficiency virus proteins: different ways to counteract host-encoded restriction. *Virology*, 424, 138-46.
- CHARLES A JANEWAY, J., PAUL TRAVERS, MARK WALPORT, AND MARK J SHLOMCHIK. 2001. *Immunobiology: The Immune System in Health and Disease. 5th edition*, United States, New York : Garland Pub., c2001.
- CHIU, Y. L. & GREENE, W. C. 2008. The APOBEC3 cytidine deaminases: an innate defensive network opposing exogenous retroviruses and endogenous retroelements. *Annu Rev Immunol*, 26, 317-53.
- CHIU, Y. L. & GREENE, W. C. 2009. APOBEC3G: an intracellular centurion. *Philos Trans R Soc Lond B Biol Sci*, 364, 689-703.
- CLAPHAM, P. R. & MCKNIGHT, A. 2002. Cell surface receptors, virus entry and tropism of primate lentiviruses. *J Gen Virol*, 83, 1809-29.
- CLOYD, M. W. 1996. Human Retroviruses. In: BARON, S. (ed.) *Medical Microbiology*. 4th ed. Galveston (TX).
- COFFIN, J., HAASE, A., LEVY, J. A., MONTAGNIER, L., OROSZLAN, S., TEICH, N., TEMIN, H., TOYOSHIMA, K., VARMUS, H., VOGT, P. & ET AL. 1986. Human immunodeficiency viruses. *Science*, 232, 697.

- COST, G. J., FENG, Q., JACQUIER, A. & BOEKE, J. D. 2002. Human L1 element target-primed reverse transcription in vitro. *EMBO J*, 21, 5899-910.
- CULLEN, B. R. 1992. Mechanism of action of regulatory proteins encoded by complex retroviruses. *Microbiol Rev*, 56, 375-94.
- CULLEN, B. R. 2006. Role and mechanism of action of the APOBEC3 family of antiretroviral resistance factors. *J Virol*, 80, 1067-76.
- DANG, Y., DAVIS, R. W., YORK, I. A. & ZHENG, Y. H. 2010a. Identification of 81LGxGxxlxW89 and 171EDRW174 domains from human immunodeficiency virus type 1 Vif that regulate APOBEC3G and APOBEC3F neutralizing activity. *J Virol*, 84, 5741-50.
- DANG, Y., WANG, X., YORK, I. A. & ZHENG, Y. H. 2010b. Identification of a critical T(Q/D/E)x5ADx2(I/L) motif from primate lentivirus Vif proteins that regulate APOBEC3G and APOBEC3F neutralizing activity. *J Virol*, 84, 8561-70.
- DANG, Y., WANG, X., ZHOU, T., YORK, I. A. & ZHENG, Y. H. 2009. Identification of a novel WxSLVK motif in the N terminus of human immunodeficiency virus and simian immunodeficiency virus Vif that is critical for APOBEC3G and APOBEC3F neutralization. *J Virol*, 83, 8544-52.
- DAPP, M. J., PATTERSON, S. E. & MANSKY, L. M. 2013. Back to the future: revisiting HIV-1 lethal mutagenesis. *Trends Microbiol*, 21, 56-62.
- DAUGHERTY, M. D. & MALIK, H. S. 2012. Rules of engagement: molecular insights from host-virus arms races. *Annu Rev Genet*, 46, 677-700.
- DAYTON, A. I., SODROSKI, J. G., ROSEN, C. A., GOH, W. C. & HASELTINE, W. A. 1986. The trans-activator gene of the human T cell lymphotropic virus type III is required for replication. *Cell*, 44, 941-7.
- DE MATOS, A. L., VAN DER LOO, W., AREAL, H., LANNING, D. K. & ESTEVES, P. J. 2011. Study of Sylvilagus rabbit TRIM5alpha species-specific domain: how ancient endoviruses could have shaped the antiviral repertoire in Lagomorpha. *BMC Evol Biol*, 11, 294.
- DEHART, J. L., BOSQUE, A., HARRIS, R. S. & PLANELLES, V. 2008. Human immunodeficiency virus type 1 Vif induces cell cycle delay via recruitment of the same E3 ubiquitin ligase complex that targets APOBEC3 proteins for degradation. *J Virol*, 82, 9265-72.
- DELEBECQUE, F., SUSPENE, R., CALATTINI, S., CASARTELLI, N., SAIB, A., FROMENT, A., WAIN-HOBSON, S., GESSAIN, A., VARTANIAN, J. P. & SCHWARTZ, O. 2006. Restriction of foamy viruses by APOBEC cytidine deaminases. *J Virol*, 80, 605-14.
- DETTENHOFER, M., CEN, S., CARLSON, B. A., KLEIMAN, L. & YU, X. F. 2000. Association of human immunodeficiency virus type 1 Vif with RNA and its role in reverse transcription. *J Virol*, 74, 8938-45.
- DIETRICH, I., MCMONAGLE, E. L., PETIT, S. J., VIJAYAKRISHNAN, S., LOGAN, N., CHAN, C. N., TOWERS, G. J., HOSIE, M. J. & WILLETT, B. J. 2011. Feline tetherin efficiently restricts release of feline immunodeficiency virus but not spreading of infection. *J Virol*, 85, 5840-52.
- DOMBROSKI, B. A., FENG, Q., MATHIAS, S. L., SASSAMAN, D. M., SCOTT, A. F., KAZAZIAN, H. H., JR. & BOEKE, J. D. 1994. An in vivo assay for the reverse transcriptase of human retrotransposon L1 in *Saccharomyces cerevisiae*. *Mol Cell Biol*, 14, 4485-92.
- DOMBROSKI, B. A., MATHIAS, S. L., NANTHAKUMAR, E., SCOTT, A. F. & KAZAZIAN, H. H., JR. 1991. Isolation of an active human transposable element. *Science*, 254, 1805-8.
- DONAHUE, J. P., VETTER, M. L., MUKHTAR, N. A. & D'AQUILA, R. T. 2008. The HIV-1 Vif PPLP motif is necessary for human APOBEC3G binding and degradation. *Virology*, 377, 49-53.
- ENDERS, J. F. & PEEBLES, T. C. 1954. Propagation in tissue cultures of cytopathogenic agents from patients with measles. *Proc Soc Exp Biol Med*, 86, 277-86.
- ENGELMAN, A. N. & CHEREPANOV, P. 2017. Retroviral intasomes arising. *Curr Opin Struct Biol*, 47, 23-29.
- ERLWEIN, O. & MCCLURE, M. O. 2010. Progress and prospects: foamy virus vectors enter a new age. *Gene Ther*, 17, 1423-9.
- FELBER, B. K., DRYSDALE, C. M. & PAVLAKIS, G. N. 1990. Feedback regulation of human immunodeficiency virus type 1 expression by the Rev protein. *J Virol*, 64, 3734-41.

- FENG, Q., MORAN, J. V., KAZAZIAN, H. H., JR. & BOEKE, J. D. 1996. Human L1 retrotransposon encodes a conserved endonuclease required for retrotransposition. *Cell*, 87, 905-16.
- FISHER, A. G., FEINBERG, M. B., JOSEPHS, S. F., HARPER, M. E., MARSELLE, L. M., REYES, G., GONDA, M. A., ALDOVINI, A., DEBOUK, C., GALLO, R. C. & ET AL. 1986. The trans-activator gene of HTLV-III is essential for virus replication. *Nature*, 320, 367-71.
- FRICKE, T., WHITE, T. E., SCHULTE, B., DE SOUZA ARANHA VIEIRA, D. A., DHARAN, A., CAMPBELL, E. M., BRANDARIZ-NUNEZ, A. & DIAZ-GRIFFERO, F. 2014. MxB binds to the HIV-1 core and prevents the uncoating process of HIV-1. *Retrovirology*, 11, 68.
- GABUZDA, D. H., LAWRENCE, K., LANGHOFF, E., TERWILLIGER, E., DORFMAN, T., HASELTINE, W. A. & SODROSKI, J. 1992. Role of vif in replication of human immunodeficiency virus type 1 in CD4+ T lymphocytes. *J Virol*, 66, 6489-95.
- GALLERANO, D., DEVANABOYINA, S. C., SWOBODA, I., LINHART, B., MITTERMANN, I., KELLER, W. & VALENTA, R. 2011. Biophysical characterization of recombinant HIV-1 subtype C virus infectivity factor. *Amino Acids*, 40, 981-9.
- GALLO, R. C., SARIN, P. S., GELMANN, E. P., ROBERT-GUROFF, M., RICHARDSON, E., KALYANARAMAN, V. S., MANN, D., SIDHU, G. D., STAHL, R. E., ZOLLA-PAZNER, S., LEIBOWITZ, J. & POPOVIC, M. 1983. Isolation of human T-cell leukemia virus in acquired immune deficiency syndrome (AIDS). *Science*, 220, 865-7.
- GARNEAU, J. E., DUPUIS, M. E., VILLION, M., ROMERO, D. A., BARRANGOU, R., BOYAVAL, P., FREMAUX, C., HORVATH, P., MAGADAN, A. H. & MOINEAU, S. 2010. The CRISPR/Cas bacterial immune system cleaves bacteriophage and plasmid DNA. *Nature*, 468, 67-71.
- GASIOR, S. L., ROY-ENGEL, A. M. & DEININGER, P. L. 2008. ERCC1/XPF limits L1 retrotransposition. *DNA Repair (Amst)*, 7, 983-9.
- GASIOR, S. L., WAKEMAN, T. P., XU, B. & DEININGER, P. L. 2006. The human LINE-1 retrotransposon creates DNA double-strand breaks. *J Mol Biol*, 357, 1383-93.
- GESSAIN, A., RUA, R., BETSEM, E., TURPIN, J. & MAHIEUX, R. 2013. HTLV-3/4 and simian foamy retroviruses in humans: discovery, epidemiology, cross-species transmission and molecular virology. *Virology*, 435, 187-99.
- GIFFORD, R. J. 2012. Viral evolution in deep time: lentiviruses and mammals. *Trends Genet*, 28, 89-100.
- GIFFORD, R. J., KATZOURAKIS, A., TRISTEM, M., PYBUS, O. G., WINTERS, M. & SHAFER, R. W. 2008. A transitional endogenous lentivirus from the genome of a basal primate and implications for lentivirus evolution. *Proc Natl Acad Sci U S A*, 105, 20362-7.
- GILBERT, C., MAXFIELD, D. G., GOODMAN, S. M. & FESCHOTTE, C. 2009. Parallel germline infiltration of a lentivirus in two Malagasy lemurs. *PLoS Genet*, 5, e1000425.
- GOLDSTONE, D. C., YAP, M. W., ROBERTSON, L. E., HAIRE, L. F., TAYLOR, W. R., KATZOURAKIS, A., STOYE, J. P. & TAYLOR, I. A. 2010. Structural and functional analysis of prehistoric lentiviruses uncovers an ancient molecular interface. *Cell Host Microbe*, 8, 248-59.
- GOODIER, J. L. & KAZAZIAN, H. H., JR. 2008. Retrotransposons revisited: the restraint and rehabilitation of parasites. *Cell*, 135, 23-35.
- GOTTLIEB, M. S., SCHROFF, R., SCHANKER, H. M., WEISMAN, J. D., FAN, P. T., WOLF, R. A. & SAXON, A. 1981. Pneumocystis carinii pneumonia and mucosal candidiasis in previously healthy homosexual men: evidence of a new acquired cellular immunodeficiency. *N Engl J Med*, 305, 1425-31.
- GOUBAU, D., DEDDOUCHE, S. & REIS, E. S. C. 2013. Cytosolic sensing of viruses. *Immunity*, 38, 855-69.
- GOUJON, C., MONCORGE, O., BAUBY, H., DOYLE, T., WARD, C. C., SCHALLER, T., HUE, S., BARCLAY, W. S., SCHULZ, R. & MALIM, M. H. 2013. Human MX2 is an interferon-induced post-entry inhibitor of HIV-1 infection. *Nature*, 502, 559-62.
- GUO, F., CEN, S., NIU, M., SAADATMAND, J. & KLEIMAN, L. 2006. Inhibition of formula-primed reverse transcription by human APOBEC3G during human immunodeficiency virus type 1 replication. *J Virol*, 80, 11710-22.

- GUO, F., CEN, S., NIU, M., YANG, Y., GORELICK, R. J. & KLEIMAN, L. 2007. The interaction of APOBEC3G with human immunodeficiency virus type 1 nucleocapsid inhibits tRNA³Lys annealing to viral RNA. *J Virol*, 81, 11322-31.
- GUO, Y., DONG, L., QIU, X., WANG, Y., ZHANG, B., LIU, H., YU, Y., ZANG, Y., YANG, M. & HUANG, Z. 2014. Structural basis for hijacking CBF-beta and CUL5 E3 ligase complex by HIV-1 Vif. *Nature*, 505, 229-33.
- HACHE, G., LIDDAMENT, M. T. & HARRIS, R. S. 2005. The retroviral hypermutation specificity of APOBEC3F and APOBEC3G is governed by the C-terminal DNA cytosine deaminase domain. *J Biol Chem*, 280, 10920-4.
- HALLER, O. 2013. Dynamins Are Forever: MxB Inhibits HIV-1. *Cell Host Microbe*, 14, 371-3.
- HAN, G. Z. & WOROBEY, M. 2012a. An endogenous foamy-like viral element in the coelacanth genome. *PLoS Pathog*, 8, e1002790.
- HAN, G. Z. & WOROBEY, M. 2012b. An endogenous foamy virus in the aye-aye (*Daubentonia madagascariensis*). *J Virol*, 86, 7696-8.
- HANCKS, D. C. & KAZAZIAN, H. H., JR. 2012. Active human retrotransposons: variation and disease. *Curr Opin Genet Dev*, 22, 191-203.
- HARE, S., GUPTA, S. S., VALKOV, E., ENGELMAN, A. & CHEREPANOV, P. 2010. Retroviral intasome assembly and inhibition of DNA strand transfer. *Nature*, 464, 232-6.
- HARRICH, D. & HOOKER, B. 2002. Mechanistic aspects of HIV-1 reverse transcription initiation. *Rev Med Virol*, 12, 31-45.
- HARRIS, R. S., BISHOP, K. N., SHEEHY, A. M., CRAIG, H. M., PETERSEN-MAHRT, S. K., WATT, I. N., NEUBERGER, M. S. & MALIM, M. H. 2003. DNA deamination mediates innate immunity to retroviral infection. *Cell*, 113, 803-9.
- HARRIS, R. S. & DUDLEY, J. P. 2015. APOBECs and virus restriction. *Virology*, 479-480, 131-45.
- HARRIS, R. S., HULTQUIST, J. F. & EVANS, D. T. 2012. The restriction factors of human immunodeficiency virus. *J Biol Chem*, 287, 40875-83.
- HARRIS, R. S., PETERSEN-MAHRT, S. K. & NEUBERGER, M. S. 2002. RNA editing enzyme APOBEC1 and some of its homologs can act as DNA mutators. *Mol Cell*, 10, 1247-53.
- HE, Z., ZHANG, W., CHEN, G., XU, R. & YU, X. F. 2008. Characterization of conserved motifs in HIV-1 Vif required for APOBEC3G and APOBEC3F interaction. *J Mol Biol*, 381, 1000-11.
- HENRIET, S., RICHER, D., BERNACCHI, S., DECROLY, E., VIGNE, R., EHRESMANN, B., EHRESMANN, C., PAILLART, J. C. & MARQUET, R. 2005. Cooperative and specific binding of Vif to the 5' region of HIV-1 genomic RNA. *J Mol Biol*, 354, 55-72.
- HENRIET, S., SINCK, L., BEC, G., GORELICK, R. J., MARQUET, R. & PAILLART, J. C. 2007. Vif is a RNA chaperone that could temporally regulate RNA dimerization and the early steps of HIV-1 reverse transcription. *Nucleic Acids Res*, 35, 5141-53.
- HERCHENRODER, O., RENNE, R., LONCAR, D., COBB, E. K., MURTHY, K. K., SCHNEIDER, J., MERGIA, A. & LUCIW, P. A. 1994. Isolation, cloning, and sequencing of simian foamy viruses from chimpanzees (SFVcpz): high homology to human foamy virus (HFV). *Virology*, 201, 187-99.
- HOHJOH, H. & SINGER, M. F. 1996. Cytoplasmic ribonucleoprotein complexes containing human LINE-1 protein and RNA. *EMBO J*, 15, 630-9.
- HOLMES, E. C. 2008. Evolutionary history and phylogeography of human viruses. *Annu Rev Microbiol*, 62, 307-28.
- HOLMES, E. C. 2011. The evolution of endogenous viral elements. *Cell Host Microbe*, 10, 368-77.
- HOLMES, R. K., MALIM, M. H. & BISHOP, K. N. 2007. APOBEC-mediated viral restriction: not simply editing? *Trends Biochem Sci*, 32, 118-28.
- HORN, A. V., KLAWITTER, S., HELD, U., BERGER, A., VASUDEVAN, A. A., BOCK, A., HOFMANN, H., HANSCHMANN, K. M., TROSEMEIER, J. H., FLORY, E., JABULOWSKY, R. A., HAN, J. S., LOWER, J., LOWER, R., MÜNK, C. & SCHUMANN, G. G. 2014. Human LINE-1 restriction by APOBEC3C is deaminase independent and mediated by an ORF1p interaction that affects LINE reverse transcriptase activity. *Nucleic Acids Res*, 42, 396-416.

- HUANG, C. R., SCHNEIDER, A. M., LU, Y., NIRANJAN, T., SHEN, P., ROBINSON, M. A., STERANKA, J. P., VALLE, D., CIVIN, C. I., WANG, T., WHEELAN, S. J., JI, H., BOEKE, J. D. & BURNS, K. H. 2010. Mobile interspersed repeats are major structural variants in the human genome. *Cell*, 141, 1171-82.
- HUANG, F., WANG, H., JING, S. & ZENG, W. 2012. Simian foamy virus prevalence in *Macaca mulatta* and zookeepers. *AIDS Res Hum Retroviruses*, 28, 591-3.
- HULTQUIST, J. F. & HARRIS, R. S. 2009. Leveraging APOBEC3 proteins to alter the HIV mutation rate and combat AIDS. *Future Virol*, 4, 605.
- HUTHOFF, H., AUTORE, F., GALLOIS-MONTBRUN, S., FRATERNALI, F. & MALIM, M. H. 2009. RNA-dependent oligomerization of APOBEC3G is required for restriction of HIV-1. *PLoS Pathog*, 5, e1000330.
- HUTTER, S., ZURNIC, I. & LINDEMANN, D. 2013. Foamy virus budding and release. *Viruses*, 5, 1075-98.
- ISKOW, R. C., MCCABE, M. T., MILLS, R. E., TORENE, S., PITTARD, W. S., NEUWALD, A. F., VAN MEIR, E. G., VERTINO, P. M. & DEVINE, S. E. 2010. Natural mutagenesis of human genomes by endogenous retrotransposons. *Cell*, 141, 1253-61.
- IWATANI, Y., CHAN, D. S., WANG, F., MAYNARD, K. S., SUGIURA, W., GRONENBORN, A. M., ROUZINA, I., WILLIAMS, M. C., MUSIER-FORSYTH, K. & LEVIN, J. G. 2007. Deaminase-independent inhibition of HIV-1 reverse transcription by APOBEC3G. *Nucleic Acids Res*, 35, 7096-108.
- IWATANI, Y., TAKEUCHI, H., STREBEL, K. & LEVIN, J. G. 2006. Biochemical activities of highly purified, catalytically active human APOBEC3G: correlation with antiviral effect. *J Virol*, 80, 5992-6002.
- IZUMI, T., IO, K., MATSUI, M., SHIRAKAWA, K., SHINOHARA, M., NAGAI, Y., KAWAHARA, M., KOBAYASHI, M., KONDOH, H., MISAWA, N., KOYANAGI, Y., UCHIYAMA, T. & TAKAORI-KONDO, A. 2010. HIV-1 viral infectivity factor interacts with TP53 to induce G2 cell cycle arrest and positively regulate viral replication. *Proc Natl Acad Sci U S A*, 107, 20798-803.
- JAGER, S., CIMERMANCIC, P., GULBAHCE, N., JOHNSON, J. R., MCGOVERN, K. E., CLARKE, S. C., SHALES, M., MERCENNE, G., PACHE, L., LI, K., HERNANDEZ, H., JANG, G. M., ROTH, S. L., AKIVA, E., MARLETT, J., STEPHENS, M., D'ORSO, I., FERNANDES, J., FAHEY, M., MAHON, C., O'DONOGHUE, A. J., TODOROVIC, A., MORRIS, J. H., MALTBY, D. A., ALBER, T., CAGNEY, G., BUSHMAN, F. D., YOUNG, J. A., CHANDA, S. K., SUNDQUIST, W. I., KORTEMME, T., HERNANDEZ, R. D., CRAIK, C. S., BURLINGAME, A., SALI, A., FRANKEL, A. D. & KROGAN, N. J. 2012a. Global landscape of HIV-human protein complexes. *Nature*, 481, 365-70.
- JAGER, S., KIM, D. Y., HULTQUIST, J. F., SHINDO, K., LARUE, R. S., KWON, E., LI, M., ANDERSON, B. D., YEN, L., STANLEY, D., MAHON, C., KANE, J., FRANKS-SKIBA, K., CIMERMANCIC, P., BURLINGAME, A., SALI, A., CRAIK, C. S., HARRIS, R. S., GROSS, J. D. & KROGAN, N. J. 2012b. Vif hijacks CBF-beta to degrade APOBEC3G and promote HIV-1 infection. *Nature*, 481, 371-5.
- JAGUVA VASUDEVAN, A. A., PERKOVIC, M., BULLIARD, Y., CICHUTEK, K., TRONO, D., HÄUSSINGER, D. & MÜNK, C. 2013. Prototype foamy virus Bet impairs the dimerization and cytosolic solubility of human APOBEC3G. *J Virol*, 87, 9030-40.
- JARMUZ, A., CHESTER, A., BAYLISS, J., GISBOURNE, J., DUNHAM, I., SCOTT, J. & NAVARATNAM, N. 2002. An anthropoid-specific locus of orphan C to U RNA-editing enzymes on chromosome 22. *Genomics*, 79, 285-96.
- JASZCZUR, M., BERTRAM, J. G., PHAM, P., SCHARFF, M. D. & GOODMAN, M. F. 2013. AID and APOBEC3G haphazard deamination and mutational diversity. *Cell Mol Life Sci*, 70, 3089-108.
- JEANG, K. T., XIAO, H. & RICH, E. A. 1999. Multifaceted activities of the HIV-1 transactivator of transcription, Tat. *J Biol Chem*, 274, 28837-40.
- JIA, X., ZHAO, Q. & XIONG, Y. 2015. HIV suppression by host restriction factors and viral immune evasion. *Curr Opin Struct Biol*, 31, 106-14.
- JONES-ENGEL, L., MAY, C. C., ENGEL, G. A., STEINKRAUS, K. A., SCHILLACI, M. A., FUENTES, A., ROMPIS, A., CHALISE, M. K., AGGIMARANGSEE, N., FEEROZ, M. M., GRANT, R., ALLAN, J. S., PUTRA, A., WANDIA, I. N., WATANABE, R., KULLER, L., THONGSAWAT, S., CHAIWARITH, R., KYES, R. C. & LINIAL, M. L. 2008. Diverse contexts of zoonotic transmission of simian foamy viruses in Asia. *Emerg Infect Dis*, 14, 1200-8.

- KANE, M., YADAV, S. S., BITZECEO, J., KUTLUAY, S. B., ZANG, T., WILSON, S. J., SCHOGGINS, J. W., RICE, C. M., YAMASHITA, M., HATZIOANNOU, T. & BIENIASZ, P. D. 2013. MX2 is an interferon-induced inhibitor of HIV-1 infection. *Nature*, 502, 563-6.
- KAO, S., GOILA-GAUR, R., MIYAGI, E., KHAN, M. A., OPI, S., TAKEUCHI, H. & STREBEL, K. 2007. Production of infectious virus and degradation of APOBEC3G are separable functional properties of human immunodeficiency virus type 1 Vif. *Virology*, 369, 329-39.
- KAO, S., KHAN, M. A., MIYAGI, E., PLISHKA, R., BUCKLER-WHITE, A. & STREBEL, K. 2003. The human immunodeficiency virus type 1 Vif protein reduces intracellular expression and inhibits packaging of APOBEC3G (CEM15), a cellular inhibitor of virus infectivity. *J Virol*, 77, 11398-407.
- KAO, S., MIYAGI, E., KHAN, M. A., TAKEUCHI, H., OPI, S., GOILA-GAUR, R. & STREBEL, K. 2004. Production of infectious human immunodeficiency virus type 1 does not require depletion of APOBEC3G from virus-producing cells. *Retrovirology*, 1, 27.
- KATZOURAKIS, A. & GIFFORD, R. J. 2010. Endogenous viral elements in animal genomes. *PLoS Genet*, 6, e1001191.
- KATZOURAKIS, A., GIFFORD, R. J., TRISTEM, M., GILBERT, M. T. & PYBUS, O. G. 2009. Macroevolution of complex retroviruses. *Science*, 325, 1512.
- KATZOURAKIS, A., TRISTEM, M., PYBUS, O. G. & GIFFORD, R. J. 2007. Discovery and analysis of the first endogenous lentivirus. *Proc Natl Acad Sci U S A*, 104, 6261-5.
- KAZAZIAN, H. H., JR., WONG, C., YOUSOUFIAN, H., SCOTT, A. F., PHILLIPS, D. G. & ANTONARAKIS, S. E. 1988. Haemophilia A resulting from de novo insertion of L1 sequences represents a novel mechanism for mutation in man. *Nature*, 332, 164-6.
- KECKESOVA, Z., YLINEN, L. M., TOWERS, G. J., GIFFORD, R. J. & KATZOURAKIS, A. 2009. Identification of a RELIK orthologue in the European hare (*Lepus europaeus*) reveals a minimum age of 12 million years for the lagomorph lentiviruses. *Virology*, 384, 7-11.
- KEHL, T., TAN, J. & MATERNIAK, M. 2013. Non-simian foamy viruses: molecular virology, tropism and prevalence and zoonotic/interspecies transmission. *Viruses*, 5, 2169-209.
- KENYON, J. C. & LEVER, A. M. 2011. XMRV, prostate cancer and chronic fatigue syndrome. *Br Med Bull*, 98, 61-74.
- KHAN, M. A., ABERHAM, C., KAO, S., AKARI, H., GORELICK, R., BOUR, S. & STREBEL, K. 2001. Human immunodeficiency virus type 1 Vif protein is packaged into the nucleoprotein complex through an interaction with viral genomic RNA. *J Virol*, 75, 7252-65.
- KHAZINA, E. & WEICHENRIEDER, O. 2009. Non-LTR retrotransposons encode noncanonical RRM domains in their first open reading frame. *Proc Natl Acad Sci U S A*, 106, 731-6.
- KIM, E. Y., BHATTACHARYA, T., KUNSTMAN, K., SWANTEK, P., KONING, F. A., MALIM, M. H. & WOLINSKY, S. M. 2010. Human APOBEC3G-mediated editing can promote HIV-1 sequence diversification and accelerate adaptation to selective pressure. *J Virol*, 84, 10402-5.
- KINOMOTO, M., KANNO, T., SHIMURA, M., ISHIZAKA, Y., KOJIMA, A., KURATA, T., SATA, T. & TOKUNAGA, K. 2007. All APOBEC3 family proteins differentially inhibit LINE-1 retrotransposition. *Nucleic Acids Res*, 35, 2955-64.
- KOBAYASHI, M., TAKAORI-KONDO, A., MIYAUCHI, Y., IWAI, K. & UCHIYAMA, T. 2005. Ubiquitination of APOBEC3G by an HIV-1 Vif-Cullin5-Elongin B-Elongin C complex is essential for Vif function. *J Biol Chem*, 280, 18573-8.
- KOLOSHA, V. O. & MARTIN, S. L. 1997. In vitro properties of the first ORF protein from mouse LINE-1 support its role in ribonucleoprotein particle formation during retrotransposition. *Proc Natl Acad Sci U S A*, 94, 10155-60.
- KOLOSHA, V. O. & MARTIN, S. L. 2003. High-affinity, non-sequence-specific RNA binding by the open reading frame 1 (ORF1) protein from long interspersed nuclear element 1 (LINE-1). *J Biol Chem*, 278, 8112-7.
- KOONIN, E. V. & KRUPOVIC, M. 2015. Evolution of adaptive immunity from transposable elements combined with innate immune systems. *Nat Rev Genet*, 16, 184-92.

- KOPIETZ, F., JAGUVA VASUDEVAN, A. A., KRAMER, M., MUCKENFUSS, H., SANZENBACHER, R., CICHUTEK, K., FLORY, E. & MÜNK, C. 2012. Interaction of human immunodeficiency virus type 1 Vif with APOBEC3G is not dependent on serine/threonine phosphorylation status. *J Gen Virol*, 93, 2425-30.
- KRISHNAN, L., LI, X., NARAHARISSETTY, H. L., HARE, S., CHEREPANOV, P. & ENGELMAN, A. 2010. Structure-based modeling of the functional HIV-1 intasome and its inhibition. *Proc Natl Acad Sci U S A*, 107, 15910-5.
- KULPA, D. A. & MORAN, J. V. 2005. Ribonucleoprotein particle formation is necessary but not sufficient for LINE-1 retrotransposition. *Hum Mol Genet*, 14, 3237-48.
- LAGUETTE, N., BREGNARD, C., HUE, P., BASBOUS, J., YATIM, A., LARROQUE, M., KIRCHHOFF, F., CONSTANTINO, A., SOBHIAN, B. & BENKIRANE, M. 2014. Premature activation of the SLX4 complex by Vpr promotes G2/M arrest and escape from innate immune sensing. *Cell*, 156, 134-45.
- LANDER, E. S., LINTON, L. M., BIRREN, B., NUSBAUM, C., ZODY, M. C., BALDWIN, J., DEVON, K., DEWAR, K., DOYLE, M., FITZHUGH, W., FUNKE, R., GAGE, D., HARRIS, K., HEAFORD, A., HOWLAND, J., KANN, L., LEHOCZKY, J., LEVINE, R., MCEWAN, P., MCKERNAN, K., MELDRIM, J., MESIROV, J. P., MIRANDA, C., MORRIS, W., NAYLOR, J., RAYMOND, C., ROSETTI, M., SANTOS, R., SHERIDAN, A., SOUGNEZ, C., STANGE-THOMANN, N., STOJANOVIC, N., SUBRAMANIAN, A., WYMAN, D., ROGERS, J., SULSTON, J., AINSCOUGH, R., BECK, S., BENTLEY, D., BURTON, J., CLEE, C., CARTER, N., COULSON, A., DEADMAN, R., DELOUKAS, P., DUNHAM, A., DUNHAM, I., DURBIN, R., FRENCH, L., GRAFHAM, D., GREGORY, S., HUBBARD, T., HUMPHRAY, S., HUNT, A., JONES, M., LLOYD, C., MCMURRAY, A., MATTHEWS, L., MERCER, S., MILNE, S., MULLIKIN, J. C., MUNGALL, A., PLUMB, R., ROSS, M., SHOWNKEEN, R., SIMS, S., WATERSTON, R. H., WILSON, R. K., HILLIER, L. W., MCPHERSON, J. D., MARRA, M. A., MARDIS, E. R., FULTON, L. A., CHINWALLA, A. T., PEPIN, K. H., GISH, W. R., CHISSOE, S. L., WENDL, M. C., DELEHAUNTY, K. D., MINER, T. L., DELEHAUNTY, A., KRAMER, J. B., COOK, L. L., FULTON, R. S., JOHNSON, D. L., MINX, P. J., CLIFTON, S. W., HAWKINS, T., BRANSCOMB, E., PREDKI, P., RICHARDSON, P., WENNING, S., SLEZAK, T., DOGGETT, N., CHENG, J. F., OLSEN, A., LUCAS, S., ELKIN, C., UBERBACHER, E., FRAZIER, M., et al. 2001. Initial sequencing and analysis of the human genome. *Nature*, 409, 860-921.
- LANDRY, S., NARVAIZA, I., LINFESTY, D. C. & WEITZMAN, M. D. 2011. APOBEC3A can activate the DNA damage response and cause cell-cycle arrest. *EMBO Rep*, 12, 444-50.
- LANGLOIS, M. A. & NEUBERGER, M. S. 2008. Human APOBEC3G can restrict retroviral infection in avian cells and acts independently of both UNG and SMUG1. *J Virol*, 82, 4660-4.
- LARUE, R. S., ANDRESDOTTIR, V., BLANCHARD, Y., CONTICELLO, S. G., DERSE, D., EMERMAN, M., GREENE, W. C., JONSSON, S. R., LANDAU, N. R., LOCHELT, M., MALIK, H. S., MALIM, M. H., MÜNK, C., O'BRIEN, S. J., PATHAK, V. K., STREBEL, K., WAIN-HOBSON, S., YU, X. F., YUHKI, N. & HARRIS, R. S. 2009. Guidelines for naming nonprimate APOBEC3 genes and proteins. *J Virol*, 83, 494-7.
- LEVIN, H. L. & MORAN, J. V. 2011. Dynamic interactions between transposable elements and their hosts. *Nat Rev Genet*, 12, 615-27.
- LI, G. & DE CLERCQ, E. 2016. HIV Genome-Wide Protein Associations: a Review of 30 Years of Research. *Microbiol Mol Biol Rev*, 80, 679-731.
- LI, L., LI, H. S., PAUZA, C. D., BUKRINSKY, M. & ZHAO, R. Y. 2005. Roles of HIV-1 auxiliary proteins in viral pathogenesis and host-pathogen interactions. *Cell Res*, 15, 923-34.
- LI, M., KAO, E., GAO, X., SANDIG, H., LIMMER, K., PAVON-ETERNOD, M., JONES, T. E., LANDRY, S., PAN, T., WEITZMAN, M. D. & DAVID, M. 2012. Codon-usage-based inhibition of HIV protein synthesis by human schlafen 11. *Nature*, 491, 125-8.
- LI, W. H., GU, Z., WANG, H. & NEKRUTENKO, A. 2001. Evolutionary analyses of the human genome. *Nature*, 409, 847-9.
- LI, X. Y., GUO, F., ZHANG, L., KLEIMAN, L. & CEN, S. 2007. APOBEC3G inhibits DNA strand transfer during HIV-1 reverse transcription. *J Biol Chem*, 282, 32065-74.

- LIN, C., YANG, L., TANASA, B., HUTT, K., JU, B. G., OHGI, K., ZHANG, J., ROSE, D. W., FU, X. D., GLASS, C. K. & ROSENFELD, M. G. 2009. Nuclear receptor-induced chromosomal proximity and DNA breaks underlie specific translocations in cancer. *Cell*, 139, 1069-83.
- LINDBLAD-TOH, K., WADE, C. M., MIKKELSEN, T. S., KARLSSON, E. K., JAFFE, D. B., KAMAL, M., CLAMP, M., CHANG, J. L., KULBOKAS, E. J., 3RD, ZODY, M. C., MAUCELLI, E., XIE, X., BREEN, M., WAYNE, R. K., OSTRANDER, E. A., PONTING, C. P., GALIBERT, F., SMITH, D. R., DEJONG, P. J., KIRKNESS, E., ALVAREZ, P., BIAGI, T., BROCKMAN, W., BUTLER, J., CHIN, C. W., COOK, A., CUFF, J., DALY, M. J., DECAPRIO, D., GNERRE, S., GRABHERR, M., KELLIS, M., KLEBER, M., BARDELEBEN, C., GOODSTADT, L., HEGER, A., HITTE, C., KIM, L., KOEPFLI, K. P., PARKER, H. G., POLLINGER, J. P., SEARLE, S. M., SUTTER, N. B., THOMAS, R., WEBBER, C., BALDWIN, J., ABEBE, A., ABOUELLEIL, A., AFTUCK, L., AIT-ZAHRA, M., ALDREDGE, T., ALLEN, N., AN, P., ANDERSON, S., ANTOINE, C., ARACHCHI, H., ASLAM, A., AYOTTE, L., BACHANTSANG, P., BARRY, A., BAYUL, T., BENAMARA, M., BERLIN, A., BESSETTE, D., BLITSHTEYN, B., BLOOM, T., BLYE, J., BOGUSLAVSKIY, L., BONNET, C., BOUKHGALTER, B., BROWN, A., CAHILL, P., CALIXTE, N., CAMARATA, J., CHESHATSANG, Y., CHU, J., CITROEN, M., COLLYMORE, A., COOKE, P., DAWOE, T., DAZA, R., DECKTOR, K., DEGRAY, S., DHARGAY, N., DOOLEY, K., DOOLEY, K., DORJE, P., DORJEE, K., DORRIS, L., DUFFEY, N., DUPES, A., EGBIREMOLEN, O., ELONG, R., FALK, J., FARINA, A., FARO, S., FERGUSON, D., FERREIRA, P., FISHER, S., FITZGERALD, M., et al. 2005. Genome sequence, comparative analysis and haplotype structure of the domestic dog. *Nature*, 438, 803-19.
- LINDEMANN, D. & GOEPFERT, P. A. 2003. The foamy virus envelope glycoproteins. *Curr Top Microbiol Immunol*, 277, 111-29.
- LINDEMANN, D. & RETHWILM, A. 2011. Foamy virus biology and its application for vector development. *Viruses*, 3, 561-85.
- LINIAL, M. 2000. Why aren't foamy viruses pathogenic? *Trends Microbiol*, 8, 284-9.
- LINIAL, M. L. 1999. Foamy viruses are unconventional retroviruses. *J Virol*, 73, 1747-55.
- LIU, B., SARKIS, P. T., LUO, K., YU, Y. & YU, X. F. 2005. Regulation of APOBEC3F and human immunodeficiency virus type 1 Vif by Vif-Cul5-ElonB/C E3 ubiquitin ligase. *J Virol*, 79, 9579-87.
- LIU, W., WOROBAY, M., LI, Y., KEELE, B. F., BIBOLLET-RUCHE, F., GUO, Y., GOEPFERT, P. A., SANTIAGO, M. L., NDJANGO, J. B., NEEL, C., CLIFFORD, S. L., SANZ, C., KAMENYA, S., WILSON, M. L., PUSEY, A. E., GROSS-CAMP, N., BOESCH, C., SMITH, V., ZAMMA, K., HUFFMAN, M. A., MITANI, J. C., WATTS, D. P., PEETERS, M., SHAW, G. M., SWITZER, W. M., SHARP, P. M. & HAHN, B. H. 2008. Molecular ecology and natural history of simian foamy virus infection in wild-living chimpanzees. *PLoS Pathog*, 4, e1000097.
- LIU, Z., PAN, Q., DING, S., QIAN, J., XU, F., ZHOU, J., CEN, S., GUO, F. & LIANG, C. 2013. The Interferon-Inducible MxB Protein Inhibits HIV-1 Infection. *Cell Host Microbe*, 14, 398-410.
- LOCHELT, M., ROMEN, F., BASTONE, P., MUCKENFUSS, H., KIRCHNER, N., KIM, Y. B., TRUYEN, U., ROSLER, U., BATTENBERG, M., SAIB, A., FLORY, E., CICHUTEK, K. & MÜNK, C. 2005. The antiretroviral activity of APOBEC3 is inhibited by the foamy virus accessory Bet protein. *Proc Natl Acad Sci U S A*, 102, 7982-7.
- LUAN, D. D., KORMAN, M. H., JAKUBCZAK, J. L. & EICKBUSH, T. H. 1993. Reverse transcription of R2Bm RNA is primed by a nick at the chromosomal target site: a mechanism for non-LTR retrotransposition. *Cell*, 72, 595-605.
- LUKIC, D. S., HOTZ-WAGENBLATT, A., LEI, J., RATHE, A. M., MUHLE, M., DENNER, J., MÜNK, C. & LOCHELT, M. 2013. Identification of the feline foamy virus Bet domain essential for APOBEC3 counteraction. *Retrovirology*, 10, 76.
- LUO, K., WANG, T., LIU, B., TIAN, C., XIAO, Z., KAPPES, J. & YU, X. F. 2007. Cytidine deaminases APOBEC3G and APOBEC3F interact with human immunodeficiency virus type 1 integrase and inhibit proviral DNA formation. *J Virol*, 81, 7238-48.
- LUO, K., XIAO, Z., EHRlich, E., YU, Y., LIU, B., ZHENG, S. & YU, X. F. 2005. Primate lentiviral virion infectivity factors are substrate receptors that assemble with cullin 5-E3 ligase through a HCCH motif to suppress APOBEC3G. *Proc Natl Acad Sci U S A*, 102, 11444-9.

- MAERTENS, G. N., HARE, S. & CHEREPANOV, P. 2010. The mechanism of retroviral integration from X-ray structures of its key intermediates. *Nature*, 468, 326-9.
- MALIM, M. H. & BIENIASZ, P. D. 2012. HIV Restriction Factors and Mechanisms of Evasion. *Cold Spring Harb Perspect Med*, 2, a006940.
- MALIM, M. H. & EMERMAN, M. 2008. HIV-1 accessory proteins--ensuring viral survival in a hostile environment. *Cell Host Microbe*, 3, 388-98.
- MALONE, C. D. & HANNON, G. J. 2009. Small RNAs as guardians of the genome. *Cell*, 136, 656-68.
- MANGEAT, B., TURELLI, P., CARON, G., FRIEDLI, M., PERRIN, L. & TRONO, D. 2003. Broad antiretroviral defence by human APOBEC3G through lethal editing of nascent reverse transcripts. *Nature*, 424, 99-103.
- MANGEAT, B., TURELLI, P., LIAO, S. & TRONO, D. 2004. A single amino acid determinant governs the species-specific sensitivity of APOBEC3G to Vif action. *J Biol Chem*, 279, 14481-3.
- MARCHETTO, M. C., NARVAIZA, I., DENLI, A. M., BENNER, C., LAZZARINI, T. A., NATHANSON, J. L., PAQUOLA, A. C., DESAI, K. N., HERAI, R. H., WEITZMAN, M. D., YEO, G. W., MUOTRI, A. R. & GAGE, F. H. 2013. Differential L1 regulation in pluripotent stem cells of humans and apes. *Nature*, 503, 525-9.
- MARCSISIN, S. R. & ENGEN, J. R. 2010. Molecular insight into the conformational dynamics of the Elongin BC complex and its interaction with HIV-1 Vif. *J Mol Biol*, 402, 892-904.
- MARCSISIN, S. R., NARUTE, P. S., EMERT-SEDLAK, L. A., KLOCZEWIAK, M., SMITHGALL, T. E. & ENGEN, J. R. 2011. On the solution conformation and dynamics of the HIV-1 viral infectivity factor. *J Mol Biol*, 410, 1008-22.
- MARIANI, R., CHEN, D., SCHROFELBAUER, B., NAVARRO, F., KONIG, R., BOLLMAN, B., MÜNK, C., NYMARK-MCMAHON, H. & LANDAU, N. R. 2003. Species-specific exclusion of APOBEC3G from HIV-1 virions by Vif. *Cell*, 114, 21-31.
- MARIN, M., ROSE, K. M., KOZAK, S. L. & KABAT, D. 2003. HIV-1 Vif protein binds the editing enzyme APOBEC3G and induces its degradation. *Nat Med*, 9, 1398-403.
- MARINO, D., PERKOVIC, M., HAIN, A., JAGUVA VASUDEVAN, A. A., HOFMANN, H., HANSCHMANN, K. M., MUHLEBACH, M. D., SCHUMANN, G. G., KONIG, R., CICHUTEK, K., HÄUSSINGER, D. & MÜNK, C. 2016. APOBEC4 Enhances the Replication of HIV-1. *PLoS One*, 11, e0155422.
- MARTIN, S. L. & BUSHMAN, F. D. 2001. Nucleic acid chaperone activity of the ORF1 protein from the mouse LINE-1 retrotransposon. *Mol Cell Biol*, 21, 467-75.
- MATHIAS, S. L., SCOTT, A. F., KAZAZIAN, H. H., JR., BOEKE, J. D. & GABRIEL, A. 1991. Reverse transcriptase encoded by a human transposable element. *Science*, 254, 1808-10.
- MATSUI, Y., SHINDO, K., NAGATA, K., IO, K., TADA, K., IWAI, F., KOBAYASHI, M., KADOWAKI, N., HARRIS, R. S. & TAKAORI-KONDO, A. 2014. Defining HIV-1 Vif residues that interact with CBFbeta by site-directed mutagenesis. *Virology*, 449, 82-7.
- MBISA, J. L., BARR, R., THOMAS, J. A., VANDEGRAAFF, N., DORWEILER, I. J., SVAROVSKAIA, E. S., BROWN, W. L., MANSKY, L. M., GORELICK, R. J., HARRIS, R. S., ENGELMAN, A. & PATHAK, V. K. 2007. Human immunodeficiency virus type 1 cDNAs produced in the presence of APOBEC3G exhibit defects in plus-strand DNA transfer and integration. *J Virol*, 81, 7099-110.
- MBISA, J. L., BU, W. & PATHAK, V. K. 2010. APOBEC3F and APOBEC3G inhibit HIV-1 DNA integration by different mechanisms. *J Virol*, 84, 5250-9.
- MCDUGALL, W. M., OKANY, C. & SMITH, H. C. 2011. Deaminase activity on single-stranded DNA (ssDNA) occurs in vitro when APOBEC3G cytidine deaminase forms homotetramers and higher-order complexes. *J Biol Chem*, 286, 30655-61.
- MEHLE, A., GONCALVES, J., SANTA-MARTA, M., MCPIKE, M. & GABUZDA, D. 2004. Phosphorylation of a novel SOCS-box regulates assembly of the HIV-1 Vif-Cul5 complex that promotes APOBEC3G degradation. *Genes Dev*, 18, 2861-6.
- MEHLE, A., THOMAS, E. R., RAJENDRAN, K. S. & GABUZDA, D. 2006. A zinc-binding region in Vif binds Cul5 and determines cullin selection. *J Biol Chem*, 281, 17259-65.
- MEIERING, C. D. & LINIAL, M. L. 2001. Historical perspective of foamy virus epidemiology and infection. *Clin Microbiol Rev*, 14, 165-76.

- MOHANRAM, V., SKOLD, A. E., BACHLE, S. M., PATHAK, S. K. & SPETZ, A. L. 2013. IFN-alpha induces APOBEC3G, F, and A in immature dendritic cells and limits HIV-1 spread to CD4+ T cells. *J Immunol*, 190, 3346-53.
- MOUINGA-ONDEME, A., BETSEM, E., CARON, M., MAKUWA, M., SALLE, B., RENAULT, N., SAIB, A., TELFER, P., MARX, P., GESSAIN, A. & KAZANJI, M. 2010. Two distinct variants of simian foamy virus in naturally infected mandrills (*Mandrillus sphinx*) and cross-species transmission to humans. *Retrovirology*, 7, 105.
- MOUINGA-ONDEME, A., CARON, M., NKOGHE, D., TELFER, P., MARX, P., SAIB, A., LEROY, E., GONZALEZ, J. P., GESSAIN, A. & KAZANJI, M. 2012. Cross-species transmission of simian foamy virus to humans in rural Gabon, Central Africa. *J Virol*, 86, 1255-60.
- MUCKENFUSS, H., HAMDORF, M., HELD, U., PERKOVIC, M., LOWER, J., CICHUTEK, K., FLORY, E., SCHUMANN, G. G. & MÜNK, C. 2006. APOBEC3 proteins inhibit human LINE-1 retrotransposition. *J Biol Chem*, 281, 22161-72.
- MULLERS, E. 2013. The foamy virus Gag proteins: what makes them different? *Viruses*, 5, 1023-41.
- MÜNK, C., BECK, T., ZIELONKA, J., HOTZ-WAGENBLATT, A., CHAREZA, S., BATTENBERG, M., THIELEBEIN, J., CICHUTEK, K., BRAVO, I. G., O'BRIEN, S. J., LOCHELT, M. & YUHKI, N. 2008. Functions, structure, and read-through alternative splicing of feline APOBEC3 genes. *Genome Biol*, 9, R48.
- MÜNK, C., JENSEN, B. E., ZIELONKA, J., HÄUSSINGER, D. & KAMP, C. 2012a. Running Loose or Getting Lost: How HIV-1 Counters and Capitalizes on APOBEC3-Induced Mutagenesis through Its Vif Protein. *Viruses*, 4, 3132-3161.
- MÜNK, C., WILLEMSSEN, A. & BRAVO, I. G. 2012b. An ancient history of gene duplications, fusions and losses in the evolution of APOBEC3 mutators in mammals. *BMC Evol Biol*, 12, 71.
- MURRAY, S. M. & LINIAL, M. L. 2006. Foamy virus infection in primates. *J Med Primatol*, 35, 225-35.
- NEIL, S. J., ZANG, T. & BIENIASZ, P. D. 2008. Tetherin inhibits retrovirus release and is antagonized by HIV-1 Vpu. *Nature*, 451, 425-30.
- NIK-ZAINAL, S., ALEXANDROV, L. B., WEDGE, D. C., VAN LOO, P., GREENMAN, C. D., RAINE, K., JONES, D., HINTON, J., MARSHALL, J., STEBBINGS, L. A., MENZIES, A., MARTIN, S., LEUNG, K., CHEN, L., LEROY, C., RAMAKRISHNA, M., RANCE, R., LAU, K. W., MUDIE, L. J., VARELA, I., MCBRIDE, D. J., BIGNELL, G. R., COOKE, S. L., SHLIEN, A., GAMBLE, J., WHITMORE, I., MADDISON, M., TARPEY, P. S., DAVIES, H. R., PAPAEMMANUIL, E., STEPHENS, P. J., MCLAREN, S., BUTLER, A. P., TEAGUE, J. W., JONSSON, G., GARBER, J. E., SILVER, D., MIRON, P., FATIMA, A., BOYALT, S., LANGEROD, A., TUTT, A., MARTENS, J. W., APARICIO, S. A., BORG, A., SALOMON, A. V., THOMAS, G., BORRESEN-DALE, A. L., RICHARDSON, A. L., NEUBERGER, M. S., FUTREAL, P. A., CAMPBELL, P. J., STRATTON, M. R. & BREAST CANCER WORKING GROUP OF THE INTERNATIONAL CANCER GENOME, C. 2012a. Mutational processes molding the genomes of 21 breast cancers. *Cell*, 149, 979-93.
- NIK-ZAINAL, S., VAN LOO, P., WEDGE, D. C., ALEXANDROV, L. B., GREENMAN, C. D., LAU, K. W., RAINE, K., JONES, D., MARSHALL, J., RAMAKRISHNA, M., SHLIEN, A., COOKE, S. L., HINTON, J., MENZIES, A., STEBBINGS, L. A., LEROY, C., JIA, M., RANCE, R., MUDIE, L. J., GAMBLE, S. J., STEPHENS, P. J., MCLAREN, S., TARPEY, P. S., PAPAEMMANUIL, E., DAVIES, H. R., VARELA, I., MCBRIDE, D. J., BIGNELL, G. R., LEUNG, K., BUTLER, A. P., TEAGUE, J. W., MARTIN, S., JONSSON, G., MARIANI, O., BOYALT, S., MIRON, P., FATIMA, A., LANGEROD, A., APARICIO, S. A., TUTT, A., SIEUWERTS, A. M., BORG, A., THOMAS, G., SALOMON, A. V., RICHARDSON, A. L., BORRESEN-DALE, A. L., FUTREAL, P. A., STRATTON, M. R., CAMPBELL, P. J. & BREAST CANCER WORKING GROUP OF THE INTERNATIONAL CANCER GENOME, C. 2012b. The life history of 21 breast cancers. *Cell*, 149, 994-1007.
- NOWARSKI, R. & KOTLER, M. 2013. APOBEC3 cytidine deaminases in double-strand DNA break repair and cancer promotion. *Cancer Res*, 73, 3494-8.
- O'SULLIVAN, T. E., SUN, J. C. & LANIER, L. L. 2015. Natural Killer Cell Memory. *Immunity*, 43, 634-45.

- OPI, S., KAO, S., GOILA-GAUR, R., KHAN, M. A., MIYAGI, E., TAKEUCHI, H. & STREBEL, K. 2007. Human immunodeficiency virus type 1 Vif inhibits packaging and antiviral activity of a degradation-resistant APOBEC3G variant. *J Virol*, 81, 8236-46.
- OPPORTUNISTIC INFECTIONS PROJECT TEAM OF THE COLLABORATION OF OBSERVATIONAL, H. I. V. E. R. I. E. I. E., YOUNG, J., PSICHOGIOU, M., MEYER, L., AYAYI, S., GRABAR, S., RAFFI, F., REISS, P., GAZZARD, B., SHARLAND, M., GUTIERREZ, F., OBEL, N., KIRK, O., MIRO, J. M., FURRER, H., CASTAGNA, A., DE WIT, S., MUNOZ, J., KJAER, J., GRARUP, J., CHENE, G. & BUCHER, H. 2012. CD4 cell count and the risk of AIDS or death in HIV-Infected adults on combination antiretroviral therapy with a suppressed viral load: a longitudinal cohort study from COHERE. *PLoS Med*, 9, e1001194.
- PASSOS, D. O., LI, M., YANG, R., REBENBURG, S. V., GHIRLANDO, R., JEON, Y., SHKRIABAI, N., KVARATSKHELIA, M., CRAIGIE, R. & LYUMKIS, D. 2017. Cryo-EM structures and atomic model of the HIV-1 strand transfer complex intasome. *Science*, 355, 89-92.
- PENG, G., GREENWELL-WILD, T., NARES, S., JIN, W., LEI, K. J., RANGEL, Z. G., MUNSON, P. J. & WAHL, S. M. 2007. Myeloid differentiation and susceptibility to HIV-1 are linked to APOBEC3 expression. *Blood*, 110, 393-400.
- PENG, G., LEI, K. J., JIN, W., GREENWELL-WILD, T. & WAHL, S. M. 2006. Induction of APOBEC3 family proteins, a defensive maneuver underlying interferon-induced anti-HIV-1 activity. *J Exp Med*, 203, 41-6.
- PERKOVIC, M., SCHMIDT, S., MARINO, D., RUSSELL, R. A., STAUCH, B., HOFMANN, H., KOPIETZ, F., KLOKE, B. P., ZIELONKA, J., STROVER, H., HERMLE, J., LINDEMANN, D., PATHAK, V. K., SCHNEIDER, G., LOCHELT, M., CICHUTEK, K. & MÜNK, C. 2009. Species-specific inhibition of APOBEC3C by the prototype foamy virus protein bet. *J Biol Chem*, 284, 5819-26.
- PERY, E., RAJENDRAN, K. S., BRAZIER, A. J. & GABUZDA, D. 2009. Regulation of APOBEC3 proteins by a novel YXXL motif in human immunodeficiency virus type 1 Vif and simian immunodeficiency virus SIVagm Vif. *J Virol*, 83, 2374-81.
- POLLARD, V. W. & MALIM, M. H. 1998. The HIV-1 Rev protein. *Annu Rev Microbiol*, 52, 491-532.
- RAZZAK, M. 2012. Genetics: Schlafen 11 naturally blocks HIV. *Nat Rev Urol*, 9, 605.
- RETHWILM, A. 2007. Foamy virus vectors: an awaited alternative to gammaretro- and lentiviral vectors. *Curr Gene Ther*, 7, 261-71.
- RETHWILM, A. 2010. Molecular biology of foamy viruses. *Med Microbiol Immunol*, 199, 197-207.
- RETHWILM, A. 2013. Specific RNA-protein interactions in the replication of foamy viruses (FVs). *Curr Opin Virol*.
- RETHWILM, A. & BODEM, J. 2013. Evolution of foamy viruses: the most ancient of all retroviruses. *Viruses*, 5, 2349-74.
- ROBERTS, S. A., LAWRENCE, M. S., KLIMCZAK, L. J., GRIMM, S. A., FARGO, D., STOJANOV, P., KIEZUN, A., KRYUKOV, G. V., CARTER, S. L., SAKSENA, G., HARRIS, S., SHAH, R. R., RESNICK, M. A., GETZ, G. & GORDENIN, D. A. 2013. An APOBEC cytidine deaminase mutagenesis pattern is widespread in human cancers. *Nat Genet*, 45, 970-6.
- ROSA, A., CHANDE, A., ZIGLIO, S., DE SANCTIS, V., BERTORELLI, R., GOH, S. L., MCCAULEY, S. M., NOWOSIELSKA, A., ANTONARAKIS, S. E., LUBAN, J., SANTONI, F. A. & PIZZATO, M. 2015. HIV-1 Nef promotes infection by excluding SERINC5 from virion incorporation. *Nature*, 526, 212-7.
- RUSSELL, R. A. & PATHAK, V. K. 2007. Identification of two distinct human immunodeficiency virus type 1 Vif determinants critical for interactions with human APOBEC3G and APOBEC3F. *J Virol*, 81, 8201-10.
- RUSSELL, R. A., WIEGAND, H. L., MOORE, M. D., SCHAFFER, A., MCCLURE, M. O. & CULLEN, B. R. 2005. Foamy virus Bet proteins function as novel inhibitors of the APOBEC3 family of innate antiretroviral defense factors. *J Virol*, 79, 8724-31.
- RUSTIGIAN, R., JOHNSTON, P. & REIHART, H. 1955. Infection of monkey kidney tissue cultures with virus-like agents. *Proc Soc Exp Biol Med*, 88, 8-16.
- SADLER, H. A., STENGLEIN, M. D., HARRIS, R. S. & MANSKY, L. M. 2010. APOBEC3G contributes to HIV-1 variation through sublethal mutagenesis. *J Virol*, 84, 7396-404.

- SAKAI, K., DIMAS, J. & LENARDO, M. J. 2006. The Vif and Vpr accessory proteins independently cause HIV-1-induced T cell cytopathicity and cell cycle arrest. *Proc Natl Acad Sci U S A*, 103, 3369-74.
- SALTER, J. D., BENNETT, R. P. & SMITH, H. C. 2016. The APOBEC Protein Family: United by Structure, Divergent in Function. *Trends Biochem Sci*, 41, 578-94.
- SALTER, J. D., KRUCINSKA, J., RAINA, J., SMITH, H. C. & WEDEKIND, J. E. 2009. A hydrodynamic analysis of APOBEC3G reveals a monomer-dimer-tetramer self-association that has implications for anti-HIV function. *Biochemistry*, 48, 10685-7.
- SALTER, J. D., LIPPA, G. M., BELASHOV, I. A. & WEDEKIND, J. E. 2012. Core-binding factor beta increases the affinity between human Cullin 5 and HIV-1 Vif within an E3 ligase complex. *Biochemistry*, 51, 8702-4.
- SCHALLER, T., GOUJON, C. & MALIM, M. H. 2012. AIDS/HIV. HIV interplay with SAMHD1. *Science*, 335, 1313-4.
- SCHARTL, M., WALTER, R. B., SHEN, Y., GARCIA, T., CATCHEN, J., AMORES, A., BRAASCH, I., CHALOPIN, D., VOLFF, J. N., LESCH, K. P., BISAZZA, A., MINX, P., HILLIER, L., WILSON, R. K., FUERSTENBERG, S., BOORE, J., SEARLE, S., POSTLETHWAIT, J. H. & WARREN, W. C. 2013. The genome of the platyfish, *Xiphophorus maculatus*, provides insights into evolutionary adaptation and several complex traits. *Nat Genet*, 45, 567-72.
- SCHUMANN, G. G., GOGVADZE, E. V., OSANAI-FUTAHASHI, M., KUROKI, A., MÜNK, C., FUJIWARA, H., IVICS, Z. & BUZDIN, A. A. 2010. Unique functions of repetitive transcriptomes. *Int Rev Cell Mol Biol*, 285, 115-88.
- SCHWANTES, A., TRUYEN, U., WEIKEL, J., WEISS, C. & LOCHELT, M. 2003. Application of chimeric feline foamy virus-based retroviral vectors for the induction of antiviral immunity in cats. *J Virol*, 77, 7830-42.
- SCHWEIZER, M., SCHLEER, H., PIETREK, M., LIEGIBEL, J., FALCONE, V. & NEUMANN-HAEFELIN, D. 1999. Genetic stability of foamy viruses: long-term study in an African green monkey population. *J Virol*, 73, 9256-65.
- SCHWEIZER, M., TUREK, R., HAHN, H., SCHLIEPHAKE, A., NETZER, K. O., EDER, G., REINHARDT, M., RETHWILM, A. & NEUMANN-HAEFELIN, D. 1995. Markers of foamy virus infections in monkeys, apes, and accidentally infected humans: appropriate testing fails to confirm suspected foamy virus prevalence in humans. *AIDS Res Hum Retroviruses*, 11, 161-70.
- SHARP, P. M. & HAHN, B. H. 2011. Origins of HIV and the AIDS pandemic. *Cold Spring Harb Perspect Med*, 1, a006841.
- SHEE, C., COX, B. D., GU, F., LUENGAS, E. M., JOSHI, M. C., CHIU, L. Y., MAGNAN, D., HALLIDAY, J. A., FRISCH, R. L., GIBSON, J. L., NEHRING, R. B., DO, H. G., HERNANDEZ, M., LI, L., HERMAN, C., HASTINGS, P., BATES, D., HARRIS, R. S., MILLER, K. M. & ROSENBERG, S. M. 2013. Engineered proteins detect spontaneous DNA breakage in human and bacterial cells. *Elife*, 2, e01222.
- SHEEHY, A. M. & ERTHAL, J. 2012. APOBEC3 versus Retroviruses, Immunity versus Invasion: Clash of the Titans. *Mol Biol Int*, 2012, 974924.
- SHEEHY, A. M., GADDIS, N. C., CHOI, J. D. & MALIM, M. H. 2002. Isolation of a human gene that inhibits HIV-1 infection and is suppressed by the viral Vif protein. *Nature*, 418, 646-50.
- SHINOHARA, M., IO, K., SHINDO, K., MATSUI, M., SAKAMOTO, T., TADA, K., KOBAYASHI, M., KADOWAKI, N. & TAKAORI-KONDO, A. 2012. APOBEC3B can impair genomic stability by inducing base substitutions in genomic DNA in human cells. *Sci Rep*, 2, 806.
- SHIRAKAWA, K., TAKAORI-KONDO, A., YOKOYAMA, M., IZUMI, T., MATSUI, M., IO, K., SATO, T., SATO, H. & UCHIYAMA, T. 2008. Phosphorylation of APOBEC3G by protein kinase A regulates its interaction with HIV-1 Vif. *Nat Struct Mol Biol*, 15, 1184-91.
- SIERRA, S., KUPFER, B. & KAISER, R. 2005. Basics of the virology of HIV-1 and its replication. *J Clin Virol*, 34, 233-44.
- SOLYOM, S. & KAZAZIAN, H. H., JR. 2012. Mobile elements in the human genome: implications for disease. *Genome Med*, 4, 12.

- SOOD, C., MARIN, M., CHANDE, A., PIZZATO, M. & MELIKYAN, G. B. 2017. SERINC5 protein inhibits HIV-1 fusion pore formation by promoting functional inactivation of envelope glycoproteins. *J Biol Chem*, 292, 6014-6026.
- STANLEY, B. J., EHRLICH, E. S., SHORT, L., YU, Y., XIAO, Z., YU, X. F. & XIONG, Y. 2008. Structural insight into the human immunodeficiency virus Vif SOCS box and its role in human E3 ubiquitin ligase assembly. *J Virol*, 82, 8656-63.
- STENGLEIN, M. D., BURNS, M. B., LI, M., LENGYEL, J. & HARRIS, R. S. 2010. APOBEC3 proteins mediate the clearance of foreign DNA from human cells. *Nat Struct Mol Biol*, 17, 222-9.
- STETSON, D. B., KO, J. S., HEIDMANN, T. & MEDZHITOV, R. 2008. Trex1 prevents cell-intrinsic initiation of autoimmunity. *Cell*, 134, 587-98.
- STEVENSON, M. 2003. HIV-1 pathogenesis. *Nat Med*, 9, 853-60.
- STOPAK, K., DE NORONHA, C., YONEMOTO, W. & GREENE, W. C. 2003. HIV-1 Vif blocks the antiviral activity of APOBEC3G by impairing both its translation and intracellular stability. *Mol Cell*, 12, 591-601.
- STREBEL, K., DAUGHERTY, D., CLOUSE, K., COHEN, D., FOLKS, T. & MARTIN, M. A. 1987. The HIV 'A' (sor) gene product is essential for virus infectivity. *Nature*, 328, 728-30.
- STREBEL, K. & KHAN, M. A. 2008. APOBEC3G encapsidation into HIV-1 virions: which RNA is it? *Retrovirology*, 5, 55.
- SUSPENE, R., AYNAUD, M. M., GUETARD, D., HENRY, M., ECKHOFF, G., MARCHIO, A., PINEAU, P., DEJEAN, A., VARTANIAN, J. P. & WAIN-HOBSON, S. 2011. Somatic hypermutation of human mitochondrial and nuclear DNA by APOBEC3 cytidine deaminases, a pathway for DNA catabolism. *Proc Natl Acad Sci U S A*, 108, 4858-63.
- SUSPENE, R., SOMMER, P., HENRY, M., FERRIS, S., GUETARD, D., POCHET, S., CHESTER, A., NAVARATNAM, N., WAIN-HOBSON, S. & VARTANIAN, J. P. 2004. APOBEC3G is a single-stranded DNA cytidine deaminase and functions independently of HIV reverse transcriptase. *Nucleic Acids Res*, 32, 2421-9.
- SUZUKI, J., YAMAGUCHI, K., KAJIKAWA, M., ICHIYANAGI, K., ADACHI, N., KOYAMA, H., TAKEDA, S. & OKADA, N. 2009. Genetic evidence that the non-homologous end-joining repair pathway is involved in LINE retrotransposition. *PLoS Genet*, 5, e1000461.
- SWANSON, C. M. & MALIM, M. H. 2008. SnapShot: HIV-1 proteins. *Cell*, 133, 742, 742 e1.
- SWITZER, W. M., BHULLAR, V., SHANMUGAM, V., CONG, M. E., PAREKH, B., LERCHE, N. W., YEE, J. L., ELY, J. J., BONEVA, R., CHAPMAN, L. E., FOLKS, T. M. & HENEINE, W. 2004. Frequent simian foamy virus infection in persons occupationally exposed to nonhuman primates. *J Virol*, 78, 2780-9.
- SWITZER, W. M., SALEMI, M., SHANMUGAM, V., GAO, F., CONG, M. E., KUIKEN, C., BHULLAR, V., BEER, B. E., VALLET, D., GAUTIER-HION, A., TOOZE, Z., VILLINGER, F., HOLMES, E. C. & HENEINE, W. 2005. Ancient co-speciation of simian foamy viruses and primates. *Nature*, 434, 376-80.
- TANAKA, Y., MARUSAWA, H., SENO, H., MATSUMOTO, Y., UEDA, Y., KODAMA, Y., ENDO, Y., YAMAUCHI, J., MATSUMOTO, T., TAKAORI-KONDO, A., IKAI, I. & CHIBA, T. 2006. Anti-viral protein APOBEC3G is induced by interferon-alpha stimulation in human hepatocytes. *Biochem Biophys Res Commun*, 341, 314-9.
- TAYLOR, B. J., NIK-ZAINAL, S., WU, Y. L., STEBBINGS, L. A., RAINE, K., CAMPBELL, P. J., RADA, C., STRATTON, M. R. & NEUBERGER, M. S. 2013. DNA deaminases induce break-associated mutation showers with implication of APOBEC3B and 3A in breast cancer kataegis. *Elife*, 2, e00534.
- TROBRIDGE, G. D. 2009. Foamy virus vectors for gene transfer. *Expert Opin Biol Ther*, 9, 1427-36.
- USAMI, Y., WU, Y. & GOTTLINGER, H. G. 2015. SERINC3 and SERINC5 restrict HIV-1 infectivity and are counteracted by Nef. *Nature*, 526, 218-23.
- VALKOV, E., GUPTA, S. S., HARE, S., HELANDER, A., ROVERSI, P., MCCLURE, M. & CHEREPANOV, P. 2009. Functional and structural characterization of the integrase from the prototype foamy virus. *Nucleic Acids Res*, 37, 243-55.

- VAN DER LOO, W., ABRANTES, J. & ESTEVES, P. J. 2009. Sharing of endogenous lentiviral gene fragments among leporid lineages separated for more than 12 million years. *J Virol*, 83, 2386-8.
- VAN MAELE, B. & DEBYSER, Z. 2005. HIV-1 integration: an interplay between HIV-1 integrase, cellular and viral proteins. *AIDS Rev*, 7, 26-43.
- VASUDEVAN, A. A., SMITS, S. H., HOPFNER, A., HÄUSSINGER, D., KOENIG, B. W. & MÜNK, C. 2013. Structural features of antiviral DNA cytidine deaminases. *Biol Chem*, 394, 1357-70.
- VENTER, J. C., ADAMS, M. D., MYERS, E. W., LI, P. W., MURAL, R. J., SUTTON, G. G., SMITH, H. O., YANDELL, M., EVANS, C. A., HOLT, R. A., GOCAYNE, J. D., AMANATIDES, P., BALLEW, R. M., HUSON, D. H., WORTMAN, J. R., ZHANG, Q., KODIRA, C. D., ZHENG, X. H., CHEN, L., SKUPSKI, M., SUBRAMANIAN, G., THOMAS, P. D., ZHANG, J., GABOR MIKLOS, G. L., NELSON, C., BRODER, S., CLARK, A. G., NADEAU, J., MCKUSICK, V. A., ZINDER, N., LEVINE, A. J., ROBERTS, R. J., SIMON, M., SLAYMAN, C., HUNKAPILLER, M., BOLANOS, R., DELCHER, A., DEW, I., FASULO, D., FLANIGAN, M., FLOREA, L., HALPERN, A., HANNENHALLI, S., KRAVITZ, S., LEVY, S., MOBARRY, C., REINERT, K., REMINGTON, K., ABU-THREIDEH, J., BEASLEY, E., BIDDICK, K., BONAZZI, V., BRANDON, R., CARGILL, M., CHANDRAMOULISWARAN, I., CHARLAB, R., CHATURVEDI, K., DENG, Z., DI FRANCESCO, V., DUNN, P., EILBECK, K., EVANGELISTA, C., GABRIELIAN, A. E., GAN, W., GE, W., GONG, F., GU, Z., GUAN, P., HEIMAN, T. J., HIGGINS, M. E., JI, R. R., KE, Z., KETCHUM, K. A., LAI, Z., LEI, Y., LI, Z., LI, J., LIANG, Y., LIN, X., LU, F., MERKULOV, G. V., MILSHINA, N., MOORE, H. M., NAIK, A. K., NARAYAN, V. A., NEELAM, B., NUSSKERN, D., RUSCH, D. B., SALZBERG, S., SHAO, W., SHUE, B., SUN, J., WANG, Z., WANG, A., WANG, X., WANG, J., WEI, M., WIDES, R., XIAO, C., YAN, C., et al. 2001. The sequence of the human genome. *Science*, 291, 1304-51.
- VON SCHWEDLER, U., SONG, J., AIKEN, C. & TRONO, D. 1993. Vif is crucial for human immunodeficiency virus type 1 proviral DNA synthesis in infected cells. *J Virol*, 67, 4945-55.
- WANG, J., SHACKELFORD, J. M., CASELLA, C. R., SHIVERS, D. K., RAPAPORT, E. L., LIU, B., YU, X. F. & FINKEL, T. H. 2007. The Vif accessory protein alters the cell cycle of human immunodeficiency virus type 1 infected cells. *Virology*, 359, 243-52.
- WANG, X., AO, Z., CHEN, L., KOBINGER, G., PENG, J. & YAO, X. 2012. The cellular antiviral protein APOBEC3G interacts with HIV-1 reverse transcriptase and inhibits its function during viral replication. *J Virol*, 86, 3777-86.
- WISSING, S., GALLOWAY, N. L. & GREENE, W. C. 2010. HIV-1 Vif versus the APOBEC3 cytidine deaminases: an intracellular duel between pathogen and host restriction factors. *Mol Aspects Med*, 31, 383-97.
- WOLFE, L. S., STANLEY, B. J., LIU, C., ELIASON, W. K. & XIONG, Y. 2010. Dissection of the HIV Vif interaction with human E3 ubiquitin ligase. *J Virol*, 84, 7135-9.
- WOLFE, N. D., SWITZER, W. M., CARR, J. K., BHULLAR, V. B., SHANMUGAM, V., TAMOUFE, U., PROSSER, A. T., TORIMIRO, J. N., WRIGHT, A., MPOUDI-NGOLE, E., MCCUTCHAN, F. E., BIRX, D. L., FOLKS, T. M., BURKE, D. S. & HENEINE, W. 2004. Naturally acquired simian retrovirus infections in central African hunters. *Lancet*, 363, 932-7.
- WOOD, N., BHATTACHARYA, T., KEELE, B. F., GIORGI, E., LIU, M., GASCHEN, B., DANIELS, M., FERRARI, G., HAYNES, B. F., MCMICHAEL, A., SHAW, G. M., HAHN, B. H., KORBER, B. & SEOIGHE, C. 2009. HIV evolution in early infection: selection pressures, patterns of insertion and deletion, and the impact of APOBEC. *PLoS Pathog*, 5, e1000414.
- WU, Z., REN, X., YANG, L., HU, Y., YANG, J., HE, G., ZHANG, J., DONG, J., SUN, L., DU, J., LIU, L., XUE, Y., WANG, J., YANG, F., ZHANG, S. & JIN, Q. 2012. Virome analysis for identification of novel mammalian viruses in bat species from Chinese provinces. *J Virol*, 86, 10999-1012.
- XIAO, Z., EHRLICH, E., YU, Y., LUO, K., WANG, T., TIAN, C. & YU, X. F. 2006. Assembly of HIV-1 Vif-Cul5 E3 ubiquitin ligase through a novel zinc-binding domain-stabilized hydrophobic interface in Vif. *Virology*, 349, 290-9.
- XIAO, Z., XIONG, Y., ZHANG, W., TAN, L., EHRLICH, E., GUO, D. & YU, X. F. 2007. Characterization of a novel Cullin5 binding domain in HIV-1 Vif. *J Mol Biol*, 373, 541-50.

- XU, F., TAN, J., LIU, R., XU, D., LI, Y., GENG, Y., LIANG, C. & QIAO, W. 2011. Tetherin inhibits prototypic foamy virus release. *Virology*, 8, 198.
- YAN, N. & CHEN, Z. J. 2012. Intrinsic antiviral immunity. *Nat Immunol*, 13, 214-22.
- YANG, N. & KAZAZIAN, H. H., JR. 2006. L1 retrotransposition is suppressed by endogenously encoded small interfering RNAs in human cultured cells. *Nat Struct Mol Biol*, 13, 763-71.
- YANG, S., SUN, Y. & ZHANG, H. 2001. The multimerization of human immunodeficiency virus type 1 Vif protein: a requirement for Vif function in the viral life cycle. *J Biol Chem*, 276, 4889-93.
- YANG, X., GONCALVES, J. & GABUZDA, D. 1996. Phosphorylation of Vif and its role in HIV-1 replication. *J Biol Chem*, 271, 10121-9.
- YIN, Z., SHI, K., BANERJEE, S., PANDEY, K. K., BERA, S., GRANDGENETT, D. P. & AIHARA, H. 2016. Crystal structure of the Rous sarcoma virus intasome. *Nature*, 530, 362-6.
- YU, F., ZINGLER, N., SCHUMANN, G. & STRATLING, W. H. 2001. Methyl-CpG-binding protein 2 represses LINE-1 expression and retrotransposition but not Alu transcription. *Nucleic Acids Res*, 29, 4493-501.
- YU, Q., KONIG, R., PILLAI, S., CHILES, K., KEARNEY, M., PALMER, S., RICHMAN, D., COFFIN, J. M. & LANDAU, N. R. 2004a. Single-strand specificity of APOBEC3G accounts for minus-strand deamination of the HIV genome. *Nat Struct Mol Biol*, 11, 435-42.
- YU, S. F., SULLIVAN, M. D. & LINIAL, M. L. 1999. Evidence that the human foamy virus genome is DNA. *J Virol*, 73, 1565-72.
- YU, X., YU, Y., LIU, B., LUO, K., KONG, W., MAO, P. & YU, X. F. 2003. Induction of APOBEC3G ubiquitination and degradation by an HIV-1 Vif-Cul5-SCF complex. *Science*, 302, 1056-60.
- YU, Y., XIAO, Z., EHRLICH, E. S., YU, X. & YU, X. F. 2004b. Selective assembly of HIV-1 Vif-Cul5-ElonginB-ElonginC E3 ubiquitin ligase complex through a novel SOCS box and upstream cysteines. *Genes Dev*, 18, 2867-72.
- ZHANG, H., POMERANTZ, R. J., DORNADULA, G. & SUN, Y. 2000. Human immunodeficiency virus type 1 Vif protein is an integral component of an mRNP complex of viral RNA and could be involved in the viral RNA folding and packaging process. *J Virol*, 74, 8252-61.
- ZHANG, H., YANG, B., POMERANTZ, R. J., ZHANG, C., ARUNACHALAM, S. C. & GAO, L. 2003. The cytidine deaminase CEM15 induces hypermutation in newly synthesized HIV-1 DNA. *Nature*, 424, 94-8.
- ZHANG, W., DU, J., EVANS, S. L., YU, Y. & YU, X. F. 2012. T-cell differentiation factor CBF-beta regulates HIV-1 Vif-mediated evasion of host restriction. *Nature*, 481, 376-9.
- ZHANG, W., HUANG, M., WANG, T., TAN, L., TIAN, C., YU, X., KONG, W. & YU, X. F. 2008. Conserved and non-conserved features of HIV-1 and SIVagm Vif mediated suppression of APOBEC3 cytidine deaminases. *Cell Microbiol*, 10, 1662-75.
- ZHOU, X., EVANS, S. L., HAN, X., LIU, Y. & YU, X. F. 2012. Characterization of the interaction of full-length HIV-1 Vif protein with its key regulator CBFbeta and CUL5 E3 ubiquitin ligase components. *PLoS One*, 7, e33495.
- ZINGLER, N., WILLHOEFT, U., BROSE, H. P., SCHODER, V., JAHNS, T., HANSCHMANN, K. M., MORRISH, T. A., LOWER, J. & SCHUMANN, G. G. 2005. Analysis of 5' junctions of human LINE-1 and Alu retrotransposons suggests an alternative model for 5'-end attachment requiring microhomology-mediated end-joining. *Genome Res*, 15, 780-9.

Chapter I

Structural features of antiviral DNA cytidine deaminases

Journal : **Biological chemistry** (published in 2013)

Own contribution to this work:

- Structural analysis of APOBEC3 proteins
- Constructed all the figures and table
- Writing of the manuscript

Review

Ananda Ayyappan Jaguva Vasudevan, Sander H.J. Smits, Astrid Höppner, Dieter Häussinger, Bernd W. Koenig and Carsten Münk*

Structural features of antiviral DNA cytidine deaminases

Abstract: The APOBEC3 (A3) family of cytidine deaminases plays a vital role for innate defense against retroviruses. Lentiviruses such as HIV-1 evolved the Vif protein that triggers A3 protein degradation. There are seven A3 proteins, A3A-A3H, found in humans. All A3 proteins can deaminate cytidines to uridines in single-stranded DNA (ssDNA), generated during viral reverse transcription. A3 proteins have either one or two cytidine deaminase domains (CD). The CDs coordinate a zinc ion, and their amino acid specificity classifies the A3s into A3Z1, A3Z2, and A3Z3. A3 proteins occur as monomers, dimers, and large oligomeric complexes. Studies on the nature of A3 oligomerization, as well as the mode of interaction of A3s with RNA and ssDNA are partially controversial. High-resolution structures of the catalytic CD2 of A3G and A3F as well as of the single CD proteins A3A and A3C have been published recently. The NMR and X-ray crystal structures show globular proteins with six α -helices and five β sheets arranged in a characteristic motif (α 1- β 1- β 2/2'- α 2- β 3- α 3- β 4- α 4- β 5- α 5- α 6). However, the detailed arrangement and extension of individual structure elements and their relevance for A3 complex formation and activity remains a matter of debate and will be highlighted in this review.

Keywords: APOBEC3G; HIV-1; homology modeling; NMR; Vif; X-ray.

*Corresponding author: Carsten Münk, Clinic for Gastroenterology, Hepatology, and Infectiology, Medical Faculty, Heinrich-Heine-University, D-40225 Düsseldorf, Germany, e-mail: carsten.muenk@med.uni-duesseldorf.de

Ananda Ayyappan Jaguva Vasudevan and Dieter Häussinger: Clinic for Gastroenterology, Hepatology, and Infectiology, Medical Faculty, Heinrich-Heine-University, D-40225 Düsseldorf, Germany

Sander H.J. Smits: Institute of Biochemistry, Heinrich-Heine-University, D-40225 Düsseldorf, Germany

Astrid Höppner: Crystal and X-Ray Facility, Heinrich-Heine-University, D-40225 Düsseldorf, Germany

Bernd W. Koenig: Institute of Structural Biochemistry (ICS-6), Research Centre Jülich, D-52425 Jülich, Germany

Introduction: APOBEC3s – mammal-specific antiviral polynucleotide cytidine deaminases with oncogenic potential

Apolipoprotein B mRNA editing enzyme, catalytic polypeptide-like (APOBEC3, A3) genes are found only in placental mammals, but might be evolutionary, as old as the origin of mammals (LaRue et al., 2008; Münk et al., 2012b). All seven human A3 proteins (A3A, A3B, A3C, A3D, A3F, A3G, and A3H, Figure 1A) are single-strand DNA (ssDNA) cytidine deaminases known to inhibit multiple retroviruses, retroelements, RNA and DNA viruses (Arias et al., 2012). Many important aspects of the biology of A3 proteins are not resolved, and it is still unknown how A3s discern self from non-self ssDNA. Recent data support a role of human A3 proteins, especially for A3B, to act oncogenic and cause C-to-T mutations in breast cancer tissue (Nik-Zainal et al., 2012; Roberts et al., 2012; Burns et al., 2013; Nowarski and Kotler, 2013; Taylor et al., 2013).

The deaminases possess either one or two conserved zinc-coordinating (Z) motifs, in which the zinc is coordinated by a histidine and two cysteines. Z motifs can be classified into three groups (Z1, Z2, Z3), but share the consensus amino acid signature H-X-E-X₂₄₋₃₁-C-X₂₋₄-C (where X can be nearly any residue) (Jarmuz et al., 2002; Conticello, 2008; LaRue et al., 2008, 2009; Münk et al., 2008, 2012b) (Figure 1B).

A3G, the best-studied A3 protein (Harris et al., 2002; Jarmuz et al., 2002), is an inhibitor of variants of HIV-1 lacking the Vif gene expression (HIV-1 Δ Vif) in peripheral blood mononuclear cells (Sheehy et al., 2002). During retroviral budding, A3G binds to the viral nucleocapsid protein, can be incorporated into HIV-1 Δ Vif progeny particles, and carried over within the virion. In the virion, A3G proteins are then processed and cleansed of an inhibitory RNA by the viral RNase H (Soros et al., 2007). After cell entry, the viral genomic (+) strand RNA is reverse

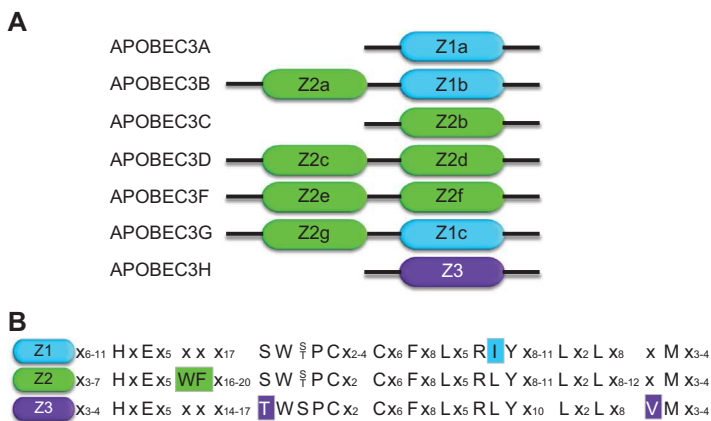


Figure 1 Human APOBEC3 proteins.

(A) Schematic representation of human APOBEC3 (A3) cytidine deaminases. All A3 proteins share at least one zinc (Z)-coordinating catalytic motif. The color code indicates the amino acid specificity of the different Z-motif-containing deaminase domains (Z1, Z2, and Z3). In humans, seven A3 proteins are detectable, A3A-A3H. (B) Amino acid sequences of indicated domains. Group-specific distinctions of Z-domains are highlighted.

transcribed into the (-) strand DNA that is the template for the (+) strand DNA synthesis, generating a complete, double-stranded viral DNA. Particle-delivered A3G proteins can inhibit HIV through multiple mechanisms early in the infection cycle, by cytidine deamination of the ssDNA and by reducing the reverse transcription and integration (for recent reviews, see Albin and Harris, 2010; Wissing et al., 2010; Münk et al., 2012a). In the virus-producer cell, Vif binding to A3G will induce polyubiquitylation and degradation of A3G, resulting in A3G-free progeny virions. To achieve polyubiquitylation and subsequent degradation of A3G, Vif acts as an A3G substrate receptor molecule by mimicking the SOCS-box component of a cellular E3 ubiquitin ligase in the Vif-Cullin5-Elongin B/C ubiquitin ligase complex (Marin et al., 2003; Sheehy et al., 2003; Yu et al., 2003, 2004; Mehle et al., 2004; Bergeron et al., 2010). Vif additionally recruits the transcription cofactor CBF- β to form this active complex (Jager et al., 2012; Zhang et al., 2012). The A3-Vif interaction is critical: Vif efficiently, but not completely, counteracts A3C, A3D, A3F, A3G, and A3H. A3 proteins that do not bind to Vif are not neutralized and likely inhibit HIV (for a review, see Münk et al., 2012a). A3 antagonists that presumably play a similar role as Vif proteins of lentiviruses have been described for other viruses, too: the Bet proteins in foamy retroviruses, the nucleocapsid protein in human T-cell lymphotropic virus type 1, and the glycosylated Gag protein (glyco-Gag) of murine leukemia virus have been implicated in the counteraction of the antiviral activity of A3 proteins (Mariani et al., 2003; Löchelt et al., 2005; Russell et al., 2005; Derse et al., 2007; Münk et al., 2008; Perkovic et al., 2009; Kolokithas et al., 2010;

Chareza et al., 2012; Ooms et al., 2012; Jaguva Vasudevan et al., 2013; Stavrou et al., 2013).

A3G is a two-domain deaminase with a Z2 and a Z1 domain (Z2g-Z1c, Figure 1B). These two functionally distinct subunits, the N-terminal pseudocatalytic domain (CD1, residues 1–196), which is more positively charged under physiological conditions, and the C-terminal catalytic domain (CD2, residues 197–384) give the protein an internal pseudosymmetry (Huthoff et al., 2009; Chelico et al., 2010; Feng and Chelico, 2011). Genetic and biochemical data illustrate that the CD2 in the context of the full-length A3G alone is responsible for the deamination activity, whereas the CD1 is more important for binding of RNA or ssDNA (Hache et al., 2005; Navarro et al., 2005; Schumacher et al., 2008; Huthoff et al., 2009; Chelico et al., 2010; Feng and Chelico, 2011). After binding randomly to ssDNA, but not to double-stranded DNA (dsDNA), A3G translocates arbitrarily in small steps by sliding along the polynucleotide and in larger steps by jumping/hopping or intersegmental transfer (Chelico et al., 2006, 2008; Nowarski et al., 2008; Shlyakhtenko et al., 2011, 2012). The deamination in the CCC motif occurs processively, i.e., one A3G molecule catalyses multiple deaminations on the same ssDNA prior to attacking a different substrate (Chelico et al., 2006, 2008). In the A3G recognition motif, the pyrimidine rings of the -2 and -1 cytidine residues are essential for motif recognition and deamination of the third (0) cytidine residue (Rausch et al., 2009). Several studies indicate that A3G deaminates predominantly in the 3'-to-5' direction, where the CD1 domain is probably required for introducing this bias (Chelico et al., 2006, 2008, 2010; Holden et al., 2008; Furukawa et al., 2009).

Oligomeric organization of APOBEC3s

What is the preferred oligomerization state of A3G and other A3 proteins in human cells? Does the cytidine deamination activity or the antiviral function of A3s require monomers, dimers, or higher-order oligomers? Questions like this have been addressed by many investigations using several different techniques.

A3G and A3F isolated by gel filtration chromatography from human or baculovirus-infected Sf9 cells revealed protein complexes of >700 kDa, implicating either homomultimerization of A3s and/or interactions with additional protein species (Chelico et al., 2006; Chiu et al., 2006; Kozak et al., 2006; Kreisberg et al., 2006). Studies also described dimerization and higher-order oligomers of A3B and A3C in living cells as well as *in vitro* (Chiu et al., 2006; Wedekind et al., 2006; Niewiadomska et al., 2007; Chen et al., 2008; Holden et al., 2008; Wang et al., 2008; Huthoff et al., 2009; Salter et al., 2009; Stauch et al., 2009; Chelico et al., 2010; Shandilya et al., 2010).

A3G can exist as monomers, dimers, or megadalton oligomers, the so-called high molecular mass (HMM) complexes (Jarmuz et al., 2002; Chiu et al., 2006; Wedekind et al., 2006; Bennett et al., 2008). Resting CD4 T cells and monocytes show low molecular mass (LMM) A3G complexes, and activation of CD4 T cells promotes the recruitment of LMM A3G and subsequent formation of HMM complexes (Kreisberg et al., 2006). A3G has RNA-binding properties (Jarmuz et al., 2002; Iwatani et al., 2006; Kozak et al., 2006; Huthoff et al., 2009). RNA digestion in cell lysates initially containing HMM complexes resulted in LMM complexes supporting the notion that HMM complexes are ribonucleoprotein complexes (Kreisberg et al., 2006). Using tandem affinity purification techniques coupled with mass spectrometry, specific components of the HMM A3G and A3F complexes were identified to bind RNA like in Staufen-containing RNA-transporting granules and in Ro ribonucleoprotein complexes (Chiu et al., 2006), poly(A)-binding proteins (Kozak et al., 2006), in P bodies (Gallois-Montbrun et al., 2007, 2008), and in stress granules (Kozak et al., 2006; Gallois-Montbrun et al., 2007, 2008). Analysis of RNAs in these complexes revealed HIV-1 RNA, Alu, small Y RNAs, certain mRNAs (such as that encoding A3G itself), and the 7SL RNA of the signal recognition particle (Chiu et al., 2006; Kozak et al., 2006; Gallois-Montbrun et al., 2008).

To obtain structural models of the A3G HMM or LMM complexes, small-angle X-ray scattering (SAXS) was applied to Sf9 cell-derived A3G (Wedekind et al., 2006).

Low-resolution molecular envelopes were derived from the SAXS data. RNase A treatment of the samples resulted in an SAXS profile consistent with an A3G dimer. The SAXS-derived molecular envelope of the untreated A3G was significantly larger and could accommodate two A3G dimer envelopes with no spatial overlap (Wedekind et al., 2006). The authors described the shape of the RNA-containing A3G oligomer, which likely presents a minimal HMM particle, as an elongated cylinder, formed by two A3G dimers. These two A3G dimers appear to associate in a tail-to-tail fashion (protein-protein interactions via the C termini) rather than in a head-to-head or head-to-tail configuration. In contrast, cross-linking experiments showed A3G dimers that appear to be arranged in a head-to-head fashion with the two N-terminal CD1 domains forming the contact. Mutating the CD1 of A3G abrogates its RNA binding and self-association potential (Navarro et al., 2005; Friew et al., 2009). Specifically, the conserved W94, Y124, and W127 within the CD1 domain mediate A3G oligomerization and packaging into HIV-1 virions (Bulliard et al., 2009; Huthoff et al., 2009). Oligomerization-deficient A3G proteins associate less efficiently with several cellular RNA molecules, supporting a model that occupation of the positively charged pocket by RNA promotes A3G oligomerization (Bulliard et al., 2009; Huthoff et al., 2009). Because native A3G can form oligomers larger than dimers, an additional oligomer interface apart from CD1-CD1 is likely to exist (Chelico et al., 2010).

The oligomerization state of A3G was analyzed by multiangle light scattering (MALS) (Chelico et al., 2010). Purified A3G is a polydisperse mixture, primarily containing dimers (~80%), along with subpopulations of monomers (~18%), and higher-order oligomers (~2%). These findings are in agreement with analytical ultracentrifugation data (Salter et al., 2009). A3G is packaged into HIV particles as a multimer, perhaps by interacting with the Alu portion of 7SL RNA or HIV RNA, but presumably not as a monomer (Burnett and Spearman, 2007; Strelb and Khan, 2008). To characterize the oligomerization state of A3G while catalyzing the deamination of HIV proviral cDNA, atomic force microscopy (AFM) was employed to investigate the dynamics and structural determinants of A3G bound to ssDNA (Chelico et al., 2008, 2010; Shlyakhtenko et al., 2011, 2012).

The first reported A3G AFM experiments suggested that A3G forms stable complexes of higher-order oligomers with ssDNA, and the stoichiometry of these complexes depended on salt concentrations and divalent cations (Chelico et al., 2008, 2010). Without salt, the binding of ssDNA appears to cause A3G dissociation from higher-order oligomers to predominantly monomers and dimers

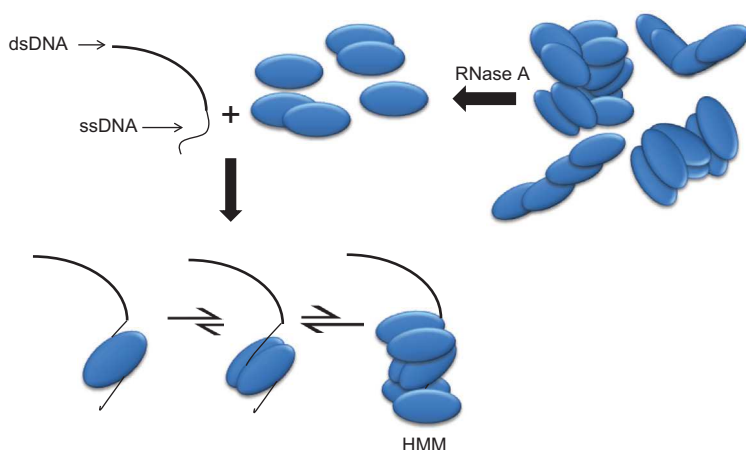


Figure 2 Possible ways of (*in vitro*) A3G-ssDNA interaction studied by AFM.

A hybrid DNA substrate made up of dsDNA (thick) and an ssDNA tail (where A3G binds). One blue oval unit represents a full-length A3G molecule. Free A3G can exist as monomers and dimers (RNase treated). A3G complexed with ssDNA is primarily dimeric, but A3G monomers or higher-order oligomers (HMM; high molecular mass complexes) can also bind ssDNA substrates (adapted from Shlyakhtenko et al., 2011).

(Chelico et al., 2008). Applying an improved hybrid ssDNA substrate Shlyakhtenko et al. demonstrated later that ssDNA-complexed A3G is mostly dimeric, unbound A3G was predominantly monomeric, and A3G monomers, dimers, and higher-order oligomers could bind ssDNA substrates in a manner independent of strand polarity and availability of free ssDNA ends (Shlyakhtenko et al., 2011, 2012). Together, these data suggest that RNA-free A3G oligomerizes upon binding ssDNA substrate, that the dimers form more stable complexes than monomers, and that oligomerization equilibrium is toward dimers (Figure 2).

NMR and crystal structures of APOBEC3s

Three nuclear magnetic resonance (NMR) structures and four X-ray crystal structures of the A3G CD2 catalytic domain have been published to date (Chen et al., 2008; Holden et al., 2008; Furukawa et al., 2009; Harjes et al., 2009; Shandilya et al., 2010; Li et al., 2012). In addition, crystal structures of the A3F CD2 catalytic domain (Bohn et al., 2013) and of A3C were determined (Kitamura et al., 2012). Very recently, the NMR structure of A3A became available (Byeon et al., 2013). However, an experimental structure of the full-length A3G is still missing.

The characteristic architecture of A3G CD2 is a hydrophobic five-stranded core β sheet surrounded by six α -helices, called β 1- β 5 and α 1- α 6, respectively, throughout this review. Please note a different

numbering scheme in two of the original papers where the N-terminal helix was missing (Chen et al., 2008) or termed α 0 (Furukawa et al., 2009). Structures have been determined for variants of different length reflecting the wild type and two CD2 mutants (dubbed A3G-2K3A and A3G-2K2A) of human A3G (see Table 1 for details). In A3G-2K3A, the solubility of the monomeric protein was increased by lysine substitutions L234K and F310K in combination with C243A, C321A, and C356A to minimize the chance of intermolecular disulfide bond formation and to promote long-term stability (Chen et al., 2008). In A3G-2K2A, C321 was not mutated in order to study C321's interaction with the inhibitor compound MN30 (Li et al., 2012). Structure elements in A3G CD2 are arranged in the order of α 1- β 1- β 2/2'- α 2- β 3- α 3- β 4- α 4- β 5- α 5- α 6 (Figure 3A). The second β strand is divided and forms a β 2-bulge- β 2' region (Chen et al., 2008; Furukawa et al., 2009; Harjes et al., 2009; Shandilya et al., 2010). Only one X-ray structure shows a continuous β 2 strand (Holden et al., 2008), resembling the distantly related APOBEC2 structure (Prochnow et al., 2007), but this continuous β 2 strand in A3G CD2 was heavily disputed and might be an artifact (Harjes et al., 2009; Shandilya et al., 2010). Autore et al. observed a general trend toward the ordered conformations of the β 2 strand during molecular dynamics (MD) simulations of the NMR structures, which had a distorted starting conformation of β 2 (Autore et al., 2010). This revealed that this distortion is dependent on preferential hydration of residues within the β 2 strand, which in turn forms a continuous β sheet in the full length CD1 and CD2 assembly.

Table 1 APOBEC3 and APOBEC2 structures with references.

Subject	Method	PDB code	Protein	Reference
Human APOBEC3G	X-ray crystallography	3E1U/ 3IQS	A3G AA 197-380	(Holden et al., 2008)
		3IR2	A3G AA 191-384 mutation 2K3A ^a	(Shandilya et al., 2010)
		3V4K	A3G AA 191-380 mutation 2K2A ^b	(Li et al., 2012)
		3V4J	A3G AA 191-384 mutation 2K3A ^a	(Li et al., 2012)
			MN30 bound	
	Solution NMR	2JYW	A3G AA 198-384 mutation 2K3A ^a	(Chen et al., 2008)
		2KBO	A3G AA 193-384	(Furukawa et al., 2009)
		2KEM	A3G AA 191-384 mutation 2K3A ^a	(Harjes et al., 2009)
			A3F	(Bohn et al., 2013)
			AA 185-373 mutation 11X ^c	
Human APOBEC3F	X-ray crystallography	4IOU	A3F	(Bohn et al., 2013)
Human APOBEC3A	Solution NMR	2M65	A3A AA 1-199	(Byeon et al., 2013)
Human APOBEC3C	X-ray crystallography	3VOW/ 3VM8	A3C AA 1-190	(Kitamura et al., 2012)
Human APOBEC2	X-ray crystallography	2NYT	A2 AA 41-224	(Prochnow et al., 2007)
Modeled structures	Homology modeling		A3G AA 1-384	(Zhang et al., 2007)
			A3G AA 1-384	(Harjes et al., 2009)
			A3G dimer model	(Bulliard et al., 2009; Huthoff et al., 2009)
			A3C AA 1-190	(Stauch et al., 2009)

^a2K3A Mutation: L234K, F310K, C243A, C321A, C356A.

^b2K2A Mutation: L234K, F310K, C243A, C356A.

^c11X Mutation: Y196D, H247G, C248R, C259A, F302K, W310D, Y314A, Q315A, K355D, K358D, F363D.

MN30, methyl-3,4-dephostatin; AA, amino acid.

The catalytic zinc is coordinated directly by H257, C288, and C291 and indirectly by the catalytic residue E259 via a water molecule (Holden et al., 2008). The zinc-coordinating active site, α 2- β 3- α 3, is anchored within the platform of β strands. The catalytic site is further supported by the α 5- and α 6-helices, which make extensive stabilizing hydrophobic contacts with the β -strand platform (Chen et al., 2008). Despite the common characteristic fold of the published A3G CD2 structures, they show conformational differences in several functionally important regions.

The first NMR structure of A3G198-384 (2K3A mutant, PDB accession 2JYW) was reported by Chen et al. (2008). Residues 198–384 of A3G were sufficient for DNA deamination. The authors also titrated ¹⁵N-labeled A3G-2K3A with a nonlabeled 21-base ssDNA and recorded a series of

2D HSQC NMR spectra of the protein to understand how A3s recognize ssDNA. Resulting changes in NMR signal position (chemical shift perturbation, CSP) or NMR signal intensity indicate binding of the ligand. The strength of the CSP observed for a given amino acid residue is often inversely related to the distance of this residue to the site of binding in the complex. Significant CSPs were detected for the conserved R215 and R313, residues adjacent to R313 within the loop between β 4 and α 4 (β 4- α 4 loop) and the catalytic E259 (Chen et al., 2008). These results suggested a DNA-binding model in which a brim of positively charged residues (arginines 213, 215, 313, 320) positions the target cytosine for catalysis that cannot access the catalytic glutamate E259 without flipping out from the phosphodiester backbone (Figure 3B). The presumable orientation of the ssDNA relative to A3G in the complex was deduced from

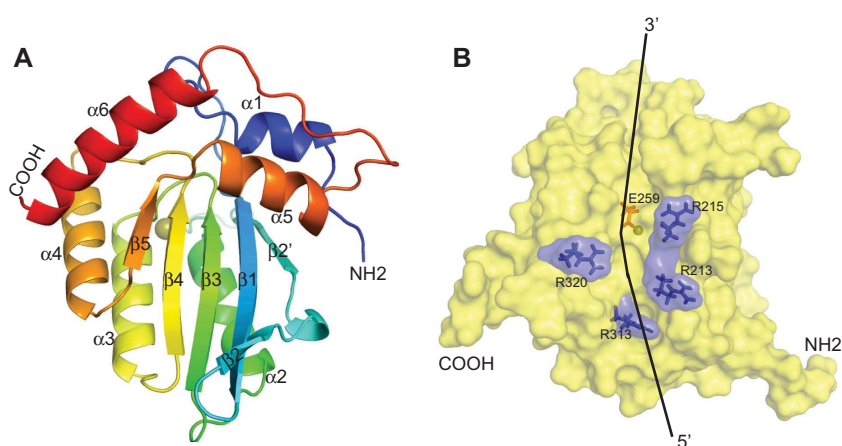


Figure 3 Structure of the CD2 (Z1c) of A3G.

(A) A3G-CD2 structure [PDB 3IR2 (Shandilya et al., 2010)] composed of a core hydrophobic five-stranded β sheets ($\beta 1$ – $\beta 5$) surrounded by six α helices ($\alpha 1$ – $\alpha 6$). The coordinating zinc atom is represented as a sphere. (B) A3G CD2 catalytic domain–DNA interaction model based on the report by Chen et al. (2008). Positively charged residues (arginines) surrounding the active site and the catalytically active E259 are labeled. Hypothetical DNA binding path and the polarity are shown in black dashed line.

previous deaminase crystal structures (Xiang et al., 1997; Teh et al., 2006; Chen et al., 2008).

The solution structure of wild-type A3G193–384 and the position of a 10-mer ssDNA in the complex were also determined in an independent NMR study (Furukawa et al., 2009) (Figure 4). CSPs were observed for residues in the $\alpha 1$ and $\beta 1$ loop (N208 and R215), in the $\beta 2'$ – $\alpha 2$ loop (C243, A246, E254, R256, and H257), in $\alpha 2$ (L260, C261, F262, L263, V265, and I266), in $\beta 4$ (V305 and S306), in the $\beta 4$ – $\alpha 4$ loop (D316 and G319), in $\beta 5$ (I337), in $\alpha 5$ (D348), and in the $\alpha 5$ – $\alpha 6$ loop (V351, D352, and D362). This CSP pattern was similar to the one observed in the above titration of A3G-2K3A with ssDNA (Chen et al., 2008). However, additional CSPs were observed upon ssDNA binding to wild-type A3G193–384 (Furukawa et al., 2009). These data imply that the substrate cytidine is positioned close to catalytic E259, conserved S284–W285–S286, and zinc-coordinating H257. The exact location of the interacting ssDNA is controversial. Three different models of the complex were proposed based on CSP data in the two NMR studies and on the crystal structure of wild-type A3G197–380 (Figure 4B) (Chen et al., 2008; Holden et al., 2008; Furukawa et al., 2009). It is possible that different modes of A3G–ssDNA interactions coexist in solution. Furukawa et al. also observed the deamination reaction of a 10-mer ssDNA carrying a C4, C5, and C6 target sequence by wild-type A3G193–384 in an NMR sample tube in real time in a series of 2D ^1H – ^{13}C HSQC spectra. Conversion of C6 to U6 was completed within 30 min. Deamination of C5 occurs on a much slower time scale of hours (Furukawa et al., 2009).

Another NMR study on the elongated A3G191–384 carrying the 2K3A mutation demonstrated that several

residues within $\alpha 1$ stabilize the catalytic core (Harjes et al., 2009). This NMR data was also used to build a model of the full-length A3G that suggested that the CD1 pseudo-active site and the CD2 catalytic domain are located on different faces of the holoenzyme (Harjes et al., 2009).

Recently, the high-resolution NMR structure of full-length human A3A, the single CD A3Z1a protein, was published (Byeon et al., 2013) (Figure 5). Comparison with other APOBEC structures reveals that the A3A solution structure most closely resembles crystal structures (see below) of A3C (Kitamura et al., 2012) and of the catalytic CD2 of A3G, in particular, of the mutated A3G-2K3A (Shandilya et al., 2010) and A3G-2K2A (Li et al., 2012) variants (Figure 5), while it shows local differences to published NMR solution structures of the A3G CD2 (Byeon et al., 2013). The A3A structure displays an interrupted $\beta 2$ strand ($\beta 2$ -bulge- $\beta 2'$) and an N-terminal helix $\alpha 1$. NMR-based analysis of A3A titrations with various ssDNA substrates showed that specific binding of the substrate involves five A3A regions: the active site, the $\beta 2'$ – $\alpha 2$ loop, the $\beta 3$ – $\alpha 3$ loop, the $\beta 4$ – $\alpha 4$ loop, and helix $\alpha 4$. These regions are situated in a localized manner and cluster around the active site in the A3A structure (Byeon et al., 2013), which strongly contrasts the mapping of ssDNA binding to the CD2 of A3G (Chen et al., 2008; Furukawa et al., 2009). In addition, NMR was used to determine binding affinity of A3A for diverse single-stranded oligonucleotides and to follow substrate deamination in real time (Byeon et al., 2013).

The first crystal structure of A3G CD2 (PDB ID: 3E1U, residues 197–380) was reported by Holden et al. (2008). This protein was soluble, but differed to full-length A3G with a 25-fold lower specific deamination activity,

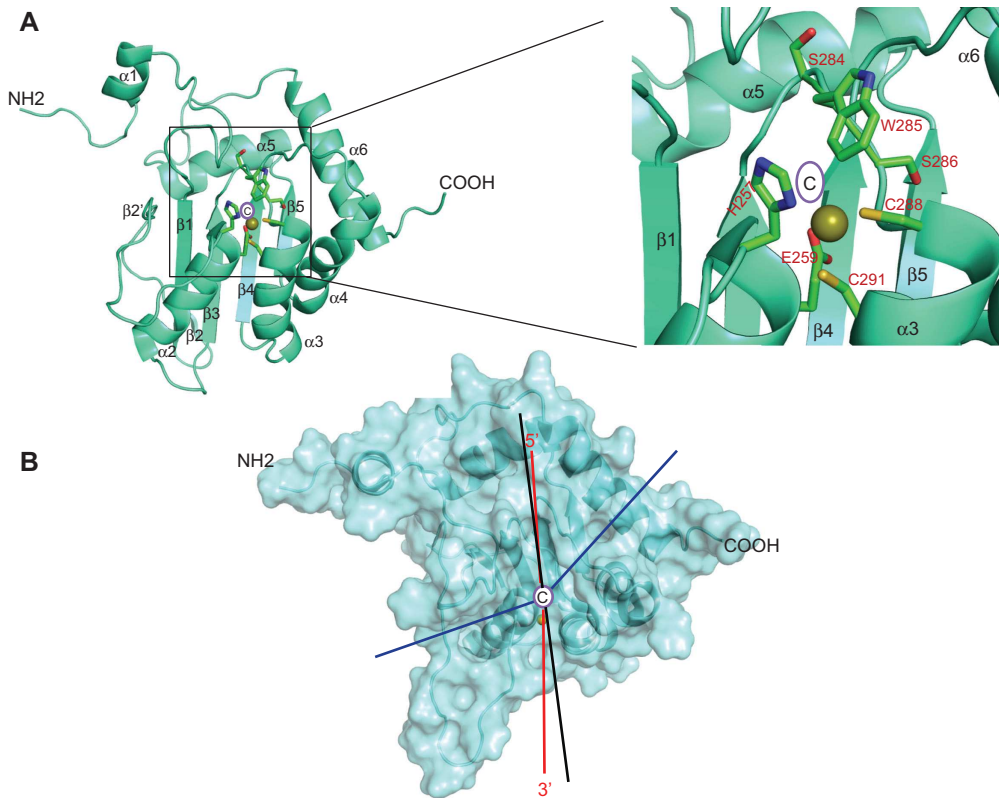


Figure 4 A3G CD2 NMR structure (Furukawa et al., 2009).

(A) Residues close to the zinc-coordinating active center are highlighted in sticks. The possible position of the substrate cytidine is highlighted by an oval shape. (B) Predicted DNA-binding path through the active center of A3G CD2. The broken lines indicate the three different positions of the ssDNA substrate proposed by Chen et al. (2008) (red), Holden et al. (2008) (blue), and Furukawa et al. (2009) (black) are collectively presented.

a twofold reduced processivity, and virtually no 3' to 5' deamination bias. The 2.3-Å resolution structure shows a core β sheet that is composed of five β strands surrounded by six α -helices (Holden et al., 2008). In the active site of A3G CD2, a zinc atom is coordinated by the residues H257, C288, and C291, plus a water molecule. In the crystal structure, the CD2 loops 1 and 3 and the regions near the active site form a continuous 'substrate groove' horizontally around the active center. The orientation of this putative substrate groove differs (by 90°) from the groove predicted by the NMR structure (A3G-2K3A) of Chen et al. (2008) (Figure 4B). The groove leads into a deep pocket where the zinc atom is located and continues toward the left side over the $\alpha 6$ -helix.

The second crystal structure of A3G CD2 (A3G residue 191-384-2K3A, PDB ID 3IR2) with a resolution of 2.25 Å was presented by Shandilya et al. (2010). This high-resolution crystal structure revealed four extensive protein interfaces (Figure 6A and B), of which one or more may be important

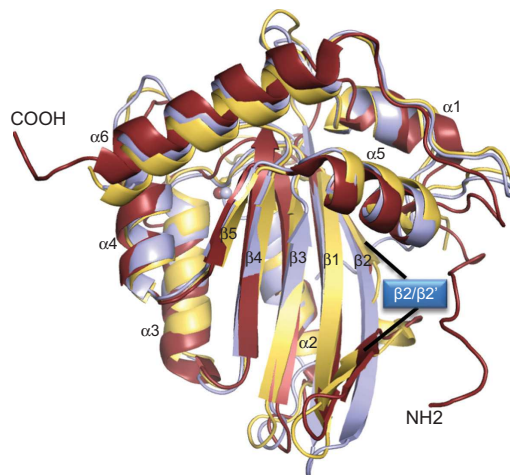


Figure 5 Structure of A3A.

NMR structure of full-length human A3A [ruby, PDB 2M65 (Byeon et al., 2013)] superimposed with the crystal structure of A3G CD2 [yellow, PDB 3IR2 (Shandilya et al., 2010)] and the crystal structure of A3C [light blue; PDB 3VOW; (Kitamura et al., 2012)]. Interrupted $\beta 2$ sheet of A3A and A3G CD2 is pointed with a dashed line.

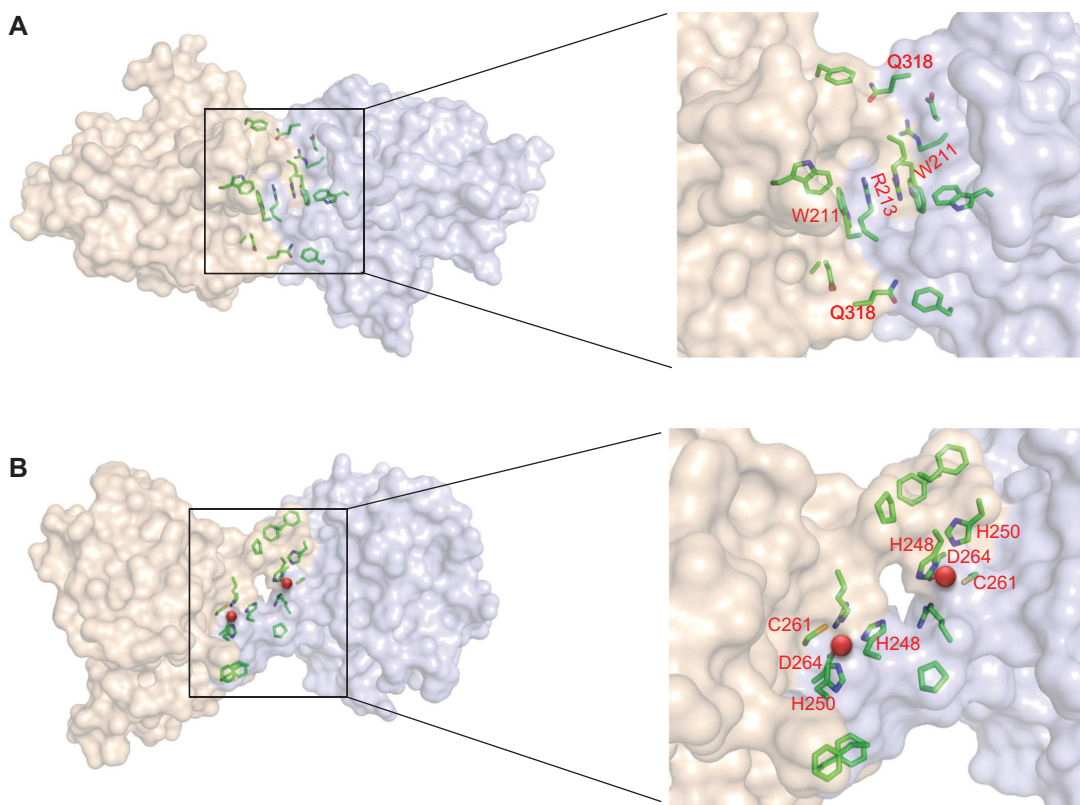


Figure 6 The interfaces of A3G CD2 (PDB 3IR2).

(A) Interface I, the largest interface between two A3G CD2 molecules in the crystal asymmetric unit (computed by PDBePISA). Residues that make this interface are shown in sticks; unique nonconserved residues (W211, R213, Q318) are labeled in red. (B) Interface II, the second largest interface, which coordinates intermolecular zinc (red sphere) through H248 and H250 of one molecule and C261 and D264 (through water-mediated H bond) of the second molecule. The structures were taken from Shandilya et al. (2010).

for A3G oligomerization and HIV restriction activity. The surfaces that form the full-length A3G oligomers remain unclear. SAXS studies have implicated that the C-terminal half of A3G takes part in oligomerization (Wedekind et al., 2006; Bennett et al., 2008). In contrast, coimmunoprecipitation studies demonstrated that N-terminal residues in CD1 are required for RNA-mediated dimerization (Frieu et al., 2009; Huthoff et al., 2009). In the A3G CD2 crystal structure (PDB ID 3IR2), the largest interaction interface is determined primarily by contacts between identical residues in the α 1-loop- β 1 region from both molecules in the asymmetric unit. The second largest interface involves the β 2'-loop- α 2 residues 247–254 in each of the two molecules of the asymmetric unit. This loop also coordinates an intermolecular zinc-binding site for a second zinc ion, indicating a metal-mediated modulation of A3G oligomerization. The third interface involves residues at N-terminal (β 1- β 2 strands) and C-terminal ends of A3G-2K3A. The fourth interface is made up of the tops of the α 5 and α 6 helices (Shandilya et al., 2010). These interaction interfaces observed between molecules in the crystal were

explored by the Protein Interfaces, Surfaces and Assemblies Service [PDBePISA (Krissinel and Henrick, 2007)]. It is likely that the residues lining the largest interaction interface (901 \AA^2) are essential for both A3G deaminase and antiviral activity and that the second largest interface (604 \AA^2) of A3G contributes to its zinc-mediated oligomerization, which may not be essential for A3G's HIV restriction activity. Using NMR, it was further shown that the addition of zinc triggers the oligomer formation, which can be reversed by chelating agents. Based on analyses of the A3G CD2 crystal 3IR2, a variety of potential surfaces could be involved in A3G oligomerization, and a full-length A3G model may give a better understanding about the oligomerization surfaces.

The highest resolution of an A3G CD2 crystal structure (A3G residue 191-384-2K2A, PDB ID 3V4K) published up to now amounts to 1.38 \AA and provides full resolution of most amino acid side chains (Li et al., 2012). In the same study, the crystal structure of A3G 191-380-2K3A in complex with the small molecule inhibitor MN30 was solved at 2.04 \AA resolution (PDB ID 3V4J). However, the position of the

inhibitor in this crystal structure does most likely not present the primary MN30-binding site in the CD2 of A3G (Li et al., 2012). The authors proposed a model in which the inhibitor molecule MN30 binds specifically to a pocket adjacent to the A3G CD2 active site, reacts covalently with C321, and pushes Y315 into the active site, thereby sterically blocking the entry of substrate DNA cytosines.

The crystal structure of catalytically active and HIV-1 Vif-binding domain of A3F CD2 (A3F residues 185-373-11X, PDB ID 4IOU) was recently solved at 2.75 Å resolution (Bohn et al., 2013). The 11-amino acid-substitution construct rendered enhanced solubility and catalytic activity of the recombinant protein. A3F CD2 has a canonical DNA cytosine deaminase fold, comprised of five β strands and six α helices with the Zn coordination catalytic motif (residues H249, C280, C283, and indirectly by the catalytic residue E251 via a water molecule) (Figure 7). The Zn-coordinating residue C283 and the catalytic residue E251, which are located in helices $\alpha 2$ and $\alpha 3$, define the catalytic pocket. Unlike the disrupted $\beta 2$ strand of most A3G CD2 structures, A3F CD2 possesses an extended sheet as in A3C and APOBEC2. Despite low sequence similarity, A3F CD2

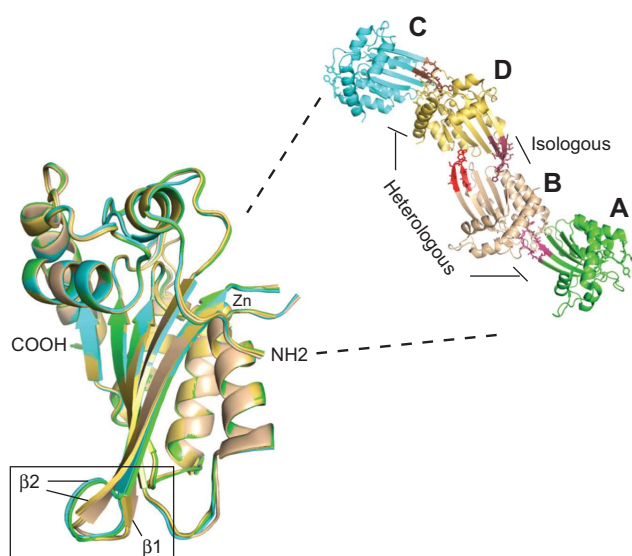


Figure 7 Structure of A3F CD2.

The crystal structure of A3F_{185-373-11X}: A3F CD2 crystal structure asymmetric unit consists of four chains (A, B, C, and D given in green, wheat, yellow, and cyan, respectively). Superimposition of A3F CD2 chains depicts the characteristic fold (five β strands and six α helices) and conformational plasticity in the $\beta 1$ - $\beta 2$ loop region of the protein (marked with a box). The conserved motif sequence 305-R L Y Y F W D-311 in the $\beta 4$ - $\alpha 4$ loop region involved in heterologous interface colored as the same as the chain color. Isologous interface motifs of $\beta 1$ - $\beta 2$ loop 223-E V V K H H S P V S-232 in chain A, B, C, D are colored as magenta, red, brown, and raspberry, respectively.

structure shares the conserved helix ($\alpha 1$ helix) and loop regions with A3G CD2 and A3C (but not with APOBEC2). Four molecules of A3F CD2 build the crystal asymmetric unit. As seen in the A3G CD2 crystal structure (PDB ID 3IR2), A3F structure possessed two unique intermolecular interfaces, but it does not contain the second Zn coordination site as in A3G CD2. The largest isologous interface formed across identical regions of the two chains B and D (Figure 7) and buries a total of 657 Å² surface area. The contacts occurred between $\beta 1$ - $\beta 2$ loop, $\alpha 2$ - $\beta 3$ loop, $\alpha 3$ - $\beta 4$ loop, and $\alpha 4$ - $\beta 5$ loop regions. The second heterologous interface was observed twice (between chains A and B and C and D) in the asymmetric unit and buries a total of 569 Å² (Figure 7). It is interesting to note that the $\beta 1$ - $\beta 2$ loop region involved in the formation of both interfaces (interface 1 and 2) exists in two distinct conformations depending on the interface.

A highly conserved sequence motif across the various human A3s is 305-R L Y Y F W D-311 in A3F-CTD ($\beta 4$ - $\alpha 4$ loop), which is also conserved across mammalian species infected by lentiviruses. This motif in CD1 and CD2 of A3F is involved in viral encapsidation (Song et al., 2012). In contrast, the less conserved motif of $\beta 1$ - $\beta 2$ loop region (223-E V V K H H S P V S-232), involved in forming both intermolecular interfaces is not conserved across A3 family members with the exception of A3D-CD2 (Bohn et al., 2013).

The negatively charged molecular surface of A3F CD2 raised some discussion about the Vif A3F interaction (Bohn et al., 2013). It was previously reported that Vif binds to negative surfaces in the $\alpha 3$ - $\alpha 4$ helices/the $\beta 4$ strand and the $\alpha 2$ - $\alpha 3$ helices/ $\beta 3$ strand of A3F CD2 (Albin et al., 2010; Smith and Pathak, 2010; Kitamura et al., 2012). This negative surface extends further into the $\beta 1$ - $\beta 2$ loop region (Bohn et al., 2013). Overall, the negative A3F CD2 surfaces are electrostatically complementary to HIV-1 Vif, a highly basic, intrinsically disordered protein. In addition, BLAST search revealed that both A3F motif sequences (305-R L Y Y F W D-311 and 223-E V V K H H S P V S-232) align closely with sequences within HIV-1 Vif: 108-H L Y Y F *D-113 and 23-S L V K H H M Y V S-32 (Bohn et al., 2013). This suggests that perhaps HIV-1 Vif evolved to mimic portions of A3F and that the molecular mimicry of Vif could play a role in modulating oligomerization or another molecular recognition event.

The crystal structure of the single CD protein A3C was presented by Kitamura et al. (2012). This structure is of interest because it contains a Vif-binding interface that is absent in A3G CD2, but present in A3G CD1. The full-length A3C protein (residues 1-190) has a core platform composed of six α -helices ($\alpha 1$ - $\alpha 6$) and five β strands

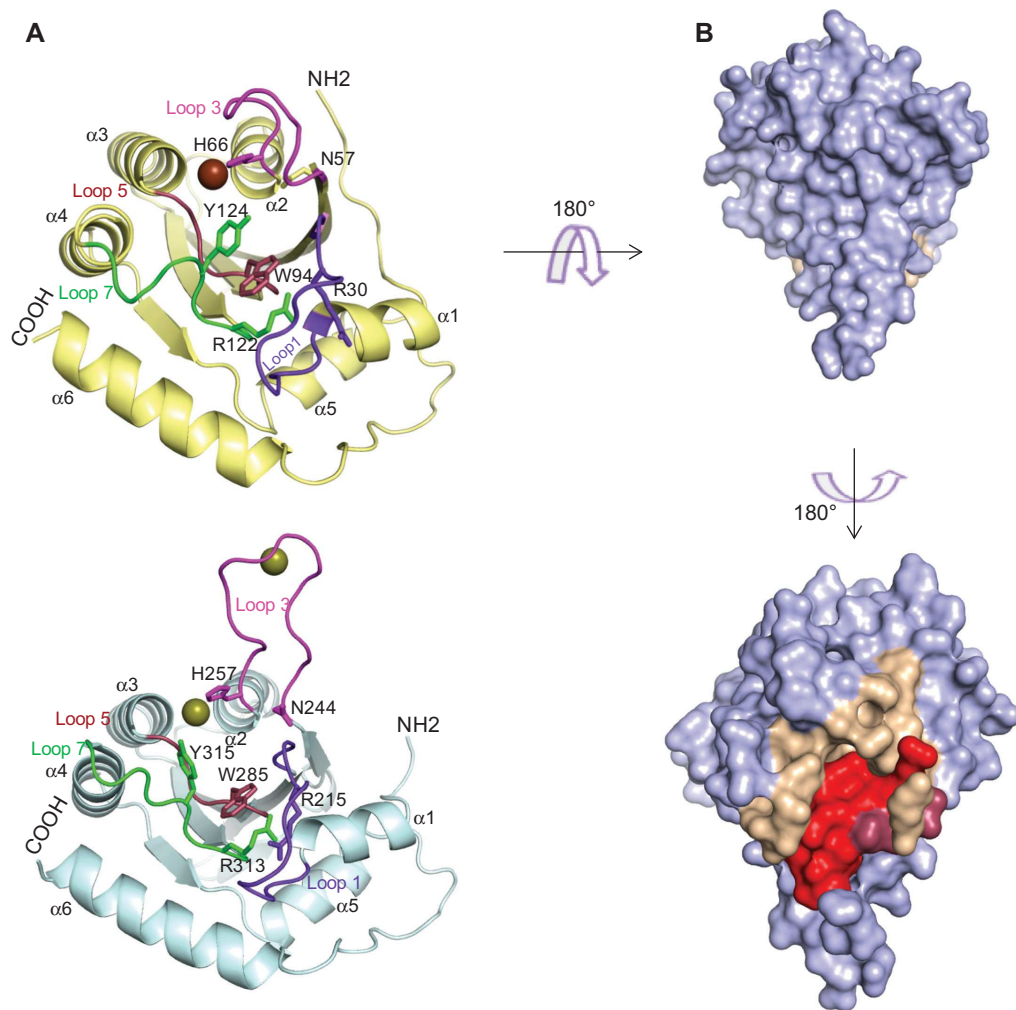


Figure 8 Comparison CD2 of A3G (Z1c) with A3C (Z2b).

(A) Comparison of A3G CD2 (cyan) [PDB 3IR2 (Shandilya et al., 2010)] and A3C (gold) [PDB 3VOW (Kitamura et al., 2012)] crystal structures, conserved amino acids in loop 1 (purple), loop 3 (magenta), loop 5 (brown), and loop 7 (green) are labeled with the residue numbers. (B) HIV-1 Vif-interacting interface on A3C. Structure-guided mutation analysis revealed the critical residues involved in Vif binding. The surface structure depicts the position of the Vif-binding interface on A3C (resides between $\alpha 2$ and $\alpha 3$; shown in wheat), color red (>50% resistance) and raspberry (40–45%) indicates the resistance levels of Vif binding to A3C when they are mutated. Arrows guide to show rotations of the A3C structure.

($\beta 1$ – $\beta 5$), with a coordinated zinc ion. Comparing the A3C structure with the structure of A3G CD2 (PDB 3IR2) shows that the core structures are highly conserved, but the loop regions, particularly loops 1, 3, 5, and 7 of the A3C and A3G CD2 structures, are distinct (Figure 8A). The A3C and A3F CD2 structures exhibit a continuous well-ordered $\beta 2$ strand that is different from the discontinuous $\beta 2$ strand of the A3G CD2 and the A3A (PDB 2M65). In contrast to the APOBEC2 crystal, where a dimer is formed by pairing two long $\beta 2$ strands (Prochnow et al., 2007), there were no indications of intermolecular contacts between $\beta 2$ strands in the A3C crystals (Kitamura et al., 2012). The Vif-binding interface was determined by structure-guided site-directed mutagenesis and revealed the involvement of 10

amino acids for Vif binding located in an area between the $\alpha 2$ and $\alpha 3$ helices, which forms a shallow cavity encompassed by hydrophobic and negatively charged residues (Figure 8B). Additional investigations demonstrated that the Vif-binding interfaces are highly conserved among human Z2-type cytidine deaminases, including A3C, A3F, and A3D, but not A3G (Kitamura et al., 2012).

Coimmunoprecipitation assays with mutants identified by a homology model indicated that aromatic residues F55 and W74 in the respective $\beta 2$ and $\alpha 2$ region of A3C are important for A3C oligomerization and cytidine deamination activity (Stauch et al., 2009). The core structure of the model A3C was quite similar to that of the experimental crystal structure. The superimposition of model structure

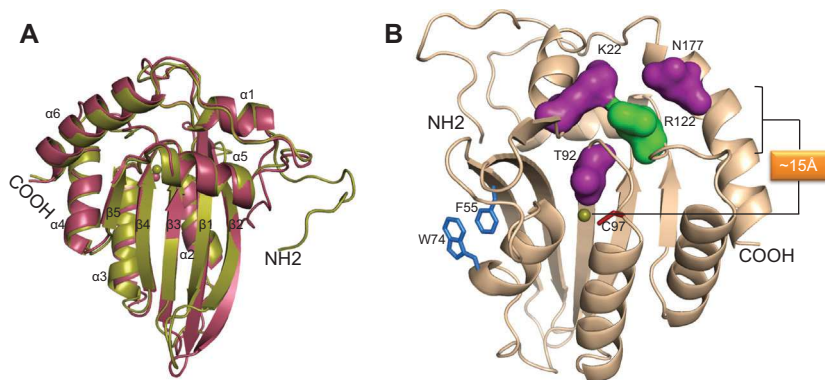


Figure 9 Model structure of A3C.

(A) Superimposition of A3C crystal [PDB 3VOW (Kitamura et al., 2012)] (brown) and model (Stauch et al., 2009) (olive) structures; spheres represent zinc. (B) Model structure of A3C showing the putative substrate-binding pocket (residues shown in surface representation; R122 is colored green), active site amino acid C97 (red) and zinc (sphere), and key dimerization residues (blue sticks).

of A3C core onto the A3C crystal structure (PDB 3VOW) for 98% of the backbone atoms exhibited a C α root mean square (RMS) deviation of 1.082 Å (187 out of 191 residues) (Figure 9A). R122 in A3C, critical for nucleic acid binding, has essential roles in the efficient RNA-dependent packaging of A3C into virions (Stauch et al., 2009). This residue is involved in the formation of a nucleic acid-binding pocket primarily consisting of loops 1, 3, 5, and 7 of A3C, which is approximately 15 Å distal from the zinc ion coordination site (Figure 9B).

Major challenges

In the last few years, advancements have been made in elucidating the structure of the CD2 catalytic domain of A3G and A3F as well as of A3C and A3A. However, an NMR or crystal structure of the full-length A3G, containing both the CD1 and CD2 domains, is still lacking and urgently needed for defining the biology of this protein. In addition to exploring the structures of all human A3s, there is a need for structures of nonhuman A3, like murine A3 or feline A3s, to describe the structural evolution of these positively selected proteins. Work has to be directed to better understand the regulation of the A3

oligomerization and the interactions with nucleic acids. Co-crystals with ssDNA/RNA and NMR titrations using selected mutants would shed light on the disputed DNA-/RNA-binding regions in A3G. Complex structures of A3s with viral antagonist like Vif or Bet or other viral proteins like the nucleocapsid protein could further expand our understanding of how the rapidly evolving A3s escape recognition by many non-adapted viral antagonists and, at the same time, recognize conserved structures of very diverse viruses. Such knowledge might help to develop new antiretroviral therapeutics that target HIV's interaction with cellular APOBEC3 proteins.

Acknowledgments: We gratefully acknowledge the support (and training) from the International NRW Research School BioStruct, granted by the Ministry of Innovation, Science and Research of the State North Rhine-Westphalia, the Heinrich-Heine-University of Düsseldorf, and the Entrepreneur Foundation at the Heinrich-Heine-University of Düsseldorf. CM is supported by the Heinz Ansmann Foundation for AIDS Research. We thank Lutz Schmitt and Dieter Willbold for their continuous support.

Received April 30, 2013; accepted June 17, 2013; previously published online June 20, 2013

References

- Albin, J.S. and Harris, R.S. (2010). Interactions of host APOBEC3 restriction factors with HIV-1 *in vivo*: implications for therapeutics. *Expert. Rev. Mol. Med* 12, e4.
- Albin, J.S., LaRue, R.S., Weaver, J.A., Brown, W.L., Shindo, K., Harjes, E., Matsuo, H., and Harris, R.S. (2010). A single amino acid in human APOBEC3F alters susceptibility to HIV-1 Vif. *J. Biol. Chem.* 285, 40785–40792.

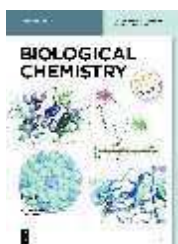
- Arias, J.F., Koyama, T., Kinomoto, M., and Tokunaga, K. (2012). Retroelements versus APOBEC3 family members: no great escape from the magnificent seven. *Front. Microbiol.* **3**, 275.
- Autore, F., Bergeron, J.R., Malim, M.H., Fraternali, F., and Huthoff, H. (2010). Rationalisation of the differences between APOBEC3G structures from crystallography and NMR studies by molecular dynamics simulations. *PLoS One.* **5**, e11515.
- Bennett, R.P., Salter, J.D., Liu, X., Wedekind, J.E., and Smith, H.C. (2008). APOBEC3G subunits self-associate via the C-terminal deaminase domain. *J. Biol. Chem.* **283**, 33329–33336.
- Bergeron, J.R., Huthoff, H., Veselkov, D.A., Beavil, R.L., Simpson, P.J., Matthews, S.J., Malim, M.H., and Sanderson, M.R. (2010). The SOCS-box of HIV-1 Vif interacts with ElonginBC by induced-folding to recruit its Cul5-containing ubiquitin ligase complex. *PLoS Pathog.* **6**, e1000925.
- Bohn, M.F., Shandilya, S.M., Albin, J.S., Kouno, T., Anderson, B.D., McDougle, R.M., Carpenter, M.A., Rathore, A., Evans, L., Davis, A.N., et al. (2013). Crystal structure of the DNA cytosine deaminase APOBEC3F: the catalytically active and HIV-1 Vif-binding domain. *Structure* **21**, 1042–1050.
- Bulliard, Y., Turelli, P., Rohrig, U.F., Zoete, V., Mangeat, B., Michielin, O., and Trono, D. (2009). Functional analysis and structural modeling of human APOBEC3G reveal the role of evolutionarily conserved elements in the inhibition of human immunodeficiency virus type 1 infection and Alu transposition. *J. Virol.* **83**, 12611–12621.
- Burnett, A. and Spearman, P. (2007). APOBEC3G multimers are recruited to the plasma membrane for packaging into human immunodeficiency virus type 1 virus-like particles in an RNA-dependent process requiring the NC basic linker. *J. Virol.* **81**, 5000–5013.
- Burns, M.B., Lackey, L., Carpenter, M.A., Rathore, A., Land, A.M., Leonard, B., Refsland, E.W., Kotandeniya, D., Tretyakova, N., Nikas, J.B., et al. (2013). APOBEC3B is an enzymatic source of mutation in breast cancer. *Nature* **494**, 366–370.
- Byeon, I.J., Ahn, J., Mitra, M., Byeon, C.H., Hercik, K., Hritz, J., Charlton, L.M., Levin, J.G., and Gronenborn, A.M. (2013). NMR structure of human restriction factor APOBEC3A reveals substrate binding and enzyme specificity. *Nat. Commun.* **4**, 1890.
- Chareza, S., Slavkovic, L.D., Liu, Y., Rathe, A.M., Münk, C., Zabogli, E., Pistello, M., and Löchelt, M. (2012). Molecular and functional interactions of cat APOBEC3 and feline foamy and immunodeficiency virus proteins: different ways to counteract host-encoded restriction. *Virology* **424**, 138–146.
- Chelico, L., Pham, P., Calabrese, P., and Goodman, M.F. (2006). APOBEC3G DNA deaminase acts processively 3'→5' on single-stranded DNA. *Nat. Struct. Mol. Biol.* **13**, 392–399.
- Chelico, L., Sacho, E.J., Erie, D.A., and Goodman, M.F. (2008). A model for oligomeric regulation of APOBEC3G cytosine deaminase-dependent restriction of HIV. *J. Biol. Chem.* **283**, 13780–13791.
- Chelico, L., Prochnow, C., Erie, D.A., Chen, X.S., and Goodman, M.F. (2010). Structural model for deoxycytidine deamination mechanisms of the HIV-1 inactivation enzyme APOBEC3G. *J. Biol. Chem.* **285**, 16195–16205.
- Chen, K.M., Harjes, E., Gross, P.J., Fahmy, A., Lu, Y., Shindo, K., Harris, R.S., and Matsuo, H. (2008). Structure of the DNA deaminase domain of the HIV-1 restriction factor APOBEC3G. *Nature* **452**, 116–119.
- Chiu, Y.L., Witkowska, H.E., Hall, S.C., Santiago, M., Soros, V.B., Esnault, C., Heidmann, T., and Greene, W.C. (2006). High-molecular-mass APOBEC3G complexes restrict Alu retrotransposition. *Proc. Natl. Acad. Sci. USA* **103**, 15588–15593.
- Coticello, S.G. (2008). The AID/APOBEC family of nucleic acid mutators. *Genome Biol.* **9**, 229.
- Derse, D., Hill, S.A., Princler, G., Lloyd, P., and Heidecker, G. (2007). Resistance of human T cell leukemia virus type 1 to APOBEC3G restriction is mediated by elements in nucleocapsid. *Proc. Natl. Acad. Sci. USA* **104**, 2915–2920.
- Feng, Y. and Chelico, L. (2011). Intensity of deoxycytidine deamination of HIV-1 proviral DNA by the retroviral restriction factor APOBEC3G is mediated by the noncatalytic domain. *J. Biol. Chem.* **286**, 11415–11426.
- Friew, Y.N., Boyko, V., Hu, W.S., and Pathak, V.K. (2009). Intracellular interactions between APOBEC3G, RNA, and HIV-1 Gag: APOBEC3G multimerization is dependent on its association with RNA. *Retrovirology* **6**, 56.
- Furukawa, A., Nagata, T., Matsugami, A., Habu, Y., Sugiyama, R., Hayashi, F., Kobayashi, N., Yokoyama, S., Takaku, H., and Katahira, M. (2009). Structure, interaction and real-time monitoring of the enzymatic reaction of wild-type APOBEC3G. *EMBO J.* **28**, 440–451.
- Gallois-Montbrun, S., Kramer, B., Swanson, C.M., Byers, H., Lynham, S., Ward, M., and Malim, M.H. (2007). Antiviral protein APOBEC3G localizes to ribonucleoprotein complexes found in P bodies and stress granules. *J. Virol.* **81**, 2165–2178.
- Gallois-Montbrun, S., Holmes, R.K., Swanson, C.M., Fernandez-Ocana, M., Byers, H.L., Ward, M.A., and Malim, M.H. (2008). Comparison of cellular ribonucleoprotein complexes associated with the APOBEC3F and APOBEC3G antiviral proteins. *J. Virol.* **82**, 5636–5642.
- Hache, G., Liddament, M.T., and Harris, R.S. (2005). The retroviral hypermutation specificity of APOBEC3F and APOBEC3G is governed by the C-terminal DNA cytosine deaminase domain. *J. Biol. Chem.* **280**, 10920–10924.
- Harjes, E., Gross, P.J., Chen, K.M., Lu, Y., Shindo, K., Nowarski, R., Gross, J.D., Kotler, M., Harris, R.S., and Matsuo, H. (2009). An extended structure of the APOBEC3G catalytic domain suggests a unique holoenzyme model. *J. Mol. Biol.* **389**, 819–832.
- Harris, R.S., Petersen-Mahrt, S.K., and Neuberger, M.S. (2002). RNA editing enzyme APOBEC1 and some of its homologs can act as DNA mutators. *Mol. Cell* **10**, 1247–1253.
- Holden, L.G., Prochnow, C., Chang, Y.P., Bransteitter, R., Chelico, L., Sen, U., Stevens, R.C., Goodman, M.F., and Chen, X.S. (2008). Crystal structure of the anti-viral APOBEC3G catalytic domain and functional implications. *Nature* **456**, 121–124.
- Huthoff, H., Autore, F., Gallois-Montbrun, S., Fraternali, F., and Malim, M.H. (2009). RNA-dependent oligomerization of APOBEC3G is required for restriction of HIV-1. *PLoS Pathog.* **5**, e1000330.
- Iwatani, Y., Takeuchi, H., Strebel, K., and Levin, J.G. (2006). Biochemical activities of highly purified, catalytically active human APOBEC3G: correlation with antiviral effect. *J. Virol.* **80**, 5992–6002.
- Jager, S., Kim, D.Y., Hultquist, J.F., Shindo, K., LaRue, R.S., Kwon, E., Li, M., Anderson, B.D., Yen, L., Stanley, D., et al. (2012). Vif hijacks CBF- β to degrade APOBEC3G and promote HIV-1 infection. *Nature* **481**, 371–375.

- Jaguva Vasudevan, A.A., Perkovic, M., Bulliard, Y., Cichutek, K., Trono, D., Haussinger, D., and Munk, C. (2013). Prototype foamy virus bet impairs the dimerization and cytosolic solubility of human APOBEC3G. *J. Virol.* 2013 Jun 12. [Epub ahead of print].
- Jarmuz, A., Chester, A., Bayliss, J., Gisbourne, J., Dunham, I., Scott, J., and Navaratnam, N. (2002). An anthropoid-specific locus of orphan C to U RNA-editing enzymes on chromosome 22. *Genomics* 79, 285–296.
- Kitamura, S., Ode, H., Nakashima, M., Imahashi, M., Naganawa, Y., Kurosawa, T., Yokomaku, Y., Yamane, T., Watanabe, N., Suzuki, A., et al. (2012). The APOBEC3C crystal structure and the interface for HIV-1 Vif binding. *Nat. Struct. Mol. Biol.* 19, 1005–1010.
- Kolokithas, A., Rosenke, K., Malik, F., Hendrick, D., Swanson, L., Santiago, M.L., Portis, J.L., Hasenkrug, K.J., and Evans, L.H. (2010). The glycosylated Gag protein of a murine leukemia virus inhibits the antiretroviral function of APOBEC3. *J. Virol.* 84, 10933–10936.
- Kozak, S.L., Marin, M., Rose, K.M., Bystrom, C., and Kabat, D. (2006). The anti-HIV-1 editing enzyme APOBEC3G binds HIV-1 RNA and messenger RNAs that shuttle between polysomes and stress granules. *J. Biol. Chem.* 281, 29105–29119.
- Kreisberg, J.F., Yonemoto, W., and Greene, W.C. (2006). Endogenous factors enhance HIV infection of tissue naive CD4 T cells by stimulating high molecular mass APOBEC3G complex formation. *J. Exp. Med.* 203, 865–870.
- Krissinel, E. and Henrick, K. (2007). Inference of macromolecular assemblies from crystalline state. *J. Mol. Biol.* 372, 774–797.
- LaRue, R.S., Jonsson, S.R., Silverstein, K.A., Lajoie, M., Bertrand, D., El-Mabrouk, N., Hotzel, I., Andresdottir, V., Smith, T.P., and Harris, R.S. (2008). The artiodactyl APOBEC3 innate immune repertoire shows evidence for a multi-functional domain organization that existed in the ancestor of placental mammals. *Mol. Biol.* 9, 104.
- LaRue, R.S., Andresdottir, V., Blanchard, Y., Conticello, S.G., Derse, D., Eberman, M., Greene, W.C., Jonsson, S.R., Landau, N.R., Löchelt, M., et al. (2009). Guidelines for naming nonprimate APOBEC3 genes and proteins. *J. Virol.* 83, 494–497.
- Li, M., Shandilya, S.M., Carpenter, M.A., Rathore, A., Brown, W.L., Perkins, A.L., Harki, D.A., Solberg, J., Hook, D.J., Pandey, K.K., et al. (2012). First-in-class small molecule inhibitors of the single-strand DNA cytosine deaminase APOBEC3G. *ACS Chem. Biol.* 7, 506–517.
- Löchelt, M., Romen, F., Bastone, P., Muckenfuss, H., Kirchner, N., Kim, Y.B., Truyen, U., Rosler, U., Battenberg, M., Saib, A., et al. (2005). The antiretroviral activity of APOBEC3 is inhibited by the foamy virus accessory Bet protein. *Proc. Natl. Acad. Sci. USA* 102, 7982–7987.
- Mariani, R., Chen, D., Schröfelbauer, B., Navarro, F., König, R., Bollman, B., Münk, C., Nymark-McMahon, H., and Landau, N.R. (2003). Species-specific exclusion of APOBEC3G from HIV-1 virions by Vif. *Cell* 114, 21–31.
- Marin, M., Rose, K.M., Kozak, S.L., and Kabat, D. (2003). HIV-1 Vif protein binds the editing enzyme APOBEC3G and induces its degradation. *Nat. Med.* 9, 1398–1403.
- Mehle, A., Goncalves, J., Santa-Marta, M., McPike, M., and Gabuzda, D. (2004). Phosphorylation of a novel SOCS-box regulates assembly of the HIV-1 Vif-Cul5 complex that promotes APOBEC3G degradation. *Genes Dev.* 18, 2861–2866.
- Münk, C., Beck, T., Zielonka, J., Hotz-Wagenblatt, A., Chareza, S., Battenberg, M., Thielebein, J., Cichutek, K., Bravo, I.G., O'Brien, S.J., et al. (2008). Functions, structure, and read-through alternative splicing of feline APOBEC3 genes. *Genome Biol.* 9, R48.
- Münk, C., Jensen, B.E., Zielonka, J., Häussinger, D., and Kamp, C. (2012a). Running loose or getting lost: how HIV-1 counters and capitalizes on APOBEC3-induced mutagenesis through its Vif protein. *Viruses* 4, 3132–3161.
- Münk, C., Willemsen, A., and Bravo, I.G. (2012b). An ancient history of gene duplications, fusions and losses in the evolution of APOBEC3 mutators in mammals. *BMC. Evol. Biol.* 12, 71.
- Navarro, F., Bollman, B., Chen, H., König, R., Yu, Q., Chiles, K., and Landau, N.R. (2005). Complementary function of the two catalytic domains of APOBEC3G. *Virology* 333, 374–386.
- Niewiadomska, A.M., Tian, C., Tan, L., Wang, T., Sarkis, P.T., and Yu, X.F. (2007). Differential inhibition of long interspersed element 1 by APOBEC3 does not correlate with high-molecular-mass-complex formation or P-body association. *J. Virol.* 81, 9577–9583.
- Nik-Zainal, S., Alexandrov, L.B., Wedge, D.C., Van, L.P., Greenman, C.D., Raine, K., Jones, D., Hinton, J., Marshall, J., Stebbings, L.A., et al. (2012). Mutational processes molding the genomes of 21 breast cancers. *Cell* 149, 979–993.
- Nowarski, R. and Kotler, M. (2013). APOBEC3 cytidine deaminases in double-strand DNA break repair and cancer promotion. *Cancer Res.* 73, 3494–3498.
- Nowarski, R., Britan-Rosich, E., Shiloach, T., and Kotler, M. (2008). Hypermutation by intersegmental transfer of APOBEC3G cytidine deaminase. *Nat. Struct. Mol. Biol.* 15, 1059–1066.
- Ooms, M., Krikoni, A., Kress, A.K., Simon, V., and Münk, C. (2012). APOBEC3A, APOBEC3B, and APOBEC3H haplotype 2 restrict human T-lymphotropic virus type 1. *J. Virol.* 86, 6097–6108.
- Perkovic, M., Schmidt, S., Marino, D., Russell, R.A., Stauch, B., Hofmann, H., Kopietz, F., Kloke, B.P., Zielonka, J., Strover, H., et al. (2009). Species-specific inhibition of APOBEC3C by the prototype foamy virus protein bet. *J. Biol. Chem.* 284, 5819–5826.
- Prochnow, C., Bransteitter, R., Klein, M.G., Goodman, M.F., and Chen, X.S. (2007). The APOBEC-2 crystal structure and functional implications for the deaminase AID. *Nature* 445, 447–451.
- Rausch, J.W., Chelico, L., Goodman, M.F., and Le Grice, S.F. (2009). Dissecting APOBEC3G substrate specificity by nucleoside analog interference. *J. Biol. Chem.* 284, 7047–7058.
- Roberts, S.A., Sterling, J., Thompson, C., Harris, S., Mav, D., Shah, R., Klimczak, L.J., Kryukov, G.V., Malc, E., Mieczkowski, P.A., et al. (2012). Clustered mutations in yeast and in human cancers can arise from damaged long single-strand DNA regions. *Mol. Cell* 46, 424–435.
- Russell, R.A., Wiegand, H.L., Moore, M.D., Schafer, A., McClure, M.O., and Cullen, B.R. (2005). Foamy virus Bet proteins function as novel inhibitors of the APOBEC3 family of innate antiretroviral defense factors. *J. Virol.* 79, 8724–8731.
- Salter, J.D., Krucinska, J., Raina, J., Smith, H.C., and Wedekind, J.E. (2009). A hydrodynamic analysis of APOBEC3G reveals a monomer-dimer-tetramer self-association that has implications for anti-HIV function. *Biochemistry* 48, 10685–10687.

- Schumacher, A.J., Hache, G., MacDuff, D.A., Brown, W.L., and Harris, R.S. (2008). The DNA deaminase activity of human APOBEC3G is required for Ty1, MusD, and human immunodeficiency virus type 1 restriction. *J. Virol.* **82**, 2652–2660.
- Shandilya, S.M., Nalam, M.N., Nalivaika, E.A., Gross, P.J., Valesano, J.C., Shindo, K., Li, M., Munson, M., Royer, W.E., Harjes, E., et al. (2010). Crystal structure of the APOBEC3G catalytic domain reveals potential oligomerization interfaces. *Structure* **18**, 28–38.
- Sheehy, A.M., Gaddis, N.C., Choi, J.D., and Malim, M.H. (2002). Isolation of a human gene that inhibits HIV-1 infection and is suppressed by the viral Vif protein. *Nature* **418**, 646–650.
- Sheehy, A.M., Gaddis, N.C., and Malim, M.H. (2003). The antiretroviral enzyme APOBEC3G is degraded by the proteasome in response to HIV-1 Vif. *Nat. Med.* **9**, 1404–1407.
- Shlyakhtenko, L.S., Lushnikov, A.Y., Li, M., Lackey, L., Harris, R.S., and Lyubchenko, Y.L. (2011). Atomic force microscopy studies provide direct evidence for dimerization of the HIV restriction factor APOBEC3G. *J. Biol. Chem.* **286**, 3387–3395.
- Shlyakhtenko, L.S., Lushnikov, A.Y., Miyagi, A., Li, M., Harris, R.S., and Lyubchenko, Y.L. (2012). Nanoscale structure and dynamics of APOBEC3G complexes with single-stranded DNA. *Biochemistry* **51**, 6432–6440.
- Smith, J.L. and Pathak, V.K. (2010). Identification of specific determinants of human APOBEC3F, APOBEC3C, and APOBEC3DE and African green monkey APOBEC3F that interact with HIV-1 Vif. *J. Virol.* **84**, 12599–12608.
- Song, C., Sutton, L., Johnson, M.E., D'Aquila, R.T., and Donahue, J.P. (2012). Signals in APOBEC3F N-terminal and C-terminal deaminase domains each contribute to encapsidation in HIV-1 virions and are both required for HIV-1 restriction. *J. Biol. Chem.* **287**, 16965–16974.
- Soros, V.B., Yonemoto, W., and Greene, W.C. (2007). Newly synthesized APOBEC3G is incorporated into HIV virions, inhibited by HIV RNA, and subsequently activated by RNase H. *PLoS Pathog.* **3**, e15.
- Stauch, B., Hofmann, H., Perkovic, M., Weisel, M., Kopietz, F., Cichutek, K., Münk, C., and Schneider, G. (2009). Model structure of APOBEC3C reveals a binding pocket modulating ribonucleic acid interaction required for encapsidation. *Proc. Natl. Acad. Sci. USA* **106**, 12079–12084.
- Stavrou, S., Nitta, T., Kotla, S., Ha, D., Nagashima, K., Rein, A.R., Fan, H., and Ross, S.R. (2013). Murine leukemia virus glycosylated Gag blocks apolipoprotein B editing complex 3 and cytosolic sensor access to the reverse transcription complex. *Proc. Natl. Acad. Sci. USA* **110**, 9078–9083. doi: 10.1073/pnas.1217399110. [Epub 2013 May 13].
- Strebel, K. and Khan, M.A. (2008). APOBEC3G encapsidation into HIV-1 virions: which RNA is it? *Retrovirology* **5**, 55.
- Taylor, B.J., Nik-Zainal, S., Wu, Y.L., Stebbings, L.A., Raine, K., Campbell, P.J., Rada, C., Stratton, M.R., and Neuberger, M.S. (2013). DNA deaminases induce break-associated mutation showers with implication of APOBEC3B and 3A in breast cancer kataegis. *Elife* **2**, e00534.
- Teh, A.H., Kimura, M., Yamamoto, M., Tanaka, N., Yamaguchi, I., and Kumasaka, T. (2006). The 1.48 Å resolution crystal structure of the homotetrameric cytidine deaminase from mouse. *Biochemistry* **45**, 7825–7833.
- Wang, T., Zhang, W., Tian, C., Liu, B., Yu, Y., Ding, L., Spearman, P., and Yu, X.F. (2008). Distinct viral determinants for the packaging of human cytidine deaminases APOBEC3G and APOBEC3C. *Virology* **377**, 71–79.
- Wedekind, J.E., Gillilan, R., Janda, A., Krucinska, J., Salter, J.D., Bennett, R.P., Raina, J., and Smith, H.C. (2006). Nanostructures of APOBEC3G support a hierarchical assembly model of high molecular mass ribonucleoprotein particles from dimeric subunits. *J. Biol. Chem.* **281**, 38122–38126.
- Wissing, S., Galloway, N.L., and Greene, W.C. (2010). HIV-1 Vif versus the APOBEC3 cytidine deaminases: an intracellular duel between pathogen and host restriction factors. *Mol. Aspects Med.* **31**, 383–397.
- Xiang, S., Short, S.A., Wolfenden, R., and Carter, C.W., Jr. (1997). The structure of the cytidine deaminase-product complex provides evidence for efficient proton transfer and ground-state destabilization. *Biochemistry* **36**, 4768–4774.
- Yu, X., Yu, Y., Liu, B., Luo, K., Kong, W., Mao, P., and Yu, X.F. (2003). Induction of APOBEC3G ubiquitination and degradation by an HIV-1 Vif-Cul5-SCF complex. *Science* **302**, 1056–1060.
- Yu, Y., Xiao, Z., Ehrlich, E.S., Yu, X., and Yu, X.F. (2004). Selective assembly of HIV-1 Vif-Cul5-ElonginB-ElonginC E3 ubiquitin ligase complex through a novel SOCS box and upstream cysteines. *Genes Dev.* **18**, 2867–2872.
- Zhang, K.L., Mangeat, B., Ortiz, M., Zoete, V., Trono, D., Telenti, A., and Michielin, O. (2007). Model structure of human APOBEC3G. *PLoS One.* **2**, e378.
- Zhang, W., Du, J., Evans, S.L., Yu, Y., and Yu, X.F. (2012). T-cell differentiation factor CBF- β regulates HIV-1 Vif-mediated evasion of host restriction. *Nature* **481**, 376–379.



RightsLink®

[Account Info](#)
[Help](#)


Title: Structural features of antiviral DNA cytidine deaminases

Author: Ananda Ayyappan Jaguva Vasudevan, Sander H.J. Smits, Astrid Höppner, et al.

Publication: Biological Chemistry

Publisher: De Gruyter

Date: Jun 20, 2013

Copyright © 2013, Walter de Gruyter GmbH

Logged in as:

Ananda Ayyappan Jaguva Vasudevan

Account #:
3000710859

[LOGOUT](#)

Order Completed

Thank you for your order.

This Agreement between Ananda Ayyappan Jaguva Vasudevan ("You") and De Gruyter ("De Gruyter") consists of your order details and the terms and conditions provided by De Gruyter and Copyright Clearance Center.

License number	Reference confirmation email for license number
License date	May, 12 2017
Licensed Content Publisher	De Gruyter
Licensed Content Publication	Biological Chemistry
Licensed Content Title	Structural features of antiviral DNA cytidine deaminases
Licensed Content Author	Ananda Ayyappan Jaguva Vasudevan, Sander H.J. Smits, Astrid Höppner, et al.
Licensed Content Date	Jun 20, 2013
Licensed Content Volume	394
Licensed Content Issue	11
Type of use	Thesis/Dissertation
Requestor type	Author of requested content
Format	Print, Electronic
Portion	chapter/article
Page range of chapter/article	1
Number of pages in chapter/article	1
Rights for	Main product
Duration of use	Life of current edition
Creation of copies for the disabled	no
With minor editing privileges	no
For distribution to	Worldwide
In the following language(s)	Original language of publication
With incidental promotional use	no
Lifetime unit quantity of new product	0 to 499
The requesting person/organization	Ananda Ayyappan Jaguva Vasudevan, Heinrich Heine University
Order reference number	
Title of your thesis / dissertation	"Dazzling APOBEC3 DNA deaminases: A mechanistic study on how A3A, A3C and A3G act on retroviruses and being counteracted by their foe"
Expected completion date	Dec 2017

Expected size (number of pages) 140

Publisher VAT

Requestor Location Ananda Ayyappan Jaguva Vasudevan
Universitätstr.1
AG Münk
Building: 23.12.U1.85
Duesseldorf, NRW 40225
Germany
Attn: Ananda Ayyappan Jaguva Vasudevan

Billing Type Invoice

Billing address Ananda Ayyappan Jaguva Vasudevan
Universitätstr.1
AG Münk
Building: 23.12.U1.85
Duesseldorf, Germany 40225
Attn: Ananda Ayyappan Jaguva Vasudevan

Total 0.00 EUR

CLOSE WINDOW

Copyright © 2017 [Copyright Clearance Center, Inc.](#) All Rights Reserved. [Privacy statement.](#) [Terms and Conditions.](#)
Comments? We would like to hear from you. E-mail us at customercare@copyright.com

Chapter II

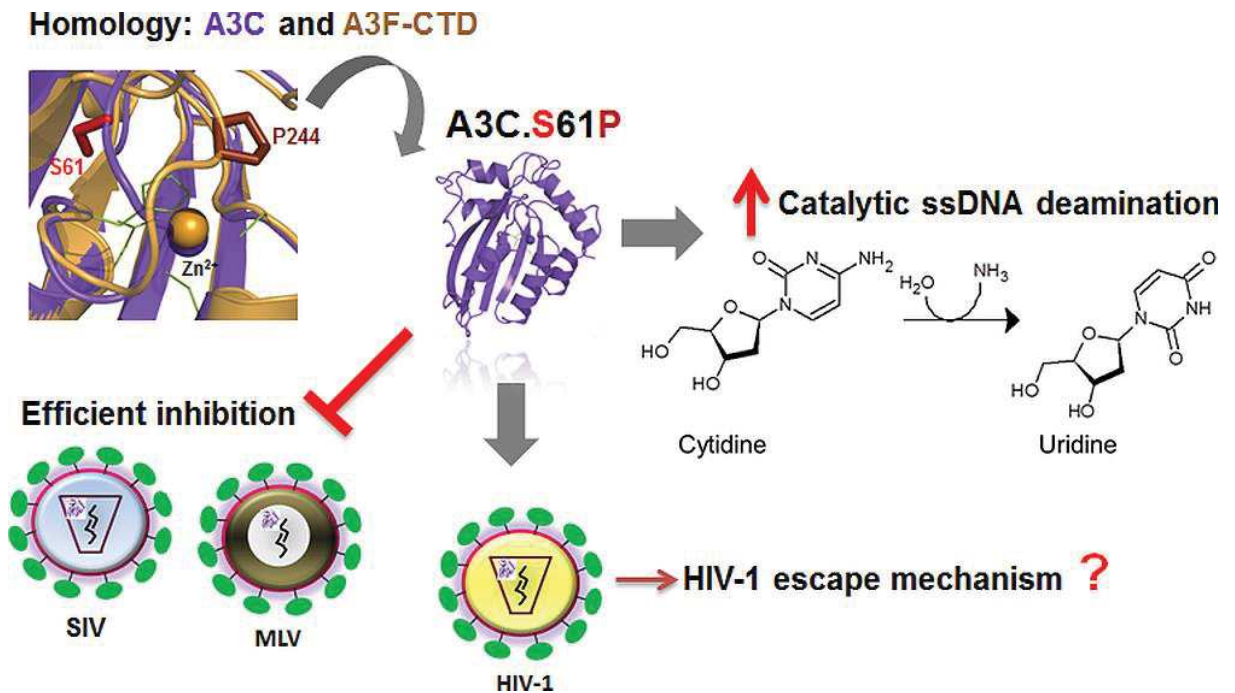
Enhancing the Catalytic Deamination Activity of APOBEC3C Is Insufficient to Inhibit Vif-Deficient HIV-1

Journal : **Journal of Molecular Biology** (published in 2017)

Own contribution to this work:

- Complete execution of experimental procedures
- Writing of the manuscript

Graphical abstract



Highlights

- Enzymatic and antiviral functions of A3C are not well studied
- This study highlights the deamination-dependent antiviral function of A3C using three viral systems
- This study identifies that S61P mutation in A3C can boost antiviral and catalytic activity
- This study confirms the preferential “deamination hotspots” of A3C, A3G and A3F in viral DNA
- Lack of the anti-HIV-1 activity of A3C.S61P indicating an unknown viral escape mechanism



Enhancing the Catalytic Deamination Activity of APOBEC3C Is Insufficient to Inhibit Vif-Deficient HIV-1

Ananda Ayyappan Jaguva Vasudevan¹, Henning Hofmann^{1,†}, Dieter Willbold^{2,3}, Dieter Häussinger¹, Bernd W. Koenig^{2,3} and Carsten Münk¹

1 - Clinic for Gastroenterology, Hepatology, and Infectiology, Medical Faculty, Heinrich-Heine-University Düsseldorf, Moorenstr. 5, 40225 Düsseldorf, Germany

2 - Institute of Complex Systems, Structural Biochemistry (ICS-6), Forschungszentrum Jülich, 52425 Jülich, Germany

3 - Institut für Physikalische Biologie, Heinrich-Heine-University Düsseldorf, Universitätsstr. 1, 40225 Düsseldorf, Germany

Correspondence to Carsten Münk: Clinic for Gastroenterology, Hepatology, and Infectiology, Medical Faculty, Heinrich-Heine-University Düsseldorf, Building 23.12.U1.82, Moorenstr. 5, 40225 Düsseldorf, Germany.

carsten.muenk@med.uni-duesseldorf.de

<http://dx.doi.org/10.1016/j.jmb.2017.03.015>

Edited by Eric O. Freed

Abstract

The retroviral restriction factors of the APOBEC3 (A3) cytidine deaminase family catalyze the deamination of cytidines in single-stranded viral DNA. APOBEC3C (A3C) is a strong antiviral factor against viral infectivity factor (*vif*)-deficient simian immunodeficiency virus Δvif , which is, however, a weak inhibitor against human immunodeficiency virus (HIV)-1 for reasons unknown. The precise link between the antiretroviral effect of A3C and its catalytic activity is incompletely understood. Here, we show that the S61P mutation in human A3C (A3C.S61P) boosted hypermutation in the viral genomes of simian immunodeficiency virus Δvif and murine leukemia virus but not in human immunodeficiency virus HIV-1 Δvif . The enhanced antiviral activity of A3C.S61P correlated with enhanced *in vitro* cytidine deamination. Furthermore, the S61P mutation did not change the substrate specificity of A3C, ribonucleoprotein complex formation, self-association, Zinc coordination, or viral incorporation features. We propose that local structural changes induced by the serine-to-proline substitution are responsible for the gain of catalytic activity of A3C.S61P. Our results are a first step toward an understanding of A3C's DNA binding capacity, deamination-dependent editing, and antiviral functions at the molecular level. We conclude that the enhanced enzymatic activity of A3C is insufficient to restrict HIV-1, indicating an unknown escape mechanism of HIV-1.

© 2017 Elsevier Ltd. All rights reserved.

Introduction

The APOBEC3 (A3) family of cytidine deaminases builds an intrinsic immune barrier against retroviruses, retrotransposons, and other viral pathogens [1–3], and recently, members of A3 were implicated in genome-wide mutation events associated with cancers [4–6] (for a review, see Ref. [7]). Humans have seven A3s (A3A–A3D, A3F–A3H). A3G, which exhibits anti HIV-1 activity, is the best-studied enzyme [8–10], and a second HIV-1 restriction factor, A3F, also displayed potent antiviral activity [11–15].

A3 enzymes mutate retroviral single-stranded DNA (ssDNA) by catalyzing the deamination of dC

residues into dU. During viral assembly, A3 proteins are incorporated into progeny virions bound to viral RNA and structural proteins [16–23] and exert an antiviral effect upon subsequent infection by causing mutations in the newly reverse transcribed viral minus strand ssDNA [2]. The dC-to-dU base modification in the minus strand DNA results in dA instead of dG in plus strands, leading to coding changes and premature stop codons in the viral genome, which abort viral replication [24–26]. Additionally, deamination-independent modes may restrict the virus, for example, by inhibiting reverse transcription or interfering with integration [27–33]. As a countermeasure, lentiviruses developed the viral infectivity factor (Vif) protein that binds A3s to

target them for polyubiquitination and proteasomal degradation [34–36], thereby preventing the incorporation of A3s into budding virions. These A3–Vif interactions are often species-specific [14,37–40].

A characteristic of mammalian A3 deaminases is the presence of either one or two conserved zinc-binding (Z) domains, in which Zn^{2+} is coordinated by a Z signature (H-X-E- X_{24-31} C- X_{2-4} C, where X can be any amino acid) motif, and these domains are further classified into Z1, Z2, and Z3 domains [41–44]. A3A (Z1), A3C (Z2), and A3H (Z3) contain a single Z domain, whereas A3B (Z2-Z1), A3D (Z2-Z2), A3F (Z2-Z2), and A3G (Z2-Z1) are double Z domain proteins. All seven human A3 genes are encoded on chromosome 22, and it was speculated that duplications of single-domain genes led to the evolution of the double domain A3s [42,44]. A3C shares a high primary sequence identity of 77.4% with the C-terminal part of A3F (termed, A3F-C-terminal domain (CTD)). Of note, both A3C and A3F-CTD proteins possess the DNA deaminase catalytic function and the HIV-1 Vif binding region [14,45–48].

A3C was reported to have antiviral activity against simian immunodeficiency virus (SIV) from the African green monkey (agm), hepatitis B virus, herpes simplex virus, certain human papillomaviruses, murine leukemia virus (MLV), and HIV-1 [37,47,49–54], but there are several contradictory findings regarding its viral packaging and deamination activity [55–59]. A3C is ubiquitously expressed in lymphoid cells [60–62]. Its mRNA expression level can be stimulated by HIV-1 infection [55,57], and it was found to be significantly elevated in HIV-1 elite controllers [63]. However, A3C has no strong antiviral activity against HIV-1 lacking *vif* gene (HIV-1 Δ *vif*) [9,52,55]. The moderate deamination activity of A3C on HIV-1 genomes was linked with the evolution of viral diversity rather than viral restriction [60]. Interestingly, the capacity of HIV-1 Vif to induce degradation of A3C is conserved in the majority of HIV-1 subtypes [64].

The structure of A3C, with putative DNA substrate binding pockets, was reported [46,47]. However, the biochemical aspects of A3C catalytic activity and their relevance for antiviral activity are not well explored [65]. The goal of this study was to understand the antiviral function and catalytic activity of A3C using three different viral systems. Here, we identified a single amino acid change (S61P) that increased A3C's antiviral function solely due to the enhancement of catalytic activity. We further report that the S61P substitution in A3C did not affect A3C's viral encapsidation, dimerization, nucleic acid binding, and target motif for cytosine deamination. Compared to the restriction of SIV Δ *vif* and MLV, HIV-1 Δ *vif* was found to be rather resistant to this A3C mutant, suggesting an elusive escape mechanism of HIV-1 Δ *vif*.

Results

Viral restriction capacity of encapsidated A3C in HIV-1 Δ *vif*, SIV Δ *vif*, and MLV

To determine the antiviral activity of human A3C (hA3C), we produced luciferase reporter viruses of HIV-1 Δ *vif*, SIVagm Δ *vif*, and MLV in the presence or absence of A3C, pseudotyped with the glycoprotein of vesicular stomatitis virus (VSV-G), and tested their infectivity. Figure 1a shows that hA3C inhibited SIV replication by about 2 orders of magnitude. In contrast, infectivity of MLV and HIV-1 Δ *vif* virions produced in the presence of A3C was only reduced to 58% and 62%, respectively, confirming the results of other studies [9,52,55]. A3C was incorporated to similar extent into all tested viruses; thus, differential encapsidation of A3C into the viral particles cannot explain the differences in antiviral activity (Fig. 1b and c).

We then compared the impact of A3C orthologs on HIV-1 infectivity. We produced HIV-1 Δ *vif* particles with A3C from chimpanzees, agm, and cat A3Z2b and with human A3F full-length or A3F-CTD (residues 184–373). Human, chimpanzee, and agm A3C proteins similarly reduced the relative infectivity of HIV-1 Δ *vif* to 60%, whereas feline A3Z2b did not inhibit HIV-1 Δ *vif* (Fig. 2a). The full-length A3F inhibited HIV-1 Δ *vif* by nearly 2 orders of magnitude relative to the control, whereas A3F-CTD resulted in weak inhibition (Fig. 2a). In contrast to A3Cs and full-length A3F, A3F-CTD expression was low, and the packaging of A3F-CTD into HIV-1 Δ *vif* was below the detection limit in our immunoblots (Fig. 2b). To possibly enhance the expression of A3F-CTD, the conserved N-terminal amino acids of A3C ¹MNPQI were inserted in A3F-CTD to replace ¹⁸⁴LKEIL. However, this variant also failed to form detectable levels of protein (data not shown), and hence, we used full-length A3F throughout this study.

Comparison of A3C and A3F-CTD structures

Because of its only moderate anti HIV-1 activity, deamination by A3C has not been extensively characterized [9,24,55]. To address why A3C is not very catalytically active [55], we compared the sequence and the three-dimensional structure of prototype Z2-domain protein A3C with those of the catalytically active C-terminal domain of the Z2-Z2 domain protein, A3F-CTD (Fig. 3a). The X-ray structures of hA3C and catalytic A3F-CTD were recently solved [46,66–68]. Superimposition of the structures of A3C (PDB ID: **3VOW**) and A3F-CTD (PDB ID: **4J4J**) exhibits a C α rmsd of 0.794 Å, and the overall canonical DNA cytosine deaminase fold is intact (Fig. 3b). Given the critical roles of conserved residues in preserving the conformation

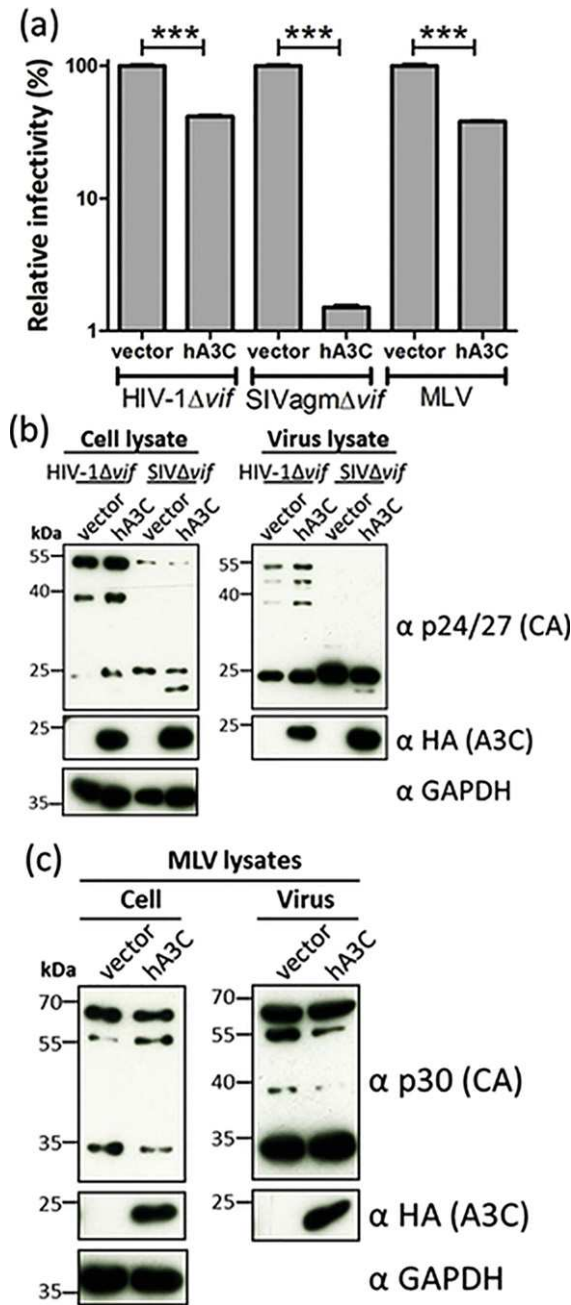


Fig. 1. Effects of encapsidated A3C on the infectivity of HIV-1Δvif, SIVΔvif, and MLV. (a) HIV-1Δvif, SIVΔvif, and MLV reporter viruses were produced in the presence and absence of hA3C. Infectivities of (RT normalized) equal amounts of viruses, relative to the virus lacking A3C, were determined by quantification of luciferase activity in 293T cells. Values are means \pm standard deviations (error bars) for three independent experiments. Unpaired *t*-tests were computed to determine whether the differences between vector and each A3 protein reach the level of statistical significance. Asterisks represent statistically significant differences: ***, $p < 0.0001$. (b) Immunoblot shows the amount A3C in cell and the viral lysates of HIV, SIV, and (c) MLV. HIV and SIV capsids (anti-p24/27), MLV capsid (anti-p30), and A3C (anti-HA) were detected with respective antibodies, and GAPDH served as a loading control. "α" represent anti-antibody.

of the catalytic center and its DNA binding properties [46,48,69–71], amino acids located close to the Zn^{2+} -coordinating motif were selected for mutagenesis to possibly impact deamination activity. The amino acid sequence regions of A3C and A3F-CTD depicted in Fig. 3a differ in four positions only (a total number of 38 differing residues present in full-length A3C compared to A3F-CTD). We replaced the two variable amino acids of A3C located most closely to the Zn^{2+} -coordinating motif with the ones found in A3F-CTD (Fig. 3a, arrow mark). Thus, in A3C, aspartate 99 in helix $\alpha 3$ was mutated to glutamate (D99E), and serine 61 in the flexible loop 3 was converted to proline (S61P). In addition, a double point mutant of A3C carrying both S61P and D99E was generated.

S61P mutation in human A3C (A3C.S61P) shows increased antiviral activity

We first tested the antiviral effect of the three A3C mutants against HIV-1Δvif, SIVΔvif, and MLV generated in the presence or absence of A3s, respectively. Compared to wild-type (WT) A3C, the D99E mutant showed slightly reduced antiviral activity against all tested viruses (Fig. 4a). In contrast, the proline mutation S61P of A3C reduced the relative infectivity of HIV, SIV, and MLV by a factor of 2, 4, and 2.5, respectively. The double mutant A3C.DS-EP showed an activity lower than that of A3C.S61P but stronger than that of WT A3C (Fig. 4a).

We next determined if the amino acid change(s) in A3C resulted in modified expression, cytosolic solubility, or viral packaging of A3C in transfected 293T cells. The amount of A3C variants in cell lysates and viral particles was determined by immunoblotting. Expression and viral packaging of WT and mutant A3C were found to be very similar in all three virus systems (Fig. 4b and c). Furthermore, A3C and A3C.S61P exhibited viral core localization in HIV-1Δvif, SIVΔvif, and MLV (Supplementary Fig. S1). To explore the role of proline 61, we constructed an alanine mutant, A3C.S61A, and compared the antiviral effects of A3C.S61A, A3C.S61P, and WT A3C. Only A3C.S61P inhibited all tested viruses effectively in a dose-dependent manner; A3C.S61A restriction was similar to or less efficient than WT A3C (Supplementary Figs. S2a and S2b). Additionally, a catalytically inactive A3C mutant A3C.C97S [47] was tested for anti HIV-1 and SIV activity in a dose-titration experiment. A3C.C97S caused no inhibition of HIV-1Δvif and a very mild inhibition of SIVΔvif at the highest transfected plasmid concentration, which suggests the involvement of an active site Zn^{2+} -coordinating residue (cysteine 97) in antiviral activity (Supplementary Fig. S2a). These observations posed the question of why the proline mutant A3C.S61P showed stronger antiviral activity than WT A3C.

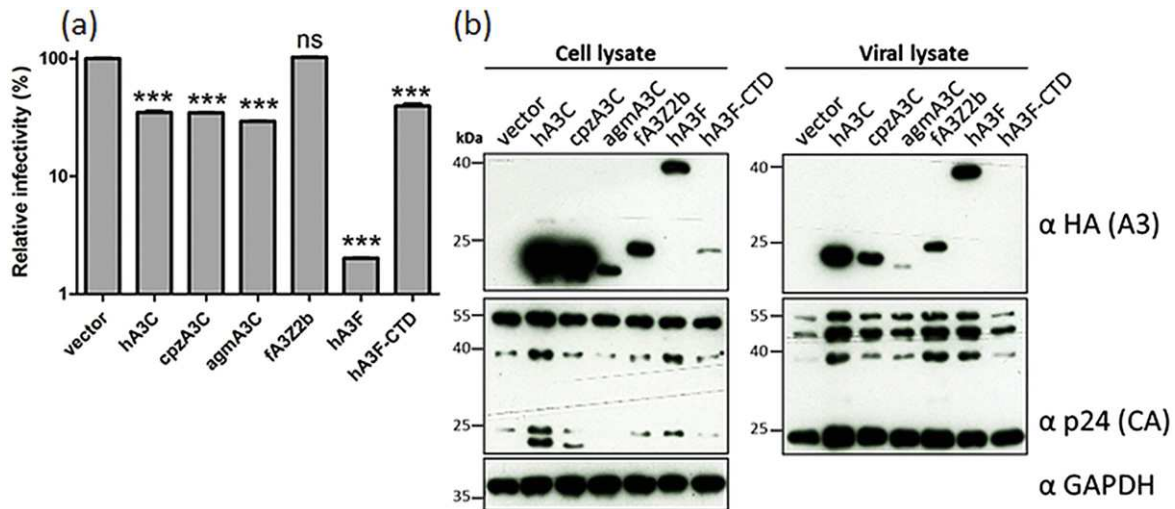


Fig. 2. Anti HIV-1 activity of A3C orthologs. (a) HIV-1 Δ vif particles were produced with A3C from human, chimpanzees (cpz), African green monkey (agm), cat A3Z2b, human A3F, and A3F-CTD (residues 184–373). Infectivities of (RT normalized) equal amounts of viruses, relative to the virus lacking A3C, were determined by the quantification of luciferase activity in 293T cells. Values are means \pm standard deviations (error bars) for three independent experiments. Unpaired *t*-tests were computed to determine whether differences between vector and each A3 protein reach the level of statistical significance. Asterisks represent statistically significant differences: ***, $p < 0.0001$; ns, not significant. (b) Amount of proteins in the cell lysate and A3 viral encapsidation were determined by immunoblotting. A3s and HIV-1 capsids were stained with anti-HA and anti-p24 antibodies, respectively. GAPDH served as a loading control. “ α ” represents anti-antibody.

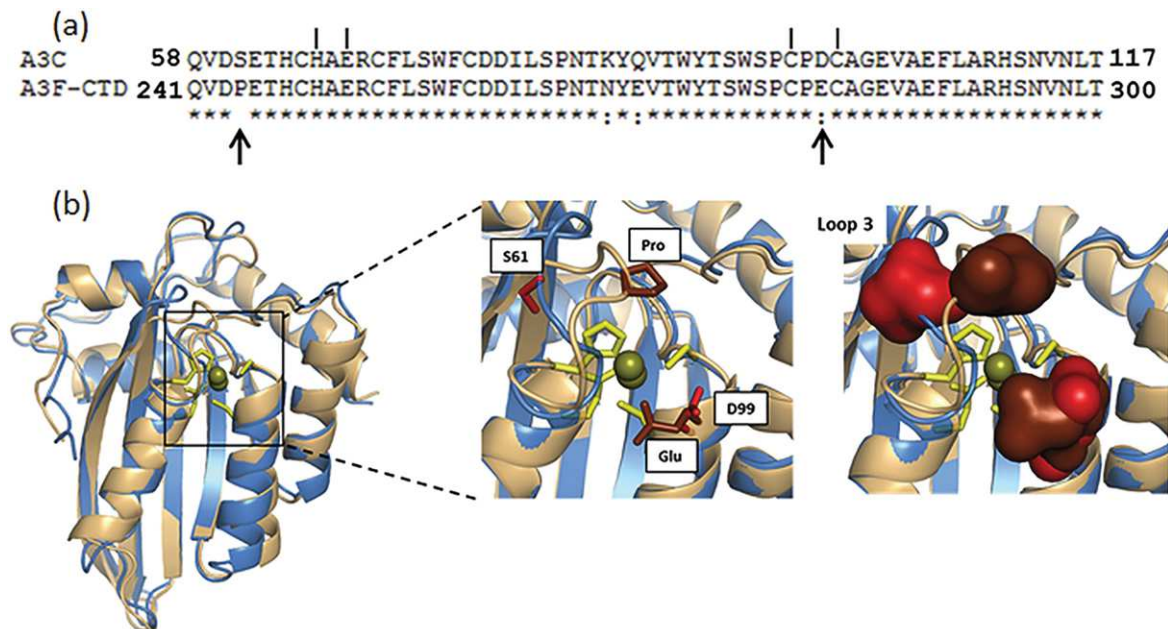


Fig. 3. Sequence and structure homology of A3C and A3F-CTD. (a) Sequence alignment of A3C and A3F-CTD amino acids spanning the active center. The vertical lines above the sequences indicate the Zn^{2+} -coordinating residues involved in catalytic activity, and the bottom arrow specifies the variable amino acids that were taken into account for this study. (b) Superimposition of A3C crystal structure (PDB 3VOW; blue) and A3F-CTD crystal structure (PDB 4J4J; pale orange) was made using Pymol software and shown in cartoon. Residues in A3C, D99 (helix α), S61 (loop 3), and its equivalent residues in A3F, E282 and P244 are displayed in sticks and surface model. Zinc atoms are represented as sphere.

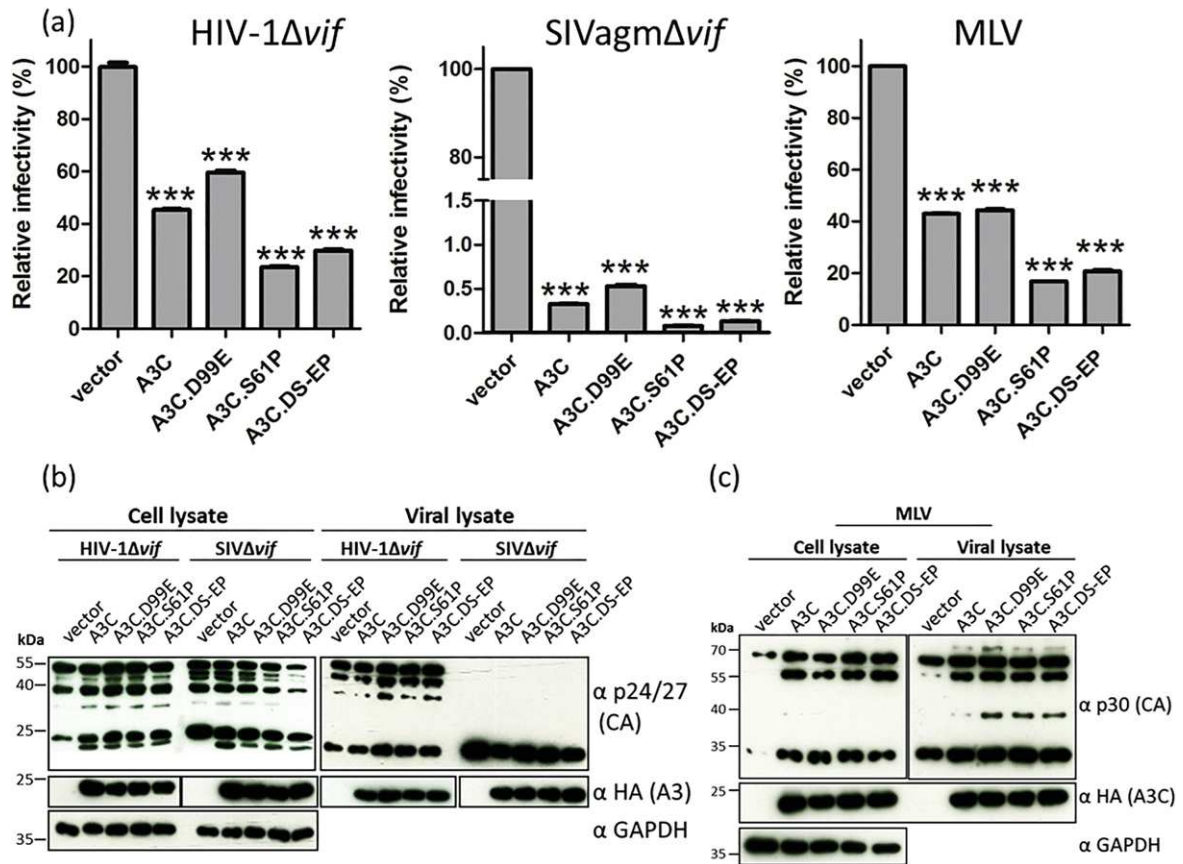


Fig. 4. A3C.S61P but not D99E mutant gained antiretroviral activity. (a) HIV-1Δvif, SIVagmΔvif, and MLV reporter viruses were produced in the presence of vector only, A3C, A3C.D99E, A3C.S61P, and double mutant A3C.DS-EP. Infectivities of (RT normalized) equal amounts of viruses, relative to the virus lacking A3C, were determined by quantification of luciferase activity in 293T cells. Please note that the break in the y-axis of SIVagmΔvif graph was made for presentation purpose. Values are means ± standard deviations (error bars) for three independent experiments. Unpaired *t*-tests were computed to determine whether differences between vector and each A3 protein reach the level of statistical significance. Asterisks represent statistically significant differences: ***, *p* < 0.0001. (b) Immunoblot shows the amount A3C in cell and viral lysates of HIV-1Δvif, SIVΔvif, and (c) MLV. HIV and SIV capsids (anti-p24/27), MLV capsid (anti-p30), and A3C (anti-HA) were detected with respective antibodies, and GAPDH served as a loading control. “α” represents anti-antibody.

Protein–RNA and protein–protein interaction features of A3C are not altered by S61P mutation

To further characterize the impact of the S61P mutation on A3C, we analyzed its tendency to form intracellular oligomers. A3C was reported to bind RNAs, which was found to be important for its activity [47,72]. A recent study on diffusional mobility of A3C fused to enhanced green fluorescent protein (EGFP) in living cells suggested the presence of A3C in higher-order molecular mass (HMM) complexes, although brightness analysis identified A3C as predominantly monomeric [73]. The cellular HMM of A3G, found as ribonucleoprotein complexes and the RNA-dependent multimerization of A3G, was correlated with viral packaging efficiency [16,48,73–78].

To explore whether A3C and A3C.S61P form similar higher-order protein species by interacting with RNA,

we performed velocity sucrose gradient centrifugation. Wild-type A3C and A3C.S61P distributed throughout the gradient and were largely found in HMM complexes, as tracked with ribosomal S6 protein (Fig. 5a). Treatment with RNase reduced the amount of higher-order molecules of both A3C and A3C.S61P in the maximum sucrose fractions and did not form low-molecular-mass complexes but instead elevated as aggregates (Fig. 5a, the last fraction) and sedimented as pellet (Fig. 5b). A3F also resides in the HMM complexes; however, unlike A3G, the A3F HMM complexes are insensitive to RNase treatment [79], suggesting that A3C forms unique HMM complexes that are stabilized by RNA molecules.

A3C oligomerization was found to be crucial for antiretroviral activity and LINE-1 inhibition, and A3C was reported to form at least dimers *in vivo* [47,72]. However, molecular brightness analysis characterized

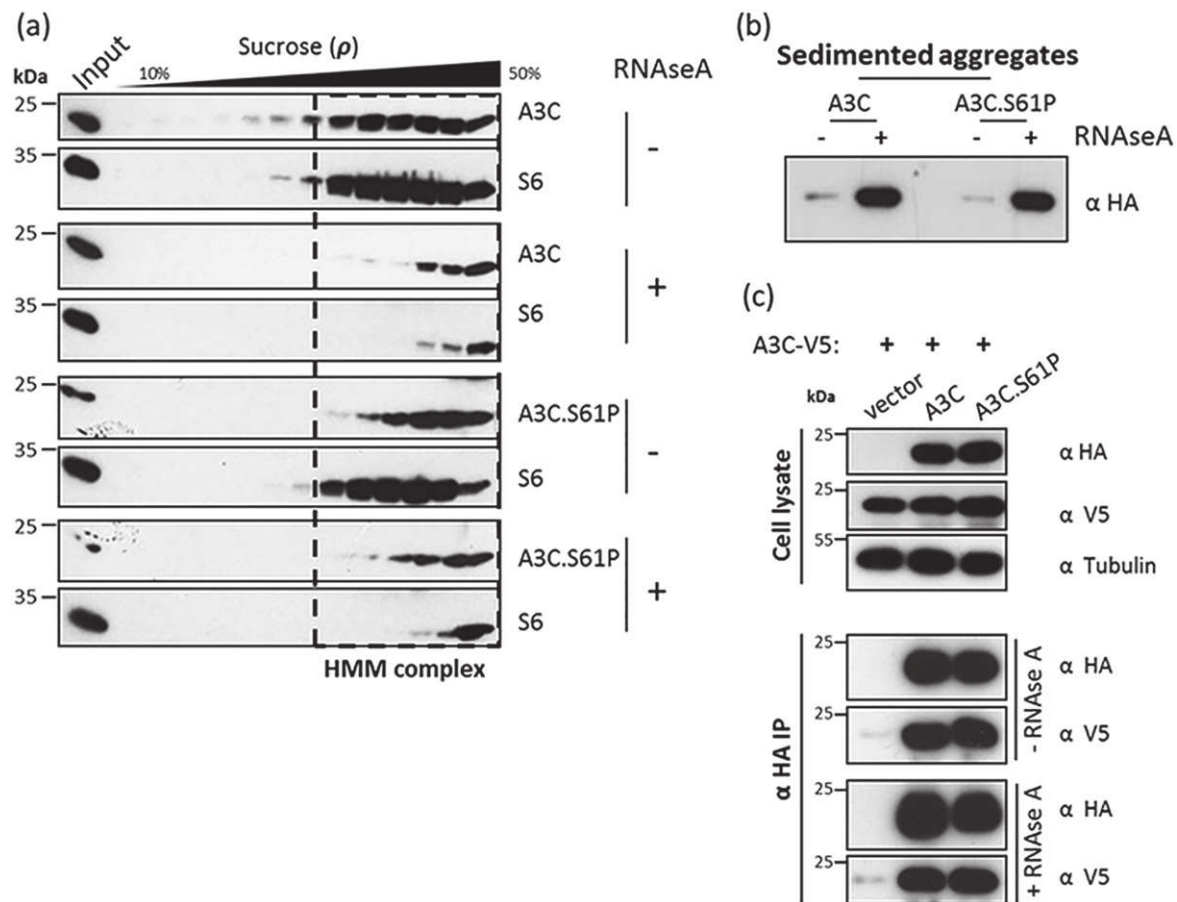


Fig. 5. A3C-RNA binding and A3C multimerization are not affected by serine-to-proline point mutation. (a) Velocity sucrose gradient fractionation of RNase-A-treated and untreated cell lysates of 293T cells that were transfected with expression plasmids for A3C and A3C.S61P through sucrose gradients (10% to 50%). Each blot panel was also loaded with cell lysate (input). Samples were examined by the use of specific antibodies: A3C and endogenous ribosomal S6 marker proteins were detected by anti-HA and anti-S6 antibody, respectively. Lanes corresponding to HMM complexes of A3C and S6 proteins were marked with a dashed box. (b) The pellet formed by A3C aggregates was dissolved by gel loading buffer, and 20% of the resulting mixture was subjected to immunoblot analysis using anti-HA antibody. (c) Pull-down assay to detect the homodimerization of A3C and A3C.S61P with and without RNase A treatment was performed. Carboxy terminal V5-tagged A3C construct was co-transfected together with an expression vector coding HA-tagged A3C and A3C.S61P. Anti-HA immunoprecipitates (IP) and the cell lysates were subjected to immunoblot analysis using anti-HA and anti-V5 antibodies. Tubulin served as loading control. “α” represents anti-antibody.

EGFP-labeled A3C to be preferentially monomeric in cells [73]. To determine whether A3C.S61P also forms dimers, we performed pull-down assays. Then, 293T cells were co-transfected with plasmids encoding V5-tagged WT A3C (A3C-V5) plus hemagglutinin (HA)-tagged WT A3C (A3C-HA), A3C.S61P-HA, or mutants A3C.F55A-HA and A3C.W74A-HA that lack the propensity to oligomerize [47]. Using experimental conditions as before [47,72], WT A3C-HA and A3C.S61P-HA co-precipitated an equal amount of A3C-V5 in cell lysates prepared with radioimmunoprecipitation assay (RIPA) buffer. Treatment with RNase A did not reduce the co-precipitation of the V5-tagged protein (Fig. 5c and Supplementary Fig. S3a), possibly suggesting that A3C complexes were not bridged by

RNA. Consistent with our previous data, A3C mutant F55A-HA did not precipitate the A3C-V5, and W74A-HA precipitated A3C-V5 weakly (Supplementary Fig. S3a). Together, these data confirm that the RNA binding and self-association of A3C are two separate functions and that the S61P mutation did not affect these inherent properties of A3C.

In addition, we performed co-immunoprecipitations (CO-IPs) using a mild lysis buffer containing 0.5% Triton X-100 to confirm the RNA-mediated A3G–A3G interaction [75,80]. Using this lysis condition, we found no precipitation of A3C-V5 by A3C-HA or A3C.S61P-HA, irrespective of RNase treatment (Supplementary Fig. S3b). This may indicate that the 0.5% Triton X-100 containing mild lysis buffer did not isolate

multimeric A3C complexes but was sufficient to isolate cytosolic localized A3G multimers (Supplementary Fig. S3b), supporting the previous observations that A3G HMMs are stabilized by both protein–protein and protein–RNA interactions [73,75,76,80,81]. In contrast, the HMM complexes of A3C were stabilized mainly by RNA, as the mild lysis condition did not isolate A3C dimers but A3C RNA–HMM complexes and RNA-deficient A3C aggregates (Fig. 5).

The S61P mutation in A3C enhances the editing of viral DNA

Yu *et al.* showed that A3C produced substantially fewer mutations than A3G in HIV-1 Δ vif and SIVagm Δ vif genomes [55]. Hence, we tested whether virion-incorporated A3C and A3C.S61P caused similar levels of DNA editing during infection. By using the sensitive 3D-PCR [82,83], we selectively amplified A3-mutagenized sequences of HIV-1 Δ vif, SIVagm Δ vif, and MLV (a 714-bp segment of the luciferase gene of the viral vector). DNA mutated by A3s contains fewer GC base pairs, resulting in a lower melting temperature during PCR. Therefore, successful amplification at lower denaturation temperature (T_d ; 83.5–87.6 °C) in 3D-PCR is an indicator of mutagenized sequences.

3D-PCR amplification with HIV-1 Δ vif/A3C samples formed amplicons until T_d is 86.3 °C, whereas HIV-1 Δ vif/A3C.S61P amplicons formed at 85.2 °C. Control reactions using virions produced with A3G and A3F resulted in amplification at lower T_d (84.2 °C; Supplementary Fig. S4a). A3C and A3C.S61P packaged in SIVagm Δ vif formed amplicons at 84.2 °C, which was comparable to A3G- and A3F-containing SIVagm Δ vif virions, indicating the possibility of hypermutation. A similar finding was obtained with MLV; in these samples, A3C.S61P formed PCR products at 84.2 °C, whereas WT A3C protein-induced mutations were detected at 85.2 °C. A3G and A3F amplicon formation appeared at 85.2 °C. Importantly, for the control experiments (no A3), PCR amplicons could be amplified only at the higher T_d (87.6 °C and weakly at 86.3 °C).

To characterize the G-to-A abundance and local nucleotide context, the amplified PCR products from the lowest denaturing temperature were cloned, and independent clones were sequenced. In cases with identical clones, only one is presented. Supplementary Fig. S4b shows the overall viral G-to-A mutation load (given as “X” %) and frequency of each tested A3 in a dinucleotide context. Supplementary Fig. S5 illustrates the extensive mutagenesis profiles observed in the presence of the respective A3s in the tested viruses.

In HIV-1 Δ vif, A3C and A3C.S61P induced a mutation rate of around 6%, whereas A3G and A3F caused a hypermutation rate of around 17% and 15%, respectively. We defined hypermutation as an overall mutation rate of >6% [84]. The majority of clones had a low

number of mutations, and only a few clones showed exceptionally high levels of G-to-A mutations (49 and 39 mutations using A3C and A3C.S61P, respectively; Supplementary Fig. S5). In contrast, A3C caused hypermutations in SIVagm Δ vif and MLV, with rates of 14% and 8%, respectively. With A3C.S61P, the amount of mutations was strongly enhanced in SIVagm Δ vif and MLV to 23% and 19%, respectively, and it surpassed the mutation rate caused by A3G and A3F in viruses. Notably, the antiviral activity of A3G and A3F against SIVagm Δ vif and MLV was lower than that of A3C and A3C.S61P (Supplementary Fig. S6a). Together, the data show that A3C is a DNA mutator enzyme of SIVagm Δ vif and MLV, but it has a much lower effect on HIV-1 Δ vif; moreover, its point mutant S61P enhances the net mutation rate (Supplementary Figs. S4b and S5). These results together with those obtained using the active site mutant A3C.C97S (Supplementary Fig. S2a) support the model that A3C inhibits SIVagm Δ vif and MLV primarily by DNA deamination.

A3 proteins preferentially deaminate selected cytidines to uridines with high specificity for a substrate dinucleotide motif. The C-to-U deamination in the viral negative strand induces the G-to-A mutation in the viral (plus strand) reverse transcripts [24,55,85]. Thus, we analyzed the nucleotide context of individual G-to-A mutations (5 nts) preceding and succeeding the G hotspot on the coding (plus) strand of the viral DNA induced by A3G, A3F, A3C, and A3C.S61P, testing all three viruses. Using the observed total mutations, the sequence logos were plotted (Fig. 6a). These plots confirmed that A3G favored the motif GG (mutated G underlined) [9,24,26,85]. In contrast, A3F preferred the sequence GAA irrespective of the virus source. A3C and A3C.S61P also favored GA predominantly, but they could mutate GG to a lesser extent (Fig. 6a and b).

A3C.S61P possesses improved *in vitro* catalytic activity

Based on the mutation signatures of A3C detected in three different viruses, we identified TTCA in the minus strand (TGAA of the viral plus strand) as an ideal target sequence of A3C. We performed *in vitro* deamination assays using A3s isolated from cell lysates and viral particles and ssDNA oligonucleotides containing the preferred motif. We adapted the PCR-based *in vitro* deamination assay described by Nowarski and Kotler [86] by using different oligonucleotides. The assay depends on a cytidine-to-uridine change in an 80-nt ssDNA by A3. A subsequent PCR generates a double-stranded DNA, replaces the uridine with thymidine, and thus generates a new restriction site. The efficiency of the restriction enzyme digestion is monitored using a similar 80-nt ssDNA containing uridine instead of a cytidine in the hotspot (Fig. 7, lane U). For cell-derived A3s, 293T cells were transfected with A3-encoding

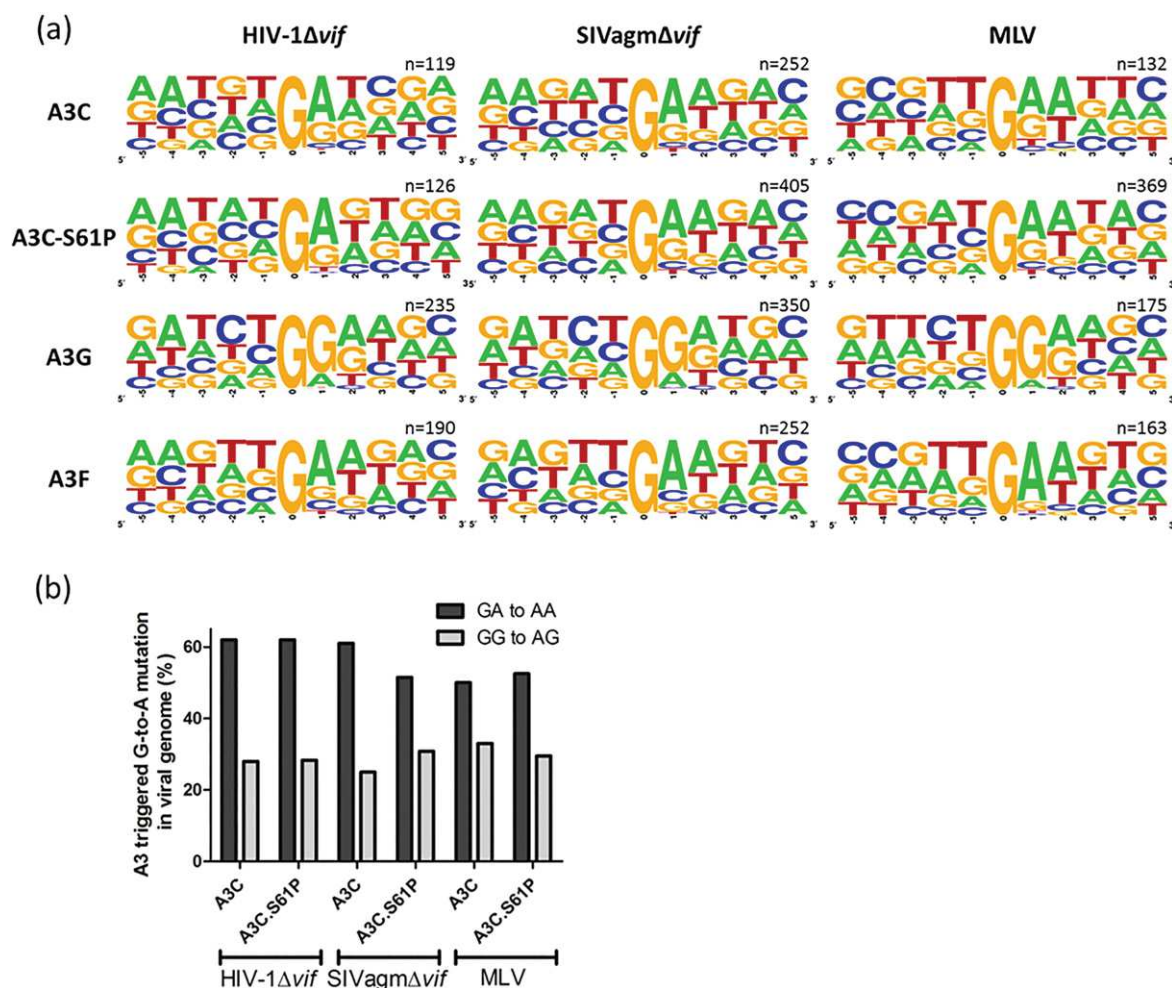


Fig. 6. The mutation pattern of A3C and A3C.S61P remains similar. (a) Sequence logos were generated from the sequence alignment of each G-to-A mutations (given as “n”) with 5 nts preceding and succeeding to the “G” hotspot. Local nucleotide sequence conservation rate at each position was analyzed using WebLogo tool. (b) The relative dinucleotide context of A3C and A3C.S61P. Histogram shows dinucleotide-specific GG-to-AG and GA-to-AA mutations elicited by A3C and A3C.S61P.

plasmids together with viral plasmids. Then, 2 days later, the cells were lysed, and HA-tagged A3s were immunoprecipitated using anti-HA beads. A portion of the beads was used for *in vitro* deamination assays (Fig. 7) and another portion for the immunoblots (Supplementary Fig. S6b). The reaction mixtures for the assay were untreated or treated with RNase A to eliminate potential inhibitory RNA [87,88]. A3G deaminated the CCCA substrate efficiently as reported previously [24,89] (Fig. 7a), and a very low-level deamination was also observed for A3C and A3C.S61P. In the experiments applying A3Cs, the deamination product was very faint, and it was only detectable after RNase A treatment. For the CCCA substrate, the gradient of activity can be expressed as A3G \gg A3C.S61P > A3C. Conversely, the cytidine in the TTCA oligonucleotide was preferentially deam-

inated by A3C and A3C.S61P, but no activity was detected with A3G (Fig. 7b). Remarkably, the deamination activity of A3C.S61P was much stronger than that of A3C in all three virus samples. Of note, similar levels of *in vitro* deamination activity were observed for the tested A3s precipitated from cell lysates that were co-expressed with viral proteins in 293T cells to produce virus particles (Fig. 7a and b).

The enzymatic activity of virion-incorporated A3 proteins may differ from that expressed in producer cells. To test this possibility, we produced viral particles packaging A3C, A3C.S61P, or A3G and subjected one fraction of the pelleted virus to immunoblot analysis (Supplementary Fig. S6b) and another fraction to the *in vitro* deamination assay (Fig. 7). With the CCCA-containing substrate, A3C and A3F deamination was hardly detectable, whereas deamination by A3C.S61P

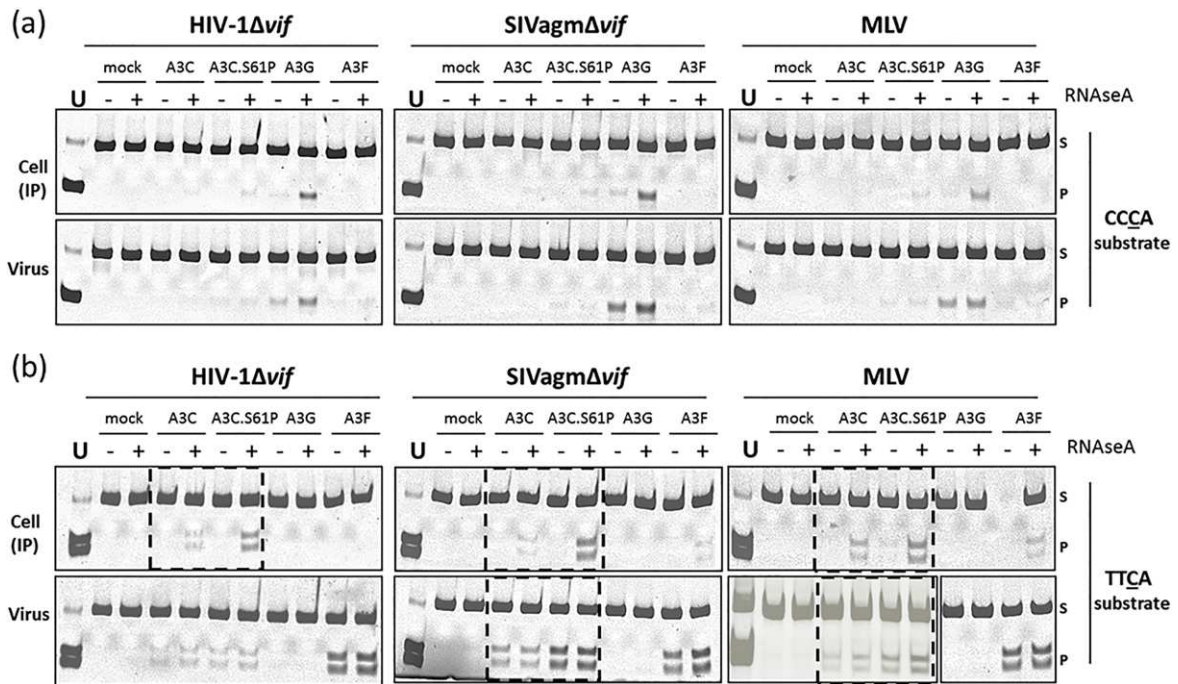


Fig. 7. *In vitro* catalytic activity of A3C.S61P is enhanced. Deamination of the activity of A3 from the cell lysate (expressed together with viral proteins) and viral particles was performed using two substrates containing (a) CCCA and (b) TTCA motif. To enrich the A3 from cell lysate, we immunoprecipitated HA-tagged A3 proteins and the HA-beads bound to the proteins were used in the activity assay (please note that A3F from IP did not yield enough protein due to less pipetted affinity beads in the HIV sample; hence, we repeated this experiment and presented it in Supplementary Fig. S8). Virions were concentrated and lysed in a mild lysis buffer and equal amount of lysate used for the assay. The amount of A3s used in the assay was shown in the immunoblot (Supplementary Fig. S6b). Evident activity enhancement of A3C.S61P was highlighted with a dashed box. RNaseA treatment was included; oligonucleotide-containing uracil (U) instead of cytosine served as a marker to denote the migration of deaminated product after restriction enzyme cleavage. S, substrate; P, product. Note that MLV/TTCA/virus experiment shown was stained with SYBR gold.

was evident, and A3G was highly active, as expected (Fig. 7a). Whereas with TTCA substrate, A3C.S61P formed more products than A3C when packaged into SIV and MLV particles, similar to the findings using proteins precipitated from transfected cells (A3F >>> A3C.S61P > A3C; Fig. 7b).

Although A3C.S61P showed increased deamination activity compared to WT A3C when isolated from cells, HIV-1 virion isolated A3C and A3C.S61P both had similar low activity (A3F >>> A3C.S61P = A3C). To further study the increased deamination activity of the A3C mutant when packaged into SIVagmΔvif virions, we evaluated the dose-dependent activity of virion-incorporated A3C and A3C.S61P (Fig. 8). When we tested the incremental amount of virion lysate (= packaged A3C), A3C.S61P showed enhanced catalytic activity, whereas A3C had fourfold lower *in vitro* deamination activity (Fig. 8). Together, these data indicate that virion-encapsidated A3C and A3C.S61P were catalytically active in SIVagmΔvif and MLV, but HIV-1Δvif evades much of the A3C-mediated deamination *in vivo* by as yet unknown mechanisms.

A3C and A3C.S61P form stable ssDNA complexes *in vitro*

To determine whether the interaction of A3C with the substrate DNA was differentially influenced by the S61P mutation, we performed electrophoretic mobility shift assays (EMSAs) using recombinant purified glutathione *S*-transferase (GST)-tagged proteins from 293T cells (Supplementary Fig. S7a). A3G is known to form three distinct DNA-protein complexes (Supplementary Fig. S7b) [81,86,90]. Recently, we established EMSAs for A3C with a 30-nt DNA oligonucleotide probe (TTCA) [91]. In a titration experiment with protein concentration ranging from 2 to 1000 nM (2, 20, 40, 80, 160, and 1000 nM), we found the formation of similar DNA-protein complexes for both A3C and A3C.S61P (Fig. 9). Importantly, the GST moiety did not affect the binding, and all DNA-protein complexes in the EMSA could be efficiently disrupted by adding the 80-nt unlabeled competitive DNA carrying the same probe sequence at 200-fold in excess [91].

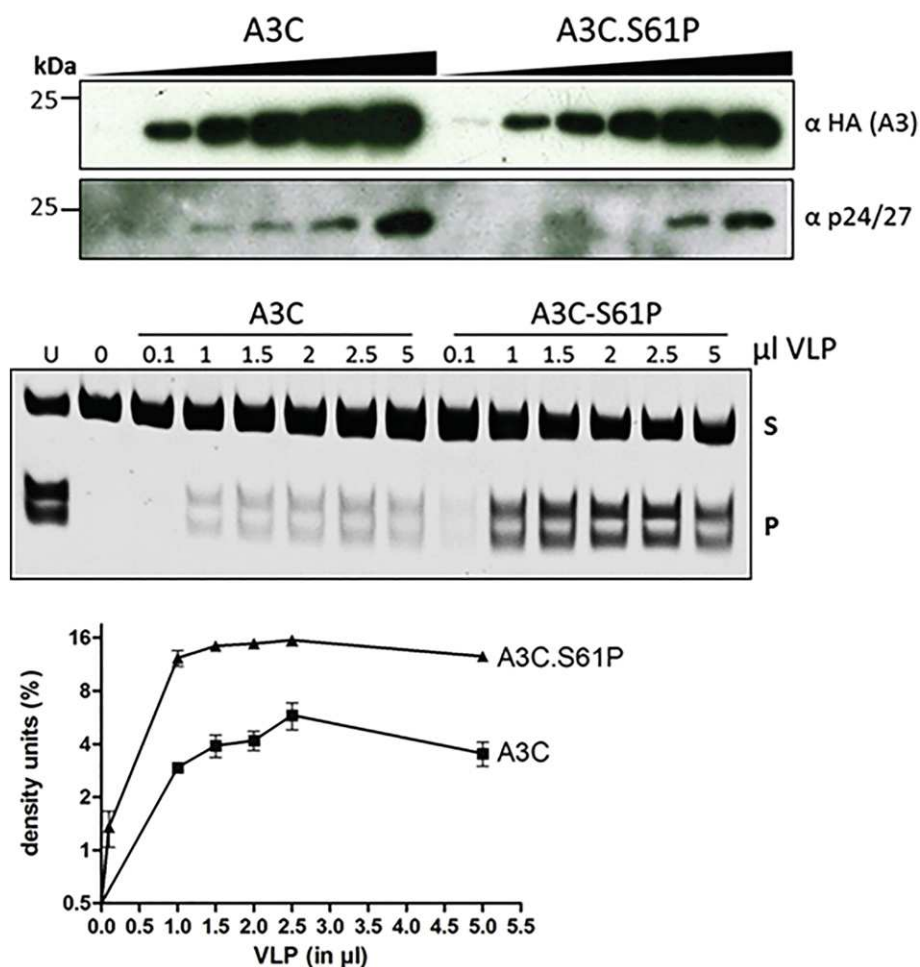


Fig. 8. Dose-dependent *in vitro* deamination activity of viral encapsidated A3C and A3C.S61P. Immunoblot shows the increasing amount of proteins derived from SIVagmΔ*vif* particles used for the subsequent titration experiment; capsid served as a loading control. Pooled particles were carefully used from a master stock to make the immunoblot and the deamination activity assay. The density signal of product (P) was calculated using Image J, and the percentages of density signals were plotted as line diagrams. Samples were treated with RNase; oligonucleotide-containing uracil (U) instead of cytosine served as a marker to denote the migration of deaminated product after restriction enzyme cleavage. S, substrate; P, product. A representative figure of three independent experiments is shown, and the error bars represent the SD obtained from three independent measurements.

Compared to A3C-GST, A3C.S61P-GST from 293T cells were found to be more catalytically active in a dose-dependent manner (Fig. 10a).

Zinc incorporation is unaltered in A3C.S61P

A recent study suggested that the addition of Zn^{2+} enhanced the catalytic activity of A3G and likely A3A due to Zn^{2+} binding at the allosteric or secondary zinc binding site in A3G [92]. Conversely, another study reported an A3F-CTD structure lacking a zinc atom at the catalytic center and suggested that zinc is not necessarily required for catalytic activity of A3F [93]. Hence, we tested the effect of zinc supplementation

and depletion on A3C catalytic activity by adding $ZnCl_2$, $ZnSO_4$, or EDTA, respectively (Fig. 10b and c). The addition of zinc enhanced the activity of A3C.S61P further and mildly of WT A3C, but even at the maximum concentration of zinc, the activity of A3C did not reach the activity of A3C.S61P (Fig. 10b). The effect of increasing the amount of EDTA to chelate the coordinated Zn^{2+} ion showed a similar dose-dependent inhibition for A3C-GST and A3C.S61P-GST activity (Fig. 10c). Using atomic absorption spectroscopy, the zinc content of A3C and A3C.S61P from 293T cells and *Escherichia coli* was found to be similar (Table 1). Together, these data demonstrate that the activity enhancement of

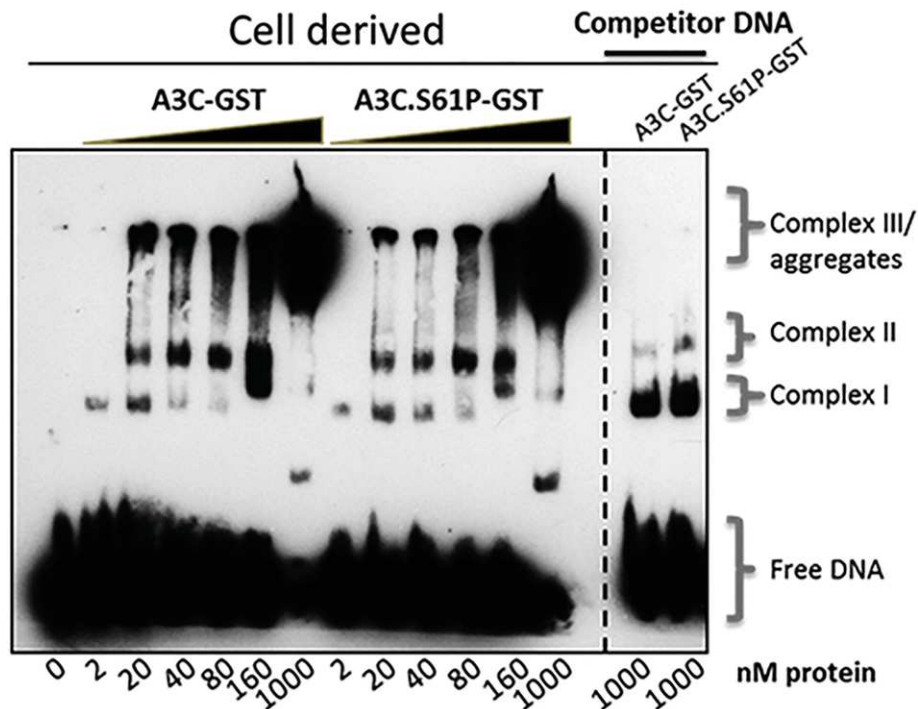


Fig. 9. A3C and A3C.S61P strongly interact with ssDNA. EMSA with 293T cells produced GST-tagged A3C, and A3C.S61P performed with 30-nt ssDNA target DNA labeled with 3'-labeled biotin. Indicated amounts of protein (at the bottom of the blot) were titrated with 10 nM of DNA. Presence of competitor DNA (unlabeled 80-nt DNA used in deamination assay, 200-fold molar excess added) used to demonstrate the specific binding of protein to DNA being causative for the shift. Purity of the recombinant proteins used was shown in Fig. S7a.

A3C.S61P was not due to the involvement of extra Zn^{2+} coordination and that the Zn^{2+} coordination is unaffected by the S61P mutation in A3C.

Mutation in P244 moderately affects the antiviral function of full-length A3F

To determine whether a mutation in analogous proline 244 can influence the antiviral properties of A3F, we tested the antiviral effect of A3F, A3F.P244S, and A3F.P244A against HIV-1 Δ vif, SIVagm Δ vif, and MLV. Mutation in P244 increased the infectivities of SIVagm Δ vif and MLV marginally but not of HIV-1 Δ vif (Supplementary Fig. S8a). Production of A3F and its mutants in cells and viral encapsidation were found to be nearly similar (Supplementary Figs. S8b and S8c). We also characterized the enzymatic activity of these proteins from 293T cells (enriched by immunoprecipitation) and HIV-1 packaged proteins. Compared to WT, A3F.P244S showed a reduction in product formation, and this trend was further diminished for A3F.P244A (Supplementary Fig. S8d).

Discussion

In contrast to A3G, knowledge about the catalytic activity and nucleic acid binding capacity of A3C is

very limited, despite the presence of a 3D structure [24,46,47,94]. Importantly, A3C is known to be a potent enzyme that restricts vif-deficient SIV [55,95], but several reports show little to no effect of hA3C on HIV-1 Δ vif [9,11,12,52,57–59,96,97]. The results of this study reveal the importance of A3C's deamination function to restrict SIVagm Δ vif and MLV [9,52,55]. The anti-MLV activity described here contrasts previous reports of resistance of MLV to inhibition by A3C [55,98] and may be explained by the use of slightly different reagents and experimental conditions.

Our findings support reports that A3C is efficiently incorporated into viral cores of HIV-1 Δ vif, SIVagm Δ vif, and MLV particles [52,55,99], but they essentially contradict other studies describing the absence of A3C in these virions [57,59,98]. Like A3C in HIV-1 Δ vif, murine A3 was reported to have limited anti-MLV activity, although it was packaged efficiently [100]. Given the level of uncertainty about A3C, we set out to identify the determinants of A3C's catalytic activity and postulated that an enhancement of A3C's activity could direct the inhibition of HIV-1 Δ vif. Using sequence and structure comparison of A3C and A3F-CTD, we identified two residues near the catalytic center in A3C that are different compared to A3F-CTD. Of those, only the S61P mutation enhanced the activity of A3C. During this manuscript preparation, Wittkopp *et al.* [101]

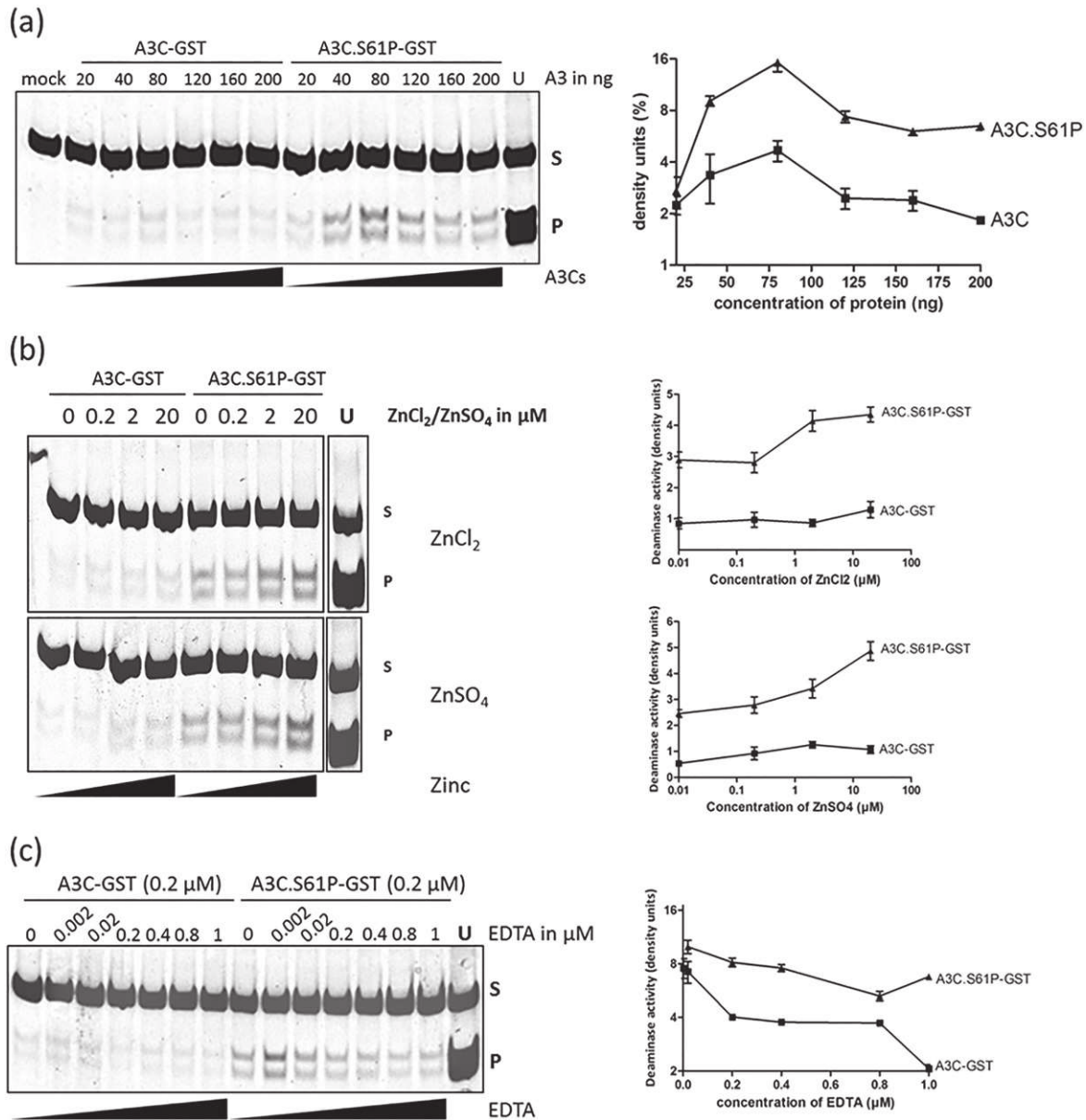


Fig. 10. *In vitro* deamination activity assay and effect of Zinc and EDTA titration. Activity assay using GST-tagged A3C, A3C.S61P, or A3F-CTD from 293T cells. (a) A titration experiment with increasing amounts of protein was made with A3C and A3C.S61P. The density signal of product (P) was calculated using Image J, and the percentage of density signals were plotted as line diagrams in all experiments (right panel). (b) Effect of Zinc addition on deamination activity. Indicated amount of ZnCl_2 or ZnSO_4 added in the reaction mixture containing 0.2 μM A3. The density signal of product (P) was calculated using Image J, and the percentages of density signals were plotted as line diagrams in all experiments (right panel). (c) EDTA titration of A3C activity assay. A representative figure of three independent experiments is presented. The density signal of product (P) was calculated using Image J, and the percentages of density signals were plotted as line diagrams in all experiments (right panel). In (a–c), samples were treated with RNase; oligonucleotide-containing uracil (U) instead of cytosine served as a marker to denote the migration of deaminated product after restriction enzyme cleavage. S, substrate. The PAGE gels in these experiments were stained with SYBR gold.

reported a single nucleotide polymorphism of A3C (serine 188 to isoleucine) that acted more antiviral. S61P is not found as a human single nucleotide polymorphism variant of A3C, while D99E is present in some humans (accession number, dbSNP:

RS143646385). The analogous proline (P244) mutation to serine or alanine in the full-length A3F did not determine its antiviral function; yet, it was required for optimal catalytic activity (Supplementary Fig. S8). A3F.P244S lost a moderate amount of its antiviral

Table 1. Zinc content in GST tagged A3Cs purified from 293T cells and *E. coli*

Sample		Concentration of Zinc mean (mg/L)	SD (mg/L)	% RSD
Cell	A3C-sample 1	0.04	0	0.42
	A3C.S61P-sample 1	0.045	0.001	2.59
	A3C-sample 2	0.042	0	0.1
	A3C.S61P-sample 2	0.042	0.001	2.06
<i>E. coli</i>	A3C	0.045	0.001	1.9
	A3C.S61P	0.044	0	1.13

Purified proteins were subjected to atomic absorption spectroscopy, and the Zinc content of the samples was calculated as described in the Materials and Method section.

activity against SIV Δ vif but not against HIV-1 Δ vif, further suggesting that the A3C interaction with SIV and HIV-1 differs.

Although many tested protein features of A3C and A3C.S61P, such as oligomerization, formation of HMM complexes, and viral core localization, were found to be similar, the deamination-based virus inhibition of A3C was enhanced markedly by the S61P mutation. Our study identified a TTC nucleotide substrate preference of A3C, which explains the weak A3C *in vitro* deamination reported previously using a CC substrate [55].

Several studies of A3 proteins have confirmed the importance of the catalytic Zn²⁺ coordination motif (H-E-C-C), but few studies have described the role of single amino acids of A3 in substrate binding and catalytic and antiviral functions [13,29,47,65,67,83,102]. Using time-resolved nuclear magnetic resonance spectroscopy, kinetic parameters of A3G's deamination within the preferred CCC motif was determined in real time [70,94,103]. H216 of A3G was found to play a key role in substrate binding through the protonation of its imidazole ring below physiological pH [103]. Interestingly, Rathore *et al.* modified the dinucleotide substrate specificity of A3G from CC to TC by replacing loop 7 with the one found in A3A; they also demonstrated that D317 was a determinant of the substrate specificity [89]. Moreover, they reported that the replacement of loop 3 enhanced A3G's enzymatic function. These data support our findings of enhanced A3C.S61P deamination activity that is governed by a residue in loop 3 of A3C.

Two models of DNA binding grooves in CTD of A3G and A3F were proposed [48,68–71], and the involvement of loop 7 present in both NTD and CTD of A3F was discussed [45]. Alanine scanning in the DNA binding groove residues of A3F-CTD resulted in reduced affinity for ssDNA, and the YYFW motif in loop 7 determined the TC substrate specificity [68]. This suggests that the similar YYFQ motif in loop 7 of A3C may have a positive regulatory role for DNA binding and TTC substrate specificity. Another report confirmed that the insertion of a tyrosine instead of

C320 in A3D (A3D.C320Y) in an equivalent CYFW motif (loop 7) resulted in a deamination-dependent antiviral effect, whereas the introduction of cysteine in the aromatic motif in A3G, A3B, and A3F abolished the antiviral function [104]. Thus, given the similarity of DNA binding sites in A3C and A3F-CTD and that the position of proline 244 in loop 3 is distal to the DNA binding region (loop 7) but in proximity to the catalytic center, we postulated that the S61P mutation in A3C might play a vital role in the enzymatic activity. We found that a proline mutation but not an alanine mutation at position 61 increased the catalytic and antiviral exertion of A3C without altering TTC specificity. Thus, we hypothesized that the presence of proline in the loop 3 contributes to changes in protein folding that in turn promote deamination.

Structurally, proline is a rigid amino (*imino*) acid (lacks an amide hydrogen) that generally occupies tight turns/coils in the protein structure, and it is widely used as a helix conformation breaker; it also contributes to favorable conformation stability in certain β -turn positions [105–110]. Proline is expected to decrease the conformational entropy of the unfolded state, thereby stabilizing energetically favored conformations [108], which are a feature favorable for many enzymes [108,111–113]. Xu *et al.* [113] noted that in cyclophilin A, Pro16 located between two beta strands distal from the catalytic site was crucial for the maintenance of structural and functional integrity. Serine 16 substitution for proline 16 correlated with increased flexibility of the loop connecting beta strands, impaired the catalytic function, and decreased the stability by making indirect contacts with a hydrophobic pocket. Likewise, we speculate that the exchange of serine 61 to proline 61 in A3C might influence the deamination activity, likely by anchoring the substrate DNA toward the catalytic center or by stabilizing the catalytic site conformation. Based on our EMSA data from 293T cells and the fact that proline 244 is not part of A3F DNA binding groove, we propose that the proline at position 61 did not influence the substrate binding in A3C.S61P. Because the DNA binding of A3C is unaltered by the S61P mutation, we assume that the enhancement of deamination and virus inhibition is a reflection of proline-induced minute structural changes around the active site of A3C. The zinc content measurement revealed that A3C and A3C.S61P coordinated similar amounts of zinc; thus, the S61P-mediated enhancement of deamination is zinc-independent.

Herein, we propose a model in which A3C packaged into retroviruses is catalytically active, although the power of inhibition varies among different viruses. The A3C.S61P variant acts similar to WT A3C but catalyzes more cytidine deamination, likely due to the rigid microenvironment provided by proline 61. Lack of anti HIV-1 activity of either A3C or A3C.S61P appears to be not due to a lack of catalytic function and needs further

investigation to understand how HIV-1 can escape from the deamination-dependent antiviral defense of A3C.

Materials and Methods

Cell culture

HEK293T cells were maintained at 37 °C in a humidified atmosphere of 5% CO₂ in Dulbecco's high-glucose modified Eagle's medium (Biochrom, Berlin, Germany), supplemented with 10% fetal bovine serum, 2 mM L-glutamine, 50 units/ml penicillin, and 50 µg/ml streptomycin.

Virus production and isolation

We transiently transfected 293T cells using Lipofectamine LTX and plus reagent (Invitrogen, Karlsruhe, Germany) with appropriate combination of viral vectors (HIV-1: 600 ng pMDLg/pRRE, 600 ng pSIN.PPT.CMV.Luc.IRES.GFP, 250 ng pRSV-Rev, 150 ng pMD.G with 600 ng A3 plasmid or pcDNA3.1; SIVagm: 1400 ng pSIV Tan-Luc Δ vif, 150 ng pMD.G with 600 ng A3 plasmid; MLV: 750 ng pHIT60, 750 ng pMP71-luc, and 150 ng pMD.G with 600 ng A3 plasmid, unless otherwise mentioned) together with A3 plasmid or as a vector control pcDNA3.1 empty vector in 6-well plate. Then, 48 h post-transfection, virion-containing supernatants were collected and concentrated by layering on 20% sucrose cushion and centrifuged for 4 h at 14,800 rpm. Viral particles were resuspended in mild lysis buffer [50 mM Tris (pH 8), 1 mM PMSF, 10% glycerol, 0.8% NP-40, 150 mM NaCl, and 1X complete protease inhibitor]. Viral lysate was used in immunoblots and *in vitro* deamination assay.

Luciferase-based infectivity assay

HIV-1, SIVagm, and Mo-MLV-based luciferase reporter viruses were used to transduce HEK293T cells. Prior to infection, the amount of reverse transcriptase (RT) in the viral particles was determined by RT assay using Cavid HS kit Lenti RT (Cavid Tech, Uppsala, Sweden). Normalized RT amount equivalent viral supernatants were transduced. Then, 72 h later, luciferase activity was measured using SteadyLiteHTS luciferase reagent substrate (Perkin Elmer, Rodgau, Germany) in black 96-well plates on a Berthold MicroLumat Plus luminometer (Berthold Detection Systems, Pforzheim, Germany). Transductions were done in triplicate, and at least three independent experiments were performed.

Plasmids

SIVagm luciferase vector system was described before [37]. The MLV packaging construct pHIT60

were kindly provided by Jonathan Stoye, which encodes the *gag-pol* of Mo-MLV [114]. The MLV luciferase reporter plasmid MP71-luc is based on the MP71 plasmid that was previously described by Schambach *et al.* [115], provided by Harald Wodrich. The MP71-luc plasmid contains the firefly luciferase gene cloned into the EcoRI endonuclease restriction of MP71. The HIV-1 packaging plasmid pMDLg/pRRE encodes *gag-pol*, and the pRSV-Rev for the HIV-1 *rev* [116]. The HIV-1 vector pSIN.PPT.CMV.-Luc.IRES.GFP expresses the firefly luciferase and GFP reported previously [117]. MLV and HIV-1 based viral vectors were pseudotyped using the pMD.G plasmid that encodes the VSV-G. All A3 constructs described here were cloned in pcDNA3.1 (+) with a C-terminal HA tag. The expression vector for A3G-HA was generously provided by Nathaniel R. Landau. Expression constructs A3C-HA and A3F-HA and the A3C point mutants A3C.C97S and A3C.F55A were described before [47,118]. A3F-CTD open reading frame region (start codon plus residues 184–373) with C-terminal HA tag was cloned using primers forward 5'-GCTAAGCTTGC-CACCATGCTAAAGGAGATTCTCAG and reverse 5'-TCAGAGAATTCTCAAGCGTAATCTGGAA-CATCGTATGGATACTCGAGAATCTCCTGCAG. In addition to clone C-terminal GST-tagged A3C, A3C.S61P, and A3F-CTD, the open reading frames were inserted between the restriction sites HindIII and XbaI in mammalian expression construct pK-GST [119] using the following primers: A3C and A3C.S61P: forward 5'-ATAAGCTTGCCACCATGAATCCACAGATCAGAAAC and reverse 5'-ATTCTAGACTGGAGACTCTCCCGTAGCCT; A3F-CTD: the same A3F-CTD forward primer and reverse 5'-ATTCTAGACTCGAGAATCTCCTGCAG. Bacterial expression vector pGEX-6P-2 (GE Healthcare, Munich, Germany) was used to generate A3C and A3F-CTD with N-terminal GST tag using the following primers: A3C: forward 5'-GGGGATCCATGAATCCACAGATCAGAAAC, and reverse 5'-TCCTCGAGTCACTGGAGACTCTCCCGTAGCC; A3F-CTD: forward 5'-ATGAATTCGCCACATGCTAAAGGAGATTCTCAG and reverse 5'-ATGCGGCCGCTCACTCGAGAATCTCCTGCAG.

A3C point mutants D99E, S61P, S61A, and double mutant A3C.DS-EP; A3F.P244S and A3F.P244A were generated by site-directed mutagenesis using following primers: D99E: forward 5'-AGCCCTTGCC-CAGAGTGTGCAGGGGAG and reverse 5'-CTCCCC TGCACACTCTGGGCAAGGGCT; S61P: forward 5'-AACCAGGTGGATCCTGAGACCCATTG and reverse 5'-CAATGGGTCTCAGGATCCACCTGGTT; S61A: forward 5'-AACCAGGTGGATGCTGAGACCCATTG and reverse 5'-CAATGGGTCTCAGCATCCACCTGGTT, A3F.P244S: forward 5'-AACCA GGTGGATTCTGAGACCCATTG and reverse 5'-CAATGGGTCTCAGAATCCACCTGGTT; A3F.P244A: forward 5'-AACCAGGTGGATGCTGAGACC

CATTG and reverse 5'- CAATGGGTCTCAGCATC CACCTGGTT.

Immunoblots

Transfected 293T cells were washed with phosphate-buffered saline and lysed in RIPA buffer [25 mM Tris (pH 8.0), 137 mM NaCl, 1% glycerol, 0.1% SDS, 0.5% sodium deoxycholate, 1% Nonidet P-40, 2 mM EDTA, and protease inhibitor cocktail set III (Calbiochem, Darmstadt, Germany)] for 20 min on ice. Lysates were clarified by centrifugation (20 min, 14,800 rpm, 4 °C). Samples (cell/viral lysate) were boiled at 95 °C for 5 min with Roti load reducing loading buffer (Carl 726 Roth, Karlsruhe, Germany) and subjected to SDS-PAGE followed by transfer (Semi-Dry Transfer Cell, Biorad, Munich, Germany) to a PVDF membrane (Merck Millipore, Schwalbach, Germany). Membranes were blocked with skimmed milk solution and probed with appropriate primary antibody, mouse anti-HA antibody (1:7500 dilution, MMS-101P, Covance, Münster, Germany); mouse α -V5 antibody (1:4000 dilution; Serotec); goat anti-GAPDH (C-terminus, 1:15,000 dilution, Everest Biotech, Oxfordshire, UK); mouse anti- α -tubulin antibody (1:4000 dilution, clone B5-1-2; Sigma-Aldrich, Taufkirchen, Germany), mouse anti-capsid p24/p27 MAb AG3.0 [120] (1:250 dilution, NIH AIDS Reagents); rabbit anti S6 ribosomal protein (5G10; 1:10³ dilution in 5% BSA, Cell Signaling Technology, Leiden, The Netherlands); antiserum against Rauscher MLV p30 [1:10⁴ dilution, NCI HD 539, (ATCC VR-1564AS-Gt)]. Secondary Abs: anti-mouse (NA931V), anti-rabbit (NA934V) horseradish peroxidase (1:10⁴ dilution, GE Healthcare) and anti-goat IgG-HRP (1:10⁴ dilution, sc-2768, Santa Cruz biotechnology, Heidelberg, Germany). Signals were visualized using ECL chemiluminescent reagent (GE Healthcare).

Sucrose density gradient centrifugation

We transfected 293T cells with expression plasmids for 1 μ g A3C-HA or A3C.S61P. After 24 h, cells were lysed with lysis buffer [0.7% NP-40, 100 mM NaCl, 50 mM potassium acetate, 10 mM EDTA, 10 mM Tris (pH 7.4), and complete protease inhibitor cocktail (Merck Calbiochem)] and then clarified by centrifugation for 10 min at 162g followed by a short spin at 18,000g for 30 s. A half portion of the sample was aliquoted to a new tube, to which RNase A (Thermo Fisher Scientific; 70 μ g/ml) was added and incubated for 30 min at 37 °C. Samples were then overlaid on top of a 10%-15%-20%-30%-50% sucrose step gradient in lysis buffer and centrifuged for 45 min at 163,000g at 4 °C in a MLS-50 rotor (Beckman Coulter, Fullerton, CA) [75,80]. After centrifugation, the samples were sequentially removed from the top of the gradient, resolved by SDS-PAGE, and analyzed by immunoblotting with

anti-HA and anti-S6 antibodies to detect A3C and endogenous S6 ribosomal protein [72], respectively.

Viral core isolation

HIV-1 Δ vif, SIVagm Δ vif, and MLV cores were isolated according to the protocol described for isolating HIV-1 cores [121]. Viral particles were produced together with the expression of A3C or A3C.S61P. Then, 2 days post-transfection, the virions were purified and concentrated by centrifuging through 20% sucrose cushion in an ultracentrifuge at 136,000g for 2 h. Viral particles resuspended in STE buffer [10 mM Tris-HCl (pH 7.4), 100 mM NaCl, and 1 mM EDTA] [79], loaded on the top of the sucrose step gradient containing a layer of buffer or 1% Triton X-100 (in 15% sucrose), followed by 20% and 60% sucrose gradient (Supplementary Fig. S1), and centrifuged at 136,000g for 1 h at 4 °C in ultra-clear centrifuge tubes (13 \times 51 mm, Beckman Coulter) in a MLS-50 rotor (Beckman Coulter). This procedure minimized the time of detergent exposure of the virus. Three fractions (F1, F2, and F3) were collected, and an aliquot of each fraction of step gradients was subjected for immunoblot analysis. Viral compartments and the A3 proteins were detected by probing the blots with appropriate antibodies [anti-p24/p27 (HIV and SIV), anti-p30 (MLV), anti-VSV-G and anti-HA].

Co-immunoprecipitation assay for A3C self-association in cells

We performed this experiment as we reported previously [47] by including the A3C.S61P and appropriate dimer mutant controls. To test whether RNase A treatment can influence the A3C-A3C interaction, we split the cell lysate made with RIPA buffer into two halves, in which one portion was treated with RNase A (70 μ g/ml) and incubated for 30 min at 37 °C, followed by 30 min at room temperature, and the immunoprecipitation assay was performed as described in [47].

Alternatively, we also did an independent CO-IP using a procedure used before [75,80]. The difference in this method is the use of mild lysis buffer containing 0.5% Triton X-100, 287 mM NaCl, 3 mM KCl, 50 mM Tris (pH 7.5), and complete protease inhibitor. At 24 h post-transfection, cells were harvested and lysed with lysis buffer. The cleared lysates were incubated with 20 μ l anti-HA affinity matrix beads for 2 h at 4 °C, with end-over-end rotation. After binding, the beads were washed twice, with lysis buffer, and half portions of the samples were aliquoted to new tubes. RNase A (70 μ g/ml) was added to one aliquot of the sample and incubated at 37 °C for 10 min and at 22 °C for 40 min. Samples were further washed thrice with lysis buffer. CO-IP products were eluted by boiling beads in SDS gel loading buffer at 95 °C for 5 min. A parallel A3G-A3G CO-IP was performed as a control.

Differential DNA denaturation (3D) PCR

We cultured 293T cells in the 6-well plates and infected it with DNase-I-treated viruses for 12 h. Cells were harvested and washed in phosphate-buffered saline; the total DNA was isolated using DNeasy DNA isolation kit (Qiagen, Hilden, Germany). A 714-bp fragment of the luciferase gene was amplified using the primers 5'-GATATGTGGATTTTCGAGTCGTC-3' and 5'-GTCATCGTCTTTCCGTGCTC-3'. For selective amplification of the hypermutated products, the PCR denaturation temperature was lowered stepwise from 87.6 °C to 83.5 °C (83.5 °C, 84.2 °C, 85.2 °C, 86.3 °C, 87.6 °C) using a gradient thermocycler. The PCR parameters were as follows: (i) 95 °C for 5 min; (ii) 40 cycles, with 1 cycle consisting of 83.5 °C to 87.6 °C for 30 s, 55 °C for 30 s, 72 °C for 1 min; (iii) 10 min at 72 °C. PCRs were performed with Dream Taq DNA polymerase (Thermo Fisher Scientific). PCR products from the lowest denaturation temperatures were cloned using CloneJET PCR Cloning Kit (Thermo Fisher Scientific) and sequenced. A3-induced hypermutations of at least eight independent clones were analyzed with the Hypermut online tool[†] [122]. Mutated sequences (clones) carrying similar base changes were omitted, and only the unique clones were presented for clarity.

The overall mutation percentage in the viral DNA was calculated as shown below:

$$\text{Overall mutation rate} = \frac{\text{no. of G} \rightarrow \text{A mutations in "n" sequences}}{\text{"n"} \times 176 \text{ (G)}}$$

Sequence logos of the nucleotide context in the G-to-A hotspot were generated by using weblogo[‡] online tool [123].

Purification of recombinant GST-tagged A3Cs from *E. coli* and 293T cells

Recombinant GST-tagged proteins were purified as described before [81,91]. Purified protein concentration was determined spectrophotometrically by measuring the A_{280} , using their (theoretical) extinction coefficient and molecular mass. Protein gels were stained with Coomassie brilliant blue stain. C-terminal GST-tagged A3 proteins from 293T cells were expressed and purified similarly and used for the following deamination assay [67,71] and EMSA.

In vitro DNA cytidine deamination assay

Deamination reactions were performed as described [80,86] in a 10- μ L reaction volume containing 25 mM Tris (pH 7.0) and 100 fmol ssDNA substrate (CCCA: 5'-GGATTGGTTGGTTATTTGTTTAAGGAAGGTGGATTAAGGCCCAAGAAGGTGATGGAAGT-TATGTTTGGTAGATTGATGG; TTCA: 5'-GGATT

GGTTGGTTATTTGTATAAGGAAGGTGGATTGAA GGTTCAAGAAGGTGATGGAAGTTATGTTTGGTA-GATTGATGG). Samples were split into halves, and in one, 50 μ g/ml RNase A (Thermo Fisher Scientific) was added. Reactions were incubated for at least 1 h at 37 °C, and the reaction was terminated by boiling at 95 °C for 5 min. We used 1 fmol of the reaction mixture for PCR amplification Dream Taq polymerase (Thermo Fisher Scientific) at 95 °C for 3 min, followed by 30 cycles of 61 °C for 30 s and 94 °C for 30 s, and the primers forward 5'-GGATTGGTTGGTTATTTGTT-TAAGGA, reverse 5'-CCATCAATCTACCAAACA-TAACTTCCA were used to amplify CCCA substrate, forward primer 5'-GGATTGGTTGGTTATTTGTTA-TAAGGA with the above reverse primer used for TTCA. PCR products of CCCA and TTCA were digested with Eco147I (Stul; Thermo Fisher Scientific) and MseI (NEB, Frankfurt/Main, Germany), respectively, and resolved on 15% PAGE, stained with ethidium bromide (7.5 μ g/ml). As a positive control substrate, oligonucleotides with CCUA and TTUA instead of respective CCCA and TTCA were used to control the restriction enzyme digestion. For the titration experiments using increasing concentrations of viral particles or purified proteins and to detect the effect of Zinc and EDTA on deamination, we made only RNase-A-containing reactions. Proteins and reagents were carefully diluted by serial dilution from the master mix. PAGE gel for titration experiments were stained with SYBR gold (1:1000 dilution, Thermo Fisher Scientific).

A3 production in 293T cells for deamination assay

We transfected 293T cells with expression plasmids carrying A3C, A3C.S61P, A3G, and A3F (and A3F mutants). Cells were lysed 48 h later with mild lysis buffer [50 mM Tris (pH 8), 1 mM PMSF, 10% glycerol, 0.8% NP-40, 150 mM NaCl, and 1X complete protease inhibitor]. HA-tagged proteins were immunoprecipitated by using 20 μ L of anti-HA Affinity Matrix Beads (Roche) by slowly rotating the lysate bead mixture for 2 h at 4 °C. A portion of beads were used for deamination assay, and the remaining was used for immunoblots.

A3 incorporation into HIV-1 Δ vif, SIVagm Δ vif, and MLV particles

Virions were produced as described above and used as input for the *in vitro* deamination assay. For the titration experiments, SIVagm with A3C and A3C.S61P were produced, and different amounts of viral lysate (0.1, 1, 1.5, 2, 2.5, 5 μ L) were used in deamination reaction treated with RNase A.

EMSA

EMSA method is adapted from Refs. [81,90,91]. Proteins were produced as described above,

brought to a buffer containing 50 mM Tris (pH –8), 50 mM NaCl, and 10% glycerol. We mixed 10 mM 3' biotinylated DNA (30-TTC-Bio-TEG purchased from Eurofins Genomics, Ebersberg Germany) with 10 mM Tris (pH –7.5), 100 mM KCl, 10 mM MgCl₂, 1 mM DTT, 2% glycerol, and the indicated amount of recombinant proteins in a 10- μ l reaction mixture, and we incubated it at 25 °C for 30 min. The protein–DNA complex was resolved on a 5% native PAGE gel on ice, and the DNA–protein complex was transferred to nylon membrane (Amersham Hybond-XL, GE healthcare) by southern blot. After the transfer, the molecules on the membrane were crosslinked by UV radiation by facing the membrane on a transilluminator equipped with 312-nm bulb. Chemiluminescent detection of biotinylated DNA was carried out according to the manufacturer's instruction (Thermo Fisher Scientific).

Quantitation of zinc content in A3C

Purified GST-tagged A3C and A3C.S61P proteins from *E. coli* and 293T cells (at concentration 1 mg/L) were subjected to atomic absorption spectroscopy using a Perkin Elmer Analyst 100. The spectrometer was equipped with a hollow-cathode lamp and acetylene flame air. The Zinc absorption spectra were measured at 213.9 nm with a 0.7 nm slit width. Zinc content in the protein was determined from a standard curve (0.01, 0.1, 0.5, and 1 mg/L zinc standard from Fluka) within the linear range.

Sequence and structure alignment

A3C and A3F-CTD amino acid sequences were aligned using the online server Clustal Omega. The structure alignment and graphical visualization presented in Fig. 3b were constructed using PyMOL (PyMOL Molecular Graphics System, version 1.5.0.4; Schrödinger, Portland, OR).

Statistical analysis

Data were represented as the mean with SD in all bar diagrams. Statistically significant differences between two groups were analyzed using the unpaired Student's *t*-test with GraphPad Prism version 5 (GraphPad software, San Diego, CA, USA). A minimum *p* value of 0.05 was considered as statistically significant.

Acknowledgments

This work was supported in part by the International NRW Research School BioStruct (to A.A.J.V.) and Heinz-Ansman foundation for AIDS research

(to C.M.). We thank Holger Gohlke and Sander Smits for helpful discussion, Shingo Kitamura and Yasumasa Iwatani for their insights on A3C purification, Wioletta Hörschken for excellent technical assistance, and Annette Ricken and Christoph Janiak for Zinc measurements. We thank Neeltje Kootstra, Nathaniel R. Landau, Bryan R Cullen, Jonathan Stoye, and Harald Wodrich for reagents. The following reagent was obtained through the NIH AIDS Research and Reference Reagent Program, Division of AIDS, NIAID, NIH: a monoclonal antibody to HIV-1 p24 (AG3.0), from Jonathan Allan.

Author contributions: A.A.J.V. performed all of the experiments, analyzed data, and drafted the manuscript, while H.H. contributed pilot cloning and cell culture experiments and analyzed data. D.W., D.H., B.W.K., and C.M. analyzed data and conceived experiments. C.M. conceived the study, wrote the manuscript, and supervised A.A.J.V. All authors reviewed and approved the final version of the manuscript. The authors declare no competing financial conflicts of interest.

Competing financial interests: The authors declare no competing financial conflicts of interest.

Appendix A. Supplementary Data

Supplementary data to this article can be found online at <http://dx.doi.org/10.1016/j.jmb.2017.03.015>.

Received 16 December 2016;

Received in revised form 8 March 2017;

Accepted 8 March 2017

Available online 16 March 2017

Keywords:

cytidine deaminase;

APOBEC3C;

deamination-dependent virus restriction;

retrovirus;

human immunodeficiency virus (HIV)

Present address: H. Hofmann, Robert Koch Institute, Division for HIV and other Retroviruses, Nordufer 20, 13353 Berlin, Germany.

†<http://www.hiv.lanl.gov/content/sequence/HYPERMUT/hypermut.html>

‡<http://weblogo.berkeley.edu/logo.cgi>

Abbreviations used:

A3, APOBEC3; ssDNA, single-stranded DNA; Vif, viral infectivity factor; Z, zinc-binding; SIV, simian immunodeficiency virus; agm, African green monkey; MLV, murine leukemia virus; hA3C, human A3C; VSV-G, glycoprotein of vesicular stomatitis virus; A3C.S61P, S61P mutation in human A3C; WT, wild-type; EGFP, enhanced green

fluorescent protein; HMM, higher-order molecular mass; A3C-V5, V5-tagged WT A3C; HA, hemagglutinin; A3C-HA, HA-tagged WT A3C; RIPA, radioimmunoprecipitation assay; T_d , denaturation temperature; EMSA, electrophoretic mobility shift assays; GST, glutathione S-transferase; RT, reverse transcriptase; CTD, C-terminal domain; CO-IPs, co-immuno precipitations.

References

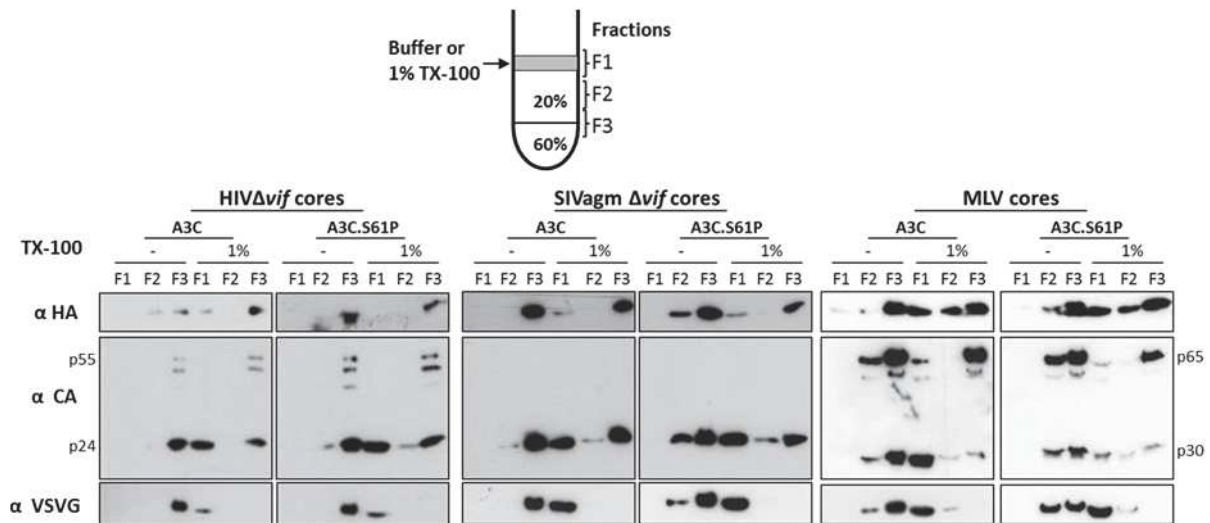
- [1] R. Goila-Gaur, K. Strebel, HIV-1 Vif, APOBEC, and intrinsic immunity, *Retrovirology* 5 (2008) 51.
- [2] R.S. Harris, J.P. Dudley, APOBECs and virus restriction, *Virology* 479–480 (2015) 131–145.
- [3] P.D. Bieniasz, Intrinsic immunity: a front-line defense against viral attack, *Nat. Immunol.* 5 (2004) 1109–1115.
- [4] M.B. Burns, L. Lackey, M.A. Carpenter, A. Rathore, A.M. Land, B. Leonard, et al., APOBEC3B is an enzymatic source of mutation in breast cancer, *Nature* 494 (2013) 366–370.
- [5] S.A. Roberts, J. Sterling, C. Thompson, S. Harris, D. Mav, R. Shah, et al., Clustered mutations in yeast and in human cancers can arise from damaged long single-strand DNA regions, *Mol. Cell* 46 (2012) 424–435.
- [6] R. Nowarski, M. Kotler, APOBEC3 cytidine deaminases in double-strand DNA break repair and cancer promotion, *Cancer Res.* 73 (2013) 3494–3498.
- [7] S. Henderson, T. Fenton, APOBEC3 genes: retroviral restriction factors to cancer drivers, *Trends Mol. Med.* 21 (2015) 274–284.
- [8] A.M. Sheehy, N.C. Gaddis, J.D. Choi, M.H. Malim, Isolation of a human gene that inhibits HIV-1 infection and is suppressed by the viral Vif protein, *Nature* 418 (2002) 646–650.
- [9] K.N. Bishop, R.K. Holmes, A.M. Sheehy, N.O. Davidson, S.J. Cho, M.H. Malim, Cytidine deamination of retroviral DNA by diverse APOBEC proteins, *Curr. Biol.* 14 (2004) 1392–1396.
- [10] H. Zhang, B. Yang, R.J. Pomerantz, C. Zhang, S.C. Arunachalam, L. Gao, The cytidine deaminase CEM15 induces hypermutation in newly synthesized HIV-1 DNA, *Nature* 424 (2003) 94–98.
- [11] H.L. Wiegand, B.P. Doehle, H.P. Bogerd, B.R. Cullen, A second human antiretroviral factor, APOBEC3F, is suppressed by the HIV-1 and HIV-2 Vif proteins, *EMBO J.* 23 (2004) 2451–2458.
- [12] Y.H. Zheng, D. Irwin, T. Kurosui, K. Tokunaga, T. Sata, B.M. Peterlin, Human APOBEC3F is another host factor that blocks human immunodeficiency virus type 1 replication, *J. Virol.* 78 (2004) 6073–6076.
- [13] J.S. Albin, W.L. Brown, R.S. Harris, Catalytic activity of APOBEC3F is required for efficient restriction of Vif-deficient human immunodeficiency virus, *Virology* 450–451 (2014) 49–54.
- [14] J.L. Smith, V.K. Pathak, Identification of specific determinants of human APOBEC3F, APOBEC3C, and APOBEC3DE and African green monkey APOBEC3F that interact with HIV-1 Vif, *J. Virol.* 84 (2010) 12,599–12,608.
- [15] B.A. Desimie, R.C. Burdick, T. Izumi, H. Doi, W. Shao, W.G. Alvord, et al., APOBEC3 proteins can copackage and comutate HIV-1 genomes, *Nucleic Acids Res.* 44 (2016) 7848–7865.
- [16] A. Burnett, P. Spearman, APOBEC3G multimers are recruited to the plasma membrane for packaging into human immunodeficiency virus type 1 virus-like particles in an RNA-dependent process requiring the NC basic linker, *J. Virol.* 81 (2007) 5000–5013.
- [17] V. Zennou, D. Perez-Caballero, H. Gottlinger, P.D. Bieniasz, APOBEC3G incorporation into human immunodeficiency virus type 1 particles, *J. Virol.* 78 (2004) 12,058–12,061.
- [18] L. Apolonia, R. Schulz, T. Curk, P. Rocha, C.M. Swanson, T. Schaller, et al., Promiscuous RNA binding ensures effective encapsidation of APOBEC3 proteins by HIV-1, *PLoS Pathog.* 11 (2015) e1004609.
- [19] H. Huthoff, M.H. Malim, Identification of amino acid residues in APOBEC3G required for regulation by human immunodeficiency virus type 1 Vif and Virion encapsidation, *J. Virol.* 81 (2007) 3807–3815.
- [20] S. Cen, F. Guo, M. Niu, J. Saadatmand, J. Defflassieux, L. Kleiman, The interaction between HIV-1 Gag and APOBEC3G, *J. Biol. Chem.* 279 (2004) 33,177–33,184.
- [21] K. Luo, B. Liu, Z. Xiao, Y. Yu, X. Yu, R. Gorelick, et al., Amino-terminal region of the human immunodeficiency virus type 1 nucleocapsid is required for human APOBEC3G packaging, *J. Virol.* 78 (2004) 11,841–11,852.
- [22] A. Schafer, H.P. Bogerd, B.R. Cullen, Specific packaging of APOBEC3G into HIV-1 virions is mediated by the nucleocapsid domain of the gag polyprotein precursor, *Virology* 328 (2004) 163–168.
- [23] E.S. Svarovskaia, H. Xu, J.L. Mbisa, R. Barr, R.J. Gorelick, A. Ono, et al., Human apolipoprotein B mRNA-editing enzyme-catalytic polypeptide-like 3G (APOBEC3G) is incorporated into HIV-1 virions through interactions with viral and nonviral RNAs, *J. Biol. Chem.* 279 (2004) 35,822–35,828.
- [24] Q. Yu, R. König, S. Pillai, K. Chiles, M. Kearney, S. Palmer, et al., Single-strand specificity of APOBEC3G accounts for minus-strand deamination of the HIV genome, *Nat. Struct. Mol. Biol.* 11 (2004) 435–442.
- [25] E.P. Browne, C. Allers, N.R. Landau, Restriction of HIV-1 by APOBEC3G is cytidine deaminase-dependent, *Virology* 387 (2009) 313–321.
- [26] R.S. Harris, K.N. Bishop, A.M. Sheehy, H.M. Craig, S.K. Petersen-Mahrt, I.N. Watt, et al., DNA deamination mediates innate immunity to retroviral infection, *Cell* 113 (2003) 803–809.
- [27] K. Strebel, APOBEC3G & HTLV-1: inhibition without deamination, *Retrovirology* 2 (2005) 37.
- [28] Y. Iwatani, D.S. Chan, F. Wang, K.S. Maynard, W. Sugiura, A.M. Gronenborn, et al., Deaminase-independent inhibition of HIV-1 reverse transcription by APOBEC3G, *Nucleic Acids Res.* 35 (2007) 7096–7108.
- [29] R.K. Holmes, F.A. Koning, K.N. Bishop, M.H. Malim, APOBEC3F can inhibit the accumulation of HIV-1 reverse transcription products in the absence of hypermutation. Comparisons with APOBEC3G, *J. Biol. Chem.* 282 (2007) 2587–2595.
- [30] J.S. Albin, R.S. Harris, Interactions of host APOBEC3 restriction factors with HIV-1 *in vivo*: implications for therapeutics, *Expert Rev. Mol. Med.* 12 (2010) e4.
- [31] C. Münk, B.E. Jensen, J. Zielonka, D. Häussinger, C. Kamp, Running loose or getting lost: how HIV-1 counters and capitalizes on APOBEC3-induced mutagenesis through its Vif protein, *Viruses* 4 (2012) 3132–3161.

- [32] J.L. Mbisa, W. Bu, V.K. Pathak, APOBEC3F and APOBEC3G inhibit HIV-1 DNA integration by different mechanisms, *J. Virol.* 84 (2010) 5250–5259.
- [33] K.N. Bishop, R.K. Holmes, M.H. Malim, Antiviral potency of APOBEC proteins does not correlate with cytidine deamination, *J. Virol.* 80 (2006) 8450–8458.
- [34] A. Mehle, B. Strack, P. Ancuta, C. Zhang, M. McPike, D. Gabuzda, Vif overcomes the innate antiviral activity of APOBEC3G by promoting its degradation in the ubiquitin-proteasome pathway, *J. Biol. Chem.* 279 (2004) 7792–7798.
- [35] A.M. Sheehy, N.C. Gaddis, M.H. Malim, The antiretroviral enzyme APOBEC3G is degraded by the proteasome in response to HIV-1 Vif, *Nat. Med.* 9 (2003) 1404–1407.
- [36] X. Yu, Y. Yu, B. Liu, K. Luo, W. Kong, P. Mao, et al., Induction of APOBEC3G ubiquitination and degradation by an HIV-1 Vif-Cul5-SCF complex, *Science* 302 (2003) 1056–1060.
- [37] R. Mariani, D. Chen, B. Schrofelbauer, F. Navarro, R. Konig, B. Bollman, et al., Species-specific exclusion of APOBEC3G from HIV-1 virions by Vif, *Cell* 114 (2003) 21–31.
- [38] H.P. Bogerd, B.P. Doehle, H.L. Wiegand, B.R. Cullen, A single amino acid difference in the host APOBEC3G protein controls the primate species specificity of HIV type 1 virion infectivity factor, *Proc. Natl. Acad. Sci. U. S. A.* 101 (2004) 3770–3774.
- [39] B. Mangeat, P. Turelli, S. Liao, D. Trono, A single amino acid determinant governs the species-specific sensitivity of APOBEC3G to Vif action, *J. Biol. Chem.* 279 (2004) 14,481–14,483.
- [40] W. Zhang, M. Huang, T. Wang, L. Tan, C. Tian, X. Yu, et al., Conserved and non-conserved features of HIV-1 and SIVagm Vif mediated suppression of APOBEC3 cytidine deaminases, *Cell. Microbiol.* 10 (2008) 1662–1675.
- [41] R.S. LaRue, V. Andresdottir, Y. Blanchard, S.G. Conticello, D. Derse, M. Emerman, et al., Guidelines for naming nonprimate APOBEC3 genes and proteins, *J. Virol.* 83 (2009) 494–497.
- [42] C. Münk, T. Beck, J. Zielonka, A. Hotz-Wagenblatt, S. Chareza, M. Battenberg, et al., Functions, structure, and read-through alternative splicing of feline APOBEC3 genes, *Genome Biol.* 9 (2008) R48.
- [43] R.S. LaRue, S.R. Jonsson, K.A. Silverstein, M. Lajoie, D. Bertrand, N. El-Mabrouk, et al., The artiodactyl APOBEC3 innate immune repertoire shows evidence for a multifunctional domain organization that existed in the ancestor of placental mammals, *BMC Mol. Biol.* 9 (2008) 104.
- [44] C. Münk, A. Willemsen, I.G. Bravo, An ancient history of gene duplications, fusions and losses in the evolution of APOBEC3 mutators in mammals, *BMC Evol. Biol.* 12 (2012) 71.
- [45] Q. Chen, X. Xiao, A. Wolfe, X.S. Chen, The *in vitro* biochemical characterization of an HIV-1 restriction factor APOBEC3F: importance of loop 7 on both CD1 and CD2 for DNA binding and deamination, *J. Mol. Biol.* 428 (2016) 2661–2670.
- [46] S. Kitamura, H. Ode, M. Nakashima, M. Imahashi, Y. Naganawa, T. Kurosawa, et al., The APOBEC3C crystal structure and the interface for HIV-1 Vif binding, *Nat. Struct. Mol. Biol.* 19 (2012) 1005–1010.
- [47] B. Stauch, H. Hofmann, M. Perkovic, M. Weisel, F. Koppitz, K. Cichutek, et al., Model structure of APOBEC3C reveals a binding pocket modulating ribonucleic acid interaction required for encapsidation, *Proc. Natl. Acad. Sci. U. S. A.* 106 (2009) 12,079–12,084.
- [48] A.A. Vasudevan, S.H. Smits, A. Hoppner, D. Haussinger, B.W. Koenig, C. Münk, Structural features of antiviral DNA cytidine deaminases, *Biol. Chem.* 394 (2013) 1357–1370.
- [49] M.M. Ahasan, K. Wakae, Z. Wang, K. Kitamura, G. Liu, M. Koura, et al., APOBEC3A and 3C decrease human papillomavirus 16 pseudovirion infectivity, *Biochem. Biophys. Res. Commun.* 457 (2015) 295–299.
- [50] T.F. Baumert, C. Rosler, M.H. Malim, F. von Weizsacker, Hepatitis B virus DNA is subject to extensive editing by the human deaminase APOBEC3C, *Hepatology* 46 (2007) 682–689.
- [51] R. Suspene, D. Guetard, M. Henry, P. Sommer, S. Wain-Hobson, J.P. Vartanian, Extensive editing of both hepatitis B virus DNA strands by APOBEC3 cytidine deaminases *in vitro* and *in vivo*, *Proc. Natl. Acad. Sci. U. S. A.* 102 (2005) 8321–8326.
- [52] M.A. Langlois, R.C. Beale, S.G. Conticello, M.S. Neuberger, Mutational comparison of the single-domain APOBEC3C and double-domain APOBEC3F/G anti-retroviral cytidine deaminases provides insight into their DNA target site specificities, *Nucleic Acids Res.* 33 (2005) 1913–1923.
- [53] J.P. Vartanian, D. Guetard, M. Henry, S. Wain-Hobson, Evidence for editing of human papillomavirus DNA by APOBEC3 in benign and precancerous lesions, *Science* 320 (2008) 230–233.
- [54] R. Suspene, M.M. Aynaud, S. Koch, D. Padeloup, M. Labetoulle, B. Gaertner, et al., Genetic editing of herpes simplex virus 1 and Epstein-Barr herpesvirus genomes by human APOBEC3 cytidine deaminases in culture and *in vivo*, *J. Virol.* 85 (2011) 7594–7602.
- [55] Q. Yu, D. Chen, R. Konig, R. Mariani, D. Unutmaz, N.R. Landau, APOBEC3B and APOBEC3C are potent inhibitors of simian immunodeficiency virus replication, *J. Biol. Chem.* 279 (2004) 53,379–53,386.
- [56] M. Bonvin, F. Achermann, I. Greeve, D. Stroka, A. Keogh, D. Inderbitzin, et al., Interferon-inducible expression of APOBEC3 editing enzymes in human hepatocytes and inhibition of hepatitis B virus replication, *Hepatology* 43 (2006) 1364–1374.
- [57] J.F. Hultquist, J.A. Lengyel, E.W. Refsland, R.S. LaRue, L. Lackey, W.L. Brown, et al., Human and rhesus APOBEC3D, APOBEC3F, APOBEC3G, and APOBEC3H demonstrate a conserved capacity to restrict Vif-deficient HIV-1, *J. Virol.* 85 (2011) 11,220–11,234.
- [58] E.W. Refsland, J.F. Hultquist, R.S. Harris, Endogenous origins of HIV-1 G-to-A hypermutation and restriction in the nonpermissive T cell line CEM2n, *PLoS Pathog.* 8 (2012) e1002800.
- [59] J.F. Hultquist, M. Binka, R.S. LaRue, V. Simon, R.S. Harris, Vif proteins of human and simian immunodeficiency viruses require cellular CBFbeta to degrade APOBEC3 restriction factors, *J. Virol.* 86 (2012) 2874–2877.
- [60] K. Bourara, T.J. Liegler, R.M. Grant, Target cell APOBEC3C can induce limited G-to-a mutation in HIV-1, *PLoS Pathog.* 3 (2007) 1477–1485.
- [61] A. Jarmuz, A. Chester, J. Bayliss, J. Gisbourne, I. Dunham, J. Scott, et al., An anthropoid-specific locus of orphan C to U RNA-editing enzymes on chromosome 22, *Genomics* 79 (2002) 285–296.
- [62] E.W. Refsland, M.D. Stenglein, K. Shindo, J.S. Albin, W.L. Brown, R.S. Harris, Quantitative profiling of the full APOBEC3 mRNA repertoire in lymphocytes and tissues: implications for HIV-1 restriction, *Nucleic Acids Res.* 38 (2010) 4274–4284.

- [63] M. Abdel-Mohsen, R.A. Raposo, X. Deng, M. Li, T. Liegler, E. Sinclair, et al., Expression profile of host restriction factors in HIV-1 elite controllers, *Retrovirology* 10 (2013) 106.
- [64] Z. Zhang, Q. Gu, A.A. Jaguva Vasudevan, M. Jeyaraj, S. Schmidt, J. Zielonka, et al., Vif proteins from diverse human immunodeficiency virus/simian immunodeficiency virus lineages have distinct binding sites in A3C, *J. Virol.* 90 (2016) 10,193–10,208.
- [65] J.D. Salter, R.P. Bennett, H.C. Smith, The APOBEC protein family: united by structure, divergent in function, *Trends Biochem. Sci.* 41 (2016) 578–594.
- [66] M.F. Bohn, S.M. Shandilya, J.S. Albin, T. Kouno, B.D. Anderson, R.M. McDougale, et al., Crystal structure of the DNA cytosine deaminase APOBEC3F: the catalytically active and HIV-1 Vif-binding domain, *Structure* 21 (2013) 1042–1050.
- [67] M. Nakashima, H. Ode, T. Kawamura, S. Kitamura, Y. Naganawa, H. Awazu, et al., Structural insights into HIV-1 Vif-APOBEC3F interaction, *J. Virol.* 90 (2016) 1034–1047.
- [68] K.K. Siu, A. Sultana, F.C. Azimi, J.E. Lee, Structural determinants of HIV-1 Vif susceptibility and DNA binding in APOBEC3F, *Nat. Commun.* 4 (2013) 2593.
- [69] K.M. Chen, E. Harjes, P.J. Gross, A. Fahmy, Y. Lu, K. Shindo, et al., Structure of the DNA deaminase domain of the HIV-1 restriction factor APOBEC3G, *Nature* 452 (2008) 116–119.
- [70] A. Furukawa, T. Nagata, A. Matsugami, Y. Habu, R. Sugiyama, F. Hayashi, et al., Structure and real-time monitoring of the enzymatic reaction of APOBEC3G which is involved in anti-HIV activity, *Nucleic Acids Symp. Ser. (Oxf.)* (2009) 87–88.
- [71] L.G. Holden, C. Prochnow, Y.P. Chang, R. Bransteitter, L. Chelico, U. Sen, et al., Crystal structure of the anti-viral APOBEC3G catalytic domain and functional implications, *Nature* 456 (2008) 121–124.
- [72] A.V. Horn, S. Klawitter, U. Held, A. Berger, A.A. Vasudevan, A. Bock, et al., Human LINE-1 restriction by APOBEC3C is deaminase independent and mediated by an ORF1p interaction that affects LINE reverse transcriptase activity, *Nucleic Acids Res.* 42 (2014) 396–416.
- [73] J. Li, Y. Chen, M. Li, M.A. Carpenter, R.M. McDougale, E.M. Luengas, et al., APOBEC3 multimerization correlates with HIV-1 packaging and restriction activity in living cells, *J. Mol. Biol.* 426 (2014) 1296–1307.
- [74] J.F. Kreisberg, W. Yonemoto, W.C. Greene, Endogenous factors enhance HIV infection of tissue naive CD4 T cells by stimulating high molecular mass APOBEC3G complex formation, *J. Exp. Med.* 203 (2006) 865–870.
- [75] H. Huthoff, F. Autore, S. Gallois-Montbrun, F. Fraternali, M.H. Malim, RNA-dependent oligomerization of APOBEC3G is required for restriction of HIV-1, *PLoS Pathog.* 5 (2009) e1000330.
- [76] J.E. Wedekind, R. Gillilan, A. Janda, J. Krucinska, J.D. Salter, R.P. Bennett, et al., Nanostructures of APOBEC3G support a hierarchical assembly model of high molecular mass ribonucleoprotein particles from dimeric subunits, *J. Biol. Chem.* 281 (2006) 38,122–38,126.
- [77] S. Gallois-Montbrun, B. Kramer, C.M. Swanson, H. Byers, S. Lynham, M. Ward, et al., Antiviral protein APOBEC3G localizes to ribonucleoprotein complexes found in P bodies and stress granules, *J. Virol.* 81 (2007) 2165–2178.
- [78] S.L. Kozak, M. Marin, K.M. Rose, C. Bystrom, D. Kabat, The anti-HIV-1 editing enzyme APOBEC3G binds HIV-1 RNA and messenger RNAs that shuttle between polysomes and stress granules, *J. Biol. Chem.* 281 (2006) 29,105–29,119.
- [79] X. Wang, P.T. Dolan, Y. Dang, Y.H. Zheng, Biochemical differentiation of APOBEC3F and APOBEC3G proteins associated with HIV-1 life cycle, *J. Biol. Chem.* 282 (2007) 1585–1594.
- [80] A.A. Jaguva Vasudevan, M. Perkovic, Y. Bulliard, K. Cichutek, D. Trono, D. Haussinger, et al., Prototype foamy virus bet impairs the dimerization and cytosolic solubility of human APOBEC3G, *J. Virol.* 87 (2013) 9030–9040.
- [81] Y. Iwatani, H. Takeuchi, K. Strebel, J.G. Levin, Biochemical activities of highly purified, catalytically active human APOBEC3G: correlation with antiviral effect, *J. Virol.* 80 (2006) 5992–6002.
- [82] R. Suspene, M. Henry, S. Guillot, S. Wain-Hobson, J.P. Vartanian, Recovery of APOBEC3-edited human immunodeficiency virus G→A hypermutants by differential DNA denaturation PCR, *J. Gen. Virol.* 86 (2005) 125–129.
- [83] M. Ooms, A. Krikoni, A.K. Kress, V. Simon, C. Münk, APOBEC3A, APOBEC3B, and APOBEC3H haplotype 2 restrict human T-lymphotropic virus type 1, *J. Virol.* 86 (2012) 6097–6108.
- [84] B. Beggel, C. Münk, M. Daumer, K. Hauck, D. Häussinger, T. Lengauer, et al., Full genome ultra-deep pyrosequencing associates G-to-A hypermutation of the hepatitis B virus genome with the natural progression of hepatitis B, *J. Viral Hepat.* 20 (2013) 882–889.
- [85] C.M. Holtz, H.A. Sadler, L.M. Mansky, APOBEC3G cytosine deamination hotspots are defined by both sequence context and single-stranded DNA secondary structure, *Nucleic Acids Res.* 41 (2013) 6139–6148.
- [86] R. Nowarski, E. Britan-Rosich, T. Shiloach, M. Kotler, Hypermutation by intersegmental transfer of APOBEC3G cytidine deaminase, *Nat. Struct. Mol. Biol.* 15 (2008) 1059–1066.
- [87] V.B. Soros, W. Yonemoto, W.C. Greene, Newly synthesized APOBEC3G is incorporated into HIV virions, inhibited by HIV RNA, and subsequently activated by RNase H, *PLoS Pathog.* 3 (2007) e15.
- [88] W.M. McDougall, H.C. Smith, Direct evidence that RNA inhibits APOBEC3G ssDNA cytidine deaminase activity, *Biochem. Biophys. Res. Commun.* 412 (2011) 612–617.
- [89] A. Rathore, M.A. Carpenter, O. Demir, T. Ikeda, M. Li, N.M. Shaban, et al., The local dinucleotide preference of APOBEC3G can be altered from 5'-CC to 5'-TC by a single amino acid substitution, *J. Mol. Biol.* 425 (2013) 4442–4454.
- [90] B. Polevoda, W.M. McDougall, B.N. Tun, M. Cheung, J.D. Salter, A.E. Friedman, et al., RNA binding to APOBEC3G induces the disassembly of functional deaminase complexes by displacing single-stranded DNA substrates, *Nucleic Acids Res.* 43 (2015) 9434–9445.
- [91] D. Marino, M. Perkovic, A. Hain, A.A. Jaguva Vasudevan, H. Hofmann, K.M. Hanschmann, et al., APOBEC4 enhances the replication of HIV-1, *PLoS One* 11 (2016) e0155422.
- [92] A. Marx, M. Galilee, A. Alian, Zinc enhancement of cytidine deaminase activity highlights a potential allosteric role of loop-3 in regulating APOBEC3 enzymes, *Sci. Rep.* 5 (2015) 18,191.
- [93] N.M. Shaban, K. Shi, M. Li, H. Aihara, R.S. Harris, 1.92 angstrom zinc-free APOBEC3F catalytic domain crystal structure, *J. Mol. Biol.* 428 (2016) 2307–2316.
- [94] A. Furukawa, K. Sugase, R. Morishita, T. Nagata, T. Kodaki, A. Takaori-Kondo, et al., Quantitative analysis of location- and sequence-dependent deamination by APOBEC3G

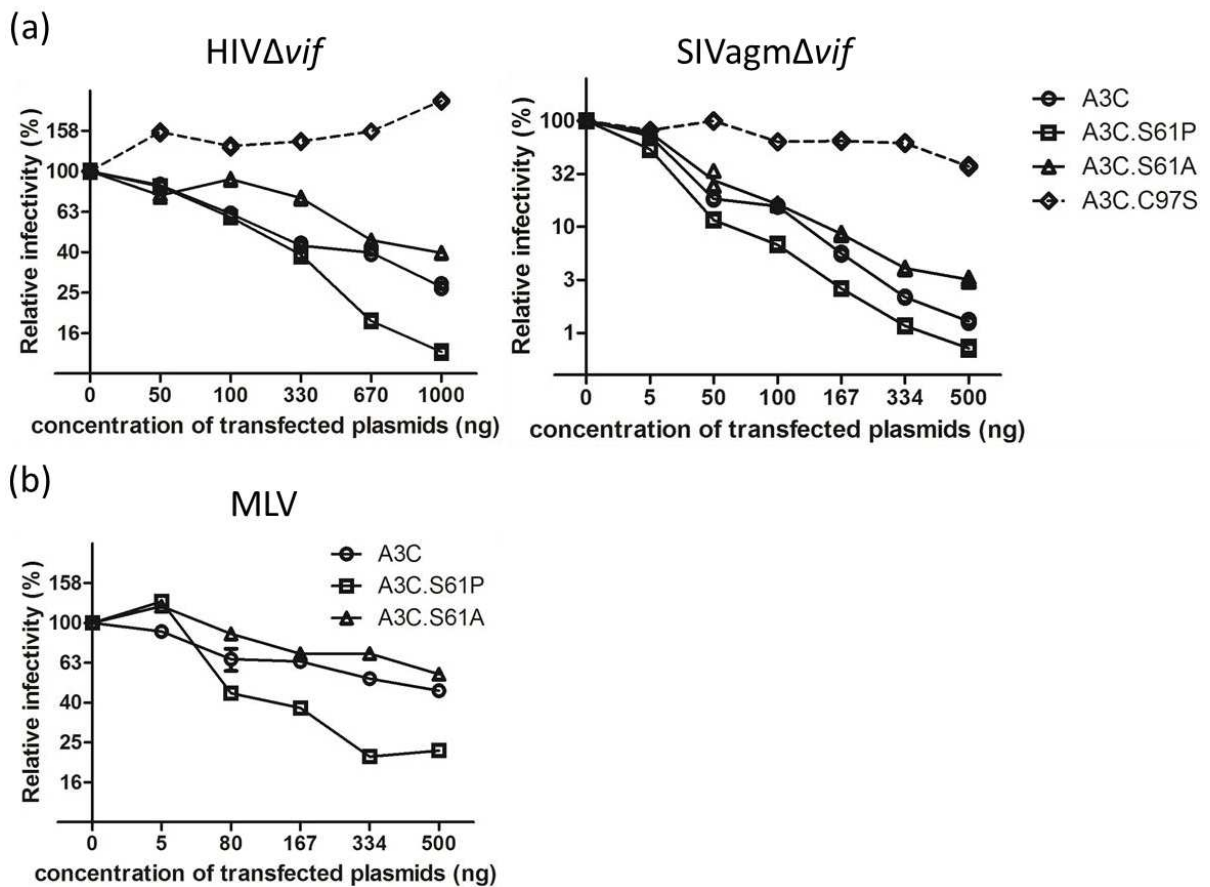
- using real-time NMR spectroscopy, *Angew. Chem. Int. Ed. Eng.* 53 (2014) 2349–2352.
- [95] M. Perkovic, S. Schmidt, D. Marino, R.A. Russell, B. Stauch, H. Hofmann, et al., Species-specific inhibition of APOBEC3C by the prototype foamy virus protein bet, *J. Biol. Chem.* 284 (2009) 5819–5826.
- [96] K.M. Rose, M. Marin, S.L. Kozak, D. Kabat, Regulated production and anti-HIV type 1 activities of cytidine deaminases APOBEC3B, 3F, and 3G, *AIDS Res. Hum. Retrovir.* 21 (2005) 611–619.
- [97] B.P. Doehle, A. Schafer, B.R. Cullen, Human APOBEC3B is a potent inhibitor of HIV-1 infectivity and is resistant to HIV-1 Vif, *Virology* 339 (2005) 281–288.
- [98] B.P. Doehle, A. Schafer, H.L. Wiegand, H.P. Bogerd, B.R. Cullen, Differential sensitivity of murine leukemia virus to APOBEC3-mediated inhibition is governed by virion exclusion, *J. Virol.* 79 (2005) 8201–8207.
- [99] T. Wang, W. Zhang, C. Tian, B. Liu, Y. Yu, L. Ding, et al., Distinct viral determinants for the packaging of human cytidine deaminases APOBEC3G and APOBEC3C, *Virology* 377 (2008) 71–79.
- [100] S. Nair, S. Sanchez-Martinez, X. Ji, A. Rein, Biochemical and biological studies of mouse APOBEC3, *J. Virol.* 88 (2014) 3850–3860.
- [101] C.J. Wittkopp, M.B. Adolph, L.I. Wu, L. Chelico, M. Emerman, A single nucleotide polymorphism in human APOBEC3C enhances restriction of lentiviruses, *PLoS Pathog.* 12 (2016) e1005865.
- [102] F. Navarro, B. Bollman, H. Chen, R. Konig, Q. Yu, K. Chiles, et al., Complementary function of the two catalytic domains of APOBEC3G, *Virology* 333 (2005) 374–386.
- [103] S. Harjes, W.C. Solomon, M. Li, K.M. Chen, E. Harjes, R.S. Harris, et al., Impact of H216 on the DNA binding and catalytic activities of the HIV restriction factor APOBEC3G, *J. Virol.* 87 (2013) 7008–7014.
- [104] Y. Dang, A. Abudu, S. Son, E. Harjes, P. Spearman, H. Matsuo, et al., Identification of a single amino acid required for APOBEC3 antiretroviral cytidine deaminase activity, *J. Virol.* 85 (2011) 5691–5695.
- [105] S.C. Li, N.K. Goto, K.A. Williams, C.M. Deber, Alpha-helical, but not beta-sheet, propensity of proline is determined by peptide environment, *Proc. Natl. Acad. Sci. U. S. A.* 93 (1996) 6676–6681.
- [106] K. Yutani, S. Hayashi, Y. Sugisaki, K. Ogasahara, Role of conserved proline residues in stabilizing tryptophan synthase alpha subunit: analysis by mutants with alanine or glycine, *Proteins* 9 (1991) 90–98.
- [107] M. Alias, S. Ayuso-Tejedor, J. Fernandez-Recio, C. Cativiela, J. Sancho, Helix propensities of conformationally restricted amino acids. Non-natural substitutes for helix breaking proline and helix forming alanine, *Org. Biomol. Chem.* 8 (2010) 788–792.
- [108] R.S. Prajapati, M. Das, S. Sreeramulu, M. Sirajuddin, S. Srinivasan, V. Krishnamurthy, et al., Thermodynamic effects of proline introduction on protein stability, *Proteins* 66 (2007) 480–491.
- [109] S.R. Trevino, S. Schaefer, J.M. Scholtz, C.N. Pace, Increasing protein conformational stability by optimizing beta-turn sequence, *J. Mol. Biol.* 373 (2007) 211–218.
- [110] D.W. Carr, A. Fujita, C.L. Stentz, G.A. Liberty, G.E. Olson, S. Narumiya, Identification of sperm-specific proteins that interact with A-kinase anchoring proteins in a manner similar to the type II regulatory subunit of PKA, *J. Biol. Chem.* 276 (2001) 17,332–17,338.
- [111] X.-D. Feng, H. Tang, B. Han, B. Lv, C. Li, Enhancing the thermostability of β -glucuronidase by rationally redesigning the catalytic domain based on sequence alignment strategy, *Ind. Eng. Chem. Res.* 55 (19) (2016) 5474–5483, <http://dx.doi.org/10.1021/acs.iecr.6b00535>.
- [112] A.M. Gilles, I. Saint-Girons, M. Monnot, S. Fermandjian, S. Michelson, O. Barzu, Substitution of a serine residue for proline-87 reduces catalytic activity and increases susceptibility to proteolysis of *Escherichia coli* adenylate kinase, *Proc. Natl. Acad. Sci. U. S. A.* 83 (1986) 5798–5802.
- [113] L.R. Xu, X. Yan, M. Luo, Y.X. Guan, S.J. Yao, Preparation, characterization and refolding *in vitro* of a recombinant human cyclophilin A mutant: effect of a single Pro/Ser substitution on cyclophilin A structure and properties, *Biotechnol. Prog.* 24 (2008) 302–310.
- [114] M. Bock, K.N. Bishop, G. Towers, J.P. Stoye, Use of a transient assay for studying the genetic determinants of Fv1 restriction, *J. Virol.* 74 (2000) 7422–7430.
- [115] A. Schambach, H. Wodrich, M. Hildinger, J. Bohne, H.G. Krausslich, C. Baum, Context dependence of different modules for posttranscriptional enhancement of gene expression from retroviral vectors, *Mol. Ther.* 2 (2000) 435–445.
- [116] T. Dull, R. Zufferey, M. Kelly, R.J. Mandel, M. Nguyen, D. Trono, et al., A third-generation lentivirus vector with a conditional packaging system, *J. Virol.* 72 (1998) 8463–8471.
- [117] A. Bähr, A. Singer, A. Hain, A.A. Vasudevan, M. Schilling, J. Reh, et al., Interferon but not MxB inhibits foamy retroviruses, *Virology* 488 (2016) 51–60.
- [118] H. Muckenfuss, M. Hamdorf, U. Held, M. Perkovic, J. Lower, K. Cichutek, et al., APOBEC3 proteins inhibit human LINE-1 retrotransposition, *J. Biol. Chem.* 281 (2006) 22,161–22,172.
- [119] R.A. Russell, H.L. Wiegand, M.D. Moore, A. Schafer, M.O. McClure, B.R. Cullen, Foamy virus Bet proteins function as novel inhibitors of the APOBEC3 family of innate antiretroviral defense factors, *J. Virol.* 79 (2005) 8724–8731.
- [120] M. Simm, M. Shahabuddin, W. Chao, J.S. Allan, D.J. Volsky, Aberrant Gag protein composition of a human immunodeficiency virus type 1 vif mutant produced in primary lymphocytes, *J. Virol.* 69 (1995) 4582–4586.
- [121] R. Goila-Gaur, M.A. Khan, E. Miyagi, S. Kao, K. Strelb, Targeting APOBEC3A to the viral nucleoprotein complex confers antiviral activity, *Retrovirology* 4 (2007) 61.
- [122] P.P. Rose, B.T. Korber, Detecting hypermutations in viral sequences with an emphasis on G \rightarrow A hypermutation, *Bioinformatics* 16 (2000) 400–401.
- [123] G.E. Crooks, G. Hon, J.M. Chandonia, S.E. Brenner, WebLogo: a sequence logo generator, *Genome Res.* 14 (2004) 1188–1190.

SUPPLEMENTARY FIGURES



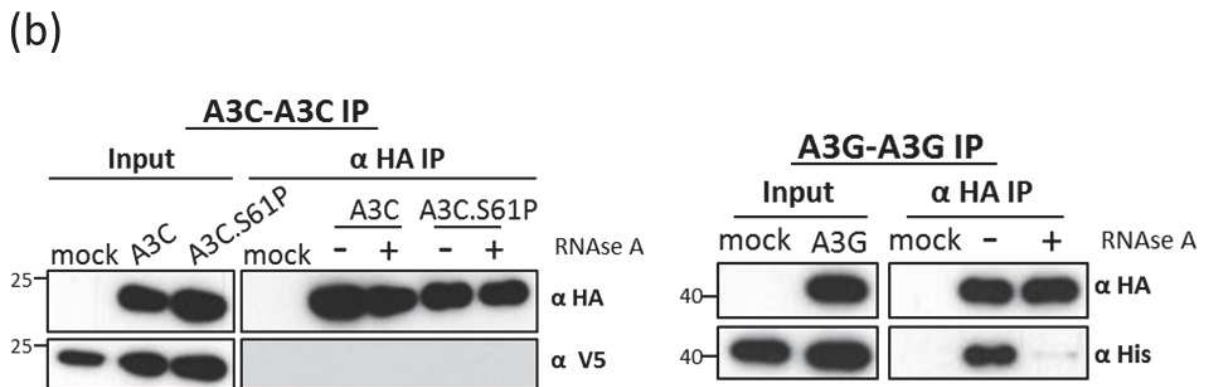
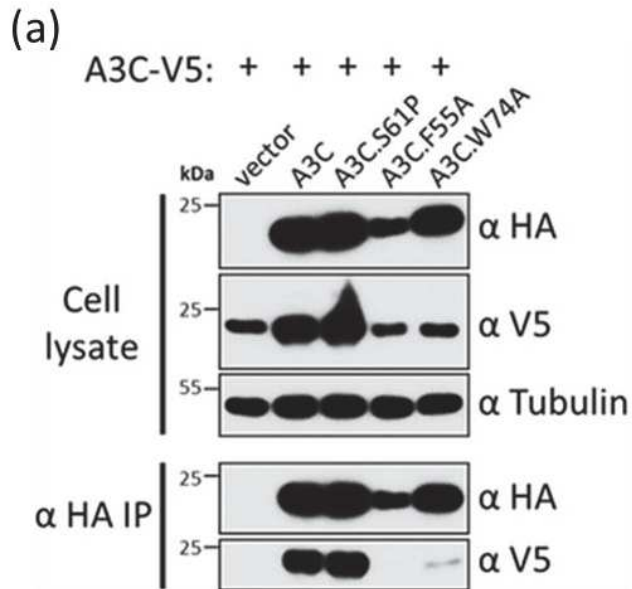
Suppl. Fig S1. Viral core localization of A3C and A3C.S61P

HIV-1 Δ vif, SIVagm and MLV virions were produced with A3C or A3C.S61P and the viral cores were isolated by 20%/60% sucrose step gradient centrifugation, where 1% triton X-100 overlaid on the top (see methods). Three fractions (F1, F2, and F3) as shown in the cartoon, were collected from the top of the gradient. F1 contains soluble proteins, F2 is a buffer fraction of 20% sucrose that separates soluble proteins from virus particles or viral cores; F3 includes the interphase of 20%:60% sucrose where viral particles (not TX-100) and viral cores (TX-100) accumulate. An aliquot of gradient fractions were subjected to immunoblot analysis, HIV and SIV capsids (anti-p24/27), MLV capsid (anti-p30), A3C (anti HA) and VSVG (anti VSVG) were detected with respective antibodies. TX-100 denotes Triton X-100. “ α ” represent anti-antibody.



Suppl. Fig S2. Dose dependent antiretroviral activity of A3C mutants

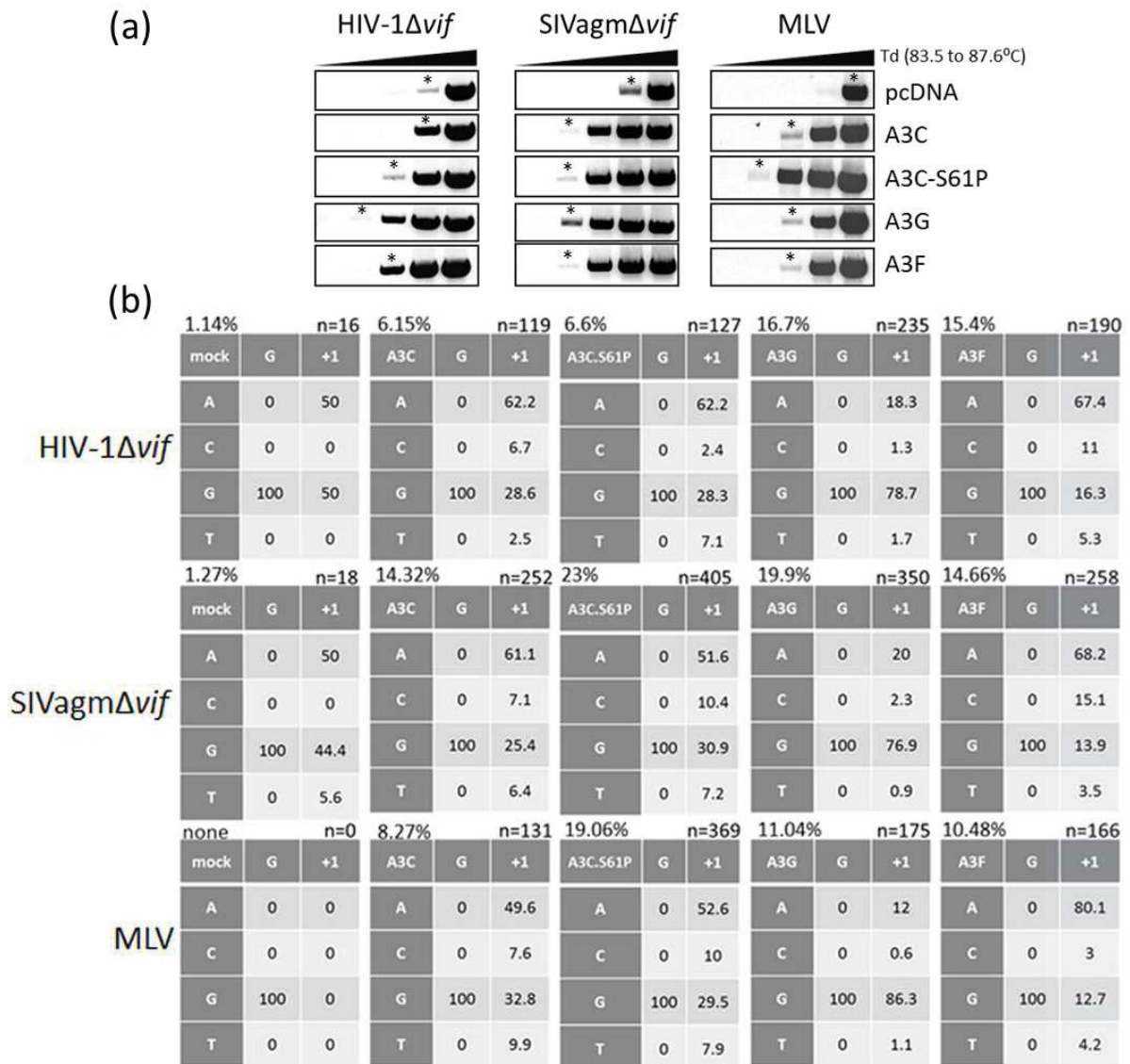
(a) HIV-1 Δ vif, SIV Δ vif reporter viruses were produced in the presence of increasing concentration of expression plasmids encoding A3C, A3C.S61P, A3C.S61A or A3C.C97S and similarly (b) MLV virions produced together with A3C, A3C.S61P, or A3C.S61A. Infectivities of (RT normalized) equal amounts of viruses, relative to the virus did not contain A3C, were determined by quantification of luciferase activity in 293T cells. Please note that, SIV Δ vif and MLV were restricted potently with 500 ng of transfected A3C. Values are means plus standard deviations (error bars) for three independent experiments. Unpaired *t* tests were computed to determine whether differences between vector and each A3 protein reach the level of statistical significance. All of the subjects had a significance of $p < 0.0001$.



Suppl. Fig S3. Protein-protein interaction experiments using two different buffers

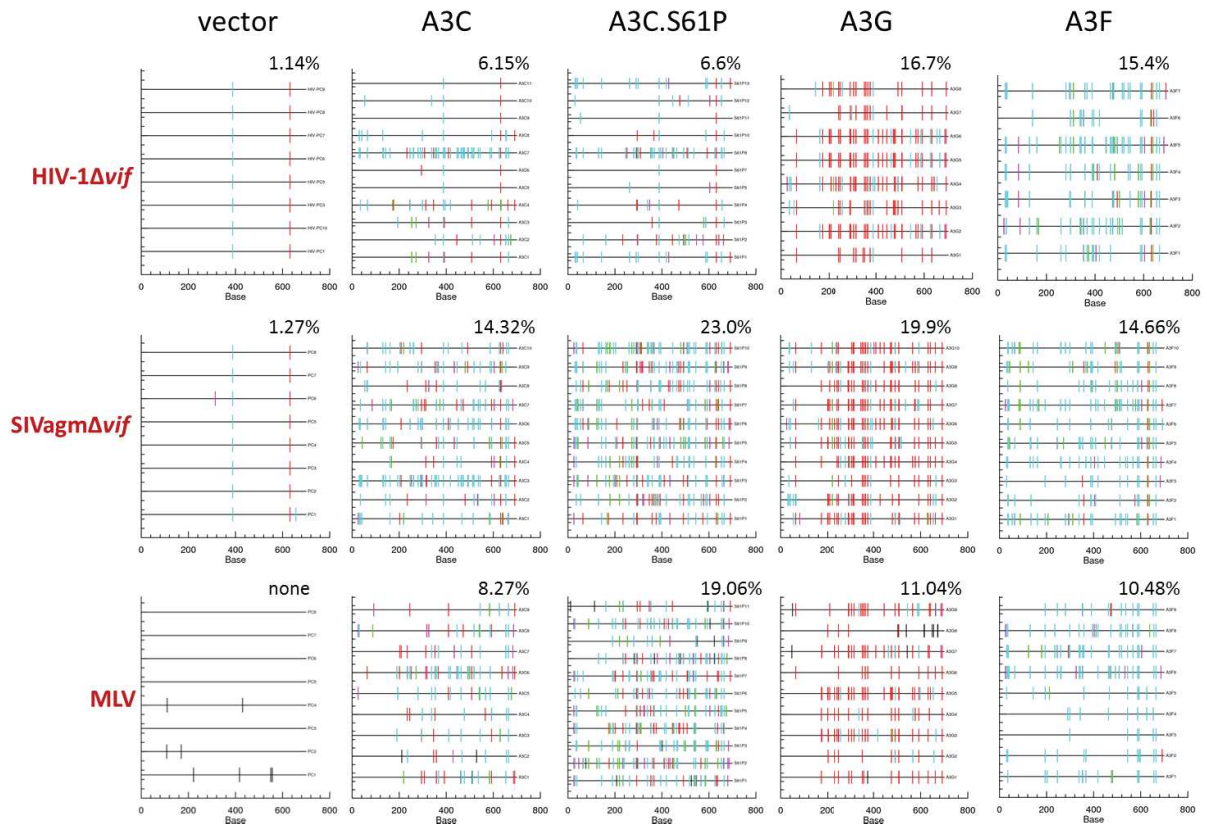
RIPA buffer: Carboxy terminal V5 tagged A3C construct were co-transfected together with an expression vector coding HA tagged A3C, A3C.S61P, A3C.F55A and A3C.W74A. Anti HA immunoprecipitates (IP) and the cell lysates were subjected to Immunoblot analysis using anti-HA and anti-V5-antibodies. Dimerization mutants A3C.F55A and A3C.W74A served as a control for this experiment. Tubulin served as loading control. “ α ” represent anti-antibody.

Triton X-100 buffer: As described in the procedure, we performed this Co-IP with and without RNaseA treatments, after binding the HA tagged protein to the beads. Cell lysates (Input) and Anit HA IP fractions were analyzed by immunblotting with respective antibodies. As a control for RNase bridged interaction, we added a parallel A3G-A3G interaction experiment.



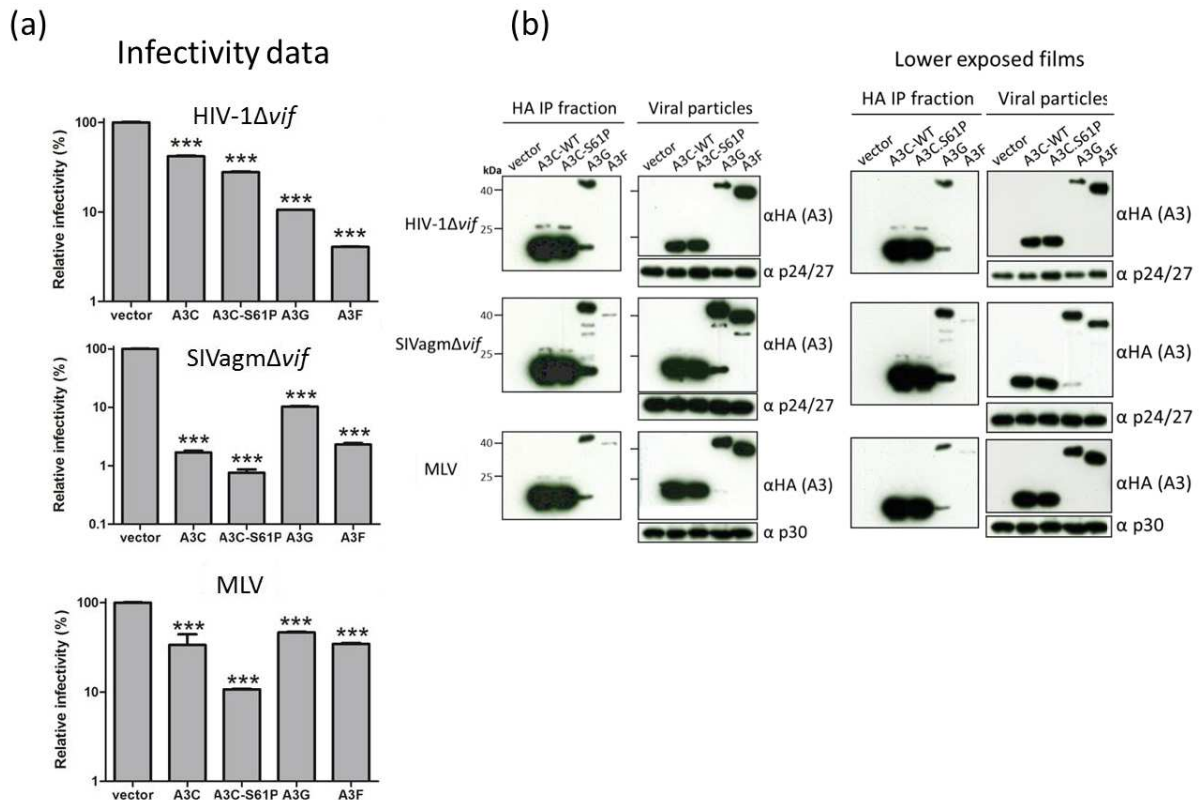
Suppl. Fig S4. A3 induced editing in HIV-1, SIVagm and MLV genomes

(a) 3D PCR: HIV-1Δvif, SIVΔvif and MLV virions produced together with pcDNA vector or A3C, A3C.S61P, A3G and A3F was used to infect 293T cells. Total DNA was extracted and a 714 bp segment of reporter viral DNA was selectively amplified using 3D PCR (Td=denaturation temperature). PCR products were stained with ethidium bromide. The infectivity data of these viruses is shown in Suppl. Fig. S6A. (b) To determine the amount mutation conferred by A3 proteins, PCR products from the lowest denaturing temperature, shown in (a) were cloned (marked with an asterisk (*)) and a number of independent clones were sequenced and analyzed. The overall mutation load (G→A) was given in the top, left side of each table, as 'x%'. The mutation rate of G→A transition (as percentage) were presented according to its local dinucleotide context. 'n' denotes the total number of independent G→A mutations found in independent sequences. The extensive deamination profiles of the relative positions of the G→A transition mutations were presented in suppl. Fig. S5.



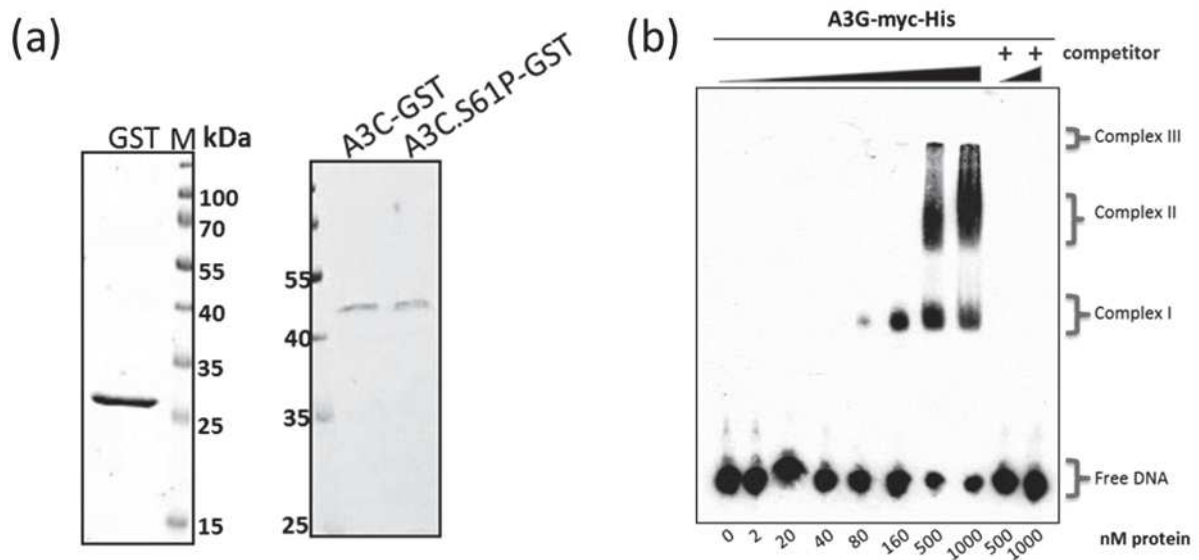
Suppl. Fig S5. A3C mediated SIVagm and MLV viral DNA hypermutation is enhanced by A3C.S61P

The data presented in Suppl. Fig. S4 were analyzed and the mutation pattern is presented using hypermut tool (note: identical clones were omitted). The percentage of G-to-A changes for each sample was indicated. Each sequence is given as a horizontal line. Mutations were denoted as small vertical lines. Red, cyan, magenta, green and black colored lines represent the GG-to-AG, GA-to-AA, GT-to-AT, GC-to-AC, and non-G-to-A mutations, respectively. Dinucleotide specific GG-to-AG and GA-to-AA of A3C and A3C.S61P derived mutations were presented as histogram in Fig. 6B.



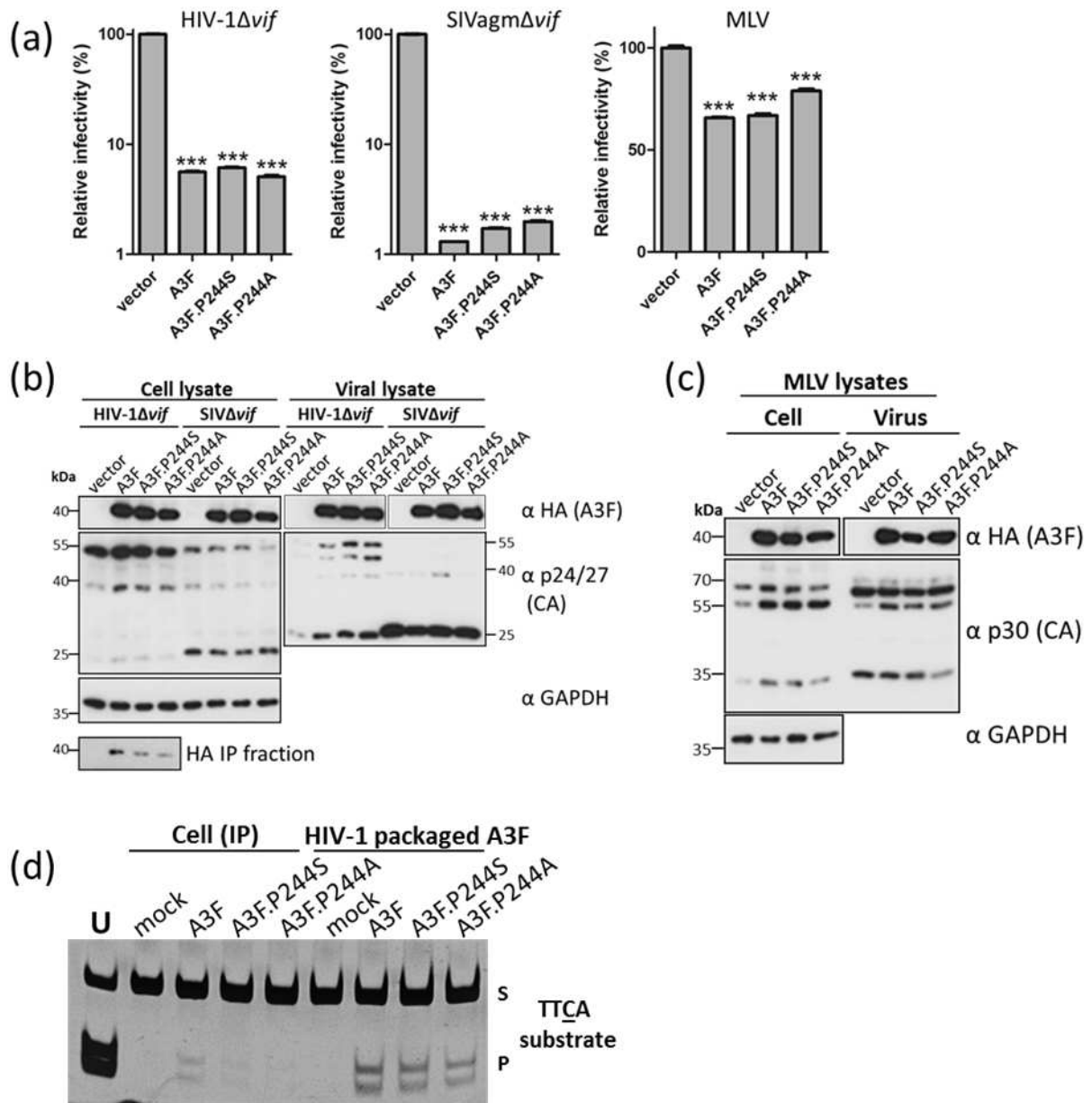
Suppl. Fig S6. Infectivity and immunoblot data of viruses used in *in vitro* activity assay and 3D PCR

(a) HIV-1 Δ vif, SIV Δ vif and MLV reporter viruses were produced in the presence and absence of A3s. Infectivities of (RT normalized) equal amounts of viruses, relative to the virus that did not contain A3, were determined by quantification of luciferase activity in 293T cells. Values are means plus standard deviations (error bars) for three independent experiments. Unpaired *t* tests were computed to determine whether differences between vector and each A3 protein reach the level of statistical significance. Asterisks represent statistically significant differences: ***, $p < 0.0001$. (b) Immunoblot shows the amount of immunoprecipitated (IP) HA tagged A3 proteins from cell lysate and encapsidated proteins from retroviral particles (please note that A3F from IP was not yielded enough protein due to less pipetted affinity beads, and not included in the *in vitro* deamination assay). HIV and SIV capsids (anti-p24/27), MLV capsid (anti-p30), A3C (anti HA) were detected with respective antibodies and GAPDH served as a loading control. “ α ” represent anti-antibody.



Suppl. Fig S7. Purity of recombinant proteins and EMSA with cell-derived A3G-myc-His

(a) Recombinantly produced and affinity purified GST, A3C-GST and A3C.S61P-GST. Purity of the proteins was determined by staining the gel with Coomassie blue. Prestained protein ladder (M) indicate the molecular mass. (b) EMSA using A3G-myc-His from 293T cells. Indicated amounts of protein (at the bottom of blot) were titrated with 10 nM of DNA. Presence of competitor DNA (unlabeled 80 nt DNA used in deamination assay, 200-fold molar excess added) used to demonstrate specific binding of protein to DNA being causative for the shift.



Suppl. Fig S8. Effect of proline 244 to serine/alanine mutation in A3F

(a) HIV-1 Δ vif, SIV Δ vif and MLV reporter viruses were produced in the presence of vector only, A3F, A3F.P244S or A3F.P244A. Infectivities of (RT normalized) equal amounts of viruses, relative to the virus did not contain A3, were determined by quantification of luciferase activity in 293T cells. Values are means plus standard deviations (error bars) for three independent reads. Unpaired *t* tests were computed to determine whether differences between vector and each A3 protein reach the level of statistical significance. Asterisks represent statistically significant differences: ***, *p* < 0.0001. (b) Immunoblot shows the amount A3 in cell and viral lysates of HIV-1 Δ vif, SIV Δ vif and (c) MLV. HIV and SIV capsids

(anti-p24/27), MLV capsid (anti-p30), A3C (anti HA) were detected with respective antibodies and GAPDH served as a loading control. "α" represent anti-antibody. (d) Deamination of activity of A3F from cell lysate (expressed together with HIV-1 proteins) and viral particles were performed using the substrates containing specific TTCA motif. To enrich the A3 from cell lysate, HA tagged A3 proteins were immunoprecipitated and the HA-beads bound to the proteins were used in the activity assay. Virions were concentrated, lysed in a mild lysis buffer and equal amount of lysate used for the assay. The amount of A3 used here was shown in the HIV-1Δ*vif* panel of immunoblots in (b). RNase treatment was included; oligonucleotide containing uracil (U) instead of cytidine served as a marker to denote the migration of deaminated product after restriction enzyme cleavage. S: substrate, P: product.

**ELSEVIER LICENSE
TERMS AND CONDITIONS**

May 04, 2017

This Agreement between Ananda Ayyappan Jaguva Vasudevan ("You") and Elsevier ("Elsevier") consists of your license details and the terms and conditions provided by Elsevier and Copyright Clearance Center.

License Number	4101940303283
License date	May 04, 2017
Licensed Content Publisher	Elsevier
Licensed Content Publication	Journal of Molecular Biology
Licensed Content Title	Enhancing the Catalytic Deamination Activity of APOBEC3C Is Insufficient to Inhibit Vif-Deficient HIV-1
Licensed Content Author	Ananda Ayyappan Jaguva Vasudevan, Henning Hofmann, Dieter Willbold, Dieter Häussinger, Bernd W. Koenig, Carsten Münk
Licensed Content Date	21 April 2017
Licensed Content Volume	429
Licensed Content Issue	8
Licensed Content Pages	21
Start Page	1171
End Page	1191
Type of Use	reuse in a thesis/dissertation
Portion	full article
Format	both print and electronic
Are you the author of this Elsevier article?	Yes
Will you be translating?	No
Order reference number	
Title of your thesis/dissertation	"Dazzling APOBEC3 DNA deaminases: A mechanistic study on how A3A, A3C and A3G act on retroviruses and being counteracted by their foe"
Expected completion date	Dec 2017
Estimated size (number of pages)	140
Elsevier VAT number	GB 494 6272 12
Requestor Location	Ananda Ayyappan Jaguva Vasudevan Universitätstr.1 AG Münk Building: 23.12.U1.85 Duesseldorf, NRW 40225 Germany Attn: Ananda Ayyappan Jaguva Vasudevan
Publisher Tax ID	GB 494 6272 12
Total	0.00 EUR
Terms and Conditions	

Chapter III

A Naturally Occurring APOBEC3C from Sooty Mangabey Potently Inhibits Human Immunodeficiency Virus Replication

Status : Manuscript under preparation

Own contribution to this work:

- Complete execution of experimental procedures
- Writing of the manuscript

A Naturally Occurring APOBEC3C from Sooty Mangabey Potently Inhibits Human Immunodeficiency Virus Replication

Ananda Ayyappan Jaguva Vasudevan¹, Zhang Zeli¹, Dieter Häussinger¹ and Carsten Münk^{1,*}

¹Clinic for Gastroenterology, Hepatology, and Infectiology, Medical Faculty, Heinrich-Heine-University Düsseldorf, Moorenstr. 5, 40225 Düsseldorf, Germany.

Short title: Sooty Mangabey A3C inhibits HIV-1

*Corresponding author:

Clinic for Gastroenterology, Hepatology, and Infectiology, Medical Faculty, Heinrich-Heine-University Düsseldorf, Building 23.12.U1.82, Moorenstr. 5, 40225 Düsseldorf, Germany, Tel: +49 (0) 211-81-10887, Fax: +49 (0) 211-81-18752, E-mail: carsten.muenk@med.uni-duesseldorf.de

ABSTRACT

The APOBEC3 (A3) family of single stranded DNA deaminases defends hosts from retroviruses, including human immunodeficiency virus (HIV)-1 lacking viral infectivity factor (*vif*) (HIV-1 Δ *vif*). A3 catalyzes the dC to dU deamination in the viral genome, causing hypermutation that abrogates the virus. Human APOBEC3C (hA3C) is known as a strong restriction factor of Vif-deficient simian immunodeficiency virus (SIV Δ *vif*), but exhibit a weak inhibition against HIV-1 Δ *vif*. The exact reason for this specificity of A3C's antiviral function remains unknown.

Here we show that A3C from a primate, sooty mangabey (smmA3C), potently restricts the replication of HIV-1 in a deamination-dependent manner. The viral incorporation tendency of smmA3C was lower than that of hA3C, but still effectively inhibited HIV-1. Moreover, like hA3C, smmA3C formed ribonucleoprotein complexes that are resistant to RNase, and possessed similar proteins self-association features. Given the protein sequence similarity, we tested chimeric proteins of human/smm A3C, and identified that replacing the N-terminal region of hA3C with that of smmA3C drastically enhances hA3C's antiviral activity against HIV-1 Δ *vif*. Our results suggest that protein-dimerization of smmA3C in the cytoplasm is not essential for its antiviral and mutagenic activities. We propose that smmA3C is an attractive target for further structural investigations, because smmA3C is not targeted by HIV-1 Vif and represses HIV-1 Δ *vif* to a level similar to A3G.

Keywords: APOBEC3C, Sooty Mangabey, cytidine deaminase, Deamination-dependent virus restriction, human immunodeficiency virus (HIV)

INTRODUCTION

The APOBEC3 (A3) family of single-stranded (ss) DNA cytidine deaminases builds an intrinsic immune defense against retroviruses, retrotransposons, and other viral pathogens (Goila-Gaur and Strebel, 2008, Harris and Dudley, 2015, Stavrou and Ross, 2015). There are seven human A3s that possess either single (A3A, A3C and A3H) or double (A3B, A3D, A3F and A3G) zinc (Z)-coordinating DNA cytosine deaminase motif, His-X-Glu-X₂₃₋₂₈-Pro-Cys-X₂₋₄-Cys (where X indicates a non-conserved position) (Jarmuz et al., 2002, Münk et al., 2012b, LaRue et al., 2008). A3G was identified as a factor capable of restricting infection of HIV-1 lacking Vif (viral infectivity factor) protein in non-permissive T cell lines whose biochemical properties and biological functions were extensively studied (Sheehy et al., 2002, Zhang et al., 2003, Bishop et al., 2004, Salter et al., 2016, Vasudevan et al., 2013).

A3 encapsidation into the viral particles is crucial for virus inhibition (Zennou et al., 2004, Luo et al., 2004, Svarovskaia et al., 2004, Huthoff and Malim, 2007, Schafer et al., 2004, Burnett and Spearman, 2007). During reverse transcription, viral core associated A3 enzymes can deaminate the cytidines (dC) on the retroviral ssDNA into uridines (dU). These base modifications in the minus DNA strand cause coding changes and premature stop codons in the plus-strand viral genome (dG→dA hypermutation), which impair or suppress viral infectivity (Browne et al., 2009, Harris et al., 2003, Yu et al., 2004b, Mangeat et al., 2003, Zhang et al., 2003, Harris and Dudley, 2015). In addition to the mutagenic activity of the viral-incorporated A3 enzyme, deaminase-independent mechanisms of restriction were also manifested by impeding reverse transcription or inhibiting DNA integration (Iwatani et al., 2007, Holmes et al., 2007, Münk et al., 2012a, Bishop et al., 2006, Mbisa et al., 2010, Strebel, 2005). To counteract A3 mediated inhibition, lentiviruses evolved the viral infectivity factor (Vif) protein that physically interacts with A3s to target them for polyubiquitination and proteasomal degradation, subsequently deplete the cellular A3s (Mehle et al., 2004, Sheehy et al., 2003, Yu et al., 2003). These A3-Vif interactions are often species-specific (Mariani et al., 2003, Bogerd et al., 2004, Mangeat et al., 2004, Zhang et al., 2008, Smith and Pathak, 2010).

A3D, A3F, A3G and A3H were shown to restrict HIV-1 lacking *vif* (HIV-1 Δ *vif*) (Harris and Dudley, 2015, Smith and Pathak, 2010, Dang et al., 2006, Wiegand et al., 2004, Zheng et al., 2004, Hultquist et al., 2011). Recently, mutation signatures resulting from the catalytic activity of A3s (especially A3A and A3B) were reported in several cancer types (Burns et al., 2013, Roberts et al., 2013) (for a review, see: (Henderson and Fenton, 2015)). Human A3C, the subject of the current study, is known to act as a potent inhibitor of SIV, and can limit the infectivity of herpes simplex virus, certain human papillomaviruses, murine leukemia virus and hepatitis B virus (Yu et al., 2004a, Langlois et al., 2005, Suspene et al., 2005a, Baumert et al., 2007, Vartanian et al., 2008, Stauch et al., 2009, Ahasan et al., 2015, Suspene et al., 2011). But the restrictive role of A3C on HIV-1 is marginal and there are several contradictory findings regarding its viral packaging and cytidine deamination activity (Hultquist et al., 2011, Yu et al., 2004a, Hultquist et al., 2012, Bonvin et al., 2006, Refsland et al., 2012). Interestingly, A3C is expressed ubiquitously in lymphoid cells (Jarmuz et al., 2002, Yu et al., 2004a, Bourara et al., 2007, Refsland et al., 2010). mRNA expression levels of A3C were found to be induced in HIV-infected CD4⁺ T lymphocytes (Hultquist et al., 2011, Yu et al., 2004a), and significantly elevated in elite controllers with respect to ART-suppressed individuals (Abdel-Mohsen et al., 2013). A3C was found to moderately deaminate HIV-1 if expressed in target cells of the virus and rather increased viral diversity than caused restriction (Bourara et al., 2007).

Recently, we have shown that increasing the catalytic activity of A3C by serine to proline substitution at position 61 was not sufficient to inhibit HIV-1 Δ *vif* (Jaguva Vasudevan et al., 2017). It is still unclear why A3C can potently restrict SIV, but not HIV-1 Δ *vif* although the wild-type enzyme possesses reasonable catalytic activity and encapsidate efficiently into retroviral particles (Jaguva Vasudevan et al., 2017). Here we identified an orthologous primate A3C from sooty mangabey (*Cercocebus torquatus lunulatus*) that restricted HIV-1 to the similar extent or higher than human A3G. Human and sooty mangabey A3C was further characterized with a focus on possibly identifying a mechanism that differently regulated to inhibit HIV-1 Δ *vif* infectivity.

RESULTS

smmA3C strongly restricts HIV-1 Δ vif

To determine whether the A3C from orthologous species can potently restrict HIV-1 Δ vif propagation, we produced HIV-1 Δ vif luciferase reporter virus particles with A3C from human, rhesus macaque, sooty mangabey (smm), chimpanzees (cpz), African green monkey (agm) or human A3G. Viral particles were pseudotyped with the glycoprotein of vesicular stomatitis virus (VSV-G) and normalized by RT activity. The luciferase enzyme assay of infected cells was quantified two days post infection. Figure 1A shows the level of relative infectivity of HIV-1 Δ vif in presence of tested A3Cs and A3G. Human, rhesus, chimpanzee, and African green monkey A3C proteins similarly reduced the relative infectivity of HIV-1 Δ vif to 60%. Conversely, smmA3C inhibited HIV-1 Δ vif replication by above one order of magnitude. Human A3G served as a positive control. Expression of the A3 in viral vector producing cells showed that smmA3C and agmA3C was lower expressed than A3Cs from human, rhesus, and cpz (Figure 1B). Viral incorporation of smmA3C was found to be very similar to hA3G, but much weaker compared to hA3C (suppl. Fig. 1 and Fig. 2).

It was recently reported that smmA3C resist HIV-1 Vif mediated depletion (Zhang et al., 2016). Because smmA3C restriction of HIV-1 Δ vif was similar or slightly stronger than restriction by A3G (Fig. 1A), we analyzed its DNA editing capacity during infection by 3D-PCR on the viral genome (Jaguva Vasudevan et al., 2017, Suspene et al., 2005b). DNA in which the cytosines are deaminated by A3s contains less GC base pairs than non-edited DNA, resulting in a lower melting temperature during PCR. Therefore, successful amplification at lower denaturation temperature (Td) (83.5 - 87.6°C) in 3D-PCR is an indicator of A3-mutagenized sequences. 3D-PCR amplification with samples of cells infected with viruses encapsidating hA3C, rhA3C, cpzA3C, or agmA3C formed amplicons until Td 86.3°C, whereas HIV-1 Δ vif/smA3C amplicons formed at 84.2°C. In control reactions using virions produced with A3G PCR amplification was detectable at lower Td (85.2°C and weakly at 84.2°C) (Fig. 1C). Importantly, with the vector control sample (no A3), PCR amplicons could be amplified only at the higher Td (87.6°C). The sequencing of the PCR products of smmA3C samples formed at 84.2°C showed common G-to-A hypermutations (data not shown). Together we

conclude that smmA3C inhibits HIV-1 by cytidine deamination causing hypermutation on the viral DNA.

Identification of a specific region in smmA3C involved in deamination-mediated HIV-1 Δ vif restriction

The amino acid sequence identity and similarity between human and sooty mangabey A3C are 77.9% and 90%, respectively (alignment is shown in suppl. Fig. S2). To possibly identify the distinct determinants, ten different hA3C/smA3C chimeras were constructed (Zhang et al., 2016) (Fig. 2A). We first tested the anti-HIV-1 Δ vif activity of hA3C, smmA3C and the chimeras. Viral particles with different chimeras were produced and their infectivity was tested. As shown in Fig. 2B, chimeras C2 and C4 and C8 strongly reduced the relative infectivity of HIV-1 Δ vif, especially C2 (hA3C with 36 residue exchange with smmA3C at the N-terminus) inhibited HIV-1 Δ vif replication by about two orders of magnitude. C6 and C9 reduced 72% of the viral infectivity, compared to vector control. All other chimeras showed the antiviral activity similar or lesser to hA3C.

Next, we determined the intracellular expression and virion incorporation efficiency of the chimeras by immunoblotting. Chimeras C2, C3, C5, C7, and C9 that contain residues 37 to 76 (marked as a box in Fig. 2A) of hA3C were stably produced (perhaps with more solubility) than C1, C4, C6, and C10. Specifically, C2 was expressed higher than hA3C and C10 was below the detection limit (Fig. 2C). Chimeras, C2, C4, C6, C7, and C9 were found to be encapsidated in HIV-1 Δ vif (Fig. 2C, viral lysate). Notably, C3 and C5 were less efficiently packed into viral particles although they had higher intracellular levels, conversely, C6 might be produced lesser but its viral incorporation is higher than C3 or C5. Taken together, C2 and C4 were the chimeras potentially restricting HIV-1 Δ vif, C6, in contrast, lost the antiviral activity, suggesting that the N-terminal region of smmA3C is crucially involved in the antiviral mechanism, but might not be the only determinant. A second domain is indicated because C6 did not repress HIV-1 Δ vif, in spite of having the N-terminal region and half of smmA3C. In addition, chimera C8 that contained more than half of the smmA3C region worked better than C6 in restricting HIV-1 Δ vif. We speculate that the parts of the hA3C residues in C2 and

C4 that are absent in C6 complemented the restriction activity of these chimeras. In addition, the low-level inhibitory activity of C8 compared to C2/C4 and the loss of C10 intracellular expression together clearly indicate the vital role of C-terminal regions of smmA3C for expression and antiviral activity.

Catalytic deamination activity of smmA3C correlates with antiviral function

To characterize whether the anti-HIV-1 activity of the hA3C/smA3C chimeras were due to the differences in catalytic activity, we compared their *in vitro* deamination activity. Transiently transfected hA3C, smmA3C and their chimeras 293T lysates were used as input in this assay (Fig. 3A). In addition, we have included a catalytic inactive mutant hA3C.C97S and an activity enhanced mutant hA3C.S61P as controls (Fig. 3B). We adapted the PCR-based *in vitro* deamination assay, which was shown to be effective in determining specific A3's activity from various samples (Nowarski et al., 2008, Jaguva Vasudevan et al., 2013, Marino et al., 2016, Jaguva Vasudevan et al., 2017). This assay depends on a site-specific cytidine to uridine deamination in an 80 nucleotide (nt) ssDNA by A3. A subsequent PCR generates a double stranded DNA, replaces the uridine with thymidine, and thus generates a new restriction site. The efficiency of the restriction enzyme digestion is monitored using a similar 80 nt ssDNA containing uridine instead of a cytidine in the hotspot. The substrate nucleotide containing TTCA was reported as an optimal A3C target motif, used for this assay (Jaguva Vasudevan et al., 2017). smmA3C elicited the stronger product formation compared to hA3C and hA3C.S61P, a mutant of hA3C that has enhanced deamination activity (Jaguva Vasudevan et al., 2017) (Fig. 3A and 3B). Remarkably, the deamination by C2 and C4 resulted in more cleavage product than the deamination by smmA3C (Fig. 3A). The catalytic activity of the chimeras can be expressed as [C2 and C4] >>> [C6 and C8] >> [C7 and C9]. Together these data suggest that the smmA3C mediated restriction of HIV-1 Δ vif is due to its robust deamination function.

smmA3C and hA3C forms intracellular RNase resistant oligomers

A3s are nucleic acid binding proteins, earlier studies suggested that RNA-dependent multimerization of A3G was essential for efficient viral encapsidation and it was shown that the cellular higher order molecular mass complexes (HMM) of A3G, found as ribonucleoprotein complexes (RNP) (Kreisberg et al., 2006, Huthoff et al., 2009, Vasudevan et al., 2013, Burnett and Spearman, 2007, Wedekind et al., 2006, Gallois-Montbrun et al., 2007, Kozak et al., 2006, Li et al., 2014). RNA bridged A3G multimers are sensitive to RNase treatment, which can form low molecular mass complexes (LMM) from HMM in presence of RNase (Huthoff et al., 2009, Jaguva Vasudevan et al., 2013), and A3G-HMMs are stabilized by both protein-protein and protein-RNA interactions (Li et al., 2014, Wedekind et al., 2006, Iwatani et al., 2006, Jaguva Vasudevan et al., 2013, Huthoff et al., 2009). We and others have reported that hA3C, (like A3F) can form unique RNA stabilized HMM complexes that are insensitive to RNase treatment (Jaguva Vasudevan et al., 2017, Li et al., 2014, Wang et al., 2007). In presence of RNase hA3C-HMM did not yield low LMM, but sedimented as insoluble protein pellet, suggesting A3C multimers are not RNA-bridged, but the overall stability of A3C-HMM complexes were RNA-dependent (Jaguva Vasudevan et al., 2017).

To test whether smmA3C possess similar inherent features as hA3C, we performed velocity sucrose gradient centrifugation. hA3C and smmA3C from the cell lysates, distributed throughout the gradient and were largely found in HMM complexes, as tracked with ribosomal S6 protein (Fig. 4A). Treatment with RNase reduced the amount of higher order molecules of both hA3C and smmA3C in the maximum sucrose fractions and did not form low molecular mass complexes but instead elevated as aggregates (Fig. 5A, and protein pellet not shown).

smmA3C and hA3C did not self-associate in the cytosol

Unlike A3G, hA3C does not form protein-protein complexes bridged by RNA (Huthoff et al., 2009, Jaguva Vasudevan et al., 2017, Jaguva Vasudevan et al., 2013) but the functional importance of dimerization of hA3C was reported earlier (Horn et al., 2014, Stauch et al.,

2009). Recently it was confirmed that cellular hA3C lysed in the mild reagent did not pull down its partner (Jaguva Vasudevan et al., 2017, Adolph et al., 2017), possibly suggesting different forms of hA3C localized in cytoplasm and nucleus.

To test whether the stronger antiviral activity of smmA3C is mediated protein self-association of cytoplasmic smmA3C, we performed pull-down assays. 293T cells were co-transfected with plasmids encoding V5-tagged smmA3C (smmA3C-V5) plus HA-tagged smmA3C (smmA3C-HA) or the empty vector. Using experimental (mild-lysis) conditions as followed before (Jaguva Vasudevan et al., 2017) smmA3C-HA was pulled down with anti-HA beads. The A3C bound beads were then split into two halves for RNase treatment. We found no co-precipitation of smmA3C-V5 by smmA3C, irrespective of RNase treatment (Fig. 4B). Parallel experiments with hA3C and hA3G were served as negative and positive controls, respectively for this CO-IP (Fig. 4B). Alternatively, we performed CO-IPs using radioimmunoprecipitation assay (RIPA) buffer. First, we treated the cell lysates with and without RNase and proceeded with anti-HA CO-IP. As expected, hA3C-HA co-precipitated hA3C-V5 independent of RNase (Fig. 4C). Interestingly, in absence of RNase treatment, smmA3C-HA did not co-precipitate smmA3C-V5 to a level similar to hA3C, but this could be improved very much by RNase treatment (Fig. 4C).

MATERIALS AND METHODS

Cell culture. HEK293T cells were maintained in Dulbecco's high-glucose modified Eagle's medium (Biochrom, Berlin, Germany), supplemented with 10% fetal bovine serum (FBS), 2 mM L-glutamine, 50 units/ml penicillin, and 50 µg/ml streptomycin at 37°C in a humidified atmosphere of 5% CO₂.

Plasmids. The HIV-1 packaging plasmid pMDLg/pRRE encodes *gag-pol*, and the pRSV-Rev for the HIV-1 *rev* (Dull et al., 1998). The HIV-1 vector pSIN.PPT.CMV.Luc.IRES.GFP expresses the

firefly luciferase and GFP reported previously (Bähr et al., 2016). HIV-1 based viral vectors were pseudotyped using the pMD.G plasmid that encodes the glycoprotein of VSV (VSV-G). All APOBEC3 constructs described here were cloned in pcDNA3.1 (+) with a C-terminal hemagglutinin (HA) tag. The smmA3C expression plasmid was generated by exon assembly from the genomic DNA of white-crowned mangabey (*Cercocebus torquatus lunulatus*), and the cloning strategy for smmA3C and the chimeras of hA3C/smmA3C plasmid construction was recently described (Zhang et al., 2016). The expression vector for A3G-HA was generously provided by Nathaniel R. Landau. Expression constructs hA3C, rhA3C, cpzA3C, agmA3C and A3C point mutants A3C.C97S were described before (Jaguva Vasudevan et al., 2017, Perkovic et al., 2009, Stauch et al., 2009). smmA3C with C-terminal V5 tag was cloned using following primers using following primers forward 5'-EcoRI-ATGAATTCGCCACCATGAATCCACAGATCAGAAAC and reverse 5'-NotI-ATGCGGCCGCCACTCGAGAATCTCCTGTAGGCGTC.

Virus production and isolation. 293T cells were transiently transfected using Lipofectamine LTX and plus reagent (Invitrogen, Karlsruhe, Germany) with appropriate combination of HIV-1 viral vectors (600 ng pMDLg/pRRE, 600 ng pSIN.PPT.CMV.Luc.IRES.GFP, 250 ng pRSV-Rev, 150 ng pMD.G with 600 ng A3 plasmid or pcDNA3.1, unless otherwise mentioned) together with A3 plasmid or as a vector control pcDNA3.1 empty vector in 6 well plate. 48 h post-transfection, virion containing supernatants were collected and concentrated by layering on 20% sucrose cushion and centrifuged for 4 h at 14,800 rpm. Viral particles were re-suspended in mild lysis buffer (50 mM Tris (pH 8), 1 mM PMSF, 10% glycerol, 0.8% NP-40, 150 mM NaCl and 1X complete protease inhibitor).

Luciferase-based infectivity assay. HIV-1 luciferase reporter viruses were used to transduce HEK293T cells. Prior infection, the amount of reverse transcriptase (RT) in the viral particles was determined by RT assay using Cavid HS kit Lenti RT (Cavid Tech, Uppsala, Sweden). Normalized RT amount equivalent viral supernatants were transduced. 48 h later, luciferase activity was measured using SteadyliteHTS luciferase reagent substrate (Perkin Elmer,

Rodgau, Germany) in black 96-well plates on a Berthold MicroLumat Plus luminometer (Berthold Detection Systems, Pforzheim, Germany). Transductions were done in triplicate and at least three independent experiments were performed.

Immunoblots. Transfected 293T Cells were washed with phosphate-buffered saline (PBS) and lysed in radioimmunoprecipitation assay buffer (RIPA, 25 mM Tris (pH 8.0), 137 mM NaCl, 1% glycerol, 0.1% SDS, 0.5% sodium deoxycholate, 1% Nonidet P-40, 2 mM EDTA, and protease inhibitor cocktail set III [Calbiochem, Darmstadt, Germany].) 20 min on ice. Lysates were clarified by centrifugation (20 min, 14800 rpm, 4°C). Samples (cell/viral lysate) were boiled at 95°C for 5 min with Roti load reducing loading buffer (Carl 726 Roth, Karlsruhe, Germany) and subjected to SDS-PAGE followed by transfer (Semi-Dry Transfer Cell, Biorad, Munich, Germany) to a PVDF membrane (Merck Millipore, Schwalbach, Germany). Membranes were blocked with skimmed milk solution and probed with appropriate primary antibody, mouse anti-hemagglutinin (anti-HA) antibody (1:7,500 dilution, MMS-101P, Covance, Münster, Germany); mouse α -V5 antibody (1: 4000 dilution; Serotec); goat anti-GAPDH (C-terminus, 1:15,000 dilution, Everest Biotech, Oxfordshire, UK); mouse anti- α -tubulin antibody (1:4,000 dilution, clone B5-1-2; Sigma-Aldrich, Taufkirchen, Germany), mouse anti-capsid p24/p27 MAb AG3.0 (Simm et al., 1995) (1:250 dilution, NIH AIDS Reagents); rabbit anti S6 ribosomal protein (5G10; 1:10³ dilution in 5% BSA, Cell Signaling Technology, Leiden, The Netherlands). Secondary Abs.: anti-mouse (NA931V), anti-rabbit (NA934V) horseradish peroxidase (1:10⁴ dilution, GE Healthcare) and anti-goat IgG-HRP (1:10⁴ dilution, sc-2768, Santa Cruz biotechnology, Heidelberg, Germany). Signals were visualized using ECL chemiluminescent reagent (GE Healthcare).

Differential DNA denaturation (3D) PCR. 293T cells were cultured in the 6-well plates and infected with DNase I treated viruses for 12 hours. Cells were harvested and washed in PBS, the total DNA was isolated using DNeasy DNA isolation kit (Qiagen, Hilden, Germany). A 714-bp fragment of the luciferase gene was amplified using the primers 5'-GATATGTGGATTTTCGAGTCGTC-3' and 5'-GTCATCGTCTTTCCGTGCTC-3'. For selective

amplification of the hypermutated products, the PCR denaturation temperature was lowered stepwise from 87.6°C to 83.5°C (83.5°C, 84.2°C, 85.2°C, 86.3°C, 87.6°C) using a gradient thermocycler. The PCR parameters were as follows: (i) 95°C for 5 min; (ii) 40 cycles, with 1 cycle consisting of 83.5°C to 87.6°C for 30 s, 55°C for 30 s, 72°C for 1 min; (iii) 10 min at 72°C. PCRs were performed with Dream Taq DNA polymerase (Thermo Fisher Scientific).

Co-immunoprecipitation assay for A3C self-association in cells. We performed this experiment as we reported previously (Stauch et al., 2009) by including the smmA3C and hA3C. To test whether RNase A treatment can influence the A3C-A3C interaction, the cell lysate made with RIPA buffer were split into two halves, in which one portion was treated with RNase A (70 µg/ml) and incubated for 30 min at 37°C followed by 30 min at room temperature and the immunoprecipitation assay was performed as described in (Stauch et al., 2009).

Alternatively, we also did an independent CO-IP using a procedure used before (Huthoff et al., 2009, Jaguva Vasudevan et al., 2013). The difference in this method is the use of mild lysis buffer containing 50 mM Tris (pH 8), 1 mM PMSF, 10% glycerol, 0.8% NP-40, 150 mM NaCl and 1X complete protease inhibitor. At 24 h post-transfection, cells were harvested and lysed with lysis buffer. The cleared lysates were incubated with 20 µl anti-HA affinity matrix beads for 2 h at 4°C, with end-over-end rotation. After binding, the beads were washed twice, with lysis buffer, and half-portions of the samples were aliquoted to new tubes. RNase A (70 µg/ml) was added to one aliquot of the sample and incubated at 37°C for 10 min and at 22°C for 40 min. Samples were further washed thrice with lysis buffer. CO-IP products were eluted by boiling beads in SDS gel loading buffer at 95°C for 5 min. A parallel A3G-A3G CO-IP was performed as a control.

Sucrose density gradient centrifugation. 293T cells were transfected with expression plasmids for 1 µg A3C or smmA3C. After 24 hours, cells were lysed with lysis buffer (0.7% NP-40, 100 mM NaCl, 50 mM potassium acetate, 10 mM EDTA, 10 mM Tris, pH 7.4, and complete protease inhibitor cocktail [Merck Calbiochem]) and then clarified by centrifugation for 10 min at 162 X *g* followed by a short spin at 18,000 X *g* for 30 s. A half

portion of the sample was aliquoted to a new tube, to which RNase A (Thermo Fisher Scientific) (70 µg/ml) was added and incubated for 30 min at 37°C. Samples were then overlaid on top of a 10%-15%-20%-30%-50% sucrose step gradient in lysis buffer and centrifuged for 45 min at 163,000X *g* at 4°C in a MLS-50 rotor (Beckman Coulter, Fullerton, CA) (Jaguva Vasudevan et al., 2013, Huthoff et al., 2009). After centrifugation, the samples were sequentially removed from the top of the gradient, resolved by SDS-PAGE, and analyzed by immunoblotting with anti-HA and anti-S6 antibodies to detect A3C and endogenous S6 ribosomal protein (Horn et al., 2014), respectively.

***In vitro* DNA cytidine deamination assay.** A3 proteins expressed in transfected 293T cells used as input. Cell lysates were prepared with mild lysis buffer after 48 h post plasmid transfection. Deamination reactions were performed as described (Nowarski et al., 2008, Jaguva Vasudevan et al., 2013) in a 10 µL reaction volume containing 25 mM Tris pH 7.0, 2 µL of cell lysate and 100 fmol single-stranded DNA substrate (TTCA: 5'-GGATTGGTTGGTTATTTGTATAAGGAAGGTGGATTGAAGGTTCAAGAAGGTGATGGAAGTTATGTTGGTAGATTGATGG). Samples were treated with 50 µg/ml RNase A (Thermo Fisher Scientific). Reactions were incubated for at least 1 h at 37°C and the reaction was terminated by boiling at 95°C for 5 min. One fmol of the reaction mixture was used for PCR amplification Dream Taq polymerase (Thermo Fisher Scientific) 95°C for 3 min, followed by 30 cycles of 61°C for 30 s and 94°C for 30 s) using primers forward 5'-GGATTGGTTGGTTATTTGTATAAGGA and reverse 5'-CCATCAATCTACCAAACATAACTTCCA. PCR products were digested with MseI (NEB, Frankfurt/Main, Germany), and resolved on 15% PAGE, stained with ethidium bromide (7.5 µg/ml). As a positive control substrate oligonucleotides with TTUA instead of TTCA were used to control the restriction enzyme digestion (Jaguva Vasudevan et al., 2017).

Statistical analysis. Data were represented as the mean with SD in all bar diagrams. Statistically significant differences between two groups were analyzed using the unpaired Student's t-test with GraphPad Prism version 5 (GraphPad Software, San Diego, CA, USA). A minimum *p* value of 0.05 was considered as statistically significant.

ACKNOWLEDGMENTS

This work was supported Heinz-Ansmann foundation for AIDS research (to CM). We thank Jörg Zielonka for help and Wioletta Hörschken for excellent technical assistance. We thank Neeltje Kootstra, Nathaniel R. Landau, Bryan R Cullen, Jonathan Stoye, Harald Wodrich for reagents. The following reagent was obtained through the NIH AIDS Research and Reference Reagent Program, Division of AIDS, NIAID, NIH: a monoclonal antibody to HIV-1 p24 (AG3.0), from Jonathan Allan.

AUTHOR CONTRIBUTIONS

AAJV performed all of the experiments, conceived the study, analyzed data and wrote the manuscript while ZZ contributed pilot cell culture experiments and analyzed data. DH and CM analyzed data. CM conceived and supervised the study, wrote the manuscript. All authors reviewed and approved the final version of the manuscript. The authors declare no competing financial conflicts of interest.

FIGURES

Figure 1

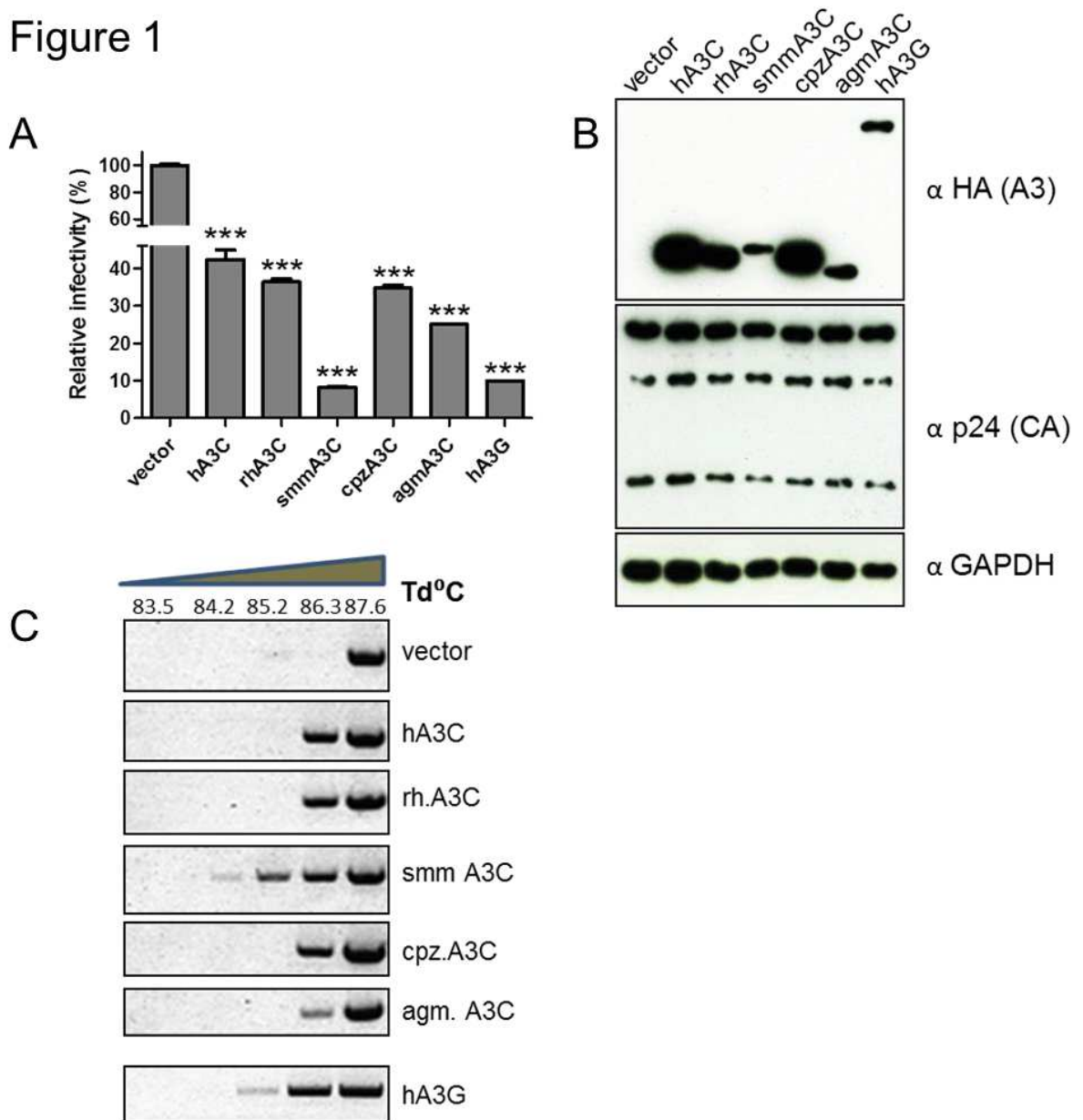


Figure 1. A3C from sooty mangabey but not from other orthologues strongly inhibits HIV-1 Δ vif

(A) HIV-1 Δ vif particles were produced with A3C from human, rhesus macaque, sooty mangabey (smm), chimpanzees (cpz), African green monkey (agm), human A3G or vector only. Infectivity of (RT-normalized) equal amounts of viruses, relative to the virus lacking A3C, was determined by quantification of luciferase activity in 293T cells. Values are means \pm standard deviations (error bars) for three independent experiments. Unpaired *t*-tests were computed to determine whether differences between vector and each A3 protein reach the level of statistical significance. Asterisks represent statistically significant differences: ***, $p < 0.0001$. (B) The amount of proteins in the cell lysate and A3 viral encapsidation were determined by immunoblotting. A3s and HIV-1 capsids were stained with anti-HA and anti-p24 antibodies, respectively. GAPDH served as a loading control. “ α ” represent anti-antibody. (C) 3D-PCR: HIV-1 Δ vif produced together A3C orthologues, hA3G or vector controls were used to transduce 293T cells. Total DNA was extracted and a 714 bp segment of reporter viral DNA was selectively amplified using 3D-PCR. Td = denaturation temperature.

Figure 2

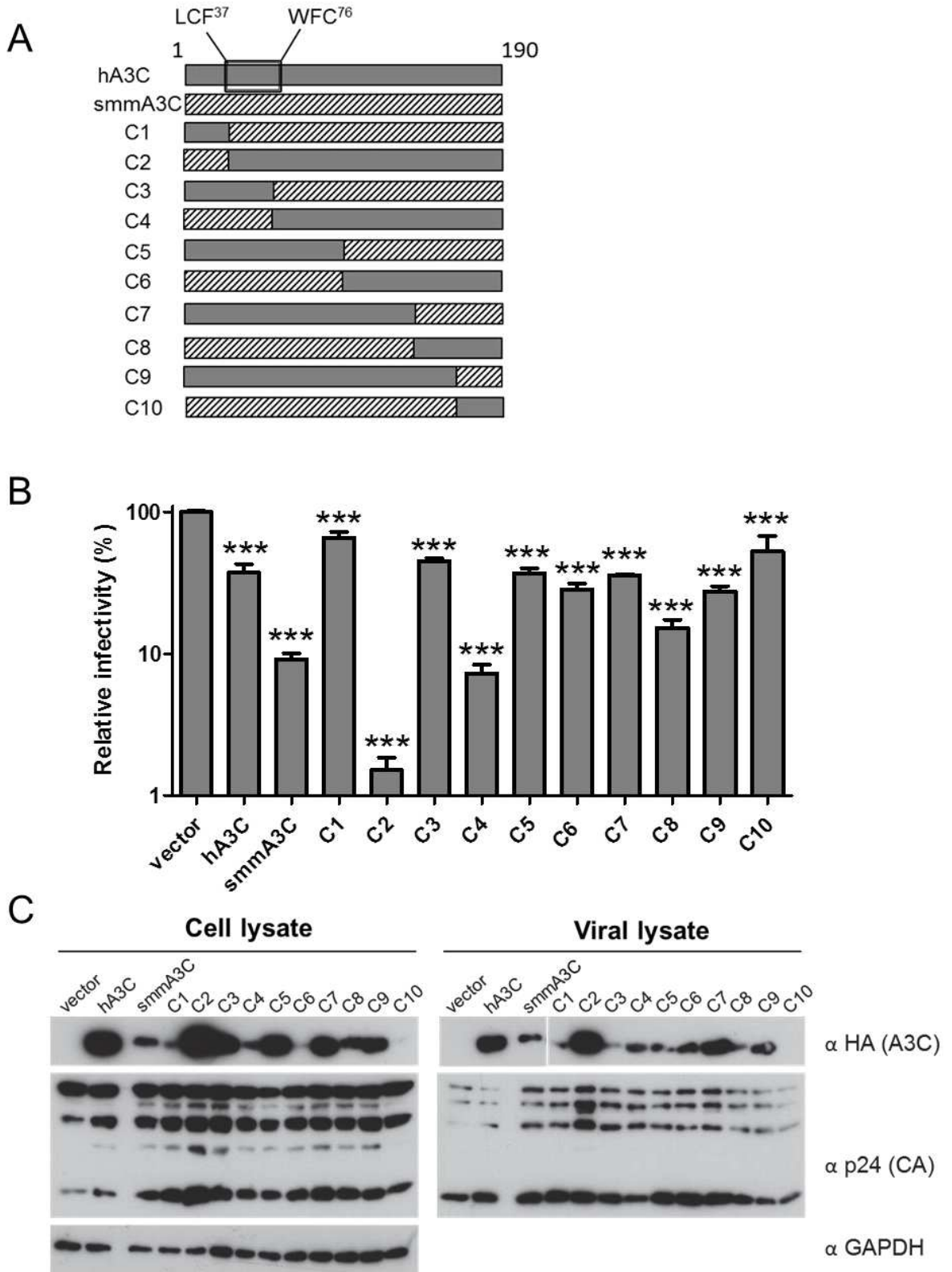
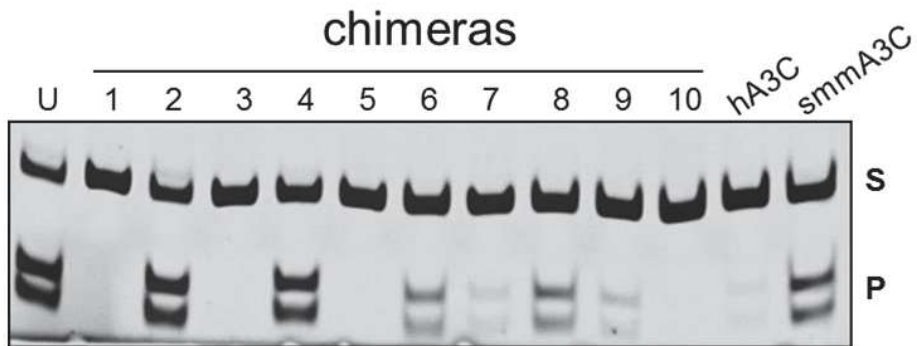
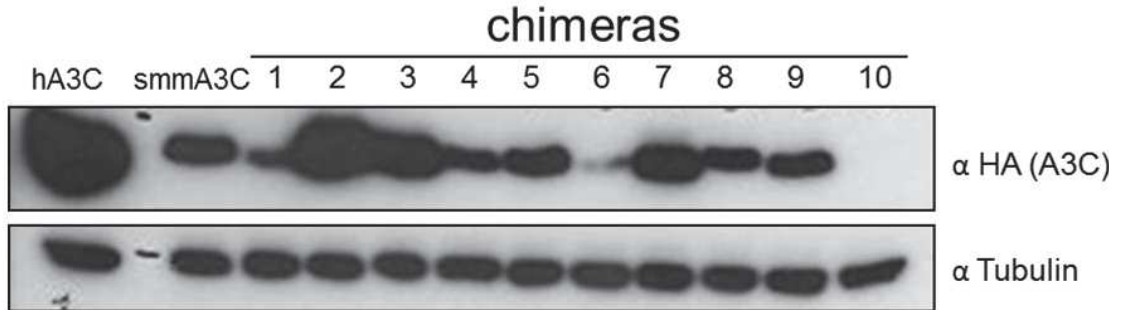


Figure 2. Anti-HIV-1 activity of human/smm A3C chimeras

(A) Illustration of ten different h/smm A3C chimeras (C = chimeras). A box in hA3C denotes the amino acids region of 37 to 76. (B) HIV-1 Δ vif particles were produced with A3C from human, smm, and h/smm chimeras or vector only. Infectivity of (RT-normalized) equal amounts of viruses, relative to the virus lacking A3C, was determined by quantification of luciferase activity in 293T cells. Values are means \pm standard deviations (error bars) for three independent experiments. Unpaired *t*-tests were computed to determine whether differences between vector and each A3 protein reach the level of statistical significance. Asterisks represent statistically significant differences: ***, $p < 0.0001$. (C) The amount of proteins in the cell lysate and A3 viral incorporation were determined by immunoblotting. A3s and HIV-1 capsids were stained with anti-HA and anti-p24 antibodies, respectively. GAPDH served as a loading control. “ α ” represent anti-antibody.

Figure 3

A



B

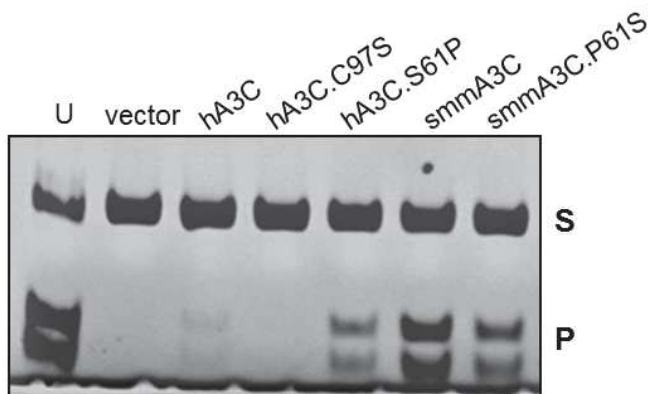
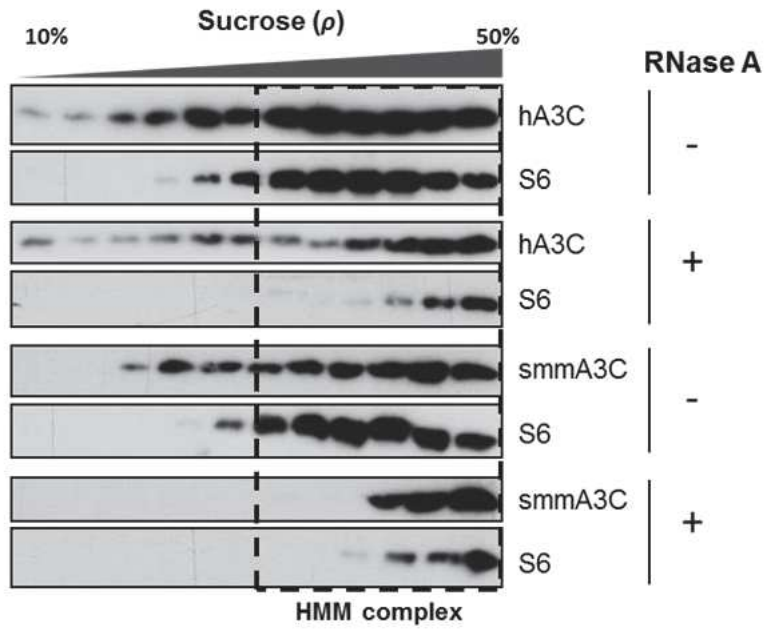


Figure 3. Cytidine deamination capacity of chimeras

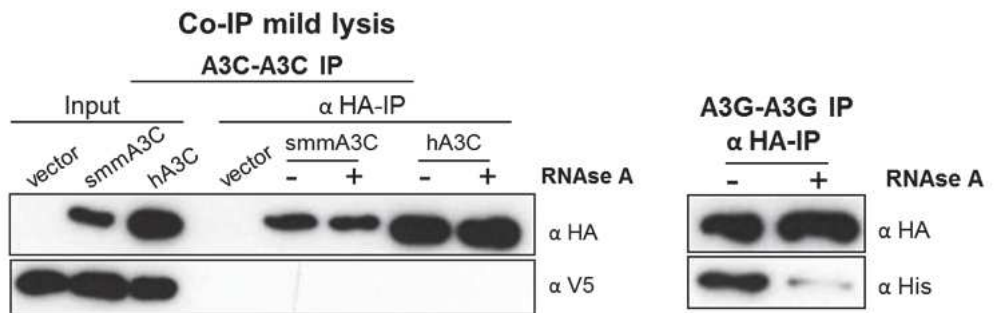
(A) 293T cells were transfected with expression plasmids encoding hA3C, smmA3C and all h/smm chimeras. Immunoblot stained with anti-HA antibody, shows the amount of A3C and chimeric-A3C in cell lysates. Tubulin served as a loading control. “ α ” represent anti-antibody. In the next panel, the *in vitro* cytidine deamination activity was shown. RNase treatment was included; oligonucleotide containing uracil (U) instead of cytosine served as a marker to denote the migration of deaminated product after restriction enzyme cleavage. S-substrate, P-product. (B) A new activity assay using hA3C, hA3C.C97S, hA3C.S61P, smmA3C, smmA3C.P61S was performed as given in (A).

Figure 4

A



B



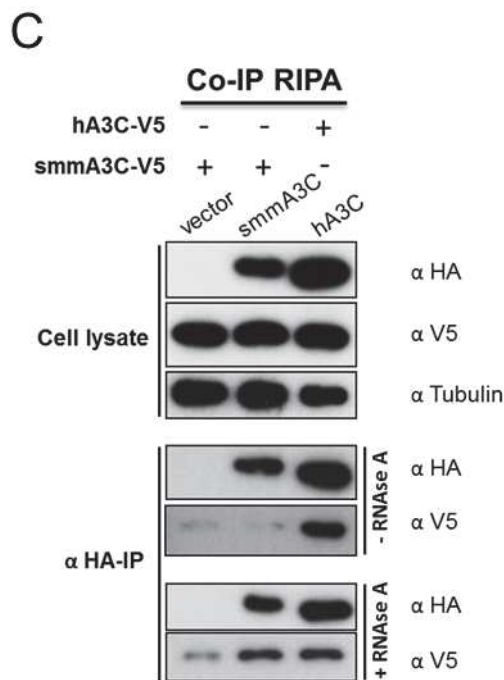
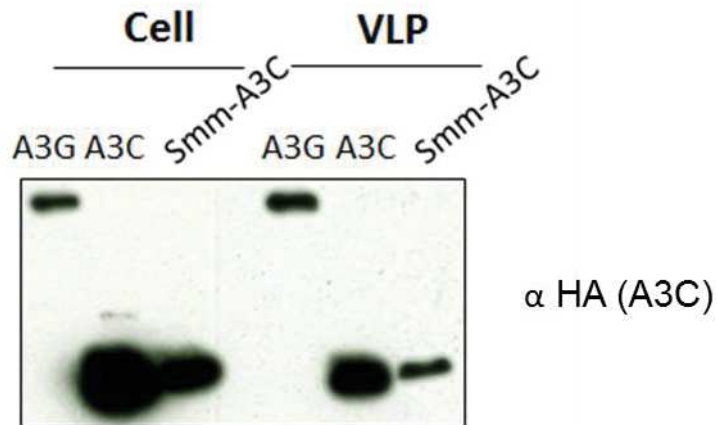


Figure 4. smmA3C forms HMM complexes and self-associates like human A3C

(A) Velocity sucrose gradient fractionation of RNase A-treated and untreated cell lysates of 293T cells that were transfected with expression plasmids for hA3C and smmA3C through sucrose gradients (10% to 50%). Samples were examined by use of specific antibodies: A3C and endogenous ribosomal S6 marker proteins were detected by anti-HA and anti-S6 antibody respectively. Lanes corresponding to HMM complexes of A3C and S6 proteins were marked with a dashed box. (B) protein-protein interaction using the mild-lysis buffer: Pull down assay to detect homo-dimerization of smmA3C was performed. Carboxy-terminal V5 tagged smmA3C construct were co-transfected together with an expression vector coding HA-tagged smmA3C. This assay was done with and without RNase A treatments, after binding the HA-tagged protein to the beads. Cell lysates (Input) and anti-HA IP fractions were subjected to immunoblot analysis using anti-HA and anti-V5 antibodies. As a control for RNase bridged interaction, parallel hA3C-A3C and A3G-A3G interaction experiment were added. (C) Using RIPA buffer, an independent pull-down assay with hA3C and smmA3C with and without RNase A treatment was performed. As described in (B) transfections and immunoblotting were followed.

Suppl. Fig. 1



Supplementary Figure 1. A comparable viral-packaging assay was performed with hA3G, hA3C, and smmA3C. The amount of A3 in cell lysate and viral particles was determined by immunoblotting using anti-HA antibody. VLP-viral like particles.

Suppl. Fig. 2

```

hA3C  MNPQIRNPMKAMYPGIFYFQFKNLWEANDRNETWLCFTVEGIKRRSVVSWKTGVFRNQVD 60
smmA3C MNPQIRNPMKAMDPHIFYFHFKNLRKAYGRNETWLCFAVEI IKQRSTVPWRTGVFRNQVD 60
***** *  **:**** :* .*****:* **:**. * *:*****

hA3C  SETHCHAERCFLSWFCDDILSPNTKYQVTWYTSWSPCPDCAGEVAEFLARHSNVNLTIFT 120
smmA3C PESHCHAERCFLSWFCEDILSPNTIDYRVTWYTSWSPCLDCAGEVAEFLARHSNVELAIFA 120
*:******:******.*:***** *****:***:

hA3C  ARLYYFQYPCYQEGLRSLSQEGVAVEIMDYEDFKYCWENFVYNDNEPFKPKWGLKTNFRL 180
smmA3C ARLYYFWDTHYQQGLRSLSEKGASVEIMGYEDFKYCRENFVCDGKPFKPKWGLKTNFRF 180
***** **:*****:*.:****.***** ** * :*.:*****:

hA3C  LKRRLRESLQ 190
smmA3C LKRRLQEILE 190
*****:* *:
    
```

77.9% identity and 90% similarity

Supplementary Figure 2.

(a) Sequence alignment of hA3C and smmA3 was done by using Clustal Omega (<http://www.ebi.ac.uk/Tools/msa/clustalo/>). A pairwise sequence alignment using LALIGN (http://embnet.vital-it.ch/software/LALIGN_form.html) was performed to learn the similarity and identity of the residues among them.

REFERENCES

- ABDEL-MOHSEN, M., RAPOSO, R. A., DENG, X., LI, M., LIEGLER, T., SINCLAIR, E., SALAMA, M. S., GHANEM HEL, D., HOH, R., WONG, J. K., DAVID, M., NIXON, D. F., DEEKS, S. G. & PILLAI, S. K. 2013. Expression profile of host restriction factors in HIV-1 elite controllers. *Retrovirology*, 10, 106.
- ADOLPH, M. B., ARA, A., FENG, Y., WITTKOPP, C. J., EMERMAN, M., FRASER, J. S. & CHELICO, L. 2017. Cytidine deaminase efficiency of the lentiviral viral restriction factor APOBEC3C correlates with dimerization. *Nucleic Acids Res*, 45, 3378-3394.
- AHASAN, M. M., WAKAE, K., WANG, Z., KITAMURA, K., LIU, G., KOURA, M., IMAYASU, M., SAKAMOTO, N., HANAOKA, K., NAKAMURA, M., KYO, S., KONDO, S., FUJIWARA, H., YOSHIZAKI, T., MORI, S., KUKIMOTO, I. & MURAMATSU, M. 2015. APOBEC3A and 3C decrease human papillomavirus 16 pseudovirion infectivity. *Biochem Biophys Res Commun*, 457, 295-9.
- BÄHR, A., SINGER, A., HAIN, A., VASUDEVAN, A. A., SCHILLING, M., REH, J., RIESS, M., PANITZ, S., SERRANO, V., SCHWEIZER, M., KÖNIG, R., CHANDA, S., HÄUSSINGER, D., KOCHS, G., LINDEMANN, D. & MÜNK, C. 2016. Interferon but not MxB inhibits foamy retroviruses. *Virology*, 488, 51-60.
- BAUMERT, T. F., ROSLER, C., MALIM, M. H. & VON WEIZSACKER, F. 2007. Hepatitis B virus DNA is subject to extensive editing by the human deaminase APOBEC3C. *Hepatology*, 46, 682-9.
- BISHOP, K. N., HOLMES, R. K. & MALIM, M. H. 2006. Antiviral potency of APOBEC proteins does not correlate with cytidine deamination. *J Virol*, 80, 8450-8.
- BISHOP, K. N., HOLMES, R. K., SHEEHY, A. M., DAVIDSON, N. O., CHO, S. J. & MALIM, M. H. 2004. Cytidine deamination of retroviral DNA by diverse APOBEC proteins. *Curr Biol*, 14, 1392-6.
- BOGERD, H. P., DOEHLE, B. P., WIEGAND, H. L. & CULLEN, B. R. 2004. A single amino acid difference in the host APOBEC3G protein controls the primate species specificity of HIV type 1 virion infectivity factor. *Proc Natl Acad Sci U S A*, 101, 3770-4.
- BONVIN, M., ACHERMANN, F., GREEVE, I., STROKA, D., KEOGH, A., INDERBITZIN, D., CANDINAS, D., SOMMER, P., WAIN-HOBSON, S., VARTANIAN, J. P. & GREEVE, J. 2006. Interferon-inducible expression of APOBEC3 editing enzymes in human hepatocytes and inhibition of hepatitis B virus replication. *Hepatology*, 43, 1364-74.
- BOURARA, K., LIEGLER, T. J. & GRANT, R. M. 2007. Target cell APOBEC3C can induce limited G-to-A mutation in HIV-1. *PLoS Pathog*, 3, 1477-85.
- BROWNE, E. P., ALLERS, C. & LANDAU, N. R. 2009. Restriction of HIV-1 by APOBEC3G is cytidine deaminase-dependent. *Virology*, 387, 313-21.

- BURNETT, A. & SPEARMAN, P. 2007. APOBEC3G multimers are recruited to the plasma membrane for packaging into human immunodeficiency virus type 1 virus-like particles in an RNA-dependent process requiring the NC basic linker. *J Virol*, 81, 5000-13.
- BURNS, M. B., LACKEY, L., CARPENTER, M. A., RATHORE, A., LAND, A. M., LEONARD, B., REFSLAND, E. W., KOTANDENIYA, D., TRETYAKOVA, N., NIKAS, J. B., YEE, D., TEMIZ, N. A., DONOHUE, D. E., MCDUGLE, R. M., BROWN, W. L., LAW, E. K. & HARRIS, R. S. 2013. APOBEC3B is an enzymatic source of mutation in breast cancer. *Nature*, 494, 366-70.
- DANG, Y., WANG, X., ESSELMAN, W. J. & ZHENG, Y. H. 2006. Identification of APOBEC3DE as another antiretroviral factor from the human APOBEC family. *J Virol*, 80, 10522-33.
- DULL, T., ZUFFEREY, R., KELLY, M., MANDEL, R. J., NGUYEN, M., TRONO, D. & NALDINI, L. 1998. A third-generation lentivirus vector with a conditional packaging system. *J Virol*, 72, 8463-71.
- GALLOIS-MONTBRUN, S., KRAMER, B., SWANSON, C. M., BYERS, H., LYNHAM, S., WARD, M. & MALIM, M. H. 2007. Antiviral protein APOBEC3G localizes to ribonucleoprotein complexes found in P bodies and stress granules. *J Virol*, 81, 2165-78.
- GOILA-GAUR, R. & STREBEL, K. 2008. HIV-1 Vif, APOBEC, and intrinsic immunity. *Retrovirology*, 5, 51.
- HARRIS, R. S., BISHOP, K. N., SHEEHY, A. M., CRAIG, H. M., PETERSEN-MAHRT, S. K., WATT, I. N., NEUBERGER, M. S. & MALIM, M. H. 2003. DNA deamination mediates innate immunity to retroviral infection. *Cell*, 113, 803-9.
- HARRIS, R. S. & DUDLEY, J. P. 2015. APOBECs and virus restriction. *Virology*, 479-480, 131-45.
- HENDERSON, S. & FENTON, T. 2015. APOBEC3 genes: retroviral restriction factors to cancer drivers. *Trends Mol Med*, 21, 274-84.
- HOLMES, R. K., KONING, F. A., BISHOP, K. N. & MALIM, M. H. 2007. APOBEC3F can inhibit the accumulation of HIV-1 reverse transcription products in the absence of hypermutation. Comparisons with APOBEC3G. *J Biol Chem*, 282, 2587-95.
- HORN, A. V., KLAWITTER, S., HELD, U., BERGER, A., VASUDEVAN, A. A., BOCK, A., HOFMANN, H., HANSCHMANN, K. M., TROSEMEIER, J. H., FLORY, E., JABULOWSKY, R. A., HAN, J. S., LOWER, J., LOWER, R., MÜNK, C. & SCHUMANN, G. G. 2014. Human LINE-1 restriction by APOBEC3C is deaminase independent and mediated by an ORF1p interaction that affects LINE reverse transcriptase activity. *Nucleic Acids Res*, 42, 396-416.
- HULTQUIST, J. F., BINKA, M., LARUE, R. S., SIMON, V. & HARRIS, R. S. 2012. Vif proteins of human and simian immunodeficiency viruses require cellular CBFbeta to degrade APOBEC3 restriction factors. *J Virol*, 86, 2874-7.
- HULTQUIST, J. F., LENGYEL, J. A., REFSLAND, E. W., LARUE, R. S., LACKEY, L., BROWN, W. L. & HARRIS, R. S. 2011. Human and rhesus APOBEC3D, APOBEC3F, APOBEC3G, and APOBEC3H demonstrate a conserved capacity to restrict Vif-deficient HIV-1. *J Virol*, 85, 11220-34.
- HUTHOFF, H., AUTORE, F., GALLOIS-MONTBRUN, S., FRATERNALI, F. & MALIM, M. H. 2009. RNA-dependent oligomerization of APOBEC3G is required for restriction of HIV-1. *PLoS Pathog*, 5, e1000330.
- HUTHOFF, H. & MALIM, M. H. 2007. Identification of amino acid residues in APOBEC3G required for regulation by human immunodeficiency virus type 1 Vif and Virion encapsidation. *J Virol*, 81, 3807-15.
- IWATANI, Y., CHAN, D. S., WANG, F., MAYNARD, K. S., SUGIURA, W., GRONENBORN, A. M., ROUZINA, I., WILLIAMS, M. C., MUSIER-FORSYTH, K. & LEVIN, J. G. 2007. Deaminase-independent inhibition of HIV-1 reverse transcription by APOBEC3G. *Nucleic Acids Res*, 35, 7096-108.
- IWATANI, Y., TAKEUCHI, H., STREBEL, K. & LEVIN, J. G. 2006. Biochemical activities of highly purified, catalytically active human APOBEC3G: correlation with antiviral effect. *J Virol*, 80, 5992-6002.
- JAGUVA VASUDEVAN, A. A., HOFMANN, H., WILLBOLD, D., HÄUSSINGER, D., KOENIG, B. W. & MÜNK, C. 2017. Enhancing the Catalytic Deamination Activity of APOBEC3C Is Insufficient to Inhibit Vif-Deficient HIV-1. *J Mol Biol*, 429, 1171-1191.

- JAGUVA VASUDEVAN, A. A., PERKOVIC, M., BULLIARD, Y., CICHUTEK, K., TRONO, D., HÄUSSINGER, D. & MÜNK, C. 2013. Prototype foamy virus Bet impairs the dimerization and cytosolic solubility of human APOBEC3G. *J Virol*, 87, 9030-40.
- JARMUZ, A., CHESTER, A., BAYLISS, J., GISBOURNE, J., DUNHAM, I., SCOTT, J. & NAVARATNAM, N. 2002. An anthropoid-specific locus of orphan C to U RNA-editing enzymes on chromosome 22. *Genomics*, 79, 285-96.
- KOZAK, S. L., MARIN, M., ROSE, K. M., BYSTROM, C. & KABAT, D. 2006. The anti-HIV-1 editing enzyme APOBEC3G binds HIV-1 RNA and messenger RNAs that shuttle between polysomes and stress granules. *J Biol Chem*, 281, 29105-19.
- KREISBERG, J. F., YONEMOTO, W. & GREENE, W. C. 2006. Endogenous factors enhance HIV infection of tissue naive CD4 T cells by stimulating high molecular mass APOBEC3G complex formation. *J Exp Med*, 203, 865-70.
- LANGLOIS, M. A., BEALE, R. C., CONTICELLO, S. G. & NEUBERGER, M. S. 2005. Mutational comparison of the single-domained APOBEC3C and double-domained APOBEC3F/G anti-retroviral cytidine deaminases provides insight into their DNA target site specificities. *Nucleic Acids Res*, 33, 1913-23.
- LARUE, R. S., JONSSON, S. R., SILVERSTEIN, K. A., LAJOIE, M., BERTRAND, D., EL-MABROUK, N., HOTZEL, I., ANDRESDOTTIR, V., SMITH, T. P. & HARRIS, R. S. 2008. The artiodactyl APOBEC3 innate immune repertoire shows evidence for a multi-functional domain organization that existed in the ancestor of placental mammals. *BMC Mol Biol*, 9, 104.
- LI, J., CHEN, Y., LI, M., CARPENTER, M. A., MCDOUGLE, R. M., LUENGAS, E. M., MACDONALD, P. J., HARRIS, R. S. & MUELLER, J. D. 2014. APOBEC3 multimerization correlates with HIV-1 packaging and restriction activity in living cells. *J Mol Biol*, 426, 1296-307.
- LUO, K., LIU, B., XIAO, Z., YU, Y., YU, X., GORELICK, R. & YU, X. F. 2004. Amino-terminal region of the human immunodeficiency virus type 1 nucleocapsid is required for human APOBEC3G packaging. *J Virol*, 78, 11841-52.
- MANGEAT, B., TURELLI, P., CARON, G., FRIEDLI, M., PERRIN, L. & TRONO, D. 2003. Broad antiretroviral defence by human APOBEC3G through lethal editing of nascent reverse transcripts. *Nature*, 424, 99-103.
- MANGEAT, B., TURELLI, P., LIAO, S. & TRONO, D. 2004. A single amino acid determinant governs the species-specific sensitivity of APOBEC3G to Vif action. *J Biol Chem*, 279, 14481-3.
- MARIANI, R., CHEN, D., SCHROFELBAUER, B., NAVARRO, F., KONIG, R., BOLLMAN, B., MÜNK, C., NYMARK-MCMAHON, H. & LANDAU, N. R. 2003. Species-specific exclusion of APOBEC3G from HIV-1 virions by Vif. *Cell*, 114, 21-31.
- MARINO, D., PERKOVIC, M., HAIN, A., JAGUVA VASUDEVAN, A. A., HOFMANN, H., HANSCHMANN, K. M., MUHLEBACH, M. D., SCHUMANN, G. G., KONIG, R., CICHUTEK, K., HÄUSSINGER, D. & MÜNK, C. 2016. APOBEC4 Enhances the Replication of HIV-1. *PLoS One*, 11, e0155422.
- MBISA, J. L., BU, W. & PATHAK, V. K. 2010. APOBEC3F and APOBEC3G inhibit HIV-1 DNA integration by different mechanisms. *J Virol*, 84, 5250-9.
- MEHLE, A., STRACK, B., ANCUITA, P., ZHANG, C., MCPRIKE, M. & GABUZDA, D. 2004. Vif overcomes the innate antiviral activity of APOBEC3G by promoting its degradation in the ubiquitin-proteasome pathway. *J Biol Chem*, 279, 7792-8.
- MÜNK, C., JENSEN, B. E., ZIELONKA, J., HÄUSSINGER, D. & KAMP, C. 2012a. Running Loose or Getting Lost: How HIV-1 Counters and Capitalizes on APOBEC3-Induced Mutagenesis through Its Vif Protein. *Viruses*, 4, 3132-3161.
- MÜNK, C., WILLEMSSEN, A. & BRAVO, I. G. 2012b. An ancient history of gene duplications, fusions and losses in the evolution of APOBEC3 mutators in mammals. *BMC Evol Biol*, 12, 71.
- NOWARSKI, R., BRITAN-ROSICH, E., SHILOACH, T. & KOTLER, M. 2008. Hypermutation by intersegmental transfer of APOBEC3G cytidine deaminase. *Nat Struct Mol Biol*, 15, 1059-66.

- PERKOVIC, M., SCHMIDT, S., MARINO, D., RUSSELL, R. A., STAUCH, B., HOFMANN, H., KOPIETZ, F., KLOKE, B. P., ZIELONKA, J., STROVER, H., HERMLE, J., LINDEMANN, D., PATHAK, V. K., SCHNEIDER, G., LOCHELT, M., CICHUTEK, K. & MÜNK, C. 2009. Species-specific inhibition of APOBEC3C by the prototype foamy virus protein bet. *J Biol Chem*, 284, 5819-26.
- REFSLAND, E. W., HULTQUIST, J. F. & HARRIS, R. S. 2012. Endogenous origins of HIV-1 G-to-A hypermutation and restriction in the nonpermissive T cell line CEM2n. *PLoS Pathog*, 8, e1002800.
- REFSLAND, E. W., STENGLEIN, M. D., SHINDO, K., ALBIN, J. S., BROWN, W. L. & HARRIS, R. S. 2010. Quantitative profiling of the full APOBEC3 mRNA repertoire in lymphocytes and tissues: implications for HIV-1 restriction. *Nucleic Acids Res*, 38, 4274-84.
- ROBERTS, S. A., LAWRENCE, M. S., KLIMCZAK, L. J., GRIMM, S. A., FARGO, D., STOJANOV, P., KIEZUN, A., KRYUKOV, G. V., CARTER, S. L., SAKSENA, G., HARRIS, S., SHAH, R. R., RESNICK, M. A., GETZ, G. & GORDENIN, D. A. 2013. An APOBEC cytidine deaminase mutagenesis pattern is widespread in human cancers. *Nat Genet*, 45, 970-6.
- SALTER, J. D., BENNETT, R. P. & SMITH, H. C. 2016. The APOBEC Protein Family: United by Structure, Divergent in Function. *Trends Biochem Sci*, 41, 578-94.
- SCHAFFER, A., BOGERD, H. P. & CULLEN, B. R. 2004. Specific packaging of APOBEC3G into HIV-1 virions is mediated by the nucleocapsid domain of the gag polyprotein precursor. *Virology*, 328, 163-8.
- SHEEHY, A. M., GADDIS, N. C., CHOI, J. D. & MALIM, M. H. 2002. Isolation of a human gene that inhibits HIV-1 infection and is suppressed by the viral Vif protein. *Nature*, 418, 646-50.
- SHEEHY, A. M., GADDIS, N. C. & MALIM, M. H. 2003. The antiretroviral enzyme APOBEC3G is degraded by the proteasome in response to HIV-1 Vif. *Nat Med*, 9, 1404-7.
- SIMM, M., SHAHABUDDIN, M., CHAO, W., ALLAN, J. S. & VOLSKY, D. J. 1995. Aberrant Gag protein composition of a human immunodeficiency virus type 1 vif mutant produced in primary lymphocytes. *J Virol*, 69, 4582-6.
- SMITH, J. L. & PATHAK, V. K. 2010. Identification of specific determinants of human APOBEC3F, APOBEC3C, and APOBEC3DE and African green monkey APOBEC3F that interact with HIV-1 Vif. *J Virol*, 84, 12599-608.
- STAUCH, B., HOFMANN, H., PERKOVIC, M., WEISEL, M., KOPIETZ, F., CICHUTEK, K., MÜNK, C. & SCHNEIDER, G. 2009. Model structure of APOBEC3C reveals a binding pocket modulating ribonucleic acid interaction required for encapsidation. *Proc Natl Acad Sci U S A*, 106, 12079-84.
- STAVROU, S. & ROSS, S. R. 2015. APOBEC3 Proteins in Viral Immunity. *J Immunol*, 195, 4565-70.
- STREBEL, K. 2005. APOBEC3G & HTLV-1: inhibition without deamination. *Retrovirology*, 2, 37.
- SUSPENE, R., AYNAUD, M. M., KOCH, S., PASDELOUP, D., LABETOULLE, M., GAERTNER, B., VARTANIAN, J. P., MEYERHANS, A. & WAIN-HOBSON, S. 2011. Genetic editing of herpes simplex virus 1 and Epstein-Barr herpesvirus genomes by human APOBEC3 cytidine deaminases in culture and in vivo. *J Virol*, 85, 7594-602.
- SUSPENE, R., GUETARD, D., HENRY, M., SOMMER, P., WAIN-HOBSON, S. & VARTANIAN, J. P. 2005a. Extensive editing of both hepatitis B virus DNA strands by APOBEC3 cytidine deaminases in vitro and in vivo. *Proc Natl Acad Sci U S A*, 102, 8321-6.
- SUSPENE, R., HENRY, M., GUILLOT, S., WAIN-HOBSON, S. & VARTANIAN, J. P. 2005b. Recovery of APOBEC3-edited human immunodeficiency virus G->A hypermutants by differential DNA denaturation PCR. *J Gen Virol*, 86, 125-9.
- SVAROVSKAIA, E. S., XU, H., MBISA, J. L., BARR, R., GORELICK, R. J., ONO, A., FREED, E. O., HU, W. S. & PATHAK, V. K. 2004. Human apolipoprotein B mRNA-editing enzyme-catalytic polypeptide-like 3G (APOBEC3G) is incorporated into HIV-1 virions through interactions with viral and nonviral RNAs. *J Biol Chem*, 279, 35822-8.

- VARTANIAN, J. P., GUETARD, D., HENRY, M. & WAIN-HOBSON, S. 2008. Evidence for editing of human papillomavirus DNA by APOBEC3 in benign and precancerous lesions. *Science*, 320, 230-3.
- VASUDEVAN, A. A., SMITS, S. H., HOPFNER, A., HÄUSSINGER, D., KOENIG, B. W. & MÜNK, C. 2013. Structural features of antiviral DNA cytidine deaminases. *Biol Chem*, 394, 1357-70.
- WANG, X., DOLAN, P. T., DANG, Y. & ZHENG, Y. H. 2007. Biochemical differentiation of APOBEC3F and APOBEC3G proteins associated with HIV-1 life cycle. *J Biol Chem*, 282, 1585-94.
- WEDEKIND, J. E., GILLILAN, R., JANDA, A., KRUCINSKA, J., SALTER, J. D., BENNETT, R. P., RAINA, J. & SMITH, H. C. 2006. Nanostructures of APOBEC3G support a hierarchical assembly model of high molecular mass ribonucleoprotein particles from dimeric subunits. *J Biol Chem*, 281, 38122-6.
- WIEGAND, H. L., DOEHLE, B. P., BOGERD, H. P. & CULLEN, B. R. 2004. A second human antiretroviral factor, APOBEC3F, is suppressed by the HIV-1 and HIV-2 Vif proteins. *EMBO J*, 23, 2451-8.
- YU, Q., CHEN, D., KONIG, R., MARIANI, R., UNUTMAZ, D. & LANDAU, N. R. 2004a. APOBEC3B and APOBEC3C are potent inhibitors of simian immunodeficiency virus replication. *J Biol Chem*, 279, 53379-86.
- YU, Q., KONIG, R., PILLAI, S., CHILES, K., KEARNEY, M., PALMER, S., RICHMAN, D., COFFIN, J. M. & LANDAU, N. R. 2004b. Single-strand specificity of APOBEC3G accounts for minus-strand deamination of the HIV genome. *Nat Struct Mol Biol*, 11, 435-42.
- YU, X., YU, Y., LIU, B., LUO, K., KONG, W., MAO, P. & YU, X. F. 2003. Induction of APOBEC3G ubiquitination and degradation by an HIV-1 Vif-Cul5-SCF complex. *Science*, 302, 1056-60.
- ZENNOU, V., PEREZ-CABALLERO, D., GOTTLINGER, H. & BIENIASZ, P. D. 2004. APOBEC3G incorporation into human immunodeficiency virus type 1 particles. *J Virol*, 78, 12058-61.
- ZHANG, H., YANG, B., POMERANTZ, R. J., ZHANG, C., ARUNACHALAM, S. C. & GAO, L. 2003. The cytidine deaminase CEM15 induces hypermutation in newly synthesized HIV-1 DNA. *Nature*, 424, 94-8.
- ZHANG, W., HUANG, M., WANG, T., TAN, L., TIAN, C., YU, X., KONG, W. & YU, X. F. 2008. Conserved and non-conserved features of HIV-1 and SIVagm Vif mediated suppression of APOBEC3 cytidine deaminases. *Cell Microbiol*, 10, 1662-75.
- ZHANG, Z., GU, Q., JAGUVA VASUDEVAN, A. A., JEYARAJ, M., SCHMIDT, S., ZIELONKA, J., PERKOVIC, M., HECKEL, J. O., CICHUTEK, K., HÄUSSINGER, D., SMITS, S. H. & MÜNK, C. 2016. Vif Proteins from Diverse Human Immunodeficiency Virus/Simian Immunodeficiency Virus Lineages Have Distinct Binding Sites in A3C. *J Virol*, 90, 10193-10208.
- ZHENG, Y. H., IRWIN, D., KUROSU, T., TOKUNAGA, K., SATA, T. & PETERLIN, B. M. 2004. Human APOBEC3F is another host factor that blocks human immunodeficiency virus type 1 replication. *J Virol*, 78, 6073-6.

Chapter IV

Glycosylated gag protects murine leukemia virus from producer cell-derived but not from target cell APOBEC3A

Status : Manuscript under preparation

Own contribution to this work:

- Complete execution of experimental procedures except for a 3D-PCR (presented in figure 5C)
- Writing of the manuscript

Glycosylated gag protects murine leukemia virus from producer cell-derived but not from target cell APOBEC3A

Ananda Ayyappan Jaguva Vasudevan¹, Aikaterini Krikoni¹, André Franken¹, Daniela Marino¹, Renate König², Gerald Schumann³, Dieter Häussinger¹, and Carsten Münk^{1,#}

¹Clinic for Gastroenterology, Hepatology, and Infectiology, Medical Faculty, Heinrich-Heine-University, 40225 Düsseldorf, Germany.

²Host-Pathogen Interactions, and ³Division of Medical Biotechnology, Paul-Ehrlich-Institute, Langen, Germany

Running title: MLV-glycogag counteracts A3A by virion exclusion

[#]corresponding author: Clinic for Gastroenterology, Hepatology, and Infectiology, Medical Faculty, Heinrich-Heine-University Düsseldorf, Building 23.12.U1.82, Moorenstr. 5, 40225 Düsseldorf, Germany, Tel: +49 (0) 211-81-10887, Fax: +49 (0) 211-81-18752, E-mail: carsten.muenk@med.uni-duesseldorf.de

ABSTRACT

The APOBEC3A (A3A) polynucleotide cytidine deaminase of the human APOBEC3 (A3) protein family has been shown to have antiviral activity against HTLV-1, but not HIV-1, when expressed in the virus producer cell. In viral target cells, high levels of endogenous A3A activity have been associated with restriction of HIV-1 during infection. Reports on the inhibition of Murine leukemia virus (MLV) by producer cell A3A have not been so clear with inhibition ranging from marginal to strong. It has also been shown that A3A can have a direct effect on transfected plasmid DNA. Therefore, we first optimized the experimental system to minimize direct A3A effects.

Here we show that A3A can block the replication of Moloney-MLV (Mo-MLV) and related AKV-derived strains of MLV in a deaminase-dependent fashion. Furthermore, our results demonstrate that glycosylated Gag (glycogag) of MLV inhibits the encapsidation of A3A, and to a lesser extent of murine A3. However, target cell A3A was not affected by glycogag and exerted deamination in viral DNA. Since glycogag expression is abundant in full-length MLV compared to the *gag-pol* packaging construct, our results may explain the controversial results in previous reports.

Keywords: glycosylated gag, Murine leukemia virus (MLV), cytidine deaminase, APOBEC3A, murine APOBEC3, A3 viral encapsidation, MDMs, and interferon

INTRODUCTION

The human family of APOBEC3 (A3) genes consists of seven members, APOBEC3A (A3A), -B, -C, -D, -F, -G, and -H (Jarmuz et al., 2002, Münk et al., 2012b). They belong to the group of cytidine deaminases that can catalyze the deamination of cytidine residues to uridine in single-stranded DNA (ssDNA) (Vasudevan et al., 2013). Members of the A3 enzymes contain one or two zinc (Z)-coordinating domains and can be classified according to the presence or absence of a Z1, Z2, or Z3 motif (LaRue et al., 2009). Different lineages of placental mammals show an individual A3 locus with a variable number of A3 genes that appears to result from specific host adaptation to viruses (LaRue et al., 2009, Münk et al., 2008, Münk et al., 2012b).

Human immunodeficiency virus type 1 (HIV-1) variants lacking expression of the *vif* gene (HIV-1 Δ *vif*), package A3G and other A3s of their producer cells into nascent viral particles. Upon subsequent infection, the incorporated A3G deaminates cytosine residues to uracil in elongating viral ssDNA during reverse transcription, leading to hypermutation that causes missense and nonsense mutations impair the production of functional viruses (Bishop et al., 2004, Harris et al., 2003, Lecossier et al., 2003, Mangeat et al., 2003, Mariani et al., 2003a, Zhang et al., 2003, Yu et al., 2004a, Browne et al., 2009), (for a review, see (Harris and Dudley, 2015)). More recent studies indicate that deaminase-independent mechanisms might also contribute to the antiviral activity of A3G (Bishop et al., 2006, Bishop et al., 2008, Holmes et al., 2007, Iwatani et al., 2007, Mbisa et al., 2007, Guo et al., 2007, Li et al., 2007, Wang et al., 2012, Strebel, 2005, Münk et al., 2012a). In the case of HIV-1, the amount of encapsidated A3G in wild-type HIV-1 virions is dramatically reduced by Vif-dependent degradation of A3G via the polyubiquitination-proteasome pathway and by degradation-independent mechanisms (Marin et al., 2003, Sheehy et al., 2003, Yu et al., 2003, Yu et al., 2004b, Kao et al., 2007, Kao et al., 2004, Opi et al., 2007, Santa-Marta et al., 2005, Britan-Rosich et al., 2011).

The Z1 domain protein A3A, was found to have no antiviral activity when tested against HIV-1 or Murine leukemia virus (MLV) by co-expression in the virus producer cells (Bishop et al., 2004, Wiegand et al., 2004, Schmitt et al., 2011, Chen et al., 2006, Aguiar et al., 2008, Doehle

et al., 2005, Bogerd et al., 2006a, Goila-Gaur et al., 2007, Hultquist et al., 2011, Ooms et al., 2012). However, a study reported that A3A inhibits MLV (Dorrschuck et al., 2011), and A3A can restrict HIV-1 if targeted to the capsid core by fusion to the viral protein Vpr or the N-terminal domain of A3G (Aguiar et al., 2008, Goila-Gaur et al., 2007).

In addition, A3A expressed in the viral producer cell inhibits other retroviruses, such as the *Human T-lymphotropic virus type 1*, the *Rous sarcoma virus*, the *Porcine endogenous retrovirus-B* and the simian-human immunodeficiency virus Δvif (Schmitt et al., 2011, Ooms et al., 2012, Dorrschuck et al., 2011, Wiegand and Cullen, 2007, Schmitt et al., 2013). A3A can also restrict hepatitis B virus as well as parvo- and papillomaviruses (Chen et al., 2006, Zielonka et al., 2009, Narvaiza et al., 2009, Vartanian et al., 2008, Bulliard et al., 2011, Henry et al., 2009, Lucifora et al., 2014) and A3A-mediated human papillomavirus 16 E2 hypermutation in oropharyngeal cancers were correlated with viral DNA integration (Kondo et al., 2017). It is a repressor of retrotransposition activity and effectively inhibits long terminal repeat (LTR)-retrotransposons through a novel deamination-independent mechanism (Chen et al., 2006, Bogerd et al., 2006a). A3A is also reported to be a potent inhibitor of human non-LTR retrotransposons, causing a reduction in LINE-1 (L1) and *Alu* retrotransposition frequencies (Chen et al., 2006, Bogerd et al., 2006b, Muckenfuss et al., 2006, Kinomoto et al., 2007, Niewiadomska et al., 2007, Lovsin and Peterlin, 2009, Khatua et al., 2010, MacDuff et al., 2009, Tan et al., 2009). A mechanism of deamination mediated L1 inhibition was recently reported in which, A3A targeted the transiently exposed ssDNA during L1 integration (Richardson et al., 2014). Other described functions of A3A include efficient deamination of 5-methylcytosine to thymine and cytosine to uracil in ssDNA substrate (Carpenter et al., 2012, Wijesinghe and Bhagwat, 2012), induction of DNA breaks, activation of the DNA damage response and induction of cell-cycle arrest (Landry et al., 2011), hypermutation of nuclear and mitochondrial DNA (Suspene et al., 2011), A3A induction by interferon (as a result of cytosolic DNA mediated innate immune signaling), can catabolize cytoplasmic ssDNA and potentially damage genomic DNA (Suspene et al., 2017) and reduction of the expression of plasmid DNA by deamination-induced destabilization (Carpenter et al., 2012, Stenglein et al., 2010). Recently, mutation signatures resulting from

the enzymatic activity of A3s (especially A3A and A3B) were reported in several cancer types (Burns et al., 2013, Roberts et al., 2013) (for a review, see (Henderson and Fenton, 2015)).

A3A is preferentially expressed in monocytes, macrophages, and dendritic cells, and interferon (IFN) can further induce its expression (Chen et al., 2006, Stenglein et al., 2010, Berger et al., 2011b, Berger et al., 2010, Koning et al., 2009, Cassetta et al., 2013, Peng et al., 2007, Refsland et al., 2010, Thielen et al., 2010, Land et al., 2013, Koning et al., 2011, Mohanram et al., 2013). Monocytes and, to a moderate extent, macrophages are refractory to HIV-1 infection. This restriction is likely caused by two inhibitors, SAMHD1 (Berger et al., 2011a, Hrecka et al., 2011, Laguette et al., 2011, Lahouassa et al., 2012) and A3A (Berger et al., 2011b, Berger et al., 2010, Cassetta et al., 2013, Peng et al., 2007, Koning et al., 2011). Silencing of A3A renders myeloid cells vulnerable to HIV-1 infection (Berger et al., 2011b, Peng et al., 2007), suggesting that A3A expressed in target cells can attack the incoming virion (Koning et al., 2011, Cassetta et al., 2013). However, ectopic expression of A3A in HeLa cells did not significantly modulate the susceptibility of these cells to HIV-1 infection (Berger et al., 2011b). Recently, it was shown that upregulation of A3A by type-I and type-II IFN are myeloid cell specific and it did not induce A3A in activated CD4+ T cells (Logue et al., 2014).

MLV encodes two different forms of the Gag polyprotein, a regular Gag precursor initiated by AUG codon and an upstream CUG primed longer version coding glycosylated Gag (glycogag) (Edwards and Fan, 1979). The function of glycogag in MLV biology is not fully understood. It was reported to be essential for MLV spreading and pathogenesis in mice but less in culture (Corbin et al., 1994). It has been shown to enhance MLV particle release through lipid rafts and stability of the mature viral capsid (Nitta et al., 2011, Nitta et al., 2010, Stavrou et al., 2013). Glycogag possesses a function similar to HIV-1 Nef, serve as an infectivity factor of MLV, and can assist Nef-deficient HIV-1's infectivity (Pizzato, 2010). It was also found that MLV glycogag, HIV-1 Nef and S2 of equine infectious anemia virus counteract the retroviral inhibition mediated by SERINC5 and SERINC3. This suggested the evolution of three independent retroviral accessory proteins to antagonize host SERINC5 and SERINC3 (Rosa et al., 2015, Usami et al., 2015, Chande et al., 2016, Ahi et al., 2016). Recent

studies demonstrated that glycogag protects MLV from A3 restriction factors (Kolokithas et al., 2010, Rosales Gerpe et al., 2015, Stavrou et al., 2013).

Here, we report that in contrast to HIV-1, Mo-MLV is restricted by producer cell A3A. We also reanalyzed the functional consequences of the presence of A3A on the expression of reporter genes encoded by plasmid DNA and confirm that A3A can inhibit plasmid-derived expression by cytidine deamination. A3A present in target cells could inhibit the incoming MLV particles by its deamination activity. In addition, the glycogag of MLV could counteract producer cell derived A3A and murine A3 by excluding them from virion packaging. However, glycogag was inefficient to protect incoming MLV against target cell A3A.

RESULTS

Interferon treatment strongly induces endogenous A3A in macrophages and inhibits the replication of MLV and HIV-1

A3 proteins were reported to be enhanced by type I and type II interferons (Liu et al., 2012, Peng et al., 2006). To verify the induction of A3A in monocyte-derived macrophages (MDMs), we treated them with IFN β and analyzed the antiviral effect of interferon on viral replication of MLV and HIV-1. Macrophages pretreated with interferon- β were infected and the reporter luciferase activity was measured three days post infection. Fig 1A shows that 100 and 1000 U/ml of interferon- β treatment can block 70% and 83% of respective MLV infectivity and 80% and 87% HIV-1 infectivity, although the Vpx can enhance the infectivity of HIV-1 to a certain level (Suppl. Fig. 1). As expected, interferon treatment boosted the A3A protein level in a dose-dependent manner while A3G was also moderately induced (Fig. 1B). This data allowed us to ask whether the enhanced expression of A3A in target cell has a role on inhibiting MLV. We performed 3D-PCR to selectively amplify the hypermutated reporter viral DNA (a 714-bp segment of the luciferase gene of the viral vector). At lower denaturation temperature (85.2°C), PCR amplicons were detectable from MDM samples treated with 100 U and 1000 U interferon, in a dose-dependent manner. Samples of

untreated MDM yielded PCR products at higher denaturation temperature (86.3°C) when compared to treated samples (Fig. 1C).

Thus, MLV infection of human macrophages can be blocked by interferon treatment. Since interferon treatment did not only raise the level of A3A but also of many interferon-induced genes (ISG) such as A3G and MxB (Fig 1B), we performed the following experiments by ectopic expression of A3A in HEK293T cells.

Effect of target cell A3A on MLV replication

To demonstrate the target cell effect of A3A on incoming MLV, we transfected 293T cells with A3A and its cytidine deaminase catalytic mutant, A3A.E72A and 24 h later, they were infected with the virus. 12-14 h post infection, total DNA was isolated and the viral reporter DNA was amplified using 3D-PCR. In addition, protein levels of A3A and A3A.E72A were determined at the same time point (Fig. 2A). Compared to the vector control or A3A.E72A, PCR products of A3A samples amplified at lower denaturation temperature (85.2°C) (Fig. 2B).

To determine G-to-A mutations potentially triggered by A3A, the PCR products generated at the lowest temperature were cloned and sequenced. The results showed several G-to-A mutations in a specific A3A-specific GA dinucleotide context and A3A caused a hypermutation rate of around 14% (Fig. 2C). Importantly we could not find any mutations in the control samples where we transfected the cells with vector plasmid or plasmid encoding A3A.E72A.

A3A mediates inhibition of plasmid expression

We first wanted to use our experimental system to provide a more quantitative assessment of whether A3A impairs the expression and integrity of co-transfected plasmids, as initially described by Stenglein et al., (Stenglein et al., 2010). Other recent studies using co-transfection systems with A3A plasmids observed either a slight (<20%) (Schmitt et al., 2011, Muckenfuss et al., 2006, Ooms et al., 2012) or a strong (2-to-4-fold) diminution of reporter

gene expression (Bulliard et al., 2011), possibly indicating a dose- and reagent-specific effect of A3A. To delineate any side effects of A3A during viral vector production, we co-transfected cells with the MLV-based luciferase transfer vector plasmid and increasing amounts (0 to 1000 ng) of A3A or A3A.E72A expression plasmids and analyzed the intracellular luciferase activity in the transfected cells two days post transfection. The results demonstrate an A3A dose-dependent inhibition of luciferase expression (Fig. 3). Notably, the mutant protein A3A.E72A increased the luciferase activity, likely due to its competitive binding to the substrate or any unknown factors. To verify this effect is not cooperatively promoted by the large T antigen expressed in the HEK293T cells, we performed a similar experiment with HEK293 cells (Fig. 3). Together, the data demonstrate that A3A's enzymatic activity inhibited the expression of plasmid-encoded luciferase in a dose-dependent manner in both 293 and 293T cell lines. Extensive hypermutation on the plasmids DNA and induction of genomic double-stranded DNA breaks (Landry et al., 2011) were observed in our experimental set up by transfected A3A wild type and not with catalytic mutant A3A.E72A.

The results demonstrate that ectopic A3A can induce cytidine deamination in plasmid DNA and likely inactivates plasmid-based expression. We conclude that the use of A3A in studies of viral replication requires a careful investigation of unwanted and possibly misleading side effects. However, compared to ectopic A3A in 293T cells, the endogenous A3A expression levels found in interferon-treated macrophages were higher (Suppl. Fig. 1B). MDMs (and not PBMCs) treated with 1000 U interferon for 24 h yielded an amount of A3A that surpasses the level of A3A produced with 1 µg plasmid DNA by transient transfection (Suppl. Fig. 1B).

Producer-cell-derived A3A restricts Mo-MLV

To test a producer cell effect of A3A, Mo-MLV was generated by transfection together with incremental amounts of expression plasmids for A3A and its catalytic mutant A3A.E72A. RT-normalized viral particles were used for transduction and the intracellular luciferase activity was determined two days post transduction. The titration experiment showed that A3A but

not the deaminase-inactive A3A.E72A efficiently restricts the replication of MLV (by up to 80%) in a dose-dependent manner (Fig. 4A).

The packaging of A3 proteins into retroviral particles is a prerequisite for targeting the early post-entry phases of infection (Mariani et al., 2003b, Münk et al., 2012a). We, therefore, analyzed A3A incorporation into the Mo-MLV particles by immunoblotting. A3A was found detectable in the Mo-MLV particles even with the lowest concentration of plasmid used (Fig. 4B), suggesting efficient encapsidation of A3A by MLV.

Encapsidated A3A resides at viral core of MLV

To understand if A3A is incorporated into the viral core, we isolated the viral cores by detergent stripping. Virions were concentrated and intact cores were fractionated with sucrose step gradient with a layer of detergent (1% Triton X-100) on top (Kotov et al., 1999, Wang et al., 2007). As a control, we purified intact virions by sucrose gradient that lacks the detergent phase. As reported, the viral core was relatively unstable, and during the process of core purification, a fraction of viral core proteins found disassembled (Fig. 4C) (Kotov et al., 1999). The detergent sensitive fraction containing VSV-G membrane proteins and digested p30 was prominently seen at the earlier fractions (soluble proteins) and the core fractions were enriched with p67 and p30 with A3A, devoid of VSV-G (Fig. 4C). This result suggests that MLV could not block encapsidation of A3A into nascent viral particles, and incorporated A3A found in viral cores.

A3A restricts Mo-MLV and AKV tropic strains

To understand whether A3A can restrict different strains of MLV, we repeated the analysis using packaging constructs derived from Mo-MLV and two variants of the related AKV MLV (N-tropic or B-tropic). The resulting virions differed only in their Gag-Pol protein. The amount of A3A plasmid was limited to 100 ng per transfection for all experiments to reduce the likelihood of mutations in plasmids and of DNA double-strand breaks. Viral supernatants

normalized by RT were subsequently used to infect feline CrFK cells that lack expression of the TRIM5 α protein (McEwan et al., 2009), and intracellular luciferase activity was measured. Using these experimental conditions, the infectivity of the Mo-MLV, N-tropic, and B-tropic particles were restricted significantly yet displayed a different level of inhibition (Fig. 5A). Whereas, the virus particles produced with catalytically inactive mutant A3A.E72A increased the luciferase activity above the level of vector control (no A3), suggesting a possible competitive effect of the catalytic mutant protein. Immunoblot analysis of cell lysates and viral particles detected expressed viral proteins and encapsulated A3A and A3A.E72A into Mo-MLV and AKV particles (Fig. 5B).

To assess the deaminase-dependent effect of A3A on viral infectivity, we used 3D-PCR to characterize the integrity of viral cDNA produced in the presence of A3A during transduction of target cells. The cDNA samples of Mo-MLV particles generated with A3A.E72A or vector control (no A3) did not result in PCR products amplified at lower denaturing temperatures (Fig. 5C). In contrast, DNA samples of cells infected with Mo-MLV particles assembled in the presence of A3A yielded PCR amplicons at the lower denaturing temperatures as an indication of A3-mutagenized sequences. PCR products from the lowest denaturing temperature of each were cloned and sequenced. Sequencing results confirmed G-to-A hypermutations caused by A3A (G-to-A changes 16%), and that none were elicited by the corresponding A3A.E72A (G-to-A changes 0.2%) (Fig. 5C). Virions made in the absence of any A3A plasmids displayed 0.14% G-to-A changes in their cDNA. The dinucleotide substitutions occurred in an A3A-specific motif of GA to AA as we found before (Fig. 2C).

Human and rhesus A3A but not deaminase-defective A3A.F75L mutant can inhibit MLV

Because it was reported that the three amino acid deletion (²⁷SVR²⁹) in A3A was acquired in hominids that do not alter its antiviral function (Schmitt et al., 2011). But the analogous deletion in rhesus A3A abrogated its antiviral activity against HIV-1 Δ vif and HTLV-1 (Schmitt et al., 2011, Ooms et al., 2012). We tested the human A3A variants containing these additional amino acids (+SV and +SVR) found in rhesus macaque. As a control, we added

rhesus A3A and the variants lacking the equivalent amino acids (Δ SV and Δ SVR). MLV viral particles were produced with the above A3A variants or vector control, and their infectivity was tested. As shown in Fig. 6A, both human and rhesus A3A potently inhibited MLV replication. Insertion of SV or SVR amino acids in human A3A did not affect its anti-MLV activity but interestingly, rhesus A3A deletion mutants SV and SVR lost 2-fold and 4-fold antiviral activities, respectively (Fig. 6A). Human and rhesus A3A variants were expressed and incorporated into MLV particles in a similar manner (Fig. 6B). This data, together with the previous observations (Schmitt et al., 2011, Ooms et al., 2012) suggest that the A3A from human and rhesus share an evolutionally conserved capacity to restrict retroviruses.

Human A3A and a deaminase-defective A3A.F75L mutant were shown to inhibit replication of the parvovirus adeno-associated virus in a deaminase-independent manner (Narvaiza et al., 2009). A non-catalytic core residue, F75 in A3A is reported to be crucial for its deaminase activity, as A3A.F75L mutant failed to deaminate cytidines (Narvaiza et al., 2009). Since we found the loss of MLV activity with active site mutant A3A.E72A in all experiments, and to rule out the possibility that this is not due to the distorted integrity of the active site in the E72A mutant, we tested the deaminase-defective A3A.F75L (Narvaiza et al., 2009). MLV particles were produced with these A3A mutants, and tested for infectivity. As expected, both enzymatically inactive A3A variants, A3A.F75L and A3A.E72A lost its capacity to inhibit MLV replication (Fig. 6C). All the tested A3A mutants were produced and encapsidated nearly similar into MLV virions (Fig. 6D). These results further indicate that A3A inhibits MLV by a deamination-dependent mechanism.

Glycogag protect MLV from A3A and mouse A3

According to Ensembl genome browser, there are 9 protein-coding transcripts of A3 reportedly found in murine cells (Aken et al., 2017), in which the full-length (429 amino acids) canonical form is made up of 9 exons. An alternatively spliced variant lacking exon 5 (396 amino acids) was shown to have more antiviral activity than its full-length counterpart (Takeda et al., 2008, Langlois et al., 2009, Okeoma et al., 2009, Li et al., 2012, Mariani et al.,

2003a). Hence, to possibly obtain variants other than the well-known clone (exon 5 deleted variant), we performed reverse transcription-PCR using spleen RNA of C57BL/6 mice. We got three different clones of mA3 lacking exon 5 (termed, mA3) in a successive PCR with mA3 specific primers. The first variant had a single amino acid change, mA3.R354W (Accession no of mA3 isoform 2: NP084531) when compared to mA3 (NIH AIDS reagent program cat. No: 10021) as previously described (Mariani et al., 2003a). Tryptophan found in this variant is analogous to the full-length mA3 (mA3 isoform 1, Accession no: NP001153887) as reported before (Takeda et al., 2008, Langlois et al., 2009). A second variant that was not reported earlier had a 39 base pair (bp) deletion in exon 7, named mA3- Δ 13. The third one had a 14 bp insertion that causing a truncation encoding a 207 amino acid long mA3, which is not included in the current study. The amino acid sequence alignment of mA3, mA3.R354W, and mA3- Δ 13 is given in Suppl. Fig. 2. These mA3 variants were used in the following experiments.

Because our primary analysis suggested very low level of glycogag proteins in MLV (pHIT60 derived) vectors (Fig. 7A), we expressed glycogag proteins *in trans* using p8065-2, a full-length glycogag coding construct and gg88 that codes only the 88 amino acids of glycogag lacking gag polyprotein (Nitta et al., 2011). To test the effect of glycogag on infectivity of MLV, we produced MLV particles together with A3A, mA3 variants or a vector control encoding no A3. In addition, we produced full-length amphotropic MLV together with the luciferase transfer vector and A3s (without any additional pseudotyping). Infectivity of RT-normalized particles was measured three days later. A3A, mA3, mA3.R354, and mA3- Δ 13 reduced the infectivity of pHIT60-derived MLV more efficiently than the infectivity of the amphotropic MLV (Fig. 7B). However, co-expression of glycogag increased the infectivity of MLV made in the presence of A3 to the level of control virus produced without A3. The level of inhibition by different A3s slightly varied, but importantly, the presence of glycogag improved the replication of A3 containing pHIT60 MLV (Fig. 7B). The successful expression of the different A3s was confirmed by immunoblotting (Fig. 7C).

Glycogag did not affect the catalytic activity of A3A

As A3A can enzymatically affect the expression of plasmid encoded luciferase (Fig. 4), we asked whether the co-expression of glycogag can rescue the plasmid DNA from the mutating activity of A3A. We performed similar experiments by co-transfecting A3A, glycogag expression plasmids, and MLV-luciferase vector. However, the dose-dependent A3A mediated inhibition of luciferase activity was equally reduced in presence and absence of glycogag (Fig. 8A).

Because we detected glycogag protein (gg88) to be packaged into MLV particles (Fig. 8B), we wanted to test if virus particle associated glycogag can counteract the target cell A3A's deamination activity in MLV infection. MLV particles without and with glycogag were produced and used to infect A3A expressing cells. Using 3D-PCR to analyze for potential mutations caused in MLV genome during the early infection phase demonstrated that glycogag cannot reduce the A3A activity on MLV genomes incoming into the cells. In both samples containing MLV with and without glycogag PCR products could be amplified at the lower denaturation temperature (85.2°C) (Fig. 8C).

Glycogag selectively excludes A3A packaging and enhance MLV infectivity

Since glycogag did not alter the A3A's enzymatic activity, we hypothesized that it may exclude the A3 packaging into MLV. To test this, we performed immunoblot analysis of cell and viral lysates of MLV produced together with glycogag or not. Immunoblots in Fig. 8D show that A3A and mA3 can incorporate into MLV in absence of glycogag but not when glycogag was co-expressed. Thus, these data suggest a model, in which glycogag counteract A3s from producer cell by preventing their packaging into viral particles. Future experiments should address the question whether glycogag has specificity for individual A3 proteins and viruses.

MATERIALS AND METHODS

Cell culture: HEK293T and CrFK (feline renal fibroblast cells) cells were maintained at 37°C in a humidified atmosphere of 5% CO₂ in Dulbecco's high-glucose modified Eagle's medium (Biochrom, Berlin, Germany), supplemented with 10% fetal bovine serum (FBS), 2 mM L-glutamine, 50 units/ml penicillin, and 50 µg/ml streptomycin.

Preparation and cultivation of human peripheral blood-derived CD14⁺ macrophages: CD14⁺ monocytes were purified and enriched from human peripheral blood mononuclear cells (PBMCs) and differentiated into macrophages in RPMI 1640 medium supplemented with antibiotics, 10% fetal calf serum and 40 ng/ml recombinant human M-CSF (Peprotech) as described before (Ehltling et al., 2015). Cells were used after 8 days of cultivation and differentiation.

Interferon β stimulation: Monocyte-derived macrophages (MDMs) were treated with 0, 10, 100 and 1000 U/ml of human interferon β, 1a (PBL assay science) for 24 h. After treatment, one set of samples were lysed with RIPA buffer for immunoblot determination. Another set of MDMs treated with (0, 100, 1000 U/ml) interferon β were transduced with HIV-1Δ*vif* and MLV viral particles and viral infectivity was evaluated by luciferase assay after 72 h as described below. To detect endogenous (total) A3 catalyzed editing of MLV viral genome, infected MDMs were collected after 12 h for DNA extraction and following PCR of viral DNA (see 3D-PCR section).

Plasmids: The MLV packaging plasmids CIG-N, CIG-B, and pHIT60 were kindly provided by Jonathan Stoye, which encode for the *gag-pol* of AKV N-tropic, AKV B-tropic, and Mo-MLV, respectively (Bock et al., 2000). The MLV luciferase reporter plasmid MP71-luc is based on the MP71 plasmid that was previously described before (Schambach et al., 2000), kindly provided by Harald Wodrich. The MP71-luc plasmid contains the firefly luciferase gene

cloned into the EcoRI endonuclease restriction of MP71. The replication competent amphoteric MLV viral vector, R675 was a gift from Carol Stocking. The APOBEC3A (A3A)-HA expression construct is coding for the human A3A with three C-terminal hemagglutinin (HA)-tags (Wiegand et al., 2004), kindly provided by Bryan Cullen. The catalytic inactive A3A.E72A mutant was previously described (Muckenfuss et al., 2006). The HIV-1 packaging plasmid pMDLg/pRRE encodes *gag-pol*, and the pRSV-Rev for the HIV-1 *rev* (Dull et al., 1998). The HIV-1 vector pSIN.PPT.CMV.Luc.IRES.GFP expresses the firefly luciferase and GFP reported previously (Bähr et al., 2016). MLV and HIV-1 based viral vectors were pseudotyped using the pMD.G plasmid that encodes the glycoprotein of VSV (VSV-G). The pTR600 APOBEC3A plasmid is a gift from Viviana Simon (Ooms et al., 2012). Human and rhesus A3A variants cloned in pTR600 was previously reported by us (Ooms et al., 2012). In addition, we constructed a point mutant, pTR600-A3A.F75L mutant by site directed mutagenesis using primers forward 5'-CGGAGCTGCGCTTGTGGACCTGGTTC and reverse 5'-CGGAGCTGCGCTTGTGGACCTGGTTC. The M-MuLV glycoag (gPr80gag) expression plasmid p8065-2 and 2XHA tagged gg88 plasmid (2xHA-gg88, which expresses 2XHA epitope tags and the 88 amino acids at the N-terminus of gPr80gag) were generously provided by Hung Fan. Note that the putative CUG start codon in both p8065-2 and gg88 plasmids were replaced with AUG by site-directed mutagenesis as described before (Nitta et al., 2011). In addition, murine A3 (mA3) isoforms were amplified from cDNA, prepared from mouse (C57BL/6 strain) spleen RNA using following primers forward 5'-EcoRI-GGTGAATTCGCCATGGGACCATTCTGTCTGGGATGC and reverse 5'-XhoI-TATCTCGAGTCAAGCGTAATCTGGAACATCGTATGGGTAAGACATCGGGGGTCCAAGCT, the two different variants of mA3 with a C-terminal HA tag was then cloned into EcoRI and XhoI restriction sites of pcDNA3.1.

Virus production and isolation: 293T cells were transiently transfected using Lipofectamine LTX and plus reagent (Invitrogen, Karlsruhe, Germany) with appropriate combination of viral and A3A plasmids (in a six-well plate, MLV: 1000 ng pHIT60 or tropic plasmids CIG-N or CIG-B, 1000 ng pMP71-luc, 150 ng pMD.G with 100 ng A3A plasmid; in a twelve well plate, MLV:

450 ng pHIT60, 600 ng pMP71-luc, 100 ng pMD.G with 100 to 1000 ng A3A plasmid (prepared for Fig. 3A); Amphoteric MLV: 500 ng R675, 500 ng with 100 ng A3A or 400 ng mA3 (unless otherwise mentioned) together with pcDNA3.1 as a vector control. Note that the overall plasmid concentration was kept constant in all transfections by adding pcDNA3.1 plasmid as required. 48 h post-transfection, virion containing supernatants were collected and concentrated by layering on 20% sucrose cushion and centrifuged for 4 h at 14,800 rpm. Viral particles were resuspended in mild lysis buffer (50 mM Tris (pH 8), 1 mM PMSF, 10% glycerol, 0.8% NP-40, 150 mM NaCl and 1X complete protease inhibitor) and proteins were subjected to immunoblotting. For experiments involving glycogag plasmids p8065-2 and pgg88 the following transfection scheme was used: 500 ng pHIT60, 500 ng pMP71-luc, 100 ng pMD.G with 100 ng A3A or 400 ng mA3, 500 ng p8065-2 or pgg88, balanced appropriately with pcDNA empty plasmid to maintain constant ng of DNA in a six well plate.

Luciferase-based infectivity assay: Mo-MLV-based luciferase reporter viruses, Amphoteric MLV were used to transduce HEK293T cells, while the experiment shown in Fig.5 with tropic strains, CrFK cells were transduced. Prior infection, the amount of reverse transcriptase (RT) in the viral particles was determined by RT assay using Cavid HS kit Lenti RT (Cavid Tech, Uppsala, Sweden). Normalized RT amount equivalent viral supernatants were transduced in all the experiments. 72 h later, and luciferase activity was measured using SteadyLite HTS luciferase reagent substrate (Perkin Elmer, Rodgau, Germany) in black 96-well plates on a Berthold MicroLumat Plus luminometer (Berthold Detection Systems, Pforzheim, Germany). Transductions were done in triplicate and at least two independent experiments were performed.

Viral core isolation: MLV cores were isolated according to the protocol described for isolating HIV-1 cores (Wang et al., 2007) Viral particles were produced by transient transfection of 293T cells (1000 ng pHIT60, 1000ng pMP71-luc, 200ng A3A and 150ng VSV-G). Two days post transfection the virions containing supernatants were purified and

concentrated by centrifuging through 20% sucrose cushion in a table top centrifuge at 14000 rpm for 4 h. Viral particles resuspended in STE buffer (10 mM Tris-HCl, pH 7.4, 100 mM NaCl, 1 mM EDTA), loaded on the top of 7.5% sucrose followed by 1% Triton X-100 layer (in 15% sucrose) and a 20–70% sucrose gradient, and centrifuged at 136,000 \times g for 16 h at 4°C in ultra-clear centrifuge tubes (13 x 51 mm, Beckman Coulter) in an MLS-50 rotor (Beckman Coulter). Next day, 12 fractions were collected and subjected for Immunoblot. Viral compartments and the A3 proteins were detected by probing the blots with appropriate antibodies (MLV anti-p30, anti-VSV-G and anti-HA).

A3A mediated inhibition of plasmid expression: HEK293T cells and HEK293 cells lacking large T-antigens (2×10^5 cells/well in a 12-well plate) were co-transfected with the luciferase expression plasmid MP71-luc (200 ng), and increasing amounts of the A3A or A3A.E72A expression plasmids (0, 0.1, 0.25, 0.5, 0.75, and 1 μ g). pcDNA3.1 empty vector was used to keep total DNA concentrations equivalent for each transfection. Two days post-transfection, luciferase activity was measured as described above. Results are representative of three independent experiments. Similar A3A titration experiment was performed in 293T cells with 100 ng of the MP71-luc plasmid with 200 ng of p8065-2 or pgg88 glycogag plasmid.

Immunoblots: Transfected 293T cells PBMCs or MDMs were washed with phosphate buffered saline (PBS) and lysed in radioimmunoprecipitation assay buffer (RIPA, 25 mM Tris (pH 8.0), 137 mM NaCl, 1% glycerol, 0.1% SDS, 0.5% sodium deoxycholate, 1% Nonidet P-40, 2 mM EDTA, and protease inhibitor cocktail set III [Calbiochem, Darmstadt, Germany].) 20 min on ice. Lysates were clarified by centrifugation (20 min, 14800 rpm, 4°C). Samples (cell or viral lysate) were boiled at 95°C for 5 min with Roti load reducing loading buffer (Carl 726 Roth, Karlsruhe, Germany) and subjected to SDS-PAGE followed by transfer (Semi-Dry Transfer Cell, Biorad, Munich, Germany) to a PVDF membrane (Merck Millipore, Schwalbach, Germany). Membranes were blocked with skimmed milk solution and probed with appropriate primary antibody, mouse anti-hemagglutinin (anti-HA) antibody (1:7,500

dilution, MMS-101P, Covance, Münster, Germany); mouse anti- α -tubulin antibody (1:4,000 dilution, clone B5-1-2; Sigma-Aldrich, Taufkirchen, Germany), mouse anti-capsid p24/p27 MAbs AG3.0 (Simm et al., 1995) (1:250 dilution, NIH AIDS Reagents); rabbit anti-ApoC17 for endogenous A3A and A3G detection (1:10⁴ dilution, NIH AIDS Reagents); goat antiserum against Rauscher murine leukemia virus p30 [1:10⁴ dilution, NCI HD 539, (ATCC VR-1564AS-Gt)] Secondary Abs.: anti-mouse (NA931V), anti-rabbit (NA934V) horseradish peroxidase (1:10⁴ dilution, GE Healthcare) and anti-goat IgG-HRP (1:10⁴ dilution, sc-2768, Santa Cruz biotechnology, Heidelberg, Germany). Signals were visualized using ECL chemiluminescent reagent (GE Healthcare).

Differential DNA denaturation (3D) PCR: 293T cells were cultured in the 6-well plates and infected with DNase I treated viruses for 12 hours. Cells were harvested and washed in PBS, the total DNA was isolated using DNeasy DNA isolation kit (Qiagen, Hilden, Germany). A 714-bp fragment of the luciferase gene was amplified using the primers 5'-GATATGTGGATTTCGAGTCGTC-3' and 5'-GTCATCGTCTTTCCGTGCTC-3'. For selective amplification of the hypermutated products, the PCR denaturation temperature was lowered stepwise from 87.6°C to 83.5°C (83.5°C, 84.2°C, 85.2°C, 86.3°C, 87.6°C) using a gradient thermocycler (Jaguva Vasudevan et al., 2017). The PCR parameters were as follows: (i) 95°C for 5 min; (ii) 40 cycles, with 1 cycle consisting of 83.5°C to 87.6°C for 30 s, 55°C for 30 s, 72°C for 1 min; (iii) 10 min at 72°C. PCRs were performed with Dream Taq DNA polymerase (Thermo Fisher Scientific). PCR products from the lowest denaturation temperatures were cloned using CloneJET PCR Cloning Kit (Thermo Fisher Scientific) and sequenced. A3 induced hypermutations of at least eight independent clones were analyzed with the Hypermut online tool (Rose and Korber, 2000) (<http://www.hiv.lanl.gov/content/sequence/HYPERMUT/hypermut.html>). Mutated sequences (clones) carrying similar base changes were omitted and only the unique clones were presented for clarity.

To assess the target cell A3A mediated DNA editing of incoming MLV, we first transfected 293T cells with 600 ng A3A. ~24 h later, DNase I treated MLV particles (prepared with no A3) were infected and 3D-PCR performed as given above.

Statistical analysis: Data were represented as the mean with SD in all bar diagrams. Statistically significant differences between two groups were analyzed using the unpaired Student's t-test with GraphPad Prism version 5 (GraphPad Software, San Diego, CA, USA). A minimum *p* value of 0.05 was considered as statistically significant.

ACKNOWLEDGMENTS

We thank Christian Ehling for providing purified CD14⁺ monocytes and helpful discussion, Prashant Shinde and Philipp Lang for a gift of murine RNA, and Wioletta Hörschken for excellent technical assistance. We thank Neeltje Kootstra, Hung Fan, Carol Stocking, Bryan R Cullen, Reuben S. Harris, Viviana Simon, Jonathan Stoye, Harald Wodrich for reagents. The following reagent was obtained through the NIH AIDS Research and Reference Reagent Program, Division of AIDS, NIAID, NIH: a monoclonal antibody to HIV-1 p24 (AG3.0), from Jonathan Allan, anti-ApoC17, from Klaus Strebler and pc-Mu-APOBEC3G-HA, from Nathaniel R. Landau. CM is supported by Heinz-Ansmann foundation for AIDS research.

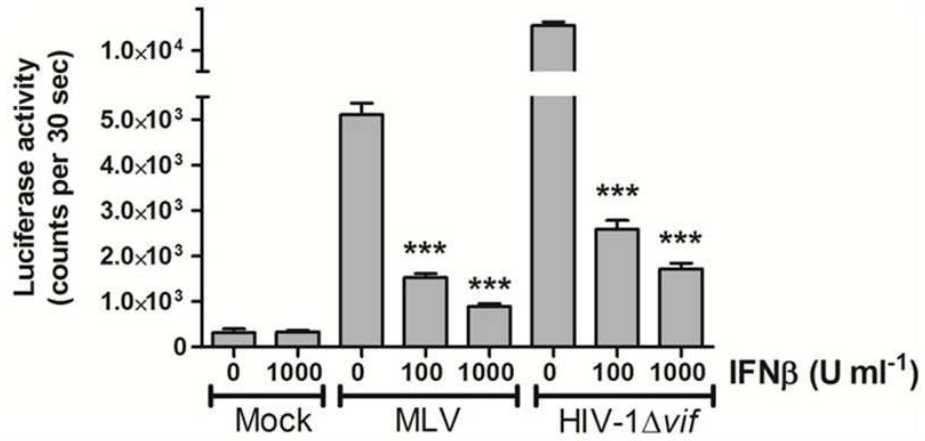
AUTHOR CONTRIBUTIONS

AAJV performed most of the experiments, conceived the study, analyzed data wrote the manuscript. AK carried out initial MLV 3D-PCR, analyzed data while AF and DM contributed pilot experiments. RK analyzed data. GS analyzed data. DH analyzed data. CM conceived and supervised the study, analyzed data and wrote the manuscript. All authors reviewed and approved the final version of the manuscript. The authors declare no competing financial conflicts of interest.

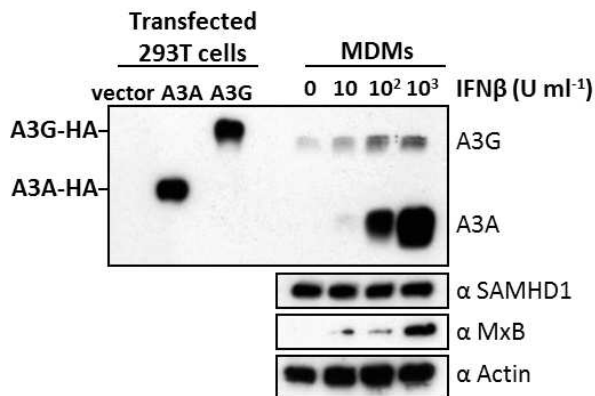
FIGURES

Figure 1

A



B



C

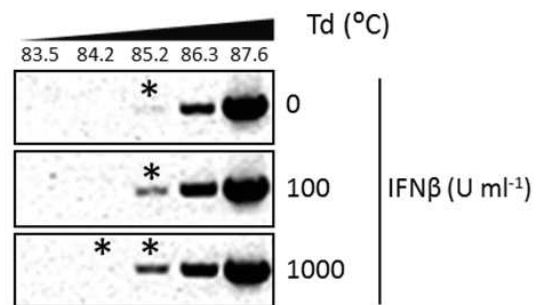


Figure 1. Effect of IFN β treatment on the infectivity of MLV and HIV-1 Δ vif

(A) Human monocyte-derived macrophages (MDMs) were treated with indicated amounts of IFN β for 24 h, before infecting them with MLV and HIV-1 Δ vif luciferase reporter viruses. Infectivity of viruses was determined by quantification of luciferase activity 72 h post infection. Values are means \pm standard deviations (error bars) for three independent experiments. Unpaired *t*-tests were computed to determine whether differences between untreated and interferon-treated samples reach the level of statistical significance. Asterisks represent statistically significant differences: ***, $p < 0.0001$. Please note that the break in the *y*-axis of the graph made for presentation purpose. (B) The amount of proteins in the cell lysate of MDMs and transfected 293T cells were determined by immunoblotting. A3G and A3A were stained with anti-A3G antiserum cross-reactive to A3A. MxB, SAMHD1 were stained with anti-SAMHD1, anti-MxB antibodies, respectively. Actin served as a loading control for MDM samples. “ α ” represent anti-antibody. (C) 3D-PCR: Total DNA of MLV infected MDMs (12 h post infection) were isolated and a 714 bp segment of reporter viral DNA was selectively amplified using 3D-PCR. Td = denaturation temperature.

Figure 2

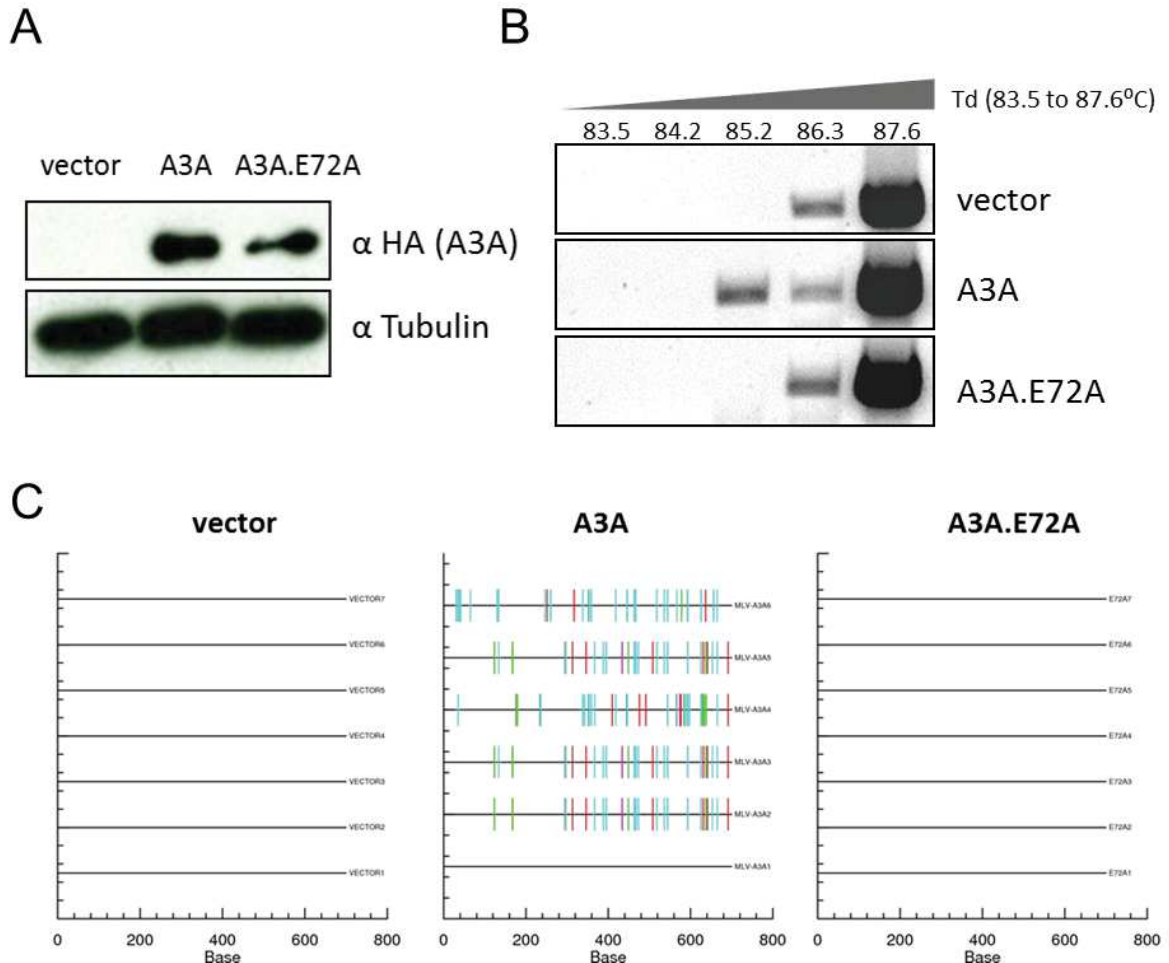


Figure 2. Target cell A3A hypermutates incoming MLV genome

(A) Ectopic expression of vector control, A3A, A3A.E72A in 293T cells. Cells were lysed after 12 h post infection of MLV, the same time point also used for subsequent 3D-PCR. (B) Following infection, half of the cells were used to extract total DNA and a 714 bp segment of reporter viral DNA was selectively amplified using 3D-PCR. Td = denaturation temperature. PCR products were stained with ethidium bromide (C) To determine the amount mutation conferred by A3 proteins, PCR products from the lowest denaturing temperature, shown in (B) were cloned (marked with an asterisk (*)) and a number of independent clones were sequenced, analyzed and the mutation pattern is presented using hypermut tool (note: identical clones were omitted). The percentage of G-to-A changes for each sample was

indicated. Each sequence is given as a horizontal line. Mutations were denoted as small vertical lines. Red, cyan, magenta, green and black colored lines represent the GG-to-AG, GA-to-AA, GT-to-AT, GC-to-AC, and non-G-to-A mutations, respectively.

Figure 3

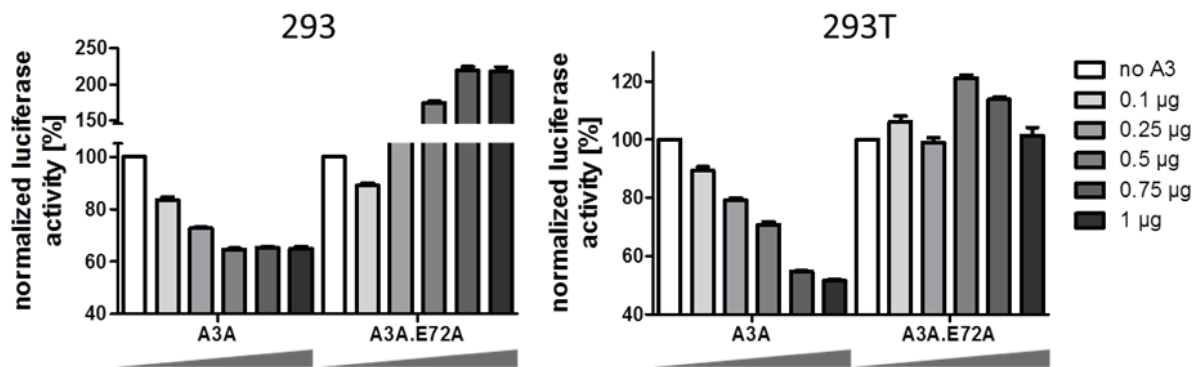


Figure 3. A3A impairs luciferase expression of transfected plasmid DNA

293 and 293T cells were cotransfected with 200 ng of MLV-luciferase vector with increasing amount of A3A or A3A.E72A expression plasmid (as indicated). Intracellular luciferase activity of these transfected cells was determined after 48 h and presented. Values are means \pm standard deviations (error bars) for three independent reads. The break in the y-axis of the graph made for presentation purpose.

Figure 4

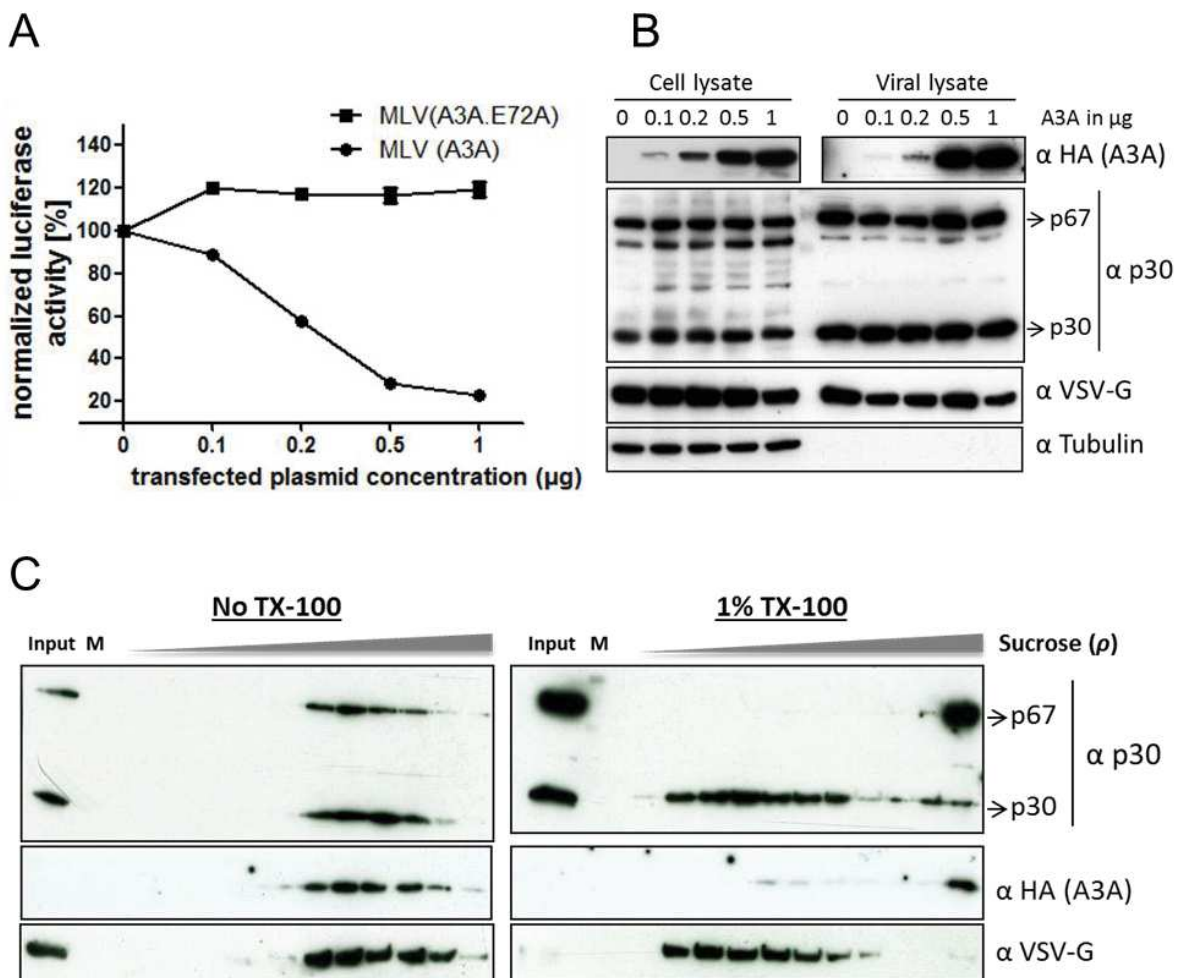
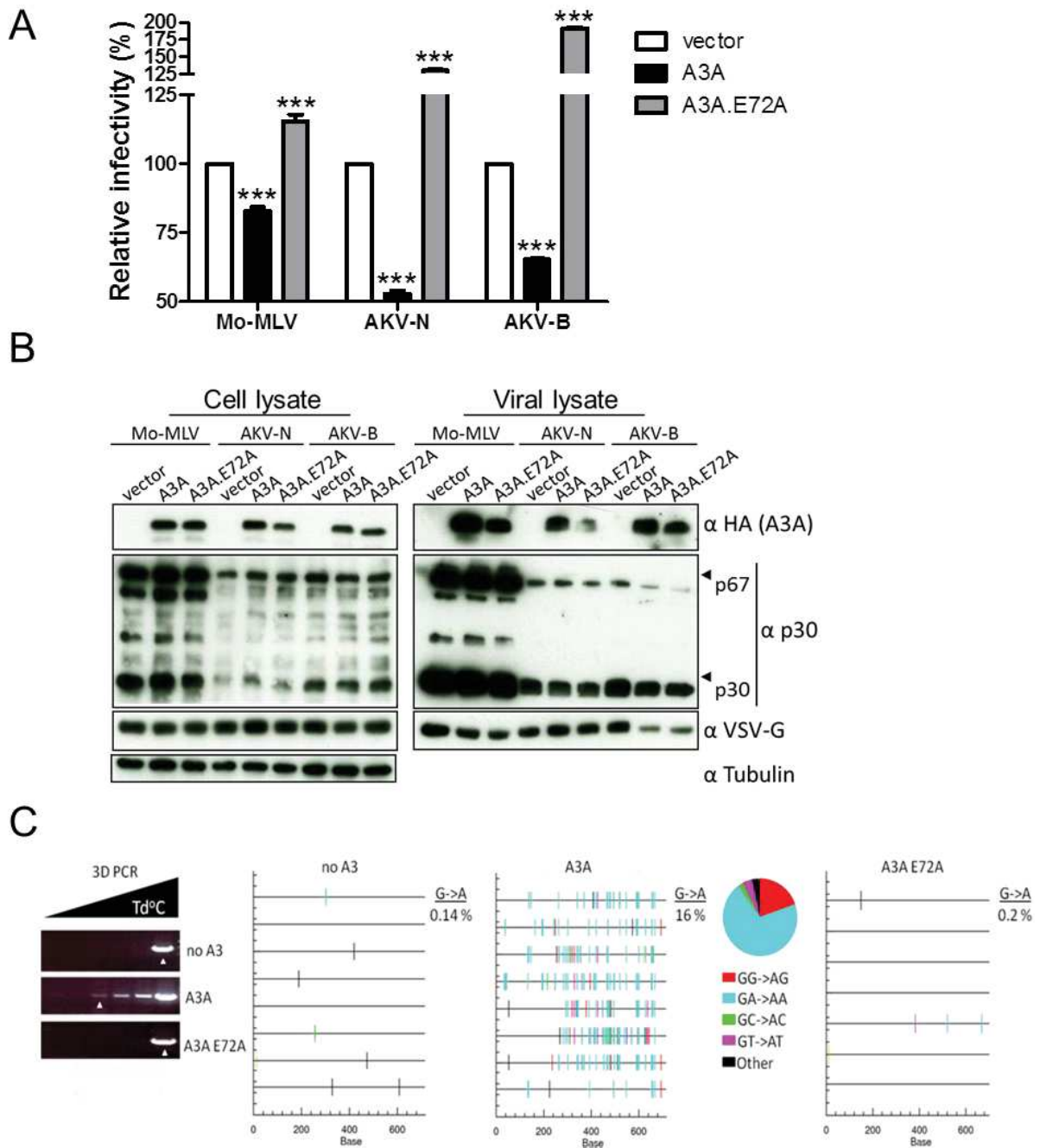


Figure 4. Producer cell A3A restrict MLV infection by associating into viral core

(A) The dose-dependent anti-MLV activity of A3A. MLV virions produced in the presence of increasing concentration of expression plasmids encoding A3A or A3A.E72A. Infectivities of (RT-normalized) the equal amount of viruses, relative to the virus did not contain A3A, were determined by quantification of luciferase activity in 293T cells. Values are means ± standard deviations (error bars) for three independent experiments. Unpaired *t*-tests were computed

to determine whether differences between vector and each A3A protein reach the level of statistical significance. All of the subjects had a significance of $p < 0.0001$. (B) Immunoblot shows the amount of A3A or A3A.E72A in cell and viral lysates of MLV. A3A (anti-HA), MLV capsid (anti-p30), VSV-G (anti-VSV-G) were detected with respective antibodies. Tubulin served as a loading control. (C) A3A viral core localization was achieved by detergent stripping. Viral capsid, VSV-G, and A3A present in the core fractions and detergent sensitive fractions were determined by immunoblotting. TX-100 and “ α ” denotes detergent Triton X-100, and anti-antibody, respectively.

Figure 5



293T cells. Values are means \pm standard deviations (error bars) for three independent experiments. Unpaired *t*-tests were computed to determine whether differences between vector and each A3A protein reach the level of statistical significance. Asterisks represent statistically significant differences: ***, $p < 0.0001$. The break in the *y*-axis of the graph made for presentation purpose. (B) Immunoblot shows the amount of A3A or A3A.E72A in cell and viral lysates of different strains of MLV. A3A (anti-HA), MLV capsid (anti-p30), VSV-G (anti-VSV-G) were detected with respective antibodies. Tubulin served as a loading control. (C) Producer cell A3A-3D-PCR: Mo-MLV virions produced together with vector, A3A or A3A.E72A was used to infect 293T cells. 12 h later, the total DNA of the infected cells was isolated and 3D-PCR was performed as stated in Fig. 2B. The percentage of G-to-A changes for each sample was indicated. Each sequence is given as a horizontal line. Mutations were denoted as small vertical lines. Red, cyan, magenta, green and black colored lines represent the GG-to-AG, GA-to-AA, GT-to-AT, GC-to-AC, and non-G-to-A mutations, respectively. The dinucleotide preference of A3A was also given as a pie chart.

Figure 6

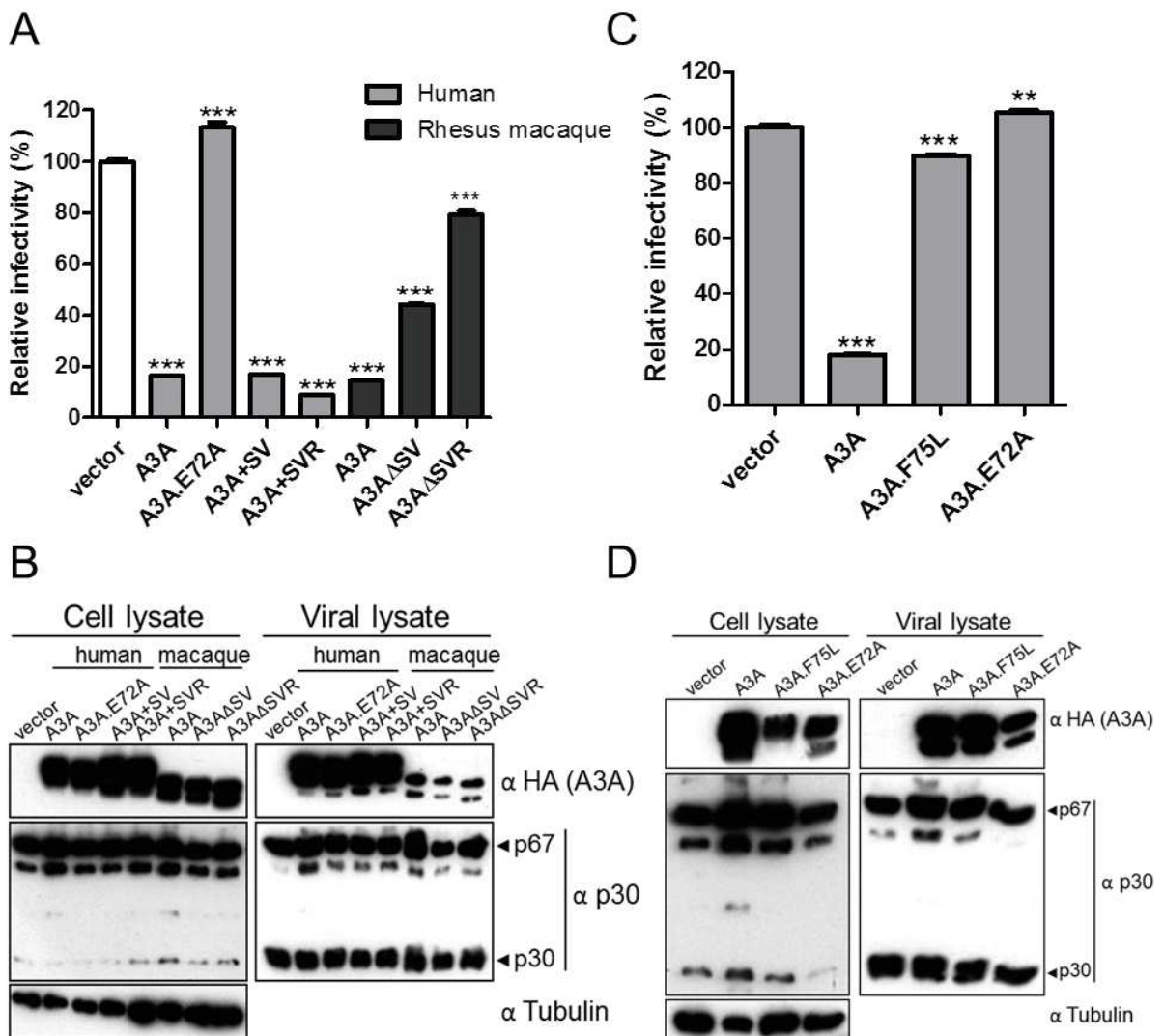
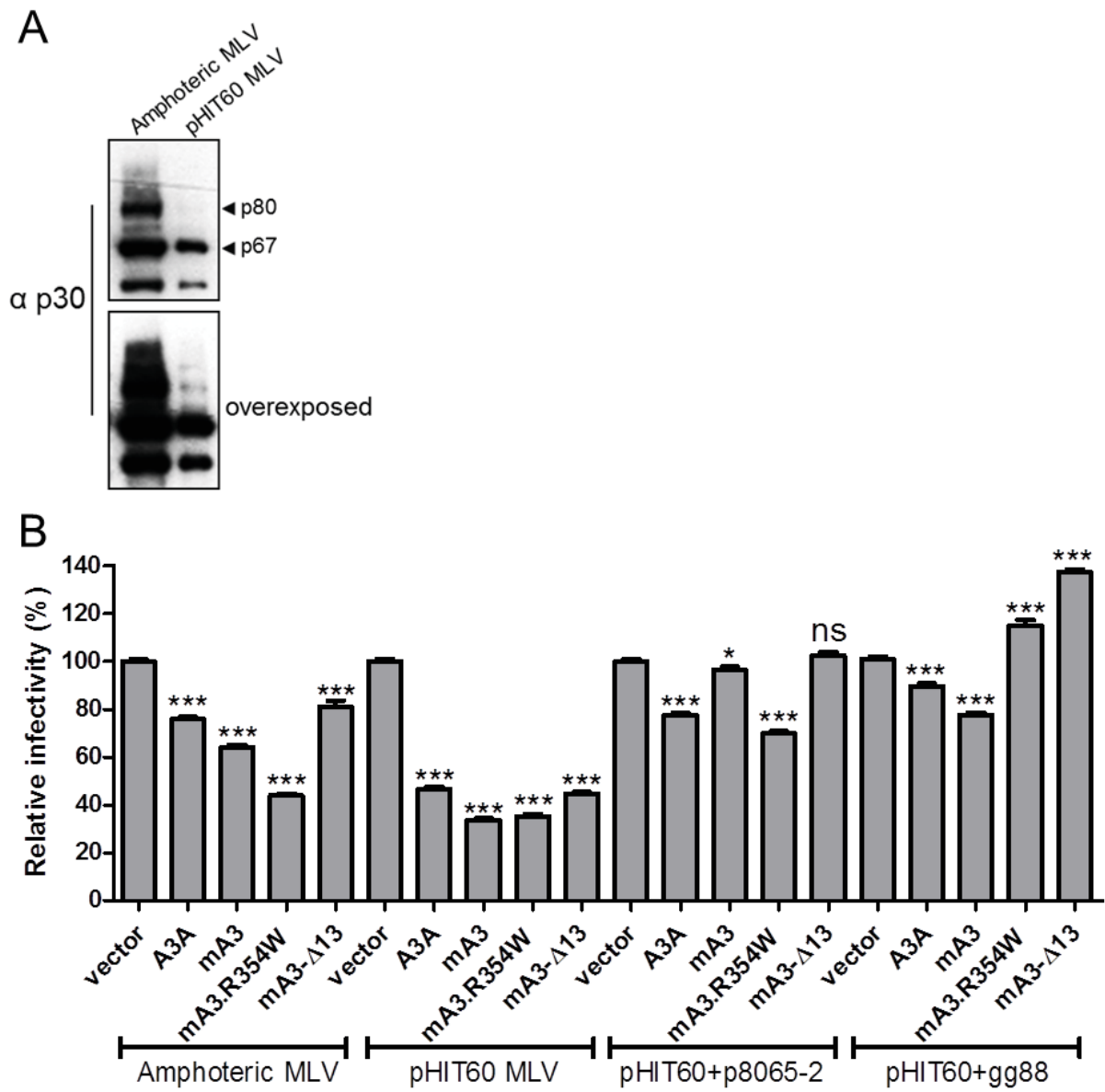


Figure 6. Deaminase-dependent MLV restriction of human and rhesus A3A

(A) MLV virions produced in the presence of vector only, human A3A, A3A.E72A, A3A+SV, A3A+SVR, rhesus A3A, A3AΔSV, and A3AΔSVR. Infectivities of (RT-normalized) the equal amount of viruses, relative to the virus did not contain A3A, were determined by quantification of luciferase activity in 293T cells. Values are means ± standard deviations (error bars) for three independent experiments. Unpaired *t*-tests were computed to determine whether differences between vector and each A3A protein reach the level of

statistical significance. Asterisks represent statistically significant differences: **, $P < 0.001$; and ***, $P < 0.0001$. (B) Immunoblot shows the amount of A3A or variants of A3A in cell and viral lysates of different strains of MLV. A3A (anti-HA), and MLV capsid (anti-p30) were detected with respective antibodies. Tubulin served as a loading control. (C) and (D) Experiments similar to (A) and (B) was carried out with vector, A3A, deaminase-defective A3A.F75L, and A3A.E72A.

Figure 7



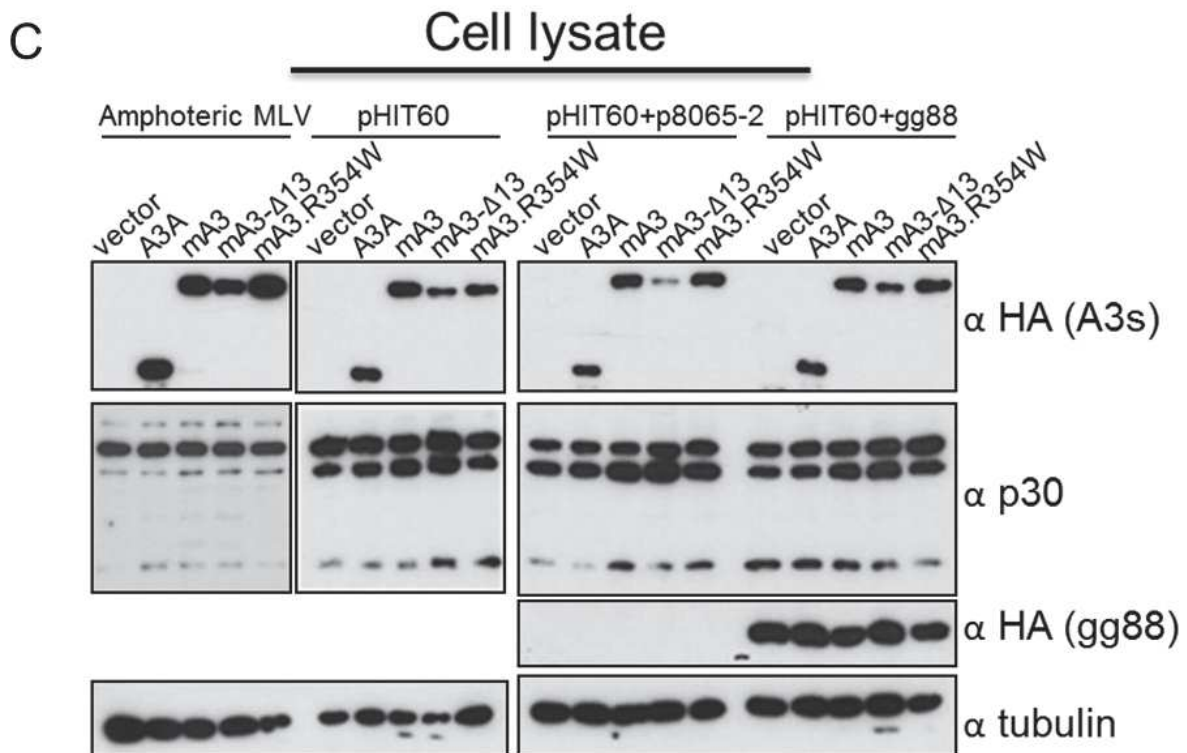


Figure 7. Effect of human and mouse A3 on the infectivity of pHIT60 and amphoteric MLV

(A) p67 (gag) and p80 (glycogag) expression found in cells transfected with the equal amount of pHIT60 and amphoteric MLV expression vectors. Blots were stained with anti-p30 antibody. An overexposed figure is also presented. (B) MLV virions produced in the presence of vector only, human A3A, and mouse A3 (mA3) variants. Four different group of MLV virions were made as indicated (Amphoteric MLV, pHIT60 MLV, and pHIT60 together with glycogag expression plasmid p8065-2 or gg88 that encodes only the 88 amino acids of glycogag lacking gag polyprotein). Infectivities of (RT-normalized) the equal amount of viruses, relative to the virus did not contain A3A, were determined by quantification of luciferase activity in 293T cells. Values are means \pm standard deviations (error bars) for three independent experiments. Unpaired *t*-tests were computed to determine whether differences between vector and each A3 protein reach the level of statistical significance. Asterisks represent statistically significant differences: *, $P < 0.05$; **, $P < 0.001$; and ***, $P < 0.0001$, and ns, not significant. (C) Immunoblot shows the amount of human A3A or mA3

variants in cell lysates. A3 (anti-HA), MLV capsid (anti-p30), gg88 (anti-HA) were detected with respective antibodies. Tubulin served as a loading control.

Figure 8

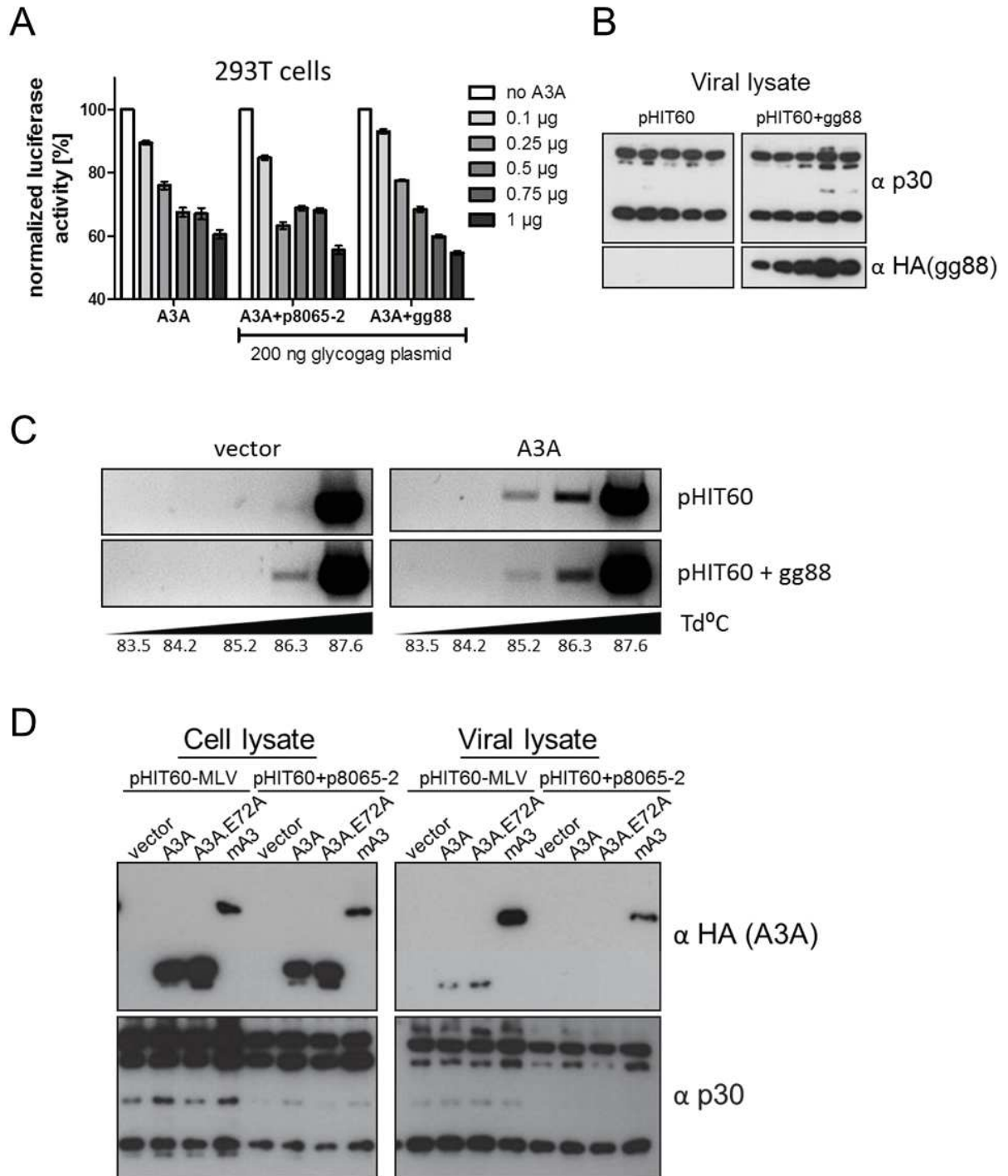
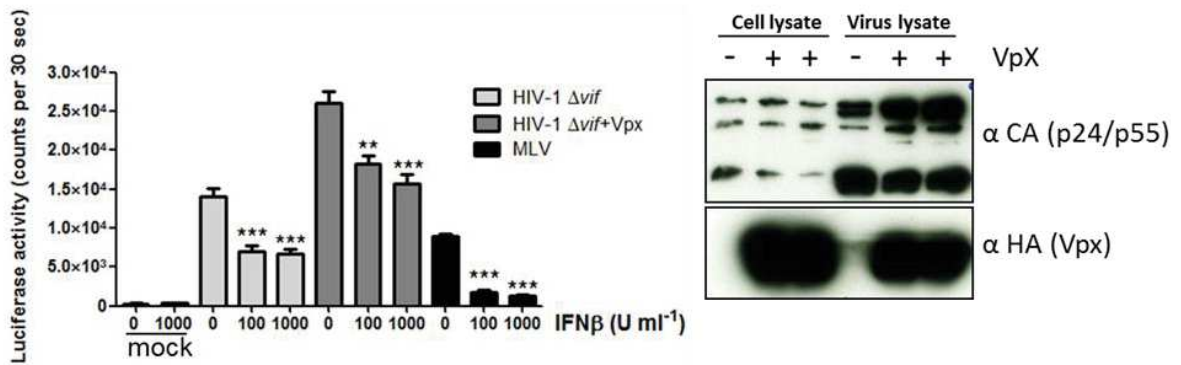


Figure 8. Glycogag counteracts A3A packaging into MLV

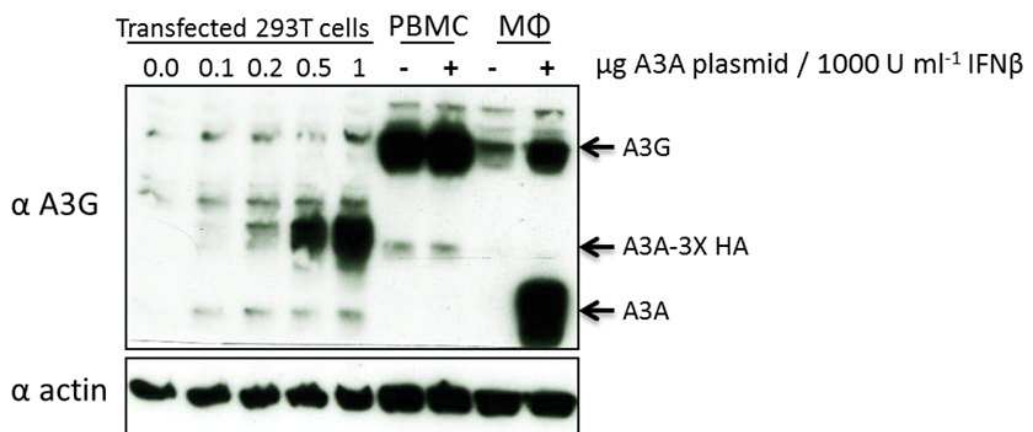
(A) An A3A titration experiment similar to Fig. 3 was made by including glycogag expression plasmids p8065-2 or gg88 in 293T cells. Intracellular luciferase activity of transfected cells was determined after 48 h and presented. Values are means \pm standard deviations (error bars) for three independent reads. (B) Immunoblot shows the amount gg88 (88 amino acids of glycogag lacking gag polyprotein) viral lysates of pHIT60 and pHIT60 + gg88 MLV. gg8 (anti-HA), MLV capsid (anti-p30) were detected with respective antibodies. (C) Target cell A3A-3D-PCR was done as mentioned in Fig. 2 with virions derived from pHIT60 and pHIT60 + gg88. Td = denaturation temperature. (D) The amount A3A, mA3, in cell and viral lysates of pHIT60 and pHIT60 + gg88 MLV was determined by immunoblotting. A3 (anti-HA), gg8 (anti-HA), MLV capsid (anti-p30) were detected with respective antibodies.

Suppl. Fig. 1

A



B



Supplementary Figure 1. Effect of Vpx on HIV-1 Δ vif infectivity and the comparison of ectopic and endogenous level of A3A

(A) An independent experiment was performed with MDMs treated with IFN β (see Fig. 1). The Vpx-mediated rescue of HIV-1 Δ vif infectivity was compared with that of virus lacking Vpx. MLV infections were also made. Vpx incorporation into HIV-1 Δ vif particles was confirmed by immunoblotting. (B) Cell lysates of 1000 units/ml IFN β treated and untreated PBMC and MDMs were run in parallel with the different concentration of A3A (with 3X carboxy-terminal HA tags) encoding plasmid transfected cell lysates. Immunoblots were stained with anti-A3G antiserum that detects A3A and A3A proteins. Actin served as a loading control.

Suppl. Fig. 2

```

mA3-Δ13      MGPFCCLGCSHRKCYSPINLISQETFKFHFKNLGYAKGRKDTFLCYEVTRKDCDSPVSLH
mA3 (Landaulab) MGPFCCLGCSHRKCYSPINLISQETFKFHFKNLGYAKGRKDTFLCYEVTRKDCDSPVSLH
mA3.R354W    MGPFCCLGCSHRKCYSPINLISQETFKFHFKNLGYAKGRKDTFLCYEVTRKDCDSPVSLH
*****

mA3-Δ13      HGVFKNKDNIAEICFLYWFDKVLKVLSPREEFKITWYMSWSPCFECAEQIVRFLATHH
mA3 (Landaulab) HGVFKNKDNIAEICFLYWFDKVLKVLSPREEFKITWYMSWSPCFECAEQIVRFLATHH
mA3.R354W    HGVFKNKDNIAEICFLYWFDKVLKVLSPREEFKITWYMSWSPCFECAEQIVRFLATHH
*****

mA3-Δ13      NLSLDIFSSRLYNVQDPETQQNLCLRVQEGAQVAAMDLYEFKKCWKKFVDNGGRRFRFPWK
mA3 (Landaulab) NLSLDIFSSRLYNVQDPETQQNLCLRVQEGAQVAAMDLYEFKKCWKKFVDNGGRRFRFPWK
mA3.R354W    NLSLDIFSSRLYNVQDPETQQNLCLRVQEGAQVAAMDLYEFKKCWKKFVDNGGRRFRFPWK
*****

mA3-Δ13      RLLTNFRYQDSKLQEILRRMDPLSEEEFYQFYNQVRVKHLCYYHRMKPYLCYQLEQFNGQ
mA3 (Landaulab) RLLTNFRYQDSKLQEILRRMDPLSEEEFYQFYNQVRVKHLCYYHRMKPYLCYQLEQFNGQ
mA3.R354W    RLLTNFRYQDSKLQEILRRMDPLSEEEFYQFYNQVRVKHLCYYHRMKPYLCYQLEQFNGQ
*****

mA3-Δ13      APLKGCLLSE-----IRSMELSQVTITCYLTWSPCPNCAWQLAAFKRDRPDL
mA3 (Landaulab) APLKGCLLSEKKGQHAIEILFLDKIRSMELSQVTITCYLTWSPCPNCAWQLAAFKRDRPDL
mA3.R354W    APLKGCLLSEKKGQHAIEILFLDKIRSMELSQVTITCYLTWSPCPNCAWQLAAFKRDRPDL
*****

mA3-Δ13      ILHIYTSRLYFHWKRPFQKGLCSLWQSGILVDVMDLPQFTDCWTN FVNPKRPFEPWKGLE
mA3 (Landaulab) ILHIYTSRLYFHWKRPFQKGLCSLWQSGILVDVMDLPQFTDCWTN FVNPKRPFEPWKGLE
mA3.R354W    ILHIYTSRLYFHWKRPFQKGLCSLWQSGILVDVMDLPQFTDCWTN FVNPKRPFEPWKGLE
*****

mA3-Δ13      IISRRTQRRLRRIKESWGLQDLVNDFGNLQLGPPMS
mA3 (Landaulab) IISRRTQRRLRRIKESWGLQDLVNDFGNLQLGPPMS
mA3.R354W    IISRRTQRRLRRIKESWGLQDLVNDFGNLQLGPPMS
*****

```

Supplementary Figure 2.

(a) Amino acid sequence alignment of mA3, mA3.R354W, and mA3-Δ13 was done by using Clustal Omega (<http://www.ebi.ac.uk/Tools/msa/clustalo/>). Differing amino acid sequences are highlighted with rectangles.

REFERENCES

- AGUIAR, R. S., LOVSIN, N., TANURI, A. & PETERLIN, B. M. 2008. Vpr.A3A chimera inhibits HIV replication. *J Biol Chem*, 283, 2518-25.
- AHI, Y. S., ZHANG, S., THAPPETA, Y., DENMAN, A., FEIZPOUR, A., GUMMULURU, S., REINHARD, B., MURIAUX, D., FIVASH, M. J. & REIN, A. 2016. Functional Interplay Between Murine Leukemia Virus Glycogag, Serinc5, and Surface Glycoprotein Governs Virus Entry, with Opposite Effects on Gammaretroviral and Ebolavirus Glycoproteins. *MBio*, 7.
- AKEN, B. L., ACHUTHAN, P., AKANNI, W., AMODE, M. R., BERNSDORFF, F., BHAI, J., BILLIS, K., CARVALHO-SILVA, D., CUMMINS, C., CLAPHAM, P., GIL, L., GIRON, C. G., GORDON, L., HOURLIER, T., HUNT, S. E., JANACEK, S. H., JUETTEMANN, T., KEENAN, S., LAIRD, M. R., LAVIDAS, I., MAUREL, T., MCLAREN, W., MOORE, B., MURPHY, D. N., NAG, R., NEWMAN, V., NUHN, M., ONG, C. K., PARKER, A., PATRICIO, M., RIAT, H. S., SHEPPARD, D., SPARROW, H., TAYLOR, K., THORMANN, A., VULLO, A., WALTZ, B., WILDER, S. P., ZADISSA, A., KOSTADIMA, M., MARTIN, F. J., MUFFATO, M., PERRY, E., RUFFIER, M., STAINES, D. M., TREVANION, S. J., CUNNINGHAM, F., YATES, A., ZERBINO, D. R. & FLICEK, P. 2017. Ensembl 2017. *Nucleic Acids Res*, 45, D635-D642.
- BÄHR, A., SINGER, A., HAIN, A., VASUDEVAN, A. A., SCHILLING, M., REH, J., RIESS, M., PANITZ, S., SERRANO, V., SCHWEIZER, M., KÖNIG, R., CHANDA, S., HÄUSSINGER, D., KOCHS, G., LINDEMANN, D. & MÜNK, C. 2016. Interferon but not MxB inhibits foamy retroviruses. *Virology*, 488, 51-60.
- BERGER, A., MÜNK, C., SCHWEIZER, M., CICHUTEK, K., SCHULE, S. & FLORY, E. 2010. Interaction of Vpx and apolipoprotein B mRNA-editing catalytic polypeptide 3 family member A (APOBEC3A) correlates with efficient lentivirus infection of monocytes. *J Biol Chem*, 285, 12248-54.
- BERGER, A., SOMMER, A. F., ZWARG, J., HAMDORF, M., WELZEL, K., ESLY, N., PANITZ, S., REUTER, A., RAMOS, I., JATIANI, A., MULDER, L. C., FERNANDEZ-SESMA, A., RUTSCH, F., SIMON, V., KONIG, R. & FLORY, E. 2011a. SAMHD1-deficient CD14+ cells from individuals with Aicardi-Goutieres syndrome are highly susceptible to HIV-1 infection. *PLoS Pathog*, 7, e1002425.
- BERGER, G., DURAND, S., FARGIER, G., NGUYEN, X. N., CORDEIL, S., BOUAZIZ, S., MURIAUX, D., DARLIX, J. L. & CIMARELLI, A. 2011b. APOBEC3A is a specific inhibitor of the early phases of HIV-1 infection in myeloid cells. *PLoS Pathog*, 7, e1002221.
- BISHOP, K. N., HOLMES, R. K. & MALIM, M. H. 2006. Antiviral potency of APOBEC proteins does not correlate with cytidine deamination. *J Virol*, 80, 8450-8.
- BISHOP, K. N., HOLMES, R. K., SHEEHY, A. M., DAVIDSON, N. O., CHO, S. J. & MALIM, M. H. 2004. Cytidine deamination of retroviral DNA by diverse APOBEC proteins. *Curr Biol*, 14, 1392-6.
- BISHOP, K. N., VERMA, M., KIM, E. Y., WOLINSKY, S. M. & MALIM, M. H. 2008. APOBEC3G inhibits elongation of HIV-1 reverse transcripts. *PLoS Pathog*, 4, e1000231.
- BOCK, M., BISHOP, K. N., TOWERS, G. & STOYE, J. P. 2000. Use of a transient assay for studying the genetic determinants of Fv1 restriction. *J Virol*, 74, 7422-30.
- BOGERD, H. P., WIEGAND, H. L., DOEHLE, B. P., LUEDERS, K. K. & CULLEN, B. R. 2006a. APOBEC3A and APOBEC3B are potent inhibitors of LTR-retrotransposon function in human cells. *Nucleic Acids Res*, 34, 89-95.
- BOGERD, H. P., WIEGAND, H. L., HULME, A. E., GARCIA-PEREZ, J. L., O'SHEA, K. S., MORAN, J. V. & CULLEN, B. R. 2006b. Cellular inhibitors of long interspersed element 1 and Alu retrotransposition. *Proc Natl Acad Sci U S A*, 103, 8780-5.
- BRITAN-ROSICH, E., NOWARSKI, R. & KOTLER, M. 2011. Multifaceted counter-APOBEC3G mechanisms employed by HIV-1 Vif. *J Mol Biol*, 410, 1065-76.

- BROWNE, E. P., ALLERS, C. & LANDAU, N. R. 2009. Restriction of HIV-1 by APOBEC3G is cytidine deaminase-dependent. *Virology*, 387, 313-21.
- BULLIARD, Y., NARVAIZA, I., BERTERO, A., PEDDI, S., ROHRIG, U. F., ORTIZ, M., ZOETE, V., CASTRO-DIAZ, N., TURELLI, P., TELENTI, A., MICHIELIN, O., WEITZMAN, M. D. & TRONO, D. 2011. Structure-function analyses point to a polynucleotide-accommodating groove essential for APOBEC3A restriction activities. *J Virol*, 85, 1765-76.
- BURNS, M. B., LACKEY, L., CARPENTER, M. A., RATHORE, A., LAND, A. M., LEONARD, B., REFSLAND, E. W., KOTANDENIYA, D., TRETYAKOVA, N., NIKAS, J. B., YEE, D., TEMIZ, N. A., DONOHUE, D. E., MCDUGLE, R. M., BROWN, W. L., LAW, E. K. & HARRIS, R. S. 2013. APOBEC3B is an enzymatic source of mutation in breast cancer. *Nature*, 494, 366-70.
- CARPENTER, M. A., LI, M., RATHORE, A., LACKEY, L., LAW, E. K., LAND, A. M., LEONARD, B., SHANDILYA, S. M., BOHN, M. F., SCHIFFER, C. A., BROWN, W. L. & HARRIS, R. S. 2012. Methylcytosine and normal cytosine deamination by the foreign DNA restriction enzyme APOBEC3A. *J Biol Chem*, 287, 34801-8.
- CASSETTA, L., KAJASTE-RUDNITSKI, A., CORADIN, T., SABA, E., DELLA CHIARA, G., BARBAGALLO, M., GRAZIANO, F., ALFANO, M., CASSOL, E., VICENZI, E. & POLI, G. 2013. M1 polarization of human monocyte-derived macrophages restricts pre and postintegration steps of HIV-1 replication. *AIDS*, 27, 1847-56.
- CHANDE, A., CUCCURULLO, E. C., ROSA, A., ZIGLIO, S., CARPENTER, S. & PIZZATO, M. 2016. S2 from equine infectious anemia virus is an infectivity factor which counteracts the retroviral inhibitors SERINC5 and SERINC3. *Proc Natl Acad Sci U S A*, 113, 13197-13202.
- CHEN, H., LILLEY, C. E., YU, Q., LEE, D. V., CHOU, J., NARVAIZA, I., LANDAU, N. R. & WEITZMAN, M. D. 2006. APOBEC3A is a potent inhibitor of adeno-associated virus and retrotransposons. *Curr Biol*, 16, 480-5.
- CORBIN, A., PRATS, A. C., DARLIX, J. L. & SITBON, M. 1994. A nonstructural gag-encoded glycoprotein precursor is necessary for efficient spreading and pathogenesis of murine leukemia viruses. *J Virol*, 68, 3857-67.
- DOEHLE, B. P., SCHAFFER, A., WIEGAND, H. L., BOGERD, H. P. & CULLEN, B. R. 2005. Differential sensitivity of murine leukemia virus to APOBEC3-mediated inhibition is governed by virion exclusion. *J Virol*, 79, 8201-7.
- DORRSCHUCK, E., FISCHER, N., BRAVO, I. G., HANSCHMANN, K. M., KUIPER, H., SPOTTER, A., MOLLER, R., CICHUTEK, K., MÜNK, C. & TONJES, R. R. 2011. Restriction of porcine endogenous retrovirus by porcine APOBEC3 cytidine deaminases. *J Virol*, 85, 3842-57.
- DULL, T., ZUFFEREY, R., KELLY, M., MANDEL, R. J., NGUYEN, M., TRONO, D. & NALDINI, L. 1998. A third-generation lentivirus vector with a conditional packaging system. *J Virol*, 72, 8463-71.
- EDWARDS, S. A. & FAN, H. 1979. gag-Related polyproteins of Moloney murine leukemia virus: evidence for independent synthesis of glycosylated and unglycosylated forms. *J Virol*, 30, 551-63.
- EHLTING, C., BOHMER, O., HAHNEL, M. J., THOMAS, M., ZANGER, U. M., GAESTEL, M., KNOEFEL, W. T., SCHULTE AM ESCH, J., HAUSSINGER, D. & BODE, J. G. 2015. Oncostatin M regulates SOCS3 mRNA stability via the MEK-ERK1/2-pathway independent of p38(MAPK)/MK2. *Cell Signal*, 27, 555-67.
- GOILA-GAUR, R., KHAN, M. A., MIYAGI, E., KAO, S. & STREBEL, K. 2007. Targeting APOBEC3A to the viral nucleoprotein complex confers antiviral activity. *Retrovirology*, 4, 61.
- GUO, F., CEN, S., NIU, M., YANG, Y., GORELICK, R. J. & KLEIMAN, L. 2007. The interaction of APOBEC3G with human immunodeficiency virus type 1 nucleocapsid inhibits tRNA³Lys annealing to viral RNA. *J Virol*, 81, 11322-31.

- HARRIS, R. S., BISHOP, K. N., SHEEHY, A. M., CRAIG, H. M., PETERSEN-MAHRT, S. K., WATT, I. N., NEUBERGER, M. S. & MALIM, M. H. 2003. DNA deamination mediates innate immunity to retroviral infection. *Cell*, 113, 803-9.
- HARRIS, R. S. & DUDLEY, J. P. 2015. APOBECs and virus restriction. *Virology*, 479-480, 131-45.
- HENDERSON, S. & FENTON, T. 2015. APOBEC3 genes: retroviral restriction factors to cancer drivers. *Trends Mol Med*, 21, 274-84.
- HENRY, M., GUETARD, D., SUSPENE, R., RUSNIOK, C., WAIN-HOBSON, S. & VARTANIAN, J. P. 2009. Genetic editing of HBV DNA by monodomain human APOBEC3 cytidine deaminases and the recombinant nature of APOBEC3G. *PLoS One*, 4, e4277.
- HOLMES, R. K., KONING, F. A., BISHOP, K. N. & MALIM, M. H. 2007. APOBEC3F can inhibit the accumulation of HIV-1 reverse transcription products in the absence of hypermutation. Comparisons with APOBEC3G. *J Biol Chem*, 282, 2587-95.
- HRECKA, K., HAO, C., GIERSZEWSKA, M., SWANSON, S. K., KESIK-BRODACKA, M., SRIVASTAVA, S., FLORENS, L., WASHBURN, M. P. & SKOWRONSKI, J. 2011. Vpx relieves inhibition of HIV-1 infection of macrophages mediated by the SAMHD1 protein. *Nature*, 474, 658-61.
- HULTQUIST, J. F., LENGUEL, J. A., REFSLAND, E. W., LARUE, R. S., LACKEY, L., BROWN, W. L. & HARRIS, R. S. 2011. Human and rhesus APOBEC3D, APOBEC3F, APOBEC3G, and APOBEC3H demonstrate a conserved capacity to restrict Vif-deficient HIV-1. *J Virol*, 85, 11220-34.
- IWATANI, Y., CHAN, D. S., WANG, F., MAYNARD, K. S., SUGIURA, W., GRONENBORN, A. M., ROUZINA, I., WILLIAMS, M. C., MUSIER-FORSYTH, K. & LEVIN, J. G. 2007. Deaminase-independent inhibition of HIV-1 reverse transcription by APOBEC3G. *Nucleic Acids Res*, 35, 7096-108.
- JAGUVA VASUDEVAN, A. A., HOFMANN, H., WILLBOLD, D., HÄUSSINGER, D., KOENIG, B. W. & MÜNK, C. 2017. Enhancing the Catalytic Deamination Activity of APOBEC3C Is Insufficient to Inhibit Vif-Deficient HIV-1. *J Mol Biol*, 429, 1171-1191.
- JARMUZ, A., CHESTER, A., BAYLISS, J., GISBOURNE, J., DUNHAM, I., SCOTT, J. & NAVARATNAM, N. 2002. An anthropoid-specific locus of orphan C to U RNA-editing enzymes on chromosome 22. *Genomics*, 79, 285-96.
- KAO, S., GOILA-GAUR, R., MIYAGI, E., KHAN, M. A., OPI, S., TAKEUCHI, H. & STREBEL, K. 2007. Production of infectious virus and degradation of APOBEC3G are separable functional properties of human immunodeficiency virus type 1 Vif. *Virology*, 369, 329-39.
- KAO, S., MIYAGI, E., KHAN, M. A., TAKEUCHI, H., OPI, S., GOILA-GAUR, R. & STREBEL, K. 2004. Production of infectious human immunodeficiency virus type 1 does not require depletion of APOBEC3G from virus-producing cells. *Retrovirology*, 1, 27.
- KHATUA, A. K., TAYLOR, H. E., HILDRETH, J. E. & POPIK, W. 2010. Inhibition of LINE-1 and Alu retrotransposition by exosomes encapsidating APOBEC3G and APOBEC3F. *Virology*, 400, 68-75.
- KINOMOTO, M., KANNO, T., SHIMURA, M., ISHIZAKA, Y., KOJIMA, A., KURATA, T., SATA, T. & TOKUNAGA, K. 2007. All APOBEC3 family proteins differentially inhibit LINE-1 retrotransposition. *Nucleic Acids Res*, 35, 2955-64.
- KOLOKITHAS, A., ROSENKE, K., MALIK, F., HENDRICK, D., SWANSON, L., SANTIAGO, M. L., PORTIS, J. L., HASENKRUG, K. J. & EVANS, L. H. 2010. The glycosylated Gag protein of a murine leukemia virus inhibits the antiretroviral function of APOBEC3. *J Virol*, 84, 10933-6.
- KONDO, S., WAKAE, K., WAKISAKA, N., NAKANISHI, Y., ISHIKAWA, K., KOMORI, T., MORIYAMA-KITA, M., ENDO, K., MURONO, S., WANG, Z., KITAMURA, K., NISHIYAMA, T., YAMAGUCHI, K., SHIGENOBU, S., MURAMATSU, M. & YOSHIZAKI, T. 2017. APOBEC3A associates with human papillomavirus genome integration in oropharyngeal cancers. *Oncogene*, 36, 1687-1697.
- KONING, F. A., GOUJON, C., BAUBY, H. & MALIM, M. H. 2011. Target cell-mediated editing of HIV-1 cDNA by APOBEC3 proteins in human macrophages. *J Virol*, 85, 13448-52.

- KONING, F. A., NEWMAN, E. N., KIM, E. Y., KUNSTMAN, K. J., WOLINSKY, S. M. & MALIM, M. H. 2009. Defining APOBEC3 expression patterns in human tissues and hematopoietic cell subsets. *J Virol*, 83, 9474-85.
- KOTOV, A., ZHOU, J., FLICKER, P. & AIKEN, C. 1999. Association of Nef with the human immunodeficiency virus type 1 core. *J Virol*, 73, 8824-30.
- LAGUETTE, N., SOBHIAN, B., CASARTELLI, N., RINGEARD, M., CHABLE-BESSIA, C., SEGERAL, E., YATIM, A., EMILIANI, S., SCHWARTZ, O. & BENKIRANE, M. 2011. SAMHD1 is the dendritic- and myeloid-cell-specific HIV-1 restriction factor counteracted by Vpx. *Nature*, 474, 654-7.
- LAHOUASSA, H., DADDACHA, W., HOFMANN, H., AYINDE, D., LOGUE, E. C., DRAGIN, L., BLOCH, N., MAUDET, C., BERTRAND, M., GRAMBERG, T., PANCINO, G., PRIET, S., CANARD, B., LAGUETTE, N., BENKIRANE, M., TRANSY, C., LANDAU, N. R., KIM, B. & MARGOTTIN-GOGUET, F. 2012. SAMHD1 restricts the replication of human immunodeficiency virus type 1 by depleting the intracellular pool of deoxynucleoside triphosphates. *Nat Immunol*, 13, 223-8.
- LAND, A. M., LAW, E. K., CARPENTER, M. A., LACKEY, L., BROWN, W. L. & HARRIS, R. S. 2013. Endogenous APOBEC3A DNA cytosine deaminase is cytoplasmic and nongenotoxic. *J Biol Chem*, 288, 17253-60.
- LANDRY, S., NARVAIZA, I., LINFESTY, D. C. & WEITZMAN, M. D. 2011. APOBEC3A can activate the DNA damage response and cause cell-cycle arrest. *EMBO Rep*, 12, 444-50.
- LANGLOIS, M. A., KEMMERICH, K., RADA, C. & NEUBERGER, M. S. 2009. The AKV murine leukemia virus is restricted and hypermutated by mouse APOBEC3. *J Virol*, 83, 11550-9.
- LARUE, R. S., ANDRESDOTTIR, V., BLANCHARD, Y., CONTICELLO, S. G., DERSE, D., EMERMAN, M., GREENE, W. C., JONSSON, S. R., LANDAU, N. R., LOCHELT, M., MALIK, H. S., MALIM, M. H., MÜNK, C., O'BRIEN, S. J., PATHAK, V. K., STREBEL, K., WAIN-HOBSON, S., YU, X. F., YUHKI, N. & HARRIS, R. S. 2009. Guidelines for naming nonprimate APOBEC3 genes and proteins. *J Virol*, 83, 494-7.
- LECOSSIER, D., BOUCHONNET, F., CLAVEL, F. & HANCE, A. J. 2003. Hypermutation of HIV-1 DNA in the absence of the Vif protein. *Science*, 300, 1112.
- LI, J., HAKATA, Y., TAKEDA, E., LIU, Q., IWATANI, Y., KOZAK, C. A. & MIYAZAWA, M. 2012. Two genetic determinants acquired late in Mus evolution regulate the inclusion of exon 5, which alters mouse APOBEC3 translation efficiency. *PLoS Pathog*, 8, e1002478.
- LI, X. Y., GUO, F., ZHANG, L., KLEIMAN, L. & CEN, S. 2007. APOBEC3G inhibits DNA strand transfer during HIV-1 reverse transcription. *J Biol Chem*, 282, 32065-74.
- LIU, S. Y., SANCHEZ, D. J., ALIYARI, R., LU, S. & CHENG, G. 2012. Systematic identification of type I and type II interferon-induced antiviral factors. *Proc Natl Acad Sci U S A*, 109, 4239-44.
- LOGUE, E. C., BLOCH, N., DHUEY, E., ZHANG, R., CAO, P., HERATE, C., CHAUVEAU, L., HUBBARD, S. R. & LANDAU, N. R. 2014. A DNA sequence recognition loop on APOBEC3A controls substrate specificity. *PLoS One*, 9, e97062.
- LOVSIN, N. & PETERLIN, B. M. 2009. APOBEC3 proteins inhibit LINE-1 retrotransposition in the absence of ORF1p binding. *Ann N Y Acad Sci*, 1178, 268-75.
- LUCIFORA, J., XIA, Y., REISINGER, F., ZHANG, K., STADLER, D., CHENG, X., SPRINZL, M. F., KOPPENSTEINER, H., MAKOWSKA, Z., VOLZ, T., REMOUCHAMPS, C., CHOU, W. M., THASLER, W. E., HUSER, N., DURANTEL, D., LIANG, T. J., MÜNK, C., HEIM, M. H., BROWNING, J. L., DEJARDIN, E., DANDRI, M., SCHINDLER, M., HEIKENWALDER, M. & PROTZER, U. 2014. Specific and nonhepatotoxic degradation of nuclear hepatitis B virus cccDNA. *Science*, 343, 1221-8.
- MACDUFF, D. A., DEMOREST, Z. L. & HARRIS, R. S. 2009. AID can restrict L1 retrotransposition suggesting a dual role in innate and adaptive immunity. *Nucleic Acids Res*, 37, 1854-67.
- MANGEAT, B., TURELLI, P., CARON, G., FRIEDLI, M., PERRIN, L. & TRONO, D. 2003. Broad antiretroviral defence by human APOBEC3G through lethal editing of nascent reverse transcripts. *Nature*, 424, 99-103.

- MARIANI, R., CHEN, D., SCHROFELBAUER, B., NAVARRO, F., KONIG, R., BOLLMAN, B., MÜNK, C., NYMARK-MCMAHON, H. & LANDAU, N. R. 2003a. Species-specific exclusion of APOBEC3G from HIV-1 virions by Vif. *Cell*, 114, 21-31.
- MARIANI, R., CHEN, D., SCHRÖFELBAUER, B., NAVARRO, F., KÖNIG, R., BOLLMAN, B., MÜNK, C., NYMARK-MCMAHON, H. & LANDAU, N. R. 2003b. Species-specific exclusion of APOBEC3G from HIV-1 virions by Vif. *Cell*, 114, 21-31.
- MARIN, M., ROSE, K. M., KOZAK, S. L. & KABAT, D. 2003. HIV-1 Vif protein binds the editing enzyme APOBEC3G and induces its degradation. *Nat Med*, 9, 1398-403.
- MBISA, J. L., BARR, R., THOMAS, J. A., VANDEGRAAFF, N., DORWEILER, I. J., SVAROVSKAIA, E. S., BROWN, W. L., MANSKY, L. M., GORELICK, R. J., HARRIS, R. S., ENGELMAN, A. & PATHAK, V. K. 2007. Human immunodeficiency virus type 1 cDNAs produced in the presence of APOBEC3G exhibit defects in plus-strand DNA transfer and integration. *J Virol*, 81, 7099-110.
- MCEWAN, W. A., SCHALLER, T., YLINEN, L. M., HOSIE, M. J., TOWERS, G. J. & WILLETT, B. J. 2009. Truncation of TRIM5 in the Feliformia explains the absence of retroviral restriction in cells of the domestic cat. *J Virol*, 83, 8270-5.
- MOHANRAM, V., SKOLD, A. E., BACHLE, S. M., PATHAK, S. K. & SPETZ, A. L. 2013. IFN-alpha induces APOBEC3G, F, and A in immature dendritic cells and limits HIV-1 spread to CD4+ T cells. *J Immunol*, 190, 3346-53.
- MUCKENFUSS, H., HAMDORF, M., HELD, U., PERKOVIC, M., LOWER, J., CICHUTEK, K., FLORY, E., SCHUMANN, G. G. & MÜNK, C. 2006. APOBEC3 proteins inhibit human LINE-1 retrotransposition. *J Biol Chem*, 281, 22161-72.
- MÜNK, C., BECK, T., ZIELONKA, J., HOTZ-WAGENBLATT, A., CHAREZA, S., BATTENBERG, M., THIELEBEIN, J., CICHUTEK, K., BRAVO, I. G., O'BRIEN, S. J., LOCHELT, M. & YUHKI, N. 2008. Functions, structure, and read-through alternative splicing of feline APOBEC3 genes. *Genome Biol*, 9, R48.
- MÜNK, C., JENSEN, B. E., ZIELONKA, J., HÄUSSINGER, D. & KAMP, C. 2012a. Running Loose or Getting Lost: How HIV-1 Counters and Capitalizes on APOBEC3-Induced Mutagenesis through Its Vif Protein. *Viruses*, 4, 3132-3161.
- MÜNK, C., WILLEMSSEN, A. & BRAVO, I. G. 2012b. An ancient history of gene duplications, fusions and losses in the evolution of APOBEC3 mutators in mammals. *BMC Evol Biol*, 12, 71.
- NARVAIZA, I., LINFESTY, D. C., GREENER, B. N., HAKATA, Y., PINTEL, D. J., LOGUE, E., LANDAU, N. R. & WEITZMAN, M. D. 2009. Deaminase-independent inhibition of parvoviruses by the APOBEC3A cytidine deaminase. *PLoS Pathog*, 5, e1000439.
- NIEWIADOMSKA, A. M., TIAN, C., TAN, L., WANG, T., SARKIS, P. T. & YU, X. F. 2007. Differential inhibition of long interspersed element 1 by APOBEC3 does not correlate with high-molecular-mass-complex formation or P-body association. *J Virol*, 81, 9577-83.
- NITTA, T., KUZNETSOV, Y., MCPHERSON, A. & FAN, H. 2010. Murine leukemia virus glycosylated Gag (gPr80gag) facilitates interferon-sensitive virus release through lipid rafts. *Proc Natl Acad Sci U S A*, 107, 1190-5.
- NITTA, T., TAM, R., KIM, J. W. & FAN, H. 2011. The cellular protein La functions in enhancement of virus release through lipid rafts facilitated by murine leukemia virus glycosylated Gag. *MBio*, 2, e00341-10.
- OKEOMA, C. M., PETERSEN, J. & ROSS, S. R. 2009. Expression of murine APOBEC3 alleles in different mouse strains and their effect on mouse mammary tumor virus infection. *J Virol*, 83, 3029-38.
- OOMS, M., KRIKONI, A., KRESS, A. K., SIMON, V. & MÜNK, C. 2012. APOBEC3A, APOBEC3B, and APOBEC3H haplotype 2 restrict human T-lymphotropic virus type 1. *J Virol*, 86, 6097-108.

- OPI, S., KAO, S., GOILA-GAUR, R., KHAN, M. A., MIYAGI, E., TAKEUCHI, H. & STREBEL, K. 2007. Human immunodeficiency virus type 1 Vif inhibits packaging and antiviral activity of a degradation-resistant APOBEC3G variant. *J Virol*, 81, 8236-46.
- PENG, G., GREENWELL-WILD, T., NARES, S., JIN, W., LEI, K. J., RANGEL, Z. G., MUNSON, P. J. & WAHL, S. M. 2007. Myeloid differentiation and susceptibility to HIV-1 are linked to APOBEC3 expression. *Blood*, 110, 393-400.
- PENG, G., LEI, K. J., JIN, W., GREENWELL-WILD, T. & WAHL, S. M. 2006. Induction of APOBEC3 family proteins, a defensive maneuver underlying interferon-induced anti-HIV-1 activity. *J Exp Med*, 203, 41-6.
- PIZZATO, M. 2010. MLV glycosylated-Gag is an infectivity factor that rescues Nef-deficient HIV-1. *Proc Natl Acad Sci U S A*, 107, 9364-9.
- REFSLAND, E. W., STENGLEIN, M. D., SHINDO, K., ALBIN, J. S., BROWN, W. L. & HARRIS, R. S. 2010. Quantitative profiling of the full APOBEC3 mRNA repertoire in lymphocytes and tissues: implications for HIV-1 restriction. *Nucleic Acids Res*, 38, 4274-84.
- RICHARDSON, S. R., NARVAIZA, I., PLANEGGER, R. A., WEITZMAN, M. D. & MORAN, J. V. 2014. APOBEC3A deaminates transiently exposed single-strand DNA during LINE-1 retrotransposition. *Elife*, 3, e02008.
- ROBERTS, S. A., LAWRENCE, M. S., KLIMCZAK, L. J., GRIMM, S. A., FARGO, D., STOJANOV, P., KIEZUN, A., KRYUKOV, G. V., CARTER, S. L., SAKSENA, G., HARRIS, S., SHAH, R. R., RESNICK, M. A., GETZ, G. & GORDENIN, D. A. 2013. An APOBEC cytidine deaminase mutagenesis pattern is widespread in human cancers. *Nat Genet*, 45, 970-6.
- ROSA, A., CHANDE, A., ZIGLIO, S., DE SANCTIS, V., BERTORELLI, R., GOH, S. L., MCCAULEY, S. M., NOWOSIELSKA, A., ANTONARAKIS, S. E., LUBAN, J., SANTONI, F. A. & PIZZATO, M. 2015. HIV-1 Nef promotes infection by excluding SERINC5 from virion incorporation. *Nature*, 526, 212-7.
- ROSALES GERPE, M. C., RENNER, T. M., BELANGER, K., LAM, C., AYDIN, H. & LANGLOIS, M. A. 2015. N-linked glycosylation protects gammaretroviruses against deamination by APOBEC3 proteins. *J Virol*, 89, 2342-57.
- ROSE, P. P. & KORBER, B. T. 2000. Detecting hypermutations in viral sequences with an emphasis on G --> A hypermutation. *Bioinformatics*, 16, 400-1.
- SANTA-MARTA, M., DA SILVA, F. A., FONSECA, A. M. & GONCALVES, J. 2005. HIV-1 Vif can directly inhibit apolipoprotein B mRNA-editing enzyme catalytic polypeptide-like 3G-mediated cytidine deamination by using a single amino acid interaction and without protein degradation. *J Biol Chem*, 280, 8765-75.
- SCHAMBACH, A., WODRICH, H., HILDINGER, M., BOHNE, J., KRAUSSLICH, H. G. & BAUM, C. 2000. Context dependence of different modules for posttranscriptional enhancement of gene expression from retroviral vectors. *Mol Ther*, 2, 435-45.
- SCHMITT, K., GUO, K., ALGAIER, M., RUIZ, A., CHENG, F., QIU, J., WISSING, S., SANTIAGO, M. L. & STEPHENS, E. B. 2011. Differential virus restriction patterns of rhesus macaque and human APOBEC3A: implications for lentivirus evolution. *Virology*, 419, 24-42.
- SCHMITT, K., GUO, K., KATUWAL, M., WILSON, D., PROCHNOW, C., BRANSTEITTE, R., CHEN, X. S., SANTIAGO, M. L. & STEPHENS, E. B. 2013. Lentivirus restriction by diverse primate APOBEC3A proteins. *Virology*, 442, 82-96.
- SHEEHY, A. M., GADDIS, N. C. & MALIM, M. H. 2003. The antiretroviral enzyme APOBEC3G is degraded by the proteasome in response to HIV-1 Vif. *Nat Med*, 9, 1404-7.
- SIMM, M., SHAHABUDDIN, M., CHAO, W., ALLAN, J. S. & VOLSKY, D. J. 1995. Aberrant Gag protein composition of a human immunodeficiency virus type 1 vif mutant produced in primary lymphocytes. *J Virol*, 69, 4582-6.
- STAVROU, S., NITTA, T., KOTLA, S., HA, D., NAGASHIMA, K., REIN, A. R., FAN, H. & ROSS, S. R. 2013. Murine leukemia virus glycosylated Gag blocks apolipoprotein B editing complex 3 and

- cytosolic sensor access to the reverse transcription complex. *Proc Natl Acad Sci U S A*, 110, 9078-83.
- STENGLEIN, M. D., BURNS, M. B., LI, M., LENGYEL, J. & HARRIS, R. S. 2010. APOBEC3 proteins mediate the clearance of foreign DNA from human cells. *Nat Struct Mol Biol*, 17, 222-9.
- STREBEL, K. 2005. APOBEC3G & HTLV-1: inhibition without deamination. *Retrovirology*, 2, 37.
- SUSPENE, R., AYNAUD, M. M., GUETARD, D., HENRY, M., ECKHOFF, G., MARCHIO, A., PINEAU, P., DEJEAN, A., VARTANIAN, J. P. & WAIN-HOBSON, S. 2011. Somatic hypermutation of human mitochondrial and nuclear DNA by APOBEC3 cytidine deaminases, a pathway for DNA catabolism. *Proc Natl Acad Sci U S A*, 108, 4858-63.
- SUSPENE, R., MUSSIL, B., LAUDE, H., CAVAL, V., BERRY, N., BOUZIDI, M. S., THIERS, V., WAIN-HOBSON, S. & VARTANIAN, J. P. 2017. Self-cytoplasmic DNA upregulates the mutator enzyme APOBEC3A leading to chromosomal DNA damage. *Nucleic Acids Res*.
- TAKEDA, E., TSUJI-KAWAHARA, S., SAKAMOTO, M., LANGLOIS, M. A., NEUBERGER, M. S., RADA, C. & MIYAZAWA, M. 2008. Mouse APOBEC3 restricts friend leukemia virus infection and pathogenesis in vivo. *J Virol*, 82, 10998-1008.
- TAN, L., SARKIS, P. T., WANG, T., TIAN, C. & YU, X. F. 2009. Sole copy of Z2-type human cytidine deaminase APOBEC3H has inhibitory activity against retrotransposons and HIV-1. *FASEB J*, 23, 279-87.
- THIELEN, B. K., MCNEVIN, J. P., MCEL RATH, M. J., HUNT, B. V., KLEIN, K. C. & LINGAPPA, J. R. 2010. Innate immune signaling induces high levels of TC-specific deaminase activity in primary monocyte-derived cells through expression of APOBEC3A isoforms. *J Biol Chem*, 285, 27753-66.
- USAMI, Y., WU, Y. & GOTTLINGER, H. G. 2015. SERINC3 and SERINC5 restrict HIV-1 infectivity and are counteracted by Nef. *Nature*, 526, 218-23.
- VARTANIAN, J. P., GUETARD, D., HENRY, M. & WAIN-HOBSON, S. 2008. Evidence for editing of human papillomavirus DNA by APOBEC3 in benign and precancerous lesions. *Science*, 320, 230-3.
- VASUDEVAN, A. A., SMITS, S. H., HOPFNER, A., HÄUSSINGER, D., KOENIG, B. W. & MÜNK, C. 2013. Structural features of antiviral DNA cytidine deaminases. *Biol Chem*, 394, 1357-70.
- WANG, X., AO, Z., CHEN, L., KOBINGER, G., PENG, J. & YAO, X. 2012. The cellular antiviral protein APOBEC3G interacts with HIV-1 reverse transcriptase and inhibits its function during viral replication. *J Virol*, 86, 3777-86.
- WANG, X., DOLAN, P. T., DANG, Y. & ZHENG, Y. H. 2007. Biochemical differentiation of APOBEC3F and APOBEC3G proteins associated with HIV-1 life cycle. *J Biol Chem*, 282, 1585-94.
- WIEGAND, H. L. & CULLEN, B. R. 2007. Inhibition of alpharetrovirus replication by a range of human APOBEC3 proteins. *J Virol*, 81, 13694-9.
- WIEGAND, H. L., DOEHLE, B. P., BOGERD, H. P. & CULLEN, B. R. 2004. A second human antiretroviral factor, APOBEC3F, is suppressed by the HIV-1 and HIV-2 Vif proteins. *EMBO J*, 23, 2451-8.
- WIJESINGHE, P. & BHAGWAT, A. S. 2012. Efficient deamination of 5-methylcytosines in DNA by human APOBEC3A, but not by AID or APOBEC3G. *Nucleic Acids Res*, 40, 9206-17.
- YU, Q., KONIG, R., PILLAI, S., CHILES, K., KEARNEY, M., PALMER, S., RICHMAN, D., COFFIN, J. M. & LANDAU, N. R. 2004a. Single-strand specificity of APOBEC3G accounts for minus-strand deamination of the HIV genome. *Nat Struct Mol Biol*, 11, 435-42.
- YU, X., YU, Y., LIU, B., LUO, K., KONG, W., MAO, P. & YU, X. F. 2003. Induction of APOBEC3G ubiquitination and degradation by an HIV-1 Vif-Cul5-SCF complex. *Science*, 302, 1056-60.
- YU, Y., XIAO, Z., EHRLICH, E. S., YU, X. & YU, X. F. 2004b. Selective assembly of HIV-1 Vif-Cul5-ElonginB-ElonginC E3 ubiquitin ligase complex through a novel SOCS box and upstream cysteines. *Genes Dev*, 18, 2867-72.

- ZHANG, H., YANG, B., POMERANTZ, R. J., ZHANG, C., ARUNACHALAM, S. C. & GAO, L. 2003. The cytidine deaminase CEM15 induces hypermutation in newly synthesized HIV-1 DNA. *Nature*, 424, 94-8.
- ZIELONKA, J., BRAVO, I. G., MARINO, D., CONRAD, E., PERKOVIC, M., BATTENBERG, M., CICHUTEK, K. & MÜNK, C. 2009. Restriction of equine infectious anemia virus by equine APOBEC3 cytidine deaminases. *J Virol*, 83, 7547-59.

Chapter V

Prototype Foamy Virus Bet Impairs the Dimerization and Cytosolic Solubility of Human APOBEC3G

Journal : **Journal of Virology** (published in 2013)

Own contribution to this work:

- Performed the following experiments, immunoblots, virus infection, establishment and optimization of *in vitro* deamination assay and protein purification strategies, protein-protein interaction, sucrose density gradient centrifugation, and subcellular localization of proteins by differential detergent fractionation
- Statistical analysis of all the data
- Shared first author of this paper and do not own the following data presented in figures 1A, 2, 5A and 5B, 6C and 6E and 7
- Writing of the manuscript

Prototype Foamy Virus Bet Impairs the Dimerization and Cytosolic Solubility of Human APOBEC3G

Ananda Ayyappan Jaguva Vasudevan,^a Mario Perković,^{a,b,*} Yannick Bulliard,^{c,*} Klaus Cichutek,^b Didier Trono,^c Dieter Häussinger,^a Carsten Münk^a

Clinic for Gastroenterology, Hepatology, and Infectiology, Medical Faculty, Heinrich Heine University, Düsseldorf, Germany^a; Division of Medical Biotechnology, Paul Ehrlich Institut, Langen, Germany^b; School of Life Sciences and Frontiers-in-Genetics National Program, Ecole Polytechnique Fédérale de Lausanne (EPFL), Lausanne, Switzerland^c

Cellular cytidine deaminases from the APOBEC3 family are potent restriction factors that are able to block the replication of retroviruses. Consequently, retroviruses have evolved a variety of different mechanisms to counteract inhibition by APOBEC3 proteins. Lentiviruses such as human immunodeficiency virus (HIV) express Vif, which interferes with APOBEC3 proteins by targeting these restriction factors for proteasomal degradation, hence blocking their ability to access the reverse transcriptase complex in the virions. Other retroviruses use less-well-characterized mechanisms to escape the APOBEC3-mediated cellular defense. Here we show that the prototype foamy virus Bet protein can protect foamy viruses and an unrelated simian immunodeficiency virus against human APOBEC3G (A3G). In our system, Bet binds to A3G and prevents its encapsidation without inducing its degradation. Bet failed to coimmunoprecipitate with A3G mutants unable to form homodimers and dramatically reduced the recovery of A3G proteins from soluble cytoplasmic cell fractions. The Bet-A3G interaction is probably a direct binding interaction and seems to be independent of RNA. Together, these data suggest a novel model whereby Bet uses two possibly complementary mechanisms to counteract A3G: (i) Bet prevents encapsidation of A3G by blocking A3G dimerization, and (ii) Bet sequesters A3G in immobile complexes, impairing its ability to interact with nascent virions.

APOBEC3G (apolipoprotein B mRNA-editing, enzyme-catalytic, polypeptide-like 3G; also called A3G) is a cytidine deaminase of the APOBEC family. There are seven A3 genes (A3A to -D and A3F to -H) found in humans and most primates, one gene in rodents, and four genes in cats, showing that the A3 genes evolved in lineage-specific compositions in placental mammals (1, 2).

Human immunodeficiency virus type 1 with a deleted *vif* gene (HIV-1 Δvif) is efficiently inhibited by A3G. Viral particle-encapsidated A3G interferes with viral replication by multiple mechanisms: it deaminates cytosines to uracils in the viral cDNA generated during reverse transcription, reduces the efficiency of reverse transcription, and impairs integration (for recent reviews, see references 3 and 4). The HIV-1 Vif protein counteracts A3G by triggering its polyubiquitination and degradation (5). Vif also employs other mechanisms to inhibit A3G. In HeLa cells, production of infectious HIV-1 was shown to be independent of A3G depletion (6–8). Vif bound to A3G might inhibit the deamination activity of A3G (9), especially when both proteins are encapsidated in virions as a complex (10). Some of the A3G molecules escape the action of Vif and can even edit wild-type HIV-1, causing mutations which may contribute to viral diversity (see reference 3 for a review).

HIV-1 is not the only virus that faces antiviral A3 proteins: retroviruses, retroelements, hepadnaviruses, and certain RNA and DNA viruses show some restriction (11). Most other lentiviruses also use their Vif proteins to destroy cellular A3s: human T cell lymphotropic virus type 1 escapes the virion encapsidation of A3G, but not that of A3A, A3B, and A3H, through its unique nucleocapsid protein (12, 13); murine leukemia virus mitigates murine A3 activity by its glycosylated Gag protein (glyco-Gag) (14, 15); and foamy retroviruses express the accessory protein Bet to counteract A3 proteins (16–20).

Species-specific foamy viruses (FVs) are found in many mammals, and simian foamy viruses (SFVs) infect Old World monkeys,

New World monkeys, and apes. In chimpanzees, the chimpanzee SFV (SFVcpz) is widely distributed, and prevalence rates from 44% to 100% have been reported (21). The prototype foamy virus (PFV) was isolated from human cell cultures but identified as a chimpanzee virus (22). Humans are occasionally infected by diverse simian foamy viruses (23–25), but neither in their natural host species nor after cross-species transmission to humans do foamy retroviruses induce disease, and infected humans are dead-end hosts (26–28). The reason that humans do not transmit FVs is not clear.

Bet is an accessory protein expressed in all foamy viruses. PFV Bet has been suggested to be involved in resistance to viral superinfection (29) and as a negative regulator of the basal activity of the internal PFV promoter (30). The feline foamy virus (FFV) Bet protein inhibits antiviral feline A3 proteins without inducing their degradation (16–18). A mechanism for FFV Bet activity has not been identified, but an interaction of FFV Bet and feline A3s was demonstrated to be important (16). For the PFV system, controversial data regarding the function of Bet as an A3G antagonist have been reported (20, 31). Russell et al. described that PFV Bet

Received 7 December 2012 Accepted 26 May 2013

Published ahead of print 12 June 2013

Address correspondence to Carsten Münk, carsten.muenk@med.uni-duesseldorf.de.

* Present address: Mario Perković, Institute for Biophysics and Buchmann Institute for Molecular Life Sciences, Johann Wolfgang Goethe University, Frankfurt, Germany; Yannick Bulliard, Novartis, Novartis Institutes for Biomedical Research, Cambridge, Massachusetts, USA.

A.A.J.V. and M.P. contributed equally to this article and are co-first authors.

Copyright © 2013, American Society for Microbiology. All Rights Reserved.

doi:10.1128/JVI.03385-12

was able to rescue the infectivity of PFV Δbet and Vif-deficient HIV-1 in the presence of A3G (20). In contrast, Delebecque et al. found that PFV is sensitive to A3G, independent of Bet (31). Like the Bet activity of FFV, the mechanism of PFV Bet's inhibition of the antiviral activity of A3G has not been resolved.

We aimed here to address whether PFV Bet can protect PFV and lentiviruses against the antiviral activity of human A3G (huA3G) and to understand the fate of A3G bound to Bet.

MATERIALS AND METHODS

Plasmids. Reporter viruses for the simian immunodeficiency virus SIV_{AGM}TAN-1 (pSIV_{AGM}-luc-R⁻E⁻ Δvif) have been described previously (32). The PFV vector pczDWP002 is a variant of the PFV Gag/Pol expression vector pczDWP001 (33) in which the NLS-LacZ sequence replaces the enhanced green fluorescent protein (EGFP) open reading frame (ORF). The PFV Env expression construct pczHFVenvEM002 has been described previously (34). Human (hu), African green monkey (AGM), and chimpanzee (cpz) A3G-HA expression constructs were kindly provided by N. R. Landau (32). Myc-tagged huA3G (pcDNA3.1 expressing human APOBEC3G-Myc-6His) has been described previously (35). Plasmids encoding huA3G Y124A, Y125A, F126L, and W127A mutants were described previously (36). pBet_{PFV} (19) was generated by insertion of the PFV Bet sequence, which was obtained from HEL299 cells (ATCC CCL-137) infected with the PFV isolated by Achong et al. (37), into the HindIII and SmaI sites of pBC12-CMV (38). pVif_{HIV-1} (39) (referred to here as pcDNA3.1Vif) and the analogous pVif_{AGM.TAN-1} plasmid were kindly provided by N. R. Landau. To generate pBet-V5-His, the forward primer KpnI 5' Bet (5'-TAGGGTACCGTATCATGGATTCTACGAA-3') and the reverse primer ApaI 3' Bet (5'-CTAGGGCCCCAAGGGTCCATCTGAGTCAC-3') were used. The amplicons were cloned into the KpnI and ApaI sites of pcDNA4/V5-HisA (Life Technologies, Darmstadt, Germany). Subsequent amplification of the 3' part of Bet containing V5 and His sequences by use of primers HFV-Bet824-844f (5'-GTTTCAAGGTAATTTATGAAG-3') and G-6xH-stop-XbaI_{rc} (5'-GCTCTAGAGCTCATGGTGATGGTGATGATG-3') generated a fragment which was cloned into pBetPFV via BglII and XbaI sites. pA3G- α (40), expressing A3G fused to the α -fragment of β -galactosidase, was a gift of N. R. Landau. The ω -fragment of β -galactosidase (pCMV- ω [41]; formerly known as pSCTZ- ω [42]) was a gift of S. Rusconi.

Cell culture. Human HOS and 293T cells were maintained in Dulbecco's modified Eagle's complete medium (PAN-Biotech, Aidenbach, Germany) supplemented with 10% fetal bovine serum (FBS), 0.29 mg/ml L-glutamine, and 100 U/ml penicillin-streptomycin at 37°C in a humidified atmosphere of 5% CO₂. Plasmid transfection into 293T cells was done with Lipofectamine LTX (Life Technologies), except that PFV plasmid transfection was accomplished with Polyfect (Qiagen, Hilden, Germany), with a DNA/Polyfect ratio of 1:2.5. Reporter lentiviruses were generated by transfection into 6-well plates with 1.5 μ g pSIV_{AGM}-luc-E⁻R⁻ Δvif , 0.5 μ g vesicular stomatitis virus G glycoprotein (VSV-G) expression plasmid pMD.G, 1 μ g A3 expression plasmid, and 2 μ g pVif_{HIV-1}, pVif_{AGM.TAN-1}, or pBet_{PFV}. PFV reporter vectors were generated in 12-well plates with 1 μ g pczDWP002, 1 μ g pczHFVenvEM02, 0.33 μ g A3 expression plasmid, and 0.66 μ g pBet_{PFV}. Total plasmid DNA (4.5 or 3 μ g) was maintained by the addition of pcDNA3.1 as needed. Reverse transcriptase (RT) activity of SIV-containing supernatants was determined using a Cavid HS Lenti RT kit or a C-type RT activity kit (Cavidi Tech, Uppsala, Sweden) for PFV vectors. For infectivity assays, HOS cells were transduced in 96-well plates in triplicate with a virus amount equivalent to 10 pg of RT for HIV or SIV vectors and 20 mU for PFV. At 3 days postinfection (dpi), luciferase activity was measured by using a Steadylite HTS kit (PerkinElmer, Rodgau, Germany), or β -galactosidase activity was determined by using a Tropix Galacto-Star system (Life Technologies). Data are presented as counts/s normalized to that for virus obtained without A3 and Bet.

α -Complementation assay. 293T cells (seeded in 96-well plates) were transfected in triplicate with an expression vector for the ω -subunit of

β -galactosidase and an APOBEC3G α -subunit expression vector (huA3G- α) in combination with Bet_{PFV}, Vif_{SIVagm}, or Vif_{HIV-1}. The activity of β -galactosidase was measured 3 days later by using a Tropix Galacto-Star system (Life Technologies).

Immunoblot analysis. To generate protein lysates, cells were washed with phosphate-buffered saline (PBS) and lysed in radioimmunoprecipitation assay (RIPA) buffer for 5 min on ice. Lysates were clarified by centrifugation. For mild cell lysis, cells were treated with mild lysis buffer (50 mM HEPES, 125 mM NaCl, 0.1 mM phenylmethylsulfonyl fluoride [PMSF], 0.2% NP-40, pH 7.5, and 1 \times complete protease inhibitor cocktail [Merck Calbiochem]) for 30 min on ice and then centrifuged (10 min, 300 \times g, 4°C), and the supernatant was separated from the pellet. The pellet was treated with RIPA buffer for 5 min on ice and then centrifuged (10 min, 300 \times g, 4°C), and the supernatant was taken. For the differential detergent fractionation of proteins from cells, a ProteoExtract subcellular proteome extraction kit (Merck, Darmstadt, Germany) was used according to the manufacturer's specifications. To generate virus lysates, supernatant samples were layered on a 2-ml 20% (wt/vol) sucrose cushion (in PBS), and virions were pelleted at 35,000 rpm (SW-41 rotor; Beckman Coulter, Krefeld, Germany) for 2 h at 4°C. Pellets were resuspended with RIPA buffer and normalized to RT values for 500 pg determined from original supernatants. The levels of p27 and hemagglutinin (HA)-tagged A3 proteins were analyzed by immunoblotting. For coimmunoprecipitation (co-IP) of Bet and A3G, cells were transfected with 2 μ g of pBet_{PFV} and 1 μ g of A3G expression plasmid. After 2 days, cells were lysed, lysates were clarified by centrifugation, and supernatants were incubated with anti-HA beads (Roche Diagnostics, Berlin, Germany) for 60 min at 4°C and washed 5 times with RIPA buffer. For immunoblot analysis, samples were boiled in NuPAGE SDS sample buffer and NuPAGE sample reducing agent (Life Technologies) and subjected to SDS-PAGE followed by transfer to a polyvinylidene difluoride (PVDF) membrane. Proteins were detected using an anti-HA antibody (Ab) (1:10⁴ dilution) (MMS-101P; Covance, Munich, Germany) or an anti-c-Myc monoclonal Ab (MAb) (1:200 dilution) (9E10; Sigma-Aldrich, Munich, Germany). For the detection of endogenous A3G, rabbit antiserum (anti-Apo C17; 1:10⁴ dilution) was used (7). For the detection of Bet_{PFV}, a Bel2/Bet-specific hyperimmune serum (1:50,000 dilution) was used (43). Equal loading of cell lysates was confirmed for immunoblots probed with anti-tubulin Ab (1:10⁴ dilution) (B5-1-2; Sigma-Aldrich), and equal loading of virions was confirmed by use of anti-p24/p27 MAb AG3.0 (44). Anti-mouse- and anti-rabbit-horseradish peroxidase (GE Healthcare, Freiburg, Germany) were used as secondary Abs. Signals were visualized using ECL reagent (GE Healthcare).

Purification of Bet-A3G complexes. To purify A3G-Bet complexes, expression plasmids for A3G-HA and Bet-V5-His were cotransfected into 293T cells. Cells were harvested at 48 h posttransfection, washed with PBS, and lysed with lysis buffer (50 mM Tris, pH 8.0, 10% glycerol, 0.8% [vol/vol] NP-40, 1 mM PMSF, and 1 \times complete protease inhibitor cocktail [Merck Calbiochem]). Cell suspensions were placed on ice for 15 min, and the debris was pelleted by centrifugation at 13,000 rpm for 20 min. Prior to RNase A (Thermo Scientific, Schwerte, Germany) treatment (50 mg/ml), the soluble fraction was adjusted to 0.8 M NaCl and incubated for 15 min at 37°C and for 1 h at 25°C. After treatment, the lysate was mixed with 20 μ l of equilibrated Ni-nitrilotriacetic acid (Ni-NTA) agarose (Life Technologies) and kept at 4°C for 2 h, turning in an end-over-end fashion. Beads were washed extensively with wash buffer (50 mM Tris, pH 8.0, 0.3 M NaCl, 10% [vol/vol] glycerol, 20 mM imidazole), and Bet-A3G complexes were eluted with elution buffer (50 mM Tris, pH 8.0, 0.3 M NaCl, 10% [vol/vol] glycerol, 250 mM imidazole).

Sequencing of viral reverse transcripts. SIV_{AGM}-luc Δvif (VSV-G) reporter viruses generated in the presence of huA3G with and without Bet and treated with 20 U/ml DNase I (Thermo Scientific) for 1 h at 37°C were used for infection of 293T cells (5 \times 10⁵). After 10 h, the cells were washed and total DNA was isolated using a DNeasy DNA blood and tissue kit (Qiagen). A 600-bp *luc* fragment was amplified with DreamTaq DNA

polymerase (Thermo Scientific) (denaturation at 95°C for 5 min followed by 30 cycles of annealing at 61°C for 30 s and denaturation at 94°C for 30 s) and primers Luc-Fw (5'-GATATGTGGATTTCGAGTCGTC-3') and Luc-Rev (5'-GTCATCGTCTTCCGTGTC-3') and then cloned into the pJet blunt cloning vector (Thermo Scientific). The nucleotide sequences of 10 independent clones were analyzed and the G-to-A conversion presented using the Hypermut online tool (<http://www.hiv.lanl.gov/content/sequence/HYPERMUT/hypermut.html>).

In vitro DNA cytidine deamination assay of A3G-Bet complexes. A3G deamination reactions were performed as described previously (45), using a 10- μ l reaction volume containing 25 mM Tris, pH 7.0, and 10 fmol single-stranded DNA (ssDNA) substrate (5'-GGATTGGTTGGTTA TTTGTTTAAGGAAGGTGGATTAAGGCCCAAGAAGGTGATGGAA GTTATGTTTGGTAGATTGATGG-3'). Reaction mixtures were incubated for 3 h at 37°C, and reactions were terminated by incubation at 95°C for 5 min. One femtomole of the reaction mixture was used for PCR amplification with DreamTaq polymerase (Thermo Scientific) (denaturation at 95°C for 3 min followed by 19 cycles of annealing at 61°C for 30 s and denaturation at 94°C for 30 s) and the following primers: forward, 5'-GGATTGGTTGGTTA TTTGTTTAAGGA-3'; and reverse, 5'-CCATC AATCTACCAAACATAACTTCCA-3'. PCR products were digested with the restriction enzyme Eco147I (StuI) (Thermo Scientific) for 1 h at 37°C, resolved by 15% PAGE, and stained with SYBR gold (Life Technologies). A positive-control substrate oligonucleotide with CCU instead of CCA was used to control the Eco147I digestion. To determine the deamination activity of purified A3G in the presence of purified Bet, A3G-Myc-His and Bet-V5-His were purified separately as described above, except that the RNase A treatment step was omitted in the Bet purification. Purified His-tagged protein concentrations were determined spectrophotometrically by measuring the A_{280} , using their (theoretical) extinction coefficients and molecular masses. The A3G deamination reaction was conducted as described above. For the titration experiments, 10 fmol single-stranded DNA substrate was mixed with 20 fmol A3G-His protein and increasing amounts of Bet protein (10 to 1,000 nM).

Sucrose density gradient centrifugation. 293T cells were transfected with expression plasmids for 2 μ g A3G-HA, 2 μ g Bet-His, or 2 μ g A3G-HA plus 2 μ g Bet-His. After 24 h, cells were lysed with lysis buffer (0.626% NP-40, 100 mM NaCl, 50 mM potassium acetate, 10 mM EDTA, 10 mM Tris, pH 7.4, and complete protease inhibitor cocktail [Merck Calbiochem]) and then clarified by centrifugation for 10 min at 162 \times g followed by a short spin at 18,000 \times g for 30 s. A half-portion of the sample was aliquoted to a new tube, to which RNase A (Thermo Scientific) (70 μ g/ml) was added and incubated for 30 min at 37°C. Samples were then overlaid on top of a 10%-15%-20%-30%-50% sucrose step gradient in lysis buffer and centrifuged for 45 min at 163,000 \times g at 4°C in an MLS-50 rotor (Beckman Coulter, Fullerton, CA). After centrifugation, the samples were sequentially removed from the top of the gradient, resolved by SDS-PAGE, and analyzed by immunoblotting with anti-HA and anti-Bet antibodies to detect A3G and Bet, respectively.

Coimmunoprecipitation assays. (i) **Interaction of purified A3G-Myc-His and Bet-V5-His proteins.** A total of 1.5 μ g of mouse monoclonal anti-Myc antibody (AbD Serotec, Düsseldorf, Germany) was mixed with purified A3G-Myc-His and Bet-V5-His proteins (1:2 ratio) in a buffer (50 mM Tris, pH 7.4, and 150 mM NaCl) and incubated overnight at 4°C with end-over-end rotation. The next day, 20 μ l of protein A/G Plus agarose (Santa Cruz, Heidelberg, Germany) was added and incubated for 3 h at 4°C. After binding, the beads were washed 4 times with the same buffer, and the Bet-A3G complexes were eluted by boiling the beads at 95°C for 5 min in native loading buffer. The supernatant was further heated at 95°C for 5 min with 2-mercaptoethanol (2-ME) before being subjected to SDS-PAGE. Immunoblots were developed using PentaHis antibody (Qiagen) analysis. For better visualization of the A3G-Bet interaction, the gel was stained with Coomassie brilliant blue staining solution after the immunoblot transfer and was destained with destaining solution.

(ii) **RNA-dependent interaction.** The protocol to assay RNA-dependent interactions was adapted from a previously described protocol (46). 293T cells were transfected with 1 μ g pcDNA3.1 (Invitrogen) empty vector (mock) and expression plasmids for 1 μ g A3G-HA plus 1 μ g A3G-Myc-His or 1 μ g A3G-HA plus 1 μ g Bet-V5-His in a six-well culture plate. At 24 h posttransfection, cells were harvested and lysed with lysis buffer (0.5% Triton X-100, 287 mM NaCl, 3 mM KCl, 50 mM Tris, pH 7.5, and Complete protease inhibitor mixture [Roche]). The cleared lysates were incubated with 30 μ l anti-HA affinity matrix beads (Roche) for A3G-A3G co-IP and with 30 μ l Ni-NTA agarose (Life Technologies) for 2 h at 4°C, with end-over-end rotation. After binding, the beads were washed twice, with lysis buffer and lysis buffer containing 20 mM imidazole for A3G-A3G and A3G-Bet, respectively, and half-portions of the samples were aliquoted to new tubes. RNase A (70 μ g/ml) was added to one aliquot of the sample and incubated at 37°C for 10 min and at 22°C for 40 min. Samples were further washed thrice with lysis buffer and lysis buffer containing 20 mM imidazole for A3G-A3G and A3G-Bet, respectively. A3G-A3G co-IP products were eluted by boiling beads in SDS gel loading buffer at 95°C for 5 min, and A3G-Bet co-IP products were eluted with an elution buffer containing 300 mM imidazole; the supernatant containing the eluate was heated at 95°C for 5 min with 2-ME before being subjected to SDS-PAGE and detected by immunoblotting with respective antibodies. Results are representative of three independent experiments.

Immunofluorescence microscopy. Immunofluorescence studies were performed in HeLa cells 2 days after transfection by applying FuGENE technology (Roche Applied Science). Cells were fixed in 4% paraformaldehyde in PBS for 20 min, washed twice in PBS, permeabilized in 0.1% Triton X-100 in PBS for 15 min, washed twice in PBS, and blocked with blocking solution (1% milk powder in PBS) for 45 min. For A3G-HA staining, cells were incubated for 1 h with an anti-HA antibody (MMS-101P; Covance) in a 1:1,000 dilution in blocking solution. Bet was stained with Bet antibody at a 1:1,000 dilution in blocking solution. Anti-mouse-Alexa Fluor 488 (Life Technologies) and anti-rabbit-Alexa Fluor 594 were used as secondary antibodies at a 1:300 dilution in blocking solution for 1 h. Subsequently, 4',6-diamidino-2-phenylindole staining (1:1,000; Millipore, Darmstadt, Germany) was performed for 10 min. Finally, cells were washed twice in PBS and analyzed by laser scanning microscopy (LSM 510 Meta; Zeiss, Göttingen, Germany). Images were acquired using a 40 \times objective.

Model structure. For structure-guided mutation analysis, the previously published homology model of the A3G N terminus-N terminus dimer interface (36) was used. This model was generated using the MODELLER program (47); the crystal structure of the human A3G C-terminal domain (48) served as the template (for detailed methods, see reference 36). The graphical visualization presented in Fig. 5C was constructed using PyMOL (PyMOL Molecular Graphics System, version 1.5.0.4; Schrödinger, Portland, OR).

Statistical analysis. Data are presented as means with standard deviations (SD) in all bar diagrams. Statistically significant differences between two groups were analyzed using unpaired Student's *t* test in GraphPad Prism, version 5 (GraphPad Software, San Diego, CA). A minimum *P* value of 0.05 was considered statistically significant.

RESULTS

PFV Bet counteracts A3G in a dose-dependent manner. Conflicting data on the functional effect of PFV Bet on the activity of A3G have been reported (20, 31). These data prompted us to further investigate possible Bet activity toward A3G. First, we tested A3G by using a Bet-deficient single-round reporter vector based on PFV and expressing the *lacZ* gene for β -galactosidase in 293T cells transfected with an expression plasmid for A3G alone and together with Bet. Normalized amounts of particles were used to transduce human osteosarcoma cells, and the β -galactosidase levels were quantified at 3 days posttransduction (Fig. 1A). A3G reduced the infectivity of PFV vectors 10-fold, and the expression of

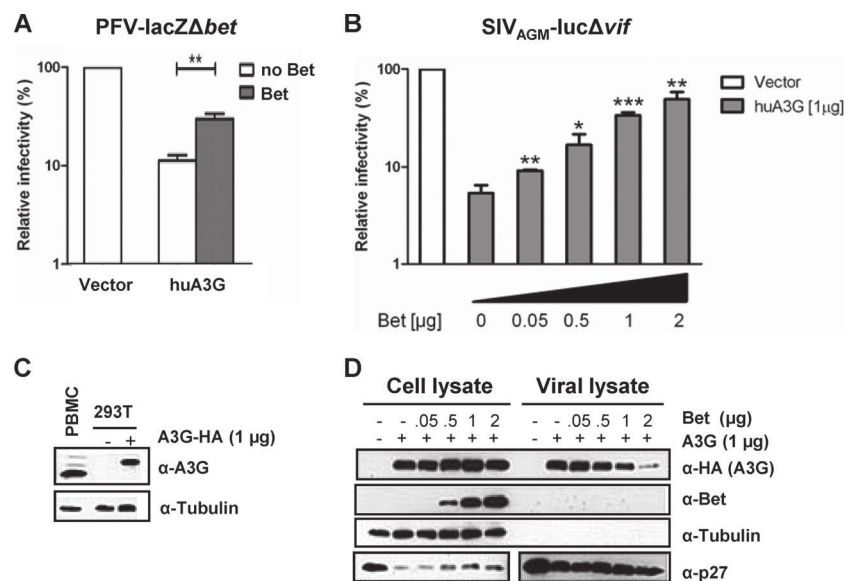


FIG 1 Bet counteracts A3G in a dose-dependent manner and independent of the virus background. (A) Bet-deficient *lacZ* reporter viruses derived from PFV were produced in the presence and absence of human APOBEC3G (huA3G) and Bet. Infectivities of viruses were determined by quantification of galactosidase expression at 3 dpi. Infectivities relative to that of the virus generated in the absence of huA3G and Bet are given. (B) *SIV_{AGM}-lucΔvif* viruses were produced in the presence and absence of huA3G and increasing amounts of Bet. Infectivities of equal amounts of viruses, relative to that of the virus generated in the absence of huA3G and Bet, were determined by quantification of luciferase activity at 3 dpi. (C) Endogenous level of A3G in activated human PBMCs compared to plasmid-derived A3G level in transfected 293T cells (1 μg A3G-HA plasmid), detected by using anti-A3G antiserum. Equal loading of cell lysate samples was confirmed with an anti-tubulin antibody. (D) Packaging of A3G in *SIV_{AGM}-lucΔvif* virions. Virions were produced in the presence of an empty expression plasmid (-; pcDNA3.1) or 1 μg A3G expression plasmid and increasing amounts of Bet expression plasmid (0 μg, 0.05 μg, 0.5 μg, 1 μg, and 2 μg). Supernatants were filtered and concentrated through a 20% sucrose cushion by centrifugation. The cell and viral lysates were analyzed by immunoblotting and were probed for A3G (α-HA, anti-HA antibody), Bet (α-Bet, anti-Bet antibody), capsid (α-p27, anti-p27 antibody), and tubulin (α-Tubulin, anti-tubulin antibody). Unpaired *t* tests were computed to determine whether differences between samples in the presence of A3G protein with and without Bet reached the level of statistical significance (*, $P < 0.05$; **, $P < 0.001$; and ***, $P < 0.0001$), using GraphPad Prism 5 software.

Bet rescued the PFV infectivity to half the levels attained by PFV vectors generated without A3G. Previously, it was shown that Bet can also protect heterologous lentiviruses against A3 proteins (19, 20). Thus, for the next experiments, we used a luciferase reporter virus based on the SIV derived from AGMs (*SIV_{AGM}*), with an inactivated *vif* gene (referred to here as *SIV_{AGM}-lucΔvif*) (32). *SIV_{AGM}-lucΔvif* was generated in the presence of 1 μg A3G plasmid and increasing amounts of Bet plasmid (0 to 2 μg). Viral particles were normalized for reverse transcription activity and used for transduction. Figure 1B shows that the SIV reporter virus could be inhibited >10-fold by A3G under these experimental conditions. The A3G expression plasmid yielded physiological levels of A3G protein compared to the level of A3G detectable in activated human peripheral blood mononuclear cells (PBMCs) (Fig. 1C). The coexpression of Bet counteracted the antiviral activity of A3G in a dose-dependent way, and virus made with A3G and 2 μg of Bet plasmid had an infectivity similar to that of SIV without A3G (Fig. 1B). Note that neither Bet expression in the PFV system nor that in the SIV system completely restored infectivity, showing that human A3G can be counteracted only partially by PFV Bet. Bet expression also caused a dose-dependent inhibition of A3G encapsidation, as demonstrated by immunoblotting of viral particles produced in the presence of 1 μg A3G plasmid and increasing amounts of Bet expression plasmid (Fig. 1D). Under these conditions, the viral particles did not package the Bet protein.

We also used the *SIV_{AGM}-lucΔvif* reporter virus to ask whether PFV Bet inhibits the antiviral activity of A3G proteins

derived from chimpanzees (cpzA3G) and AGMs (AGM.A3G). To control for specificity, we directly compared Bet to HIV-1 Vif and *SIV_{AGM}* Vif. All three A3Gs inhibited the SIV reporter virus 10- to 100-fold, and Bet completely counteracted cpzA3G and largely counteracted AGM.A3G and human A3G (Fig. 2A). HIV-1 Vif inhibited and degraded huA3G and cpzA3G but was not active on AGM.A3G. Only *SIV_{AGM}* Vif was active upon and degraded AGM.A3G, as seen previously (32). In contrast to the sensitivity of A3Gs to Vif, immunoblots of the viral producer cells showed no degradation of A3Gs in samples where Bet was produced (Fig. 2B). To further support the absence of A3G degradation by Bet, we applied the α-complementation assay to A3G (40). This assay is based on α-complementation, the ability of β-galactosidase fragments to complement in *trans*. Figure 2C shows that A3G fused to the α-peptide complemented a coexpressed ω-fragment of β-galactosidase. HIV-1 Vif synthesis reduced the galactosidase activity 10-fold, likely due to A3G degradation, as described previously (40). In contrast, neither *SIV_{AGM}* Vif nor PFV Bet reduced the β-galactosidase activity, further indicating the lack of a Bet-triggered degradation of A3G.

In summary, PFV Bet has a broad A3G tropism, does not deplete cellular A3G proteins of human, chimpanzee, or AGM origin, and can rescue the infectivity of PFV and of a heterologous lentivirus produced in the presence of A3G.

Bet prevents antiviral editing but does not inhibit A3G enzymatic activity. Next, we were interested in studying the functional consequences of the Bet interaction with A3G. Published data

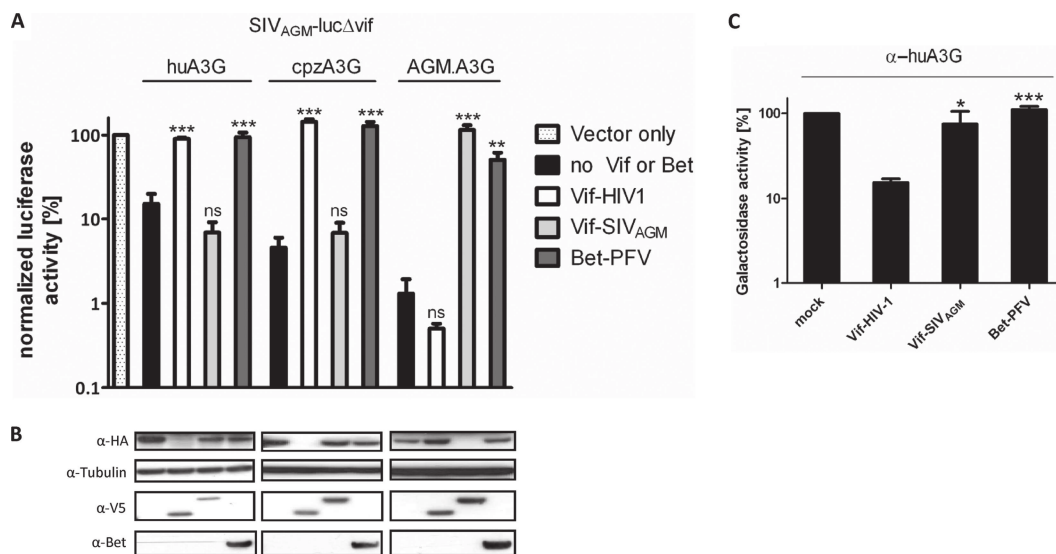


FIG 2 Bet exhibits a broader spectrum of anti-A3G activity than Vif, without leading to A3G degradation. (A) SIV_{AGM} -luc Δvif viruses were produced in the presence and absence (vector only) of the indicated HA-tagged A3G, V5-tagged HIV-1 Vif and SIV_{AGM} Vif, and PFV Bet expression plasmids. Relative infectivities (relative to the virus generated in the absence of A3G and Bet) of equal amounts of the reporter viruses are shown. (B) Immunoblot analysis performed with lysates of virus-producing cells. A3G was detected with an anti-HA MAb, tubulin with an anti-tubulin MAb, Vif with an anti-V5 MAb, and Bet with Bet antiserum. (C) α -Complementation assay of β -galactosidase. 293T cells were transfected in triplicate with the ω -subunit expression plasmid of β -galactosidase and an α -subunit-A3G expression plasmid in combination with PFV Bet, SIV_{AGM} Vif, or HIV-1 Vif. The activity of β -galactosidase was measured 3 days later. Unpaired t tests were computed to determine whether differences between samples in the presence of A3G, with and without Vif or Bet, reached the level of statistical significance (*, $P < 0.05$; **, $P < 0.001$; ***, $P < 0.0001$; and ns, not significant), using GraphPad Prism 5 software.

support Bet binding to A3G, so one could postulate that Bet might impair the enzymatic activity of A3G. To test A3G-induced genome editing, SIV_{AGM} -luc Δvif reporter particles were generated with A3G alone and with A3G and Bet. We used these virions to infect 293T cells, isolated the viral genomic DNA by PCR at 10 h postinfection, and analyzed the sequence for signs of G-to-A mutations on the positive (+) strand, which are indicative of cytidine deaminations in DNA of the viral negative (-) strand. A3G induced G-to-A changes at a mutation rate of 2.6%, in contrast to virions made without A3G, which had a very low G-to-A mutation rate of 0.26% (Fig. 3A). The viral cDNA prepared from virions made in the presence of A3G and Bet showed a reduced but important G-to-A mutation rate of 0.9%, supporting the conclusion that Bet partially counteracts the antiviral activity of A3G (Fig. 3A).

To test whether Bet can inhibit the cytidine deaminase activity of A3G, we purified Bet by immunoprecipitation from 293T cells producing either Bet alone or Bet together with A3G. These experiments were performed using His-tagged Bet that showed full anti-APOBEC3 activity (data not shown). The immunoprecipitated samples were subjected to Western blotting (Fig. 3B) and an *in vitro* deamination assay (45) (Fig. 3C). We tested two different conditions and transfected either 0.5 μ g or 1 μ g Bet expression plasmid together with an expression plasmid for A3G (A3G-HA). Immunoprecipitated Bet protein showed binding to A3G as demonstrated with an anti-A3G antibody (Fig. 3B, α -His-IP panel). We used different volumes (0.1, 1, and 3 μ l) of the immunoprecipitated protein samples and asked whether A3G bound to Bet is able to deaminate single-stranded DNA *in vitro* (Fig. 3C). In addition, we treated the 1- μ l samples with RNase A to remove potential inhibitory RNA (49). As a positive control for *in vitro* cytidine deamination, we directly immunoprecipitated A3G hav-

ing a His tag (A3G-Myc-6XHis). This sample contained several-fold more A3G protein than the amount of A3G immunoprecipitated by Bet. The PCR-based deamination assay depends on the sequence change caused by A3G converting a cytidine to uridine in an 80-nucleotide (nt) ssDNA substrate. Deamination of C to U by A3G is then followed by a PCR that replaces the uridine with thymidine, generating a StuI restriction site. The efficiency of StuI digestion is monitored by using a similar 80-nt ssDNA substrate containing a uridine instead of a cytidine in the StuI recognition site (Fig. 3C, lane U). Polyacrylamide gel electrophoresis separates deaminated from nondeaminated DNA substrates after StuI cleavage of the PCR product. While we found a faint band after StuI cleavage in the 3- μ l input of the sample generated with 0.5 μ g Bet plasmid, much more cleavage product was detectable using the 3- μ l input of cells transfected with 1 μ g Bet plasmid (Fig. 3C). Smaller volumes (0.1 and 1 μ l) of this sample showed a reduced, dose-dependent deamination of cytidine. Immunoprecipitated Bet-A3G complexes treated with RNase A displayed little change in deamination activity compared to the corresponding sample prepared without RNase A treatment (Fig. 3C). Very importantly, immunoprecipitated Bet protein from cells that did not produce A3G did not show cytidine deamination activity, irrespective of RNase A treatment. Similar results were obtained using chimpanzee A3G instead of human A3G (data not shown). In addition, recombinant A3G and Bet proteins were purified from 293T cells by use of Ni-NTA agarose (Fig. 3D), and the *in vitro* deamination assay was conducted with a constant level of A3G (2 nM) and a gradient of Bet (Fig. 3E). A deamination activity chart (Fig. 3F) was plotted according to the corresponding density units (Fig. 3E) and illustrates the activity of A3G in the presence of Bet. The slightly reduced activity (to 83%) at the 100 nM Bet concentration may have been due to precipitation of Bet proteins. Using even

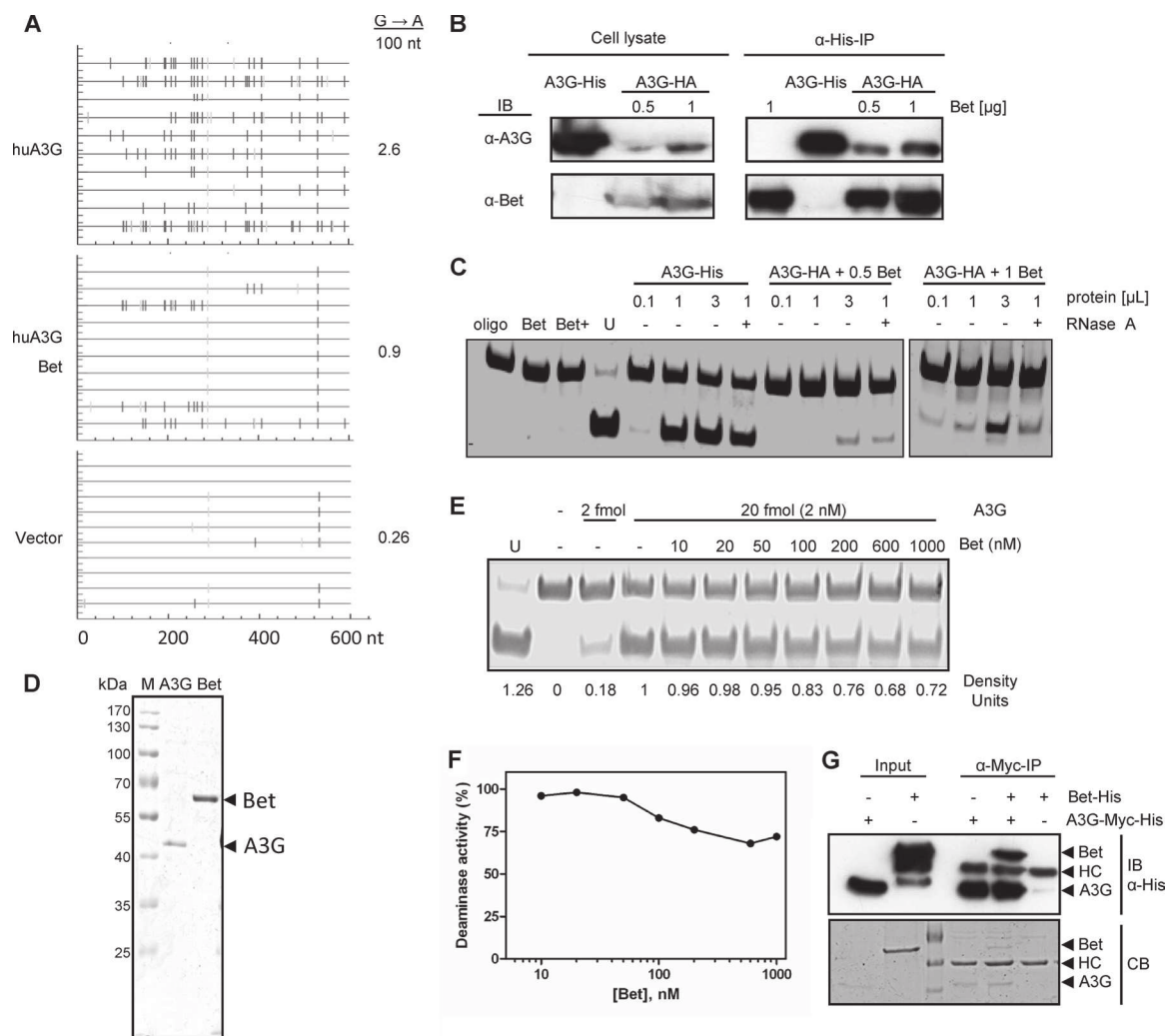


FIG 3 Bet reduces antiviral editing of A3G but does not affect enzymatic activity of A3G. (A) A fragment of the *luciferase* gene was amplified from reverse transcripts of SIV_{AGM}-*lucΔvif* viruses, generated in the presence and absence of huA3G in combination with Bet, at 12 h postinfection. Ten independent nucleotide sequences were determined. The G-to-A conversions (vertical lines) are shown for each clone (horizontal line). (B) The A3G cytidine deamination activity of Bet-A3G complexes was analyzed in Bet-precipitated complexes. For immunoprecipitation of Bet-A3G complexes, 0.5 μg or 1 μg of Bet-V5-His expression plasmid was transfected alone or together with a constant amount (0.5 μg) of A3G-HA into 293T cells. Blots were probed separately with anti-Bet antibody and anti-A3G antibody. (C) Immunoprecipitated complexes and A3G-His and Bet alone were tested in the *in vitro* deamination assay. Protein complexes (0.1 μL, 1 μL, and 3 μL) were used with each Bet concentration (for cells transfected with either 0.5 μg or 1 μg Bet expression plasmid). In addition, 1 μL was purified after RNase A treatment (+) and compared with the untreated sample. An oligonucleotide with CCU in place of CCA served as a marker/digestion control (U). A3G-His (0.5 μg) served as a positive control for the cytidine deamination reaction, whereas Bet alone was the negative control. (D) Coomassie blue-stained SDS-PAGE gel indicating the purity of huA3G-Myc-His and Bet-V5-His proteins after purification from transfected 293T cells by use of Ni-NTA agarose. (E) *In vitro* deamination assay using 293T cell-purified huA3G and Bet proteins. The A3G-Myc-His activity of 20 fmol (2 nM) of protein was tested in the presence of increasing amounts of Bet-His (0 to 1,000 μM). (F) Deaminase activities determined in panel E, in terms of density units plotted against the concentration of Bet. The plot represents relative deaminase activities, with 100% activity adjusted to deamination in the absence of Bet. (G) Anti-Myc immunoprecipitation (IP) shows the interaction of purified A3G-Myc-His and Bet-His *in vitro*. HC, anti-Myc antibody heavy chain. (Top) Immunoblot (IB) of IP and input samples, using anti-His antibody. (Bottom) The same SDS-PAGE gel stained with Coomassie blue (CB).

higher Bet concentrations, a further minor drop in deamination activity, to about 70%, was seen. The interaction between the separately purified A3G and Bet proteins was confirmed by coimmunoprecipitation using an anti-Myc antibody. The Myc antibody bound to protein A/G Plus agarose precipitated A3G-Myc-His and Bet-V5-His complexes but not Bet-V5-His alone, as shown in the anti-His immunoblot and Coomassie blue-stained gel (Fig. 3G). Together, these observations indicate that A3G bound to Bet is not inhibited in its cytidine deamination activity.

Bet interaction is RNA independent. Since A3G-A3G interac-

tion is known to be bridged by RNAs (46), we asked whether A3G-Bet interaction follows a similar phenomenon. To test this, we first performed velocity sedimentation of cell lysates containing A3G alone, A3G with Bet, or Bet alone, with and without RNase A treatment. 293T cells were transfected with expression vectors for A3G alone or together with Bet. Part of the lysates was subjected to RNase A treatment for an hour, and all samples were layered on 10 to 50% sucrose gradients. A3G without Bet showed the expected high-molecular-mass (HMM) complexes that were sensitive to RNase A (Fig. 4A) (50). In contrast, Bet was distrib-

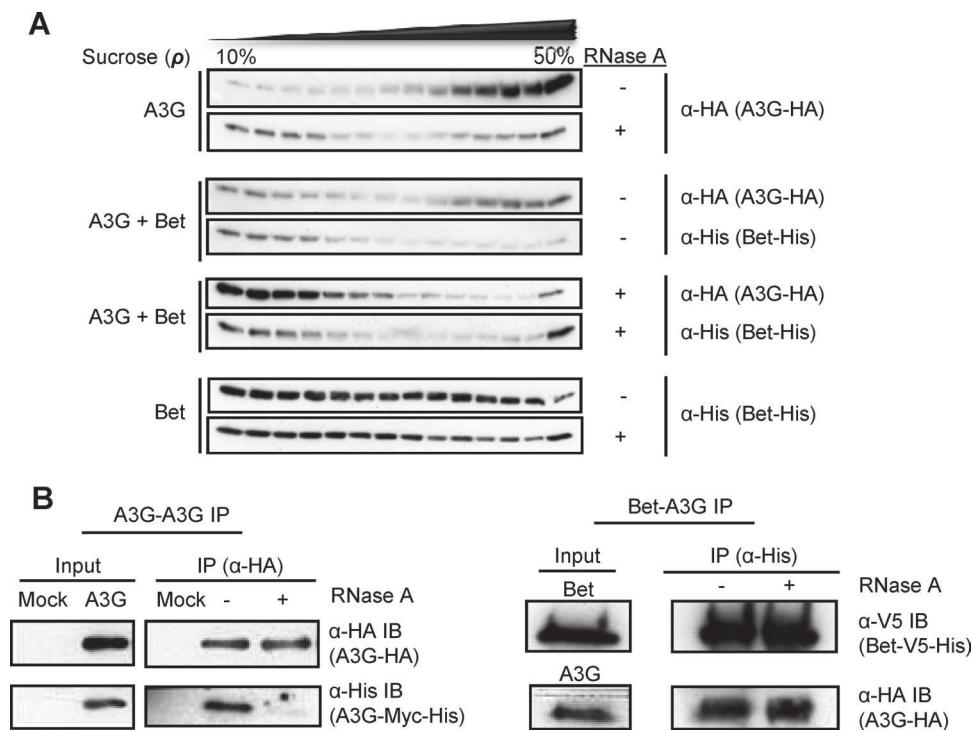


FIG 4 A3G-Bet interaction is RNA independent. (A) Velocity sedimentation of RNase A-treated and untreated cell lysates of 293T cells that were transfected with expression plasmids for A3G alone, A3G and Bet, or Bet alone through sucrose gradients (10% to 50%). Samples were examined by use of specific antibodies: A3G was detected with an anti-HA MAb, and Bet was detected with an anti-His antibody. (B) 293T cells were cotransfected with expression plasmids for A3G-HA and A3G-Myc-His for A3G-A3G immunoprecipitation (IP) and with Bet-V5-His and A3G-HA expression plasmids for Bet-A3G IP. Immunoblots (IB) were incubated with specific antibodies: A3G was detected with an anti-HA MAb, and Bet was detected with an anti-His antibody. IP samples were treated with RNase A or left untreated while binding to the beads.

uted throughout the fractions, irrespective of RNase A treatment, indicating that Bet forms complexes of various molecular masses that are RNA independent. Cell lysates of A3G with Bet showed that A3G was found partially in HMM complexes but also in lower-molecular-mass (LMM) complexes. In the presence of A3G, the Bet protein delocalized from HMM to LMM complexes, consistent with a Bet-A3G interaction. RNase A did not change the detection of Bet in the coexpressing cells but removed the HMM complexes of A3G that did not show copurification with Bet (Fig. 4A). While Bet oligomerization appears to be RNA independent, Bet could require RNA to bind to A3G. To directly check the influence of RNA on A3G-Bet interaction, we performed a co-IP analysis of A3G-HA and Bet-V5-His produced in 293T cells with and without RNase treatment. The cell lysates were allowed to bind to Ni-NTA agarose first and then split into two parts for RNase A treatment. The immunoblot indicates no difference between RNase-treated and untreated Bet-A3G samples (Fig. 4B, right panel), demonstrating that Bet does not bind to A3G via an RNA molecule. In contrast, the parallel A3G-A3G co-IP with anti-HA beads showed a dramatic reduction of A3G-A3G interaction when lysates were treated with RNase A (Fig. 4B, left panel).

Bet prevents A3G-A3G interaction. We recently reported that PFV Bet binds to A3C and reduces A3C dimer formation (19). To determine if Bet also inhibits A3G-A3G complex formation, we studied the oligomerization of A3G in the presence of Bet. Coprecipitation experiments were done with HA-tagged A3G and Myc-tagged A3G. As expected, A3G-HA coprecipitated with A3G-Myc (Fig. 5A), but interestingly, this A3G-A3G interaction was not

detectable when Bet was coexpressed. The observation that Bet prevented A3G dimerization allowed us to identify relevant residues in A3G regulating the Bet interaction. Amino acids in the putative A3G dimer interface were recently described (36, 46), so we tested the Y124A, Y125A, F126L, and W127A A3G mutants (36) that partake in stabilizing the A3G dimer for interaction with Bet. Of these mutants, the W127A mutant is unable to homodimerize and to inhibit HIV-1 Δ vif due to a lack of encapsidation (36, 46).

The Y124A and F126L A3G mutants coimmunoprecipitated with Bet, like wild-type A3G, whereas the F126A and W127A A3G mutants showed partial and complete loss of coimmunoprecipitation, respectively (Fig. 5B). The predicted localization of the analyzed amino acids is shown in Fig. 5C, using a head-to-head structural model of the A3G homodimer (36, 48). Together, these data suggest that Bet interacts with A3G and disrupts its ability to dimerize.

Bet impairs the cytosolic solubility of A3G. Pilot experiments indicated that the choice of cell lysis buffer strongly affected immunoblot detection of A3G in Bet-cotransfected cells (data not shown). To describe any Bet-dependent recovery of A3G under mild lysis conditions, we performed a Western blot titration experiment. After cotransfection of A3G and different amounts of Bet plasmid (0.5 to 2 μ g in experiment I and 0.1 to 2 μ g in experiment II), we used a mild lysis buffer, separated the soluble and insoluble fractions by centrifugation, and solubilized the insoluble fraction with RIPA buffer. Normalized protein samples were analyzed by SDS electrophoresis and immunoblotting (Fig. 6A). In-

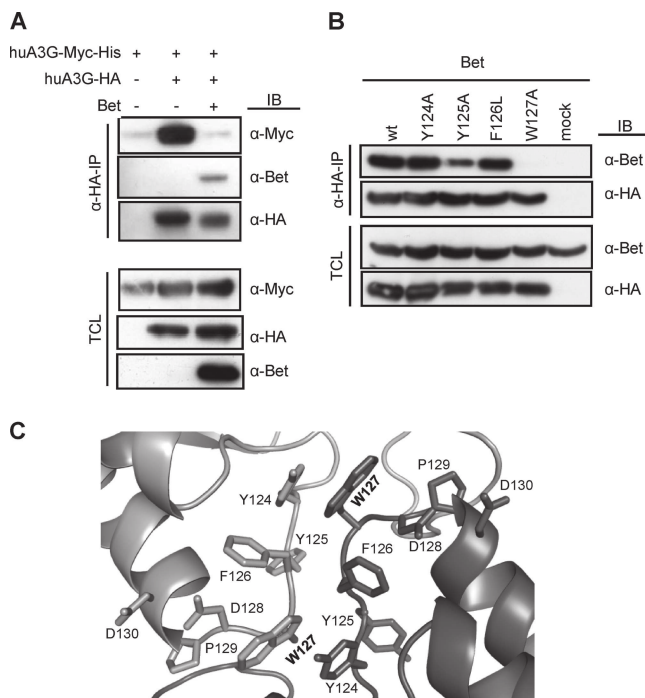


FIG 5 Bet prevents A3G dimerization. (A) Cells were transfected with Myc-tagged huA3G alone or also with HA-tagged huA3G in the presence and absence of Bet. Cell lysates were prepared, and anti-HA immunoprecipitation (α -HA-IP) was performed. huA3G-Myc was coprecipitated with HA-tagged A3G, Bet was detected by immunoblot (IB) analysis using Bet antibody, and A3G-Myc was detected using an anti-Myc MAb. The HA-tagged A3G protein was detected with an anti-HA MAb. TCL, total cell lysate. (B) Cells were transfected with Bet alone or with expression plasmids for HA-tagged wild-type (wt) huA3G or the Y124A, Y125A, F126L, or W127A mutant. Cell lysates were prepared, and anti-HA immunoprecipitation (α -HA-IP) was performed. A3G-associated Bet was detected by immunoblot (IB) analysis using Bet anti-serum. A3G proteins were detected in anti-HA IP samples and in cell lysates by use of anti-HA MAbs, as well as Bet and tubulin antibodies in cell lysates (TCL). (C) Model of A3G N-terminal dimeric interface. The cartoon representation of the A3G dimer interface depicts the spatial arrangements of amino acids 124 to 127, which are involved in dimerization, and HIV-1 Vif binding residues 128 to 130. Dark gray and light gray represent separate N-terminal parts of two A3G proteins, and the Trp127 residue is highlighted in bold.

creasing amounts of Bet protein reduced the detectable amount of A3G in the soluble fraction in a dose-dependent way, and the sample generated with 2 μ g Bet plasmid lost most of the A3G signal (Fig. 6A to C). In contrast, the insoluble cell fractions showed no A3G depletion, but rather an increased amount of A3G with increased expression of Bet. The Bet protein itself was detectable in the soluble as well as insoluble cell fraction.

To determine whether the presence of Bet affects the subcellular recovery of A3G, proteins were fractionated according to their subcellular locations by applying a ProteoExtract subcellular proteome extraction kit. For this approach, proteomes of 293T cells containing A3G in combination with Bet were separated by taking advantage of the different solubilities of certain subcellular compartments in four selected reagents. This system, also known as differential detergent fractionation (DDF), uses different detergents to sequentially extract cellular proteins prior to homogenization while keeping the cell architecture intact (51). Interestingly, using DDF, the resulting fractions reflect not only the characteristics of the protein's solubility but also its localization within the

cell (52). The cellular fractions of proteins in their native state, representing enriched samples of cytosolic proteins (F1; digitonin extraction), proteins of membranes and organelles (F2; Triton X-100 extraction), soluble and DNA-associated nuclear proteins (F3; Tween 20/deoxycholate extraction), and cytoskeleton proteins (F4; SDS extraction), were analyzed by immunoblotting for the presence of A3G and Bet. Proper fractionation was controlled by the use of MAbs specific for the cytosolic proteins glyceraldehyde-3-phosphate dehydrogenase (GAPDH), calpain, and calnexin, the mitochondrial protein cytochrome P450 reductase, and the nuclear histone proteins. The results show that Bet reduced the amount of A3G in the cytosolic (F1), membrane/organelle (F2), and cytoskeleton (F4) fractions while increasing the amount of A3G protein in the nuclear (F3) fraction (Fig. 6D). Bet was found in all fractions, independent of the presence or absence of A3G (Fig. 6E), with the largest amounts in the nuclear fraction (F3). The control proteins GAPDH, calpain, calnexin, cytochrome P450 reductase, and histones were detected only in the expected fractions (Fig. 6D to F), and their recovery was not influenced by Bet or A3G (data not shown). To rule out the possibility that an artificially elevated level of A3G was modulating its detection, we performed immunoblot analysis of subcellular fractions derived from human PBMCs, which possess endogenous A3G. The results revealed that endogenous A3G was localized predominately in fractions F1 and F2 (Fig. 6F), similar to the localization of A3G in transfected 293T cells (Fig. 6D).

To further characterize whether Bet modifies the subcellular localization of A3G, we analyzed cells expressing huA3G together with Bet by confocal microscopy. Using anti-HA antibodies directed against HA-tagged A3G, immunofluorescence studies with transiently transfected HeLa cells showed that huA3G was distributed in the cytoplasm (Fig. 7A). In the presence of Bet, the cytoplasmic localization of A3G did not change. The Bet protein was detectable only in the cytoplasm, and expression of A3G did not affect its localization (Fig. 7A and data not shown). Because both A3G and Bet showed a cytoplasmic localization, we also tested A3C in the presence of Bet (Fig. 7B). A3C has a cytoplasmic and nuclear localization and is sensitive to Bet (19). Interestingly, in the presence of Bet, the nuclear A3C was removed, indicating that complexes of Bet and A3C proteins change their subcellular localization. Taking the data together, we concluded that Bet either modulates the subcellular localization of A3G via sequestration to a not yet identified cytoplasmic region or impairs its solubility, thus reducing its capacity for encapsidation.

DISCUSSION

In this study, we extend previous reports that PFV Bet can counteract human APOBEC3 proteins (19, 20). Our data are in full agreement with those of Russell et al., who reported that PFV Bet antagonizes A3G and can protect foamy viral and unrelated lentiviral particles (20). In our study, we showed that SIV_{AGM} Δ vif can be defended by Bet from A3Gs of human, chimpanzee, and AGM origin (Fig. 2). We also confirmed a molecular interaction between Bet and A3G that does not induce degradation of A3G. We found that Bet showed anti-A3G activity in a dose-dependent manner but that even the largest transfectable amounts of Bet expression plasmid could not fully restore viral infectivity (Fig. 1B). Thus, it is likely that the expression levels of Bet, like the case for A3G, are critical for the replication of wild-type PFV. The

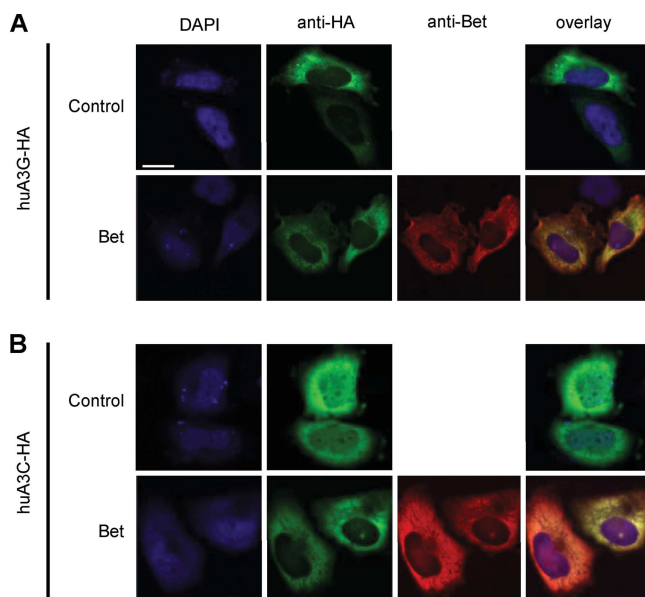


FIG 7 Influence of Bet on subcellular localization of APOBEC3G. HeLa cells were transfected with expression plasmids for HA-tagged huA3G and huA3G with Bet (A) or HA-tagged human APOBEC3C (huA3C-HA) and huA3C-HA with Bet (B). To detect APOBEC3 (green) and Bet (red), immunofluorescence staining was performed with anti-HA antibodies and Bet antiserum, respectively. Nuclei (blue) were visualized by 4',6-diamidino-2-phenylindole (DAPI) staining. Bar = 20 μ m.

Very similarly, blocking the Vif-mediated degradation of A3G by inhibition of NEDD8 conjugation of the Cullin-5 compound of the ubiquitin ligase restored the restriction of HIV-1 by A3G and the viral A3G encapsidation (56). In a different system, Vif inhibited the packaging of a degradation-resistant mutant of A3G (A3G.C97A), suggesting that Vif, like Bet, might be able to interfere with the encapsidation of A3G without inducing A3G degradation (8).

Because A3G most likely interacts with nascent virions in the cytoplasm to become encapsidated, we were interested in the subcellular fate of A3G in the presence of Bet. We found that A3G disappeared from cytoplasmic extracts in a Bet-dependent manner (Fig. 6). Immunofluorescence microscopy did not display Bet-dependent redistribution of A3G within the cell as was seen for A3C (Fig. 7). It remains unknown whether Bet drags A3G to a subcellular compartment that resists simple detection in the microscope and sequesters it away from progeny virions or forms insoluble protein aggregates that inhibit the interaction with assembling viral proteins. Our data revealed the intriguing possibility that Bet uses a second mechanism to counteract A3G, sequestering A3G in insoluble complexes.

Because the A3 genes have undergone a turbulent evolution and are found only in placental mammals (2), the recent discoveries of endogenous foamy viruses in the aye-aye (*Daubentonia madagascariensis*, a strepsirrhine primate) and the two-toed sloth (*Choloepus hoffmanni*) and of foamy virus-like insertions within the genome of a "living fossil," the coelacanth (*Latimeria chalumnae*), provide a unique opportunity to study the evolution of the foamy virus *bet* gene in species with and without A3 genes (57–59).

ACKNOWLEDGMENTS

We thank Nathaniel R. Landau, Dirk Lindemann, Martin Löchelt, and Sandro Rusconi for reagents and Wioletta Hörschken and Marion Battenberg for excellent technical assistance. The following reagents were obtained through the NIH AIDS Research and Reference Reagent Program, Division of AIDS, NIAID, NIH: a monoclonal antibody to HIV-1 p24 (AG3.0), from Jonathan Allan; anti-ApoC17, from Klaus Strebel; and pcDNA3.1 human APOBEC3G-Myc-6XHis, from David Kabat.

This project was funded by DFG grant MU 1608/3-1. M.P. was also supported by the Forschungskommission of the Medical Faculty, Heinrich Heine University Düsseldorf. A.A.J.V. was supported by the International NRW Research School BioStruct, under a grant from the Ministry of Innovation, Science and Research of the North Rhine-Westphalia State, by the Heinrich Heine University Düsseldorf, and by the Entrepreneur Foundation at the Heinrich Heine University Düsseldorf. C.M. was supported by the Heinz-Ansmann Foundation for AIDS Research.

REFERENCES

- LaRue RS, Jonsson SR, Silverstein KA, Lajoie M, Bertrand D, El-Mabrouk N, Hotzel I, Andresdottir V, Smith TP, Harris RS. 2008. The artiodactyl APOBEC3 innate immune repertoire shows evidence for a multi-functional domain organization that existed in the ancestor of placental mammals. *BMC Mol. Biol.* 9:104. doi:10.1186/1471-2199-9-104.
- Münk C, Willemsen A, Bravo IG. 2012. An ancient history of gene duplications, fusions and losses in the evolution of APOBEC3 mutators in mammals. *BMC Evol. Biol.* 12:71. doi:10.1186/1471-2148-12-71.
- Münk C, Jensen BE, Zielonka J, Häussinger D, Kamp C. 2012. Running loose or getting lost: how HIV-1 counters and capitalizes on APOBEC3-induced mutagenesis through its Vif protein. *Viruses* 4:3132–3161.
- Sheehy AM, Erthal J. 2012. APOBEC3 versus retroviruses, immunity versus invasion: clash of the titans. *Mol. Biol. Int.* 2012:974924. doi:10.1155/2012/974924.
- Chiu YL, Greene WC. 2009. APOBEC3G: an intracellular centurion. *Philos. Trans. R. Soc. Lond. B Biol. Sci.* 364:689–703.
- Kao S, Goila-Gaur R, Miyagi E, Khan MA, Opi S, Takeuchi H, Strebel K. 2007. Production of infectious virus and degradation of APOBEC3G are separable functional properties of human immunodeficiency virus type 1 Vif. *Virology* 369:329–339.
- Kao S, Miyagi E, Khan MA, Takeuchi H, Opi S, Goila-Gaur R, Strebel K. 2004. Production of infectious human immunodeficiency virus type 1 does not require depletion of APOBEC3G from virus-producing cells. *Retrovirology* 1:27. doi:10.1186/1742-4690-1-27.
- Opi S, Kao S, Goila-Gaur R, Khan MA, Miyagi E, Takeuchi H, Strebel K. 2007. Human immunodeficiency virus type 1 Vif inhibits packaging and antiviral activity of a degradation-resistant APOBEC3G variant. *J. Virol.* 81:8236–8246.
- Santa-Marta M, da Silva FA, Fonseca AM, Goncalves J. 2005. HIV-1 Vif can directly inhibit apolipoprotein B mRNA-editing enzyme catalytic polypeptide-like 3G-mediated cytidine deamination by using a single amino acid interaction and without protein degradation. *J. Biol. Chem.* 280:8765–8775.
- Britan-Rosich E, Nowarski R, Kotler M. 2011. Multifaceted counter-APOBEC3G mechanisms employed by HIV-1 Vif. *J. Mol. Biol.* 410:1065–1076.
- Arias JF, Koyama T, Kinomoto M, Tokunaga K. 2012. Retroelements versus APOBEC3 family members: no great escape from the magnificent seven. *Front. Microbiol.* 3:275. doi:10.3389/fmicb.2012.00275.
- Derse D, Hill SA, Princler G, Lloyd P, Heidecker G. 2007. Resistance of human T cell leukemia virus type 1 to APOBEC3G restriction is mediated by elements in nucleocapsid. *Proc. Natl. Acad. Sci. U. S. A.* 104:2915–2920.
- Ooms M, Krikoni A, Kress AK, Simon V, Münk C. 2012. APOBEC3A, APOBEC3B, and APOBEC3H haplotype 2 restrict human T-lymphotropic virus type 1. *J. Virol.* 86:6097–6108.
- Kolokithas A, Rosenke K, Malik F, Hendrick D, Swanson L, Santiago ML, Portis JL, Hasenkrug KJ, Evans LH. 2010. The glycosylated Gag protein of a murine leukemia virus inhibits the antiretroviral function of APOBEC3. *J. Virol.* 84:10933–10936.
- Stavrou S, Nitta T, Kotla S, Ha D, Nagashima K, Rein AR, Fan H, Ross SR. 2013. Murine leukemia virus glycosylated Gag blocks apolipoprotein B editing complex 3 and cytosolic sensor access to the reverse transcription complex. *Proc. Natl. Acad. Sci. U. S. A.* 110:9078–9083.

16. Chareza S, Slavkovic LD, Liu Y, Rathe AM, Münk C, Zabogli E, Pistello M, Löchelt M. 2012. Molecular and functional interactions of cat APOBEC3 and feline foamy and immunodeficiency virus proteins: different ways to counteract host-encoded restriction. *Virology* 424:138–146.
17. Löchelt M, Romen F, Bastone P, Muckenfuss H, Kirchner N, Kim YB, Truyen U, Rosler U, Battenberg M, Saib A, Flory E, Cichutek K, Münk C. 2005. The antiretroviral activity of APOBEC3 is inhibited by the foamy virus accessory Bet protein. *Proc. Natl. Acad. Sci. U. S. A.* 102:7982–7987.
18. Münk C, Beck T, Zielonka J, Hotz-Wagenblatt A, Chareza S, Battenberg M, Thielebein J, Cichutek K, Bravo IG, O'Brien SJ, Löchelt M, Yuhki N. 2008. Functions, structure, and read-through alternative splicing of feline APOBEC3 genes. *Genome Biol.* 9:R48. doi:10.1186/gb-2008-9-3-r48.
19. Perkovic M, Schmidt S, Marino D, Russell RA, Stauch B, Hofmann H, Kopietz F, Kloke BP, Zielonka J, Strover H, Hermle J, Lindemann D, Pathak VK, Schneider G, Löchelt M, Cichutek K, Münk C. 2009. Species-specific inhibition of APOBEC3C by the prototype foamy virus protein Bet. *J. Biol. Chem.* 284:5819–5826.
20. Russell RA, Wiegand HL, Moore MD, Schafer A, McClure MO, Cullen BR. 2005. Foamy virus Bet proteins function as novel inhibitors of the APOBEC3 family of innate antiretroviral defense factors. *J. Virol.* 79:8724–8731.
21. Liu W, Worobey M, Li Y, Keele BF, Bibollet-Ruche F, Guo Y, Goepfert PA, Santiago ML, Ndjango JB, Neel C, Clifford SL, Sanz C, Kamunya S, Wilson ML, Pusey AE, Gross-Camp N, Boesch C, Smith V, Zamma K, Huffman MA, Mitani JC, Watts DP, Peeters M, Shaw GM, Switzer WM, Sharp PM, Hahn BH. 2008. Molecular ecology and natural history of simian foamy virus infection in wild-living chimpanzees. *PLoS Pathog.* 4:e1000097. doi:10.1371/journal.ppat.1000097.
22. Herchenroder O, Renne R, Loncar D, Cobb EK, Murthy KK, Schneider J, Mergia A, Luciw PA. 1994. Isolation, cloning, and sequencing of simian foamy viruses from chimpanzees (SFVcpz): high homology to human foamy virus (HFV). *Virology* 201:187–199.
23. Locatelli S, Peeters M. 2012. Cross-species transmission of simian retroviruses: how and why they could lead to the emergence of new diseases in the human population. *AIDS* 26:659–673.
24. Sandstrom PA, Phan KO, Switzer WM, Fredeking T, Chapman L, Heneine W, Folks TM. 2000. Simian foamy virus infection among zoo keepers. *Lancet* 355:551–552.
25. Switzer WM, Bhullar V, Shanmugam V, Cong ME, Parekh B, Lerche NW, Yee JL, Ely JJ, Boneva R, Chapman LE, Folks TM, Heneine W. 2004. Frequent simian foamy virus infection in persons occupationally exposed to nonhuman primates. *J. Virol.* 78:2780–2789.
26. Heneine W, Schweizer M, Sandstrom P, Folks T. 2003. Human infection with foamy viruses. *Curr. Top. Microbiol. Immunol.* 277:181–196.
27. Khan AS. 2009. Simian foamy virus infection in humans: prevalence and management. *Expert Rev. Anti Infect. Ther.* 7:569–580.
28. Linal M. 2000. Why aren't foamy viruses pathogenic? *Trends Microbiol.* 8:284–289.
29. Bock M, Heinkelein M, Lindemann D, Rethwilm A. 1998. Cells expressing the human foamy virus (HFV) accessory Bet protein are resistant to productive HFV superinfection. *Virology* 250:194–204.
30. Meiering CD, Linal ML. 2002. Reactivation of a complex retrovirus is controlled by a molecular switch and is inhibited by a viral protein. *Proc. Natl. Acad. Sci. U. S. A.* 99:15130–15135.
31. Delebecque F, Suspene R, Calattini S, Casartelli N, Saib A, Froment A, Wain-Hobson S, Gessain A, Vartanian JP, Schwartz O. 2006. Restriction of foamy viruses by APOBEC cytidine deaminases. *J. Virol.* 80:605–614.
32. Mariani R, Chen D, Schröfelbauer B, Navarro F, König R, Bollman B, Münk C, Nymark-McMahon H, Landau NR. 2003. Species-specific exclusion of APOBEC3G from HIV-1 virions by Vif. *Cell* 114:21–31.
33. Duda A, Stange A, Luftenegger D, Stanke N, Westphal D, Pietschmann T, Eastman SW, Linal ML, Rethwilm A, Lindemann D. 2004. Prototype foamy virus envelope glycoprotein leader peptide processing is mediated by a furin-like cellular protease, but cleavage is not essential for viral infectivity. *J. Virol.* 78:13865–13870.
34. Pietschmann T, Heinkelein M, Heldmann M, Zentgraf H, Rethwilm A, Lindemann D. 1999. Foamy virus capsids require the cognate envelope protein for particle export. *J. Virol.* 73:2613–2621.
35. Marin M, Rose KM, Kozak SL, Kabat D. 2003. HIV-1 Vif protein binds the editing enzyme APOBEC3G and induces its degradation. *Nat. Med.* 9:1398–1403.
36. Bulliard Y, Turelli P, Rohrig UF, Zoete V, Mangeat B, Michielin O, Trono D. 2009. Functional analysis and structural modeling of human APOBEC3G reveal the role of evolutionarily conserved elements in the inhibition of human immunodeficiency virus type 1 infection and Alu transposition. *J. Virol.* 83:12611–12621.
37. Achong BG, Mansell PW, Epstein MA, Clifford P. 1971. An unusual virus in cultures from a human nasopharyngeal carcinoma. *J. Natl. Cancer Inst.* 46:299–307.
38. Cullen BR. 1986. Trans-activation of human immunodeficiency virus occurs via a bimodal mechanism. *Cell* 46:973–982.
39. Muckenfuss H, Kaiser JK, Krebil E, Battenberg M, Schwer C, Cichutek K, Münk C, Flory E. 2007. Sp1 and Sp3 regulate basal transcription of the human APOBEC3G gene. *Nucleic Acids Res.* 35:3784–3796.
40. Fang L, Landau NR. 2007. Analysis of Vif-induced APOBEC3G degradation using an alpha-complementation assay. *Virology* 359:162–169.
41. Holland AU, Munk C, Lucero GR, Nguyen LD, Landau NR. 2004. Alpha-complementation assay for HIV envelope glycoprotein-mediated fusion. *Virology* 319:343–352.
42. Moosmann P, Rusconi S. 1996. Alpha complementation of LacZ in mammalian cells. *Nucleic Acids Res.* 24:1171–1172.
43. Löchelt M, Zentgraf H, Flugel RM. 1991. Construction of an infectious DNA clone of the full-length human spumaretrovirus genome and mutagenesis of the bet1 gene. *Virology* 184:43–54.
44. Simm M, Shahabuddin M, Chao W, Allan JS, Volsky DJ. 1995. Aberrant Gag protein composition of a human immunodeficiency virus type 1 vif mutant produced in primary lymphocytes. *J. Virol.* 69:4582–4586.
45. Nowarski R, Britan-Rosich E, Shiloach T, Kotler M. 2008. Hypermutation by intersegmental transfer of APOBEC3G cytidine deaminase. *Nat. Struct. Mol. Biol.* 15:1059–1066.
46. Huthoff H, Autore F, Gallois-Montbrun S, Fraternali F, Malim MH. 2009. RNA-dependent oligomerization of APOBEC3G is required for restriction of HIV-1. *PLoS Pathog.* 5:e1000330. doi:10.1371/journal.ppat.1000330.
47. Sali A, Blundell TL. 1993. Comparative protein modelling by satisfaction of spatial restraints. *J. Mol. Biol.* 234:779–815.
48. Holden LG, Prochnow C, Chang YP, Bransteitter R, Chelico L, Sen U, Stevens RC, Goodman MF, Chen XS. 2008. Crystal structure of the anti-viral APOBEC3G catalytic domain and functional implications. *Nature* 456:121–124.
49. Soros VB, Yonemoto W, Greene WC. 2007. Newly synthesized APOBEC3G is incorporated into HIV virions, inhibited by HIV RNA, and subsequently activated by RNase H. *PLoS Pathog.* 3:e15. doi:10.1371/journal.ppat.0030015.
50. Kreisberg JF, Yonemoto W, Greene WC. 2006. Endogenous factors enhance HIV infection of tissue naive CD4 T cells by stimulating high molecular mass APOBEC3G complex formation. *J. Exp. Med.* 203:865–870.
51. Ramsby M, Makowski G. 2011. Differential detergent fractionation of eukaryotic cells. *Cold Spring Harb. Protoc.* 2011:prot5592. doi:10.1101/pdb.prot5592.
52. Ramsby ML, Makowski GS. 1999. Differential detergent fractionation of eukaryotic cells. Analysis by two-dimensional gel electrophoresis. *Methods Mol. Biol.* 112:53–66.
53. Khan MA, Goila-Gaur R, Kao S, Miyagi E, Walker RC, Jr, Strebel K. 2009. Encapsidation of APOBEC3G into HIV-1 virions involves lipid raft association and does not correlate with APOBEC3G oligomerization. *Retrovirology* 6:99. doi:10.1186/1742-4690-6-99.
54. Huthoff H, Malim MH. 2007. Identification of amino acid residues in APOBEC3G required for regulation by human immunodeficiency virus type 1 Vif and virion encapsidation. *J. Virol.* 81:3807–3815.
55. Yu X, Yu Y, Liu B, Luo K, Kong W, Mao P, Yu XF. 2003. Induction of APOBEC3G ubiquitination and degradation by an HIV-1 Vif-Cul5-SCF complex. *Science* 302:1056–1060.
56. Stanley DJ, Bartholomeussen K, Crosby DC, Kim DY, Kwon E, Yen L, Cartozo NC, Li M, Jager S, Mason-Herr J, Hayashi F, Yokoyama S, Krogan NJ, Harris RS, Peterlin BM, Gross JD. 2012. Inhibition of a NEDD8 cascade restores restriction of HIV by APOBEC3G. *PLoS Pathog.* 8:e1003085. doi:10.1371/journal.ppat.1003085.
57. Han GZ, Worobey M. 2012. An endogenous foamy virus in the aye-aye (*Daubentonia madagascariensis*). *J. Virol.* 86:7696–7698.
58. Han GZ, Worobey M. 2012. An endogenous foamy-like viral element in the coelacanth genome. *PLoS Pathog.* 8:e1002790. doi:10.1371/journal.ppat.1002790.
59. Katzourakis A, Gifford RJ, Tristem M, Gilbert MT, Pybus OG. 2009. Macroevolution of complex retroviruses. *Science* 325:1512. doi:10.1126/science.1174149.

AMERICAN
SOCIETY FOR
MICROBIOLOGY

Title: Prototype Foamy Virus Bet Impairs the Dimerization and Cytosolic Solubility of Human APOBEC3G

Author: Ananda Ayyappan Jaguva Vasudevan, Mario Perković, Yannick Bulliard et al.

Publication: Journal of Virology

Publisher: American Society for Microbiology

Date: Aug 15, 2013

Copyright © 2013, American Society for Microbiology

Logged in as:
Ananda Ayyappan Jaguva
Vasudevan
Account #:
3000710859

LOGOUT

Permissions Request

Authors in ASM journals retain the right to republish discrete portions of his/her article in any other publication (including print, CD-ROM, and other electronic formats) of which he or she is author or editor, provided that proper credit is given to the original ASM publication. ASM authors also retain the right to reuse the full article in his/her dissertation or thesis. For a full list of author rights, please see: http://journals.asm.org/site/misc/ASM_Author_Statement.xhtml

BACK

CLOSE WINDOW

Copyright © 2017 Copyright Clearance Center, Inc. All Rights Reserved. [Privacy statement](#). [Terms and Conditions](#).

Comments? We would like to hear from you. E-mail us at customercare@copyright.com

Chapter VI

Detection of APOBEC3 proteins and catalytic activity in urothelial carcinoma

Journal : A book chapter on “Urothelial Carcinoma”, to be published in the lab protocol series, *Methods in Molecular Biology*, published by Springer (2017) in press.

Own contribution to this work:

- Complete execution of experimental procedures
- Writing of the manuscript

With the permission from the series editors:

W. A. Schulz, PhD

Günter Niegisch, MD

Michèle J. Hoffmann, PhD

Dept. of Urology

Heinrich Heine University

Duesseldorf, Germany

Phone +49 (0) 211 81 15845 (WAS) or -15847 (MJH)

Detection of APOBEC3 proteins and catalytic activity in urothelial carcinoma

Ananda Ayyappan Jaguva Vasudevan^{1, 2}, Wolfgang Göring^{2, 3}, Dieter Häussinger¹, and Carsten Münk^{1, #}

¹Clinic for Gastroenterology, Hepatology, and Infectiology, ² Department of Urology, and

³Institute of Pathology, Medical Faculty, Heinrich Heine University Düsseldorf, Germany

Running head: Characterization of endogenous APOBEC3s in UC

[#]corresponding author: Clinic for Gastroenterology, Hepatology, and Infectiology, Medical Faculty, Heinrich Heine University Düsseldorf, Building 23.12.U1.82, Moorenstr. 5, 40225 Düsseldorf, Germany, Tel: +49 (0) 211-81-10887, Fax: +49 (0) 211-81-18752, E-mail: carsten.muenk@med.uni-duesseldorf.de

Abstract

Members of the APOBEC3 (A3) family of enzymes were shown to act in an oncogenic manner in several cancer types. Immunodetection of APOBEC3A (A3A), APOBEC3B (A3B) and APOBEC3G (A3G) proteins is particularly challenging due to the large sequence homology of these proteins and limited availability of antibodies. Here we combine independent immunoblotting with an *in vitro* activity assay technique, to detect and categorize specific A3s expressed in urothelial bladder cancer and other cancer cells.

Keywords APOBEC3, cytidine deaminase, urothelial bladder cancer, mutation, deamination assay, cancer cell

1. Introduction

APOBEC3G (apolipoprotein B mRNA-editing, enzyme-catalytic, polypeptide-like 3G; referred to as A3G), one of the cellular polynucleotide cytidine deaminases of the APOBEC3 (A3) family, is extensively studied as a retroviral (HIV-1) restriction factor (Sheehy et al., 2002, Bishop et al., 2004, Zhang et al., 2003). On infection, A3 proteins encapsidated into the virus catalyze the deamination of cytidines to uridines in single stranded viral cDNA generated during reverse transcription in the target cells, thereby hypermutating the viral genome and subsequently inhibiting productive infection (for reviews on antiviral role of A3s and their protein features, see: (Harris and Dudley, 2015, Chiu and Greene, 2008, Vasudevan et al., 2013)). The preferred dinucleotides of A3G and other A3s are CC and TC in the DNA substrate, respectively (Yu et al., 2004, Burns et al., 2013, Henderson and Fenton, 2015, Burns et al., 2015). A3 act only on single-stranded DNA and can deaminate the cytosines on the substrate molecule in a processive manner in 3'→5' direction (Chelico et al., 2006, Nowarski et al., 2008). To counter A3-mediated mutagenesis, lentiviruses acquired the accessory protein Vif (viral infectivity factor) that anchors A3s to target them for polyubiquitylation and proteasomal degradation (Sheehy et al., 2003, Yu et al., 2003).

Recently, mutation signatures resulting from catalytic activity of A3s (especially A3A and A3B) were reported in several cancer types, including bladder, cervical, head and neck, breast and lung cancers (Burns et al., 2013, Roberts et al., 2012, Nik-Zainal et al., 2012, Roberts et al., 2013, Cancer Genome Atlas Research, 2014). Specifically, mRNA levels of A3B were found to be elevated in breast, urothelial and several other cancer tissues (Burns et al., 2013, Hedegaard et al., 2016) positively correlating with overall mutation loads in the respective tumor genomes (Burns et al., 2013, Roberts et al., 2013). Even though the mRNA levels of A3B appear to be much higher (Hedegaard et al., 2016), the mutation spectrum in the bladder tumor patient cohort was found to be two times more A3A specific (YTCA) than A3B specific (RTCA) (Hedegaard et al., 2016, Chan et al., 2015). Interestingly, an A3B deletion polymorphism was reported to increase the risk of breast cancers (Long et al., 2013, Xuan et al., 2013) and further analysis revealed that the fusion form of protein A3A_B (A3A coding sequence with A3B 3' UTR) tends to be more mutagenic (Caval et al., 2014, Nik-Zainal et al., 2014). In addition, the haplotype I of APOBEC3H (A3H) was recently linked to breast and lung cancer mutagenesis (Starrett et al., 2016).

In experimental research, A3 proteins are often fused to an epitope tag (such as hemagglutinin (HA), V5, or FLAG), which is then used for detection of the particular proteins from the cell and virus lysates using tag specific antibodies. Although antibodies raised against A3G and A3B are available, they broadly detect A3A, A3B, and A3G due to their high sequence homology (for example A3A and A3B C-terminal domains share >90% identity at nucleotide and amino acid level). This makes it difficult to quantitatively determine the endogenous A3(s) as well as to study the localization of A3s by immunohistochemistry (Henderson and Fenton, 2015, Burns et al., 2015). However, the approximate molecular weight of A3A, A3B and A3G are 23, 45.9 and 46.4 kDa, respectively. Because of this difficulty in assessing A3 family members using mRNA expression profile and available antibodies, an additional independent method to validate endogenous enzymatic activity of A3s in cancer research is crucial. This validation is important to understand whether A3 borne mutations in the genome are a consequence of malignancy and whether this mutation load drives tumor development (Henderson and Fenton, 2015).

Our method involves immunodetection of A3s and determining deamination activity of the A3s using different substrate nucleotides from cell lysates (Figure 1). We adapted the PCR-

based *in vitro* deamination assay described by Nowarski *et al.* (Nowarski *et al.*, 2008) which depends on a cytidine to uridine conversion in an 80 nt ssDNA by A3. A subsequent PCR generates a double stranded DNA, replaces the uridine with thymidine, and thus generates a new restriction site (Figure 1). The efficiency of the restriction enzyme digestion is monitored using a similar 80 nt ssDNA containing uridine instead of a cytidine in the hotspot. This method was shown to be effective in determining specific A3 activity from various samples (Jaguva Vasudevan *et al.*, 2013, Marino *et al.*, 2016). Here we used two different bladder cancer cell lines (UMUC-3 and VMCUB-1) to demonstrate our method. As a source of defined cell-derived A3s, 293T cells transiently transfected with A3-encoding plasmids were used.

2. Materials

Prepare all buffers using ultrapure water and analytical grade reagents. Prepare and store all reagents at room temperature (unless indicated otherwise). Diligently follow all waste disposal regulations when disposing waste materials (*see Note 1*). Note that we did not include the operating procedure for SDS-PAGE and immunoblotting in this chapter, as it follows commonly used standard protocols.

2.1 Cells and immunoblotting

1. Cell culture: Bladder cancer cell lines of interest and HEK293T cells for transient transfection (*see Note 2*).
2. Complete Dulbecco's Modified Eagle Medium (DMEM). For 293T: Dulbecco's high-glucose modified Eagle's medium (DMEM), supplemented with 10% fetal bovine serum (FBS), 2 mM L-glutamine, 50 units/ml penicillin, and 50 µg/ml streptomycin. For bladder cancer cell lines: DMEM plus 10% FBS and 2 mM L-glutamine.
3. Phosphate buffered saline (PBS).
4. Trypsin-EDTA.
5. Transfection reagent such as Lipofectamine.
6. Human APOBEC3 expression plasmids for A3B or A3G can be obtained from the NIH AIDS reagent program (www.aidsreagent.org/).

7. Mild lysis buffer (1X): 50 mM Tris, pH 8, 1 mM phenylmethylsulfonyl fluoride (PMSF), 10% glycerol, 0.8% NP-40, 150 mM NaCl and 1X complete protease inhibitor cocktail. Store at 4°C (see **Note 3**).

8. Materials needed for standard SDS-PAGE and immunoblotting (semi-dry or wet blotting).

The data presented here was obtained using Mini PROTEAN[®] 3 System glass plates and semi-dry blotting procedure (Biorad). It is also expected to work in a similar way with other glass plates and wet blotting.

9. PVDF membrane (see **Note 4**)

10. TBST (1X): 10 mM Tris, pH 8, 150 mM NaCl and 0.05% Tween-20, adjust the pH to 8 using 1 M hydrochloric acid. TBST can be prepared as 10X stock, store at room temperature.

11. Blocking solution: 5% skimmed-milk powder in 1X TBST (see **Note 5**). Store at 4°C.

12. A plastic container to handle blot.

13. Anti-HA antibody (1:7,500 dilution, MMS-101P, Covance) and anti-APOBEC3G antiserum (NIH catalog number 9906) (see **Note 6**).

14. Appropriate anti-mouse and anti-rabbit secondary antibodies (see **Note 7**).

15. Chemiluminescent reagent (see **Note 8**).

2.2 *In vitro* DNA deamination assay

1. Single stranded oligonucleotide DNA substrates (ss DNA), and control oligonucleotides as given in Table 1 (see **Note 9**).

2. 250 mM Tris buffer; adjust the pH to 7.0 using 1 M hydrochloric acid, store at room temperature.

3. RNase A.

4. Thermoblock.

5. Standard thermocycler

6. PCR reaction tubes.

7. PCR components: Taq DNA polymerase and its buffer, 10 mM dNTPs, 10 μM forward and reverse primers (Table 1).

8. Restriction enzymes: Eco147I and MseI

2.3 Native-PAGE electrophoresis of DNA

1. In-house, native-PAGE gel: 10X TBE buffer: 890 mM Tris (pH 8), 890 mM borate and 20 mM EDTA (can be diluted from 0.5 M EDTA, pH 8), store at room temperature. (see **Note 10**).
2. Aqueous 30% acrylamide and bisacrylamide stock solution at a ratio of 37.5:1, store at 4°C (see **Note 11**).
3. Ammonium persulfate (APS): 10% solution in water
4. N,N,N',N'-tetramethylethylenediamine, 1,2-bis(dimethylamino)-ethane (TEMED), store at 4°C.
5. Ethidium bromide staining solution in water, 7.5 µg/ml final concentration (see **Note 12**).
6. UV-detection and documentation system

3. Methods

Perform the following procedures at room temperature unless otherwise specified.

3.1 Cell lysis and immunoblotting

1. Maintain HEK293T cells and bladder cancer cell lines at 37°C in a humidified atmosphere of 5% CO₂ in complete DMEM as specified in 2.1. Treat the cancer cell line of interest as required.
2. Seed 6 x 10⁵ 293T cells per well in a 6 well plate. Next day, transfect 293T cells with 1 µg of A3B or A3G expression plasmids using a suitable transfection reagent. Incubate the cells for 2 days.
3. Lyse with 250-300 µl mild lysis buffer, incubate on ice for at least 15 min and clarify the lysate at 21,000 x g for 20 min at 4°C, transfer the soluble fraction into a new tube (see **Note 13**).
4. Determine the protein concentration in the cell lysate using BCA assay.

5. Load 20 µg of total protein on the 12% SDS-PAGE gel after heating the protein at 95 °C for 5 min with loading dye containing denaturing agent.
6. Run the gel at a constant 40 mA/gel until the bromophenol blue dye front has reached the bottom of the gel.
7. Transfer the protein onto a PVDF membrane using blotting technique.
8. Block the membrane with 5% milk in TBST for 30 min (in a blot shaker).
9. Incubate the blot with the primary antibody (anti-HA or anti-A3G antiserum) for overnight at 4 °C or in a cold room with slight shaking.
10. Next day, wash 3X with TBST, 10 min each time.
11. Probe the blot with appropriate secondary antibody and incubate it for 1 h at room temperature.
12. Wash 3X with TBST, 10 min each time.
13. Detect the signals using appropriate chemiluminescent reagent, image on the X-ray film or direct imaging system (Figure 2A).

3.2 *In vitro* DNA cytidine deamination assay

1. Set up the deamination reaction as follows: 100 fmol ssDNA, 1 µl of 250 mM Tris, pH 7, 2 µl of cell lysate, make up to 10 µl volume with water and mix gently (*see Note 14*).
2. Split the reaction mixture into two halves; to one tube add 50 µg/ml RNase A (final concentration) (*see Note 15*).
3. Incubate the reaction mixture at 37 °C for at least 1 h and then terminate by boiling at 95 °C for 5 min (*see Note 16*).
4. Dilute the reaction mixture to 1/10 with water, in order to get the substrate concentration to 1 fmol/µl. Use 1 µl of this as template DNA in the subsequent PCR reaction.

5. Set the PCR reaction (to a total volume 25 μ l) with 1 μ l of template, 1 μ l of each appropriate forward and reverse primers (stock 10 μ M) (Table 1), 1 μ l of dNTPs (10 mM), 2.5 μ l Taq polymerase buffer containing MgCl₂ (10X), 1.5 units Taq DNA polymerase (see **Note 17**). The PCR parameters are 95°C for 3 min, followed by 30 cycles of 61°C for 30 s and 94°C for 30 s (see **Note 18**).
6. As a control for restriction enzyme digestion, include parallel PCR reactions with CU and TU oligos (1 fmol) together.
7. Add 10 units of the respective restriction enzyme Eco147I or MseI to the PCR reactions, mix thoroughly and incubate for at least 1 h at 37°C (see **Note 19**).

3.3 Native page and visualization of DNA

1. Prepare a 15% NATIVE-PAGE gel as follows: Add 10 ml of 30% acrylamide-bisacrylamide solution, 8 ml water, 2 ml 10X TBE, 165 μ l APS and add finally 16.6 μ l TEMED. Quickly mix the casting solution by swirling the container and pour between the glass plates placed in the casting frame. Insert a comb immediately without introducing air bubbles (see **Note 20**).
2. When polymerization is complete, immediately transfer the gel to a running container, fill with 1X TBE buffer, and pre-run the gel in 1X TBE for 30 min at 100 V before adding any sample (see **Note 21**).
3. To avoid heat formation in the gel tank and buffer, running the native gel in a cold room or on ice is recommended. Load the digested PCR products with 6X loading dye.
4. Following electrophoresis, pry the gel plates open using a gel releaser, stain with ethidium bromide solution in water for 5 min at room temperature
5. Detect the DNA signal using a 320 nm UV-lamp and appropriate documentation system (Figure 2B).

Notes

1. Wear laboratory safety equipment such as goggles, nitrile gloves, mask and lab coat, follow the safety instructions suggested by the manufacturer of chemicals and the local legal regulations.
2. We used UMUC-3 and VMCUB-1 bladder cancer cell lines as a model in this chapter. Our method can be used for any other cancer cell line as required. Cell lines can also be subjected to drug treatment, ectopic co-expression of another factor or downregulation by siRNA. Maintain the cells with appropriate medium and conditions as required. HEK293T cells were used for transient transfection of A3 since these cells are easily transfectable using Lipofectamine reagent.
3. Prepare mild lysis buffer without adding the PMSF and 1X protease inhibitor cocktail. It is suggested to make an aliquot of the buffer and freshly add the above components for cell lysis.
4. We obtained optimum results using Immobilon-P Membrane, 0.45 μm from Millipore.
5. We routinely use 5% milk in TBST for blocking and diluting primary and secondary antibodies. It doesn't mean that you must not use 5% BSA in TBST. Empirically determine the better one suits for your antibody and detection method.
6. The NIH antibody was obtained through the NIH AIDS reagent program. Researchers can request reagents through their website (www.aidsreagent.org/).
7. We used anti-mouse, anti-rabbit antibody from GE healthcare at dilution of 1: 10,000 as final concentration.
8. Our immunoblot was developed using ECL prime reagent and X-ray film (both from GE healthcare). It should also work in a similar manner with other reagents or imaging systems. Note that different cell lines may have higher or lower A3 protein levels; hence the detection reagent must be chosen accordingly to avoid capturing saturated signal.
9. We recommend HPLC-purified standard oligonucleotides for this assay. Salt-purified oligonucleotides may result in unspecific DNA amplification.

10. 10X TBE buffer on long storage often tends to precipitate. This complication can be resolved by warming up the buffer for a while prior to use or by using a 5X TBE stock.
11. Due to the neurotoxicity of acrylamide, we prefer buying this reagent rather than preparing it ourselves. Handle this solution inside the hood while making gels.
12. Alternatively, SYBR gold (1:1,000 dilution) nucleic acid gel stain from Thermo Fischer Scientific can be used, which better stains weak signals. Note that the number of PCR cycles then needs to be reduced to 18 (instead of 30) for optimal amplification and staining.
13. We use mild lysis buffer for keeping the protein content native for activity assay, but it is also good to try using other harsh buffers such as RIPA if required for the cell lysis. Choose the same buffer and conditions throughout for all the cell lines.
14. If required, for convenient sample handling, the 15 µl reaction volume can be made up with the same substrate concentration.
15. It is easy to dilute the RNase A to a concentration 10 times higher than the final working concentration required in 25 mM Tris buffer, pH 7. RNase treatment is important to release the A3 protein from the higher mass RNA complexes.
16. Spin the tube shortly to settle down the contents immediately after boiling.
17. Archaeal DNA polymerases such as the Pfu enzyme bind tightly to template-strand uracil and stall replication (Fogg et al., 2002) unless a point mutation V93Q is introduced (Firbank et al., 2008)).
18. The PCR reaction volume was kept within 20-25 µl, because it facilitates loading the complete products on the gel after restriction digestion.
19. Following PCR, add the restriction enzyme directly to the PCR product. PCR purification is not suggested (and not needed) because the columns may not be able to bind the 80 bp ds DNA fragments. Specific restriction enzyme buffers may not be required as well. We do this incubation in a PCR machine, by setting 1 h at 30°C and then 4°C indefinitely.
20. Given here is a composition to make a mini-gel with 1.5 mm thick glass plates from Biorad. The volumes can be scaled according to the need. Note that here we have only one layer of gel to cast, unlike stacking and separating gels of SDS-PAGE.

21. It is suggested to wash each well of the gel before and after pre-run with a syringe (to remove unwanted gel fragments). This ensures the convenient loading of samples.

Acknowledgments

We would like to thank Klaus Strebel and the NIH AIDS Research and Reference Reagent Program for anti-ApoC17 (A3G) antibody. We are grateful to W. A. Schulz for his constant support. CM is supported by the Heinz Ansmann foundation.

References

- BISHOP, K. N., HOLMES, R. K., SHEEHY, A. M., DAVIDSON, N. O., CHO, S. J. & MALIM, M. H. 2004. Cytidine deamination of retroviral DNA by diverse APOBEC proteins. *Curr Biol*, 14, 1392-6.
- BURNS, M. B., LACKEY, L., CARPENTER, M. A., RATHORE, A., LAND, A. M., LEONARD, B., REFSLAND, E. W., KOTANDENIYA, D., TRETAKOVA, N., NIKAS, J. B., YEE, D., TEMIZ, N. A., DONOHUE, D. E., MCDUGLE, R. M., BROWN, W. L., LAW, E. K. & HARRIS, R. S. 2013. APOBEC3B is an enzymatic source of mutation in breast cancer. *Nature*, 494, 366-70.
- BURNS, M. B., LEONARD, B. & HARRIS, R. S. 2015. APOBEC3B: pathological consequences of an innate immune DNA mutator. *Biomed J*, 38, 102-10.
- CANCER GENOME ATLAS RESEARCH, N. 2014. Comprehensive molecular characterization of urothelial bladder carcinoma. *Nature*, 507, 315-22.
- CAVAL, V., SUSPENE, R., SHAPIRA, M., VARTANIAN, J. P. & WAIN-HOBSON, S. 2014. A prevalent cancer susceptibility APOBEC3A hybrid allele bearing APOBEC3B 3'UTR enhances chromosomal DNA damage. *Nat Commun*, 5, 5129.
- CHAN, K., ROBERTS, S. A., KLIMCZAK, L. J., STERLING, J. F., SAINI, N., MALC, E. P., KIM, J., KWIATKOWSKI, D. J., FARGO, D. C., MIECZKOWSKI, P. A., GETZ, G. & GORDENIN, D. A. 2015. An APOBEC3A hypermutation signature is distinguishable from the signature of background mutagenesis by APOBEC3B in human cancers. *Nat Genet*, 47, 1067-72.
- CHELICO, L., PHAM, P., CALABRESE, P. & GOODMAN, M. F. 2006. APOBEC3G DNA deaminase acts processively 3' → 5' on single-stranded DNA. *Nat Struct Mol Biol*, 13, 392-9.
- CHIU, Y. L. & GREENE, W. C. 2008. The APOBEC3 cytidine deaminases: an innate defensive network opposing exogenous retroviruses and endogenous retroelements. *Annu Rev Immunol*, 26, 317-53.
- FIRBANK, S. J., WARDLE, J., HESLOP, P., LEWIS, R. J. & CONNOLLY, B. A. 2008. Uracil recognition in archaeal DNA polymerases captured by X-ray crystallography. *J Mol Biol*, 381, 529-39.
- FOGG, M. J., PEARL, L. H. & CONNOLLY, B. A. 2002. Structural basis for uracil recognition by archaeal family B DNA polymerases. *Nat Struct Biol*, 9, 922-7.
- HARRIS, R. S. & DUDLEY, J. P. 2015. APOBECs and virus restriction. *Virology*, 479-480, 131-45.
- HEDEGAARD, J., LAMY, P., NORDENTOFT, I., ALGABA, F., HOYER, S., ULHOI, B. P., VANG, S., REINERT, T., HERMANN, G. G., MOGENSEN, K., THOMSEN, M. B., NIELSEN, M. M., MARQUEZ, M., SEGERSTEN, U., AINE, M., HOGLUND, M., BIRKENKAMP-DEMTRODER, K., FRISTRUP, N., BORRE, M., HARTMANN, A., STOHR, R., WACH, S., KECK, B., SEITZ, A. K., NAWROTH, R., MAURER, T., TULIC, C., SIMIC, T., JUNKER, K., HORSTMANN, M., HARVING, N., PETERSEN, A. C., CALLE, M. L., STEYERBERG, E. W., BEUKERS, W., VAN KESSEL, K. E., JENSEN, J. B., PEDERSEN, J. S., MALMSTROM, P. U., MALATS, N., REAL, F. X., ZWARTHOF, E. C., ORNTOFT,

- T. F. & DYRSKJOT, L. 2016. Comprehensive Transcriptional Analysis of Early-Stage Urothelial Carcinoma. *Cancer Cell*, 30, 27-42.
- HENDERSON, S. & FENTON, T. 2015. APOBEC3 genes: retroviral restriction factors to cancer drivers. *Trends Mol Med*, 21, 274-84.
- JAGUVA VASUDEVAN, A. A., PERKOVIC, M., BULLIARD, Y., CICHUTEK, K., TRONO, D., HÄUSSINGER, D. & MÜNK, C. 2013. Prototype foamy virus Bet impairs the dimerization and cytosolic solubility of human APOBEC3G. *J Virol*, 87, 9030-40.
- LONG, J., DELAHANTY, R. J., LI, G., GAO, Y. T., LU, W., CAI, Q., XIANG, Y. B., LI, C., JI, B. T., ZHENG, Y., ALI, S., SHU, X. O. & ZHENG, W. 2013. A common deletion in the APOBEC3 genes and breast cancer risk. *J Natl Cancer Inst*, 105, 573-9.
- MARINO, D., PERKOVIC, M., HAIN, A., JAGUVA VASUDEVAN, A. A., HOFMANN, H., HANSCHMANN, K. M., MUHLEBACH, M. D., SCHUMANN, G. G., KONIG, R., CICHUTEK, K., HÄUSSINGER, D. & MÜNK, C. 2016. APOBEC4 Enhances the Replication of HIV-1. *PLoS One*, 11, e0155422.
- NIK-ZAINAL, S., ALEXANDROV, L. B., WEDGE, D. C., VAN LOO, P., GREENMAN, C. D., RAINE, K., JONES, D., HINTON, J., MARSHALL, J., STEBBINGS, L. A., MENZIES, A., MARTIN, S., LEUNG, K., CHEN, L., LEROY, C., RAMAKRISHNA, M., RANCE, R., LAU, K. W., MUDIE, L. J., VARELA, I., MCBRIDE, D. J., BIGNELL, G. R., COOKE, S. L., SHLIEN, A., GAMBLE, J., WHITMORE, I., MADDISON, M., TARPEY, P. S., DAVIES, H. R., PAPAEMMANUIL, E., STEPHENS, P. J., MCLAREN, S., BUTLER, A. P., TEAGUE, J. W., JONSSON, G., GARBER, J. E., SILVER, D., MIRON, P., FATIMA, A., BOYALT, S., LANGEROD, A., TUTT, A., MARTENS, J. W., APARICIO, S. A., BORG, A., SALOMON, A. V., THOMAS, G., BORRESEN-DALE, A. L., RICHARDSON, A. L., NEUBERGER, M. S., FUTREAL, P. A., CAMPBELL, P. J., STRATTON, M. R. & BREAST CANCER WORKING GROUP OF THE INTERNATIONAL CANCER GENOME, C. 2012. Mutational processes molding the genomes of 21 breast cancers. *Cell*, 149, 979-93.
- NIK-ZAINAL, S., WEDGE, D. C., ALEXANDROV, L. B., PETLJAK, M., BUTLER, A. P., BOLLI, N., DAVIES, H. R., KNAPPSKOG, S., MARTIN, S., PAPAEMMANUIL, E., RAMAKRISHNA, M., SHLIEN, A., SIMONIC, I., XUE, Y., TYLER-SMITH, C., CAMPBELL, P. J. & STRATTON, M. R. 2014. Association of a germline copy number polymorphism of APOBEC3A and APOBEC3B with burden of putative APOBEC-dependent mutations in breast cancer. *Nat Genet*, 46, 487-91.
- NOWARSKI, R., BRITAN-ROSICH, E., SHILOACH, T. & KOTLER, M. 2008. Hypermutation by intersegmental transfer of APOBEC3G cytidine deaminase. *Nat Struct Mol Biol*, 15, 1059-66.
- ROBERTS, S. A., LAWRENCE, M. S., KLIMCZAK, L. J., GRIMM, S. A., FARGO, D., STOJANOV, P., KIEZUN, A., KRYUKOV, G. V., CARTER, S. L., SAKSENA, G., HARRIS, S., SHAH, R. R., RESNICK, M. A., GETZ, G. & GORDENIN, D. A. 2013. An APOBEC cytidine deaminase mutagenesis pattern is widespread in human cancers. *Nat Genet*, 45, 970-6.
- ROBERTS, S. A., STERLING, J., THOMPSON, C., HARRIS, S., MAV, D., SHAH, R., KLIMCZAK, L. J., KRYUKOV, G. V., MALC, E., MIECZKOWSKI, P. A., RESNICK, M. A. & GORDENIN, D. A. 2012. Clustered mutations in yeast and in human cancers can arise from damaged long single-strand DNA regions. *Mol Cell*, 46, 424-35.
- SHEEHY, A. M., GADDIS, N. C., CHOI, J. D. & MALIM, M. H. 2002. Isolation of a human gene that inhibits HIV-1 infection and is suppressed by the viral Vif protein. *Nature*, 418, 646-50.
- SHEEHY, A. M., GADDIS, N. C. & MALIM, M. H. 2003. The antiretroviral enzyme APOBEC3G is degraded by the proteasome in response to HIV-1 Vif. *Nat Med*, 9, 1404-7.
- STARRETT, G. J., LUENGAS, E. M., MCCANN, J. L., EBRAHIMI, D., TEMIZ, N. A., LOVE, R. P., FENG, Y., ADOLPH, M. B., CHELICO, L., LAW, E. K., CARPENTER, M. A. & HARRIS, R. S. 2016. The DNA cytosine deaminase APOBEC3H haplotype I likely contributes to breast and lung cancer mutagenesis. *Nat Commun*, 7, 12918.
- VASUDEVAN, A. A., SMITS, S. H., HOPFNER, A., HÄUSSINGER, D., KOENIG, B. W. & MÜNK, C. 2013. Structural features of antiviral DNA cytidine deaminases. *Biol Chem*, 394, 1357-70.
- XUAN, D., LI, G., CAI, Q., DEMING-HALVERSON, S., SHRUBSOLE, M. J., SHU, X. O., KELLEY, M. C., ZHENG, W. & LONG, J. 2013. APOBEC3 deletion polymorphism is associated with breast cancer risk among women of European ancestry. *Carcinogenesis*, 34, 2240-3.

- YU, Q., KONIG, R., PILLAI, S., CHILES, K., KEARNEY, M., PALMER, S., RICHMAN, D., COFFIN, J. M. & LANDAU, N. R. 2004. Single-strand specificity of APOBEC3G accounts for minus-strand deamination of the HIV genome. *Nat Struct Mol Biol*, 11, 435-42.
- YU, X., YU, Y., LIU, B., LUO, K., KONG, W., MAO, P. & YU, X. F. 2003. Induction of APOBEC3G ubiquitination and degradation by an HIV-1 Vif-Cul5-SCF complex. *Science*, 302, 1056-60.
- ZHANG, H., YANG, B., POMERANTZ, R. J., ZHANG, C., ARUNACHALAM, S. C. & GAO, L. 2003. The cytidine deaminase CEM15 induces hypermutation in newly synthesized HIV-1 DNA. *Nature*, 424, 94-8.

Table 1

Designation	Oligonucleotide sequence
CC	5'- GGATTGGTTGGTTATTTGTTTAAGGAAGGTGGATTAAAGGCC <u>C</u> AAGAAGGTGATG GAAGTTATGTTTGGTAGATTGATGG
CU	5'- GGATTGGTTGGTTATTTGTTTAAGGAAGGTGGATTAAAGGCC <u>U</u> AAGAAGGTGATG GAAGTTATGTTTGGTAGATTGATGG
TC	5'- GGATTGGTTGGTTATTTGTATAAGGAAGGTGGATTGAAGGTT <u>C</u> AAGAAGGTGATG GAAGTTATGTTTGGTAGATTGATGG
TU	5'- GGATTGGTTGGTTATTTGTATAAGGAAGGTGGATTGAAGGTT <u>U</u> AAGAAGGTGATG GAAGTTATGTTTGGTAGATTGATGG
CC-forward	5'-GGATTGGTTGGTTATTTGTTTAAGGA
Common reverse	5'-CCATCAATCTACCAAACATAACTTCCA
TC-forward	5'-GGATTGGTTGGTTATTTGTATAAGGA

Table 1

Oligonucleotides used in the deamination assay (substrate DNA and PCR primers) are listed. Note that the underlined cytosine is the target base for deamination by A3. A3G and A3B prefers **CC** and **TC** motif in the ssDNA, respectively. Uracil containing modified DNA (**CU** and **TU**) oligonucleotides were used as a control to denote the restriction enzyme digestion.

Figure 1

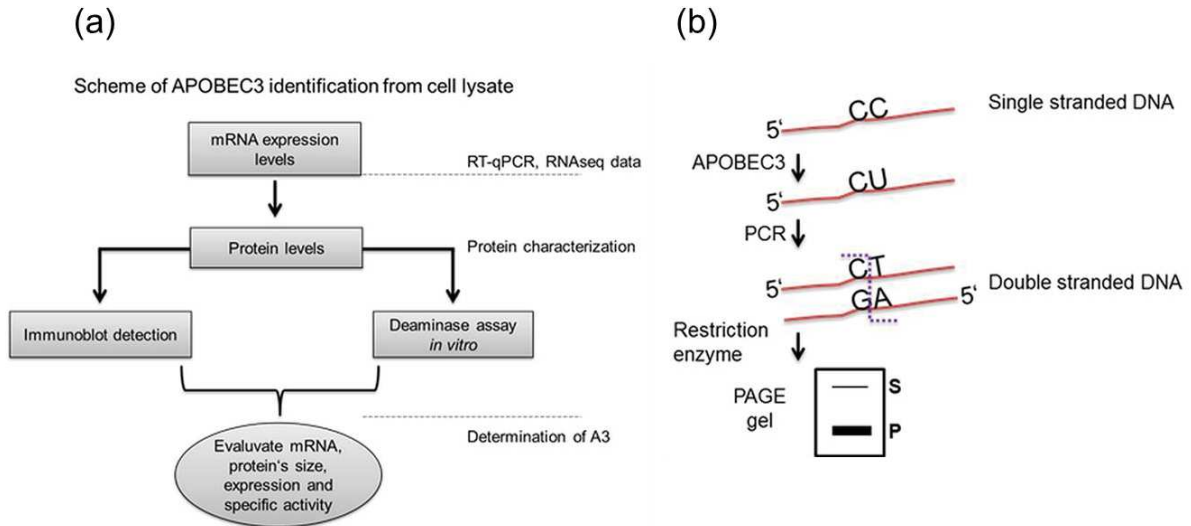


Figure 1

(a) Flow chart representing the combination of techniques used for the characterization of endogenous APOBEC3 from bladder cancer cell lines. (b) Principle of DNA deamination assay adapted from Nowarski *et al.* Incubation of ssDNA with A3 results in deamination of cytidine to uridine in the target motif (CC→CU), generating a specific restriction site following PCR. S-substrate; P-product; RE-restriction enzyme.

Figure 2

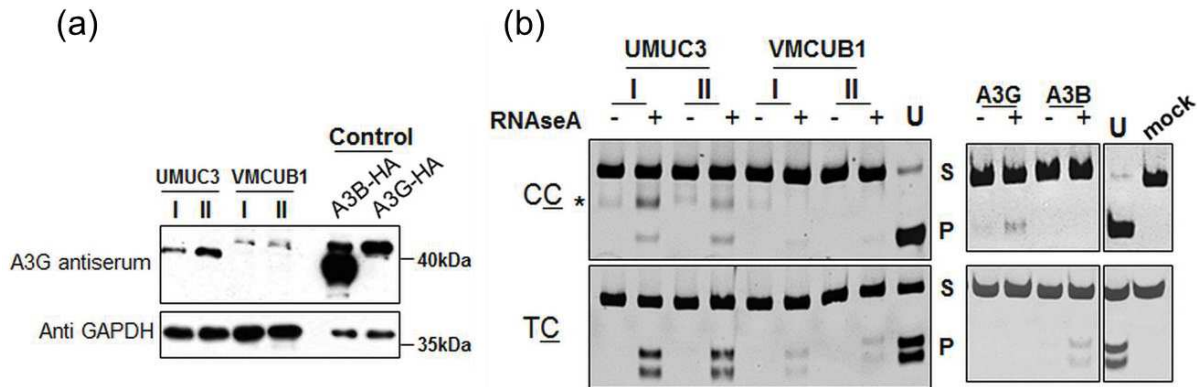


Figure 2

(a) Immunodetection of endogenous A3 from bladder cancer cell lines UMUC-3 and VMCUB-1 lysates and detection of ectopically expressed HA-tagged A3B and A3G from 293T cells. Blot was stained with anti A3G antiserum, where GAPDH served as a loading control. I and II represent two independent samples. (b) Deamination activity of endogenous A3 proteins was tested on two different oligonucleotide substrates containing either CC or TC. RNase A treatment was performed to derive physiologically active A3 proteins from higher mass RNA complexes. Deamination substrate band (S) and product band (P) were marked. "U" specifies the cleavage of CU or TU substrate by its respective restriction enzyme to be used as a marker to denote deaminated product. "*" indicates an unspecific band. In a separate panel, activity assay gel image representing A3G and A3B protein derived from 293T cells was included.

Chapter VII

APOBEC4 Enhances the Replication of HIV-1

Journal : PLoS ONE (published in 2016)

Own contribution to this work:

- A shared first author of this paper, performed the following experiments, immunoblots, a semi-quantitative RT-PCR, establishment and optimization of *in vitro* deamination assay, protein purification strategies from *E. coli* and 293T cells (cloned some plasmids for the same), immunoprecipitation, and Electrophoretic mobility shift assay; Virion isolation to assess A3/A4 encapsidation. These data are presented in figures 1A, 9, 10, 11A and 11B
- Writing of the manuscript

RESEARCH ARTICLE

APOBEC4 Enhances the Replication of HIV-1

Daniela Marino^{1,2}, Mario Perković^{1,2}[✉], Anika Hain¹, Ananda A. Jaguva Vasudevan¹, Henning Hofmann^{1,2}[✉], Kay-Martin Hanschmann³, Michael D. Mühlebach^{2,4}, Gerald G. Schumann², Renate König^{5,6}, Klaus Cichutek², Dieter Häussinger¹, Carsten Münk^{1,2,*}

1 Clinic for Gastroenterology, Hepatology, and Infectiology, Medical Faculty, Heinrich-Heine-University Düsseldorf, Düsseldorf, Germany, **2** Division of Medical Biotechnology, Paul-Ehrlich-Institute, Langen, Germany, **3** Biostatistics, Paul-Ehrlich-Institute, Langen, Germany, **4** Product Testing of Immunological Medicinal Products for Veterinary Uses, Paul-Ehrlich-Institute, Langen, Germany, **5** Host-Pathogen Interactions, Paul-Ehrlich-Institute, Langen, Germany, **6** Sanford Burnham Prebys Medical Discovery Institute, Immunity and Pathogenesis Program, La Jolla, California, United States of America

 These authors contributed equally to this work.

[✉] Current address: TRON (Translational Oncology at the University Medical Center), Johannes Gutenberg University Mainz, Mainz, Germany

[✉] Current address: Robert Koch Institute, Division for HIV and other Retroviruses, Berlin, Germany

* carsten.muenk@med.uni-duesseldorf.de



Abstract

APOBEC4 (A4) is a member of the AID/APOBEC family of cytidine deaminases. In this study we found a high mRNA expression of A4 in human testis. In contrast, there were only low levels of A4 mRNA detectable in 293T, HeLa, Jurkat or A3.01 cells. Ectopic expression of A4 in HeLa cells resulted in mostly cytoplasmic localization of the protein. To test whether A4 has antiviral activity similar to that of proteins of the APOBEC3 (A3) subfamily, A4 was co-expressed in 293T cells with wild type HIV-1 and HIV-1 luciferase reporter viruses. We found that A4 did not inhibit the replication of HIV-1 but instead enhanced the production of HIV-1 in a dose-dependent manner and seemed to act on the viral LTR. A4 did not show detectable cytidine deamination activity *in vitro* and weakly interacted with single-stranded DNA. The presence of A4 in virus producer cells enhanced HIV-1 replication by transiently transfected A4 or stably expressed A4 in HIV-susceptible cells. APOBEC4 was capable of similarly enhancing transcription from a broad spectrum of promoters, regardless of whether they were viral or mammalian. We hypothesize that A4 may have a natural role in modulating host promoters or endogenous LTR promoters.

OPEN ACCESS

Citation: Marino D, Perković M, Hain A, Jaguva Vasudevan AA, Hofmann H, Hanschmann K-M, et al. (2016) APOBEC4 Enhances the Replication of HIV-1. PLoS ONE 11(6): e0155422. doi:10.1371/journal.pone.0155422

Editor: Javier Marcelo Di Noia, Institut de Recherches Cliniques de Montréal (IRCM), CANADA

Received: April 5, 2016

Accepted: April 28, 2016

Published: June 1, 2016

Copyright: © 2016 Marino et al. This is an open access article distributed under the terms of the [Creative Commons Attribution License](https://creativecommons.org/licenses/by/4.0/), which permits unrestricted use, distribution, and reproduction in any medium, provided the original author and source are credited.

Data Availability Statement: All relevant data are within the paper.

Funding: CM is supported by the Heinz-Ansmann foundation for AIDS research

Competing Interests: The authors have declared that no competing interests exist.

Introduction

The AID/APOBEC (apolipoprotein B mRNA-editing enzyme, catalytic polypeptide-like) polynucleotide (deoxy) cytidine deaminases family consists of AICDA (activation-induced cytidine deaminase, AID), APOBEC1 (A1), APOBEC2 (A2), APOBEC3 (A3), which has the following seven paralogues in humans: A3A–A3D, A3F–A3H, and APOBEC4 (A4) [1–5]. These enzymes have a diverse range of functions and substrate specificities. Cytidine deamination of single-stranded DNA or RNA was shown to be the principal activity of the AID, A1, and A3 proteins in biochemical and cell culture assays, but such evidence is lacking for A2 and A4 proteins.

Cytidine deaminases of the A3 gene family can inhibit long terminal repeat (LTR)—and non-LTR-retrotransposons and have broad antiviral activity against retroviruses such as HIV and murine leukemia virus (MLV), hepadnaviruses, and non-related viruses [6–21]. A3s mainly act by deaminating cytosine into uracil using single-stranded DNA as a substrate (for review, see [22]). DNA editing introduces hypermutations of the viral genome that eventually render the target genome inactive. Conversely, retroviruses have evolved countermeasures to prevent encapsidation of A3s into viral particles. For example, the Vif protein in lentiviruses, the Bet protein in foamyviruses, the glycosylated Gag (glyco-Gag) protein in MLV, and the nucleocapsid protein in Human T-cell lymphotropic virus accomplish this counteraction using different mechanisms [17, 19, 20, 22–28].

AID is a B lymphoid protein that deaminates chromosomal DNA, thereby inducing somatic hypermutations and gene conversion. Furthermore, AID stimulates class switch recombination in B cells [29–35]. AID can restrict LINE-1 (L1) retrotransposition [15, 36, 37], but it is inactive against HIV-1 [38–40]. A1 catalyzes the cytosine-to-uracil editing of apolipoprotein B mRNA in the intestine [41, 42]. Editing generates a premature stop codon, which is translated to produce a truncated form of apolipoprotein B protein, termed *apoB48*, that has distinct functions in lipid transport [43]. The editing mechanism is highly specific for residue C6666 and works in conjunction with A1 complementation factor [44]. Other mRNA targets for A1 editing were recently identified [45]. A1s of rabbit and rodents inhibit both MLV and HIV-1 by mutating the viral RNA and DNA; in contrast human A1 does not edit *in vitro* [39, 46–49]. In addition, L1 retrotransposons can be restricted by A1s derived from rodents and rabbits, but this effect is weak for human A1 [15, 50]. A2 plays an important role in regulating and maintaining muscle development in mammals [51]. A2 did not exhibit cytosine deaminase activity of DNA substrates in bacterial or yeast mutation assays [52, 53]. Human A2 lacks inhibitory activity against retrotransposons [9, 54, 55] and HIV-1 [38, 40], and murine A2 does not inhibit or edit MLV [46].

A4 protein is more closely related to A1 than to the other APOBECs, and the A4 gene is conserved in chimpanzee, rhesus monkey, dog, cow, mouse, rat, chicken, and frog [3]. A4 is considered to be a putative cytosine-to-uracil editing enzyme. However, experiments conducted using A4 overexpression in yeast and bacteria failed to show cytosine deamination activity in DNA [52]. In mice, the A4 gene is expressed primarily in testis [3], which suggests that it may be involved in spermatogenesis. Whether human A4 participates in intrinsic immunity against HIV as demonstrated for A3s and A1 is unknown, but these anti-viral activities of its sister proteins suggest that it might be possible. Therefore we set out to evaluate the effect of human A4 on the replication of HIV-1 *in vitro*.

Results

Analysis of A4 expression in cell lines and human testis tissue

Based on information of public repositories (e.g. GenBank) A4 is detectable mainly in human testis, and neither full length A4 mRNAs nor expressed sequence tags (ESTs) have been identified in blood cells, lymphoid tissues, T cells or macrophages. To functionally test A4 in cell culture, we first wanted to determine whether widely used human cell lines express A4. To this end, semi-quantitative RT PCRs on total RNA from the 293T, HeLa, A3.01 T, and Jurkat T cell lines were conducted and the weakly detected PCR products were cloned and sequence verified (Fig 1A). We further compared the A4 expression levels of these cell lines to A4 expression in human testis tissue by quantitative real-time RT PCR on total RNA. Data demonstrate that A4 expression levels in testis are approximately 30- to 50-fold higher than those in the tested cell lines (Fig 1B). A4 expression plasmids were generated with either N-terminal or C-terminal

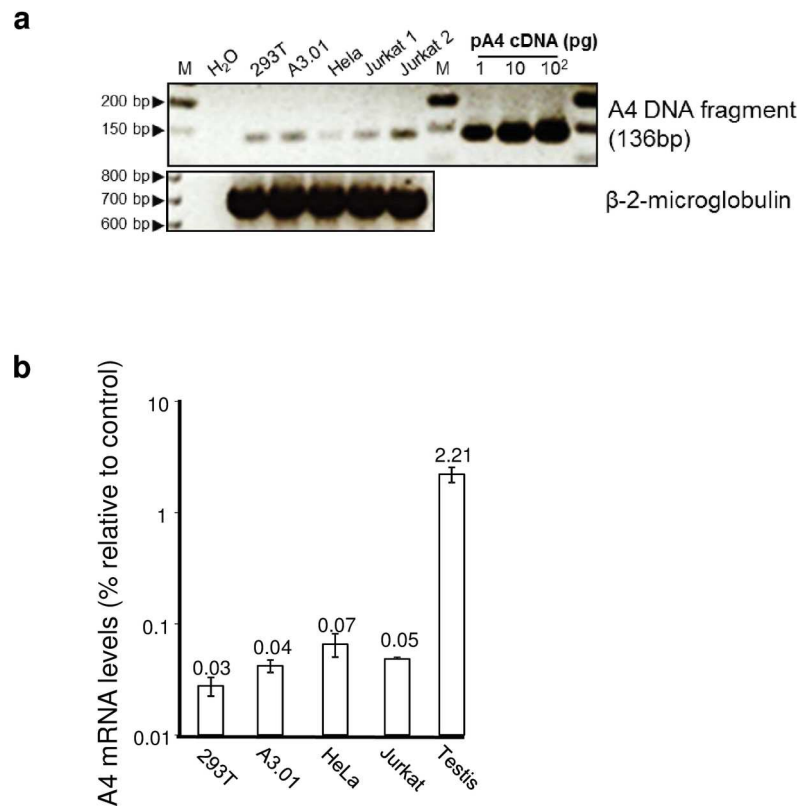


Fig 1. Differential expression of A4. (a) A4 expression was determined by semi-quantitative RT-PCR. Low level A4 amplification by PCR using equal amount of cDNA prepared from total RNA of 293T, A3.01, HeLa, and Jurkat cell lines. As a control, β-2-microglobulin (β-2-M) cDNA was amplified. Water instead of template served as a background control and a plasmid coding for A4 cDNA (pA4 cDNA) served as a positive control. M: 50 bp DNA ladder. (b) Levels of A4 expression were determined by quantitative real-time RT-PCR and measured relative to endogenous HPRT1 RNA levels. A4 is expressed at a high level in human testis tissue, while 293T, HeLa, A3.01 and Jurkat cells exhibit very low A4 expression. Error bars indicate standard deviation.

doi:10.1371/journal.pone.0155422.g001

HA-tags or without any tag (HA-A4, A4-HA, A4, Fig 2A). A4 constructs expressed 10- to 100-fold less protein than A3 plasmids expressed from the same vector as shown for A4-HA (3xHA-tag) in comparison with A3G-HA (1xHA-tag) and A3A-HA (3xHA-tag) (Fig 2B). To study the subcellular localization of the differently tagged A4 proteins, we analyzed the expression of these proteins in transfected HeLa cells using confocal microscopy. HA-A4 was localized in both cytoplasm and nucleus (Fig 3A and 3B). A4-HA exhibited a predominantly cytoplasmic distribution (Fig 3C and 3D). Untagged A4 could not be detected, because there was no A4-specific antibody available. To analyze if the characteristic polylysine stretch (KKKKKGKK) at the C-terminus is important for nuclear localization of A4, an N-terminal HA-tagged mutant lacking the polylysine domain (HA-A4ΔKK, Fig 2A) was tested. Only few cells showed expression of this protein, however, if expressed, HA-A4ΔKK was detectable in nucleus and cytoplasm, suggesting that the polylysine stretch does not function as a nuclear localization motif (Fig 3F).

A4 expression results in an increased HIV-1 particle yield

To determine the effect of A4 on HIV-1 particle production, we co-transfected increasing amounts of the HA-A4 expression plasmid with a constant amount of HIV-1 expression

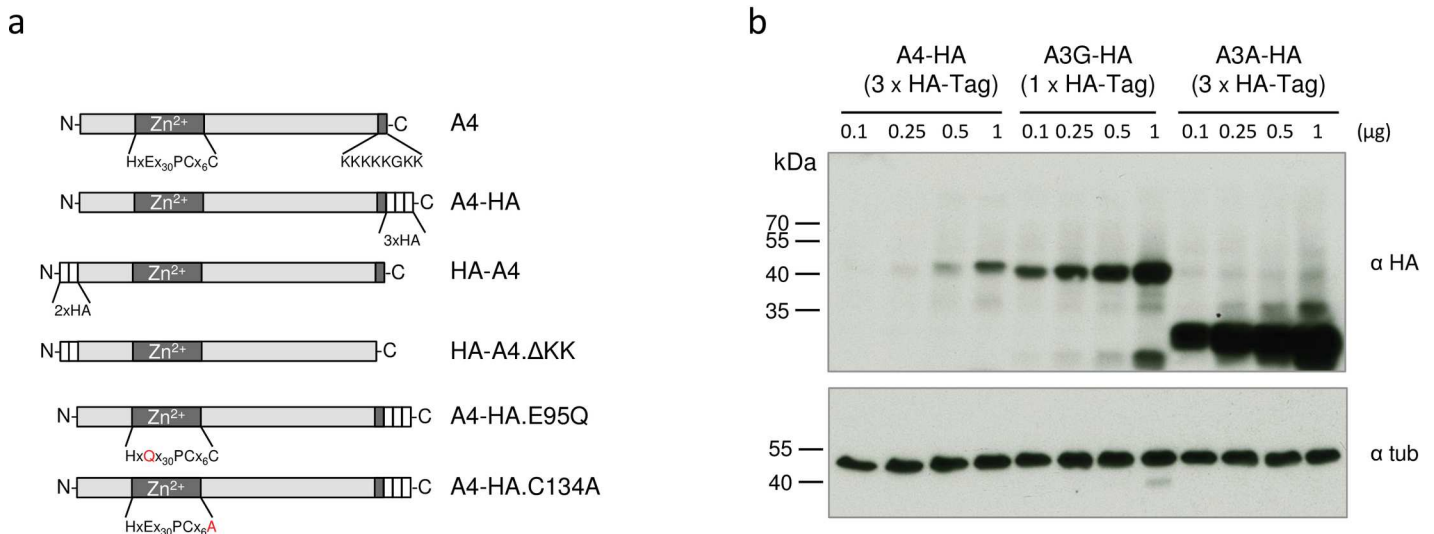


Fig 2. Expression of the A4-HA fusion proteins. (a) Schematic representation of protein domains and motifs found in the human A4 protein and tested variants. Zn²⁺: presumed zinc-binding domain. HA (white boxes): HA-tag. KKKKKKGKK: polylysine domain. (b) Increasing amounts of A4-HA (3xHA-tags), A3G-HA (1xHA-tag) and A3A-HA (3xHA-tags) expression plasmids were transfected into 293T cells followed by immunoblot analysis of the transfected cells using an anti-HA antibody. Immunoblot analysis with anti-tubulin (tub) antibody served as loading control. α, anti.

doi:10.1371/journal.pone.0155422.g002

plasmid (pNL4-3 [56]). The total amount of transfected DNA was kept constant by replacing HA-A4 with the empty expression plasmid (pcDNA3.1zeo). Two days post transfection, we quantified virus production by measuring viral reverse transcriptase (RT) activity in the cell culture supernatant (Fig 4A) and tested the cell lysate for expression of HIV-1 Gag (p24) by immunoblot analysis (Fig 4B). Transfection of incremental amounts of HA-A4 plasmid caused a 2.5-fold increase in the amount of released viral particles as reflected by the RT activity detected in cell culture supernatants. Immunoblot analyses of viral lysates concentrated from the cell culture supernatant also demonstrated the A4 stimulating effect on virus expression (Fig 4B). This positive effect of HA-A4 on late stage HIV-1 particle production was highly reproducible, as demonstrated by data from four independent experiments (Fig 4C). These results were consistent with experimental findings using untagged A4 protein (data not shown).

Production but not infectivity of HIV-1-luciferase is enhanced by A4 expression

We used VSV-G pseudotyped HIV-1 luciferase virus (NL.Luc R^E [57]) to test whether increasing the levels of expressed A4 influences HIV-1 production and infectivity. Co-transfection of A4 expression plasmids (data are shown for A4 and A4-HA plasmids in Fig 5A) and NL-Luc resulted in a dose-dependent increase of intracellular virus-encoded luciferase activity in transfected 293T cells. Presence or absence of the viral Vif protein (using the *vif*-deficient NL.Luc R^EΔ*vif*/VSV-G in the same set of experiments) had no detectable effect on the A4-induced stimulation of NL.Luc (data not shown). Immunoblot analysis of lysates isolated from the transfected cells confirmed the A4 dose-dependent expression of viral capsid p24 (Fig 5B). Fig 5C shows that co-expression of HA-A4 with NL.Luc also caused a similar boost of Gag expression, indicating that the location of the HA tag did not influence virus production enhancement by A4. Results from 28, 16, and seven independent experiments using different amounts of the A4-HA plasmid together with NL.Luc are summarized in Fig 5D, 5E and 5F, respectively. These results confirmed a significant increase in NL-Luc-mediated luciferase

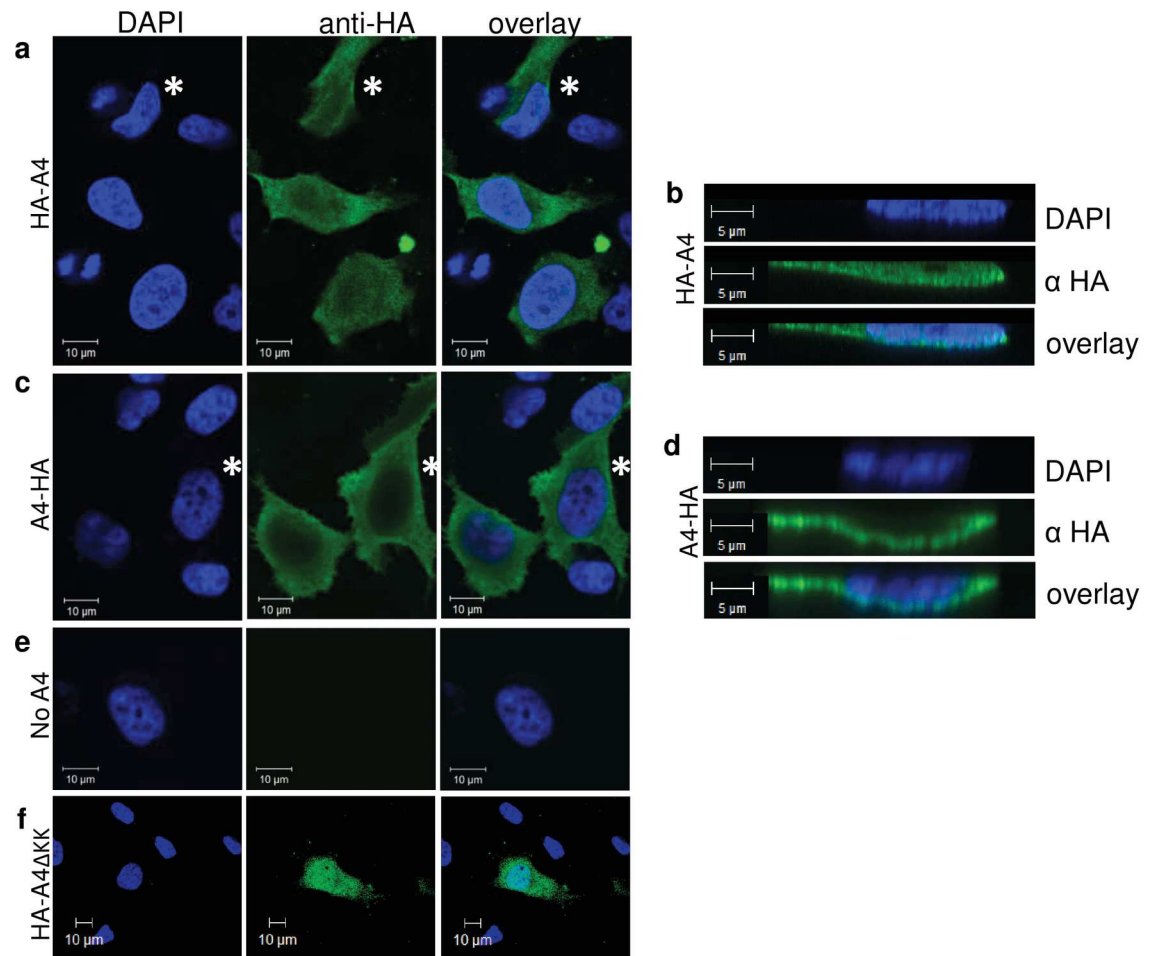


Fig 3. Subcellular localization of A4 in transfected cells. Immunofluorescence confocal laser scanning microscopy images of HeLa cells transfected with N- or C-terminal HA-tagged A4 (HA-A4 and A4-HA). (a, b) HA-A4 proteins show cytoplasmic and nuclear localization. (c, d) A4-HA proteins show cytoplasmic localization. (a, c, e, f) x-y optical sections. (b, d) x-z vertical scanning image of indicated cells (see asterisks). (e) Mock transfected cells (no A4). (f) HA-A4ΔKK transfected cells show cytoplasmic and nuclear localization. To detect A4 (green) immunofluorescence, cells were stained with an anti-HA antibody. Nuclei (blue) were visualized by DAPI staining. α , anti.

doi:10.1371/journal.pone.0155422.g003

activity in the transfected virus producer cells (Fig 5D). When testing equal volumes of cell culture supernatants for the presence of infectious HIV reporter virions, we also detected a dose-dependent increase in luciferase activity in infected cells (Fig 5E). However, when equal concentrations of viral particles normalized for RT activity were used escalating levels of A4-HA did not cause a significant increase in infectivity (Fig 5F). The summarized individual experiments did not always cover all ranges of applied plasmid concentrations (Fig 5D), and single virus samples obtained from a subset of experiments were used to study particle infectivity (Fig 5E and 5F). Taken together, these data indicate that A4 expression enhances the production of HIV-1, but does not change its infectivity.

Stable A4 expression enhances multiple-cycle replication of HIV-1

To test whether A4 can also enhance production of CCR5-tropic HIV-1, we co-transfected the replication competent HIV-1 NL-BaL plasmid [58] with A4 expression plasmid and measured the infectivity of RT value normalized particles using the HIV-reporter cell line TZM-bl [59].

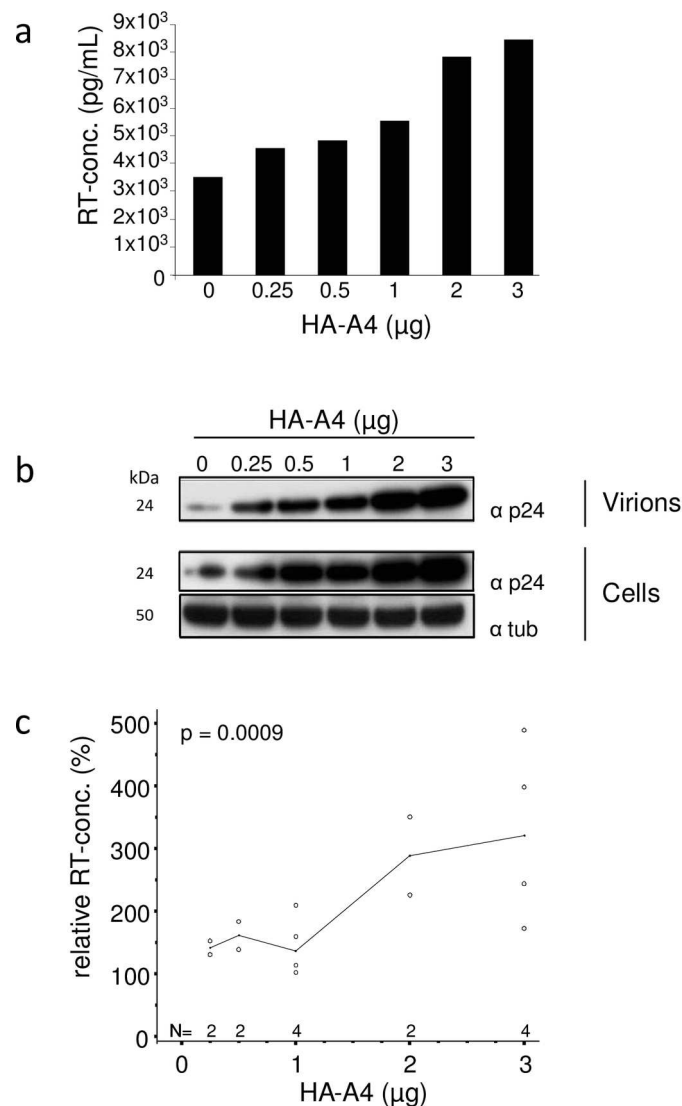


Fig 4. A4 enhances the expression of HIV-1. (a) HIV-1 genome expression plasmid was co-transfected with increasing amounts of HA-A4 expression plasmid, as indicated. A4 increases the production of HIV-1 particles as measured by the RT activity in the supernatant of the transfected cells. (b) Immunoblot analysis of virions and transfected 293T cells (same cells as in (a)). Immunoblots of virions and cell lysates were probed with anti-p24 (capsid) antibody. Anti-tubulin (tub) antibody served as loading control. α, anti. (c) RT concentrations in the supernatant of cells co-transfected with HA-A4 and HIV-1 plasmids relative to supernatant of cells co-transfected with empty vector and HIV-1, as in (a), summary of four independent experiments, median indicated. Evaluation of RT activity data was performed by means of a multifactorial analysis of variance (ANOVA).

doi:10.1371/journal.pone.0155422.g004

The expression of A4-HA resulted in enhanced expression of NL-BaL, as demonstrated by immunoblots probed for viral capsid p24 and Vif proteins (Fig 6A). The viral particles harvested from this experiment demonstrated similar infectivity after normalization for RT activity (Fig 6B).

To analyze whether A4 expression can also enhance spreading replication of HIV-1, we generated a stable A4-HA expressing cell line derived from HOS.CD4.CCR5 cells [60] using a G418-selectable retroviral A4-expressing vector (Fig 7A). As a control, we generated HOS.CD4.CCR5.neo cells transduced with a retroviral vector just encoding the G418-resistance

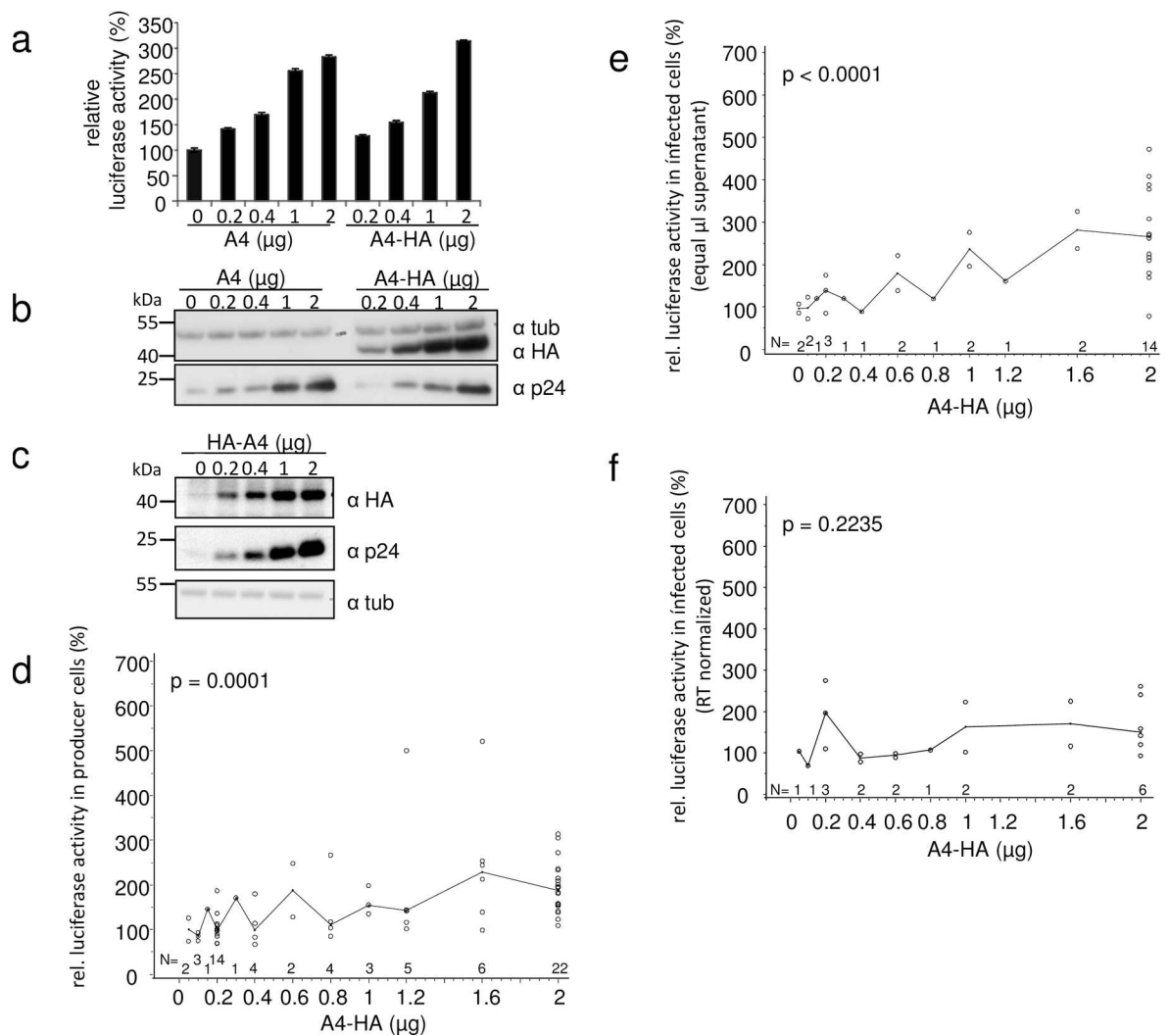


Fig 5. Presence of A4 does not affect HIV-1 infectivity. HIV-1 reporter virus NL-Luc R'E' (VSV-G) was produced in 293T cells in the presence of increasing amounts of A4 (no tag) and A4-HA (C-terminal HA-tag). A4 and A4-HA increase in a dose-dependent manner both (a) the virus-encoded luciferase activity and (b) the expression of intracellular viral capsid (p24) in the transfected virus producing cells as demonstrated by immunoblot analysis (same cell lysates used in (a) and (b)). Error bars indicate standard deviation. (c) Immunoblot analysis of intracellular viral p24 (capsid) expression. Similar as in (a) and (b), NL-Luc R'E'/VSV-G was co-transfected with increasing amounts of HA-A4 plasmid (N-terminal HA-tag), as indicated. Immunoblots of cells were probed with anti-p24 (capsid) antibody. A4-HA expression in transfected cells was detected by immunoblotting using anti-HA antibody. Anti-tubulin (tub) antibody served as loading control. α , anti. (d) Relative viral luciferase activity in cells co-transfected with A4-HA and HIV-1 plasmids, as in (a). Summary of 28 independent experiments, median indicated. A4-HA was transfected in increasing amounts. (e) Equal volumes of supernatants of cells co-transfected with NL-Luc R'E'/VSV-G and increasing amounts of A4-HA were used to infect HOS cells. Intracellular luciferase activities were determined in infected cells; summary of 16 experiments (a subset of the experiments shown in (d)), median is indicated. (f) A subset of samples (seven experiments) used in (e) was quantified for RT concentrations. RT normalized supernatants of cells co-transfected with NL-Luc R'E'/VSV-G and increasing amounts of A4-HA were used to infect HOS cells. Intracellular luciferase activities determined in infected cells, median is indicated. (d–f) Statistical evaluation of reporter luciferase activity data was performed by means of a multifactorial ANOVA.

doi:10.1371/journal.pone.0155422.g005

gene. The cell lines were infected with NL-BaL, and virus spread was monitored for 20 days (Fig 7B). HIV-1 showed comparable overall virus replication kinetics in both cell lines; however, HIV-1 replicated in the A4 expressing cells more efficiently resulting in 2–3 fold increased virus titers. These data are consistent with our finding that A4 stimulated HIV expression in

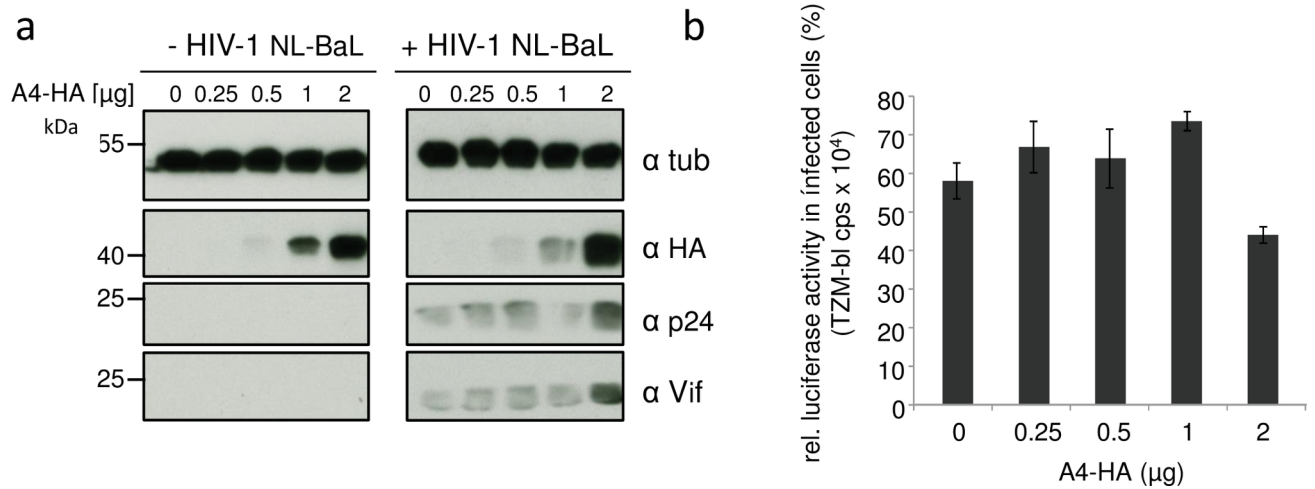


Fig 6. A4 enhances expression of CCR5-tropic HIV-1. (a) Increasing amounts of A4-HA expression plasmid were co-transfected with HIV-1 NL-BaL and immunoblot analysis of co-transfected 293T cells were performed. Immunoblots were probed with anti-p24 (capsid), anti-Vif, anti-HA and anti-tubulin (tub) antibodies. α, anti. (b) Infectivity of RT-normalized viral supernatant of the transfected cells from (a) were used to infect TzM-bl luciferase reporter cells. cps, counts per second. Data are represented as the mean with SD. Statistically significant differences between no A4 and A4 groups were analyzed using the unpaired Student's t-test with GraphPad Prism version 5 (GraphPad software, San Diego, CA, USA). Validity of the null hypothesis was verified with significance level at α value = 0.05. NS: not significant.

doi:10.1371/journal.pone.0155422.g006

the transient transfection experiments, supporting the premise that A4 modulates HIV-1 replication.

HIV enhancement is not mediated by cytidine deamination

To test whether cytidine deamination activity is associated with the described A4 effect, we generated the active site mutants E95Q and C134A, in which the zinc-coordinating motif HxEx₃₀PCx₆C (E95 and C134 underlined, x can be any amino acid) was mutated (Fig 2A). Unexpectedly, only the A4-E95Q construct expressed detectable protein, precluding A4-C134A mutant from functional studies (Fig 8A). To analyze if the active site mutation has

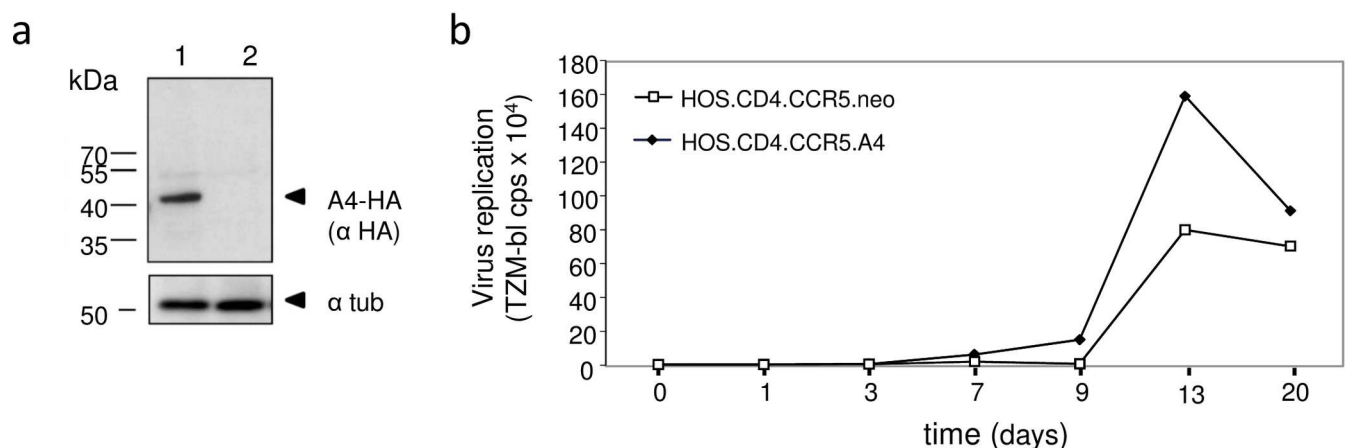


Fig 7. A4 enhances multiple cycle replication of HIV-1. (a) Immunoblot analysis of A4-HA expressing HOS.CD4.CCR5.A4 cells (1) and empty retroviral vector just encoding G418-resistance containing HOS.CD4.CCR5.neo cells (2) using an anti-HA antibody. Cell lysates were also analyzed for equal amounts of total proteins by using anti-tubulin antibody. (b) HOS.CD4.CCR5.A4 and HOS.CD4.CCR5.neo cells were infected with HIV-1 clone NL-BaL, MOI of 0.01. Virus replication was monitored by testing the cell supernatants on TzM-bl cells and measuring luciferase activity.

doi:10.1371/journal.pone.0155422.g007

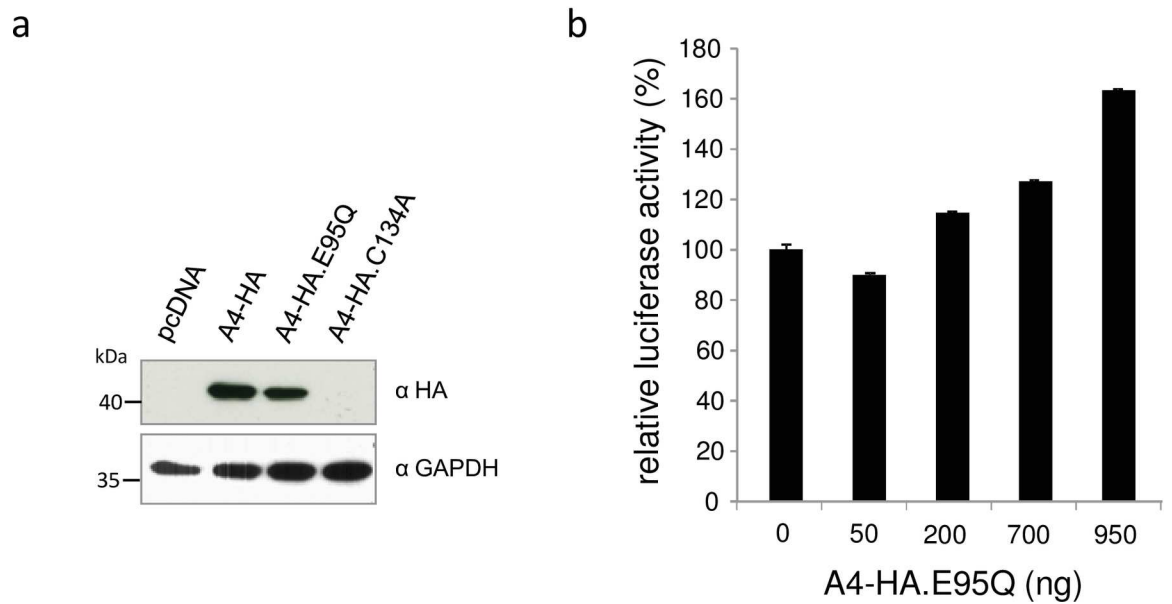


Fig 8. Active site mutation has no influence on A4 activity. (a) Protein expression of A4-HA, A4-HA.E95Q and A4-HA.C134A detected by anti-HA immuno blot analysis, showing equal amounts of A4-HA and A4-HA.E95Q, but lack of A4-HA.C134A expression in transfected cells. (b) HIV-1 reporter virus (NL-Luc R'E') was co-transfected with increasing amounts of expression plasmid for A4-HA.E95Q. Virus encoded luciferase activity in the transfected cells was enhanced by A4-HA.E95Q in a dose-dependent manner.

doi:10.1371/journal.pone.0155422.g008

any effect on virus production, HIV-1 luciferase plasmid (NL-Luc R'E') was co-transfected with increasing amounts of A4-HA.E95Q expression plasmid and luciferase activity was measured in virus producer cells (Fig 8B). 293T cells showed higher virus-encoded luciferase activity after transfection of A4-HA.E95Q in a dose-dependent manner, comparable with the luciferase enhancement after transfection of wildtype A4 (Fig 5A), indicating that cytidine deamination activity of A4 protein is dispensable for the described HIV enhancing effect.

A4 lacks detectable cytidine deaminase activity

To evaluate the cytidine deaminase activity of A4 directly, we performed *in vitro* cytidine deamination assays as described before [61, 62]. We expressed and purified GST-tagged fusion proteins (GST-A3C, GST-A4, GST-A4ΔKK and free GST) from *E. coli* (Fig 9) and used them for activity assays (Fig 10) and DNA binding experiments (Fig 11). In parallel, A3G-His was purified from transfected 293T cells [62] (Fig 9) and used as a positive control for deamination of CCC to CCU. Because the target preference for A4 is not known, we used two different oligonucleotide substrates containing either CCCA/G or TTCA in the central region. If deamination of cytidine to uridine occurred, a 40-nt DNA product is generated after restriction enzyme cleavage and detectable after separation of the digested substrate on a polyacrylamide gel. This method demonstrated cytidine deamination of CCC oligonucleotide substrates by A3G-His protein but not by GST-A4 (Fig 10A and 10B). Since *E. coli*-derived GST-proteins might not be optimally folded and may differ in deamination activity or DNA binding due to the GST-tag, we additionally tested APOBEC proteins encapsidated in virions, protein lysates of transfected 293T cells or APOBEC proteins immunoprecipitated from transfected cells (Fig 10C and 10E) for their deamination activity (Fig 10D and 10F). We performed *in vitro* editing experiments with HA-tagged A4, A4-ΔKK, A3F and A3G. In contrast to A3 proteins, A4 were not detected in HIV-1 particles (Fig 10C). Similarly, only minor amounts of 3xHA-A4 were detectable in

lysate of transfected 293T cells, but this could be enhanced by immunoprecipitation with HA affinity beads (Fig 10E). We saw deamination of CCC to CCU and TTC to TTU only by A3G and A3F, respectively. A4 did not deaminate in any of the above experiments irrespective of its protein source, tags or target DNA (Fig 10D and 10F).

A4 weakly interacts with single stranded DNA

For A3 proteins such as A3G, interaction with single-stranded DNA (ss-DNA) and the formation of multiple DNA-protein complexes was shown [61, 63, 64]. We purified GST, GST-A4 and as a control, GST-A3C from *E. coli* to characterize whether GST-A4 interacts with ss-DNA. Electrophoretic mobility shift assays (EMSA) were carried out with a biotinylated end-labelled 30 nt DNA oligo (TTCA). GST as a background control protein did not cause any characteristic shift. GST-A3C formed complex I, but a greater proportion shifted on the top of the blot (complex II) at the highest protein concentration (1 μM) (Fig 11A). However, the addition of detergent NP-40 aided to form the stable complex I at 10 nM GST-A3C and complex II at higher protein concentrations, suggesting a strong GST-A3C interaction with DNA. Importantly, the GST moiety did not affect the binding (Fig 11A). GST-A4 did not cause a shift at low protein concentration like A3C or A3G [64], but at the highest amount of protein used (500–1000 nM) a minor proportion of complex I was formed. All the DNA-protein complexes in the EMSA were disrupted by adding the 80 nt unlabeled competitive DNA in 200-fold molar excess. In contrast, GST-A4ΔKK failed to form any complexes (Fig 11B).

Crosslinking DNA-A3G studies previously showed that the deamination activity on ss-DNA was facilitated when A3G formed dimers and tetramers [65]. These observations suggested analyzing the capacity of A4 to form dimers. To demonstrate that A4 protein multimerizes in human cells, cleared cell lysate was incubated with different concentrations of the cross linking reagent disuccinimidyl suberate (DSS). Immunoblot analysis of cross-linked samples dose-dependently revealed the existence of A4 running at the molecular weight expected for dimers, indicating that primary amines which can be crosslinked with DSS are present within the A4 dimerization interface (Fig 11C).

A4 enhances expression of HIV-1 LTR and other promoters

To test whether A4 enhances specifically HIV-1 production, we performed comparative expression analysis of HIV-1 LTR and other viral and cellular promoters with and without A4

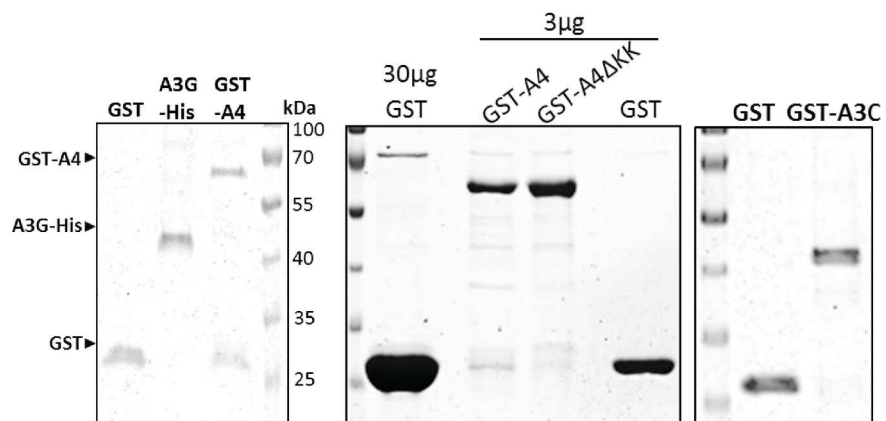


Fig 9. Recombinantly produced and affinity purified *E. coli*-derived GST, GST-A3C, GST-A4, GST-A4-ΔKK proteins and 293T cell-derived A3G-His protein were resolved on a 10% SDS gel. Purity of the proteins was determined by staining the gel with Coomassie blue. GST-A4, A3G-His and GST proteins are indicated according to their molecular mass.

doi:10.1371/journal.pone.0155422.g009

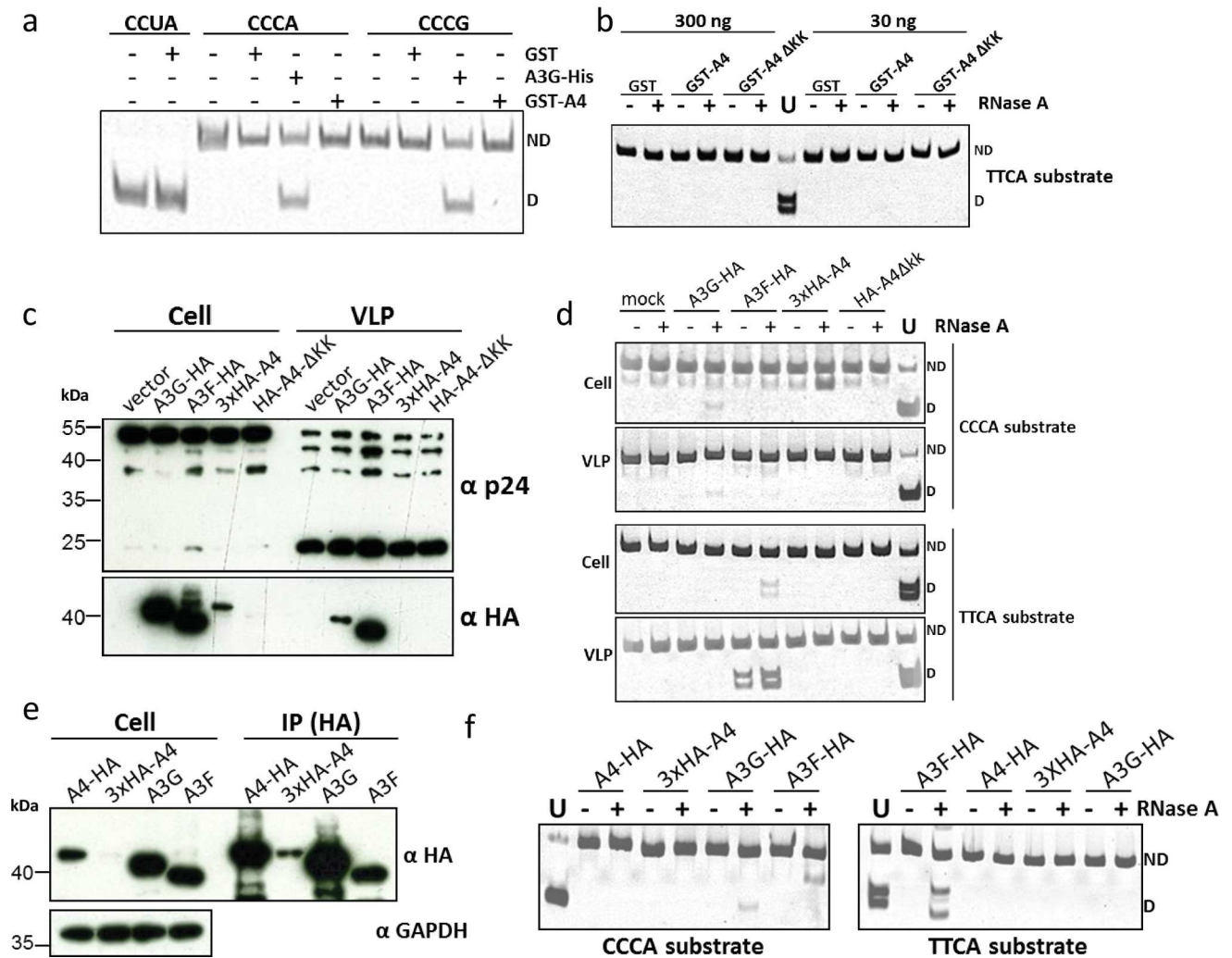


Fig 10. A4 does not deaminate single stranded DNA. (a) Deamination activity of A4 was tested on two different oligonucleotide substrates containing nucleotide sequences CCCA or CCG. The A3G-His fusion protein was incubated with CCCA and CCG containing substrates and served as positive control for deamination resulting in 40-bp DNA fragments. Oligonucleotide CUA served as a marker to denote the deaminated product after Eco1471 cleavage; ND: not deaminated; D: deaminated. (b) Deamination experiment using TTCA containing oligonucleotide and GST-purified A4 proteins, RNase A treatment was included; ND: not deaminated; D: deaminated. (c) Immuno blot analysis of cell lysates and virus lysate of A3G-HA, A3F-HA, 3xHA-A4 and HA-A4-ΔKK expressing cells and HIV virus like particles (VLP), respectively. Anti-HA staining indicates the presence of HA-tagged A3 and A4 proteins, while anti-p24 antibody detects HIV-1 capsid proteins. (d) Deamination assay using transfected 293T cell lysate (from experiment shown in (c)). RNase A treatment was included; ND: not deaminated; D: deaminated. (e) Immuno blot analysis of cell lysate and immunoprecipitate (IP) fraction of A3 and A4 proteins. (f) Deamination assay using the immunoprecipitated APOBEC proteins (from experiment shown in (e)). RNase A treatment was included; ND: not deaminated; D: deaminated.

doi:10.1371/journal.pone.0155422.g010

in the same cell. To this end, we co-transfected the NL-Luc plasmid expressing the firefly luciferase gene which is located in the *nef* gene together with the Herpes simplex virus (HSV) thymidine kinase (TK) promoter-driven *Renilla* luciferase (HSV-RLuc) reporter plasmid and different amounts of A4-HA expression plasmids. Both luciferases were measured sequentially from single samples. The results revealed an A4 dose-dependent increase in both luciferase activities (up to 2.5-fold for NL-Luc expression and up to 1.5-fold for the HSV driven luciferase) (Fig 12A). To test whether A4 affects HIV expression by acting on the viral LTR, luciferase reporter constructs with the HIV-1 LTR (LTR-Luc, firefly luciferase) and HSV-RLuc were co-

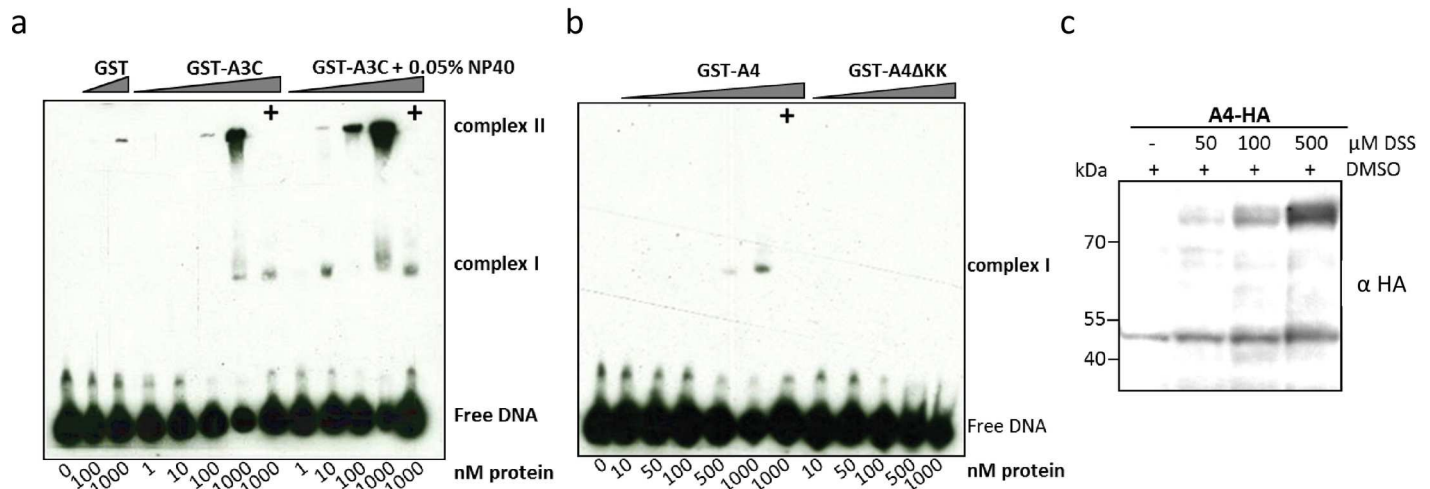


Fig 11. A4 interacts weakly with single-stranded DNA. EMSA with purified, GST-A3C (a), GST-A4 and GST-A4ΔKK (b) performed with 30 nt single stranded target DNA labeled with 3'-labeled with biotin. Indicated amounts of protein (at the bottom of blot) were titrated with 10 nM of DNA. (+) indicates presence of competitor DNA, which is unlabeled 80 nt DNA (200-fold molar excess), as used for deamination assay to demonstrate specific binding of protein to DNA being causative for the shift. For GST-A3C (a) a separate panel was added for reactions containing 0.05% NP-40 detergent. (c) A4-HA crosslinking by DSS. DSS was added to the cleared cell lysates to reach the indicated DSS concentrations. The blot was probed with anti HA antibody to detect monomeric and dimeric forms of A4-HA.

doi:10.1371/journal.pone.0155422.g011

transfected with increasing amounts of A4-HA expression plasmid with or without addition of an HIV-1 Tat expression plasmid. As expected, the presence of Tat enhanced the expression of the LTR-Luc construct (by 19-fold) relative to LTR-Luc expression in the absence of the Tat plasmid (Fig 12B). A4 expression in the absence of Tat stimulated the LTR-Luc expression by up to 2.6-fold and by up to 1.6-fold in the presence of Tat. The thymidine kinase promoter of HSV was not sensitive to the presence of Tat. In contrast, A4 enhanced the HSV-RLuc expression by up to 2.8-fold when Tat was not co-transfected. In the next experiment, we tested firefly luciferase expression constructs driven by promoters of HSV-TK, LINE1 (P850 L1), probasin, or prostate-specific antigen (PSA), together with NL-Luc. Co-transfection with 2 μg A4-HA expression plasmid enhanced the luciferase activity of all these constructs from 3.5-fold to 5-fold, whereas HIV-LTR expression was enhanced by 7-fold (Fig 12C). Based on these results, we conclude that A4 might directly or indirectly enhance the transcription of HIV and other promoters.

Discussion

Herein we report the first study addressing the potential function of the A4 protein in human cells. A4 is the most recently identified and the least studied APOBEC protein [3, 52]. It is more closely related to A1 than to the A3 proteins [3]. Knowledge about the A4 protein is very limited; it is unknown if A4 binds to RNA or DNA or possesses any enzymatic activity, and no biochemical and structural information about A4 is available to date. Our data show for the first time biological activity of A4, which enhances the expression of HIV-1.

As part of this study, we established mammalian expression plasmids for A4 and we also generated bacterially expressed GST-A4 fusion proteins to test for their enzymatic activity. Under experimental conditions that readily detect cytidine deamination by A3G, purified GST-A4 did not carry out any detectable cytidine deamination. We also tested A4 isolated from transfected human cells and similarly found no cytidine deamination activity. These findings are in agreement with the previously reported absence of cytidine deamination of A4 using a cellular mutation assay in bacteria and yeast [52]. In addition, we found that mutating

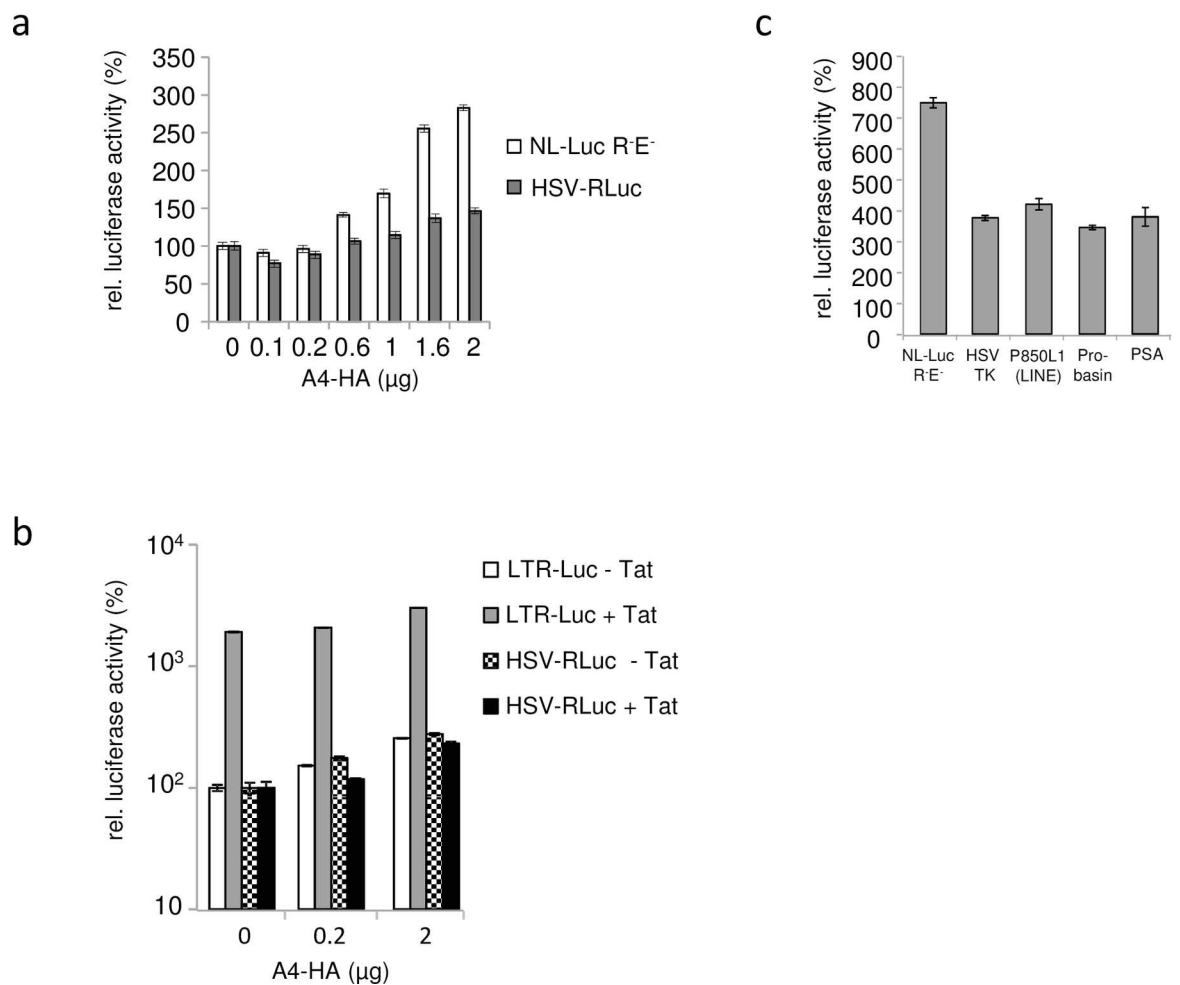


Fig 12. A4 enhances expression of luciferase reporter genes driven by various viral and cellular promoters. (a) Dual luciferase reporter assay was performed two days post co-transfection of NL-Luc R'E⁻ and HSV-TK promoter *Renilla* luciferase (HSV-RLuc) with and without A4-HA, relative luciferase activities are shown. (0) indicates transfections in the absence of A4-HA plasmid. A4-HA was transfected in increasing amounts. (b) Relative luciferase activities after co-transfection of LTR-Luc (LTR of HIV-1 driving firefly luciferase) with A4-HA or HSV-TK promoter *Renilla* luciferase (HSV-RLuc) with A4-HA and with and without Tat expression plasmid (c) Luciferase activities driven by various viral (LTR, HSV TK) or cellular promoters (LINE, Probasin, PSA) in presence of the transfected A4-HA expression plasmid, relative to luciferase activity in cells without A4 expression. Total amounts of luciferase expression plasmid and total plasmid DNA was kept constant within all experiments. Error bars indicate standard deviation.

doi:10.1371/journal.pone.0155422.g012

the zinc-coordinating domain of A4 did not abolish the HIV-enhancing activity of A4. Nevertheless, these observations do not mean that A4 is catalytically inactive, A4 may just have different substrate specificity and cytidine deamination may not be the A4 function required for enhancement of HIV expression.

The deamination activity of A3 proteins such as A3G on ss-DNA is facilitated by A3G dimers and tetramers [65]. A4 formed at least dimers, but did weakly bind to ss-DNA only. This weak DNA binding was lost, if the characteristic polylysine stretch (KKKKKGKK) at the C-terminus of A4 was deleted (A4ΔKK), supporting the hypothesis that the net positive charge rendered by polylysines confer some capacity to interact with DNA [66]. Thus, the weak interaction of A4 with ss-DNA may be one reason for the lack of detectable deamination.

We speculated that the polylysine domain would be involved in nuclear localization of A4 and that a C-terminal HA-tag would obstruct this activity, because A4 with an N-terminal

HA-tag (HA-A4) localized to both cytoplasm and nucleus of transfected cells, while A4-HA with a C-terminal HA-tag was detected only in the cytoplasm. However, HA-A4ΔKK also localized to both compartments, cytoplasm and nucleus, suggesting that the polylysine domain is not important for nuclear localization. C-terminal stretches of lysines are also found in other proteins unrelated to A4 e.g. in the GTPase KRas (KRAS, K-Ras4B, NP_004976) and FAM133B (NP_001035146). In KRas, the polylysine region (KKKKKKSK) contributes to the interaction of KRas with Ca²⁺/calmodulin and strongly influences its binding to the plasma membrane by electrostatic interactions with the membrane anionic lipids [67, 68]. Whether A4 specifically interacts with membranes or Ca²⁺/calmodulin is not known.

We demonstrated that A4 mRNA is highly expressed in human testis, but is barely detectable in 293T, HeLa, A3.01 T and Jurkat T cell lines. Analysis of protein expression of endogenous A4 was precluded, due to the non-availability of any A4-specific antibody. In light of the sexual transmission of HIV-1 and the possibility of sanctuary sites for HIV-1 in the male genital tract, the origin of seminal HIV-1 is a topic of ongoing discussion [69–76]. Human testicular tissue is described to be susceptible to HIV-1 [69, 72, 77–80] and macaque testis and epididymis are found to be infected by SIV in several studies [70, 73, 76, 81, 82]. Since we do not know whether CD4⁺ cells in testis express A4, we cannot make a statement concerning modulation of HIV infection in testis by A4. A4 also enhanced the expression of firefly luciferase which is controlled by the HIV-1 LTR in a manner similar to that of the unrelated HSV promoter driven *Renilla* luciferase and A4 expression increased the expression of luciferase constructs driven by cellular promoters. However, our results do not clearly demonstrate that A4 is a factor that enhances LTR-mediated transcription. Indeed, it is thus likely that HIV benefits from a broad activity of A4. We hypothesize that A4 creates a cellular/nuclear environment that stimulates for example the expression of HIV-1. A4 may boost expression or activity of a factor important for HIV or reduce the expression or activity of a negative regulator of HIV. It is very well possible that the observed enhancing activity of A4 to HIV is relevant for the expression of cellular promoters and endogenous retroviruses in testis [83]. Future studies investigating the interactome of A4 may help to reveal the A4 pathway and its enhancing activity.

Material and Methods

Plasmids

pA4-HA (pA4-3xHA) expresses APOBEC4 (A4, GenBank NM_203454.2) fused to three C-terminal HA-tags; pMH-A4_3xHA (obtained from Matthias Hamdorf) was used to excise A4-3xHA using EcoRI x NotI, cloned into EcoRI / NotI of pcDNA3.1zeo(+) (Life Technologies, Darmstadt, Germany). pA4-HA-E95Q was generated by site-directed mutagenesis of the pA4-HA plasmid, the mutation was confirmed by sequencing. pA4 expresses A4 without an epitope tag. pA4 was cloned by PCR (pA4-HA as template) using primers hA4 5' (5'-CGGATCCCTAGCAATGGAGCCCATATATG) and hA4 3' (5'-GAATTCCTTTATTTCTTCCCTTTCCTTCTTCTTC), the PCR product was cloned via BamHI / EcoRI into pcDNA3.1zeo(+). HA-A4 (p2xHA-A4): expresses A4 with two N-terminal HA-tags, a pcDNA3.1zeo(+)-based plasmid with one N-terminal HA-tag of A4 was generated by PCR using primers HA-hA4 5' (5'-CGGATCCCTAGCAATGGGATATCCATACGATGTTCCAGATTACGCTGAGCCCATATATGAGGAGTACC) and hA4 3' (5'-GAATTCCTTTATTTCTTCCCTTTCCTTCTTCTTCTTC); this plasmid served as template for a second PCR using primers for_2xHA-A4 (5'-CGGGATCCCTAGCAATGGGATATCCATACGATGTTCCAGATTACGCTGGCTATCCATACGATGTTCCAGATTACGCTGGCTATCCATACGATGTTCCAGATTACGCT) and rev rc_hA4 (5'-GCCGGAATTCTTATTTCTTCCCTTTCCTTCTTCTTCTTC). The product was cloned via

BamHI / EcoRI into pcDNA3.1zeo(+). pGST-A4: A4 with an N-terminal GST-tag in pGEX-6-P1 (GE Healthcare, Munich, Germany), A4 was cloned via BamHI / EcoRI by excising A4 from pA4. Similarly pGST-A4-ΔKK was cloned in pGEX-6-P1 (GE Healthcare, Freiburg, Germany) using forward primer 5'-ATCGGATCCATGGAGCCCATATATGAGGAG and reverse primer 5'-CGGCGAATTCTTATTCATCTGCCTCCTTGCTACT. pMSCV.A4: a murine leukemia virus-based vector to express A4 fused with three C-terminal HA-tags; it was cloned by PCR using template pA4-3xHA and primers A4_fw_RI (5'-TGGAATTCGCCCTT CAGGCGGTACCAGCCTGGAGACAAATTGATG) and A4_rv_RI (5'-TAGAATTCTCAGT TAGCCGGCGTAG) via EcoRI into pMSCV.neo (Clonetech, Takara Bio Europe/SAS, Saint-Germain-en-Laye, France). pLTR-Luc (pGL3-bas-NL43LTR-luc): containing the LTR region of HIV-1 pNL4-3, cloned by PCR of U3, R, and TAR elements using primers NL4-3-U3(+) (5'-CTCGGCAGATCTCTGGAAGGGCTAATTCCTCC) and U3/R/TAR(-) (5'-GCTCGG AAGCTTGGCTTAAGCAGTGGGTTCCCTAG); amplicons were cloned via HindIII and BglII (partial digest) into pGL3-Basic (Promega, Mannheim, Germany). P850 luciferase plasmid with LINE Promotor (P850 L1) [84] and reporter constructs with androgen responsive promoters probasin (pGL3Eprob) and PSA (pPSA61-luc) [85] were kindly provided by Wolfgang A. Schulz. APOBEC3G (A3G)-HA expression construct was kindly provided by Nathaniel R. Landau [17]. His-tagged huA3G (A3G-Myc-6His) has been described previously [86]. APOBEC3A (A3A)-HA expression plasmid was obtained from Bryan R. Cullen [87]. pTat (pBS-KRSPA-Tat NL4-3), expressing Tat protein of HIV-1 NL4-3 was a gift of Heide Muckenfuss and Egbert Flory. For cloning of pTat, both Tat exons were amplified and fused by PCR using pNL4-3 [56] as template, and cloned into XhoI / SpeI of pBS-kRSPA [88]. pHSV-RLuc (pRG-TK, Promega), *Renilla reniformes* luciferase expressed by the *Herpes simplex virus type 1* thymidine kinase promoter.

Cells, transfections and infections

HOS (ATCC CRL-1543), HOS.CD4.CCR5 [60], HeLa (ATCC CCL-2), TZM-bl [59] and 293T (ATCC CRL-3216) cells, were maintained in Dulbecco's modified Eagle's medium complete (PAN-Biotech, Aidenbach, Germany); A3.01 T cells [89] and Jurkat T cells clone E61 (ATCC TIB152) were cultured in Roswell Park Memorial Institute (RPMI) 1640 medium (PAN-Biotech) supplemented with 10% FBS, 0.29 mg/ml L-glutamine, and 100 U/ml penicillin/streptomycin at 37°C in a humidified atmosphere of 5% CO₂. Plasmid transfections into 293T cells were performed with Lipofectamine LTX (Life technologies). HIV-1 and reporter lentiviruses were generated by transfection in 6-well plates with 200 ng pNL.Luc R⁻E⁻ (pNL4-3.Luc.R⁻E⁻) [57] plus 50 ng vesicular stomatitis virus G glycoprotein (VSV-G) expression plasmid pMD.G or with 1 μg pNL4-3 [56] and different amounts of A4 expression plasmid. Total transfected plasmid DNA was maintained by adding appropriate amounts of pcDNA3.1zeo(+) plasmid DNA where needed. To produce NL4.3 with the *env* BaL, pNL-BaL [58] was transfected in 293T cells. Reverse-transcriptase (RT) activity was determined using the Cavidis HS kit Lenti RT (Cavidis Tech, Uppsala, Sweden). For infectivity assays, 4x10³ HOS cells were transduced in 96-well plates in triplicate with a virus amount equivalent to 10 pg of RT for HIV. Three days post infection, luciferase activity was measured using the Steadylite HTS kit (PerkinElmer, Rodgau, Germany). To quantify firefly and *Renilla* luciferase in the same cell lysate, the dual-Luciferase reporter assay (Promega) was applied. All luciferase assays in transfected cells were performed two days post transfection. To generate stable A4-expressing HOS.CD4.CCR5.A4 and control HOS.CD4.CCR5.neo cells, pMSCV.A4 or pMSCV.neo plasmid was co-transfected together with pHIT60 [90] and pMD.G for generation of murine leukemia viral vector particles. Vector particles were used to transduce HOS.CD4.CCR5 cells; G418 resistant cells were

pooled and characterized for CD4 and CCR5 receptor and A4 expression. Spreading virus replication with NL-BaL was quantified over 20 days infecting HOS.CD4.CCR5.neo or HOS.CD4.CCR5.A4 cells using a multiplicity of infection of 0.01 and testing the culture supernatants with the HIV reporter cell line TZM-bl [59]. Transfection efficiency was monitored by cotransfection of 100 ng Monster Green fluorescent protein expression plasmid hMGFP (Promega).

Immunoblot analysis

Cells were lysed in radioimmunoprecipitation assay buffer (RIPA, (25 mM Tris (pH 8.0), 137 mM NaCl, 1% glycerol, 0.1% SDS, 0.5% Na-deoxycholat, 1% Nonidet P-40, 2 mM EDTA, and protease inhibitor cocktail set III [Calbiochem, Darmstadt, Germany].) buffer, 20 min on ice. Lysates were clarified by centrifugation (10 min, 300 g, 4°C). Samples were boiled in NuPAGE SDS Sample Buffer and NuPAGE Sample Reducing Agent (Life technologies) and subjected to SDS-PAGE followed by transfer to a PVDF membrane. A3G and A4 Proteins were detected using an anti-HA antibody (Ab) (1:10⁴ dilution, MMS-101P; Covance, BioLegend, Fell, Germany), HIV-1 p24 Gag was detected applying HIV-1 p24 monoclonal Ab (1:250 dilution, AG3.0, NIH AIDS REAGENTS, Germantown, USA) [91]. Cell lysates were probed with α -tubulin Ab (1:10⁴ dilution, B5-1-2; Sigma-Aldrich, Munich, Germany) and virions with α -p24 monoclonal Ab 183-H12-5C. Vif protein was detected with HIV-1 Vif monoclonal antibody (1:5x10³ dilution, #319, NIH AIDS REAGENTS) [92]. Secondary Abs.: anti-mouse (NA931V) and anti-rabbit (NA934V) horseradish peroxidase (1:10⁴ dilution, GE Healthcare). Signals were visualized using ECL reagent (GE Healthcare).

Chemical cross linking

293T cells were transfected with pA4-HA and lysed two days after transfection with RIPA buffer. Soluble fraction was clarified by centrifugation at 13,000 rpm and 4°C. To chemically cross link the amines of the protein, the lysate was treated with various concentrations of disuccinimidyl suberate (DSS) (Thermo Scientific, Braunschweig, Germany) dissolved in DMSO to make a final concentration of 50, 100 and 500 μ M and the reaction mixture was incubated for 20 min on ice. To quench the reaction, 20 mM of Tris (final concentration) was added and lysates were subjected to immunoblot analysis without addition of reducing reagent. The presence of A4 monomers and dimers were detected by anti HA antibody.

PCR

Total RNA was isolated using RNeasy mini kit (Qiagen, Hilden, Germany). Human testis RNA (DNase free, HR-401) was obtained from Zyagen (San Diego, USA). RNA was reverse transcribed with QuantiTect Reverse Transcription (Qiagen). Semi-quantitative PCR analyses of A4 mRNA: The A4 fragments were amplified from cDNA by Dream-Taq polymerase (Thermo Scientific) and the primers Origene_for (5'-CAAGCCTGGAGACAAATTGATGG) x Origene_rev (5'-GCAATCGAGAGAGAAGCTTAGCC). As a control, β -2-microglobulin cDNA was amplified in the same PCR reaction applying primer β -2-Mikroglobulin A_for (5'-CTCGCTCCGTGGCCTTAGCTGTGCTCGCGC) x β -2-Mikroglobulin A_rev (5'-TAACTTATGCACGCTTA ACTATC): Initial denaturation at 95°C for 5 min followed by 39 cycles of 95°C for 1 min, 56°C for 1 min, 72°C for 1 min and final extension 72°C for 15 min. Water instead of template served as a background control and a plasmid coding for A4 cDNA (pA4 cDNA) served as a positive control. The identity of the PCR fragments was confirmed by cloning and sequencing. Quantitative real-time PCR analyses of A4 mRNA: The A4 fragments were amplified from cDNA using SYBR green PCR Master Mix (Applied Biosystems, Warrington, United Kingdom) with an Applied Biosystems 7500 Real-Time PCR system (Applied Biosystems,

Foster City, CA) and primers: A4_909_for (5'-ACCAATGCATATGGGCCAAA) x A4_906_rev rc (5'-GTGCCTTACGATATTCCTGGGT). After initial incubations at 50°C for 2 min and 95°C for 10 min, 40 cycles of amplification were carried out for 15 s at 95°C, followed by 1 min at 60°C. The amplification product was normalized to that of HPRT1 using PCR Primers HPRT1_for (5'-GCTTTCCTTGGTACAGGCAGT) x HPRT1_rev rc (5'-GCTTGCGACCTTGACCATCT).

Purification of A3 and A4 proteins from *E. coli* and 293T cells

A3G-His was expressed in 293T cells and purified by immobilized metal affinity chromatography (IMAC) using Ni-nitrilotriacetic acid (Ni-NTA) agarose (Life Technologies) as described [62]. GST-A3C, GST-A4, GST-A4ΔKK and GST proteins were overexpressed in *E. coli* Rosetta (DE3) cells (Millipore, Merck Chemicals, Darmstadt, Germany) and purified by affinity chromatography using Glutathione Sepharose 4B beads (GE healthcare). After the growth of transformants containing pGEX4T2-GST-A4 until 0.6 OD₆₀₀, cells were induced with 1 mM isopropyl-beta-D-thiogalactopyranoside (IPTG) and 1 μM ZnSO₄ and cultured at 18°C overnight. A4 harboring cells were washed with PBS and lysed with 1X Bug buster protein extraction reagent (Millipore) containing 50 mM Tris (pH 7.0), 10% glycerol, 1 M NaCl and 5 mM 2-mercaptoethanol (2-ME), clarified by centrifugation (14,800 rpm for 20 min at 4°C) and the soluble fraction was mixed with glutathione sepharose beads. After 3 h incubation at 4°C in end-over-end rotation, the beads were washed twice with wash buffer containing 50 mM Tris (pH 8.0), 5 mM 2-ME, 10% glycerol and 500 mM NaCl. The bound GST-A4 protein was eluted with wash buffer containing 20 mM reduced glutathione. Purified protein concentration was determined spectrophotometrically by measuring the A₂₈₀, using their (theoretical) extinction coefficient and molecular mass.

In vitro DNA cytidine deamination assay

Deamination reactions were performed as described [61, 62] in a 10 μL reaction volume containing 25 mM Tris pH 7.0, and 100 fmol single stranded DNA substrate (CCCA: 5'-GGATTGTTGGTTATTTGTTAAGGAAGGTGGATTAAGGCCCAAGAAGGTGATGGAAGTTATGTTTGGTAGATTGATGG; CCCG: 5'-GGATTGGTTGGTTATTTGTTAAGGAAGGTGATTAAGGCCCAAGAAGGTGATGGAAGTTATGTTTGGTAGATTGATGG and TTCA: 5'-GGATTGGTTGGTTATTTGTATAAGGAAGGTGGATTGAAGGTTCAAGAAGGTGATGGAAGTTATGTTTGGTAGATTGATGG). Samples were splitted into two halves; in one half 50 μg/ml RNase A (Thermo Scientific) was added. Reactions were incubated for at least 1 h at 37°C and the reaction was terminated by boiling at 95°C for 5 min. One fmol of the reaction mixture was used for PCR amplification (Dream Taq polymerase (Thermo Scientific) 95°C for 3 min, followed by 19 cycles of 61°C for 30 sec and 94°C for 30 sec) and the primers forward 5'-GGATTGGTTGGTTATTTGTTAAGGA, reverse 5'-CCATCAATCTACCAAACATAACTTCCA used to amplify CCC(A/G) substrate, forward primer 5'-GGATTGGTTGGTTATTTGTATAAGGA with the above reverse primer used for TTCA. PCR products of CCC(A/G) and TTCA were digested with Eco147I (StuI) (Thermo Scientific) and MseI (NEB, Frankfurt/Main, Germany), respectively, resolved on 15% PAGE, stained with ethidium bromide (5 μg/ml). As a positive control substrate oligonucleotides with CUA and TUA instead of respective CCCA and TTCA were used to control the restriction enzyme digestion.

APOBEC incorporation into HIV-1: HIV-1 vectors were produced with 250 ng A3 plasmids and 1000 ng A4 constructs. 48 h later virion containing supernatants were concentrated by layering on 20% sucrose cushion and centrifuged for 4 h at 14,800 rpm. Viral particles were re-suspended in mild lysis buffer (50 mM Tris (pH 8), 1 mM PMSF, 10% glycerol, 0.8% NP-40,

150 mM NaCl and 1X complete protease inhibitor) and used as input for the *in vitro* deamination assay.

Deamination assay using immunoprecipitated protein from 293T cells: 293T cells were transfected with expression plasmids encoding A4-HA, 3xHA-A4, A3G-HA or A3F-HA. Cells were lysed 48 h post transfection with mild lysis buffer (50 mM Tris (pH 8.0), 1 mM PMSF, 10% glycerol, 0.8% NP-40, 150 mM NaCl and protease inhibitor (protease inhibitor cocktail set III, Calbiochem). HA-tagged proteins were immunoprecipitated using 20 μ l of anti-HA Affinity Matrix Beads (Roche Diagnostics, Mannheim, Germany) by slowly rotating the lysate bead mixture for 2 h at 4°C. One third of the beads were used for deamination assay and the remaining was used for immunoblot analysis.

Electrophoretic mobility shift assay (EMSA) with GST-A3C and GST-A4

EMSA method is adapted from [63, 64]. Proteins were produced as described above, kept in protein buffer (final concentration 50 mM Tris (pH 8.0), 50 mM NaCl, and 10% glycerol). 10 mM 3' biotinylated DNA (30-TTC-Bio-TEG purchased from Eurofins Genomics, Ebersberg Germany) was mixed with 10 mM Tris (pH 7.5), 100 mM KCl, 10 mM MgCl₂, 1 mM DTT, 2% glycerol, and desired amount of recombinant proteins in a 10 μ l reaction mixture, and incubated at 25°C for 30 min. The protein-DNA complex was resolved on a 5% native PAGE gel on ice, and then transferred onto nylon membrane (Amersham Hybond-XL, GE healthcare) by southern blot. After transfer, the molecules on the membrane were crosslinked by UV-radiation using a transilluminator at 312 nm for 15 min. Chemiluminescent detection of biotinylated DNA was carried out according to the manufacturer's instruction (Thermo scientific).

Confocal microscopy

1 x 10⁵ HeLa cells grown on coverslips (Marienfeld, Lauda Königshofen, Germany) were transfected with 500 ng A4 expression plasmids by applying Lipofectamine LTX transfection reagent. At day two post transfection, cells were fixed in 4% paraformaldehyde in PBS for 30 min, permeabilized in 0.1% Triton X-100 in PBS for 45 min, incubated in blocking solution (10% donkey antiserum (Sigma-Aldrich) in PBS) for 1 h, and treated with anti-HA Ab (MMS-101P; Covance) in blocking solution for 1 h. Donkey anti-mouse Alexa Fluor 488 (Life Technologies) was used as secondary Ab in a 1:300 dilution in blocking solution for 1 h. Finally, nuclei were stained using DAPI (4', 6'-diamidino-2-phenylindole; 1:1000 in PBS) (Merck Millipore, Darmstadt, Germany) for 5 min. Coverslips were mounted on glass microscope slide (Marienfeld) using Fluorescent Mounting Medium (DAKO, Hamburg, Germany). The images were captured by using a 63x objective on a Zeiss LSM 510 Meta laser scanning confocal microscope. x-z optical sections were acquired from 0.28 μ m layers.

Statistics

Evaluation of RT or reporter activity data was performed by means of a multifactorial analysis of variance (ANOVA) with fixed factor *plasmid ratio*. Additionally a random factor *day* was included, if more than one determination were obtained from one day in order to model day-to-day variability. The statistical analysis was performed with SAS/STAT software, version 9.3, SAS System for Windows (Cary, USA).

Acknowledgments

We thank Wioletta Hörschken for excellent technical assistance, Jan Stindt for helpful discussion, Nathaniel Landau for A3G-HA plasmid, Wolfgang Göhring and Wolfgang A. Schulz for

promotor reporter constructs, Heide Muckenfuss and Egbert Flory for the Tat expression plasmid, Bryan R. Cullen for the A3A and Matthias Hamdorf for the pMH-A43xHA plasmid. The following reagents were obtained through the National Institutes of Health (NIH) AIDS Research and Reference Reagent Program, Division of AIDS, NIAID, NIH: monoclonal antibody to HIV-1 p24 (AG3.0) from Jonathan Allan, HIV-1 Vif Monoclonal Antibody (#319) from Michael Malim, HOS.CD4.CCR5 cells and pNL4-3.Luc.R⁻E⁻ from Nathaniel Landau, A3.01 cells from Thomas Folks, and APOBEC3G-Myc-6Xhis from David Kabat.

Author Contributions

Conceived and designed the experiments: DM MP GGS RK KC CM. Performed the experiments: DM MP AH AAJV HH KMH. Analyzed the data: DM MP AH AAJV MDM KMH RK KC DH CM. Contributed reagents/materials/analysis tools: MDM. Wrote the paper: MDM GGS CM.

References

1. Jarmuz A, Chester A, Bayliss J, Gisbourne J, Dunham I, Scott J, et al. An anthropoid-specific locus of orphan C to U RNA-editing enzymes on chromosome 22. *Genomics*. 2002; 79(3):285–96. PMID: [11863358](#)
2. Navaratnam N, Sarwar R. An overview of cytidine deaminases. *International journal of hematology*. 2006; 83(3):195–200. doi: [10.1532/IJH97.06032](#) PMID: [16720547](#).
3. Rogozin IB, Basu MK, Jordan IK, Pavlov YI, Koonin EV. APOBEC4, a new member of the AID/APOBEC family of polynucleotide (deoxy)cytidine deaminases predicted by computational analysis. *Cell Cycle*. 2005; 4(9):1281–5. PMID: [16082223](#).
4. Prohaska KM, Bennett RP, Salter JD, Smith HC. The multifaceted roles of RNA binding in APOBEC cytidine deaminase functions. *Wiley interdisciplinary reviews RNA*. 2014; 5(4):493–508. doi: [10.1002/wrna.1226](#) PMID: [24664896](#); PubMed Central PMCID: PMC4062598.
5. Münk C, Willemsen A, Bravo IG. An ancient history of gene duplications, fusions and losses in the evolution of APOBEC3 mutators in mammals. *BMC evolutionary biology*. 2012; 12:71. doi: [10.1186/1471-2148-12-71](#) PMID: [22640020](#); PubMed Central PMCID: PMC3495650.
6. Vartanian JP, Guetard D, Henry M, Wain-Hobson S. Evidence for editing of human papillomavirus DNA by APOBEC3 in benign and precancerous lesions. *Science*. 2008; 320(5873):230–3. doi: [10.1126/science.1153201](#) PMID: [18403710](#)
7. Vartanian JP, Henry M, Marchio A, Suspene R, Aynaud MM, Guetard D, et al. Massive APOBEC3 editing of hepatitis B viral DNA in cirrhosis. *PLOS Pathog*. 2010; 6(5):e1000928. doi: [10.1371/journal.ppat.1000928](#) PMID: [20523896](#)
8. Chiu YL, Greene WC. The APOBEC3 cytidine deaminases: an innate defensive network opposing exogenous retroviruses and endogenous retroelements. *Annu Rev Immunol*. 2008; 26:317–53.
9. Chen H, Lilley CE, Yu Q, Lee DV, Chou J, Narvaiza I, et al. APOBEC3A is a potent inhibitor of adeno-associated virus and retrotransposons. *Curr Biol*. 2006; 16(5):480–5.
10. Tsuge M, Noguchi C, Akiyama R, Matsushita M, Kunihiro K, Tanaka S, et al. G to A hypermutation of TT virus. *Virus research*. 2010; 149(2):211–6. doi: [10.1016/j.virusres.2010.01.019](#) PMID: [20138932](#).
11. Peng ZG, Zhao ZY, Li YP, Wang YP, Hao LH, Fan B, et al. Host apolipoprotein B messenger RNA-editing enzyme catalytic polypeptide-like 3G is an innate defensive factor and drug target against hepatitis C virus. *Hepatology*. 2011; 53(4):1080–9. doi: [10.1002/hep.24160](#) PMID: [21480314](#).
12. Suspene R, Aynaud MM, Koch S, Pasdeloup D, Labetoulle M, Gaertner B, et al. Genetic Editing of Herpes Simplex Virus 1 and Epstein-Barr Herpesvirus Genomes by Human APOBEC3 Cytidine Deaminases in Culture and In Vivo. *J Virol*. 2011; 85(15):7594–602. [pii]; doi: [10.1128/JVI.00290-11](#)
13. Fehrholz M, Kendl S, Prifert C, Weissbrich B, Lemon K, Rennick L, et al. The innate antiviral factor APOBEC3G targets replication of measles, mumps and respiratory syncytial viruses. *The Journal of general virology*. 2012; 93(Pt 3):565–76. doi: [10.1099/vir.0.038919-0](#) PMID: [22170635](#).
14. Muckenfuss H, Hamdorf M, Held U, Perkovic M, Löwer J, Cichutek K, et al. APOBEC3 proteins inhibit human LINE-1 retrotransposition. *JBiolChem*. 2006; 281(31):22161–72.
15. Schumann GG, Gogvadze EV, Osanai-Futahashi M, Kuroki A, Münk C, Fujiwara H, et al. Unique functions of repetitive transcriptomes. *Int Rev Cell Mol Biol*. 2010; 285:115–88.

16. Lucifora J, Xia Y, Reisinger F, Zhang K, Stadler D, Cheng X, et al. Specific and nonhepatotoxic degradation of nuclear hepatitis B virus cccDNA. *Science*. 2014; 343(6176):1221–8. doi: [10.1126/science.1243462](https://doi.org/10.1126/science.1243462) PMID: [24557838](https://pubmed.ncbi.nlm.nih.gov/24557838/).
17. Mariani R, Chen D, Schröfelbauer B, Navarro F, König R, Bollman B, et al. Species-specific exclusion of APOBEC3G from HIV-1 virions by Vif. *Cell*. 2003; 114(1):21–31. PMID: [12859895](https://pubmed.ncbi.nlm.nih.gov/12859895/)
18. Münk C, Jensen BE, Zielonka J, Häussinger D, Kamp C. Running Loose or Getting Lost: How HIV-1 Counters and Capitalizes on APOBEC3-Induced Mutagenesis through Its Vif Protein. *Viruses*. 2012; 4(11):3132–61. [pii]; doi: [10.3390/v4113132](https://doi.org/10.3390/v4113132) PMID: [23202519](https://pubmed.ncbi.nlm.nih.gov/23202519/)
19. Löchelt M, Romén F, Bastone P, Muckenfuss H, Kirchner N, Kim YB, et al. The antiretroviral activity of APOBEC3 is inhibited by the foamy virus accessory Bet protein. *Proc Natl Acad Sci USA*. 2005; 102(22):7982–7.
20. Perkovic M, Schmidt S, Marino D, Russell RA, Stauch B, Hofmann H, et al. Species-specific inhibition of APOBEC3C by the prototype foamy virus protein bet. *JBiolChem*. 2009; 284(9):5819–26.
21. Beggel B, Münk C, Daumer M, Hauck K, Häussinger D, Lengauer T, et al. Full genome ultra-deep pyrosequencing associates G-to-A hypermutation of the hepatitis B virus genome with the natural progression of hepatitis B. *Journal of viral hepatitis*. 2013; 20(12):882–9. doi: [10.1111/jvh.12110](https://doi.org/10.1111/jvh.12110) PMID: [24304458](https://pubmed.ncbi.nlm.nih.gov/24304458/).
22. Vasudevan AA, Smits SH, Hoppner A, Häussinger D, Koenig BW, Münk C. Structural features of antiviral DNA cytidine deaminases. *Biological chemistry*. 2013; 394(11):1357–70. doi: [10.1515/hsz-2013-0165](https://doi.org/10.1515/hsz-2013-0165) PMID: [23787464](https://pubmed.ncbi.nlm.nih.gov/23787464/).
23. Sheehy AM, Gaddis NC, Choi JD, Malim MH. Isolation of a human gene that inhibits HIV-1 infection and is suppressed by the viral Vif protein. *Nature*. 2002; 418(6898):646–50. PMID: [12167863](https://pubmed.ncbi.nlm.nih.gov/12167863/)
24. Russell RA, Wiegand HL, Moore MD, Schafer A, McClure MO, Cullen BR. Foamy virus Bet proteins function as novel inhibitors of the APOBEC3 family of innate antiretroviral defense factors. *JVirology*. 2005; 79(14):8724–31.
25. Derse D, Hill SA, Princler G, Lloyd P, Heidecker G. Resistance of human T cell leukemia virus type 1 to APOBEC3G restriction is mediated by elements in nucleocapsid. *Proc Natl Acad Sci USA*. 2007; 104(8):2915–20.
26. Stavrou S, Nitta T, Kotla S, Ha D, Nagashima K, Rein AR, et al. Murine leukemia virus glycosylated Gag blocks apolipoprotein B editing complex 3 and cytosolic sensor access to the reverse transcription complex. *Proc Natl Acad Sci USA*. 2013. [pii]; doi: [10.1073/pnas.1217399110](https://doi.org/10.1073/pnas.1217399110)
27. Kolokithas A, Rosenke K, Malik F, Hendrick D, Swanson L, Santiago ML, et al. The glycosylated Gag protein of a murine leukemia virus inhibits the antiretroviral function of APOBEC3. *Journal of virology*. 2010; 84(20):10933–6. doi: [10.1128/JVI.01023-10](https://doi.org/10.1128/JVI.01023-10) PMID: [20702647](https://pubmed.ncbi.nlm.nih.gov/20702647/); PubMed Central PMCID: PMC2950561.
28. Stavrou S, Blouch K, Kotla S, Bass A, Ross SR. Nucleic Acid recognition orchestrates the anti-viral response to retroviruses. *Cell host & microbe*. 2015; 17(4):478–88. doi: [10.1016/j.chom.2015.02.021](https://doi.org/10.1016/j.chom.2015.02.021) PMID: [25816774](https://pubmed.ncbi.nlm.nih.gov/25816774/); PubMed Central PMCID: PMC4393365.
29. Muramatsu M, Sankaranand VS, Anant S, Sugai M, Kinoshita K, Davidson NO, et al. Specific expression of activation-induced cytidine deaminase (AID), a novel member of the RNA-editing deaminase family in germinal center B cells. *The Journal of biological chemistry*. 1999; 274(26):18470–6. PMID: [10373455](https://pubmed.ncbi.nlm.nih.gov/10373455/).
30. Muramatsu M, Kinoshita K, Fagarasan S, Yamada S, Shinkai Y, Honjo T. Class switch recombination and hypermutation require activation-induced cytidine deaminase (AID), a potential RNA editing enzyme. *Cell*. 2000; 102(5):553–63. PMID: [11007474](https://pubmed.ncbi.nlm.nih.gov/11007474/).
31. Arakawa H, Hauschild J, Buerstedde JM. Requirement of the activation-induced deaminase (AID) gene for immunoglobulin gene conversion. *Science*. 2002; 295(5558):1301–6. doi: [10.1126/science.1067308](https://doi.org/10.1126/science.1067308) PMID: [11847344](https://pubmed.ncbi.nlm.nih.gov/11847344/).
32. Petersen-Mahrt SK, Harris RS, Neuberger MS. AID mutates *E. coli* suggesting a DNA deamination mechanism for antibody diversification. *Nature*. 2002; 418(6893):99–103. doi: [10.1038/nature00862](https://doi.org/10.1038/nature00862) PMID: [12097915](https://pubmed.ncbi.nlm.nih.gov/12097915/).
33. Harris RS, Sale JE, Petersen-Mahrt SK, Neuberger MS. AID is essential for immunoglobulin V gene conversion in a cultured B cell line. *Current biology: CB*. 2002; 12(5):435–8. PMID: [11882297](https://pubmed.ncbi.nlm.nih.gov/11882297/).
34. Okazaki IM, Kinoshita K, Muramatsu M, Yoshikawa K, Honjo T. The AID enzyme induces class switch recombination in fibroblasts. *Nature*. 2002; 416(6878):340–5. doi: [10.1038/nature727](https://doi.org/10.1038/nature727) PMID: [11875397](https://pubmed.ncbi.nlm.nih.gov/11875397/).
35. Revy P, Muto T, Levy Y, Geissmann F, Plebani A, Sanal O, et al. Activation-induced cytidine deaminase (AID) deficiency causes the autosomal recessive form of the Hyper-IgM syndrome (HIGM2). *Cell*. 2000; 102(5):565–75. PMID: [11007475](https://pubmed.ncbi.nlm.nih.gov/11007475/).

36. MacDuff DA, Demorest ZL, Harris RS. AID can restrict L1 retrotransposition suggesting a dual role in innate and adaptive immunity. *Nucleic Acids Res.* 2009; 37(6):1854–67. doi: [10.1093/nar/gkp030](https://doi.org/10.1093/nar/gkp030) PMID: [19188259](https://pubmed.ncbi.nlm.nih.gov/19188259/)
37. Metzner M, Jack HM, Wabl M. LINE-1 retroelements complexed and inhibited by activation induced cytidine deaminase. *PLOS one.* 2012; 7(11):e49358. doi: [10.1371/journal.pone.0049358](https://doi.org/10.1371/journal.pone.0049358) PMID: [23133680](https://pubmed.ncbi.nlm.nih.gov/23133680/); PubMed Central PMCID: PMC3487726.
38. Yu Q, Chen D, Konig R, Mariani R, Unutmaz D, Landau NR. APOBEC3B and APOBEC3C are potent inhibitors of simian immunodeficiency virus replication. *J Biol Chem.* 2004; 279(51):53379–86. [pii]; doi: [10.1074/jbc.M408802200](https://doi.org/10.1074/jbc.M408802200) PMID: [15466872](https://pubmed.ncbi.nlm.nih.gov/15466872/)
39. Bishop KN, Holmes RK, Sheehy AM, Davidson NO, Cho SJ, Malim MH. Cytidine deamination of retroviral DNA by diverse APOBEC proteins. *Curr Biol.* 2004; 14(15):1392–6.
40. Zheng YH, Irwin D, Kurosu T, Tokunaga K, Sata T, Peterlin BM. Human APOBEC3F is another host factor that blocks human immunodeficiency virus type 1 replication. *Journal of virology.* 2004; 78(11):6073–6. doi: [10.1128/JVI.78.11.6073-6076.2004](https://doi.org/10.1128/JVI.78.11.6073-6076.2004) PMID: [15141007](https://pubmed.ncbi.nlm.nih.gov/15141007/); PubMed Central PMCID: PMC415831.
41. Teng B, Burant CF, Davidson NO. Molecular cloning of an apolipoprotein B messenger RNA editing protein. *Science.* 1993; 260(5115):1816–9. PMID: [8511591](https://pubmed.ncbi.nlm.nih.gov/8511591/).
42. Navaratnam N, Morrison JR, Bhattacharya S, Patel D, Funahashi T, Giannoni F, et al. The p27 catalytic subunit of the apolipoprotein B mRNA editing enzyme is a cytidine deaminase. *The Journal of biological chemistry.* 1993; 268(28):20709–12. PMID: [8407891](https://pubmed.ncbi.nlm.nih.gov/8407891/).
43. Powell LM, Wallis SC, Pease RJ, Edwards YH, Knott TJ, Scott J. A novel form of tissue-specific RNA processing produces apolipoprotein-B48 in intestine. *Cell.* 1987; 50(6):831–40. PMID: [3621347](https://pubmed.ncbi.nlm.nih.gov/3621347/).
44. Mehta A, Kinter MT, Sherman NE, Driscoll DM. Molecular cloning of apobec-1 complementation factor, a novel RNA-binding protein involved in the editing of apolipoprotein B mRNA. *Molecular and cellular biology.* 2000; 20(5):1846–54. PMID: [10669759](https://pubmed.ncbi.nlm.nih.gov/10669759/); PubMed Central PMCID: PMC85365.
45. Rosenberg BR, Hamilton CE, Mwangi MM, Dewell S, Papavasiliou FN. Transcriptome-wide sequencing reveals numerous APOBEC1 mRNA-editing targets in transcript 3' UTRs. *Nature structural & molecular biology.* 2011; 18(2):230–6. doi: [10.1038/nsmb.1975](https://doi.org/10.1038/nsmb.1975) PMID: [21258325](https://pubmed.ncbi.nlm.nih.gov/21258325/); PubMed Central PMCID: PMC3075553.
46. Petit V, Guetard D, Renard M, Keriel A, Sitbon M, Wain-Hobson S, et al. Murine APOBEC1 is a powerful mutator of retroviral and cellular RNA in vitro and in vivo. *Journal of molecular biology.* 2009; 385(1):65–78. doi: [10.1016/j.jmb.2008.10.043](https://doi.org/10.1016/j.jmb.2008.10.043) PMID: [18983852](https://pubmed.ncbi.nlm.nih.gov/18983852/).
47. Bishop KN, Holmes RK, Sheehy AM, Malim MH. APOBEC-mediated editing of viral RNA. *Science.* 2004; 305(5684):645. doi: [10.1126/science.1100658](https://doi.org/10.1126/science.1100658) PMID: [15286366](https://pubmed.ncbi.nlm.nih.gov/15286366/).
48. Ikeda T, Ohsugi T, Kimura T, Matsushita S, Maeda Y, Harada S, et al. The antiretroviral potency of APOBEC1 deaminase from small animal species. *Nucleic Acids Res.* 2008; 36(21):6859–71. [pii]; doi: [10.1093/nar/gkn802](https://doi.org/10.1093/nar/gkn802) PMID: [18971252](https://pubmed.ncbi.nlm.nih.gov/18971252/)
49. Ikeda T, Ong EB, Watanabe N, Sakaguchi N, Maeda K, Koito A. Creation of chimeric human/rabbit APOBEC1 with HIV-1 restriction and DNA mutation activities. *Scientific reports.* 2016; 6:19035. doi: [10.1038/srep19035](https://doi.org/10.1038/srep19035) PMID: [26738439](https://pubmed.ncbi.nlm.nih.gov/26738439/); PubMed Central PMCID: PMC4704027.
50. Ikeda T, Abd El Galil KH, Tokunaga K, Maeda K, Sata T, Sakaguchi N, et al. Intrinsic restriction activity by apolipoprotein B mRNA editing enzyme APOBEC1 against the mobility of autonomous retrotransposons. *Nucleic acids research.* 2011; 39(13):5538–54. doi: [10.1093/nar/gkr124](https://doi.org/10.1093/nar/gkr124) PMID: [21398638](https://pubmed.ncbi.nlm.nih.gov/21398638/); PubMed Central PMCID: PMC3141244.
51. Sato Y, Probst HC, Tatsumi R, Ikeuchi Y, Neuberger MS, Rada C. Deficiency in APOBEC2 leads to a shift in muscle fiber type, diminished body mass, and myopathy. *The Journal of biological chemistry.* 2010; 285(10):7111–8. doi: [10.1074/jbc.M109.052977](https://doi.org/10.1074/jbc.M109.052977) PMID: [20022958](https://pubmed.ncbi.nlm.nih.gov/20022958/); PubMed Central PMCID: PMC2844160.
52. Lada AG, Krick CF, Kozmin SG, Mayorov VI, Karpova TS, Rogozin IB, et al. Mutator effects and mutation signatures of editing deaminases produced in bacteria and yeast. *Biochemistry Biokhimiia.* 2011; 76(1):131–46. PMID: [21568845](https://pubmed.ncbi.nlm.nih.gov/21568845/); PubMed Central PMCID: PMC3906858.
53. Harris RS, Petersen-Mahrt SK, Neuberger MS. RNA editing enzyme APOBEC1 and some of its homologs can act as DNA mutators. *MolCell.* 2002; 10(5):1247–53. S1097276502007426 [pii].
54. Esnault C, Millet J, Schwartz O, Heidmann T. Dual inhibitory effects of APOBEC family proteins on retrotransposition of mammalian endogenous retroviruses. *Nucleic Acids Res.* 2006; 34(5):1522–31. PMID: [16537839](https://pubmed.ncbi.nlm.nih.gov/16537839/)
55. Niewiadomska AM, Tian C, Tan L, Wang T, Sarkis PT, Yu XF. Differential inhibition of long interspersed element 1 by APOBEC3 does not correlate with high-molecular-mass-complex formation or P-body association. *J Virol.* 2007; 81(17):9577–83.

56. Adachi A, Gendelman HE, Koenig S, Folks T, Willey R, Rabson A, et al. Production of acquired immunodeficiency syndrome-associated retrovirus in human and nonhuman cells transfected with an infectious molecular clone. *J Virol*. 1986; 59(2):284–91.
57. Connor RI, Chen BK, Choe S, Landau NR. Vpr is required for efficient replication of human immunodeficiency virus type-1 in mononuclear phagocytes. *Virology*. 1995; 206(2):935–44. doi: [10.1006/viro.1995.1016](https://doi.org/10.1006/viro.1995.1016) PMID: [7531918](https://pubmed.ncbi.nlm.nih.gov/7531918/).
58. Mariani R, Rasala BA, Rutter G, Wieggers K, Brandt SM, Krausslich HG, et al. Mouse-human heterokaryons support efficient human immunodeficiency virus type 1 assembly. *J Virol*. 2001; 75(7):3141–51.
59. Wei X, Decker JM, Liu H, Zhang Z, Arani RB, Kilby JM, et al. Emergence of resistant human immunodeficiency virus type 1 in patients receiving fusion inhibitor (T-20) monotherapy. *Antimicrobial agents and chemotherapy*. 2002; 46(6):1896–905. PMID: [12019106](https://pubmed.ncbi.nlm.nih.gov/12019106/); PubMed Central PMCID: PMC127242.
60. Deng H, Liu R, Ellmeier W, Choe S, Unutmaz D, Burkhart M, et al. Identification of a major co-receptor for primary isolates of HIV-1. *Nature*. 1996; 381(6584):661–6. doi: [10.1038/381661a0](https://doi.org/10.1038/381661a0) PMID: [8649511](https://pubmed.ncbi.nlm.nih.gov/8649511/)
61. Nowarski R, Britan-Rosich E, Shiloach T, Kotler M. Hypermutation by intersegmental transfer of APOBEC3G cytidine deaminase. *Nat Struct Mol Biol*. 2008; 15(10):1059–66. [pii]; doi: [10.1038/nsmb.1495](https://doi.org/10.1038/nsmb.1495)
62. Jaguva Vasudevan AA, Perkovic M, Bulliard Y, Cichutek K, Trono D, Häussinger D, et al. Prototype foamy virus Bet impairs the dimerization and cytosolic solubility of human APOBEC3G. *Journal of virology*. 2013; 87(16):9030–40. doi: [10.1128/JVI.03385-12](https://doi.org/10.1128/JVI.03385-12) PMID: [23760237](https://pubmed.ncbi.nlm.nih.gov/23760237/); PubMed Central PMCID: PMC3754047.
63. Polevoda B, McDougall WM, Tun BN, Cheung M, Salter JD, Friedman AE, et al. RNA binding to APOBEC3G induces the disassembly of functional deaminase complexes by displacing single-stranded DNA substrates. *Nucleic acids research*. 2015; 43(19):9434–45. doi: [10.1093/nar/gkv970](https://doi.org/10.1093/nar/gkv970) PMID: [26424853](https://pubmed.ncbi.nlm.nih.gov/26424853/); PubMed Central PMCID: PMC4627094.
64. Iwatani Y, Takeuchi H, Strebel K, Levin JG. Biochemical activities of highly purified, catalytically active human APOBEC3G: correlation with antiviral effect. *J Virol*. 2006; 80(12):5992–6002. [pii]; doi: [10.1128/JVI.02680-05](https://doi.org/10.1128/JVI.02680-05) PMID: [16731938](https://pubmed.ncbi.nlm.nih.gov/16731938/)
65. McDougall WM, Okany C, Smith HC. Deaminase activity on single-stranded DNA (ssDNA) occurs in vitro when APOBEC3G cytidine deaminase forms homotetramers and higher-order complexes. *The Journal of biological chemistry*. 2011; 286(35):30655–61. doi: [10.1074/jbc.M111.269506](https://doi.org/10.1074/jbc.M111.269506) PMID: [21737457](https://pubmed.ncbi.nlm.nih.gov/21737457/); PubMed Central PMCID: PMC3162426.
66. Wagner E, Cotten M, Foisner R, Birnstiel ML. Transferrin-polycation-DNA complexes: the effect of polycations on the structure of the complex and DNA delivery to cells. *Proceedings of the National Academy of Sciences of the United States of America*. 1991; 88(10):4255–9. PMID: [2034670](https://pubmed.ncbi.nlm.nih.gov/2034670/); PubMed Central PMCID: PMC51637.
67. Jang H, Abraham SJ, Chavan TS, Hitchinson B, Khavrutskii L, Tarasova NI, et al. Mechanisms of membrane binding of small GTPase K-Ras4B farnesylated hypervariable region. *The Journal of biological chemistry*. 2015; 290(15):9465–77. doi: [10.1074/jbc.M114.620724](https://doi.org/10.1074/jbc.M114.620724) PMID: [25713064](https://pubmed.ncbi.nlm.nih.gov/25713064/); PubMed Central PMCID: PMC4392252.
68. Wu LJ, Xu LR, Liao JM, Chen J, Liang Y. Both the C-terminal polylysine region and the farnesylation of K-RasB are important for its specific interaction with calmodulin. *PLOS one*. 2011; 6(7):e21929. doi: [10.1371/journal.pone.0021929](https://doi.org/10.1371/journal.pone.0021929) PMID: [21750741](https://pubmed.ncbi.nlm.nih.gov/21750741/); PubMed Central PMCID: PMC3130059.
69. Paranjpe S, Craigo J, Patterson B, Ding M, Barroso P, Harrison L, et al. Subcompartmentalization of HIV-1 quasispecies between seminal cells and seminal plasma indicates their origin in distinct genital tissues. *AIDS Res Hum Retroviruses*. 2002; 18(17):1271–80. doi: [10.1089/088922202320886316](https://doi.org/10.1089/088922202320886316) PMID: [12487815](https://pubmed.ncbi.nlm.nih.gov/12487815/).
70. Le Tortorec A, Le Grand R, Denis H, Satie AP, Mannioui K, Roques P, et al. Infection of semen-producing organs by SIV during the acute and chronic stages of the disease. *PLOS one*. 2008; 3(3):e1792. doi: [10.1371/journal.pone.0001792](https://doi.org/10.1371/journal.pone.0001792) PMID: [18347738](https://pubmed.ncbi.nlm.nih.gov/18347738/); PubMed Central PMCID: PMC2268241.
71. Lowe SH, Sankatsing SU, Repping S, van der Veen F, Reiss P, Lange JM, et al. Is the male genital tract really a sanctuary site for HIV? Arguments that it is not. *AIDS*. 2004; 18(10):1353–62. PMID: [15199311](https://pubmed.ncbi.nlm.nih.gov/15199311/).
72. Roulet V, Satie AP, Ruffault A, Le Tortorec A, Denis H, Guist'hau O, et al. Susceptibility of human testis to human immunodeficiency virus-1 infection in situ and in vitro. *The American journal of pathology*. 2006; 169(6):2094–103. PMID: [17148672](https://pubmed.ncbi.nlm.nih.gov/17148672/); PubMed Central PMCID: PMC1762481.
73. Fieni F, Stone M, Ma ZM, Dutra J, Fritts L, Miller CJ. Viral RNA levels and env variants in semen and tissues of mature male rhesus macaques infected with SIV by penile inoculation. *PLOS one*. 2013; 8(10):e76367. doi: [10.1371/journal.pone.0076367](https://doi.org/10.1371/journal.pone.0076367) PMID: [24146859](https://pubmed.ncbi.nlm.nih.gov/24146859/); PubMed Central PMCID: PMC3795772.
74. Houzet L, Matusali G, Dejuccq-Rainsford N. Origins of HIV-infected leukocytes and virions in semen. *J Infect Dis*. 2014; 210 Suppl 3:S622–30. doi: [10.1093/infdis/jiu328](https://doi.org/10.1093/infdis/jiu328) PMID: [25414416](https://pubmed.ncbi.nlm.nih.gov/25414416/).

75. Bednar MM, Hauser BM, Ping LH, Dukhovlinova E, Zhou S, Arrildt KT, et al. R5 Macrophage-Tropic HIV-1 in the Male Genital Tract. *Journal of virology*. 2015; 89(20):10688–92. doi: [10.1128/JVI.01842-15](https://doi.org/10.1128/JVI.01842-15) PMID: [26223642](https://pubmed.ncbi.nlm.nih.gov/26223642/); PubMed Central PMCID: PMC4580182.
76. Matusali G, Dereuddre-Bosquet N, Le Tortorec A, Moreau M, Satie AP, Mahe D, et al. Detection of Simian Immunodeficiency Virus in Semen, Urethra, and Male Reproductive Organs during Efficient Highly Active Antiretroviral Therapy. *Journal of virology*. 2015; 89(11):5772–87. doi: [10.1128/JVI.03628-14](https://doi.org/10.1128/JVI.03628-14) PMID: [25833047](https://pubmed.ncbi.nlm.nih.gov/25833047/); PubMed Central PMCID: PMC4442442.
77. Muciaccia B, Uccini S, Filippini A, Ziparo E, Paraire F, Baroni CD, et al. Presence and cellular distribution of HIV in the testes of seropositive subjects: an evaluation by in situ PCR hybridization. *FASEB journal: official publication of the Federation of American Societies for Experimental Biology*. 1998; 12(2):151–63. PMID: [9472980](https://pubmed.ncbi.nlm.nih.gov/9472980/).
78. Nuovo GJ, Becker J, Simsir A, Margiotta M, Khalife G, Shevchuk M. HIV-1 nucleic acids localize to the spermatogonia and their progeny. A study by polymerase chain reaction in situ hybridization. *The American journal of pathology*. 1994; 144(6):1142–8. PMID: [8203455](https://pubmed.ncbi.nlm.nih.gov/8203455/); PubMed Central PMCID: PMC1887452.
79. Muciaccia B, Filippini A, Ziparo E, Colelli F, Baroni CD, Stefanini M. Testicular germ cells of HIV-seropositive asymptomatic men are infected by the virus. *J Reprod Immunol*. 1998; 41(1–2):81–93. PMID: [10213302](https://pubmed.ncbi.nlm.nih.gov/10213302/).
80. Shevchuk MM, Nuovo GJ, Khalife G. HIV in testis: quantitative histology and HIV localization in germ cells. *J Reprod Immunol*. 1998; 41(1–2):69–79. PMID: [10213301](https://pubmed.ncbi.nlm.nih.gov/10213301/).
81. Shehu-Xhilaga M, Kent S, Batten J, Ellis S, Van der Meulen J, O'Bryan M, et al. The testis and epididymis are productively infected by SIV and SHIV in juvenile macaques during the post-acute stage of infection. *Retrovirology*. 2007; 4:7. doi: [10.1186/1742-4690-4-7](https://doi.org/10.1186/1742-4690-4-7) PMID: [17266752](https://pubmed.ncbi.nlm.nih.gov/17266752/); PubMed Central PMCID: PMC1805449.
82. Santangelo PJ, Rogers KA, Zurla C, Blanchard EL, Gumber S, Strait K, et al. Whole-body immunoPET reveals active SIV dynamics in viremic and antiretroviral therapy-treated macaques. *Nature methods*. 2015. doi: [10.1038/nmeth.3320](https://doi.org/10.1038/nmeth.3320) PMID: [25751144](https://pubmed.ncbi.nlm.nih.gov/25751144/).
83. Crowell RC, Kiessling AA. Endogenous retrovirus expression in testis and epididymis. *Biochem Soc Trans*. 2007; 35(Pt 3):629–33. doi: [10.1042/BST0350629](https://doi.org/10.1042/BST0350629) PMID: [17511667](https://pubmed.ncbi.nlm.nih.gov/17511667/).
84. Steinhoff C, Schulz WA. Transcriptional regulation of the human LINE-1 retrotransposon L1.2B. *Mol Genet Genomics*. 2003; 270(5):394–402. doi: [10.1007/s00438-003-0931-2](https://doi.org/10.1007/s00438-003-0931-2) PMID: [14530963](https://pubmed.ncbi.nlm.nih.gov/14530963/).
85. Cronauer MV, Schulz WA, Burchardt T, Ackermann R, Burchardt M. Inhibition of p53 function diminishes androgen receptor-mediated signaling in prostate cancer cell lines. *Oncogene*. 2004; 23(20):3541–9. doi: [10.1038/sj.onc.1207346](https://doi.org/10.1038/sj.onc.1207346) PMID: [15077179](https://pubmed.ncbi.nlm.nih.gov/15077179/).
86. Marin M, Rose KM, Kozak SL, Kabat D. HIV-1 Vif protein binds the editing enzyme APOBEC3G and induces its degradation. *NatMed*. 2003; 9(11):1398–403.
87. Wiegand HL, Doehle BP, Bogerd HP, Cullen BR. A second human antiretroviral factor, APOBEC3F, is suppressed by the HIV-1 and HIV-2 Vif proteins. *EMBO J*. 2004; 23(12):2451–8. PMID: [15152192](https://pubmed.ncbi.nlm.nih.gov/15152192/)
88. Hoffmeyer A, Grosse-Wilde A, Flory E, Neufeld B, Kunz M, Rapp UR, et al. Different mitogen-activated protein kinase signaling pathways cooperate to regulate tumor necrosis factor alpha gene expression in T lymphocytes. *The Journal of biological chemistry*. 1999; 274(7):4319–27. PMID: [9933633](https://pubmed.ncbi.nlm.nih.gov/9933633/).
89. Folks T, Benn S, Rabson A, Theodore T, Hoggan MD, Martin M, et al. Characterization of a continuous T-cell line susceptible to the cytopathic effects of the acquired immunodeficiency syndrome (AIDS)-associated retrovirus. *Proceedings of the National Academy of Sciences of the United States of America*. 1985; 82(13):4539–43. PMID: [2989831](https://pubmed.ncbi.nlm.nih.gov/2989831/); PubMed Central PMCID: PMC391138.
90. Soneoka Y, Cannon PM, Ramsdale EE, Griffiths JC, Romano G, Kingsman SM, et al. A transient three-plasmid expression system for the production of high titer retroviral vectors. *Nucleic acids research*. 1995; 23(4):628–33. PMID: [7899083](https://pubmed.ncbi.nlm.nih.gov/7899083/); PubMed Central PMCID: PMC306730.
91. Simm M, Shahabuddin M, Chao W, Allan JS, Volsky DJ. Aberrant Gag protein composition of a human immunodeficiency virus type 1 vif mutant produced in primary lymphocytes. *J Virol*. 1995; 69(7):4582–6. PMID: [7769728](https://pubmed.ncbi.nlm.nih.gov/7769728/)
92. Simon JH, Southerling TE, Peterson JC, Meyer BE, Malim MH. Complementation of vif-defective human immunodeficiency virus type 1 by primate, but not nonprimate, lentivirus vif genes. *Journal of virology*. 1995; 69(7):4166–72. PMID: [7769676](https://pubmed.ncbi.nlm.nih.gov/7769676/); PubMed Central PMCID: PMC189153.

Chapter VIII

Vif Proteins from Diverse Human Immunodeficiency Virus/Simian Immunodeficiency Virus Lineages Have Distinct Binding Sites in A3C

Journal : **Journal of Virology** (published in 2016)

Own contribution to this work:

- Construction of ten different human/smm A3C chimeric plasmids, amplification and sequence analysis of Vif variant plasmids obtained from Viviana Simon, initial vif mediated A3 degradation (Fig. 7A, column 3 for example) and do not own any other experiments. Analysis of data

Vif Proteins from Diverse Human Immunodeficiency Virus/Simian Immunodeficiency Virus Lineages Have Distinct Binding Sites in A3C

Zeli Zhang,^a Qinyong Gu,^a Ananda Ayyappan Jaguva Vasudevan,^a Manimehalai Jeyaraj,^a Stanislaw Schmidt,^{b*} Jörg Zielonka,^{a**} Mario Perković,^{a,b*} Jens-Ove Heckel,^c Klaus Cichutek,^b Dieter Häussinger,^a Sander H. J. Smits,^d Carsten Münk^a

Clinic for Gastroenterology, Hepatology, and Infectiology, Medical Faculty, Heinrich-Heine-Universität Düsseldorf, Düsseldorf, Germany^a; Department of Medical Biotechnology, Paul-Ehrlich-Institut, Langen, Germany^b; Zoo Landau in der Pfalz, Landau in der Pfalz, Germany^c; Institute of Biochemistry, Heinrich-Heine-Universität Düsseldorf, Düsseldorf, Germany^d

ABSTRACT

Lentiviruses have evolved the Vif protein to counteract APOBEC3 (A3) restriction factors by targeting them for proteasomal degradation. Previous studies have identified important residues in the interface of human immunodeficiency virus type 1 (HIV-1) Vif and human APOBEC3C (hA3C) or human APOBEC3F (hA3F). However, the interaction between primate A3C proteins and HIV-1 Vif or natural HIV-1 Vif variants is still poorly understood. Here, we report that HIV-1 Vif is inactive against A3Cs of rhesus macaques (rhA3C), sooty mangabey monkeys (smmA3C), and African green monkeys (agmA3C), while HIV-2, African green monkey simian immunodeficiency virus (SIVagm), and SIVmac Vif proteins efficiently mediate the depletion of all tested A3Cs. We identified that residues N/H130 and Q133 in rhA3C and smmA3C are determinants for this HIV-1 Vif-triggered counteraction. We also found that the HIV-1 Vif interaction sites in helix 4 of hA3C and hA3F differ. Vif alleles from diverse HIV-1 subtypes were tested for degradation activities related to hA3C. The subtype F-1 Vif was identified to be inactive for degradation of hA3C and hA3F. The residues that determined F-1 Vif inactivity in the degradation of A3C/A3F were located in the C-terminal region (K167 and D182). Structural analysis of F-1 Vif revealed that impairing the internal salt bridge of E171-K167 restored reduction capacities to A3C/A3F. Furthermore, we found that D101 could also form an internal interaction with K167. Replacing D101 with glycine and R167 with lysine in NL4-3 Vif impaired its counteractivity to A3F and A3C. This finding indicates that internal interactions outside the A3 binding region in HIV-1 Vif influence the capacity to induce degradation of A3C/A3F.

IMPORTANCE

The APOBEC3 restriction factors can serve as potential barriers to lentiviral cross-species transmissions. Vif proteins from lentiviruses counteract APOBEC3 by proteasomal degradation. In this study, we found that monkey-derived A3C, rhA3C and smmA3C, were resistant to HIV-1 Vif. This was determined by A3C residues N/H130 and Q133. However, HIV-2, SIVagm, and SIVmac Vif proteins were found to be able to mediate the depletion of all tested primate A3C proteins. In addition, we identified a natural HIV-1 Vif (F-1 Vif) that was inactive in the degradation of hA3C/hA3F. Here, we provide for the first time a model that explains how an internal salt bridge of E171-K167-D101 influences Vif-mediated degradation of hA3C/hA3F. This finding provides a novel way to develop HIV-1 inhibitors by targeting the internal interactions of the Vif protein.

Simian immunodeficiency virus (SIV) naturally infects many Old World primate species in Africa. The pandemic of human immunodeficiency virus (HIV) originated from cross-species transmission events of SIVs to humans. HIV-1 was introduced into the human population by multiple transmissions of a chimpanzee (cpz) virus, which is known as SIVcpz. The less virulent human lentivirus, HIV-2, was derived from SIVsmm, which was obtained from sooty mangabey monkeys (smm) (1).

The cellular restriction factors of the APOBEC3 (A3) family of DNA cytidine deaminases are an important arm of the innate immune defense system which can potentially serve as a barrier to lentiviral cross-species transmissions (recently reviewed in references 2 and 3). Human A3s include seven genes that contain either one (A3A, A3C, and A3H) or two (A3B, A3D, A3F, and A3G) zinc (Z)-binding domains with the conserved motifs of HXE(X)_{23–28}CXXC (X can be any residue) (4, 5). Among these seven genes, A3D, A3F, A3G, and A3H inhibit HIV-1ΔVif replication by deamination of cytidines in the viral single-strand DNA that is formed during reverse transcription, thereby introducing G-to-A hypermutations in the coding strand (6–12). Additionally, some A3s inhibit virus replication by deaminase-indepen-

dent mechanisms affecting reverse transcription and integration steps (13–18). Human A3A and A3C are not antiviral against HIV-1, but human A3C could effectively restrict SIVmacΔVif and

Received 27 July 2016 Accepted 25 August 2016

Accepted manuscript posted online 31 August 2016

Citation Zhang Z, Gu Q, Jaguva Vasudevan AA, Jeyaraj M, Schmidt S, Zielonka J, Perković M, Heckel J-O, Cichutek K, Häussinger D, Smits SHJ, Münk C. 2016. Vif proteins from diverse human immunodeficiency virus/simian immunodeficiency virus lineages have distinct binding sites in A3C. *J Virol* 90:10193–10208. doi:10.1128/JVI.01497-16.

Editor: S. R. Ross, University of Illinois at Chicago

Address correspondence to Carsten Münk, carsten.muenk@med.uni-duesseldorf.de.

* Present address: Stanislaw Schmidt, Division of Pediatric Hematology and Oncology, Hospital for Children and Adolescents, Johann Wolfgang Goethe-Universität, Frankfurt, Germany; Jörg Zielonka, Roche Glycart AG, Schlieren, Switzerland; Mario Perković, TRON (Translational Oncology at the University Medical Center), Johannes Gutenberg-Universität Mainz, Mainz, Germany. Z.Z. and Q.G. contributed equally to this work.

Copyright © 2016, American Society for Microbiology. All Rights Reserved.

SIVagm Δ Vif (11, 19–23), and both A3A and A3C could decrease human papillomavirus infectivity (24, 25). However, some studies found that A3C inhibited HIV-1 Δ Vif by around 50% (26–28). Human A3B is a potent inhibitor against HIV-1, SIV, and human T cell leukemia virus (HTLV) (19, 29–32). In addition, human A3B was reported to be upregulated in several cancer cells and found to be degraded by virion infectivity factor (Vif) from several SIV lineages (33–39).

To counteract the antiviral functions of A3, all lentiviruses except the equine infectious anemia virus encode the Vif that interacts with A3 proteins and then recruit them to an E3 ubiquitin ligase complex containing Cullin5 (CUL5), Elongin B/C (ELOB/C), RING-box protein RBX2, and CBF β to induce degradation of the bound A3s by the proteasome (40–42). The Bet of foamy viruses, the nucleocapsid of HTLV-1, and the glycosylated Gag (glyco-Gag) of murine leukemia virus (MLV) are also shown to have the ability to counteract A3s (21, 43–47). In many cases, this counteraction is species specific and depends on several specific A3/Vif interfaces. For example, HIV-1 Vif efficiently neutralizes human A3G, but it does not inactivate African green monkey A3G (agmA3G) and rhesus macaque A3G (rhA3G) despite a sequence identity of almost 75% (10, 48–50). The amino acid 128 of A3G determines this species-specific counteraction: human A3G with D128 is sensitive to HIV-1 Vif, while A3G.K128 is susceptible to SIVagm Vif (48–50). However, residue 129 in human A3G, but not adjacent position 128, determines the sensitivity to degradation by SIVsmm and HIV-2 Vif proteins (51). Several other cross-species counteractions were also observed: SIVmac Vif mediates the degradation not only of human A3s and rhesus macaque A3s but also of cat A3Z2Z3 (52–57); maedi-visna virus (MVV) Vif can induce the degradation of both sheep and human A3Z3s (58).

Although hA3G, hA3H hapII, and hA3F share a conserved zinc coordination motif, HIV-1 Vif targets different sites in these A3 proteins for degradation. For example, the ¹²⁸DPDY¹³¹ motif in hA3G is involved in direct interaction with the ¹⁴YRHHY¹⁷ domain of HIV-1 Vif (59, 60). The E121 residue in hA3H hapII determines its sensitivity to HIV-1 Vif derived from the NL4-3 strain (61, 62). hA3C and the C-terminal domain (CTD) of hA3F are conserved homologous Z2-typed A3s (4, 5), and 10 equivalent residues in these Z2-typed A3s are identified as being involved in HIV-1 Vif interaction (63). Additionally, A3F.E289 and HIV-1 Vif.R15 show a strong interaction by applying molecular docking (64). The equivalent residue E106 in A3C also determines A3-Vif binding (65). In contrast to this conserved A3-Vif interaction, it was also demonstrated that E324 in A3F is essential for HIV-1 Vif interaction but the equivalent residue E141 in A3C is not, which suggests that the Vif interaction interface differs between A3C and A3F (63, 66). In addition, previous studies have proved that these two glutamic acids vary in primate A3Fs and therefore determined the distinct sensitivities of primate A3F to HIV-1 Vif (67–69). However, the interaction between primate A3Cs and lentiviral Vifs is still less clear.

The N-terminal part of HIV-1 Vif is mainly involved in interaction with human A3s. For example, the ⁴⁰YRHHY⁴⁴ box is reported to be essential for A3G degradation, while the ¹⁴DRMR¹⁷ motif determines A3F degradation (70). Vif derived from HIV-1 clone LAI, but not that of NL4-3, could induce the degradation of hA3H hapII, which is determined by residues F39 and H48 (71). The C terminus of HIV-1 Vif consists of one zinc coordination motif that interacts with CUL5, one SLQ BC box that binds to

ELOB/C, and one Vif dimerization domain (reviewed in reference 72). Previously, it was also reported that the ¹⁷¹EDRW¹⁷⁵ motif in the C terminus of Vif determines the degradation of A3F (66, 73). However, A3 interaction sites in SIV Vif have not yet been identified. Recently, it was reported that the ¹⁶PXXME...PHXXV⁴⁷ domain and G48 of HIV-2 Vif and SIVsmm Vif are involved in the interaction with A3F and A3G, respectively (74).

In this study, we tested the sensitivities of primate A3Cs to several primate lentiviral Vif proteins. HIV-1 Vif had a distinct and restricted degradation profile for primate A3C proteins, while HIV-2, SIVagm, and SIVmac Vif degraded all tested A3C proteins. Additionally, three residues (106, 130, and 133) were identified in rhA3C and smmA3C that determined their resistance to HIV-1 Vif. We demonstrated that the equivalent residues in A3F (313 and 316) were unimportant for HIV-1 Vif sensitivity. Furthermore, two additional residues in the C terminus of the HIV-1 F-1 subtype Vif were identified as being involved in the interaction between HIV-1 Vif and hA3C/F. These observations suggest that Vif proteins from diverse HIV/SIV lineages have distinct interaction interfaces with A3C which mediate their degradation.

MATERIALS AND METHODS

Plasmids. HIV-1, HIV-2, SIVagm, and SIVmac Vif genes were inserted into pcWPRE containing a C-terminal V5 tag (75). SIVpts1 (Tan1; SIVCPZTAN1.910) and SIVpts2 (Tan2; SIVCPZTAN2.69) Vifs were amplified from a full-length molecular clone of SIVcpz (76). Amplicons were digested by EcoRI and NotI and inserted into pcWPRE containing a C-terminal V5 tag. The 21 different HIV-1 strain Vif expression plasmids were kindly provided by Viviana Simon (71). Recently described A3 expression plasmids for hA3C, hA3G, and hA3F (77) as well as rhA3C agmA3C (21) were used. According to the cpzA3C sequence in NCBI (NM_001251910.1), K85, D99, E103, and N115 in hA3C were replaced by N85, E99, K103, and K155 using overlapping PCR, which produced the cpzA3C expression plasmid. All A3s were inserted into pcDNA3.1(+) (Life Technologies, Darmstadt, Germany) expressing a C-terminal hemagglutinin (HA) tag. All A3 chimeras and mutants and Vif mutants were generated by overlapping PCR. PCR primers are shown in Table 1. A3 chimeras were inserted into pcDNA3.1(+), and Vif mutants were inserted into pCRV1 as described previously (78). The expression plasmid of smmA3C was generated by exon assembly from white-crowned mangabey (*Cercocebus torquatus lunulatus*) genomic DNA. Three fragments were amplified separately using the primer pairs SmA3C-1.fw (5'-TAA GCGGAATTCGAACATGAATCCACAGATCAGAAACCCG-3') and SmA3C-2.rv (5'-GATCGACCTGGTTTCGGAAG-3'), SmA3C-3.fw (5'-CTTCCGAAACCAGGTCGATC-3') and SmA3C-4.rv (5'-CAATATTTA AAATCTTCGTAGCCC-3'), and SmA3C-5.fw (5'-GGGCTACGAAGA TTTTAAATATTG-3') and SmA3C-6HA.rv (5'-AGGATAT CTCAAGCGTAATCTGGAACATCGTATGGATACTCGAGAATCT CCTG-3'). The fragments were fused through overlapping extension PCR, and the final fragment was amplified by using the forward SmA3C-1.fw and reverse SmA3C-6HA.rv primers. The amplicon was cloned into restriction sites EcoRI and EcoRV of the pcDNA3.1(+) plasmid and the sequence was verified. SIVmac-Luc (R-E-) and SIVmac-Luc (R-E-) Δ Vif were provided by N. R. Landau (10). The HIV-1-Luc reporter system was described previously (79).

Cells, transfections, and infections. HEK293T (293T; ATCC CRL-3216) cells were maintained in Dulbecco's high-glucose modified Eagle's medium (DMEM; Biochrom, Berlin, Germany) supplemented with 10% fetal bovine serum (FBS), 2 mM L-glutamine, penicillin (100 U/ml), and streptomycin (100 μ g/ml). A3 degradation experiments were performed in 24-well plates, and 1×10^5 293T cells were transfected with 150 ng hA3G, 150 ng hA3F, or 50 ng hA3C expression plasmids together with 350 ng HIV-1, SIVagm, or SIVmac Vif; pcDNA3.1(+) was used to increase the total transfected plasmid DNA to 500 ng. To produce SIVmac-luciferase

TABLE 1 Primers used in this study

Primer name	Product	Sequence (5'–3')
PrrmrRhAPO3C		TATAAGCTTTGAAGAGGAATGAATCCACAGATCAGAAACC
PrrmrRhAPOend		AGCTCGAGTCAAGCGTAATCTGGAACATCGTATGGATACTGAAGAATCTCCCGTAGGCG
CM28		AGCTCGAGTCAAGCGTAATCTGGAACATCGTATGGATACTGGAGACTCTCCCGTAGCCTT
PrrmrRhehu 9.1	rh/hA3C9	AAGGGCTCCAAGATGTGTAC
PrrmrRhehu 9.2		GTACACATCTTGGAGCCCTT
PrrmrRhehu 11.1	rh/hA3C11	CCACCTCCCCTGCACA
PrrmrRhehu 11.2		TGTGCAGGGGAGGTGG
PrrmrRhehu 1.1	rh/hA3C13	TCCACGGTGAAGCACAGC
PrrmrRhehu 1.2		GCTGTGCTTACCCTGGA
PrrmrRhehu 3.1		GTGAGATTCACGTTGCTGTGCCTGGCCAGGAACTTGG
PrrmrRhehu 3.2		CCAAGTTCCTGGCCAGGCACAGCAACGTGAATCTCAC
PrrmrRhehu 1.1	rh/hA3C15	TCCACGGTGAAGCACAGC
PrrmrRhehu 1.2		GCTGTGCTTACCCTGGA
PrrmrRhehu 11.1		CCACCTCCCCTGCACA
PrrmrRhehu 11.2		TGTGCAGGGGAGGTGG
PrrmrRhehu 1.1	rh/hA3C17	TCCACGGTGAAGCACAGC
PrrmrRhehu 1.2		GCTGTGCTTACCCTGGA
PrrmrRhehu 9.1		AAGGGCTCCAAGATGTGTAC
PrrmrRhehu 9.2		GTACACATCTTGGAGCCCTT
PrrmrRhehu 7.1	rh/hA3C31	AGGAAGCACCTTTCTGCATG
PrrmrRhehu 7.2		CATGCAGAAAGGTGCTTCTCT
PrrmrRhehu 3.1		GTGAGATTCACGTTGCTGTGCCTGGCCAGGAACTTGG
PrrmrRhehu 3.2		CCAAGTTCCTGGCCAGGCACAGCAACGTGAATCTCAC
HuA3C-EcoRI-F		ATGAATTCGCCACCATGAATCCACAGATCAGAAAC
HA-NotI-R		ATGCGGCCGCTCAAGCGTAATCTGGAACATC
HuSmmC1 + 2-F	smm/hA3C1 + 2	TCGGAACGAAACTTGGCTGTGCTTC
HuSmmC1 + 2-R		GAAGCACAGCCAAGTTTCGTTCCGA
HuSmmC3 + 4-F	smm/hA3C3 + 4	CCATTGTCATGCAGAAAGGTGCTTCTCTC
HuSmmC3 + 4-R		GAGAGGAAGCACCTTTCTGCATGACAAATGG
HuSmmC5 + 6-F	smm/hA3C5 + 6	TGCAGGGGAGGTGGCCGAGTTCCTGGCCAGG
HuSmmC5 + 6-R		CCTGGCCAGGAACTCGGCCACCTCCCCTGCA
HuSmmC7 + 8-F	smm/hA3C-7 + 8	AGATTTTAAATATTTGTTGGGAAACTTTTGTG
HuSmmC7 + 8-R		CACAAAGTTTCCCAACAATATTTAAATCT
HuSmmC9 + 10-F	smm/hA3C-9 + 10	ATGAGCCATTCAAGCCTTGAAGGGA
HuSmmC9 + 10-R		TCCCTTCCAAGGCTTGAATGGCTCAT
RhA3CCE+QE-F	rhA3C-CE+QE	CAGTATCCGTGTTACCAGGAGGGGCTCCGCAGCCTGAGTCAGGAAGGAGTC
RhA3CCE+QE-R		GACTCCTTCTGACTCAGGCTGCGGAGCCCCTCCTGGTAACACGGATACTG
SmmA3CCE+QE-F	smmA3C-CE+QE	GGGATACATGTTACCAGGAGGGGCTCCGCAGCCTGAGTCAGGAAGGG
SmmA3CCE+QE-R		CCCTTCTGACTCAGGCTGCGGAGCCCCTCCTGGTAACATGTATCCC
HuA3CE106K-F	hA3C E106K	GGAGGTGGCCAAAGTTCCTGGC
HuA3CE106K-R		GCCAGGAACCTTGCCACCTCC
HuA3CQE-EK-F	hA3C QE-EK	AGCCTGAGTGAGAAAGGGGTCGCTG
HuA3CQE-EK-R		CAGCGACCCCTTTCTCACTCAGGCT
HuA3CNQ+EK-F	hA3C NQ+EK	CAGTATCCAAATTACCAGCAGGGGCTCCGCAGCCTGAGTGAGAAAGGG
HuA3CNQ+EK-R		CCCTTTCTCACTCAGGCTGCGGAGCCCCTGCTGGTAATTTGGATACTG
HuA3FDE-HQ-F	hA3F DE-HQ	CTGGGATACACATTACCAGCAGGGGCTC
HuA3FDE-HQ-R		GAGCCCCTGCTGGTAATGTGTATCCAG
HuA3FQE-EK-F	hA3F QE-EK	GCAGCCTGAGTGAGAAAGGGGCTCCG
HuA3FQE-EK-R		CGGAGGCCCTTTCTCACTCAGGCTGC
HIV1Vif-EcorI-F		ATGAATTCGCCACCATGGAAAACAGATGGCAGG
HIV1Vif-NotI-R		ATGCGGCCGCTAGTGTCCATTCAATTGTATGG
F1D-G-NotI-R	F-1 D-G	ATGCGGCCGCTAGTGTCCATTCAATTGTATGGCTCCCTCTGTGGCCCTTGGTC
F1KD-RG-F	F-1K D-RG	AAGCCACCTTTGCCAGTGTTA
F1KD-RG-R		TAACACTGGGCAAAGGTGGCTT
F1K-R-F	F-1 K-R	GCCAGTGTAGGAAACTGACAGAG
F1K-R-R		CTCTGTCAAGTTTCCCTAACACTGGGC
HIV1VIFRR-AA-F	B-NL4-3 RR-AA	GCAAGTAGACGCGATGGCGATTAACACATGG
HIV1VIFRR-AA-R		CCATGTGTTAATCGCCATCGCGTCTACTTGC
HIV1VIFED-AA-F	B-NL4-3 ED-AA	GAAACTGACAGCGGCCAGATGGAAC
HIV1VIFED-AA-R		GTTCCATCTGGCCGCTGTCAGTTTC
HIV1VIFD101G-F	B-NL4-3 D-G	CACAAGTAGACCCTGGCCTAGCAGACC
HIV1VIFD101G-R		GGTCTGCTAGGCCAGGGTCTACTTGTG

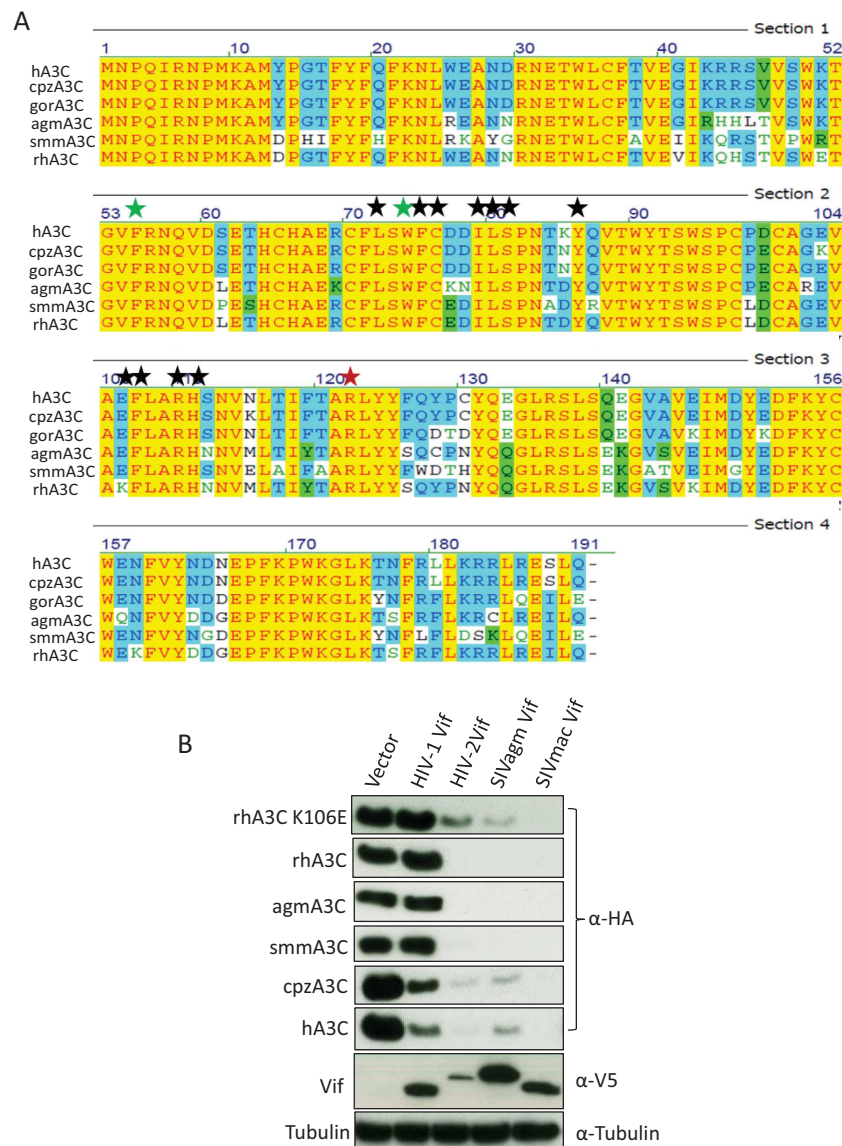


FIG 1 Sensitivity of primate A3C to lentiviral Vifs. (A) Sequence alignment of primate A3C proteins. Black stars represent important residues for HIV-1 Vif interaction. Green stars indicate the dimerization of A3C protein and anti-SIV activity. The red star is the A3C RNA binding site and indicates its viral incorporation. (B) 293T cells were cotransfected with A3C and HIV-1, HIV-2, SIVagm, or SIVmac Vif expression plasmids. Expression of A3Cs, Vifs, and tubulin was detected by immunoblotting using anti-HA, anti-V5, and anti-tubulin antibodies, respectively. h, cpz, gor, agm, smm, and rh represent human, chimpanzee, gorilla, African green monkey, sooty mangabey monkey, and rhesus monkey, respectively.

viruses, 293T cells were cotransfected with 650 ng SIVmac-Luc (R-E-) or SIVmac-Luc (R-E-)ΔVif, 150 ng A3C expression plasmid, 25 ng vesicular stomatitis virus glycoprotein (VSV-G) plasmid (pMD.G), or 200 ng HIV-1 Vif expression plasmid; in some experiments pcDNA3.1(+) was used instead of Vif or A3C expression plasmids. For HIV-1-luciferase viruses, transfection experiments in 6-well plates consisted of 300 ng of the HIV-1 packaging construct pMDLg/RRE, 130 ng of HIV-1 Rev expression plasmid pRSV-Rev, 300 ng of the HIV-1 reporter vector pSIN.PPT.CMV.Luc.IRES.GFP, 100 ng of the VSV-G expression plasmid pMD.G, and 800 ng HIV-1 Vif together with 800 ng hA3F expression plasmids. pcDNA3.1(+) was used instead of HIV-1 Vif or hA3F. At 48 h posttransfection, cells and supernatants were collected. The reverse transcriptase (RT) activity of SIVmac and HIV-1 was quantified by using the Cavid HS lenti RT kit (Cavidi Tech, Uppsala, Sweden). For reporter virus infection, 293T cells were seeded in 96-well plates 1 day before transduction. After

normalizing for RT activity, the same amounts of viruses were used for infection. Two days posttransduction, firefly luciferase activity was measured with the SteadyLite HTS reporter gene assay system (Perkin-Elmer, Cologne, Germany) according to the manufacturer's instructions on a MicroLumat Plus luminometer (Berthold Detection Systems, Pforzheim, Germany). Each sample was analyzed in triplicate; the error bars for each triplicate are shown.

Immunoblot analysis. Transfected 293T cells were lysed in radioimmunoprecipitation assay (RIPA) buffer (25 mM Tris-HCl [pH 8.0], 137 mM NaCl, 1% NP-40, 1% glycerol, 0.5% sodium deoxycholate, 0.1% sodium dodecyl sulfate [SDS], 2 mM EDTA, and protease inhibitor cocktail set III [Calbiochem, Darmstadt, Germany]). To pellet virions, culture supernatants were centrifuged at 12,000 rpm for 10 min, subjected to centrifugation through a 20% sucrose cushion at 35,000 rpm in an SW40 Ti rotor for 1.5 h, and resuspended in RIPA buffer. The solution was

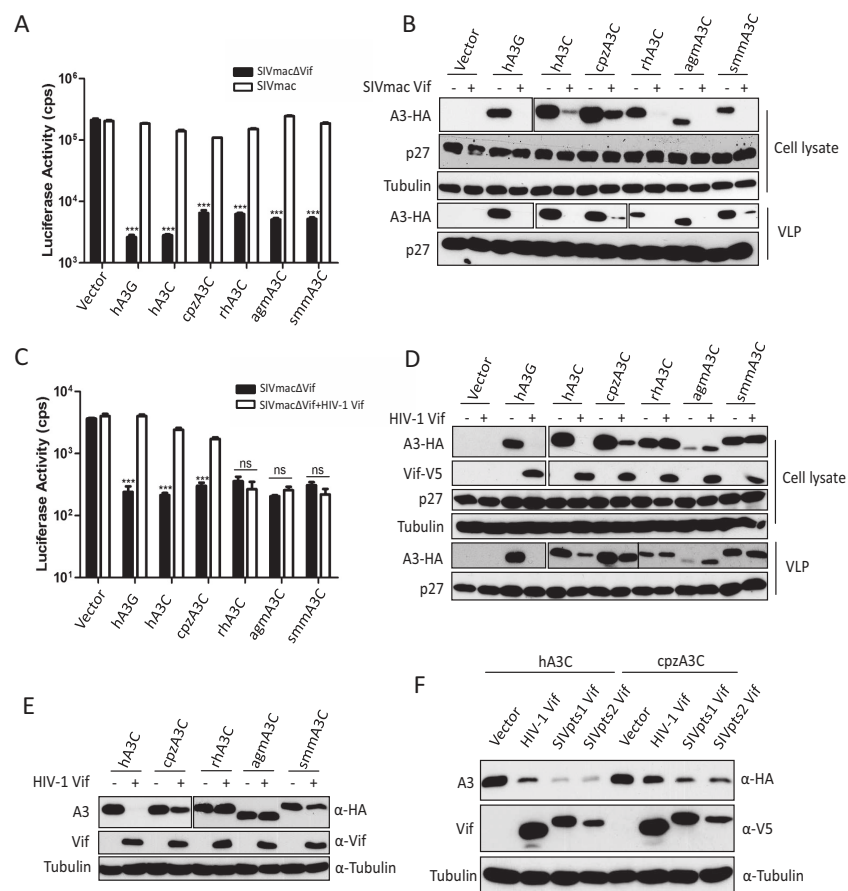


FIG 2 SIVmac Vif, but not HIV-1 Vif, counteracts primate A3Cs. (A and C) 293T cells were transfected with expression plasmids for SIVmacΔVif-Luc or SIVmac-Luc (A) or SIVmacΔVif-Luc or SIVmacΔVif-Luc plus HIV-1 Vif (C), together with expression plasmids for hA3G and primate A3Cs. pcDNA3.1(+) was used as a control (vector). After normalizing for reverse transcriptase activity, viral infectivity was determined by quantification of luciferase activity in 293T cells. (B and D) Lysates of SIVmac producer cells were used to detect the expression of A3s, SIVmac capsid (p27), or HIV-1 Vif by anti-HA, anti-p27, or anti-V5 antibody, respectively. Tubulin served as a loading control. Encapsidation of A3s into SIVmac was detected by anti-HA antibody. (E) Primate A3Cs and HIV-1 Vif (without tag) expression plasmids were cotransfected into 293T cells. The expression of A3C and HIV-1 Vif was detected by anti-HA and anti-Vif antibodies. (F) Expression plasmids for hA3C and cpzA3C were cotransfected with HIV-1 Vif or SIVcpz Vif into 293T cells. The expression of A3C and Vif was detected by anti-HA and anti-V5 antibodies. Pts, *Pan troglodytes schweinfurthii*. cps, counts per second. VLP, virus-like particle. Asterisks represent statistically significant differences: ***, $P < 0.001$; ns, no significance (Dunnett's t test).

boiled at 95°C for 5 min with Roti load-reducing loading buffer (Carl Roth, Karlsruhe, Germany) and resolved on an SDS-PAGE gel. The expression of A3s and lentivirus Vif was detected by mouse anti-HA antibody (1:7,500 dilution; MMS-101P; Covance, Münster, Germany) and mouse anti-V5 antibody (1:4,500 dilution; MCA1360; ABD Serotec, Düsseldorf, Germany) separately. HIV-1 Vifs from different subtype strains were detected by rabbit anti-Vif polyclonal antibody (1:1,000 dilution; catalog no. 2221; NIH AIDS Research and Reference Reagent Program) (80). Tubulin, SIVmac, and HIV-1 capsid proteins were detected using mouse anti- α -tubulin antibody (1:4,000 dilution; clone B5-1-2; Sigma-Aldrich, Taufkirchen, Germany) and mouse anti-capsid p24/p27 monoclonal antibody AG3.0 (1:50 dilution) separately (81), followed by horseradish peroxidase-conjugated rabbit anti-mouse or donkey anti-rabbit antibody (α -mouse or rabbit-IgG-horseradish peroxidase; GE Healthcare, Munich, Germany), and developed with ECL chemiluminescence reagents (GE Healthcare).

IP. To determine Vif and A3 binding, 293T cells were cotransfected with 1 μ g HIV-1 Vif.SLQ-AAA and 1 μ g wild-type or mutant A3 or with pcDNA3.1(+). Forty-eight hours later, the cells were lysed in immunoprecipitation (IP) lysis buffer (50 mM Tris-HCl pH 8, 1 mM phenylmethylsulfonyl fluoride [PMSF], 10% glycerol, 0.8% NP-40, 150 mM NaCl,

and complete protease inhibitor; Roche, Penzberg, Germany). The lysates were cleared by centrifugation. The supernatant were incubated with 20 μ l α -HA affinity matrix beads (Roche) at 4°C for 2 h. The samples were washed 5 times with lysis buffer. Bound proteins were eluted by boiling the beads for 5 min at 95°C in SDS loading buffer. Immunoblot analysis and detection were done as described above.

Model structure. To analyze the interaction surface between HIV-1 Vif and hA3C/A3F, the hA3C (PDB entry 3VOW), hA3F C-terminal (PDB entry 4J4J), and HIV-1 Vif (PDB entry 4N9F) structures were used. The structural models of F-1 Vif and mutants were built by the SWISS-MODEL online server (<http://www.swissmodel.expasy.org/>) (82) using B-NL4-3 Vif (PDB entry 4N9F) as a template. The graphical visualizations shown in Fig. 8 and 9 were constructed using PyMOL (PyMOL Molecular Graphics System, version 1.5.0.4; Schrödinger, Portland, OR).

Statistical analysis. Data are represented as the means with standard deviations (SD) in all bar diagrams. Statistically significant differences between two groups were analyzed using the unpaired Student's t test with GraphPad Prism, version 5 (GraphPad Software, San Diego, CA, USA). A minimum P value of 0.05 was considered statistically significant. A P value of <0.001 was extremely significant (***) , 0.001 to 0.01 very significant (**), 0.01 to 0.05 significant (*), and >0.05 not significant (ns).

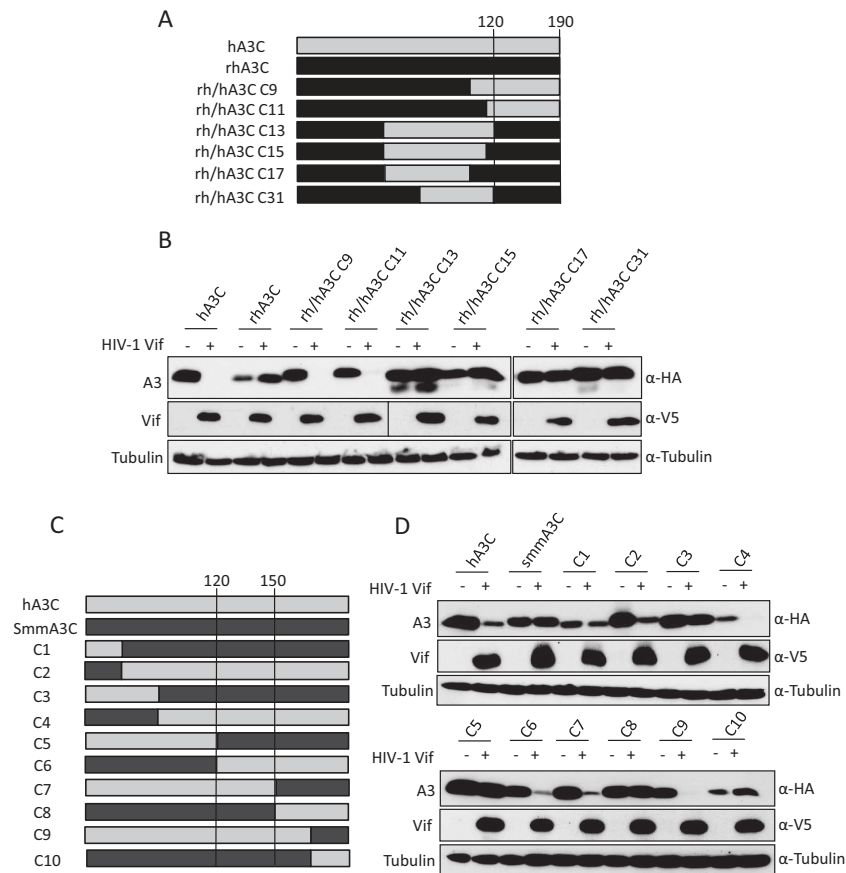


FIG 3 Sensitivity of rh/hA3C and h/smmA3C chimeras to HIV-1 Vif-mediated depletion. (A and C) Schematic structure of rh/hA3C and h/smmA3C chimeras. Amino acid positions 120, 150, and 190 in hA3C are indicated. (B and D) Immunoblots of protein lysates of cotransfected cells displaying the A3's sensitivity to HIV-1 Vif-triggered degradation. The expression of A3s and HIV-1 Vif were analyzed by using anti-HA and anti-V5 antibodies. Tubulin served as a loading control. +, with HIV-1 Vif; -, without HIV-1 Vif.

Accession number(s). Sequences for human A3C (NM_014508.2), chimpanzee A3C (NM_001251910.1), gorilla A3C (AH013821.1), African green monkey A3C (EU381232.1), sooty mangabey monkey A3C (KX405162), rhesus monkey A3C (JF714486.1), SIVpts1 (Tan1) (EF394356.1), and SIVpts2 (Tan2) (EF394357.1) were deposited in NCBI.

RESULTS

The sensitivity of primate A3C to lentiviral Vif. A previous study has identified several residues in the hydrophobic V-shaped groove formed by the $\alpha 2$ and $\alpha 3$ helices of A3C involved in HIV-1 Vif interaction (63). This interaction interface is conserved in primate A3C proteins, although rhA3C has one substitution (E to K) at position 106 (Fig. 1A). To test the sensitivities of these A3C proteins to HIV-1 Vif, cotransfections of expression plasmids for A3Cs and HIV-1 Vif were performed. A3C steady-state levels were assessed by immunoblotting protein lysates of coexpressing cells. Previous studies demonstrated that both SIVagm and HIV-1 Vif were able to induce the degradation of human A3C by the proteasome (83). Based on this finding, we assume that the dominant mechanism of Vif against A3C in our study is Vif-triggered degradation of A3 as well. Results show that HIV-1 Vif reduced the stability of hA3C and cpzA3C, while smmA3C, agmA3C, and rhA3C were resistant (Fig. 1B). smmA3C was cloned from a white-crowned mangabey (*Cercocebus torquatus lunulatus*), which is one of the three subspecies of sooty mangabey monkeys.

The resistance of smmA3C to HIV-1 Vif was unexpected, because the previously identified HIV-1 Vif interaction sites were identical between smmA3C and hA3C (Fig. 1A). HIV-1 Vif's block to deplete rhA3C may be caused by an E-to-K substitution at position 106. To prove this, we made a K106-to-E mutation in rhA3C and tested its sensitivity to HIV-1 Vif. However, the results showed that rhA3C.K106E still could not be degraded by HIV-1 Vif (Fig. 1B). These observations indicate that sites in addition to the already characterized residues in A3C are involved in the HIV-1 Vif interaction. We also observed that HIV-2, SIVmac, and SIVagm Vif depleted all A3C proteins, including rhA3C.K106E (Fig. 1B). These data suggest that Vif proteins from diverse HIV/SIV lineages have distinct binding sites in A3C which mediate its degradation.

We next tested the anti-SIVmac activities of these primate A3C proteins in the presence of SIVmac or HIV-1 Vif proteins. Luciferase reporter viruses of SIVmac, SIVmac Δ Vif, and SIVmac Δ Vif plus Vif of HIV-1 were produced with hA3G, hA3C, cpzA3C, rhA3C, agmA3C, or smmA3C. The Vif-proficient virus SIVmac-Luc expresses Vif in its natural expression context; however, Vif lacks an epitope tag for detection. Viral particles were normalized by RT activity, and the luciferase activity of infected cells was quantified 2 days postinfection. All A3C proteins strongly inhibited the infectivity of Vif-deficient SIVmac, which was fully coun-

teracted by SIVmac Vif, as was hA3G (Fig. 2A). The immunoblots of virus-producing cells indicated that SIVmac Vif reduced the stability of hA3G and all primate A3C proteins, which resulted in viral particles with much reduced A3 content (Fig. 2B). However, HIV-1 Vif counteracted the anti-SIVmac activity of hA3G, hA3C, and cpzA3C, and rhA3C, agmA3C, and smmA3C displayed resistance to HIV-1 Vif (Fig. 2C). The immunoblots showed that HIV-1 Vif decreased the protein level of hA3G, hA3C, and cpzA3C in cell lysates and viral particles but not that of rhA3C, agmA3C, and smmA3C (Fig. 2D). Since the HIV-1 Vif we used here contained a C-terminal V5 tag, we wondered whether the V5 tag in Vif would contribute to the Vif resistance of rhA3C, agmA3C, and smmA3C. We then tested the sensitivity of A3Cs to untagged HIV-1 Vif. We found that hA3C and cpzA3C were sensitive to antagonization by untagged HIV-1 Vif, whereas rhA3C, agmA3C, and smmA3C still were not degraded (Fig. 2E). Thus, the V5 tag in Vif did not contribute to the HIV-1 Vif resistance of rhA3C, agmA3C, and smmA3C. It is important to point out that cpzA3C was less efficiently depleted from cells by HIV-1 Vif (untagged and V5 tagged) than hA3C (Fig. 2D and E). The immunoblotting results showed that SIVcpz (SIVpts1 and SIVpts2) Vifs displayed stronger activity against hA3C and cpzA3C than HIV-1 Vif (Fig. 2F).

Identification of specific rh/smmA3C residues involved in resistance to HIV-1 Vif. The results from Fig. 1B suggest that additional sites in hA3C are involved in the interaction with HIV-1 Vif. To identify the additional determinants, several rh/hA3C chimeras were constructed. Structures of A3 chimeras are shown in Fig. 3A, and their sensitivities to HIV-1 Vif were determined by immunoblotting of cell lysates expressing Vif and individual A3 constructs. The results showed that hA3C chimera 9 and chimera 11 were sensitive to HIV-1 Vif-mediated depletion, while rhA3C chimeras 13, 15, 17, and 31 were resistant and not degraded (Fig. 3B). The composition of the chimeras indicated that the C terminus (from amino acids 120 to 190) of rhA3C determined the resistance to HIV-1 Vif. smmA3C was also resistant to HIV-1 Vif-induced degradation (Fig. 1A). To narrow the scope of residues in A3C that are involved in the HIV-1 Vif interaction, 10 chimeras of human A3C and smmA3C were produced. The structures of smm/hA3C chimeras are displayed in Fig. 3C. We found that hA3C chimeras 2, 4, 6, 7, and 9 could be depleted by HIV-1 Vif, while smmA3C and other chimeras evidently were not degraded (Fig. 3D). Based on these results, amino acids 120 to 150 of smmA3C were identified as an essential domain that confers resistance to HIV-1 Vif.

To identify the residues in rhA3C and smmA3C that are important for resistance to HIV-1 Vif-mediated counteraction, we compared the amino acids from 120 to 150 in primate A3C proteins, and four residues (130, 133, 140, and 141) were selected for further characterization. In hA3C and cpzA3C these residues are C130, E133, and 140QE141, while in agmA3C, rhA3C, and smmA3C these four positions are N/H130, Q133, and 140EK141, respectively (Fig. 1A). Thus, we mutated N130, Q133, and 140EK141 in rhA3C to the residues found in hA3C, termed rhA3C.CE+QE. Based on this construct, we performed the single-amino-acid substitution K106E, named rhA3C.K106E-CE+QE (Fig. 4A), because E106 in hA3C indicates it is binding to HIV-1 Vif (65). For smmA3C, four amino acid substitutions were produced, and the construct was termed smmA3C.CE+QE (Fig. 4A). The sensitivities of these constructs together with wild-type hA3C, rhA3C, and smmA3C to HIV-1 Vif-triggered de-

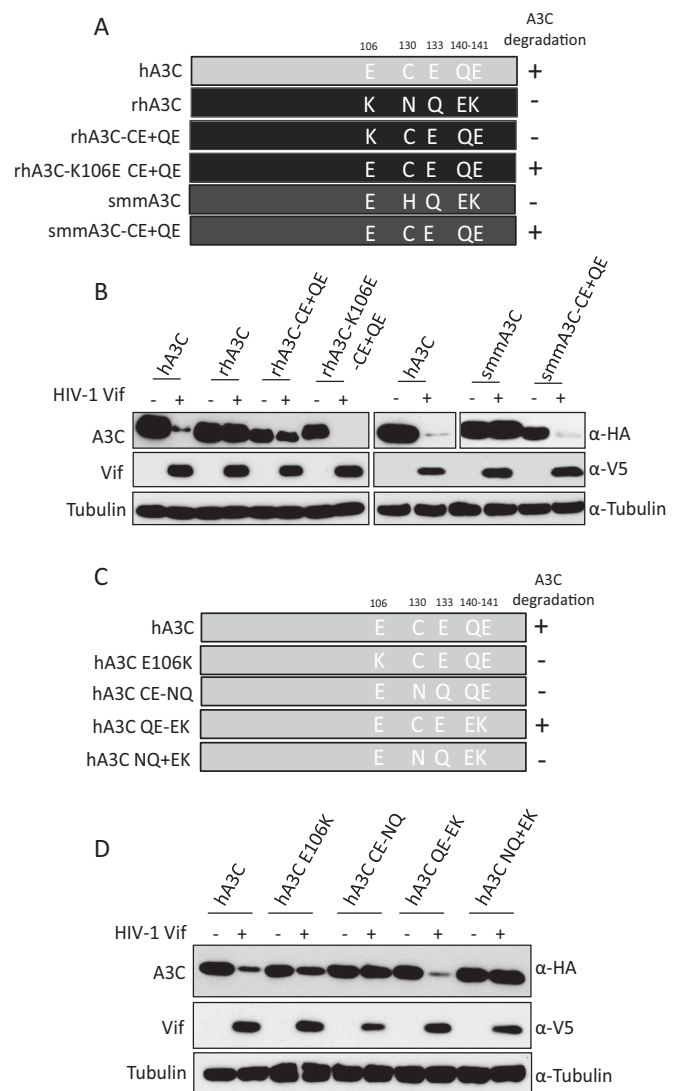


FIG 4 Identification of determinants in rhA3C and smmA3C that confer resistance to HIV-1 Vif. (A) The schematic structure of rhA3C and smmA3C mutants. The numbers represent amino acid positions in A3C. +, sensitive to HIV-1 Vif-induced degradation; -, resistant to HIV-1 Vif-induced degradation. (B and D) hA3C, rhA3C, smmA3C, or A3C mutants were cotransfected with HIV-1 Vif into 293T cells. A3, HIV-1 Vif, and tubulin were detected by using anti-HA, anti-V5, and anti-tubulin antibodies, respectively. (C) Schematic structure of hA3C mutants.

pletion were tested by immunoblotting. The results showed that rhA3C.CE+QE was still resistant to HIV-1 Vif, but rhA3C.K106E-CE+QE was sensitive to hA3C (Fig. 4B). This result confirmed the importance of E106 in hA3C involvement in the HIV-1 Vif interaction. The smmA3C.CE+QE protein was depleted by HIV-1 Vif, which suggests that C130, E133, and 140QE141 are also important for HIV-1 Vif-mediated degradation. In addition, the equivalent residues (C130, E133, and 140QE141) in hA3C were replaced by N130, Q133, and 140EK141, respectively, producing hA3C.CE-NQ, hA3C.QE-EK, and hA3C.NQ+QE (Fig. 4C). hA3C.E106K, which could not be antagonized by HIV-1 Vif, was used as a control. The results showed that hA3C.E106K was partially resistant to HIV-1 Vif but that hA3C.QE-EK was depleted (Fig. 4D), showing consis-

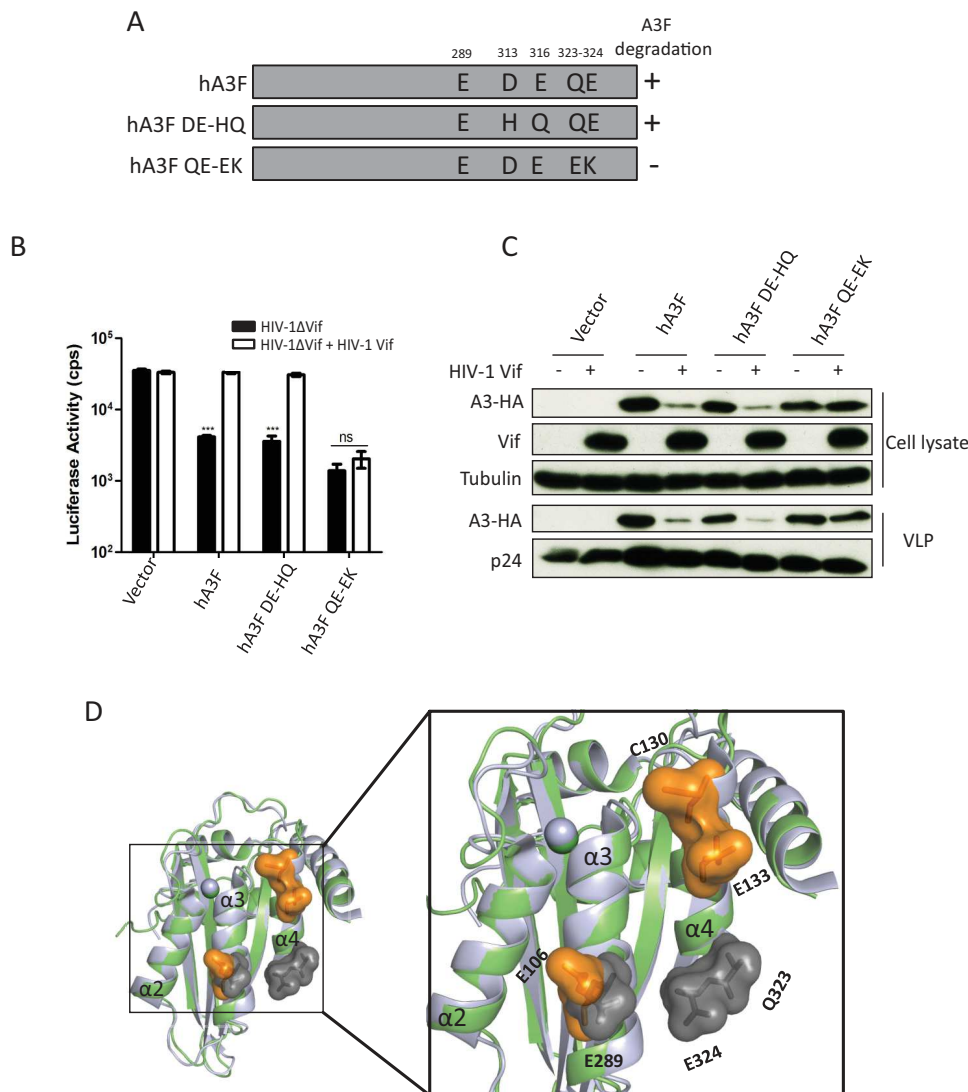


FIG 5 hA3F residues and HIV-1 Vif-induced depletion. (A) The schematic structure of hA3F mutants. +, sensitive to HIV-1 Vif induced degradation; -, resistant to HIV-1 Vif-induced degradation. (B) HIV-1 Δ Vif luciferase or HIV-1 Δ Vif luciferase plus HIV-1 Vif were produced in 293T cells in the presence of A3F or mutants. After normalizing for reverse transcriptase activity, viral infectivity was determined by quantification of luciferase activity in 293T cells. (C) A3s in HIV-1 producer cells and HIV-1 viral particles were detected by using anti-HA antibody. HIV-1 Vif and capsid (p24) were detected by anti-Vif and anti-p24 antibodies, respectively. Tubulin served as a loading control. (D) Superimposition of A3C crystal structure (PDB entry 3VOW) (green) and A3F-CTD crystal structure (PDB entry 4J4J) (light blue). Key residues E106, C130, and E133 are shown as orange surfaces in A3C with labels, and the essential residues (E289, Q323, and E324) in A3F are highlighted with gray surfaces and labels. cps, counts per second. Asterisks represent statistically significant differences: ***, $P < 0.001$; ns, no significance (Dunnett's t test).

tency with previous studies (63). Moreover, we found that hA3C.CE-NQ and hA3C.NQ+EK were resistant to HIV-1 Vif-mediated degradation (Fig. 4D). Taken together, these results demonstrate that residues 106, 130, and 133 of primate A3C proteins determine their sensitivities to HIV-1 Vif, but residues 140QE141 were unimportant for HIV-1 Vif interaction.

A3F and A3C have distinct Vif interaction interfaces. After identification of the residues C130 and E133 in hA3C as being important for interaction with HIV-1 Vif, we expanded our experiments to hA3F. The equivalent residues (D313 and E316) in hA3F were replaced by H313 and Q316, which were present in rhA3F. In addition, we altered amino acids Q323E and E324K in hA3F (Fig. 5A). We analyzed the anti-HIV-1 activity of these hA3F

mutants in the presence of HIV-1 Vif. HIV-1 Vif restored the infectivity in the presence of hA3F and hA3F.DE-HQ, while hA3F.QE-EK displayed antiviral activity in the presence and absence of HIV-1 Vif (Fig. 5B). The corresponding immunoblots of virus-producing cells showed that HIV-1 Vif reduced the steady-state level of hA3F and hA3F.DE-HQ but not of hA3F.QE-EK (Fig. 5C). Q323E and E324K alterations in hA3F impaired HIV-1 Vif-mediated depletion, consistent with previous studies (63, 67). However, we and other groups also observed that the equivalent residues (Q140 and E141) in hA3C were unimportant for HIV-1 Vif interaction (63) (Fig. 4D). We then compared the structures of hA3C and the C-terminal domain of hA3F and highlighted the HIV-1 Vif interaction surface investigated in our study. As shown

in Fig. 5D, residue E106 in hA3C and the corresponding residue E289 in hA3F, which are located in the $\alpha 3$ helices, were involved in HIV-1 Vif interaction. In the $\alpha 4$ helices, the HIV-1 Vif interaction surface differs in hA3C and hA3F, shifting from the top to the bottom of $\alpha 4$ helices (Fig. 5D). Taken together, these results indicate that the Vif-A3 interaction interfaces in hA3C and hA3F are different.

To clarify whether the identified residues of A3C and A3F were directly involved in Vif binding, coimmunoprecipitation (co-IP) assays of Vif.SLQ/AAA, which binds A3s without inducing their degradation, were performed with HA-tagged A3C and A3F. Because the expression levels of primate A3C and several mutants were distinct, ImageJ software was used to evaluate the band density of A3C and Vif from immunoprecipitation. The ratio of Vif to A3 was calculated as A3-Vif binding activity in which we set wild-type A3C-Vif or wild-type A3F-Vif binding activity as 100%. As shown in Fig. 6, rhA3C and its mutant, rhA3C-K106E-CE+QE, which was sensitive to HIV-1 Vif, immunoprecipitated with HIV-1 Vif (Fig. 6A); however, binding was much reduced compared to Vif binding to hA3C. The smmA3C and smmA3C.CE+QE protein levels were much lower in the cell lysates, so they precipitated less than hA3C in co-IP complexes, whereas the amount of detected HIV-1 Vif was similar to that of the hA3C-Vif complex (Fig. 6A), indicating that smmA3C has high binding activity to HIV-1 Vif (Fig. 6B). The hA3C.E106K and hA3C.QE-EK mutants showed very low HIV-1 Vif binding, which was consistent with a previous study (63). However, hA3C.CE-NQ, which was not degraded by HIV-1 Vif, pulled down similar amounts of Vif compared to the wild-type hA3C-Vif complex (Fig. 6A). The HIV-1 Vif binding capacities of hA3F and hA3F.DE-HQ were similar, corresponding to similar sensitivities to HIV-1 Vif (Fig. 5B and 6B). Significantly reduced amounts of Vif were pulled down by hA3F.QE-EK, suggesting hA3F residues 323QE324 were involved in Vif binding. RhA3C and smmA3C were totally resistant to HIV-1 Vif-induced degradation (Fig. 4B and D); however, both of these proteins showed robust binding to HIV-1 Vif, suggesting that the Vif binding detected by co-IPs is unrelated to Vif-mediated degradation.

Internal salt bridge of Vif protein influences degradation of hA3C/F. Previous studies have identified three motifs of HIV-1 Vif specifically involved in the interaction with hA3F: the F1 box (14DRMR17), F2 box (74TGEDW79), and F3 box (171EDRW174) (66, 84). To identify additional determinants in HIV-1 Vif relevant for interaction with hA3C/F, 21 HIV-1 Vif alleles (71) were used for detecting their hA3C counteractivity, including five Vifs isolated from HIV-1 N and O subtypes. All Vif alleles were detectable by anti-Vif polyclonal antibody (Fig. 7A). The Vif variants (C1, C2, and C3) displayed lower-level signals in the immunoblots than the other Vifs, which might be caused by weaker antibody recognition (Fig. 7A). The 21 Vif alleles depleted hA3C to various degrees. To evaluate the degree of this counteraction, ImageJ was used to calculate the density of hA3C bands in which hA3C cotransfected with empty vector plasmid was set as the control (100% expression). The results showed that 10 Vif variants (A2, B-NL4-3, B-LAI, C3, D2, F-3, F-4, O-119, O-127, and N-116) strongly depleted hA3C (Fig. 7A and B). All other Vif variants, except Vif from F-1, moderately reduced the protein level of hA3C. The F-1 Vif had an expression level similar to those of B-NL4-3 and B-LAI Vif, but almost 80% of hA3C could be detected in the presence of F-1 Vif (Fig. 7A and B). A previous

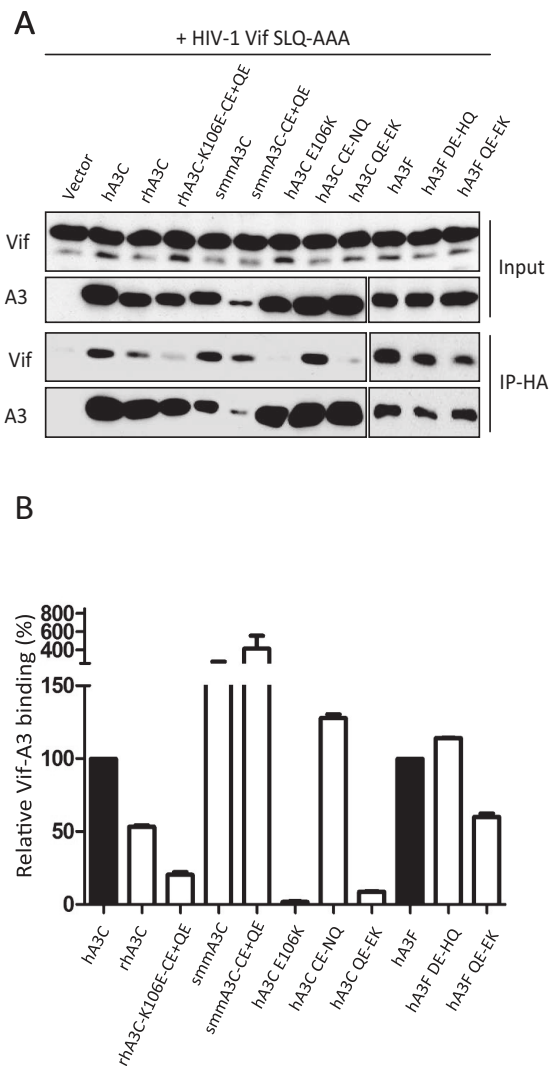


FIG 6 HIV-1 Vif binding to A3C and A3F mutants. (A) Coimmunoprecipitation of HIV-1 Vif SLQ/AAA with A3C and A3F mutants. Protein cell lysates (Input) and immunoprecipitated complexes (IP) were analyzed by immunoblotting with anti-Vif for HIV-1 Vif or anti-HA for A3. (B) ImageJ was used to evaluate the band density of A3C and Vif from immunoprecipitation. The ratio of Vif to A3 was calculated as A3-Vif binding activity. WT A3C-Vif and WT A3F-Vif binding activity was set as 100%.

study demonstrated that F-1 Vif, but not Vif from F-2 and B-NL4-3, could mediate the degradation of hA3H hapII (71). To understand whether the resistance of hA3C to F-1 Vif is specific, three Vif variants (B-NL4-3, F-1, and F-2) were tested for counteraction of hA3H hapII, hA3G, hA3F, and hA3C. The results showed that the protein levels of both hA3C and hA3F could be reduced by B-NL4-3 and F-2 Vif but displayed resistance to F-1 Vif. hA3G was strongly depleted by these three Vif variants, while hA3H hapII was resistant to B-NL4-3 and F-2 Vif but sensitive to F-1 Vif (Fig. 7C), consistent with previous data (71). Taken together, these results indicated that the differences between F-1, F-2, and B-NL4-3 Vifs determine specific degradation of hA3C/F.

After analyzing the sequences of B-NL4-3, F-1, and F-2 Vif, six residues outside the CUL5 and BC boxes were identified (positions 39, 48, 61, 62, 167, and 182) where all three Vifs differed from

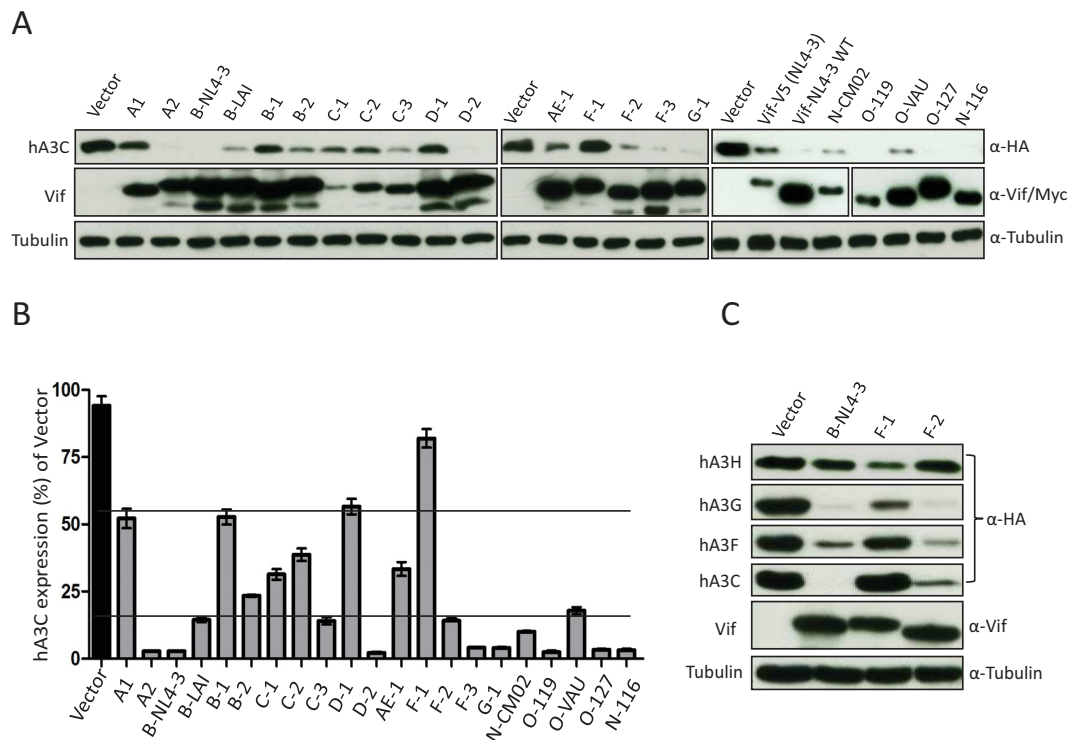


FIG 7 hA3C depletion activities of HIV-1 Vif alleles. (A) The 21 HIV-1 Vif alleles induced depletion of hA3C to various degrees. hA3C and Vif alleles were cotransfected into 293T cells. Protein extracts of transfected cells were used for detecting the expression of hA3C, Vif, and tubulin by anti-HA, anti-Vif, and anti-tubulin antibodies, respectively. Vifs from N and O subtypes were detected by anti-myc antibody. This A3C experiment was repeated at least three times with similar results. (B) ImageJ was used to evaluate the band density of A3C and tubulin. The ratio of A3C to tubulin was calculated as A3C expression efficiency. A3C plasmid cotransfected with empty vector plasmid was set as 100% expression. (C) hA3C, hA3F, hA3G, and hA3H hapII expression plasmids were transfected together with B-NL4-3 expression plasmids and F-1 and F-2 Vif variants. A3 and Vif were detected by using anti-HA and anti-Vif antibodies. Tubulin served as a loading control.

each other. Residues F39 and H48 in Vif determine the interaction with hA3H hapII (71). Based on the structure of Vif, residues 61 and 62 are on the other side of the F box that was identified for the interaction with hA3F. Thus, we focused on residues 167 and 182 in F-1 Vif. K167 and D182 in F-1 Vif were mutated to R and G, which are the corresponding residues in B-NL4-3 Vif both separately and in combination (Fig. 8A). Wild-type Vif and Vif mutants were tested in coexpression experiments for their effect on the steady-state levels of hA3C and hA3F. The immunoblot showed that replacing K167 with arginine recovered the F-1 Vif depletion activity against hA3C, while the introduction of glycine at position 182 did not help much to enhance A3C reduction (Fig. 8B). However, both K167R and D182G exchanges activated F-1 Vif counteraction of hA3F, which suggests that G182 is important for degradation of hA3F but not hA3C (Fig. 8B). We next replaced K167 in F-1 Vif by a negatively charged amino acid, D/E, as well as a nonpolar alanine, and analyzed their hA3C/hA3F inhibitory activities. We found that mutants K167A, K167D, and K167E depleted hA3C/hA3F as efficiently as B-NL4-3 Vif (Fig. 8C). The F3 box (171EDRW174) that interacts with hA3C/F is conserved in B-NL4-3 and F-1 Vif (Fig. 8A). Thus, we wondered whether the F3 box in F-1 Vif is still essential for inhibition of hA3C/hA3F. To address this question, 171ED172 to 171AA172 mutations were generated in both F-1 wild-type Vif and F-1 Vif.K167R constructs. The immunoblot revealed that replacing K167 with R recovered the F-1 Vif activity against hA3C/hA3F, but mutations in the F3

box together with K167R impaired degradation, suggesting that the F3 box in F-1 Vif is still key to the function of interaction with hA3C/hA3F (Fig. 8D). The Vifs from B-NL4-3 and F-1 share 90.3% identical residues. Thus, we modeled the structures of F-1 Vif and its mutants using the structure of B-NL4-3 Vif (PDB entry 4N9F) as a template and analyzed the interactions of residues 171 and 167 within these model variants. We found that E171 and K167 displayed a strong interaction in the F-1 Vif, while the models of K167A, K167D, and K167E displayed no interaction (Fig. 8E). Taken together, these results suggest that the side-chain interaction of E171 and K167 affect hA3C/hA3F-Vif interaction induced by E171, resulting in an F-1 Vif being inactive in the induction of the degradation of hA3C/hA3F.

Additionally, we exchanged R167 and G182 in B-NL4-3 Vif for K and D, which were found in F-1 Vif. As controls we included F2 and F3 box mutants (B-NL4-3.RR-AA and B-NL4-3.ED-AA). Wild-type Vif and Vif mutants were tested for affecting the protein stability of hA3C, hA3F, and hA3G in Vif/A3 coexpression experiments. The results showed that mutations in the F2 box and the F3 box indeed impaired Vif activity against hA3C and hA3F but not against hA3G (Fig. 9A). Surprisingly, substitution R167K or G182D or the combination of both mutations did not impair depletion of hA3C, hA3F, and hA3G by B-NL4-3 Vif (Fig. 9A). To analyze the internal structural changes of the R167K Vif mutant, we modeled the structures of B-NL4-3 Vif.R167K and analyzed the E171-K167 interaction. We found that residue K167 in

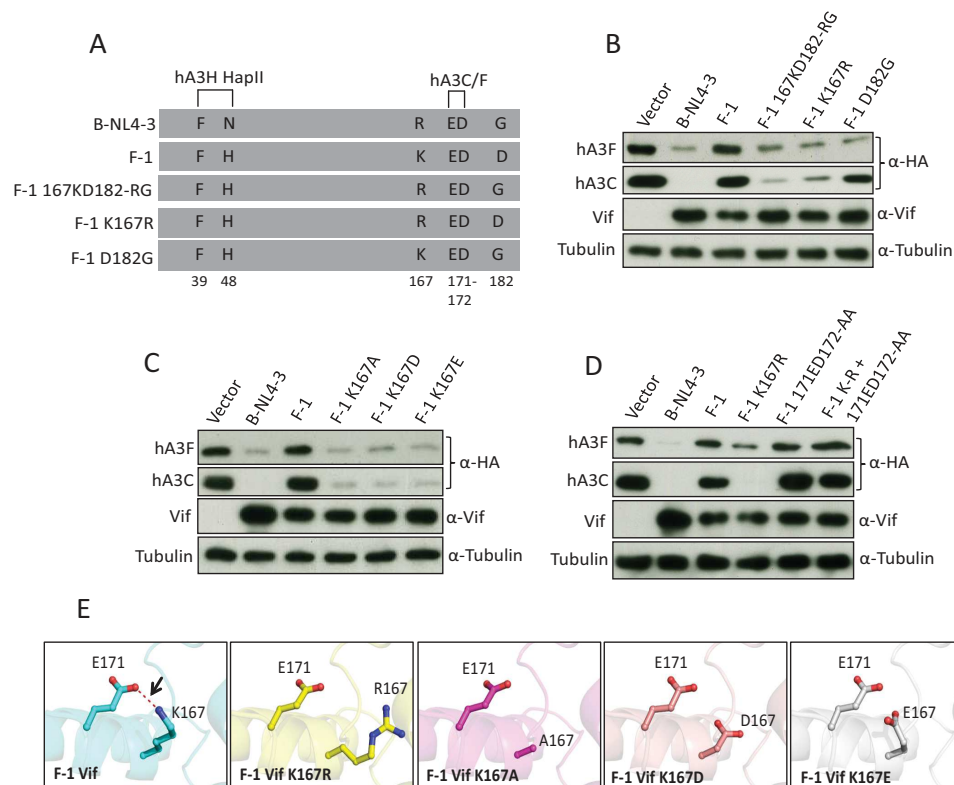


FIG 8 Identification of important residues in subtype F-1 Vif that determine its counteraction of hA3C/F. (A) Schematic structure of F-1 Vif mutants. The N-terminal hA3H hapII box and C-terminal hA3C/F box are shown. (B, C, and D) hA3C and hA3F were transfected into 293T cells together with B-NL4-3 Vif or with F-1 Vif or F-1 Vif mutant. A3 and Vif were detected by using anti-HA and anti-Vif antibodies. Tubulin served as a loading control. (E) The structures of wild-type F-1 Vif and F-1 Vif mutants were modeled by SWISS modeling. The internal interaction between residues 171 and 167 was analyzed by PyMOL and is shown as a red dashed line.

B-NL4-3 Vif.R167K preferred to interact with D101 but not with E171 (Fig. 9B). In F-1 Vif, a glycine was present at position 101 which had no chance to form an internal interaction with K167 (Fig. 9B). Thus, replacing D101 in B-NL4-3 Vif.R167K with glycine could rebuild the connection of E171-K167 (Fig. 9B). To test this hypothesis, we analyzed the counteractivity of B-NL4-3 Vif.D101G and B-NL4-3 Vif.D101G+R107K against different amounts of hA3C- or hA3F-transfected (150 ng, 250 ng, or 350 ng) expression plasmid. We found that B-NL4-3 Vif.D101G+R107K reduced the capacity to induce depletion of hA3F and hA3C compared with B-NL4-3 wild-type Vif (Fig. 9C). As shown in Fig. 9D, three discontinuous motifs (shown in red) in Vif (B-NL4-3) formed the hA3F and hA3C interaction surface, while the residues R167 and D101, which determined internal interaction with the F3 box, are shown in magenta (Fig. 9D). Taken together, these results suggest that internal interactions in the Vif protein can also influence the Vif-A3 interaction.

DISCUSSION

The antiviral activity of A3C against HIV-1 Δ Vif is not as potent as that of A3G and A3F. While several studies found no antiviral activity of hA3C, others reported that the infectivity of HIV-1 Δ Vif can be reduced by 50% by hA3C and restored by its Vif protein (11, 19–23, 26–28). We do not know whether Δ Vif mutants of the various HIV-1 subtypes differ in their sensitivity to hA3C. However, of the 21 Vif isolates we tested here from HIV-1 group M, N,

and O subtypes, only four Vifs (A-1, B-1, D-1, and F-1) showed reduced counteractivity to hA3C. Thus, the capacity of HIV-1 Vifs to counteract hA3C is highly conserved. Our data indicate that HIV-1 Vif uses a different binding surface to interact with A3C and the related A3F and that impairing the anti-A3C/A3F activity does not prevent the counteraction of A3G.

A previous study identified several hydrophobic or negatively charged residues between the α 2 and α 3 helix of hA3C that bind to HIV-1 Vif (63), and it was also reported that C130A, C130L, and E133A substitutions in hA3C did not impair HIV-1 Vif-induced degradation. However, in our study, replacement of C130 and E133 in hA3C with residues N130 and Q133, which are found in rhA3C (hA3C CE-NQ mutant in Fig. 4C), resulted in resistance to HIV-1 Vif (Fig. 4D). Both cysteine and asparagine residues belong to polar amino acids, but the E133Q substitution alters the residue from negatively polar acidic to uncharged (whereas alanine is nonpolar). These observations suggest that the charge of residue 133 in hA3C is important for the interaction with HIV-1 Vif. In addition, we demonstrated the E324 of hA3F is essential for HIV-1 Vif interaction, while the equivalent residue E141 in hA3C is not. These results are consistent with Kitamura et al. (63). In the Vif protein, a recent study described that mutations in a basic Vif interface patch (R17, E171, and R173) had distinct influence on degradation of hA3C and hA3F (66). In our experiments, we found that the additional residue G182 of HIV-1 Vif had different effects on the counteraction of hA3C and

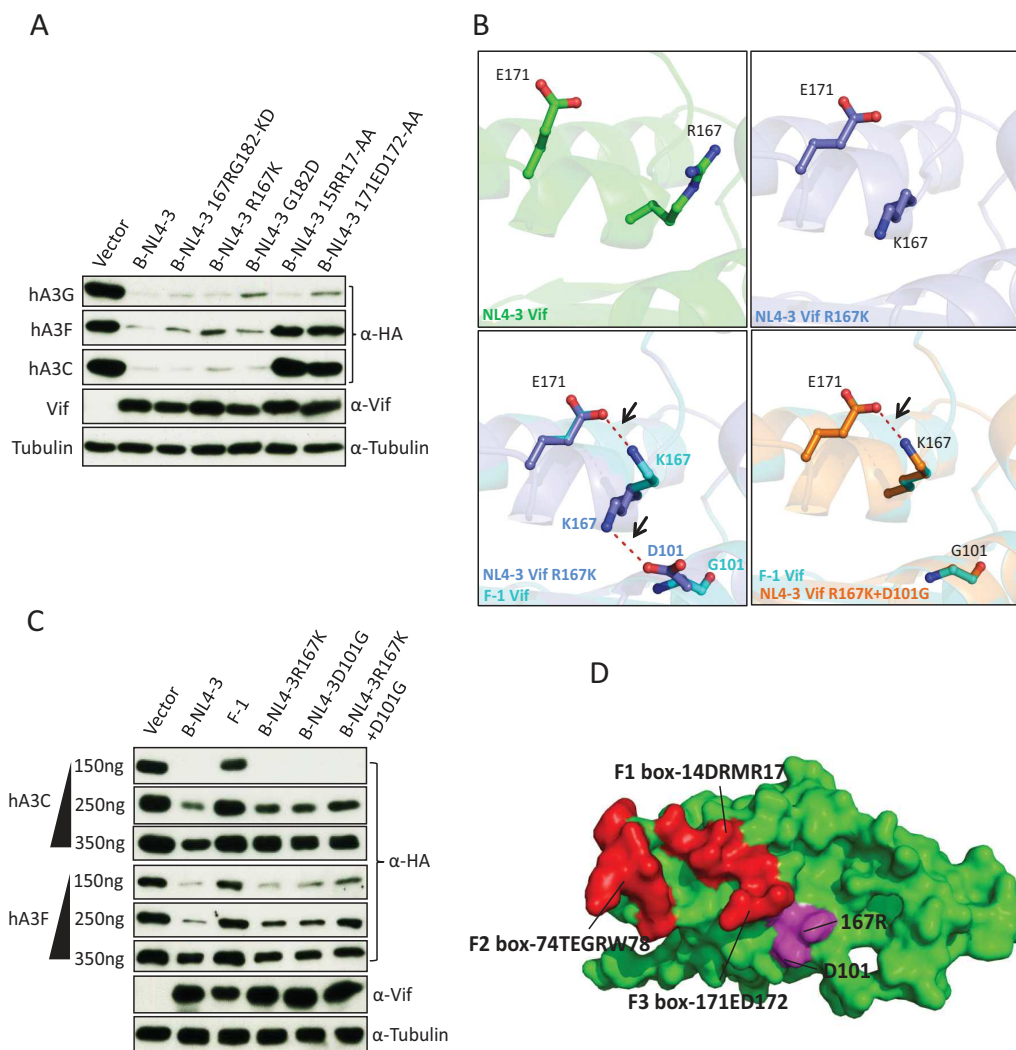


FIG 9 Structural differences between B-NL4-3 Vif and F-1 Vif. (A and C) hA3C and hA3F or hA3G expression plasmids were cotransfected together with B-NL4-3 Vif and its mutants. A3 and Vif were detected by using anti-HA and anti-Vif antibodies. Tubulin served as a loading control. (B) The structures of B-NL4-3, F-1 Vif, and their variants were modeled by SWISS modeling. The internal interaction between residues 171, 167, and 101 were analyzed by PyMOL, and the distances between interacting side chains are between 3.4 and 3.8 Å. The internal interaction is shown as a red dashed line. (D) Structure analysis of HIV-1 Vif (PDB entry 4N9F) for hA3C/hA3F interaction sites. Three discontinuous HIV-1 Vif motifs (F1 box, F2 box, and F3 box) that interact with hA3C/F are shown in red. 167R that contacted the F3 box is shown in magenta.

hA3F (Fig. 8B and 9C). These findings strongly support that HIV-1 Vif interaction interfaces in hA3C and hA3F are not identical.

A recent study reported that amino acids P16, M19, E20, P44, H45, and V47 of HIV-2 Vif are important for interaction with A3F, whereas the 140AGARV144 motif in the N-terminal half of A3F is critical for interaction with HIV-2 Vif (74). Here, we found that all tested A3C proteins were sensitive to HIV-2, SIVagm, and SIVmac Vif. hA3C and the C terminus of hA3F are homologous (5). A3C proteins are strong inhibitors of SIVΔVif, while SIVagm and SIVmac Vifs reduced the protein levels of hA3C, cpzA3C, smmA3C, agmA3C, and rhA3C (Fig. 1B and 2). This counteraction might promote SIV cross-species transmissions between primates. Compared to HIV-1 Vif, SIVcpz Vif is more active against hA3C and cpzA3C (Fig. 2F). The role of the human A3C protein during SIVcpz transmission to the human population is currently

unclear. Letko et al. reported that gorilla A3G resists degradation of HIV-1 and most SIV Vifs, serving as a barrier to SIV transmission (51). Compared to the sequence of cpzA3C or hA3C, the region of amino acids 128 to 133 of gorA3C is quite different (128YPCYQE133 presents in cpzA3C and hA3C, 128DTDYQE133 in gorA3C). Whether the replacement of 128YPC130 with 128DTD130 affects gorA3C degradation by HIV-1 or SIV Vifs needs further investigation.

Here, we found that rhA3C and smmA3C were resistant to HIV-1 Vif (Fig. 1B). However, coimmunoprecipitation assays showed that rhA3C, smmA3C, and the hA3C.CE-NQ mutant, which was insensitive to HIV-1 Vif, still bound to HIV-1 Vif. These results indicate that binding detected by co-IPs is not a proper reporter for Vif-mediated counteraction affecting the protein levels. Indeed, several previous studies reported that binding of Vif and A3 is not the only determinant for complete Vif-mediated

ated degradation (53, 57, 83–85). Kitamura et al. identified several residues between $\alpha 2$ and $\alpha 3$ helices of A3C binding to HIV-1 Vif (63). These residues are conserved in smmA3C (Fig. 1A), which might be the reason that binding of smmA3C to HIV-1 Vif was observed in our study. Recently a wobble model of the evolution of the Vif-A3 interaction was presented (64), implicating that among the Vif-A3 interactions, some binding sites are essential while others provide additional stabilizing contacts. Based on this idea, where only Vif forms a sufficient network of interactions with A3s, a functional interaction is formed. Suboptimal, destabilized interactions could be restored by the evolution of compensatory changes in the Vif-A3 interface. Thus, it is possible that the Vif interaction sites in hA3C identified by Kitamura et al. are the main interactions (63), while C130 and E133 in hA3C represent one of the relevant additional interacting points for hA3C-Vif complex formation.

Previous studies have identified three discontinuous motifs of HIV-1 Vif specifically involved in interaction with hA3F: F1-(14DRMR17), F2-(74TGEDW79), and F3-(171EDRW174) (66, 84). In addition, conserved tryptophans in Vif outside the F1, F2, and F3 box have been reported to be important for hA3F degradation (86). Here, we identified HIV-1 Vif subtype F-1, which did not degrade hA3C and hA3F, as was determined by residue K167. Our experimental results suggest that the A3-Vif interaction surface differs in Vif proteins of B-NL4-3 and F-1. Structure modeling suggested that E171, K167, and D101 in HIV-1 Vif can form internal noncovalent interactions, while the mechanism of how this internal interaction influences the Vif-A3 interaction needs further investigation, especially due to its intrinsic disordered nature (87). Vif proteins of different F-1 isolates show variability at 101 and 167 sites (G101D or K167Q/R), but E171 is conserved (data not shown). The hA3F/hA3C degradation activities of these F-1 Vif variants require further investigation. Interestingly, Vif from the F-1 subtype did not degrade hA3C and hA3F, whereas it counteracted hA3G and hA3H hapII (Fig. 7C) (71). It is unknown how the F-1 subtype virus, an isolate from Brazil, escapes the restriction of hA3F. Recently, single-nucleotide polymorphism (SNP) haplotypes of hA3F were reported, and an I231V variant with an allele (V) frequency of 48% in European Americans was associated with significantly lower set-point viral load and lower rate of progression to AIDS (88). Thus, it is possible that the hA3F of the host of our F-1 subtype had a unique haplotype that can be counteracted by F-1 Vif.

In summary, we found that rhA3C and smmA3C were resistant, but hA3C was sensitive, to HIV-1 Vif-triggered depletion, which was regulated by residues 130 and 133. Moreover, we identified that the Vif of HIV-1 F-1 subtype could not degrade hA3C as well as hA3F but was counteractive against hA3G and hA3H hapII. Residues 167 and 182 of F-1 Vif were critical for its inactivity against hA3C and hA3F, which was due to the intramolecular interaction with the F3 box. These findings provide an important addition to the model of the HIV-1 Vif and hA3C/F interaction and also advance our understanding of host-virus interactions during cross-species transmission and viral evolution.

ACKNOWLEDGMENTS

We thank Wioletta Hörschken for excellent technical assistance. We thank Neeltje Kootstra, Nathaniel R. Landau, and Viviana Simon for reagents. The following reagents were obtained through the NIH AIDS

Research and Reference Reagent Program, Division of AIDS, NIAID, NIH: HIV-1 HXB2 Vif antiserum (number 2221) from Dana Gabuzda, monoclonal antibody to HIV-1 p24 (AG3.0) from Jonathan Allan, and SIVCPZTAN1.910 (number 11496) and SIVCPZTAN2.69 (number 11497) from Jun Takehisa, Matthias H. Kraus, and Beatrice H. Hahn.

FUNDING INFORMATION

This work, including the efforts of Carsten Münk, was funded by Heinz Ansmann Foundation. This work, including the efforts of Zeli Zhang and Qinyong Gu, was funded by China Scholarship Council (CSC).

REFERENCES

- Sharp PM, Hahn BH. 2011. Origins of HIV and the AIDS pandemic. *Cold Spring Harb Perspect Med* 1:a006841.
- Harris RS, Dudley JP. 2015. APOBECs and virus restriction. *Virology* 479-480:131–145.
- Simon V, Bloch N, Landau NR. 2015. Intrinsic host restrictions to HIV-1 and mechanisms of viral escape. *Nat Immunol* 16:546–553. <http://dx.doi.org/10.1038/ni.3156>.
- LaRue RS, Andresdottir V, Blanchard Y, Conticello SG, Derse D, Emerman M, Greene WC, Jonsson SR, Landau NR, Löchelt M, Malik HS, Malim MH, Münk C, O'Brien SJ, Pathak VK, Strebel K, Wain-Hobson S, Yu XF, Yuhki N, Harris RS. 2009. Guidelines for naming nonprimate APOBEC3 genes and proteins. *J Virol* 83:494–497. <http://dx.doi.org/10.1128/JVI.01976-08>.
- Münk C, Willemsen A, Bravo IG. 2012. An ancient history of gene duplications, fusions and losses in the evolution of APOBEC3 mutators in mammals. *BMC Evol Biol* 12:71. <http://dx.doi.org/10.1186/1471-2148-12-71>.
- Ooms M, Brayton B, Letko M, Maio SM, Pilcher CD, Hecht FM, Barbour JD, Simon V. 2013. HIV-1 Vif adaptation to human APOBEC3H haplotypes. *Cell Host Microbe* 14:411–421. <http://dx.doi.org/10.1016/j.chom.2013.09.006>.
- Refsland EW, Hultquist JF, Harris RS. 2012. Endogenous origins of HIV-1 G-to-A hypermutation and restriction in the nonpermissive T cell line CEM2n. *PLoS Pathog* 8:e1002800. <http://dx.doi.org/10.1371/journal.ppat.1002800>.
- Zhang H, Yang B, Pomerantz RJ, Zhang C, Arunachalam SC, Gao L. 2003. The cytidine deaminase CEM15 induces hypermutation in newly synthesized HIV-1 DNA. *Nature* 424:94–98. <http://dx.doi.org/10.1038/nature01707>.
- Mangate B, Turelli P, Caron G, Friedli M, Perrin L, Trono D. 2003. Broad antiretroviral defence by human APOBEC3G through lethal editing of nascent reverse transcripts. *Nature* 424:99–103. <http://dx.doi.org/10.1038/nature01709>.
- Mariani R, Chen D, Schröfelbauer B, Navarro F, König R, Bollman B, Münk C, Nymark-McMahon H, Landau NR. 2003. Species-specific exclusion of APOBEC3G from HIV-1 virions by Vif. *Cell* 114:21–31. [http://dx.doi.org/10.1016/S0092-8674\(03\)00515-4](http://dx.doi.org/10.1016/S0092-8674(03)00515-4).
- Hultquist JF, Lengyel JA, Refsland EW, LaRue RS, Lackey L, Brown WL, Harris RS. 2011. Human and rhesus APOBEC3D, APOBEC3F, APOBEC3G, and APOBEC3H demonstrate a conserved capacity to restrict Vif-deficient HIV-1. *J Virol* 85:11220–11234. <http://dx.doi.org/10.1128/JVI.05238-11>.
- Wiegand HL, Doehle BP, Bogerd HP, Cullen BR. 2004. A second human antiretroviral factor, APOBEC3F, is suppressed by the HIV-1 and HIV-2 Vif proteins. *EMBO J* 23:2451–2458. <http://dx.doi.org/10.1038/sj.emboj.7600246>.
- Iwatani Y, Chan DS, Wang F, Maynard KS, Sugiura W, Gronenborn AM, Rouzina I, Williams MC, Musier-Forsyth K, Levin JG. 2007. Deaminase-independent inhibition of HIV-1 reverse transcription by APOBEC3G. *Nucleic Acids Res* 35:7096–7108. <http://dx.doi.org/10.1093/nar/gkm750>.
- Mbisa JL, Bu W, Pathak VK. 2010. APOBEC3F and APOBEC3G inhibit HIV-1 DNA integration by different mechanisms. *J Virol* 84:5250–5259. <http://dx.doi.org/10.1128/JVI.02358-09>.
- Wang X, Ao Z, Chen L, Kobinger G, Peng J, Yao X. 2012. The cellular antiviral protein APOBEC3G interacts with HIV-1 reverse transcriptase and inhibits its function during viral replication. *J Virol* 86:3777–3786. <http://dx.doi.org/10.1128/JVI.06594-11>.
- Holmes RK, Koning FA, Bishop KN, Malim MH. 2007. APOBEC3F can inhibit the accumulation of HIV-1 reverse transcription products in the

- absence of hypermutation. Comparisons with APOBEC3G. *J Biol Chem* 282:2587–2595.
17. Mbisa JL, Barr R, Thomas JA, Vandegraaff N, Dorweiler IJ, Svarovskaia ES, Brown WL, Mansky LM, Gorelick RJ, Harris RS, Engelman A, Pathak VK. 2007. Human immunodeficiency virus type 1 cDNAs produced in the presence of APOBEC3G exhibit defects in plus-strand DNA transfer and integration. *J Virol* 81:7099–7110. <http://dx.doi.org/10.1128/JVI.00272-07>.
 18. Gillick K, Pollpeter D, Phalora P, Kim EY, Wolinsky SM, Malim MH. 2013. Suppression of HIV-1 infection by APOBEC3 proteins in primary human CD4(+) T cells is associated with inhibition of processive reverse transcription as well as excessive cytidine deamination. *J Virol* 87:1508–1517. <http://dx.doi.org/10.1128/JVI.02587-12>.
 19. Yu Q, Chen D, Konig R, Mariani R, Unutmaz D, Landau NR. 2004. APOBEC3B and APOBEC3C are potent inhibitors of simian immunodeficiency virus replication. *J Biol Chem* 279:53379–53386. <http://dx.doi.org/10.1074/jbc.M408802200>.
 20. Stauch B, Hofmann H, Perkovic M, Weisel M, Kopietz F, Cichutek K, Münk C, Schneider G. 2009. Model structure of APOBEC3C reveals a binding pocket modulating ribonucleic acid interaction required for encapsidation. *Proc Natl Acad Sci U S A* 106:12079–12084. <http://dx.doi.org/10.1073/pnas.0900979106>.
 21. Perkovic M, Schmidt S, Marino D, Russell RA, Stauch B, Hofmann H, Kopietz F, Kloke BP, Zielonka J, Strover H, Hermle J, Lindemann D, Pathak VK, Schneider G, Löchelt M, Cichutek K, Münk C. 2009. Species-specific inhibition of APOBEC3C by the prototype foamy virus protein bet. *J Biol Chem* 284:5819–5826. <http://dx.doi.org/10.1074/jbc.M808853200>.
 22. Chaipan C, Smith JL, Hu WS, Pathak VK. 2013. APOBEC3G restricts HIV-1 to a greater extent than APOBEC3F and APOBEC3DE in human primary CD4+ T cells and macrophages. *J Virol* 87:444–453. <http://dx.doi.org/10.1128/JVI.00676-12>.
 23. Dang Y, Wang X, Esselman WJ, Zheng YH. 2006. Identification of APOBEC3DE as another antiretroviral factor from the human APOBEC family. *J Virol* 80:10522–10533. <http://dx.doi.org/10.1128/JVI.01123-06>.
 24. Warren CJ, Xu T, Guo K, Griffin LM, Westrich JA, Lee D, Lambert PF, Santiago ML, Pyeon D. 2015. APOBEC3A functions as a restriction factor of human papillomavirus. *J Virol* 89:688–702. <http://dx.doi.org/10.1128/JVI.02383-14>.
 25. Ahasan MM, Wakae K, Wang Z, Kitamura K, Liu G, Koura M, Imayasu M, Sakamoto N, Hanaoka K, Nakamura M, Kyo S, Kondo S, Fujiwara H, Yoshizaki T, Mori S, Kukimoto I, Muramatsu M. 2015. APOBEC3A and 3C decrease human papillomavirus 16 pseudovirion infectivity. *Biochem Biophys Res Commun* 457:295–299. <http://dx.doi.org/10.1016/j.bbrc.2014.12.103>.
 26. Marin M, Golem S, Rose KM, Kozak SL, Kabat D. 2008. Human immunodeficiency virus type 1 Vif functionally interacts with diverse APOBEC3 cytidine deaminases and moves with them between cytoplasmic sites of mRNA metabolism. *J Virol* 82:987–998. <http://dx.doi.org/10.1128/JVI.01078-07>.
 27. Bishop KN, Holmes RK, Sheehy AM, Davidson NO, Cho SJ, Malim MH. 2004. Cytidine deamination of retroviral DNA by diverse APOBEC proteins. *Curr Biol* 14:1392–1396. <http://dx.doi.org/10.1016/j.cub.2004.06.057>.
 28. Langlois MA, Beale RC, Conticello SG, Neuberger MS. 2005. Mutational comparison of the single-domain APOBEC3C and double-domain APOBEC3F/G anti-retroviral cytidine deaminases provides insight into their DNA target site specificities. *Nucleic Acids Res* 33:1913–1923. <http://dx.doi.org/10.1093/nar/gki343>.
 29. Ooms M, Krikoni A, Kress AK, Simon V, Münk C. 2012. APOBEC3A, APOBEC3B, and APOBEC3H haplotype 2 restrict human T-lymphotropic virus type 1. *J Virol* 86:6097–6108. <http://dx.doi.org/10.1128/JVI.06570-11>.
 30. Doehle BP, Schafer A, Cullen BR. 2005. Human APOBEC3B is a potent inhibitor of HIV-1 infectivity and is resistant to HIV-1 Vif. *Virology* 339:281–288. <http://dx.doi.org/10.1016/j.virol.2005.06.005>.
 31. Bogerd HP, Wiegand HL, Doehle BP, Cullen BR. 2007. The intrinsic antiretroviral factor APOBEC3B contains two enzymatically active cytidine deaminase domains. *Virology* 364:486–493. <http://dx.doi.org/10.1016/j.virol.2007.03.019>.
 32. Mahieux R, Suspene R, Delebecque F, Henry M, Schwartz O, Wain-Hobson S, Vartanian JP. 2005. Extensive editing of a small fraction of human T-cell leukemia virus type 1 genomes by four APOBEC3 cytidine deaminases. *J Gen Virol* 86:2489–2494.
 33. Burns MB, Temiz NA, Harris RS. 2013. Evidence for APOBEC3B mutagenesis in multiple human cancers. *Nat Genet* 45:977–983. <http://dx.doi.org/10.1038/ng.2701>.
 34. Land AM, Wang J, Law EK, Aberle R, Kirmaier A, Krupp A, Johnson WE, Harris RS. 2015. Degradation of the cancer genomic DNA deaminase APOBEC3B by SIV Vif. *Oncotarget* 6:39969–39979.
 35. Roberts SA, Lawrence MS, Klimczak LJ, Grimm SA, Fargo D, Stojanov P, Kiezun A, Kryukov GV, Carter SL, Saksena G, Harris S, Shah RR, Resnick MA, Getz G, Gordenin DA. 2013. An APOBEC cytidine deaminase mutagenesis pattern is widespread in human cancers. *Nat Genet* 45:970–976. <http://dx.doi.org/10.1038/ng.2702>.
 36. Alexandrov LB, Nik-Zainal S, Wedge DC, Aparicio SA, Behjati S, Biankin AV, Bignell GR, Bolli N, Borg A, Borresen-Dale AL, Boyault S, Burkhardt B, Butler AP, Caldas C, Davies HR, Desmedt C, Eils R, Eyfjord JE, Foekens JA, Greaves M, Hosoda F, Hutter B, Ilicic T, Imbeaud S, Imielinski M, Jager N, Jones DT, Jones D, Knappskog S, Kool M, Lakhani SR, Lopez-Otin C, Martin S, Munshi NC, Nakamura H, Northcott PA, Pajic M, Papaemmanuil E, Paradiso A, Pearson JV, Puente XS, Raine K, Ramakrishna M, Richardson AL, Richter J, Rosenstiel P, Schlesner M, Schumacher TN, Span PN, Teague JW, Totoki Y, Tutt AN, Valdes-Mas R, van Buuren MM, van't Veer L, Vincent-Salomon A, Waddell N, Yates LR, Australian Pancreatic Cancer Genome Initiative, ICGC Breast Cancer Consortium, ICGC MML-Seq Consortium, ICGC PedBrain I, Zucman-Rossi J, Futreal PA, McDermott U, Lichter P, Meyerson M, Grimmond SM, Siebert R, Campo E, Shibata T, Pfister SM, Campbell PJ, Stratton MR. 2013. Signatures of mutational processes in human cancer. *Nature* 500:415–421. <http://dx.doi.org/10.1038/nature12477>.
 37. Nik-Zainal S, Wedge DC, Alexandrov LB, Petljak M, Butler AP, Bolli N, Davies HR, Knappskog S, Martin S, Papaemmanuil E, Ramakrishna M, Shlien A, Simonic I, Xue Y, Tyler-Smith C, Campbell PJ, Stratton MR. 2014. Association of a germline copy number polymorphism of APOBEC3A and APOBEC3B with burden of putative APOBEC-dependent mutations in breast cancer. *Nat Genet* 46:487–491. <http://dx.doi.org/10.1038/ng.2955>.
 38. Taylor BJ, Nik-Zainal S, Wu YL, Stebbings LA, Raine K, Campbell PJ, Rada C, Stratton MR, Neuberger MS. 2013. DNA deaminases induce break-associated mutation showers with implication of APOBEC3B and 3A in breast cancer kataegis. *eLife* 2:e00534.
 39. Xu R, Zhang X, Zhang W, Fang Y, Zheng S, Yu XF. 2007. Association of human APOBEC3 cytidine deaminases with the generation of hepatitis virus B x antigen mutants and hepatocellular carcinoma. *Hepatology* 46:1810–1820. <http://dx.doi.org/10.1002/hep.21893>.
 40. Yu X, Yu Y, Liu B, Luo K, Kong W, Mao P, Yu XF. 2003. Induction of APOBEC3G ubiquitination and degradation by an HIV-1 Vif-Cul5-SCF complex. *Science* 302:1056–1060. <http://dx.doi.org/10.1126/science.1089591>.
 41. Jager S, Kim DY, Hultquist JF, Shindo K, LaRue RS, Kwon E, Li M, Anderson BD, Yen L, Stanley D, Mahon C, Kane J, Franks-Skiba K, Cimermanic P, Burlingame A, Sali A, Craik CS, Harris RS, Gross JD, Krogan NJ. 2012. Vif hijacks CBF-beta to degrade APOBEC3G and promote HIV-1 infection. *Nature* 481:371–375.
 42. Zhang W, Du J, Evans SL, Yu Y, Yu XF. 2012. T-cell differentiation factor CBF-beta regulates HIV-1 Vif-mediated evasion of host restriction. *Nature* 481:376–379.
 43. Derse D, Hill SA, Princler G, Lloyd P, Heidecker G. 2007. Resistance of human T cell leukemia virus type 1 to APOBEC3G restriction is mediated by elements in nucleocapsid. *Proc Natl Acad Sci U S A* 104:2915–2920. <http://dx.doi.org/10.1073/pnas.0609444104>.
 44. Löchelt M, Romen F, Bastone P, Muckenfuss H, Kirchner N, Kim YB, Truyen U, Rosler U, Battenberg M, Saib A, Flory E, Cichutek K, Münk C. 2005. The antiretroviral activity of APOBEC3 is inhibited by the foamy virus accessory Bet protein. *Proc Natl Acad Sci U S A* 102:7982–7987. <http://dx.doi.org/10.1073/pnas.0501445102>.
 45. Stavrou S, Nitta T, Kotla S, Ha D, Nagashima K, Rein AR, Fan H, Ross SR. 2013. Murine leukemia virus glycosylated Gag blocks apolipoprotein B editing complex 3 and cytosolic sensor access to the reverse transcription complex. *Proc Natl Acad Sci U S A* 110:9078–9083. <http://dx.doi.org/10.1073/pnas.1217399110>.
 46. Rosales Gerpe MC, Renner TM, Belanger K, Lam C, Aydin H, Langlois MA. 2015. N-linked glycosylation protects gammaretroviruses against

- deamination by APOBEC3 proteins. *J Virol* 89:2342–2357. <http://dx.doi.org/10.1128/JVI.03330-14>.
47. Jaguva Vasudevan AA, Perkovic M, Bulliard Y, Cichutek K, Trono D, Häussinger D, Münk C. 2013. Prototype foamy virus Bet impairs the dimerization and cytosolic solubility of human APOBEC3G. *J Virol* 87:9030–9040. <http://dx.doi.org/10.1128/JVI.03385-12>.
 48. Bogerd HP, Doehle BP, Wiegand HL, Cullen BR. 2004. A single amino acid difference in the host APOBEC3G protein controls the primate species specificity of HIV type 1 virion infectivity factor. *Proc Natl Acad Sci U S A* 101:3770–3774. <http://dx.doi.org/10.1073/pnas.0307713101>.
 49. Schröfelbauer B, Chen D, Landau NR. 2004. A single amino acid of APOBEC3G controls its species-specific interaction with virion infectivity factor (Vif). *Proc Natl Acad Sci U S A* 101:3927–3932. <http://dx.doi.org/10.1073/pnas.0307132101>.
 50. Xu H, Svarovskaia ES, Barr R, Zhang Y, Khan MA, Strebel K, Pathak VK. 2004. A single amino acid substitution in human APOBEC3G anti-retroviral enzyme confers resistance to HIV-1 virion infectivity factor-induced depletion. *Proc Natl Acad Sci U S A* 101:5652–5657. <http://dx.doi.org/10.1073/pnas.0400830101>.
 51. Letko M, Silvestri G, Hahn BH, Bibollet-Ruche F, Gokcumen O, Simon V, Ooms M. 2013. Vif proteins from diverse primate lentiviral lineages use the same binding site in APOBEC3G. *J Virol* 87:11861–11871. <http://dx.doi.org/10.1128/JVI.01944-13>.
 52. Yoshikawa R, Takeuchi JS, Yamada E, Nakano Y, Ren F, Tanaka H, Münk C, Harris RS, Miyazawa T, Koyanagi Y, Sato K. 2015. Vif determines the requirement for CBF-beta in APOBEC3 degradation. *J Gen Virol* 96:887–892.
 53. Stern MA, Hu C, Saenz DT, Fadel HJ, Sims O, Peretz M, Poeschla EM. 2010. Productive replication of Vif-chimeric HIV-1 in feline cells. *J Virol* 84:7378–7395. <http://dx.doi.org/10.1128/JVI.00584-10>.
 54. Dang Y, Wang X, York IA, Zheng YH. 2010. Identification of a critical T(Q/D/E)x5ADx2(I/L) motif from primate lentivirus Vif proteins that regulate APOBEC3G and APOBEC3F neutralizing activity. *J Virol* 84:8561–8570. <http://dx.doi.org/10.1128/JVI.00960-10>.
 55. Gaur R, Strebel K. 2012. Insights into the dual activity of SIVmac239 Vif against human and African green monkey APOBEC3G. *PLoS One* 7:e48850. <http://dx.doi.org/10.1371/journal.pone.0048850>.
 56. Hatzioannou T, Princiotta M, Piatak M, Jr, Yuan F, Zhang F, Lifson JD, Bieniasz PD. 2006. Generation of simian-tropic HIV-1 by restriction factor evasion. *Science* 314:95. <http://dx.doi.org/10.1126/science.1130994>.
 57. Zhang Z, Gu Q, Jaguva Vasudevan AA, Hain A, Kloke BP, Hasheminasab S, Mulnaes D, Sato K, Cichutek K, Häussinger D, Bravo IG, Smits SH, Gohlke H, Münk C. 2016. Determinants of FIV and HIV Vif sensitivity of feline APOBEC3 restriction factors. *Retrovirology* 13:46. <http://dx.doi.org/10.1186/s12977-016-0274-9>.
 58. Larue RS, Lengyel J, Jonsson SR, Andresdottir V, Harris RS. 2010. Lentiviral Vif degrades the APOBEC3Z3/APOBEC3H protein of its mammalian host and is capable of cross-species activity. *J Virol* 84:8193–8201. <http://dx.doi.org/10.1128/JVI.00685-10>.
 59. Huthoff H, Malim MH. 2007. Identification of amino acid residues in APOBEC3G required for regulation by human immunodeficiency virus type 1 Vif and virion encapsidation. *J Virol* 81:3807–3815. <http://dx.doi.org/10.1128/JVI.02795-06>.
 60. Letko M, Booiman T, Kootstra N, Simon V, Ooms M. 2015. Identification of the HIV-1 Vif and human APOBEC3G protein interface. *Cell Rep* 13:1789–1799. <http://dx.doi.org/10.1016/j.celrep.2015.10.068>.
 61. Zhen A, Wang T, Zhao K, Xiong Y, Yu XF. 2010. A single amino acid difference in human APOBEC3H variants determines HIV-1 Vif sensitivity. *J Virol* 84:1902–1911. <http://dx.doi.org/10.1128/JVI.01509-09>.
 62. Ooms M, Letko M, Binka M, Simon V. 2013. The resistance of human APOBEC3H to HIV-1 NL4-3 molecular clone is determined by a single amino acid in Vif. *PLoS One* 8:e57744. <http://dx.doi.org/10.1371/journal.pone.0057744>.
 63. Kitamura S, Ode H, Nakashima M, Imahashi M, Naganawa Y, Kurosawa T, Yokomaku Y, Yamane T, Watanabe N, Suzuki A, Sugiura W, Iwatani Y. 2012. The APOBEC3C crystal structure and the interface for HIV-1 Vif binding. *Nat Struct Mol Biol* 19:1005–1010. <http://dx.doi.org/10.1038/nsmb.2378>.
 64. Richards C, Albin JS, Demir O, Shaban NM, Luengas EM, Land AM, Anderson BD, Holten JR, Anderson JS, Harki DA, Amaro RE, Harris RS. 2015. The binding interface between human APOBEC3F and HIV-1 Vif elucidated by genetic and computational approaches. *Cell Rep* 13:1781–1788. <http://dx.doi.org/10.1016/j.celrep.2015.10.067>.
 65. Smith JL, Pathak VK. 2010. Identification of specific determinants of human APOBEC3F, APOBEC3C, and APOBEC3DE and African green monkey APOBEC3F that interact with HIV-1 Vif. *J Virol* 84:12599–12608. <http://dx.doi.org/10.1128/JVI.01437-10>.
 66. Nakashima M, Ode H, Kawamura T, Kitamura S, Naganawa Y, Awazu H, Tsuzuki S, Matsuoka K, Nemoto M, Hachiya A, Sugiura W, Yokomaku Y, Watanabe N, Iwatani Y. 2016. Structural insights into HIV-1 Vif-APOBEC3F interaction. *J Virol* 90:1034–1047. <http://dx.doi.org/10.1128/JVI.02369-15>.
 67. Albin JS, LaRue RS, Weaver JA, Brown WL, Shindo K, Harjes E, Matsuo H, Harris RS. 2010. A single amino acid in human APOBEC3F alters susceptibility to HIV-1 Vif. *J Biol Chem* 285:40785–40792. <http://dx.doi.org/10.1074/jbc.M110.173161>.
 68. Land AM, Shaban NM, Evans L, Hultquist JF, Albin JS, Harris RS. 2014. APOBEC3F determinants of HIV-1 Vif sensitivity. *J Virol* 88:12923–12927. <http://dx.doi.org/10.1128/JVI.02362-14>.
 69. Zennou V, Bieniasz PD. 2006. Comparative analysis of the antiretroviral activity of APOBEC3G and APOBEC3F from primates. *Virology* 349:31–40. <http://dx.doi.org/10.1016/j.virol.2005.12.035>.
 70. Russell RA, Pathak VK. 2007. Identification of two distinct human immunodeficiency virus type 1 Vif determinants critical for interactions with human APOBEC3G and APOBEC3F. *J Virol* 81:8201–8210. <http://dx.doi.org/10.1128/JVI.00395-07>.
 71. Binka M, Ooms M, Steward M, Simon V. 2012. The activity spectrum of Vif from multiple HIV-1 subtypes against APOBEC3G, APOBEC3F, and APOBEC3H. *J Virol* 86:49–59. <http://dx.doi.org/10.1128/JVI.06082-11>.
 72. Salter JD, Morales GA, Smith HC. 2014. Structural insights for HIV-1 therapeutic strategies targeting Vif. *Trends Biochem Sci* 39:373–380. <http://dx.doi.org/10.1016/j.tibs.2014.07.001>.
 73. Dang Y, Davis RW, York IA, Zheng YH. 2010. Identification of 81LGxGxx-IxW89 and 171EDRW174 domains from human immunodeficiency virus type 1 Vif that regulate APOBEC3G and APOBEC3F neutralizing activity. *J Virol* 84:5741–5750. <http://dx.doi.org/10.1128/JVI.00079-10>.
 74. Smith JL, Izumi T, Borbet TC, Hagedorn AN, Pathak VK. 2014. HIV-1 and HIV-2 Vif interact with human APOBEC3 proteins using completely different determinants. *J Virol* 88:9893–9908. <http://dx.doi.org/10.1128/JVI.01318-14>.
 75. Zielonka J, Marino D, Hofmann H, Yuhki N, Löchelt M, Münk C. 2010. Vif of feline immunodeficiency virus from domestic cats protects against APOBEC3 restriction factors from many felids. *J Virol* 84:7312–7324. <http://dx.doi.org/10.1128/JVI.00209-10>.
 76. Takehisa J, Kraus MH, Decker JM, Li Y, Keele BF, Bibollet-Ruche F, Zammit KP, Weng Z, Santiago ML, Kamenya S, Wilson ML, Pusey AE, Bailes E, Sharp PM, Shaw GM, Hahn BH. 2007. Generation of infectious molecular clones of simian immunodeficiency virus from fecal consensus sequences of wild chimpanzees. *J Virol* 81:7463–7475. <http://dx.doi.org/10.1128/JVI.00551-07>.
 77. Muckenfuss H, Hamdorf M, Held U, Perkovic M, Lower J, Cichutek K, Flory E, Schumann GG, Münk C. 2006. APOBEC3 proteins inhibit human LINE-1 retrotransposition. *J Biol Chem* 281:22161–22172. <http://dx.doi.org/10.1074/jbc.M601716200>.
 78. Zennou V, Perez-Caballero D, Gottlinger H, Bieniasz PD. 2004. APOBEC3G incorporation into human immunodeficiency virus type 1 particles. *J Virol* 78:12058–12061. <http://dx.doi.org/10.1128/JVI.78.21.12058-12061.2004>.
 79. Bähr A, Singer A, Hain A, Vasudevan AA, Schilling M, Reh J, Riess M, Panitz S, Serrano V, Schweizer M, König R, Chanda S, Häussinger D, Kochs G, Lindemann D, Münk C. 2016. Interferon but not Mx2 inhibits foamy retroviruses. *Virology* 488:51–60. <http://dx.doi.org/10.1016/j.virol.2015.10.034>.
 80. Goncalves J, Jallepalli P, Gabuzda DH. 1994. Subcellular localization of the Vif protein of human immunodeficiency virus type 1. *J Virol* 68:704–712.
 81. Simm M, Shahabuddin M, Chao W, Allan JS, Volsky DJ. 1995. Aberrant Gag protein composition of a human immunodeficiency virus type 1 vif mutant produced in primary lymphocytes. *J Virol* 69:4582–4586.
 82. Bordoli L, Kiefer F, Arnold K, Benkert P, Battey J, Schwede T. 2009. Protein structure homology modeling using SWISS-MODEL workspace. *Nat Protoc* 4:1–13.
 83. Zhang W, Huang M, Wang T, Tan L, Tian C, Yu X, Kong W, Yu XF. 2008. Conserved and non-conserved features of HIV-1 and SIVagm Vif mediated suppression of APOBEC3 cytidine deaminases. *Cell Microbiol* 10:1662–1675. <http://dx.doi.org/10.1111/j.1462-5822.2008.01157.x>.

84. He Z, Zhang W, Chen G, Xu R, Yu XF. 2008. Characterization of conserved motifs in HIV-1 Vif required for APOBEC3G and APOBEC3F interaction. *J Mol Biol* 381:1000–1011. <http://dx.doi.org/10.1016/j.jmb.2008.06.061>.
85. Baig TT, Feng Y, Chelico L. 2014. Determinants of efficient degradation of APOBEC3 restriction factors by HIV-1 Vif. *J Virol* 88:14380–14395. <http://dx.doi.org/10.1128/JVI.02484-14>.
86. Tian C, Yu X, Zhang W, Wang T, Xu R, Yu XF. 2006. Differential requirement for conserved tryptophans in human immunodeficiency virus type 1 Vif for the selective suppression of APOBEC3G and APOBEC3F. *J Virol* 80:3112–3115. <http://dx.doi.org/10.1128/JVI.80.6.3112-3115.2006>.
87. Auclair JR, Green KM, Shandilya S, Evans JE, Somasundaran M, Schiffer CA. 2007. Mass spectrometry analysis of HIV-1 Vif reveals an increase in ordered structure upon oligomerization in regions necessary for viral infectivity. *Proteins* 69:270–284. <http://dx.doi.org/10.1002/prot.21471>.
88. An P, Penugonda S, Thorball CW, Bartha I, Goedert JJ, Donfield S, Buchbinder S, Binns-Roemer E, Kirk GD, Zhang W, Fellay J, Yu XF, Winkler CA. 2016. Role of APOBEC3F gene variation in HIV-1 disease progression and pneumocystis pneumonia. *PLoS Genet* 12:e1005921. <http://dx.doi.org/10.1371/journal.pgen.1005921>.

AMERICAN
SOCIETY FOR
MICROBIOLOGY

Title: Vif Proteins from Diverse Human Immunodeficiency Virus/Simian Immunodeficiency Virus Lineages Have Distinct Binding Sites in A3C

Author: Zeli Zhang, Qinyong Gu, Ananda Ayyappan Jaguva Vasudevan et al.

Publication: Journal of virology

Publisher: American Society for Microbiology

Date: Nov 15, 2016

Copyright © 2016, American Society for Microbiology

Logged in as:
Ananda Ayyappan Jaguva Vasudevan
Account #: 3000710859

[LOGOUT](#)

Permissions Request

Authors in ASM journals retain the right to republish discrete portions of his/her article in any other publication (including print, CD-ROM, and other electronic formats) of which he or she is author or editor, provided that proper credit is given to the original ASM publication. ASM authors also retain the right to reuse the full article in his/her dissertation or thesis. For a full list of author rights, please see: http://journals.asm.org/site/misc/ASM_Author_Statement.xhtml

[BACK](#)[CLOSE WINDOW](#)

Copyright © 2017 Copyright Clearance Center, Inc. All Rights Reserved. [Privacy statement](#). [Terms and Conditions](#).

Comments? We would like to hear from you. E-mail us at customercare@copyright.com

Chapter IX

Interaction of human immunodeficiency virus type 1 Vif with APOBEC3G is not dependent on serine/threonine phosphorylation status

Journal : **Journal of General Virology** (published in 2012)

Own contribution to this work:

- A3G-Vif interaction by coimmunoprecipitation (Figure 3d) and analysis of data
- Phosphorylation induction of Stat3 and Erk, recombinant Vif protein purification, these supporting experiments were not included in the paper but presented to the peer reviewers

Short Communication

Interaction of human immunodeficiency virus type 1 Vif with APOBEC3G is not dependent on serine/threonine phosphorylation status

Ferdinand Kopietz,¹ Ananda Ayyappan Jaguva Vasudevan,² Melanie Krämer,² Heide Muckenfuss,¹ Ralf Sanzenbacher,¹ Klaus Cichutek,¹ Egbert Flory¹ and Carsten Münk²

Correspondence

Carsten Münk
carsten.muenk@med.uni-
duesseldorf.de

¹Division of Medical Biotechnology, Paul-Ehrlich-Institut, Langen, Germany

²Clinic for Gastroenterology, Hepatology and Infectiology, Medical Faculty, Heinrich-Heine-University, Düsseldorf, Germany

The human immunodeficiency virus type 1 accessory protein Vif is important for viral infectivity because it counteracts the antiviral protein APOBEC3G (A3G). ³²P metabolic labelling of stimulated cells revealed *in vivo* phosphorylation of the control protein, whereas no serine/threonine phosphorylation was detected for Vif or the A3G protein. These data were confirmed by *in vitro* kinase assays using active recombinant kinase. Mitogen-activated protein kinase/extracellular signal-regulated kinase 2 efficiently phosphorylated its target ELK, but failed to phosphorylate Vif. Putative serine/threonine phosphorylation point mutations in Vif (T96, S144, S165, T188) using single-round infection assays demonstrated that these mutations did not alter Vif activity, with the exception of Vif.T96E. Interestingly, T96E and not T96A was functionally impaired, indicating that this residue is critical for Vif–A3G physical interaction and activity. Our data suggest that Vif and A3G are not serine/threonine phosphorylated in human cells and phosphorylation is not linked to their functional activities.

Received 27 March 2012

Accepted 9 August 2012

Vif is a protein of human immunodeficiency virus type 1 (HIV-1) that is required for replication in non-permissive cells and primary peripheral mononuclear cells that express antiviral APOBEC3G (A3G) (Courcoul *et al.*, 1995; Fisher *et al.*, 1987; Gabuzda *et al.*, 1992; Strebel *et al.*, 1987; von Schwedler *et al.*, 1993). In addition to HIV-1, most other lentiviruses also possess *vif* genes. HIV-1 Vif targets A3G for polyubiquitination and subsequent degradation through a proteasome-dependent pathway. Vif binds A3G and acts as an A3G substrate receptor molecule by mimicking the SOCS-box component of a cellular E3 ubiquitin ligase in the Vif–Cul5–EloB/C ubiquitin ligase complex (Marin *et al.*, 2003; Mehle *et al.*, 2004; Sheehy *et al.*, 2003; Yu *et al.*, 2003, 2004). The SOCS-box in Vif (residues 144–173, Fig. 1), which consists of the BC-box and the Cullin-box, is required for multimerization. The BC-box recruits EloC and the Cullin-box interacts with Cul5 (Donahue *et al.*, 2008; Mehle *et al.*, 2004; Stanley *et al.*, 2008; Wolfe *et al.*, 2010; Yang *et al.*, 2001; Yu *et al.*, 2004). The binding of Cul5 to Vif is also mediated by the zinc-binding HCCH-box (residues 108–139) and the T(Q/D/E)_xAD_x₂(I/L) motif (residues 96–107) (Dang *et al.*, 2010b; Luo *et al.*, 2005; Mehle *et al.*, 2006; Wolfe *et al.*, 2010; Xiao *et al.*, 2006, 2007; Yu *et al.*, 2004). The interaction of Vif with A3G is organized by the G-box (residues 40–44), together with the WxSLVK motif

(residues 21–26), the FG-box (residues 55–72), the LGxGxxIxW motif (residues 81–89) and the T(Q/D/E)_xAD_x₂(I/L) motif (Fig. 1) (Dang *et al.*, 2009, 2010a, b; He *et al.*, 2008; Pery *et al.*, 2009; Russell & Pathak, 2007). Vif mutants that have a defect in binding to either A3G, Cul5 or EloC are unable to counteract the antiviral activity of A3G. However, other reports indicate that the physical assembly of Vif to A3G without subsequent degradation is sufficient to inhibit cytidine deamination, particle encapsidation or translation of A3G (Kao *et al.*, 2003, 2004, 2007; Opi *et al.*, 2007; Santa-Marta *et al.*, 2005; Stopak *et al.*, 2003).

Several putative phosphorylation sites in Vif have been described (Yang *et al.*, 1996; Yang & Gabuzda, 1998), suggesting that serine/threonine phosphorylation of Vif at Ser144, Thr155, Thr188, Thr96 and Ser165 may occur *in vivo* in cultures of human cells (Fig. 1). In addition, two studies suggested that A3G can be phosphorylated by protein kinase A (PKA) at Thr32 (Shirakawa *et al.*, 2008) or at Thr218 by PKA and calcium calmodulin-dependent kinase II (CaMKII) (Demorest *et al.*, 2011).

To determine whether Vif is phosphorylated *in vivo*, we radiolabelled Vif [derived from HIV-1 strain NL4-3, not codon-optimized, containing a C-terminal V5 tag (Zielonka *et al.*, 2010)] via metabolic labelling with

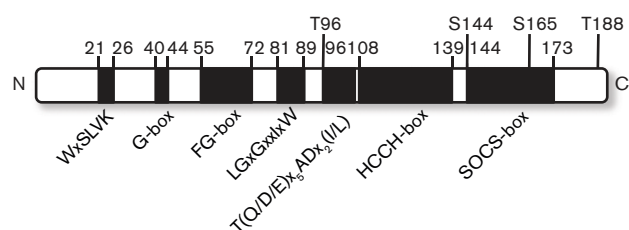


Fig. 1. Schematic representation of the functional domains in HIV-1 Vif and amino acids mutated in this study. Various domains are required for interaction with A3G [WxSLVK motif, G-box, FG-box, LGxGxIxW motif and T(Q/D/E)₅ADx₂(I/L) motif], as well as with Cul5 [T(Q/D/E)₅ADx₂(I/L) motif, HCCH-box and SOCS-box] and EloC (SOCS-box). N, N terminus; C, C terminus.

³²P-orthophosphate (³²P_i). Phosphorylation was investigated in HEK-293T cells transfected with the Vif expression plasmid, incubated with ³²P_i-containing medium and stimulated with 12-O-tetradecanoylphorbol-13-acetate (TPA) to initiate the mitogen-activated protein kinase/extracellular signal-regulated kinase (MAPK/ERK) cascade or di-butryl cAMP (dB-cAMP), which induces activation of PKA. Ten hours post-transfection, the medium was replaced with medium containing 2% FCS (Biochrome). At 36 h post-transfection, cells were labelled with ³²P_i (Hartmann Analytik) at 0.4 mCi ml⁻¹ (14.8 MBq ml⁻¹) in phosphate-free medium containing 10% dialysed FCS for 4 h. Cells were stimulated with TPA (100 ng ml⁻¹) for 10 min or with dB-cAMP (500 μM; Sigma-Aldrich) for 4 h, washed with ice-cold PBS and lysed with ice-cold RIPA buffer [25 mM Tris (pH 8.0), 137 mM NaCl, 1% (w/v) glycerol, 0.1% SDS, 0.5% sodium deoxycholate, 1% Nonidet P-40, complete phosphatase inhibitor mixture (PhosSTOP; Roche) and a protease inhibitor mixture (Roche)]. To isolate Vif, the lysates were pre-adsorbed with protein-A agarose beads (Roche) for 3 h to remove non-specific binding proteins, followed by incubation of the pre-cleared lysates with the anti-V5 antibody (1:300, MCA1360; AbD Serotec) for 1 h. Afterwards, the lysates were supplemented with protein-A agarose beads and incubated at 4 °C overnight. The transcription factor PU.1 [C-terminally haemagglutinin (HA)-tagged] was used as the control for *in vivo* phosphorylation and immunoprecipitated with anti-HA affinity matrix beads (Roche). The proteins were examined using SDS-PAGE and subjected to autoradiography. The results show that in contrast with PU.1, immunoprecipitated Vif protein was not radiolabelled (Fig. 2a). Immunoblot analysis performed as described by Zielonka *et al.* (2010) confirmed the expression and successful immunoprecipitation of Vif and PU.1 (Fig. 2a). We thus conclude that Vif is not phosphorylated *in vivo* on serine/threonine residues in HEK-293T cells.

Yang & Gabuzda (1998) previously showed that recombinant Vif expressed in *Escherichia coli* can be phosphorylated *in vitro* by ERK2. To investigate the role of ERK2 in

the phosphorylation of Vif, we performed *in vitro* kinase assays using recombinant active ERK2. The Vif protein, derived from transfected HEK-293T cells, was immunoprecipitated and eluted [using V5-peptides (1 μg μl⁻¹) at 20 °C for 30 min], and was incubated with 2.5 ng active ERK2 (p42 MAPK, Upstate) for 20 min at 30 °C in kinase reaction mixture [10 μl Vif protein and 10 μCi [γ -³³P]ATP (370 kBq) in kinase buffer (10 mM Tris/HCl, pH 7.5, 150 mM NaCl, 10 mM MgCl₂, 0.5 mM DTT), PhosSTOP (Roche) and a protease inhibitor mixture (Roche)]. ELK1, which is a standard phosphorylation substrate of ERK2, served as a positive kinase reaction control. A signal derived from protein phosphorylation was only detected for ELK1 (Fig. 2b) and not for Vif, suggesting that Vif is not a substrate for phosphorylation by ERK2.

We also analysed the phosphorylation status of A3G by performing kinase assays *in vivo*. A3G [with a C-terminal HA tag (Mariani *et al.*, 2003)] was expressed by transfection in HEK-293T cells and labelled with ³²P_i. Cell lysis was performed using RIPA. After immunoprecipitation of A3G and separation by SDS-PAGE, phosphorylation was examined by autoradiography. There was no detectable phosphorylation of A3G upon stimulation by dB-cAMP or by TPA (Fig. 2c). Identical results were obtained in experiments without dB-cAMP or TPA stimulation (data not shown).

Two studies suggest that Vif is phosphorylated at multiple serine/threonine residues (Yang *et al.*, 1996; Yang & Gabuzda, 1998). These reports motivated us to investigate the role of the putative phosphorylated amino acids in a quantitative single-round infection assay using the HIV-1 luciferase reporter virus HIVΔvif,luc [pNL4-3-luc R⁻E⁻Δvif (Mariani *et al.*, 2003)]. Expression plasmids of Vif containing mutations in single threonine or serine residues (T96A, T96E, S144A, S144E, S165A, S165E, T188A and T188E) were generated by fusion PCR. Alanine mutations in those sites prevent a potential phosphorylation and the negatively charged glutamate residues may mimic a constitutive phosphorylation. To functionally test the Vif serine/threonine point mutants, HEK-293T cells were cotransfected with HIVΔvif,luc together with A3G and Vif plasmids, along with a VSV-G expression plasmid (pMD.G) as described by Zielonka *et al.* (2010). Two days post-transfection, the virus-containing supernatants were collected, human osteosarcoma (HOS) cells were transduced with equal amounts of each virus [normalized for reverse transcription activity (Zielonka *et al.*, 2010)] and 3 days later the infectivity of these viruses was determined by quantification of intracellular luciferase activity, as described by Zielonka *et al.* (2010). Substitution of the putative phosphorylated amino acids for alanine did not modulate the ability of Vif to counteract A3G (Fig. 3a), which is in agreement with data reported by Mehle *et al.* (2004) for T96A, S144A and T188A. However, the ability of Vif to counteract A3G was impaired by the glutamate substitution of T96 (Vif.T96E), as was reported by Yang & Gabuzda (1998), resulting in reporter virus transductions

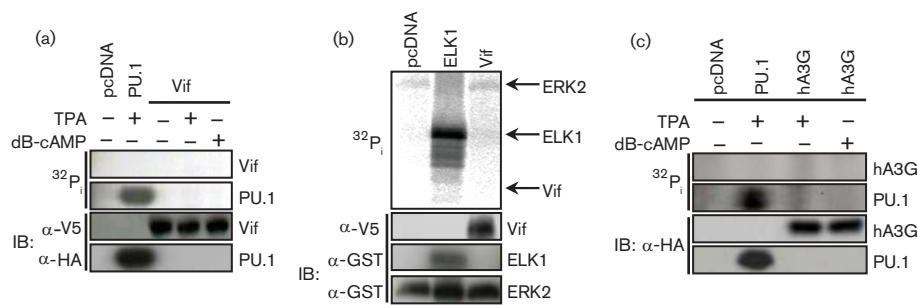


Fig. 2. Absence of *in vivo* and *in vitro* phosphorylation of HIV-1 Vif and A3G. (a) To investigate *in vivo* phosphorylation of Vif, HEK-293T cells were transfected with a Vif (V5 tag) expression plasmid. Transcription factor PU.1 (HA tag) was used as a control for the radiolabelling reaction. Cells were serum-starved, labelled with ³²P_i and stimulated with TPA or dB-cAMP. Afterwards, cells were lysed and Vif and PU.1 were purified by immunoprecipitation and detected by autoradiography or immunoblotting (IB) with anti-V5 or anti-HA antibody, respectively. (b) *In vitro* kinase assays were performed using active recombinant ERK2. ERK2 was incubated with immunoprecipitated Vif and recombinant ELK1 as the positive control in kinase buffer with [γ -³²P]ATP. Vif, ELK1 and ERK2 were analysed by autoradiography and detected by immunoblotting with anti-V5 (for Vif) and anti-glutathione S-transferase (GST) (for ELK1 and ERK2) antibodies. (c) To investigate *in vivo* phosphorylation of A3G, 293T cells were transfected with an A3G expression plasmid. Cells were serum-starved, then labelled with ³²P_i and stimulated with TPA or dB-cAMP. Transcription factor PU.1 was used as a control for the radiolabelling reaction. A3G was isolated by immunoprecipitation, analysed by autoradiography and detected by immunoblotting with the anti-HA antibody.

with significantly reduced infectivity. Supporting the importance of this residue, Dang *et al.* (2010b) recently reported that changing T96 to either D (negatively charged) or R (positively charged) prevented the interaction of Vif with A3G. In contrast, glutamate exchanges at S144, S165 and T188 did not alter the capacity of Vif to inhibit A3G (Fig. 3a). Immunoblots of transfected cells and viral particles demonstrated that Vif.T96E reduced the amount of cellular A3G less efficiently than did wild type (wt) Vif (see cell lysates in Fig. 3b, c). A3G was barely detectable in virions produced in the presence of wt and mutant Vifs (see virus lysates in Fig. 3b). HIV particles made with Vif.T96E contained slightly more A3G than particles derived from wt Vif transfections (Fig. 3b).

To determine whether residue T96 modulates the interaction of Vif with A3G, A3G was pulled down by HA beads (Roche), and bead-associated proteins were identified by immunoblotting (Fig. 3c). We found that wt, T96A and T96E mutants interacted with A3G, but Vif.T96E bound more weakly (~25% less) than wt Vif to A3G (data from two independent experiments, shown in Fig. 3c, d). Vif.T96E itself, expressed without A3G, did not reduce the infectivity of HIV-1 (Fig. 3e). The hampered neutralization of A3G by Vif.T96E supports the theory that the charge is very important in the T(Q/D/E)_X5AD_X2(I/L) motif (Fig. 1) and that the Vif interaction with A3G depends on electrostatic interaction (Dang *et al.*, 2010b). The T96E Vif mutant did not completely lose the ability to bind and induced degradation of A3G. These observations are similar to the unexplained activity of YFP-Vif (yellow fluorescent protein fused to Vif) that effectively degraded A3G but was severely impaired in its ability to direct the production of infectious HIV-1 particles from A3G-expressing cells (Kao *et al.*, 2007).

In contrast with previous studies of Vif and A3G that reported phosphorylation of both proteins on serine/threonine residues (Demorest *et al.*, 2011; Shirakawa *et al.*, 2008; Yang *et al.*, 1996; Yang & Gabuzda, 1998), our results do not support the theory that serine/threonine residues of Vif or A3G undergo phosphorylation. It is unclear why our results differ from those of previous studies. Possible explanations include the use of different expression and detection systems. Yang *et al.* (1996) and Yang & Gabuzda (1998) analysed histidine-tagged Vif strongly overexpressed from a vaccinia virus expression system and used *E. coli* recombinant Vif for *in vitro* kinase assays. In contrast, our *in vivo* phosphorylation assay was based on transient expression of Vif by a plasmid carrying the cytomegalovirus promoter, which expresses amounts of Vif similar to full-length HIV-1 (data not shown). To reduce the Rev-dependency of the *vif* RNA, we included a post-transcriptional regulatory element of the woodchuck hepatitis virus (Donello *et al.*, 1996) in the 3' untranslated region of the *vif* mRNA (Zielonka *et al.*, 2010). In addition, our *in vitro* kinase assays used Vif protein immunoprecipitated from human cells and active recombinant ERK2. If Vif is subject to phosphorylation by ERK2 as reported by Yang & Gabuzda (1998), our *in vitro* kinase assay should have detected it. Thus, based on results of *in vivo* phosphorylation and single point mutations in the putative phosphorylated serine/threonine residues in Vif, we conclude that Vif is probably not a phosphoprotein.

Shirakawa *et al.* (2008) detected putative A3G phosphorylation with antibodies against phospho-PKA substrates, but they did not perform mass spectrometry detection of phosphorylation or metabolic labelling in cell culture. Demorest *et al.* (2011) showed that an A3G-derived peptide (12 aa) containing the predicted Thr218 can be

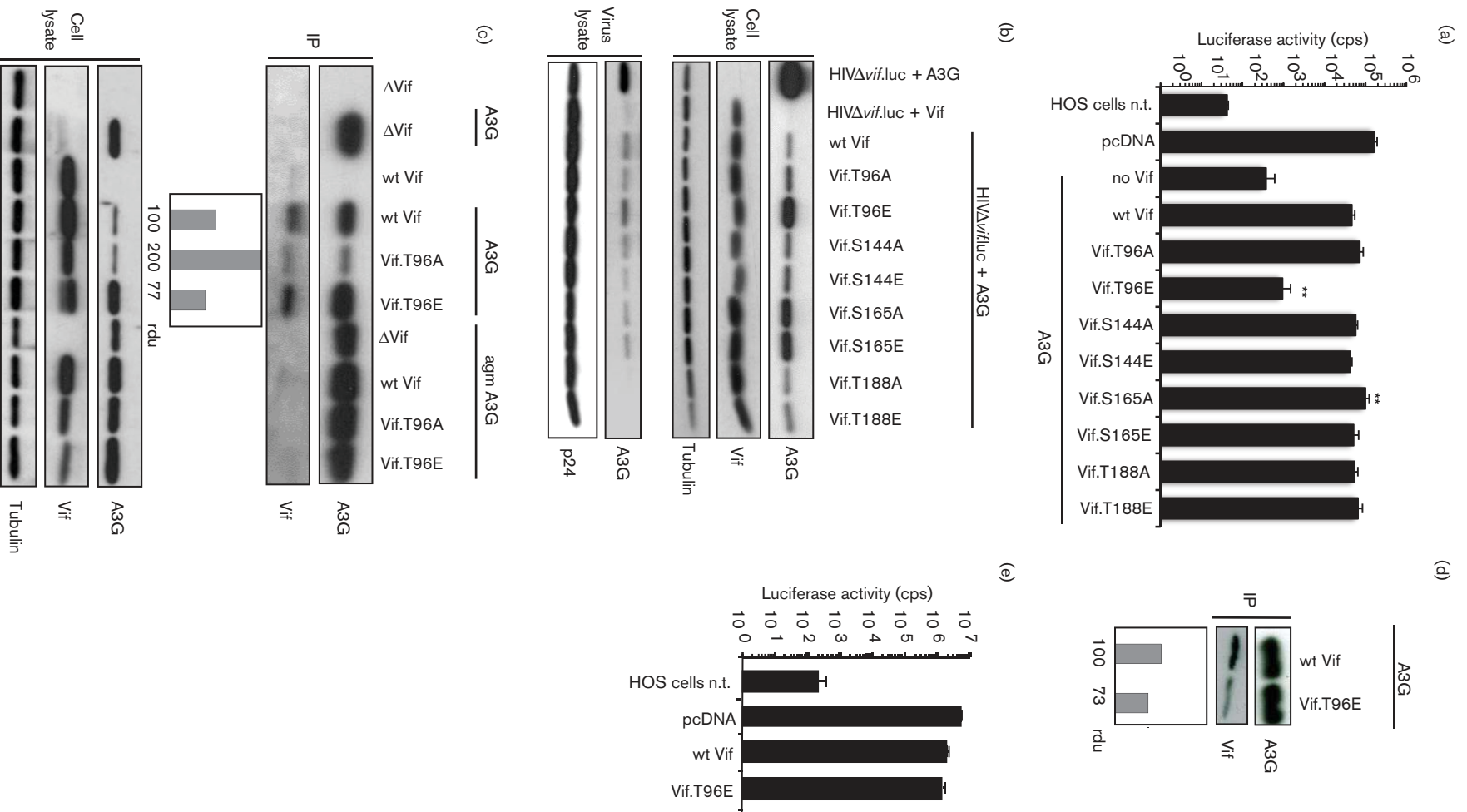


Fig. 3. Expression and activity of putative phosphorylation mutants of Vif. (a) HIV Δ vif.luc reporter viruses were produced in the presence or absence of A3G, wt Vif and Vif mutants or empty vector (pcDNA). Infectivity of normalized amounts of virus particles was determined in transduced HOS cells by quantification of the intracellular luciferase activity 3 days post-transduction. n.t., Not transduced. Asterisks represent statistically significant differences [$**P < 0.01$, Dunnett's *t* test as described by Zielonka *et al.* (2010)] relative to wt Vif activity. Errors bars are SD. (b) Immunoblots of reporter virus producer cells and viral particles. The anti-HA antibody was used for the detection of A3G and the anti-Vif antibody for the detection of Vif. Equal loading of cell lysate samples and viral particles was confirmed using anti-tubulin and anti-p24 antibodies, respectively. (c) Vif binding to A3G was determined by immunoprecipitation (IP). wt Vif or mutants T96A or T96E were co-expressed with human A3G or A3G from African green monkey (agm A3G) in HEK-293T cells. Proteins were pulled down with anti-HA beads and analysed by immunoblotting. Anti-HA antibodies were used for the detection of A3G and anti-Vif antibodies for the detection of Vif. rdu, Relative density units (software CP Atlas 2.0). (d) An independent second immunoprecipitation (IP) of wt Vif or mutant T96E with A3G. (e) HIV Δ vif.luc reporter viruses were produced in the absence of A3G, absence or presence of wt Vif and Vif.T96E or empty vector (pcDNA). Infectivity of normalized amounts of virus particles was determined as stated in (a). Errors bars are SD.

phosphorylated *in vitro* with recombinant PKA and CaMKII. However, prior to our study, no one had tested for the phosphorylation of A3G with radiolabelling. Our approach to radiolabel A3G expressed in HEK-293T is in principle a non-ambiguous and sensitive assay. We cannot rule out that very small and undetectable subpopulations of A3G or Vif proteins may be phosphorylated, even at different residues than those studied herein. However, based on our findings, the majority of Vif and A3G proteins are not subject to serine/threonine phosphorylation in HEK-293T cells. Our results indicate that the serine/threonine phosphorylation of Vif and A3G is not required for the interaction of Vif with A3G for Vif-dependent degradation of A3G and the antiviral activity of A3G. The potential specific functional consequences of any Vif or A3G phosphorylation are therefore unclear. Whether phosphorylation of Vif or A3G in human cells occurs under more physiological conditions (e.g. in primary cells) remains an open question.

Acknowledgements

We thank Matthias Hamdorf (Paul-Ehrlich Institute, Langen), Ute Albrecht (Clinic for Gastroenterology, Hepatology and Infectiology, Düsseldorf) and Nathaniel R. Landau (New York University, New York) for reagents, Wioletta Hörschken for excellent technical assistance and Dieter Häussinger (both from the Clinic for Gastroenterology, Hepatology and Infectiology, Düsseldorf) for support. The project was funded by the Deutsche Forschungsgemeinschaft grant MU 1608/3-1. C. M. was supported by the Heinz-Ansmann Foundation for AIDS Research.

References

Courcoul, M., Patience, C., Rey, F., Blanc, D., Harmache, A., Sire, J., Vigne, R. & Spire, B. (1995). Peripheral blood mononuclear cells produce normal amounts of defective Vif- human immunodeficiency virus type 1 particles which are restricted for the prero-transcription steps. *J Virol* **69**, 2068–2074.

Dang, Y., Wang, X., Zhou, T., York, I. A. & Zheng, Y. H. (2009). Identification of a novel WxSLVK motif in the N terminus of human immunodeficiency virus and simian immunodeficiency virus Vif that is critical for APOBEC3G and APOBEC3F neutralization. *J Virol* **83**, 8544–8552.

Dang, Y., Davis, R. W., York, I. A. & Zheng, Y. H. (2010a). Identification of 81LGxGxxIxW89 and 171EDRW174 domains from human immunodeficiency virus type 1 Vif that regulate APOBEC3G and APOBEC3F neutralizing activity. *J Virol* **84**, 5741–5750.

Dang, Y., Wang, X., York, I. A. & Zheng, Y. H. (2010b). Identification of a critical T(Q/D/E)x5ADx2(I/L) motif from primate lentivirus Vif proteins that regulate APOBEC3G and APOBEC3F neutralizing activity. *J Virol* **84**, 8561–8570.

Demorest, Z. L., Li, M. & Harris, R. S. (2011). Phosphorylation directly regulates the intrinsic DNA cytidine deaminase activity of activation-induced deaminase and APOBEC3G protein. *J Biol Chem* **286**, 26568–26575.

Donahue, J. P., Vetter, M. L., Mukhtar, N. A. & D'Aquila, R. T. (2008). The HIV-1 Vif PPLP motif is necessary for human APOBEC3G binding and degradation. *Virology* **377**, 49–53.

Donello, J. E., Beeche, A. A., Smith, G. J., Ill, Lucero, G. R. & Hope, T. J. (1996). The hepatitis B virus posttranscriptional regulatory element is composed of two subelements. *J Virol* **70**, 4345–4351.

Fisher, A. G., Ensoli, B., Ivanoff, L., Chamberlain, M., Petteway, S., Ratner, L., Gallo, R. C. & Wong-Staal, F. (1987). The *sor* gene of HIV-1 is required for efficient virus transmission *in vitro*. *Science* **237**, 888–893.

Gabuzda, D. H., Lawrence, K., Langhoff, E., Terwilliger, E., Dorfman, T., Haseltine, W. A. & Sodroski, J. (1992). Role of vif in replication of human immunodeficiency virus type 1 in CD4+ T lymphocytes. *J Virol* **66**, 6489–6495.

He, Z., Zhang, W., Chen, G., Xu, R. & Yu, X. F. (2008). Characterization of conserved motifs in HIV-1 Vif required for APOBEC3G and APOBEC3F interaction. *J Mol Biol* **381**, 1000–1011.

Kao, S., Khan, M. A., Miyagi, E., Plishka, R., Buckler-White, A. & Strebel, K. (2003). The human immunodeficiency virus type 1 Vif protein reduces intracellular expression and inhibits packaging of APOBEC3G (CEM15), a cellular inhibitor of virus infectivity. *J Virol* **77**, 11398–11407.

Kao, S., Miyagi, E., Khan, M. A., Takeuchi, H., Opi, S., Goila-Gaur, R. & Strebel, K. (2004). Production of infectious human immunodeficiency virus type 1 does not require depletion of APOBEC3G from virus-producing cells. *Retrovirology* **1**, 27.

Kao, S., Goila-Gaur, R., Miyagi, E., Khan, M. A., Opi, S., Takeuchi, H. & Strebel, K. (2007). Production of infectious virus and degradation of APOBEC3G are separable functional properties of human immunodeficiency virus type 1 Vif. *Virology* **369**, 329–339.

Luo, K., Xiao, Z., Ehrlich, E., Yu, Y., Liu, B., Zheng, S. & Yu, X. F. (2005). Primate lentiviral virion infectivity factors are substrate receptors that assemble with cullin 5-E3 ligase through a HCCH

- motif to suppress APOBEC3G. *Proc Natl Acad Sci U S A* **102**, 11444–11449.
- Mariani, R., Chen, D., Schröfelbauer, B., Navarro, F., König, R., Bollman, B., Münk, C., Nymark-McMahon, H. & Landau, N. R. (2003). Species-specific exclusion of APOBEC3G from HIV-1 virions by Vif. *Cell* **114**, 21–31.
- Marin, M., Rose, K. M., Kozak, S. L. & Kabat, D. (2003). HIV-1 Vif protein binds the editing enzyme APOBEC3G and induces its degradation. *Nat Med* **9**, 1398–1403.
- Mehle, A., Goncalves, J., Santa-Marta, M., McPike, M. & Gabuzda, D. (2004). Phosphorylation of a novel SOCS-box regulates assembly of the HIV-1 Vif-Cul5 complex that promotes APOBEC3G degradation. *Genes Dev* **18**, 2861–2866.
- Mehle, A., Strack, B., Ancuta, P., Zhang, C., McPike, M. & Gabuzda, D. (2004). Vif overcomes the innate antiviral activity of APOBEC3G by promoting its degradation in the ubiquitin-proteasome pathway. *J Biol Chem* **279**, 7792–7798.
- Mehle, A., Thomas, E. R., Rajendran, K. S. & Gabuzda, D. (2006). A zinc-binding region in Vif binds Cul5 and determines cullin selection. *J Biol Chem* **281**, 17259–17265.
- Opi, S., Kao, S., Goila-Gaur, R., Khan, M. A., Miyagi, E., Takeuchi, H. & Strebel, K. (2007). Human immunodeficiency virus type 1 Vif inhibits packaging and antiviral activity of a degradation-resistant APOBEC3G variant. *J Virol* **81**, 8236–8246.
- Pery, E., Rajendran, K. S., Brazier, A. J. & Gabuzda, D. (2009). Regulation of APOBEC3 proteins by a novel YXXL motif in human immunodeficiency virus type 1 Vif and simian immunodeficiency virus SIVagm Vif. *J Virol* **83**, 2374–2381.
- Russell, R. A. & Pathak, V. K. (2007). Identification of two distinct human immunodeficiency virus type 1 Vif determinants critical for interactions with human APOBEC3G and APOBEC3F. *J Virol* **81**, 8201–8210.
- Santa-Marta, M., da Silva, F. A., Fonseca, A. M. & Goncalves, J. (2005). HIV-1 Vif can directly inhibit apolipoprotein B mRNA-editing enzyme catalytic polypeptide-like 3G-mediated cytidine deamination by using a single amino acid interaction and without protein degradation. *J Biol Chem* **280**, 8765–8775.
- Sheehy, A. M., Gaddis, N. C. & Malim, M. H. (2003). The antiretroviral enzyme APOBEC3G is degraded by the proteasome in response to HIV-1 Vif. *Nat Med* **9**, 1404–1407.
- Shirakawa, K., Takaori-Kondo, A., Yokoyama, M., Izumi, T., Matsui, M., Ito, K., Sato, T., Sato, H. & Uchiyama, T. (2008). Phosphorylation of APOBEC3G by protein kinase A regulates its interaction with HIV-1 Vif. *Nat Struct Mol Biol* **15**, 1184–1191.
- Stanley, B. J., Ehrlich, E. S., Short, L., Yu, Y., Xiao, Z., Yu, X. F. & Xiong, Y. (2008). Structural insight into the human immunodeficiency virus Vif SOCS box and its role in human E3 ubiquitin ligase assembly. *J Virol* **82**, 8656–8663.
- Stopak, K., de Noronha, C., Yonemoto, W. & Greene, W. C. (2003). HIV-1 Vif blocks the antiviral activity of APOBEC3G by impairing both its translation and intracellular stability. *Mol Cell* **12**, 591–601.
- Strebel, K., Daugherty, D., Clouse, K., Cohen, D., Folks, T. & Martin, M. A. (1987). The HIV A (*src*) gene product is essential for virus infectivity. *Nature* **328**, 728–730.
- von Schwedler, U., Song, J., Aiken, C. & Trono, D. (1993). Vif is crucial for human immunodeficiency virus type 1 proviral DNA synthesis in infected cells. *J Virol* **67**, 4945–4955.
- Wolfe, L. S., Stanley, B. J., Liu, C., Eliason, W. K. & Xiong, Y. (2010). Dissection of the HIV Vif interaction with human E3 ubiquitin ligase. *J Virol* **84**, 7135–7139.
- Xiao, Z., Ehrlich, E., Yu, Y., Luo, K., Wang, T., Tian, C. & Yu, X. F. (2006). Assembly of HIV-1 Vif-Cul5 E3 ubiquitin ligase through a novel zinc-binding domain-stabilized hydrophobic interface in Vif. *Virology* **349**, 290–299.
- Xiao, Z., Xiong, Y., Zhang, W., Tan, L., Ehrlich, E., Guo, D. & Yu, X. F. (2007). Characterization of a novel Cullin5 binding domain in HIV-1 Vif. *J Mol Biol* **373**, 541–550.
- Yang, X. & Gabuzda, D. (1998). Mitogen-activated protein kinase phosphorylates and regulates the HIV-1 Vif protein. *J Biol Chem* **273**, 29879–29887.
- Yang, X., Goncalves, J. & Gabuzda, D. (1996). Phosphorylation of Vif and its role in HIV-1 replication. *J Biol Chem* **271**, 10121–10129.
- Yang, S., Sun, Y. & Zhang, H. (2001). The multimerization of human immunodeficiency virus type I Vif protein: a requirement for Vif function in the viral life cycle. *J Biol Chem* **276**, 4889–4893.
- Yu, X., Yu, Y., Liu, B., Luo, K., Kong, W., Mao, P. & Yu, X. F. (2003). Induction of APOBEC3G ubiquitination and degradation by an HIV-1 Vif-Cul5-SCF complex. *Science* **302**, 1056–1060.
- Yu, Y., Xiao, Z., Ehrlich, E. S., Yu, X. & Yu, X. F. (2004). Selective assembly of HIV-1 Vif-Cul5-ElonginB-ElonginC E3 ubiquitin ligase complex through a novel SOCS box and upstream cysteines. *Genes Dev* **18**, 2867–2872.
- Zielonka, J., Marino, D., Hofmann, H., Yuhki, N., Löchelt, M. & Münk, C. (2010). Vif of feline immunodeficiency virus from domestic cats protects against APOBEC3 restriction factors from many felids. *J Virol* **84**, 7312–7324.



Confirmation Number: 11642338
Order Date: 05/04/2017

Customer Information

Customer: Ananda Ayyappan Jaguva
Vasudevan
Account Number: 3000710859
Organization: Ananda Ayyappan Jaguva
Vasudevan
Email: ayyappan86@gmail.com
Phone: +49 2116110889
Payment Method: Invoice

This is not an invoice

Order Details

The Journal of general virology

Billing Status:
N/A

Order detail ID: 70413074	Permission Status: Granted
ISSN: 0022-1317	Permission type: Republish or display content
Publication Type: Journal	Type of use: Republish in a thesis/dissertation
Volume:	Order License Id: 4101960327313
Issue:	Requestor type: Academic institution
Start page:	Format: Print, Electronic
Publisher: Microbiology Society	Portion: chapter/article
Author/Editor: FEDERATION OF EUROPEAN MICROBIOLOGICAL SOCIETIES ; SOCIETY FOR GENERAL MICROBIOLOGY	Title or numeric reference of the portion(s): Interaction of human immunodeficiency virus type 1 Vif with APOBEC3G is not dependent on serine/threonine phosphorylation status
	Title of the article or chapter the portion is from: Interaction of human immunodeficiency virus- type 1 Vif with APOBEC3G is not dependent on serine/threonine phosphorylation status
	Editor of portion(s): N/A
	Author of portion(s): Ferdinand Kopietz, Ananda Ayyappan Jaguva Vasudevan, Melanie Krämer, Heide Muckenfuss, Ralf Sanzenbacher, Klaus Cichutek, Egbert Flory, Carsten Münk
Volume of serial or monograph:	Journal of General Virology 93: 2425-2430
Issue, if republishing an article from a serial:	Journal of General Virology 93: 2425-2430
Page range of portion:	
Publication date of portion:	01/11/2012
Rights for:	Main product
Duration of use:	Current edition and up to 5 years

Note: This item was invoiced separately through our RightsLink service. More info

\$ 0.00

Total order items: 1

Order Total: \$0.00

Chapter X

Human LINE-1 restriction by APOBEC3C is deaminase independent and mediated by an ORF1p interaction that affects LINE reverse transcriptase activity

Journal : **Nucleic Acids Research** (published in 2014)

Own contribution to this work:

- Velocity sucrose gradient fractionation (Figure 5) and A3C coimmunoprecipitation (Supplementary Figure S3)

Human LINE-1 restriction by APOBEC3C is deaminase independent and mediated by an ORF1p interaction that affects LINE reverse transcriptase activity

Axel V. Horn^{1,2}, Sabine Klawitter³, Ulrike Held³, André Berger³,
Ananda Ayyappan Jaguva Vasudevan⁴, Anja Bock³, Henning Hofmann³,
Kay-Martin O. Hanschmann⁵, Jan-Hendrik Trösemeier⁵, Egbert Flory⁵,
Robert A. Jabulowsky¹, Jeffrey S. Han², Johannes Löwer¹, Roswitha Löwer¹,
Carsten Münk^{3,4} and Gerald G. Schumann^{1,3,*}

¹Section PR2/Retroelements, Paul-Ehrlich-Institut, Paul-Ehrlich-Strasse 51-59, 63225 Langen, Germany,

²Department of Embryology, Carnegie Institution of Washington, 3520 San Martin Drive, Baltimore, MD 21218, USA, ³Division of Medical Biotechnology, Paul-Ehrlich-Institut, Paul-Ehrlich-Strasse 51-59, 63225 Langen, Germany, ⁴Clinic for Gastroenterology, Hepatology and Infectiology, Medical Faculty, Heinrich-Heine-University, 40225 Düsseldorf, Germany and ⁵Biostatistics Section, Paul-Ehrlich-Institut, Paul-Ehrlich-Strasse 51-59, 63225 Langen, Germany

Received May 23, 2012; Revised and Accepted September 13, 2013

ABSTRACT

LINE-1 (L1) retrotransposons are mobile genetic elements whose extensive proliferation resulted in the generation of ~34% of the human genome. They have been shown to be a cause of single-gene diseases. Moreover, L1-encoded endonuclease can elicit double-strand breaks that may lead to genomic instability. Mammalian cells adopted strategies restricting mobility and deleterious consequences of uncontrolled retrotransposition. The human APOBEC3 protein family of polynucleotide cytidine deaminases contributes to intracellular defense against retroelements. APOBEC3 members inhibit L1 retrotransposition by 35–99%. However, genomic L1 retrotransposition events that occurred in the presence of L1-restricting APOBEC3 proteins are devoid of detectable G-to-A hypermutations, suggesting one or multiple deaminase-independent L1 restricting mechanisms. We set out to uncover the mechanism of APOBEC3C (A3C)-mediated L1 inhibition and found that it is deaminase independent, requires an intact dimerization site and the

RNA-binding pocket mutation R122A abolishes L1 restriction by A3C. Density gradient centrifugation of L1 ribonucleoprotein particles, subcellular co-localization of L1-ORF1p and A3C and co-immunoprecipitation experiments indicate that an RNA-dependent physical interaction between L1 ORF1p and A3C dimers is essential for L1 restriction. Furthermore, we demonstrate that the amount of L1 complementary DNA synthesized by L1 reverse transcriptase is reduced by ~50% if overexpressed A3C is present.

INTRODUCTION

LINE-1 (L1) retrotransposon activity can cause disease by insertional mutagenesis, recombination, providing enzymatic activities for other non-long terminal repeat (non-LTR) retrotransposons, and perhaps by transcriptional over-activation and epigenetic effects [reviewed in (1,2)]. Since L1 elements were discovered as mutagenic insertions in 1988 (3), 96 disease-causing mutations in humans have been attributed to L1-mediated retrotransposition events [reviewed in (4)]. Recent reports also suggest that L1

*To whom correspondence should be addressed. Tel: +49 6103 773 105; Fax: +49 6103 771 280; Email: Gerald.Schumann@pei.de
Present addresses:

Robert A. Jabulowsky, Georg-Speyer-Haus, Paul-Ehrlich-Strasse 42-44, D-60596 Frankfurt, Germany.

Henning Hofmann, Microbiology Department, New York University School of Medicine, New York City, NY 1006, USA.

The authors wish it to be known that, in their opinion, the first three authors should be regarded as Joint First Authors.

endonuclease may have a general function in facilitating chromosomal breaks and genome instability (5,6). To limit such deleterious effects of retrotransposition, host genomes have adopted several strategies to curb the proliferation of transposable elements. Mechanistic strategies used by the host to restrict the mobilization of transposable elements include DNA methylation (7–9), small-RNA-based mechanisms (10–12), DNA repair factors (13,14) and L1 restriction by TREX1 DNA exonuclease (15) and members of the human APOBEC3 (*Apolipoprotein B mRNA Editing Enzyme Catalytic Polypeptide 3*, A3) protein family of cytidine deaminases [reviewed in (16)].

The human A3 protein family comprises seven members that include either one (APOBEC3A [A3A], APOBEC3C [A3C], APOBEC3H [A3H]) or two (APOBEC3B [A3B], APOBEC3D [A3D], APOBEC3F [A3F], APOBEC3G [A3G]) cytidine deaminase (CDA) domains containing a conserved zinc-binding motif (C/H)-X-E-X₂₃₋₂₈-P-C-X₂₋₄-C (17–20). Multiple A3 genes were reported to be expressed constitutively in most types of cells and tissues (21). A3 proteins can restrict the replication of various retroviruses and LTR retrotransposons by deaminating cytidines during the first-strand complementary DNA (cDNA) synthesis, which leads to either cDNA degradation or the integration of a mutated provirus or LTR retrotransposon, respectively (22,23). All A3 enzymes exhibit specificity for single-stranded DNA. Since the reaction product is deoxyuridine, A3 activity results in DNA peppered with C→U substitutions, referred to as hypermutants. The degree of editing can range from a few cytidine targets per kilobase to ~90% of all cytidine residues (24–31). All A3 enzymes preferentially edit single-stranded DNA when the edited base is 5'-flanked by thymidine or cytidine, i.e. TpC and CpC [summarized in (32)]. However, recent studies have provided evidence suggesting that A3 proteins can inhibit retroviruses by editing-independent processes (33). For instance, antiviral activities of wild-type (WT) and catalytically inactive A3F and A3G proteins were reported to correspond well with reductions in the accumulation of viral reverse transcriptase (RT) products (34).

The different A3 family members were reported to inhibit the human non-LTR retrotransposons L1 and *Alu* with varying degrees of efficiency [reviewed in (23)]. The relatively high expression level of A3 proteins in human testis, ovary (A3G, A3F and A3C) and embryonic stem cells (A3B, A3C, A3D, A3F and A3G) points to a physiologically relevant role for these DNA deaminases in these cells in the protection from potentially deleterious effects caused by endogenous retroelement mobilization [reviewed in (23)]. Although both A3A and A3C include only one single CDA domain, A3A was demonstrated to be the most potent inhibitor of non-LTR retrotransposon mobilization. A3A restricted L1 and *Alu* retrotransposition frequencies by 85–99% and 75–98% (35), respectively, while A3C inhibited L1 and *Alu* by only 40–75% and 50–70%, respectively. There is no evidence for A3-mediated editing of members of the currently mobilized human-specific L1 subfamily L1Hs (36–38), and the mechanisms through which A3 proteins inhibit

L1Hs retrotransposition are unclear to date. The CDA activity of many A3 proteins does not appear to be required since CDA mutants continue to inhibit L1 retrotransposition (36,39,40). Localization of the A3 proteins also does not appear to play a key role since both cytosolic and nuclear-localized A3 proteins effectively inhibit L1 retrotransposition (36,37,41).

Although there was no enhanced rate of G-to-A hypermutations detectable in L1 *de novo* insertions that occurred in the presence of A3A, mutating the catalytically active residues E72, C101 and C106 not only abolished the L1-inhibiting activity of A3A but even increased the L1 retrotransposition frequencies by 40 (E72A) to 70% (C101A/C106A) (37,42). It was hypothesized that the inactive A3A mutants relieve part of the L1 repression by blocking the binding of endogenous A3C and/or A3B proteins to L1 compounds (37). A3A can also restrict mobilization of the LTR-retrotransposon intracisternal A particle (IAP) (35) in cell culture assays, and it is active against the parvoviruses *Adeno-associated virus type 2* and *Minute virus of mouse* (43–45). Although A3A exerts its restricting effects on viral and retroviral targets primarily by mutating their genomes, and editing seems to be at the heart of many of these effects, A3A mutants devoid of detectable *in vitro* deaminase activity have been identified that can still restrict parvovirus (44). Also, in the presence of A3A, replicating viral genomes are decreased in *Adeno-associated virus type 2* producer cells (43), which mirrors the reduced levels of L1 reverse transcripts observed in A3A-expressing cells (46).

A3C is the most abundantly expressed of all the A3 genes across a wide range of tissues (17). All previously described A3C-mediated inhibitory effects such as the restriction of SIV_{agm}Δ*vif* (47), HTLV-1 (48) and HIVΔ*vif* and HBV (49) are a consequence of cytidine deamination. The presence of G-to-A hypermutations in these viral genomes indicates that cytidine deamination plays a major role in the inhibition of these viruses. Whereas A3C is packaged into Δ*vif* HIV with a weak antiviral effect (50), A3C is a strong inhibitor of SIVΔ*vif* (47). A3C-encoded CDA activity can induce limited G-to-A mutations in HIV-1 that do not block viral replication, but rather contribute to viral diversity (51). Even though A3C, as well as A3A, A3B, A3F and mouse (m)A3, can inhibit mouse retroelements IAP and MusD, the involvement of editing is ambiguous (33). While A3C, A3G and A3F have been found to inhibit Ty1, concomitant G-to-A mutations have been found only in the case of A3G and A3F (52,53). A3C can cause extensive G-to-A mutations in the majority of the newly synthesized HBV DNA genomes but has little effect on HBV DNA synthesis (54,55). A3C can edit transfected *human papillomavirus* DNA and mitochondrial DNA (56,57). *Herpes simplex virus-1* is particularly vulnerable to the editing effects of A3C both in tissue culture and *in vivo* because it can impact both the titer and particle/PFU ratio (58).

We set out to elucidate the mechanism responsible for A3C-mediated inhibition of L1 retrotransposition by 40–75% (37,46,59,60) because A3C is the most abundantly expressed of all A3 genes across a wide range of tissues and cell types. We demonstrate that A3C-mediated

L1 restriction is CDA independent and requires A3C dimerization. Two out of the three single mutations in the RNA-binding pocket caused a significant loss of L1 inhibition by A3C. A3C binds to L1 ORF1p in the presence of RNA, suggesting an interaction between A3C and L1 ribonucleoprotein particles (L1 RNPs). Furthermore, the amount of L1 cDNA synthesized by L1 RT is reduced by ~50% if overexpressed A3C is present. Taken together, our data suggest that A3C dimers restrict L1 by means of a CDA-independent mechanism that is based on an RNA-dependent A3C/ORF1p interaction that inhibits the processivity of L1 RT.

MATERIALS AND METHODS

Plasmids

L1 retrotransposition reporter plasmids pJM101/L1_{RP} (61) and pDK101 (62) as well as the expression plasmids encoding C-terminally hemagglutinin (HA)-tagged A3A and A3C WT proteins and the A3A mutants E72A and C101A/C106A (37) have been described recently. Plasmids expressing HA-tagged A3C mutant proteins H66R, E68Q, C100S, K22A, F55A, W74A, R122A and N177A were generated by inserting the respective HindIII/XhoI fragments of the recently described pcDNA3.1(+)-based expression plasmids (63) into the pcDNA3.1/Zeo(+) multiple cloning site (Invitrogen) after HindIII/XhoI restriction.

Cell culture, L1 retrotransposition reporter assays and statistical analyses

HeLa-JVM cells (64) were cultured in Dulbecco's modified Eagle's medium (DMEM) High Glucose (Biochrom AG) supplemented with 5% FCS (Biowest), 2 mM L-glutamine and 20 U/ml penicillin/streptomycin (Invitrogen). Osteosarcoma 143Btk- cells were grown in DMEM high glucose supplemented with 10% FCS, 2 mM L-glutamine, 20 U/ml penicillin/streptomycin and 1 mM nonessential amino acids. All cells were incubated in a humidified 5% CO₂ incubator at 37°C and passaged using standard cell culture techniques. L1 retrotransposition frequencies were determined applying the rapid and quantitative transient L1 retrotransposition reporter assay described previously (37,65). Briefly, for each transfection, 2 × 10⁵ HeLa cells/well were seeded in six-well tissue culture dishes. The following day, each well was co-transfected with 0.5 μg of reporter plasmid pJM101/L1_{RP} and 0.5 μg of the respective mutant or A3C WT expression plasmid using 3 μl of FuGENE 6 transfection reagent (Roche Diagnostics) according to manufacturer's instructions. For the titration experiment (Figure 4), 0.25–1.5 μg of the plasmid DNA encoding the R122A mutant or A3C-WT were each filled up to a total mass of 1.5 μg plasmid DNA using the empty vector pcDNA3.1/Zeo(+). Subsequently, each of the 1.5 μg-plasmid DNA samples was co-transfected with 0.5 μg of the pJM101/L1_{RP} reporter using 6 μl of FuGENE HD transfection reagent (Promega). Seventy-two hours after transfection, cells were selected for L1 retrotransposition events in 800 μg/ml G418 (Invitrogen) for 10–12 days. G418^R colonies were fixed and stained

with Giemsa (Merck, Darmstadt, Germany) as described previously. Each co-transfection was performed once or twice in quadruplicate: In each case, three co-transfection experiments were used to quantify L1 retrotransposition activities in presence or absence of the respective WT or mutant A3 expression plasmid. The fourth co-transfection was used to isolate cell lysates to analyze expression of both L1 reporter element and WT or mutated A3 expression cassette. For each co-transfection that was performed in quadruplicate, transfection efficiency was monitored by co-transfecting 0.5 μg of plasmid pHMGFP (expressing green fluorescent protein; Promega), 0.5 μg of pJM101/L1_{RP} and 0.5 μg of the respective mutant or WT A3 expression plasmid into 2 × 10⁵ HeLa cells seeded in parallel using FuGENE 6. EGFP-expressing cells were counted 24 h after transfection by flow cytometry. The percentage of green fluorescent cells was used to determine the transfection efficiency of each sample (66,67), which reproducibly ranged from 64 to 70%.

Comparisons of the effects of different WT and mutant A3 proteins on L1 retrotransposition frequencies were performed applying Student's *t*-test with *P*-values adjusted for multiple comparisons according to the Bonferroni method. The statistical analysis was performed with SAS[®]/STAT software, version 9.3 SAS System for Windows. *P*-values, which were determined to measure the significance of the L1 inhibiting effect of each A3C mutant relative to the empty A3C expression plasmid (mock) or the A3C-WT protein, respectively, are listed in Supplementary Table S1.

Toxicity assay

Toxicity assays were performed as previously described (35,37). Briefly, 2 × 10⁵ JM-HeLa cells were seeded per well of a six-well dish. The following day, cells were co-transfected with 0.5 μg of pcDNA3.1(+) (Invitrogen) expressing the neomycin resistance gene, and 0.5 μg of the A3C-WT or mutant expression plasmid or the empty vector pcDNA3.1/Zeo(+), respectively, using FuGene-HD transfection reagent (Promega) according to manufacturer's instructions. Only in the case of the A3C mutant R122A, 1.5 μg of plasmid DNA were co-transfected with 0.5 μg of pcDNA3.1(+) to assure R122A protein levels comparable with the remaining A3C mutant proteins. Two days after transfection, G418 selection (800 μg/ml) was initiated and continued for 10 days. G418^R colonies were stained with Giemsa and counted. Each co-transfection experiment was performed in quadruplicate: The arithmetic mean of the number of G418^R colonies of three independent co-transfection experiments was determined and error bars were calculated. To also control for comparable expression levels of the different A3C-WT and mutant proteins, the fourth co-transfection was performed. Hence, one well of each co-transfection was used to isolate cell lysate 3 days after transfection.

Immunoblot analysis

To analyze expression of WT and mutant A3 proteins, and of the tagged L1 reporter element, co-transfected HeLa cells were lysed 48 h after transfection using triple

lysis buffer (20 mM Tris/HCl, pH 7.5; 150 mM NaCl; 10 mM EDTA; 0.1% sodium dodecyl sulphate (SDS); 1% Triton X-100; 1% deoxycholate; 1× complete protease inhibitor cocktail [Roche]), and lysates were cleared by centrifugation. Twenty micrograms of each protein lysate were boiled in Laemmli buffer, loaded on 12% polyacrylamide gels, subjected to SDS-polyacrylamide gel electrophoresis (PAGE) and electroblotted onto nitrocellulose membranes. After protein transfer, membranes were blocked for 2 h at room temperature in a 10% solution of nonfat milk powder in 1× PBS-T [137 mM NaCl, 3 mM KCl, 16.5 mM Na₂HPO₄, 1.5 mM KH₂PO₄, 0.05% Tween 20 (Sigma-Aldrich Chemie GmbH)], washed in 1× PBS-T and incubated overnight with the respective primary antibody at 4°C. HA-tagged A3 proteins and L1 ORF1p were detected using an anti-HA antibody (Cat.# MMS-101P; Covance Inc.) in a 1:5000 dilution and the polyclonal rabbit-anti-L1 ORF1p antibody #984 (68) in a 1:2000 dilution, respectively, in 1× PBS-T containing 5% milk powder. Subsequently, membranes were washed thrice in 1× PBS-T. As secondary antibodies to detect HA-tagged A3 proteins and L1 ORF1p, we used horseradish peroxidase (HRP)-conjugated anti-mouse IgG antibody at a dilution of 1:7500, and HRP-conjugated anti-rabbit IgG antibody (Amersham Biosciences Europe GmbH) at a dilution of 1:30 000, respectively, in 1× PBS-T/1.67% milk powder and incubated the membrane for 2 h. Subsequently, the membrane was washed thrice for 10 min in 1× PBS-T. β-actin expression was detected using a monoclonal anti-β-actin antibody (clone AC-74, Sigma-Aldrich Chemie GmbH) at a dilution of 1:30 000 as primary antibody, and an anti-mouse HRP-linked species-specific antibody (from sheep) at a dilution of 1:10 000 as secondary antibody. For the detection of endogenous S6 ribosomal protein in sucrose gradient fractions, blots were probed with anti S6 ribosomal protein rabbit mAb (5G10; 1:10³ dilution in 5% bovine serum albumin dissolved in TBST; Cell Signaling Technology), for 1 h at room temperature. Anti-rabbit HRP (1:10⁴ dilution, GE Healthcare) was used as secondary antibody. Immunocomplexes were visualized using lumino-based ECL immunoblot reagent (Amersham Biosciences Europe GmbH).

Immunofluorescence microscopy

For immunofluorescence studies in HeLa cells and 143Btk- cells, 10⁵ cells/well were seeded on coverslips in 12-well cell culture dishes. Next day, cells of each well were transfected with 3.3 μg of plasmid DNA applying FuGENE HD (Promega) according to manufacturer's instructions. Three days after transfection, cells were washed once with Dulbecco's phosphate-buffered saline (Biochrom AG). Cells were fixed in 4% paraformaldehyde in phosphate buffered saline (PBS) for 15 min at room temperature, washed in PBS and permeabilized in 1% Triton-X-100/PBS for 10 min. Subsequently, cells were washed thrice for 2 min in PBS, blocked in 0.1% PBS-Triton X-100/5% Albumin Fraction V for 30 min at room temperature and finally incubated with primary

antibodies in 5% Albumin Fraction V-PBS for 1 h at room temperature.

For the staining of L1 ORF1p-T7 expressed from pDK101, cells were incubated with an anti-T7 antibody (Abcam) at a dilution of 1:250. Subsequently, cells were washed thrice for 5 min with PBS. To stain for the expression of HA-tagged A3C-WT and mutant proteins, cells were incubated with an fluorescein isothiocyanate-labeled anti-HA antibody (GenScript) in a 1:500 dilution together with the secondary antibody for L1 ORF1p-T7 detection in 5% Albumin Fraction V-PBS for 30 min and washed thrice for 5 min in PBS. The secondary antibody used for the detection of L1 ORF1p-T7 was an anti-rabbit Alexa647 antibody (Invitrogen/Life Technologies) at a 1:1000 dilution. Nuclei were stained with DAPI (1 μg/ml) for 1 min, followed by washing three times for 10 min in PBS. Coverslips were mounted in Fluoromount-G (SouthernBiotech). Finally, cellular protein expression was analyzed by confocal microscopy. Images were acquired on a fully automated Axio-ObserverZ1 microscope equipped with an ApoTome optical sectioning unit (Carl Zeiss, Jena, Germany). From each culture grown on *n* coverslips (*n* = 3 for each co-expressed A3C mutant; *n* = 5 for co-expressed A3C-WT), one high-resolution image per coverslip culture was assembled by acquisition of 25 adjacent fields of view per coverslip culture using the MosaiX module (Carl Zeiss). Morphometric analysis for A3C-WT (or mutant)/ORF1p-co-localization as well as nuclei quantification was performed using the CellProfiler Cell Image Analysis Software [www.cellprofiler.org; Broad Institute, Cambridge, MA, USA; (69)] and post-processed with the help of APOCELL (<https://pypi.python.org/pypi/apocell>).

To analyze for potential co-localization of L1 ORF1p-T7 or A3C-HA fusion proteins with the stress granule marker G3BP, the following primary and secondary antibodies and dilutions were applied: anti-T7 antibody (1:500 dilution; Novagen/Merck AG, Darmstadt, Germany), anti-HA antibody (1:250 dilution; Novus Biologicals). As secondary antibodies, anti-mouse Alexa488 (1:500 dilution; Molecular Probes) or anti-mouse Alexa594 (1:500 dilution; Invitrogen) and anti-goat Alexa546 (1:500 dilution; Molecular Probes) were used, respectively. To detect the stress granule marker G3BP, anti-G3BP antibody (1:250 dilution; Sigma-Aldrich) and secondary antibody anti-rabbit Alexa488 (1:500 dilution; Molecular Probes) were used.

To evaluate whether the P-body-specific marker rck/p54 co-localizes with L1 ORF1p-T7 or A3C-HA fusion proteins, the following antibodies and dilutions were used: anti-T7 antibody (1:500; Novagen; anti-mouse Alexa488/1:500; Molecular Probes), anti-HA (1:250; Novus Biologicals; anti-goat Alexa546/1:500; Molecular Probes) and anti-rck/p54 (1:100; MBL International; anti-rabbit Alexa647/1:500; Molecular Probes).

Velocity sucrose gradient fractionation

To generate cell lysates to be fractionated by velocity sucrose gradient centrifugation, 2 × 10⁶ HeLa cells per co-transfection were seeded in a T-75 cell culture flask.

Twenty-four hours later, cells were co-transfected with 10 µg of the L1 reporter plasmid pJM101/L1_{RP} and 10 µg of the A3C-WT or mutant expression plasmid or the empty expression vector pcDNA 3.1/Zeo(+), respectively, using FuGENE HD. Three days later, cells were washed twice with cold PBS, detached with Trypsin EDTA pelleted for 5 min at 3000g and 4°C and incubated on ice for 5 min in lysis buffer [1.5 mM KCl, 2.5 mM MgCl₂, 20 mM Tris-HCl, pH 7.4, 1% deoxycholate, 1% Triton X-100 and 1× complete EDTA-free protease inhibitor cocktail (Roche) (62)]. The lysates were cleared by centrifugation in a benchtop centrifuge at 162g for 10 min followed by 18 000g for 30 s. Subsequent sucrose gradient centrifugation was performed as described by Huthoff *et al.* (70). Briefly, cell lysates (110 µl each) were loaded on top of a 10–15–20–30–50% sucrose step gradient in a buffer [80 mM NaCl, 5 mM MgCl₂, 20 mM Tris-HCl, pH 7.4, 1 mM DTT, 1× complete EDTA-free Protease Inhibitor Cocktail (Roche) (62)] in ultra-clear centrifuge tubes (13 × 51 mm, Beckman Coulter) and centrifuged for 2 h at 39 000g at 4°C in an MLS-50 rotor (Beckman Coulter). After centrifugation, the samples were sequentially removed from the top of the gradient as 12 different fractions (84 µl per fraction). Sucrose concentrations of the different fractions were measured using a refractometer (AFAB Enterprises). Thirty microliters of each fraction were loaded per lane on a protein gel, separated by SDS-PAGE and subjected to immunoblot analysis.

Isolation of L1 RNPs

To isolate L1 RNPs, HeLa cells were plated at 6×10^6 cells per T-175 cell culture flask. Cells were transfected 24 h later with 20 µg L1 reporter plasmid pDK101 (71) per flask using FuGENE 6 or FuGENE HD transfection reagent. Three days after transfection, medium was replaced by DMEM-complete supplemented with 200 µg/ml hygromycin B and exchanged daily until day 7 after transfection. When hygromycin selection was complete, selection medium was replaced by DMEM-complete, and each T-175 culture was transfected with 20 µg of A3 expression plasmid using FuGENE 6. On the same day, one T-175 flask was seeded with 6×10^6 untransfected HeLa cells to be used as negative control. Three days later, transfected and untransfected cells were harvested and whole-cell lysates were prepared as described recently (71). Preparation of the sucrose cushion and ultracentrifugation were performed as reported previously (71). As additional negative controls, one sucrose cushion was layered only with lysis buffer or with H₂O, respectively, and subjected to the same procedures.

Co-immunoprecipitation

For co-immunoprecipitation, 1.6×10^6 HeLa cells were seeded in T-75 cell culture flasks 1 day before transfection using 8 µg of L1 reporter plasmid and FuGENE 6 according to the manufacturer's protocol. Three days later, cells were subjected to hygromycin B selection (0.2 mg/ml). After 4 days of selection, cells were transfected with 8 µg of the A3 expression plasmid using FuGENE 6 or

FuGENE HD transfection reagent. Three days later, cells were washed twice with cold phosphate-buffered saline/5% PMSF (PBSP), detached with a cell scraper in 10 ml PBSP and pelleted for 5 min at 3000g and 4°C. Cells were incubated on ice for 5 min in lysis buffer [25 mM Tris-HCl, pH 7.5, 150 mM NaCl, 5 mM MgCl₂, 5% Glycerol, 1% IGEPAL CA-630, 1 mM DTT, 1× complete protease inhibitor cocktail (Roche)]. To precipitate HA-tagged A3 proteins, the cleared lysates were incubated with 50 µl of anti-HA Affinity Matrix Beads (Roche) overnight or 1 h at 4°C under gentle agitation. For RNase treatment, the cleared lysate was incubated with 50 µl of anti-HA Affinity Matrix Beads and RNase A (Qiagen) at a final concentration of 50 µg/ml. The beads were washed five times with ice-cold lysis buffer. Subsequently, the pelleted beads were boiled in SDS loading buffer for 8 min at 95°C before separation by SDS-PAGE.

RNA isolation, reverse transcriptase-polymerase chain reaction and L1 element amplification protocol reaction

RNA isolation, reverse transcriptase-polymerase chain reaction (RT-PCR) and L1 element amplification protocol (LEAP) reaction procedures were adopted from (71) with the following modifications: A 50 µl of aliquot of each pelleted sample was used to isolate RNA using TRIzol reagent (Invitrogen) according to the manufacturer's protocol. The RNA was resuspended in 20 µl DEPC-treated water and quantified applying standard spectrophotometric methods. RNA (0.25 µg) in DEPC-treated water (8 µl) was treated with DNase I (Promega), incubated at 65°C for 10 min and chilled on ice. Next, RNA was reverse transcribed using SuperScript III RT (Invitrogen) and 0.8 mM LEAP primer (5'-GAGCACA GAATTAATACGACTCACTATAGGTTTTTTTTTTT TVN-3') according to the manufacturer's instructions in a final volume of 20 µl. As a negative control for the RT reaction, RNA was omitted from one RT reaction (Figure 8C, no RNP/RNA). Subsequently, 0.5 µl of each RT reaction were used in PCR reactions applying primers LINKER (5'-GCGAGCACAGAATTAATACGACT-3') and 'L1 3' end' [5'-GGGTTTCGAAATCGATAAGCTTG GATCCAGAC-3' (71)]. Thirty microliters of PCR products were run per lane on a 2% agarose gel.

The LEAP reaction was performed as described previously (71) with the following modifications: a 1-µl aliquot of each pelleted sample was incubated with 50 mM Tris-HCl (pH 7.5), 50 mM KCl, 5 mM MgCl₂, 10 mM DTT, 0.4 mM LEAP primer, 20 U RNaseOut (Invitrogen), 0.2 mM dNTPs and 0.05% Tween 20 in a final volume of 50 µl for 1 h at 37°C. Reactions with RNPs from untransfected HeLa cells (HeLa) or in the absence of RNPs (No RNP/RNA) were used as negative controls. After incubation, 1 µl of each LEAP reaction was used in a standard 30 µl of PCR using AmpliTaq DNA polymerase (Applied Biosystems) and 0.4 mM of each linker PCR primer and L1.3 end primer (71) according to the manufacturer's protocol. As 'No template' control, LEAP cDNA was omitted from one reaction (No template). PCR conditions were the following: one cycle 94°C for 3 min, 35 cycles 94°C for 30 s at 56°C, one cycle 10 min

at 72°C. The complete reaction was visualized on a 2% agarose gel. Quantification of the LEAP products was performed by applying the program Bio-1D Version 12.11 (Vilber Lourmat, Marne-la-Vallée, France).

RESULTS

Deaminase-deficient A3C retains its L1-restricting effect

To elucidate the mechanism that is responsible for the restriction of L1 retrotransposition by A3C [reviewed in (23)], we first investigated whether an intact CDA domain was required for A3C-mediated L1 inhibition. To answer the question of whether the presumed catalytic active site of A3C (H-X-E-X₂₇-P-C-X₂-C) is involved in the inhibition of L1 retrotransposition, we introduced mutations that were reported to abolish the editing activity in the context of A3G (72) and the L1-inhibiting effect of A3A (37) (Figure 1A).

A3G active-site mutants H257R, E259Q, C288S and C291S exhibit CDA activities that are decreased by 90–95% relative to A3G-WT (73). Mutating the corresponding A3A active-site residues H70, E72 and C106 to E72Q, H70R and C106S abolishes deaminase activity and the L1-restricting effect of A3A (43,44). Thus, we mutated the corresponding residues H66, E68 and C100 in A3C (Figure 1A) to H66R, E68Q and C100S, respectively, expecting elimination of A3C CDA activity. Simultaneously mutating the Zn²⁺-coordinating Cys residues at position 97 and 100 to Ser (C97S/C100S) did not affect A3C-mediated L1 restriction significantly ($P = 0.328$, Figure 2A and Supplementary Table S1), and mutating both Cys residues separately even slightly increased the L1 inhibition from 54 to 87% ($P = 0.0023$) or 71% ($P = 0.0349$), respectively (Figure 2C and Supplementary Table S1). These findings clearly provide evidence that deaminase activity is not required for A3C-mediated L1 restriction. Replacing Glu68 by Gln (E68Q) still resulted in a significant inhibition of L1 by ~40% ($P = 0.0044$, Figure 2A). In contrast, mutating the same Cys and Glu residues in the CDA domain of A3A (C101A/C106A, E72A) not only abrogated A3A-mediated L1 restriction but even increased the number of detectable retrotransposition events by 60–70% (C101A/C106A; Figure 2A), as reported previously (37). Replacing His66 by Arg led to the A3C CDA mutant H66R, and made no significant difference (Figure 2C) to the L1-inhibiting properties of A3C ($P = 1.0$). Since our *Escherichia coli* mutation assays demonstrate that the A3C CDA mutants H66R, E68Q, C97S, C100S and C97S/C100S are devoid of any meaningful DNA-editing activity relative to A3C-WT (Supplementary Figure S2), the retrotransposition reporter assays (Figure 2) show that, in contrast to A3A, A3C does not require an enzymatically active CDA domain to restrict L1 retrotransposition.

To exclude the possibility that the observed differences in retrotransposition frequencies can be attributed to varying L1 and/or A3 protein levels, we assessed L1 ORF1p and A3 expression in a parallel set of co-transfected HeLa cell cultures (Figure 2B and D). Immunoblot analysis of cell extracts isolated 48 h after transfection

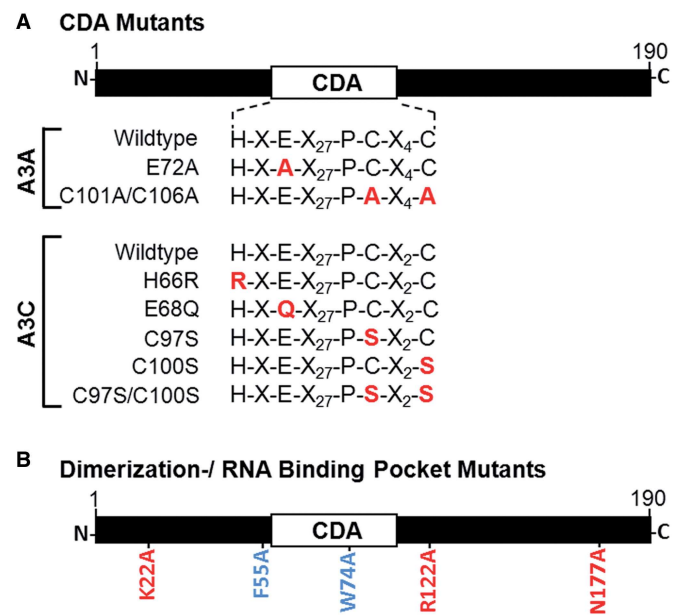


Figure 1. Schematic representation of A3A and A3C mutant constructs used in this study. (A) CDA mutants. A3A and A3C include the CDA motif HXEX₂₇PCX₂C. Point mutations were introduced into the A3A- and A3C-encoding DNAs resulting in mutations in the putative CDA domains. (B) Dimerization domain and RNA-binding pocket mutants of A3C. Blue font, mutations F55A and W74A that are located in the dimerization domain; Red font, mutations K22A, R122A and N177A that are located in the RNA-binding pocket domain. To evaluate whether A3C-WT and/or the mutant derivatives used in this study have any off target effects that might impact cell viability, and, as a consequence, hamper the identification of potential direct effects of any mutant proteins on L1 retrotransposition, we conducted toxicity assays in HeLa cells (37) (Supplementary Figure S1). Results indicate that none of the overexpressed WT or mutant A3C proteins has any considerable effect on cell viability.

showed that comparable amounts of L1 ORF1p as well as mutant and WT A3A and A3C proteins were expressed in the experiments comparing the different effects of corresponding A3A and A3C CDA mutants with each other (Figure 2B). Although the expression level of A3C-WT exceeded those of the A3C mutants C100S, C97S and H66R (Figure 2D), the mutants were still inhibiting L1 by 50–87% (Figure 2C), emphasizing that an intact CDA domain is not required for A3C-mediated L1 restriction.

A3C dimerization is required for L1 restriction

Next, we wanted to investigate whether L1-restricting A3C activity requires protein multimerization because oligomerization is essential for the inhibition of SIVΔ*vif* replication (63). For that purpose, we chose the dimerization-deficient A3C mutants F55A and W74A (Figure 1B) because it was demonstrated that amino acid residues F55 and W74 are essential for dimerization and/or oligomerization of A3C, respectively (Supplementary Figure S3). Mutating these residues was also reported to abolish the capability of A3C to introduce G-to-A hypermutations in an *E. coli* mutation assay (63). To determine whether L1 inhibition requires oligomerization of A3C, expression plasmids encoding A3C-WT and mutant proteins F55A

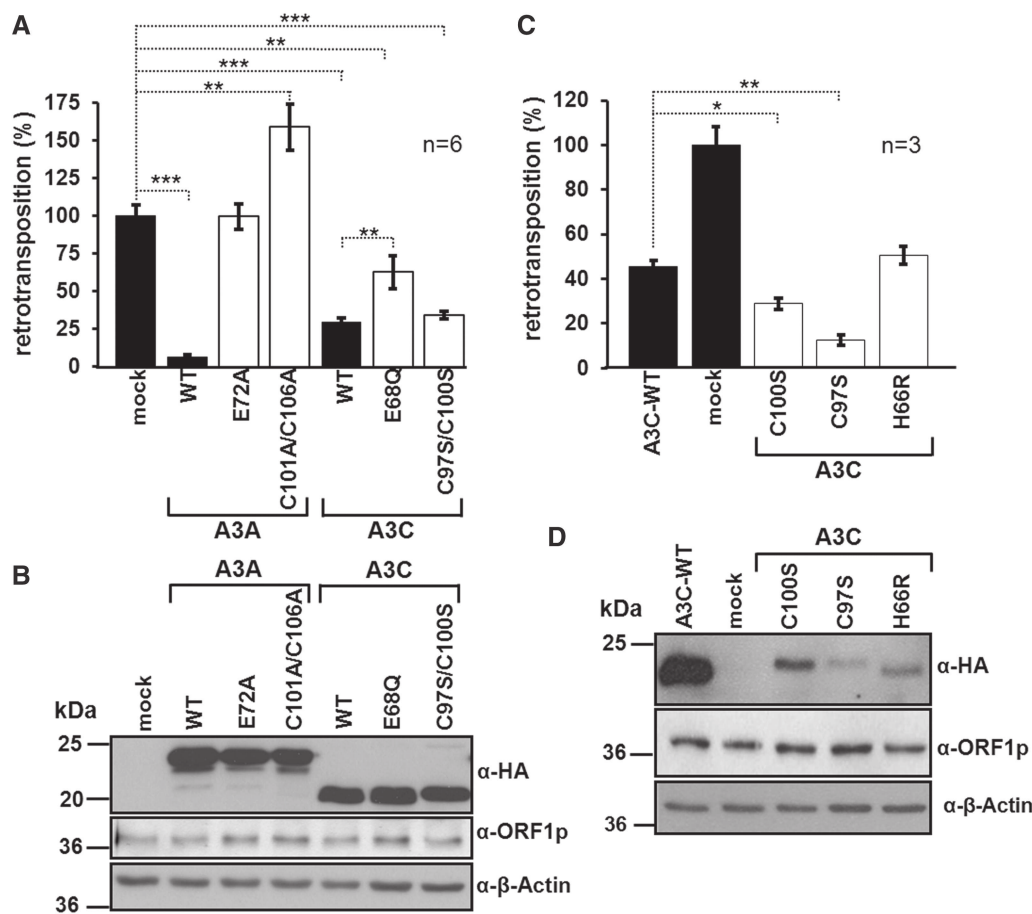


Figure 2. A3C does not require an intact CDA domain for L1 restriction. (A) Relative L1 retrotransposition frequencies in the presence of A3A, A3C and their corresponding CDA single and double mutants. HeLa cells were co-transfected with 0.5 μ g of both L1 reporter plasmid pJM101/L1_{RP} and WT or mutant A3 expression plasmids. The number of retrotransposition events in the presence of the empty expression plasmid pcDNA3.1/Zeo+ (mock) was set as 100%. Each co-transfection experiment and subsequent retrotransposition reporter assay was carried out twice in triplicates. Each bar depicts the arithmetic mean \pm SD of the relative retrotransposition frequencies obtained from six individual co-transfection experiments ($n = 6$). Absolute retrotransposition frequencies and P -values ($*P < 0.05$, $**P < 0.01$, $***P < 0.001$) are listed in Supplementary Table S1. (B) Immunoblot analysis to control for comparable expression levels of WT and mutant A3A and A3C proteins. Each lane was loaded with 20 μ g of cell lysate isolated from HeLa cells 48 h after co-transfection of A3 expression plasmid and pJM101/L1_{RP}. Expression of HA-tagged A3 proteins and L1 ORF1p was detected with anti-HA and anti-ORF1p antibodies, respectively. β -actin (~ 42 kDa) expression served as loading control. (C) Effects of A3C-CDA domain mutants C97S, C100S and H66R on L1 retrotransposition frequencies. HeLa cells were co-transfected with 0.5 μ g of both L1 reporter plasmid pJM101/L1_{RP} and WT or mutant A3C expression plasmids. The number of retrotransposition events in the presence of the empty expression plasmid (mock) was set as 100%. Each co-transfection experiment, and subsequent retrotransposition reporter assay, was performed thrice (no replicates). Each bar depicts the arithmetic mean \pm SD of the relative retrotransposition frequencies obtained from three individual co-transfection experiments ($n = 3$). Absolute retrotransposition frequencies and P -values are listed in Supplementary Table S1. (D) Immunoblot analysis of L1 ORF1p, A3C-WT, C97S, C100S and H66R mutant expression after co-transfection of the L1 retrotransposition reporter plasmid and WT or mutant A3C expression plasmids. Twenty micrograms of whole-cell extract were loaded per lane. Expression of HA-tagged A3C proteins and L1 ORF1p was detected with anti-HA and anti-ORF1p antibodies, respectively. β -actin expression served as loading control.

and W74A were separately co-transfected with the L1 retrotransposition reporter plasmid pJM101/L1_{RP}, and the effect of the mutant proteins on L1 retrotransposition was analyzed (Figure 3A). We found that in contrast to the A3C-WT protein, dimerization-deficient mutants F55A and W74A (63) were unable to restrict L1 retrotransposition (Figure 3A and Supplementary Table S1; F55A versus Mock: $P = 0.1$; W74A versus Mock: $P = 0.1$), indicating that A3C oligomerization is required for A3C-mediated L1 restriction. To evaluate the possibility that the numbers of L1 retrotransposition events in A3C-WT and F55A or W74A-transfected cells is a consequence of discrepancies in WT and mutant A3C protein levels, we

assessed expression levels of WT and mutant A3C proteins in a parallel set of co-transfected HeLa cells. Immunoblot analysis of cell extracts isolated 2 days after co-transfection showed that comparable amounts of A3C proteins were expressed (Figure 3B).

R122A mutation in the putative RNA-binding pocket of A3C abrogates L1 inhibition by A3C

By using a structure-based algorithm for automated pocket extraction, a putative RNA-binding pocket was recently located distal from the Zn²⁺-coordinating deaminase motif of A3C (63). Since evidence for binding

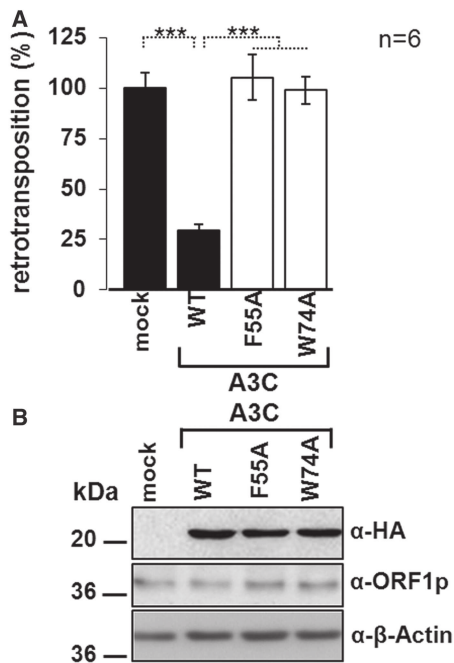


Figure 3. A3C dimerization is required for L1 restriction by A3C. (A) L1 retrotransposition reporter assays in the presence of A3C dimerization mutant proteins F55A and W74A. The L1 reporter plasmid pJM101/L1_{RP} was co-transfected with expression plasmids coding for A3C-WT or its mutants F55A and W74A. G418^R selection for retrotransposition events followed 1 day after transfection. L1 retrotransposition frequencies were determined by counting G418^R HeLa colonies. Each co-transfection experiment, and subsequent retrotransposition reporter assay, was carried out twice in triplicates. Relative retrotransposition frequencies are indicated as bar diagram. The number of retrotransposition events obtained after co-transfection of pJM101/L1_{RP} with the empty expression plasmid (mock) was set as 100%. Each bar depicts the arithmetic mean \pm SD of the relative retrotransposition frequencies obtained from six individual co-transfection experiments ($n = 6$). Absolute retrotransposition frequencies and P -values ($*P < 0.05$, $**P < 0.01$, $***P < 0.001$) are listed in Supplementary Table S1. (B) Immunoblot analysis of A3C and L1 ORF1p expression in HeLa cells after co-transfection of the L1 reporter plasmid with the respective A3C-WT and mutant A3C expression construct (F55A, W74A). Whole-cell lysates were prepared 2 days after co-transfection and subjected to immunoblot analysis using antibodies against L1 ORF1p (α -ORF1p) or HA-tag (α -HA). An amount of 20 μ g of whole-cell extract was loaded per lane. β -actin protein levels were analyzed as loading controls.

of 5.8S ribosomal RNA (rRNA) and 7SL RNA to this substrate-binding pocket has been provided (63), we evaluated whether it plays a role in A3C-mediated L1 inhibition. We tested the same mutant A3C proteins—i.e. K22A, R122A and N177A—that contain mutations near the RNA-binding pocket (Figure 1B) and were analyzed for their inhibitory effect on WT and SIV Δ vif replication recently (63). We found that A3C-WT and its N177A mutant inhibited L1 retrotransposition similarly by \sim 62 and 54%, respectively. The N177A mutation did not affect A3C-mediated L1 restriction significantly ($P = 0.1$). However, the K22A mutation reduced the L1 restricting effect to only \sim 29% relative to mock-transfected cells ($P = 0.0015$, Figure 4A and Supplementary Table S1). Initial retrotransposition reporter assays also suggested that the R122A mutation in A3C not only fully

restored the retrotransposition activity of the L1 reporter to 100% (defined as the number of L1 retrotransposition events in the absence of overexpressed A3C in HeLa cells) (Figure 4A), but actually significantly increased retrotransposition frequency by \sim 65% relative to the empty expression vector ($P = 0.0328$, Figure 4A). These data suggest that the RNA-binding pocket domain of A3C plays a role in L1 inhibition. However, immunoblot analysis of cell extracts isolated from HeLa cells that were co-transfected with the L1 reporter plasmid pJM101/L1_{RP} and WT or mutant A3C expression constructs, revealed poor R122A expression levels (Figure 4B), which may at least in part account for the absence of any L1-restricting effect of R122A.

To evaluate whether, with equal amounts of actual protein expressed, L1 retrotransposition is restored in the presence of the R122A mutant, we titrated A3C-WT and R122A mutant protein levels against the resulting L1 reporter retrotransposition activities in HeLa cells (Figure 4C and Supplementary Table S1). Expression of comparable amounts of R122A and A3C-WT protein (0.75 μ g of R122A plasmid DNA versus 0.25 μ g of A3C-WT plasmid DNA; Figure 4D) led to a significant \sim 1.8-fold increase ($P = 0.0151$) and an \sim 7-fold decrease ($P = 0.0003$) of L1 retrotransposition, respectively (Figure 4C). Increasing the expression of comparable amounts of both proteins by transfecting 1.5 μ g of R122A plasmid DNA and 0.5 μ g of A3C-WT plasmid DNA resulted in similar effects: R122A enhanced L1 retrotransposition by \sim 1.7-fold ($P = 0.1022$), whereas A3C-WT inhibited L1 by \sim 4-fold ($P = 0.0035$). These data confirmed that the restoration of the relative L1 retrotransposition frequency of 100%, observed after co-expression of the R122A mutant (Figure 4A and C), is not the consequence of minor R122A expression levels (Figure 4B and D), but is due to the R122A mutation that affects the putative RNA-binding pocket. There were no significant differences between L1-enhancing effects resulting from the transfection of increasing amounts (0.5, 0.75 and 1.5 μ g) of R122A plasmid DNA ($P = 0.5866$) nor between L1-restricting effects of increasing A3C-WT protein levels resulting from transfection of 0.25, 0.5, 1 or 1.5 μ g A3C-WT plasmid DNA ($P = 0.4190$). The 1.7- to 2-fold increase of L1 retrotransposition resulting from co-transfection of 0.5–1.5 μ g of the R122A expression construct (Figure 4C and D) suggests that R122A mutant proteins may relieve part of the L1 repression caused by endogenously expressed A3C-WT in HeLa cells by forming dimers with A3C-WT (37,74) and thus blocking their L1-inhibiting effects. Interestingly, 0.25 μ g of the R122A-expressing plasmid only restored L1 retrotransposition frequency but did not enhance L1 mobilization relative to mock-transfected cells ($P = 0.1$, Figure 4C and D), suggesting that the R122A level in the co-transfected cells is too low to affect the L1-inhibiting effect of endogenously expressed A3C-WT.

Taken together, we could show that the L1 restricting effect of the RNA-binding pocket mutant N177A is only slightly attenuated relative to A3C-WT, while the K22A mutant protein reduced L1 retrotransposition frequency

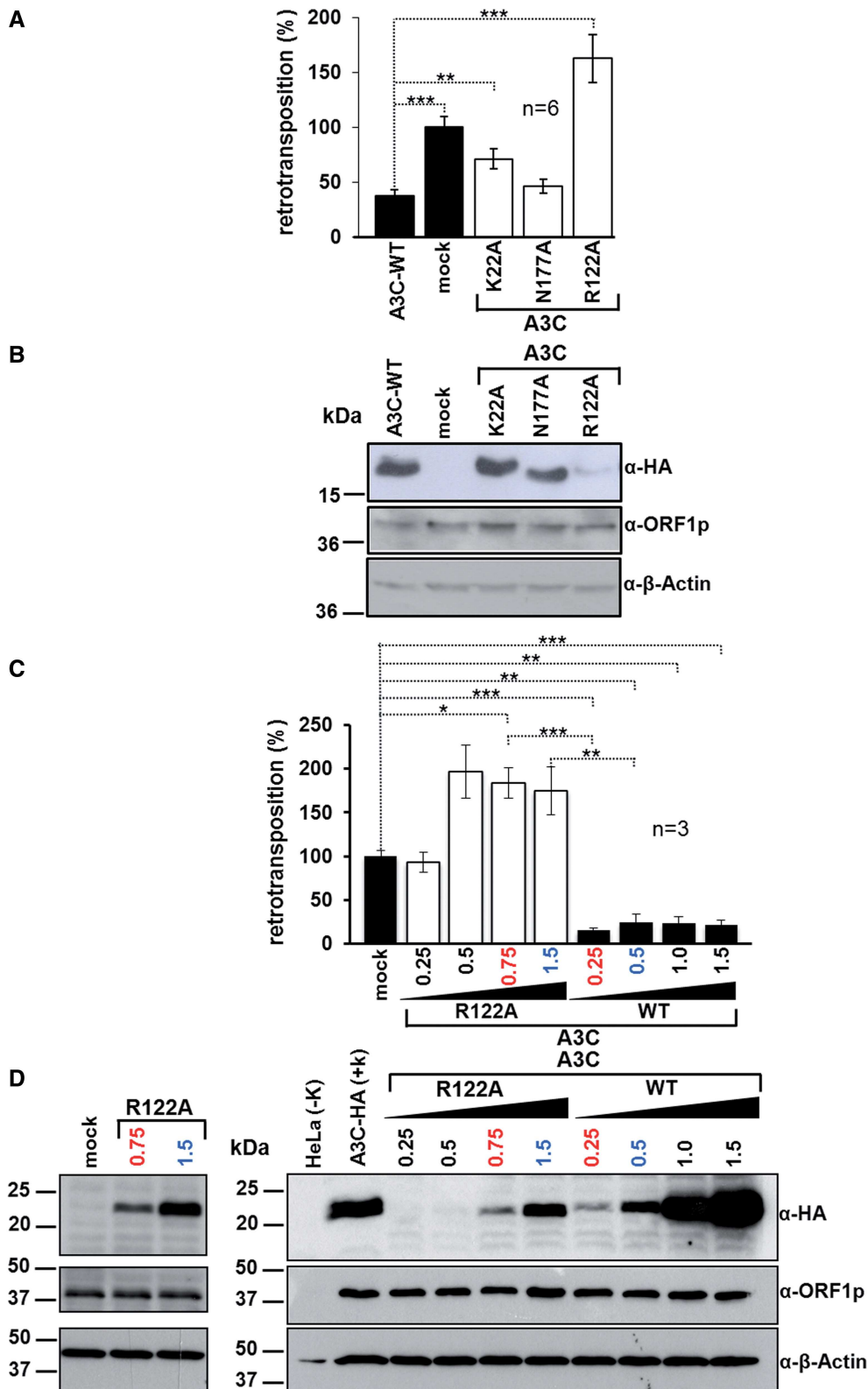


Figure 4. Effects of mutations in the putative RNA-binding pocket of A3C on L1 restriction. (A) Relative L1 retrotransposition frequencies in the presence of ectopically expressed A3C-WT and the mutant proteins K22A, N177A and R122A. HeLa cells were co-transfected with 0.5 μ g of both L1 reporter pJM101/L1_{RP} and WT or mutant A3C expression plasmids. After 11 days of G418 selection, the number of G418^R colonies was determined. The number of retrotransposition events in the presence of the empty A3C expression plasmid (mock) was set as 100%. Each co-transfection experiment, and subsequent retrotransposition reporter assay, was carried out twice in triplicates. Each bar depicts the arithmetic mean \pm SD of the relative retrotransposition frequencies obtained from six individual co-transfection experiments ($n = 6$). Absolute retrotransposition frequencies and P -values ($*P < 0.05$, $**P < 0.01$, $***P < 0.001$) are listed in Supplementary Table S1. (B) Immunoblot analysis of the expression of A3C-WT and the mutants K22A, N177A

(continued)

by only ~29%. The R122A mutation not only abolished the L1-inhibiting effect of A3C-WT entirely, but also even increased L1 retrotransposition frequencies by 62–96% (Figure 4). These data suggest that the ability to bind RNA is crucial for the L1-restricting activity of A3C.

Ectopic expression of A3C causes a shift of L1 ORF1p to sucrose gradient fractions of lower molecular mass

To explore the hypothesis that human A3C proteins exhibit their L1-restricting effect after they associate with components of the L1 RNP complex, HeLa cells were co-transfected with L1 reporter plasmid pJM101/L1_{RP} and expression plasmids for A3C-WT or its mutants W74A, R122A or C97S/C100S. Whole-cell lysates of the co-transfected HeLa cells were analyzed by centrifugation in 10–50% continuous sucrose gradients in the presence of Mg²⁺. To identify fractions containing ORF1p and/or HA-tagged A3C-WT or mutant proteins, the 12 fractions of each gradient were analyzed by immunoblotting with anti-L1-ORF1p and anti-HA antibodies (Figure 5). Consistent with a previous report (62), ORF1p was detected throughout the gradient in the absence of ectopically expressed A3C, although the majority of ORF1 proteins formed high-molecular-mass (HMM) complexes, tracked with ribosomal S6 protein (Figure 5). Ectopic co-expression of ORF1p and A3C-WT resulted in a shift of ORF1p to fractions 5–7, which cover the upper portion of the gradient (Figure 5). Co-expression of ORF1p and the CDA double-mutant C97S/C100S, which inhibits L1 transposition to the same degree as A3C-WT, led to the same shift of ORF1p in the gradient. In contrast, in extracts of cells co-transfected with the A3C mutants W74A or R122A, which do not have any L1-restricting effect, the majority of ORF1p signal accumulated in fraction 1 characterized by the highest sucrose concentration of the gradient (Figure 5). Overexpressed A3C-WT or its mutant proteins were detected throughout the gradient, irrespective of whether ectopically expressed ORF1p was present (Figure 5) or not (data not shown). A shift in L1-ORF1p-containing complexes to fractions of lower molecular mass only when A3C-WT or mutant C97S/C100S is present, is consistent with an interaction of A3C-WT or C97S/C100S with either ORF1p alone or the L1 RNP complex and suggests that both proteins are part of complexes that purify mostly in fractions 5–7. The shift could be

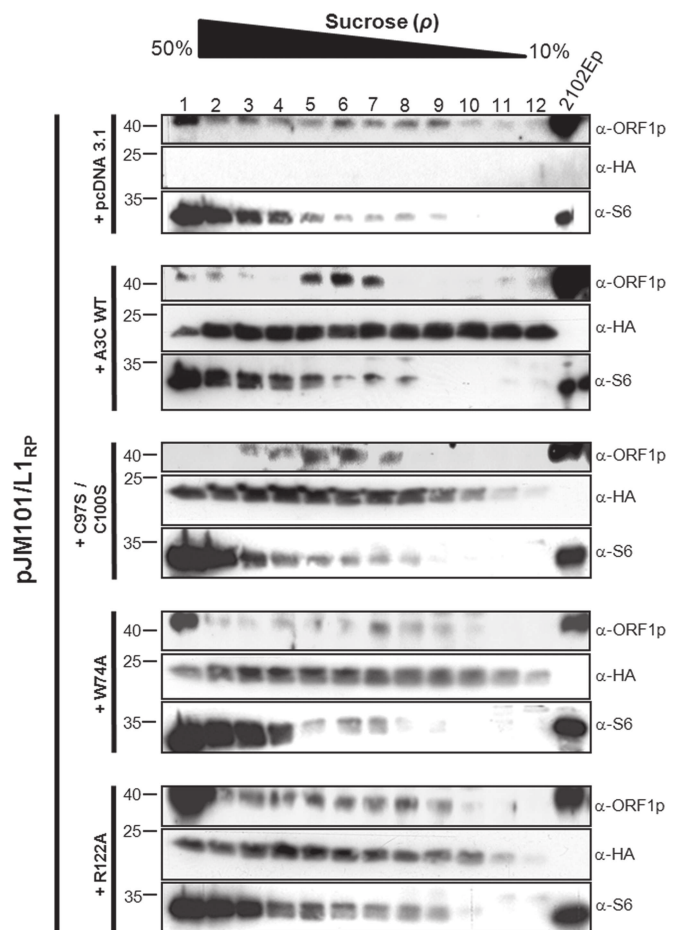


Figure 5. Velocity sucrose gradient fractionation of A3C-WT or mutant proteins and L1 ORF1p containing complexes. Whole-cell lysates from HeLa cells co-transfected with plasmids expressing WT or mutant A3C proteins and L1 reporter plasmid pJM101/L1_{RP} were layered over 10–50% sucrose containing Mg²⁺. The lowest number fraction corresponds to the bottom of the gradient. ORF1p (40 kDa), A3C WT or mutant (24 kDa) and S6 ribosomal marker proteins (32 kDa) were detected by immunoblot analysis using anti-ORF1p, anti-HA and anti-S6 antibodies, respectively. In the absence of ectopically expressed A3C proteins (pcDNA 3.1) and in the presence of overexpressed W74A or R122A mutant proteins, ORF1p co-localizes predominantly with ribosomes and polyribosomes in the bottom portion of the gradient. Co-expression of ORF1p and A3C-WT or C97S/C100S mutant protein shifted ORF1p to fractions 5, 6 and 7 (13–19% sucrose) in which ORF1p and A3C-WT or C97S/C100S mutant containing complexes were detectable. Cell lysates from 2102EP cells expressing endogenous L1 ORF1p were loaded as positive control for ORF1p expression.

Figure 4. Continued

and R122A after co-transfection with the L1 reporter pJM101/L1_{RP}. Expression of the L1 reporter and A3C proteins was detected using antibodies against L1 ORF1p (α -ORF1p) or HA-tag (α -HA), respectively. An amount of 20 μ g of whole-cell extracts was loaded per lane. β -actin protein levels were analyzed as loading controls. (C) Titration of A3C-WT and A3C-mutant R122A protein levels against L1 retrotransposition. HeLa cells were co-transfected with 0.5 μ g of pJM101/L1_{RP} and variable amounts of A3C-WT (0.25, 0.5, 1 or 1.5 μ g) of A3C-R122A mutant-encoding plasmid DNA (0.25, 0.5, 0.75 or 1.5 μ g). The total amount of co-transfected plasmid DNA was maintained at 2 μ g by adding empty parental A3C expression vector pcDNA3.1/Zeo(+). Following 11 days of G418 selection, the number of G418^R colonies was determined. The number of retrotransposition events in the presence of the empty expression plasmid (mock) was set as 100%. Data represent arithmetic means \pm SD of three independent experiments. Absolute retrotransposition frequencies and *P*-values are listed in Supplementary Table S1. (D) Immunoblot analysis of A3C-WT and R122A protein expression during titration. Cell lysates were isolated 3 days after co-transfection of pJM101/L1_{RP} and 0.25–1.5 μ g of A3C-WT or the R122A mutant expression plasmid. Expression of the L1 reporter and A3C proteins was detected using antibodies against L1 ORF1p (α -ORF1p) or HA-tag (α -HA), respectively. An amount of 20 μ g of whole-cell extracts was loaded per lane. β -actin protein levels were analyzed as loading controls. Comparable amounts of A3C-WT and R122A mutant proteins were observed after transfection of 0.25 μ g of A3C-WT and 0.75 μ g of R122A expression construct (numbers in red) or after transfection of 0.5 μ g of A3C-WT and 1.5 μ g of R122A expression construct (numbers in blue), respectively.

explained by the interference of A3C proteins with ORF1p multimer-based HMM complexes by an interaction between A3C and ORF1p.

A3C mutations interfere with the co-localization of ORF1p and A3C-WT in cytoplasmic granules

If co-fractionation of ORF1p and A3C is based on an interaction between both proteins, cellular co-localization of both proteins at some stage during the L1 replication cycle would be expected. To further investigate whether ORF1p and A3C-WT interact with each other, we next tested for co-localization of both proteins in HeLa and 143Btk- cells, which are both known to support retrotransposition of engineered human L1 reporter constructs (75,76). For that purpose, HeLa and 143Btk- cells were co-transfected with the A3C-WT expression plasmid and the reporter construct pDK101, which carries an L1 retrotransposition reporter cassette coding for a T7-tagged L1 ORF1p (62).

By applying confocal immunofluorescence microscopy, we demonstrate, in accordance with previous reports, that ectopically expressed ORF1p localizes predominantly to cytoplasmic granules in HeLa and 143Btk- cells (Figure 6A and B), which were recently identified as stress granules (77–79). Furthermore, we confirmed nucleocytoplasmic distribution of ectopically expressed A3C-HA proteins in HeLa and 143Btk- cells (37,46) (Figure 6A and B). We found that by far the majority of A3C-HA proteins accumulated in cytoplasmic foci, which we identified in $\geq 90\%$ of A3C-HA-expressing HeLa cells and is consistent with a previous report (80). Only a much smaller amount was located equally distributed in the nucleus (Figure 6A and B). While it is well established that endogenous as well as ectopically expressed ORF1p nucleates the formation of cytoplasmic granules (78,79,81), it is, to our knowledge, currently unknown whether endogenous A3C accumulates in subcellular compartments. Therefore, we cannot exclude the possibility that the observed formation of cytoplasmic A3C foci is a consequence of A3C overexpression. We found that co-expression of the tagged A3C and ORF1 proteins resulted in a predominant cytoplasmic localization of both proteins in cytoplasmic granules (Figure 6A and B; ORF1p-T7/A3C-HA) in HeLa and 143Btk- cells. Quantitative analyses showed that $\sim 34\%$ ($\sim 21\%$) of all cytoplasmic ORF1p granules in those HeLa (143Btk-) cells that co-express ORF1p and A3C-WT ectopically co-localize with A3C-WT foci (Figure 6C and D).

To challenge the hypothesis that an interaction between A3C and ORF1p was responsible for the co-localization of both proteins in the same cytoplasmic granules, we evaluated whether critical mutations in the CDA, dimerization and RNA-binding-pocket domains of A3C affect A3C/ORF1p co-localization. Quantification of the percentage of ORF1p foci co-localizing with A3C mutant proteins (Figure 6C, Supplementary Table S2 and Supplementary Figure S4) showed that the incidence of co-localization drops significantly to ~ 5.6 – 15.9% for the A3C mutant proteins tested. Interestingly, the most prominent drop (by 83 and 78%) was observed for the R122A

and W74A mutations, respectively, which were both shown earlier to abolish the L1-restricting effect of A3C entirely (Figures 3 and 4).

Data are consistent with an interaction between A3C-WT and ORF1p, which might direct both proteins to the same cytoplasmic compartment. Results suggest that this interaction may be disturbed by specific mutations introduced into the A3C domains that significantly reduce the incidence of co-localization of ORF1p and A3C foci by variable degrees.

Both ORF1p and A3C cytoplasmic foci co-localize with stress granule marker G3BP

Since we observed that A3C foci co-localize with ORF1p granules in the cytoplasmic compartment (Figure 6A and B), and endogenous as well as ectopically expressed ORF1p was previously demonstrated to nucleate the formation of stress granules (78,79), we hypothesized that both ORF1p and A3C are directed to the same stress granules. To confirm that the cytoplasmic foci in which ORF1p and A3C co-localize (Figure 6A and B) represent stress granules, we tested whether ORF1p and A3C separately localize to stress granule marker G3BP. To this end, 143Btk- cells were co-transfected with L1 reporter plasmid pDK101 and A3C expression plasmid. ORF1p, A3C and the stress granule-specific marker G3BP were visualized by immunofluorescence microscopy using an α -T7 tag, α -HA tag and an α -G3BP antibody, respectively (Figure 6E). We found that $\sim 65\%$ of HA-tagged A3C-expressing cells and $\geq 90\%$ of ORF1p-expressing cells were characterized by detectable cytoplasmic foci. In our double-labeling experiments, 73% of the cytoplasmic A3C foci, and 78% of the ORF1p foci, co-stain with the stress granule marker. Co-localization of cytoplasmic ORF1p foci with G3BP (Figure 6E) confirms the recent finding that ORF1p is found in stress granules (78). The observation that the majority of stress granules in the cytoplasm of co-transfected 143Btk- cells also co-localize with A3C foci (Figure 6E) would be consistent with the sequestration of potential ORF1p/A3C complexes in stress granules. However, not all visible ORF1p foci nor all A3C foci were associated with stress granules (Figure 6E). This could be explained by the dynamic processes involved in building and maintaining RNA-containing compartments like stress granules. Unfortunately, co-staining of the same cell culture sample/foci for all three proteins (ORF1p, A3C and G3BP) was not possible owing to objective technical restrictions. Co-staining with the processing (P) body marker RCK/p54 (82) did not uncover any co-localization of A3C or L1 ORF1p with P-bodies in immunofluorescence experiments (data not shown).

L1 ORF1p interacts with A3A and A3C

The shift of ORF1p to sucrose gradient fractions of lower molecular mass if A3C is present (Figure 5), and cytoplasmic co-localization of ORF1p and A3C in human cells (Figure 6), suggests that A3C interacts with ORF1p alone or as part of the L1 RNP complex. To elucidate whether A3C and ORF1p physically interact with each other, HeLa cells were transfected with the L1 reporter

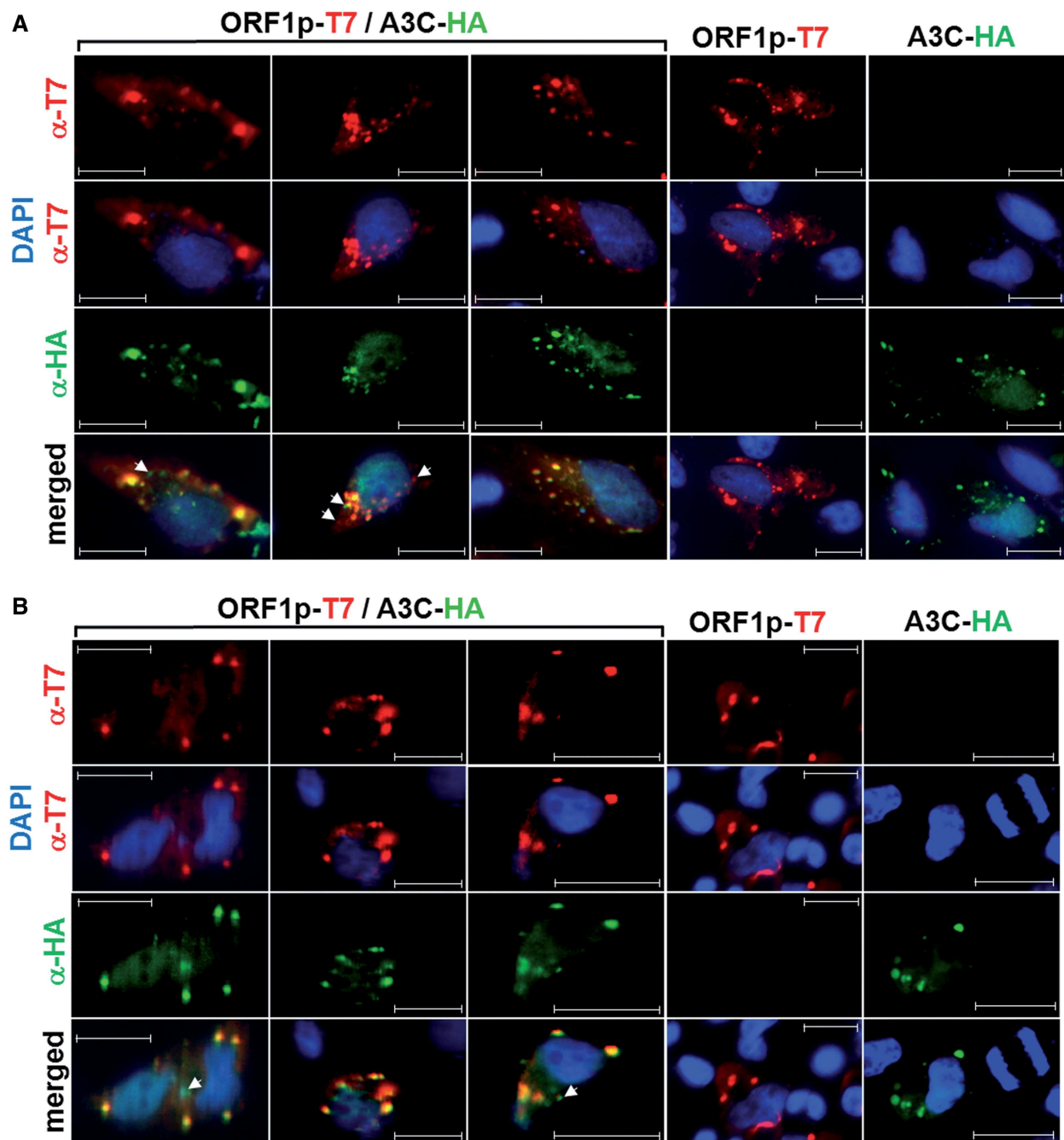


Figure 6. Ectopically co-expressed L1 ORF1p and A3C-WT co-localize in cytoplasmic granules of HeLa and 143Btk- cells. Subcellular localization of T7-tagged L1 ORF1p and HA-tagged A3C-WT proteins in HeLa (A) and 143Btk- (B) cells was determined by immunofluorescence analysis. ORF1p-T7 and A3C-HA were either co-expressed (ORF1p-T7/A3C-HA) or separately expressed (ORF1p-T7 or A3C-HA). ORF1p-T7 and A3C-HA were stained using α -T7- (red) and α -HA-tag (green) antibodies, respectively. White arrowheads indicate A3C-HA foci or ORF1p granules that do not co-localize with ORF1p granules or A3C-HA foci. Nuclei were visualized with DAPI. Scale bar, 20 μ m. (C) Mutations in the CDA, dimerization and RNA-binding pocket domains reduce the incidence of co-localization of L1 ORF1p and A3C foci in HeLa cells significantly by variable degrees. Presented are Box-and-Whisker plots of the percentages of ORF1p foci in ORF1p and A3C WT or mutant proteins co-expressing cells that co-localize with HA-tagged WT or mutant A3C foci. Percentages of ORF1p foci co-localizing with mutants of RNA-binding pocket (R122A, N177A), dimerization domain (W74A) and CDA domain (C97S/C100S) are presented. Co-localization of both proteins is most prominent in the case of A3C-WT and absent after transfection with the empty A3C expression vector pcDNA3.1/Zeo(+). Co-localization of each mutant protein with ORF1p is significantly reduced relative to A3C-WT, but dropped most severely after co-expression with R122A and W74A. N, number of analyzed images, each carrying 10–13 cells, which ectopically co-express ORF1p and A3C-WT or mutant proteins. (D) Box-and-Whisker plot of the percentages of ORF1p foci that co-localize with HA-tagged A3C-WT foci in ORF1p and A3C-WT co-expressing 143Btk- cells. (E) ORF1p and A3C co-localize with stress granule marker protein G3BP. T7-tagged ORF1p encoded by L1 reporter plasmid pDK101 was co-expressed with HA-tagged A3C in 143Btk- cells (A3C-HA/ORF1p-T7). Co-localization of L1 ORF1p with stress granules was shown by immunofluorescence staining using α -T7 (purple) and α -G3BP (yellow) antibodies, respectively (upper panel). Co-localization of A3C with stress granules was demonstrated separately by confocal microscopy using α -HA (green) and α -G3BP (yellow) antibodies, respectively (lower panel). Nuclei were counterstained using DAPI.

(continued)

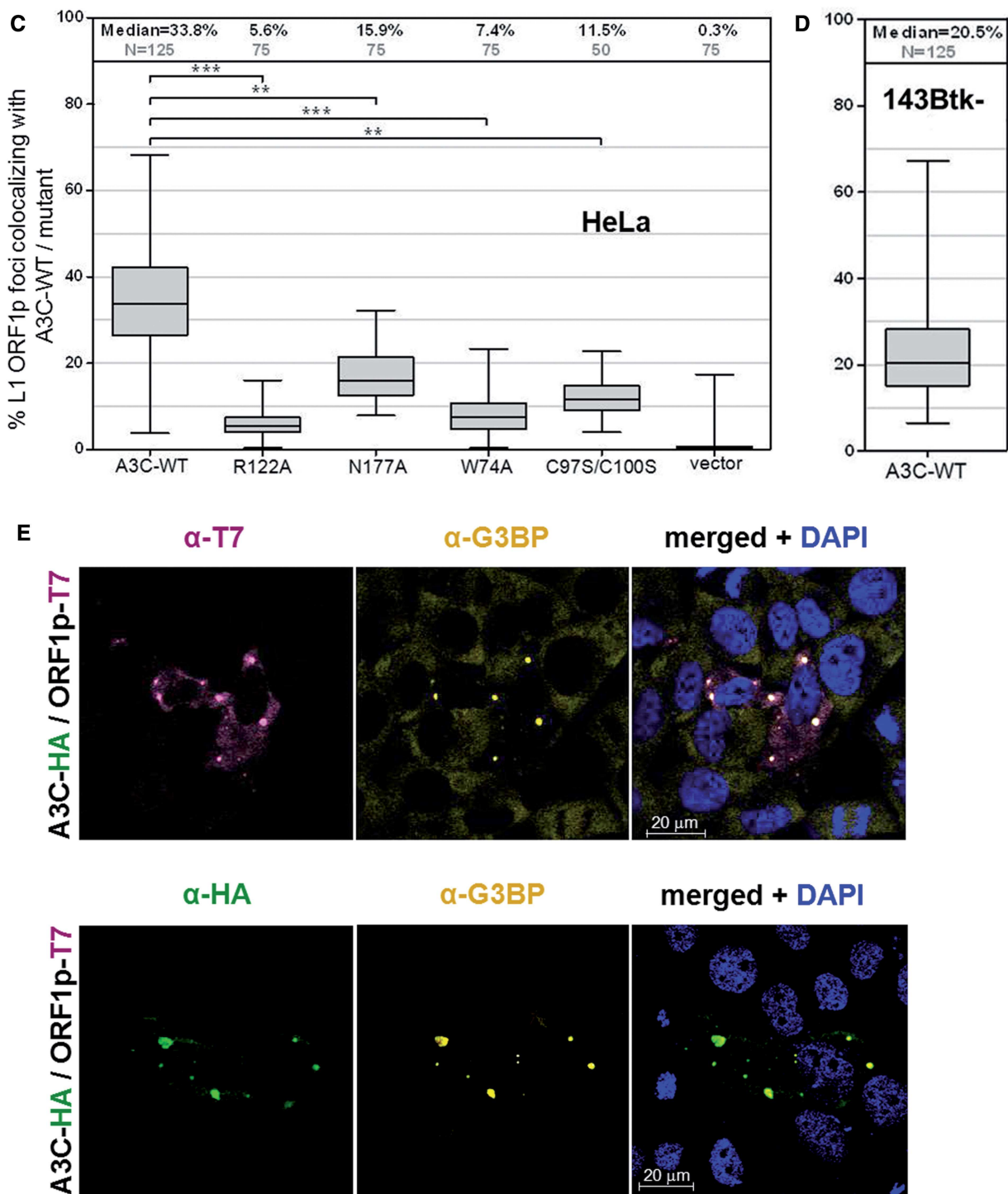


Figure 6. Continued

plasmid pDK101. After 11 days of hygromycin selection for the presence of the L1 expression plasmid, cells were separately transfected with expression plasmids encoding A3C- and A3A-WT or A3C mutants R122A, N177A, W74A or C97S/C100S. Three days later, cell lysates were isolated and HA-tagged A3 expression as well as L1 ORF1p expression was controlled for by immunoblot analysis (Figure 7A, cell lysates). HA-tagged A3 proteins

were immunoprecipitated using anti-HA affinity matrix beads. Efficient immunoprecipitation (IP) was controlled for by immunoblot analysis of the precipitated proteins with the α -HA antibody (Figure 7A, IP). ORF1p was pulled down only if overexpressed A3A or A3C was present, while ORF1p was not precipitated in the absence of APOBEC3 proteins (Figure 7A). To test whether the observed ORF1p-A3C interaction is RNA-bridged, we

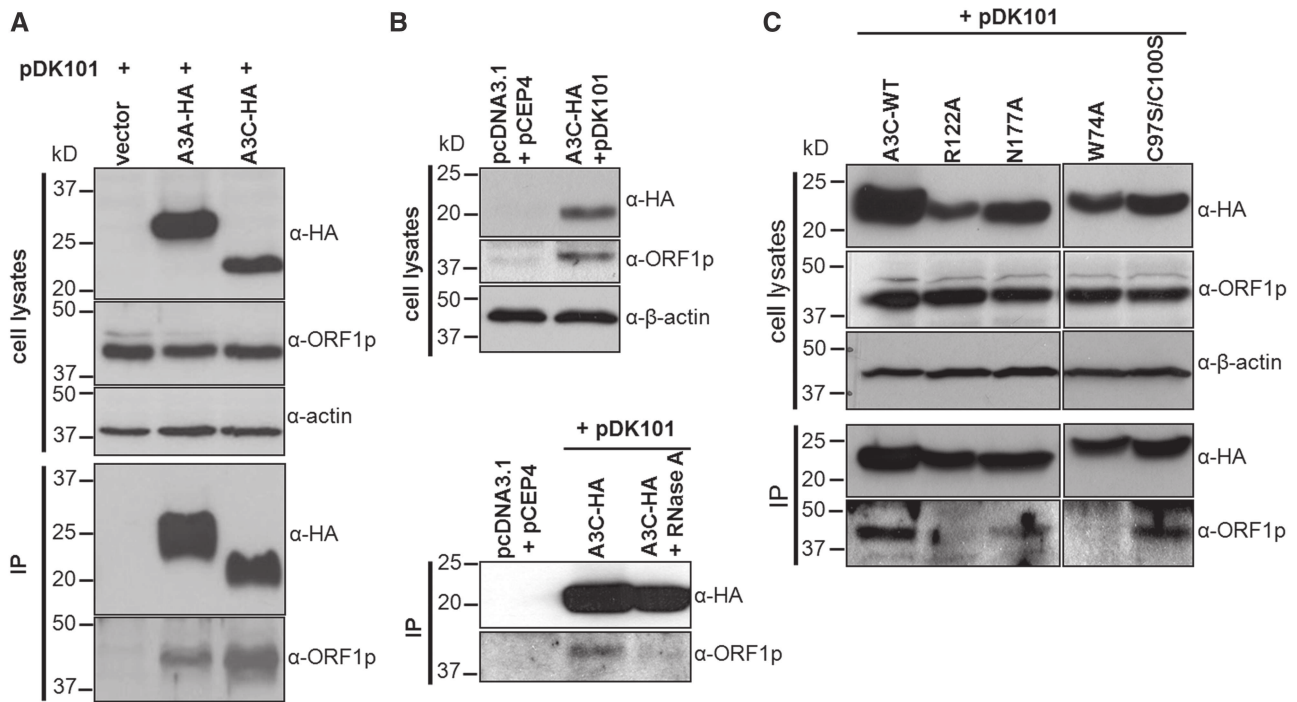


Figure 7. Complex formation between L1 ORF1p and A3C requires bridging RNA molecules. (A) ORF1p coprecipitates with ectopically expressed A3A and A3C. Immunoblot analysis of cell lysates isolated from HeLa cells that were consecutively transfected with pDK101 and A3A-HA, A3C-HA or the empty expression vector pcDNA3.1/Zeo(+) (vector), respectively, and their derived immunoprecipitates. The presence of HA-tagged A3A and A3C or L1 ORF1p in cell lysates and immunoprecipitates (IP) was demonstrated using α -HA and α -ORF1p antibodies, respectively. β -actin expression served as loading control. (B) RNase A treatment of the cell lysate abolishes the interaction between A3C and L1 ORF1p. Immunoblot analysis of cell lysates isolated from HeLa cells that were co-transfected with pDK101 and A3C-HA or the empty expression vectors (pcDNA3.1 + pCEP4), respectively (upper panel). The cleared cell lysate was split in half and RNase A was added to one half to a final concentration of 50 μ g/ml. After incubation of RNase-treated and untreated lysates with α -HA Affinity Matrix Beads, immunoprecipitates were submitted to immunoblot analyses (lower panel). (C) RNA-binding pocket mutation R122A abolishes the A3C/L1 ORF1p interaction. Immunoblot analysis of cell lysates isolated from HeLa cells that were co-transfected with pDK101 and expression plasmids encoding A3C-WT, R122A, N177A or C97S/C100S mutant proteins, respectively (upper panel, cell types), and their derived immunoprecipitates (lower panel, IP). In contrast to R122A, RNA-binding pocket mutation N177A does only moderately affect A3C/ORF1p complex formation. While mutating the A3C dimerization site (W74A) abolishes A3C/ORF1p interaction almost entirely, the CDA double-mutant C97S/C100S still exhibits significant interaction with L1 ORF1p. Lysates and immunoprecipitates obtained from W74A- and C97S/C100S-expressing HeLa cells were loaded on a different gel than the remaining lysates and immunoprecipitates.

added RNase A to an aliquot of the cleared cell lysate before IP was performed. RNaseA treatment clearly abolished the interaction between A3C and ORF1p (Figure 7B), suggesting that this interaction is RNA bridged. The finding that the RNA-binding pocket mutation R122A abolishes the A3C-ORF1p interaction (Figure 7C) further supports the existence of an RNA-bridged interaction between A3C-WT and ORF1p. Candidate RNAs that might form an RNA bridge are 5S, 5.8S and/or 7SL RNA, which were demonstrated to interact with A3C-WT, while the R122A mutant was only able to weakly interact with 7SL RNA [Supplementary Figure S5; (63)]. In contrast, the RNA-binding pocket mutation N177A has only a minor effect on A3C/ORF1p interaction. While the CDA domain double-mutation C97S/C100S does not affect the interaction with ORF1p, the W74A mutation in the dimerization domain abolishes the A3C/ORF1p interaction, suggesting that A3C dimerization is required (Figure 7C). Co-immunoprecipitation data are consistent with the percentage of co-localization of WT and mutant A3C proteins with L1 ORF1p (Figure 6).

Taken together, these data suggest an interaction between L1 ORF1p and A3C dimers, which requires RNA binding to A3C. Since both A3C-WT and the CDA domain double-mutant interact with ORF1p and similarly restrict L1 retrotransposition, the interaction with ORF1p seems to be crucial for L1 restriction by A3C. Results also imply that A3A and A3C are incorporated into L1 RNPs via ORF1p interaction.

The presence of A3C inhibits L1 RT activity

A3G has been reported to be incorporated into budding HIV-1 particles and to inhibit HIV-1 replication by blocking initiation of reverse transcription by the tRNA^{Lys3} primer, physically interacting with the RT, and interacting with the HIV integrase, which was shown to prevent the assembly of a functional pre-integration complex (83–86). Therefore, we next tested the hypothesis that the interaction of A3C with ORF1p and/or L1 RNPs inhibits L1 retrotransposition by interfering with the target-primed reverse transcription of L1 mRNA. For that purpose, we applied the LEAP assay that was established recently to mimic the initial stages

of target-primed reverse transcription, where the L1 RT acts to extend a 3'-hydroxyl that has been liberated by the L1 endonuclease (71).

We set out to compare the L1 RT activity of L1 RNPs that assembled in the presence and absence of overexpressed A3C. For that purpose, HeLa cells were transfected with the L1 reporter plasmid pDK101 or its parental empty vector pCEP4 (Invitrogen), and were then hygromycin selected for the presence of the respective plasmid for 11 days (Figure 8A). Then, hyg^R-selected cells were transfected with the A3C-expressing plasmid or its empty expression vector pcDNA3.1/Zeo(+). Three days later, the cleared cell lysate was centrifuged through a sucrose cushion and the resultant L1 RNP-containing pellet was resuspended (71). Whole-cell lysates and resuspended L1 RNP-containing pellets were assayed for the presence of ectopically expressed ORF1p and A3C-HA proteins (Figure 8B). Immunoblot analyses showed that similar amounts of ORF1p are both expressed in HeLa cells that were co-transfected with pDK101 (Figure 8B, upper panel) and present in associated RNP pellets (Figure 8B, lower panel). Comparable amounts of A3C-HA were detectable between cell lysates from HeLa cells co-transfected with A3C-HA and pDK101 expression plasmid or with the A3C-HA expression plasmid and the empty pCEP4 expression vector (Figure 8B, upper panel, α -HA). However, only those RNP pellets contain significant amounts of A3C-HA that were formed in the presence of ectopically expressed L1 ORF1p encoded by the transfected pDK101 plasmid (Figure 8B, lower panel, α -HA). In contrast, only negligible amounts of A3C-HA were detectable in RNP pellets from HeLa cells that were not co-transfected with pDK101 and expressed exclusively minor amounts of endogenous L1 ORF1p. The detection of A3C in the RNP pellet is consistent with the incorporation of A3C into L1 RNPs (Figure 8B).

Analysis of RNP pellets by qualitative RT-PCR using SuperScriptTM III RT (Figure 8C, upper gel, Superscript III L1) and the same oligonucleotides as primers that were used in the LEAP assay (Figure 8C, lower gel, LEAP-L1), demonstrates the presence of L1 mRNA, which is indicative for the presence of functional L1 RNPs. The RT-PCR experiment indicated that L1 RNA was present at comparable levels in the RNP fraction of HeLa cells that were co-transfected with the empty expression vector and those co-transfected with the A3C-HA expression plasmid. Sequence analysis of the 207-bp SuperScript III RT-PCR product obtained from cells transfected with pDK101 (Figure 8C, upper gel) confirmed the presence of the 3' end of the pDK101-encoded polyadenylated L1 message. Sequencing of the minor amounts of an unexpectedly observed ~200-bp RT-PCR product obtained from HeLa cells that were consecutively transfected with the empty expression vector pCEP4 and the A3C-HA expression plasmid (Figure 8C, upper gel, lane A3C-HA) showed that this PCR product was a consequence of unspecific annealing of the PCR primer *L1 3' end* (62) between positions 650 and 680 of the pCEP4 sequence,

which is part of the CMV-promoter-controlled transcribed region (data not shown).

Next, we applied the LEAP assay to determine whether those isolated RNPs contained L1-specific RT activity and whether the associated A3C proteins interfere with L1 RT activity. Consistent with previous studies (71,87), a diffuse set of LEAP products that ranged in size from ~220 to 400 bp was detected in RNPs isolated from HeLa cells that were co-transfected with pDK101 and A3C expression plasmid or with the empty expression vector (Figure 8C, lower gel). Quantification of the LEAP products obtained from the two RNP samples showed that the presence of A3C reduced the amount of L1 cDNA by ~50% (Figure 8C, lower gel). To evaluate which A3C domains are required for A3C-mediated inhibition of L1 RT, we also performed LEAP assays with RNP fractions carrying the A3C mutant proteins R122A, W74A or C97S/C100S or A3C-WT in parallel. We were able to express reasonable amounts of WT and mutant A3C proteins in HeLa cells, and could demonstrate the presence of A3C-WT in the L1 RNP fraction from HeLa cells co-expressing A3C-WT and pDK101. However, we could not identify any of the mutant A3C proteins R122A, W74A or C97S/C100S in the respective L1 RNP fractions isolated from HeLa cells expressing sufficient amounts of the different A3C mutant proteins (Supplementary Figure S6) and were therefore not able to evaluate any potential effect of the A3C mutants on L1 RNP-associated L1 RT activity. The absence of R122A and W74A from the RNP fractions is consistent with their inability to interact with L1 ORF1p (Figure 7C).

Taken together, our data suggest that A3C-mediated L1 restriction requires an RNA-bridged interaction between A3C dimers and ORF1p of L1 RNP complexes that interfere with the processivity of L1 RT.

DISCUSSION

Higher eukaryotes have evolved various defense mechanisms to protect their genomes from potential mutagenic effects caused by uncontrolled proliferation of transposable elements. Members of the A3 protein family were reported to inhibit L1 and/or *Alu* retrotransposition by 30–99% [reviewed in (23,74)]. However, no direct evidence for the inhibition of the currently mobilized L1Hs subfamily by cytidine deamination of L1Hs cDNA or any kind of editing of L1 nucleic acid sequences has yet been reported. This strongly suggests that CDA-independent mechanisms are involved in A3-mediated L1 restriction. Since A3C is the most abundantly expressed A3 protein across a wide range of human tissues and cells, we set out to elucidate the A3C-mediated mechanism of L1 restriction.

A3C-mediated L1 restriction does not require a catalytically functional CDA domain

Using a set of well-characterized A3C CDA mutants, we showed that CDA-activity of A3C does not play any role in A3C-mediated L1 restriction. This is the first example of an A3C-mediated inhibitory effect that is clearly deaminase independent. We also confirmed the previous finding that

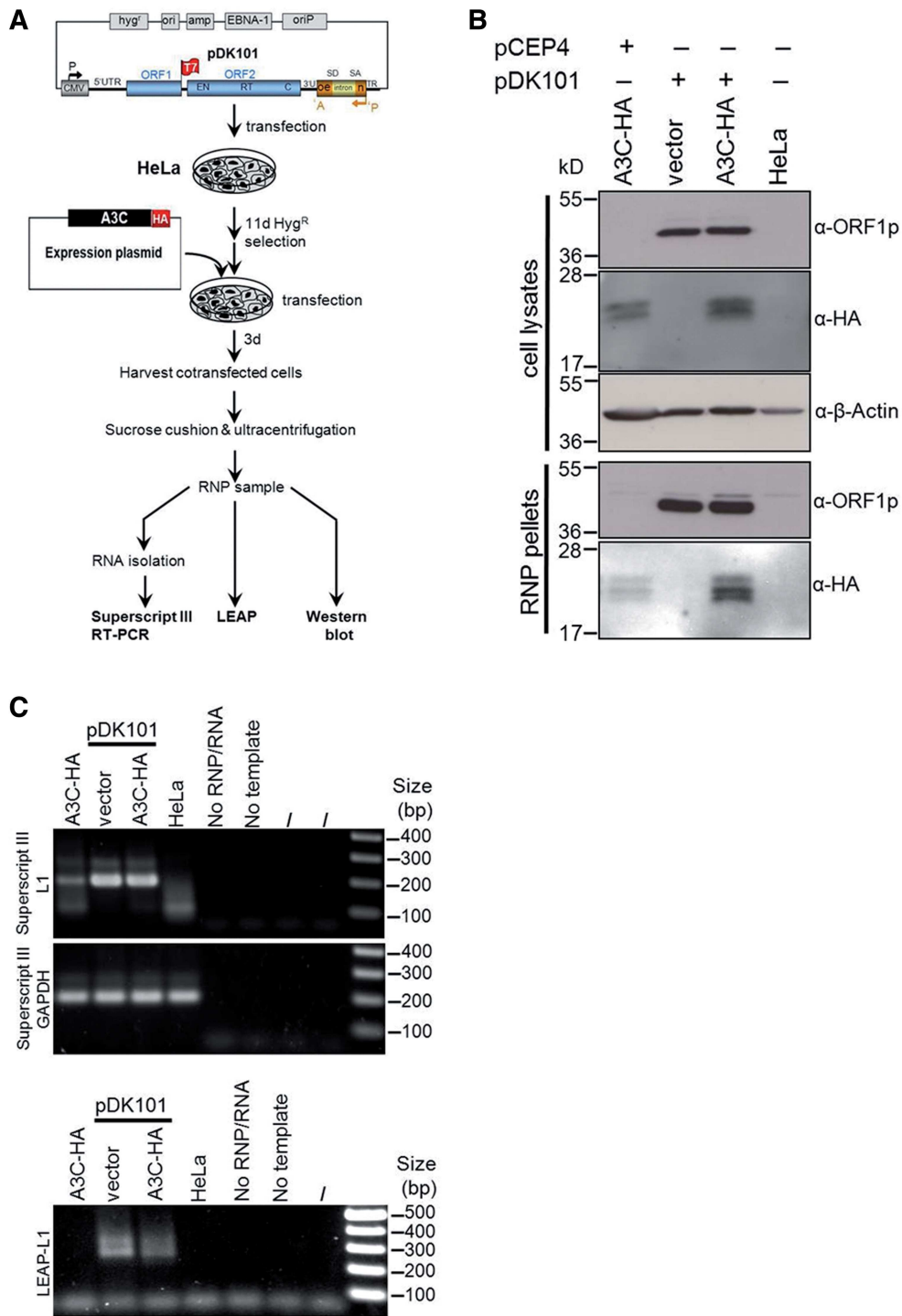


Figure 8. L1 RNPs that assembled in the presence of overexpressed A3C exhibit reduced L1 RT activity. (A) Flow chart of the experimental setup. HeLa cells were transfected with the L1 reporter plasmid pDK101 or its empty vector pCEP4, hyg^R-selected for 11 days and subsequently transfected with the A3C-HA expression plasmid or its empty vector plasmid pcDNA3.1/Zeo(+). Three days after the last transfection, RNPs were isolated from the lysed cells. Total cell lysates and RNP pellets were obtained from cells consecutively transfected with pCEP4 and the A3C-HA plasmid, pDK101 and A3C-HA or pDK101 and pcDNA3.1/Zeo(+), and from untransfected cells (HeLa). Subsequently cell lysates and RNP pellets were submitted to immunoblot analysis with α-HA and α-ORF1p antibodies. (B) Immunoblot analysis of cell lysates and RNP pellets isolated from HeLa cells overexpressing the L1 protein machinery and/or A3C-HA. β-actin expression served as loading control. Cell lysates and RNP pellets isolated from untransfected HeLa cells and after co-transfection of pDK101 and the empty expression plasmid (vector) served as negative controls. (C) LEAP assay to detect L1-specific RT activity. LEAP products are detectable using RNPs from cells, which were co-transfected with pDK101 and A3C-HA or the empty expression vector. Reactions with RNPs from untransfected HeLa cells (HeLa), without template (No template) or RNPs (No RNP/RNA) were used as negative controls. Upper gel: The 207-bp L1-specific SuperScriptIII RT-PCR product is highly abundant in samples from pDK101-transfected cells and absent from HeLa samples. Middle gel: the 198-bp GAPDH SuperScriptIII RT-PCR product is a cellular mRNA marker for all RNP preparations and confirms comparable amounts of RNPs per sample. Lower gel: LEAP products (LEAP-L1).

in contrast corresponding catalytically defective A3A mutants are largely inactive against L1 (37,43). Similar to enzymatically inactive A3C mutants, catalytically inactive mutants of A3B, A3G and AID also maintain L1 inhibition activity (36,42). It was suggested that A3B accomplishes editing-independent inhibition of retroelement mobility by direct interaction with L1 ORF2p through a common domain that interferes with L1 *cis*- and *Alu trans*-mobilization (36). A3C also modestly inhibits *Alu trans*-mobilization with G-to-A mutations being absent from *de novo Alu* insertions that occurred in the presence of overexpressed A3C (39). This observation is consistent with our results indicating that A3C interferes with L1 RT activity. *Alu* retrotransposition can also be inhibited by A3G WT and catalytically inactive mutants, which also suggests a CDA-independent mechanism for A3G action (64,88). It was shown that A3G sequesters *Alu* RNAs in cytoplasmic HMM complexes, particularly Staufen-containing RNA granules, denying these retroelements access to the nuclear L1 protein machinery (88). This inhibitory mechanism differs from the A3A- and A3B-mediated inhibition of *Alu* retrotransposition, where the A3 proteins alter the activity of the L1 machinery in the nucleus (39).

A3C dimerization and an intact RNA-binding pocket are required for L1 restriction by A3C

To answer the question of whether A3C needs to oligomerize to inhibit L1 mobilization, the effects of the dimerization-deficient A3C mutants F55A and W74A on A3C-mediated L1 inhibition were determined. As observed for SIV Δ *vif* replication (63), we found that A3C-oligomerization is required for the restriction of L1 replication. Similarly, dimerization-deficient A3G deletion mutants cannot restrict HIV Δ *vif* replication (70,89,90). Consistently, structure models of AID, A3C and A3G, as well as the APOBEC2 crystal structure, suggest that APOBEC proteins generally act as dimers or tetramers (63,70,91,92).

While mutating the critical residues K22 or R122 of the putative A3C RNA-binding pocket caused a significant loss of L1 inhibition ($p_{K22A} = 0.0015$; $p_{R122A} = 0.0001$) to only ~29% or even restored and enhanced L1 retrotransposition activity, respectively, the N177A mutation did not affect L1 inhibition by A3C significantly ($p_{N177A} = 1$). The L1-restricting effect of A3C-WT and its mutant proteins K22A and N177A, as well as the absence of any L1-inhibiting effect of R122A, correlates well with the antiretroviral effects of K22A and N177A and the loss of any inhibitory effect of R122A against SIV Δ *vif* reported previously (63). In contrast to the remaining RNA-binding pocket mutants, R122A abolished the L1-inhibiting effect entirely. It was reported recently that R122A is critically relevant for SIV particle packaging but not for the antiviral activity of A3C, and that the R122A mutation has only a minor inhibiting effect on A3C deaminase activity (63). Furthermore, A3C-WT was shown to interact with 7SL, 5.8S and 5S rRNA, while the R122A mutant maintained only the capability to bind 7SL rRNA [Supplementary Figure S5; (63)]. A strong RNA-bridge candidate is 7SL RNA because it

was demonstrated to interact with A3C-WT [Supplementary Figure S5; (63)] and was recently detected in L1 RNP immunoprecipitates (93). Since SRP14, which together with SRP9, forms a complex with 7SL RNA (94), was also reported to be associated with L1 RNPs (93), 7SL RNA could well be an RNA that the ORF1p/A3C interaction depends on.

Our observation that the expression of 0.5–1.5 μ g of the mutant R122A expression construct increased the number of L1 retrotransposition events by ~60–100% can be explained by a potential dominant-negative effect of R122A. Since A3C is endogenously expressed in HeLa cells (37), we hypothesize that R122A mutant proteins oligomerize with intact A3C proteins forming nonfunctional A3C dimers or tetramers, thereby abolishing the L1-inhibiting effect of endogenous A3C-WT. In contrast, expression of the mutant proteins K22A and N177A still restricts L1 activity. We hypothesize that L1 restriction by A3C oligomers requires efficient RNA binding to all involved A3C monomers. This could have the consequence that overexpressed K22A and/or N177A proteins, which were not demonstrated to have any RNA-binding deficiencies, oligomerize with endogenous A3C proteins forming functional RNA-binding oligomers that are still able to restrict L1. This hypothesis is supported by the finding that, in contrast to R122A, the N177A mutant is still able to form complexes with L1 ORF1p (Figure 7C), which requires RNA binding (Figure 7B). Taken together, we conclude that RNA binding to A3C is required for the L1-inhibiting effect of A3C, and that RNA binding to ORF1p is also essential for the observed interaction of A3C with L1 ORF1p. To date, it is unclear which RNA A3C needs to interact with to inhibit L1. Candidate RNAs for A3C interaction are 7SL RNA and 5.8S rRNA, L1 RNA or any host-encoded RNA. Recently it was demonstrated that A3A recognizes and interacts with L1 RNA and is associated with L1 RNA in HMM complexes (46). Interestingly, the ability of A3A to recognize L1 RNA required its catalytic domain. It could well be that the A3C oligomerization that is required for L1 inhibition is RNA dependent. This would be reminiscent of A3G oligomerization that was recently shown to be RNA dependent and required for restriction of HIV-1 (70). It was also reported that, specifically through its RNA-binding properties (17,73,95), A3G sequesters *Alu* and Y RNAs in cytoplasmic HMM complexes away from the nuclear L1 machinery, thereby interdicting the retrotransposition cycle (88).

A3C interacts with L1 ORF1p and co-localizes with L1 RNPs

Our finding that ORF1p shifts to sucrose gradient fractions of lower molecular mass in the presence of ectopically expressed A3C and the observation that L1 ORF1p and A3C co-localize in HeLa and 143Btk- cells is consistent with an interaction between A3C and ORF1p or L1 RNPs. These data further suggest that A3C and ORF1p are part of HMM complexes (88) and are consistent with the recently reported presence of A3C in HMM complexes of 293T cells (46,96). The physical interaction

between ORF1p and A3C or A3A was additionally confirmed by co-immunoprecipitation experiments that strongly imply that both A3 proteins are incorporated into L1 RNPs and exert their inhibiting effects on L1 by interacting with L1 ORF1p or L1 RNPs. Our data strongly suggest that the observed A3C/L1 ORF1p complex results from an RNA-bridged interaction, which means A3C and ORF1p are connected by binding the same RNA molecule (e.g. 7SL RNA). This is further supported by the following facts: (i) both A3C and ORF1p are RNA-binding proteins (63,97,98), and (ii) an intact RNA-binding pocket is required for A3C-mediated restriction of both SIV Δ vif and L1 replication. Furthermore, RNA binding was shown to be crucial for the interaction between A3C and SIV-NC (63), and A3B and mA3 were reported to bind to L1 ORF1p via an RNA bridge (99). It is conceivable that A3C binds L1 RNA that is interacting with ORF1p, thereby preventing the nuclear import of L1 RNPs. Taken together, we provide direct evidence for an RNA-bridged association of A3C proteins with L1 ORF1p or L1 RNPs.

Association of A3C with stress granules

In accordance with previous reports, we demonstrate that overexpressed ORF1p localizes predominantly to cytoplasmic granules in HeLa and 143Btk- cells (Figure 6A and B), which were recently identified as stress granules (77–79). Ectopic co-expression of A3C-HA led to nucleocytoplasmic distribution of A3C-HA proteins and their accumulation in cytoplasmic foci, which is consistent with the A3C distribution observed when A3C is expressed alone (37,46,80). We found that in HeLa cells co-expressing both proteins, 34% of all cytoplasmic ORF1p granules co-localize with A3C-HA foci, suggesting that A3C may block the entry of a subset of L1 RNPs into the nucleus by A3C-mediated sequestration of L1 RNPs. Since our data show that both A3C and L1 ORF1p localize with stress granules, it is most likely that A3C and L1 ORF1p also co-localize at least in a subset of stress granules. Our findings are consistent with the recent identification of L1 ORF1p together with polyadenylated RNA in stress granules (78,87). Co-localization of A3C and L1 ORF1p in stress granules would support the hypothesis that A3C mediates the transport of functional L1 RNPs into stress granules. It is also consistent with a recently proposed mechanism whereby the cell may mitigate the potential mutagenic effects of retrotransposition by sequestering L1 RNPs and possibly targeting them for degradation (78). While we could not find any evidence for A3C localization to P-bodies, A3G, A3B and A3F were reported to be located to P-bodies (88,100–102).

A3C interferes with L1 RT activity

Since our data suggest the incorporation of A3C into L1 RNPs, we tested whether the L1 RT activity of L1 RNPs that are associated with A3C is impaired. We found that the presence of A3C led to a decrease of L1 cDNAs by ~50%, which roughly corresponds to the reduction of the number of detectable L1 retrotransposition events in

HeLa cells by ~50–75% when overexpressed A3C is present. This is reminiscent of the nonenzymatic form of inhibition of HIV-1 Δ vif infectivity by A3G, which likely involves physical impairment of RT activity (73,86,103). Taken together, we uncovered a novel deaminase-independent mechanism of L1 inhibition by A3C that is mediated by the interaction of A3C with L1 ORF1p, requires the binding of RNA, and interferes with L1 RT activity. Impairment of L1 RT activity not only inhibits *cis*-mobilization of L1 elements but also *trans*-mobilization of *Alu* and SVA elements as well as processed pseudogene formation. Our data also provide some evidence for an additional mechanism of L1 restriction based on A3C-mediated transport of functional L1 RNPs into stress granules where they might be targeted for degradation. The near-ubiquitous expression of A3C may underline its significant biological role in the repression of potentially deleterious L1-mediated retrotransposition events.

While there is no evidence for A3-mediated editing of members of the currently mobilized L1Hs subfamily, ~1300 edited members of the L1 subfamilies L1PA2, L1PA3, L1PA5 and L1PA6 were recently identified, covering only ~0.1% of L1 elements (104). This suggests that A3-mediated editing of L1 elements occurred between 5.6 and 34 Myrs ago (105). Surprisingly, it was also reported that 20.1% of all SVA elements including 238 human-specific elements and 16 polymorphic elements carry G-to-A hypermutations, indicating that, in spite of everything, A3-mediated DNA editing of non-LTR retrotransposons is a still ongoing process in humans (104).

SUPPLEMENTARY DATA

Supplementary Data are available at NAR Online.

ACKNOWLEDGEMENTS

The authors thank John Moran for providing HeLa-JVM cells, plasmid pDK101 and supporting us to establish the LEAP assay. The authors are grateful to John Goodier and Haig Kazazian for providing the osteosarcoma cell line 143Btk-, and plasmid pJM101/L1_{RP}, to Bryan Cullen for the A3A expression plasmid. They also thank Klaus Cichutek, and Dieter Häussinger for constant support.

FUNDING

Deutsche Forschungsgemeinschaft [DA 545/2-1 to G.G.S.]; Heinz Ansmann Foundation for AIDS Research (to C.M.); Stiftung zur Erforschung infektiös-immunologischer Erkrankungen (to H.H.). Funding for open access charge: Paul-Ehrlich-Institut.

Conflict of interest statement. None declared.

REFERENCES

- Goodier, J.L. and Kazazian, H.H. Jr (2008) Retrotransposons revisited: the restraint and rehabilitation of parasites. *Cell*, **135**, 23–35.

2. Solyom,S. and Kazazian,H.H. Jr (2012) Mobile elements in the human genome: implications for disease. *Genome Med.*, **4**, 12.
3. Kazazian,H.H. Jr, Wong,C., Youssoufian,H., Scott,A.F., Phillips,D.G. and Antonarakis,S.E. (1988) Haemophilia A resulting from de novo insertion of L1 sequences represents a novel mechanism for mutation in man. *Nature*, **332**, 164–166.
4. Hancks,D.C. and Kazazian,H.H. Jr (2012) Active human retrotransposons: variation and disease. *Curr. Opin. Genet. Dev.*, **22**, 191–203.
5. Gasiior,S.L., Wakeman,T.P., Xu,B. and Deininger,P.L. (2006) The human LINE-1 retrotransposon creates DNA double-strand breaks. *J. Mol. Biol.*, **357**, 1383–1393.
6. Lin,C., Yang,L., Tanasa,B., Hutt,K., Ju,B.G., Ohgi,K., Zhang,J., Rose,D.W., Fu,X.D., Glass,C.K. *et al.* (2009) Nuclear receptor-induced chromosomal proximity and DNA breaks underlie specific translocations in cancer. *Cell*, **139**, 1069–1083.
7. Yu,F., Zingler,N., Schumann,G. and Stratling,W.H. (2001) Methyl-CpG-binding protein 2 represses LINE-1 expression and retrotransposition but not Alu transcription. *Nucleic Acids Res.*, **29**, 4493–4501.
8. Bourc'his,D. and Bestor,T.H. (2004) Meiotic catastrophe and retrotransposon reactivation in male germ cells lacking Dnmt3L. *Nature*, **431**, 96–99.
9. Yoder,J.A., Walsh,C.P. and Bestor,T.H. (1997) Cytosine methylation and the ecology of intragenomic parasites. *Trends Genet.*, **13**, 335–340.
10. Yang,N. and Kazazian,H.H. Jr (2006) L1 retrotransposition is suppressed by endogenously encoded small interfering RNAs in human cultured cells. *Nat. Struct. Mol. Biol.*, **13**, 763–771.
11. Malone,C.D. and Hannon,G.J. (2009) Small RNAs as guardians of the genome. *Cell*, **136**, 656–668.
12. Aravin,A.A., Sachidanandam,R., Girard,A., Fejes-Toth,K. and Hannon,G.J. (2007) Developmentally regulated piRNA clusters implicate MILI in transposon control. *Science*, **316**, 744–747.
13. Suzuki,J., Yamaguchi,K., Kajikawa,M., Ichianagi,K., Adachi,N., Koyama,H., Takeda,S. and Okada,N. (2009) Genetic evidence that the non-homologous end-joining repair pathway is involved in LINE retrotransposition. *PLoS Genet.*, **5**, e1000461.
14. Gasiior,S.L., Roy-Engel,A.M. and Deininger,P.L. (2008) ERCC1/XPF limits L1 retrotransposition. *DNA Repair*, **7**, 983–989.
15. Stenson,D.B., Ko,J.S., Heidmann,T. and Medzhitov,R. (2008) Trex1 prevents cell-intrinsic initiation of autoimmunity. *Cell*, **134**, 587–598.
16. Levin,H.L. and Moran,J.V. (2011) Dynamic interactions between transposable elements and their hosts. *Nat. Rev. Genet.*, **12**, 615–627.
17. Jarmuz,A., Chester,A., Bayliss,J., Gisbourne,J., Dunham,I., Scott,J. and Navaratnam,N. (2002) An anthropoid-specific locus of orphan C to U RNA-editing enzymes on chromosome 22. *Genomics*, **79**, 285–296.
18. Conticello,S.G., Harris,R.S. and Neuberger,M.S. (2003) The Vif protein of HIV triggers degradation of the human antiretroviral DNA deaminase APOBEC3G. *Curr. Biol.*, **13**, 2009–2013.
19. Conticello,S.G., Thomas,C.J., Petersen-Mahrt,S.K. and Neuberger,M.S. (2005) Evolution of the AID/APOBEC family of polynucleotide (deoxy)cytidine deaminases. *Mol. Biol. Evol.*, **22**, 367–377.
20. Münk,C., Willemsen,A. and Bravo,I.G. (2012) An ancient history of gene duplications, fusions and losses in the evolution of APOBEC3 mutators in mammals. *BMC Evol. Biol.*, **12**, 71.
21. Refsland,E.W., Stenglein,M.D., Shindo,K., Albin,J.S., Brown,W.L. and Harris,R.S. (2010) Quantitative profiling of the full APOBEC3 mRNA repertoire in lymphocytes and tissues: implications for HIV-1 restriction. *Nucleic Acids Res.*, **38**, 4274–4284.
22. Chiu,Y.L. and Greene,W.C. (2008) The APOBEC3 cytidine deaminases: an innate defensive network opposing exogenous retroviruses and endogenous retroelements. *Annu. Rev. Immunol.*, **26**, 317–353.
23. Schumann,G.G., Gogvadze,E.V., Osanai-Futahashi,M., Kuroki,A., Münk,C., Fujiwara,H., Ivics,Z. and Buzdin,A.A. (2010) Unique functions of repetitive transcriptomes. *Int. Rev. Cell Mol. Biol.*, **285**, 115–188.
24. Beale,R.C., Petersen-Mahrt,S.K., Watt,I.N., Harris,R.S., Rada,C. and Neuberger,M.S. (2004) Comparison of the differential context-dependence of DNA deamination by APOBEC enzymes: correlation with mutation spectra *in vivo*. *J. Mol. Biol.*, **337**, 585–596.
25. Bishop,K.N., Holmes,R.K., Sheehy,A.M., Davidson,N.O., Cho,S.J. and Malim,M.H. (2004) Cytidine deamination of retroviral DNA by diverse APOBEC proteins. *Curr. Biol.*, **14**, 1392–1396.
26. Harris,R.S., Bishop,K.N., Sheehy,A.M., Craig,H.M., Petersen-Mahrt,S.K., Watt,I.N., Neuberger,M.S. and Malim,M.H. (2003) DNA deamination mediates innate immunity to retroviral infection. *Cell*, **113**, 803–809.
27. Lecossier,D., Bouchonnet,F., Clavel,F. and Hance,A.J. (2003) Hypermutation of HIV-1 DNA in the absence of the Vif protein. *Science*, **300**, 1112.
28. Mangeat,B., Turelli,P., Caron,G., Friedli,M., Perrin,L. and Trono,D. (2003) Broad antiretroviral defence by human APOBEC3G through lethal editing of nascent reverse transcripts. *Nature*, **424**, 99–103.
29. Mariani,R., Chen,D., Schrofelbauer,B., Navarro,F., König,R., Bollman,B., Münk,C., Nymark-McMahon,H. and Landau,N.R. (2003) Species-specific exclusion of APOBEC3G from HIV-1 virions by Vif. *Cell*, **114**, 21–31.
30. Suspene,R., Sommer,P., Henry,M., Ferris,S., Guetard,D., Pochet,S., Chester,A., Navaratnam,N., Wain-Hobson,S. and Vartanian,J.P. (2004) APOBEC3G is a single-stranded DNA cytidine deaminase and functions independently of HIV reverse transcriptase. *Nucleic Acids Res.*, **32**, 2421–2429.
31. Vartanian,J.P., Henry,M., Marchio,A., Suspene,R., Aynaud,M.M., Guetard,D., Cervantes-Gonzalez,M., Battiston,C., Mazzaferro,V., Pineau,P. *et al.* (2010) Massive APOBEC3 editing of hepatitis B viral DNA in cirrhosis. *PLoS Pathog.*, **6**, e1000928.
32. Stenglein,M.D., Burns,M.B., Li,M., Lengyel,J. and Harris,R.S. (2010) APOBEC3 proteins mediate the clearance of foreign DNA from human cells. *Nat. Struct. Mol. Biol.*, **17**, 222–229.
33. Holmes,R.K., Malim,M.H. and Bishop,K.N. (2007) APOBEC-mediated viral restriction: not simply editing? *Trends Biochem. Sci.*, **32**, 118–128.
34. Holmes,R.K., Koning,F.A., Bishop,K.N. and Malim,M.H. (2007) APOBEC3F can inhibit the accumulation of HIV-1 reverse transcription products in the absence of hypermutation. Comparisons with APOBEC3G. *J. Biol. Chem.*, **282**, 2587–2595.
35. Bogerd,H.P., Wiegand,H.L., Doehle,B.P., Lueders,K.K. and Cullen,B.R. (2006) APOBEC3A and APOBEC3B are potent inhibitors of LTR-retrotransposon function in human cells. *Nucleic Acids Res.*, **34**, 89–95.
36. Stenglein,M.D. and Harris,R.S. (2006) APOBEC3B and APOBEC3F inhibit L1 retrotransposition by a DNA deamination-independent mechanism. *J. Biol. Chem.*, **281**, 16837–16841.
37. Muckenfuss,H., Hamdorf,M., Held,U., Perkovic,M., Löwer,J., Cichutek,K., Flory,E., Schumann,G.G. and Münk,C. (2006) APOBEC3 proteins inhibit human LINE-1 retrotransposition. *J. Biol. Chem.*, **281**, 22161–22172.
38. Gilbert,N., Lutz,S., Morrish,T.A. and Moran,J.V. (2005) Multiple fates of L1 retrotransposition intermediates in cultured human cells. *Mol. Cell. Biol.*, **25**, 7780–7795.
39. Bogerd,H.P., Wiegand,H.L., Hulme,A.E., Garcia-Perez,J.L., O'Shea,K.S., Moran,J.V. and Cullen,B.R. (2006) Cellular inhibitors of long interspersed element 1 and Alu retrotransposition. *Proc. Natl Acad. Sci. USA*, **103**, 8780–8785.
40. Bogerd,H.P., Wiegand,H.L., Doehle,B.P. and Cullen,B.R. (2007) The intrinsic antiretroviral factor APOBEC3B contains two enzymatically active cytidine deaminase domains. *Virology*, **364**, 486–493.
41. Pak,V., Heidecker,G., Pathak,V.K. and Derse,D. (2011) The role of amino-terminal sequences in cellular localization and antiviral activity of APOBEC3B. *J. Virol.*, **85**, 8538–8547.
42. MacDuff,D.A., Demorest,Z.L. and Harris,R.S. (2009) AID can restrict L1 retrotransposition suggesting a dual role in innate and adaptive immunity. *Nucleic Acids Res.*, **37**, 1854–1867.
43. Chen,H., Lilley,C.E., Yu,Q., Lee,D.V., Chou,J., Narvaiza,I., Landau,N.R. and Weitzman,M.D. (2006) APOBEC3A is a potent

- inhibitor of adeno-associated virus and retrotransposons. *Curr. Biol.*, **16**, 480–485.
44. Narvaiza, I., Linfesty, D.C., Greener, B.N., Hakata, Y., Pintel, D.J., Logue, E., Landau, N.R. and Weitzman, M.D. (2009) Deaminase-independent inhibition of parvoviruses by the APOBEC3A cytidine deaminase. *PLoS Pathog.*, **5**, e1000439.
 45. Zielonka, J., Bravo, I.G., Marino, D., Conrad, E., Perkovic, M., Battenberg, M., Cichutek, K. and Münk, C. (2009) Restriction of equine infectious anemia virus by equine APOBEC3 cytidine deaminases. *J. Virol.*, **83**, 7547–7559.
 46. Niewiadomska, A.M., Tian, C., Tan, L., Wang, T., Sarkis, P.T. and Yu, X.F. (2007) Differential inhibition of long interspersed element 1 by APOBEC3 does not correlate with high-molecular-mass-complex formation or P-body association. *J. Virol.*, **81**, 9577–9583.
 47. Yu, Q., Chen, D., König, R., Mariani, R., Unutmaz, D. and Landau, N.R. (2004) APOBEC3B and APOBEC3C are potent inhibitors of simian immunodeficiency virus replication. *J. Biol. Chem.*, **279**, 53379–53386.
 48. Mahieux, R., Suspene, R., Delebecque, F., Henry, M., Schwartz, O., Wain-Hobson, S. and Vartanian, J.P. (2005) Extensive editing of a small fraction of human T-cell leukemia virus type 1 genomes by four APOBEC3 cytidine deaminases. *J. Gen. Virol.*, **86**, 2489–2494.
 49. Henry, M., Guetard, D., Suspene, R., Rusniok, C., Wain-Hobson, S. and Vartanian, J.P. (2009) Genetic editing of HBV DNA by monodomain human APOBEC3 cytidine deaminases and the recombinant nature of APOBEC3G. *PLoS One*, **4**, e4277.
 50. Langlois, M.A., Beale, R.C., Conticello, S.G. and Neuberger, M.S. (2005) Mutational comparison of the single-domained APOBEC3C and double-domained APOBEC3F/G anti-retroviral cytidine deaminases provides insight into their DNA target site specificities. *Nucleic Acids Res.*, **33**, 1913–1923.
 51. Bourara, K., Liegler, T.J. and Grant, R.M. (2007) Target cell APOBEC3C can induce limited G-to-A mutation in HIV-1. *PLoS Pathog.*, **3**, 1477–1485.
 52. Dutko, J.A., Schafer, A., Kenny, A.E., Cullen, B.R. and Curcio, M.J. (2005) Inhibition of a yeast LTR retrotransposon by human APOBEC3 cytidine deaminases. *Curr. Biol.*, **15**, 661–666.
 53. Schumacher, A.J., Nissley, D.V. and Harris, R.S. (2005) APOBEC3G hypermutates genomic DNA and inhibits Ty1 retrotransposition in yeast. *Proc. Natl Acad. Sci. USA*, **102**, 9854–9859.
 54. Baumert, T.F., Rosler, C., Malim, M.H. and von Weizsacker, F. (2007) Hepatitis B virus DNA is subject to extensive editing by the human deaminase APOBEC3C. *Hepatology*, **46**, 682–689.
 55. Kock, J. and Blum, H.E. (2008) Hypermutation of hepatitis B virus genomes by APOBEC3G, APOBEC3C and APOBEC3H. *J. Gen. Virol.*, **89**, 1184–1191.
 56. Suspene, R., Aynaud, M.M., Guetard, D., Henry, M., Eckhoff, G., Marchio, A., Pineau, P., Dejean, A., Vartanian, J.P. and Wain-Hobson, S. (2011) Somatic hypermutation of human mitochondrial and nuclear DNA by APOBEC3 cytidine deaminases, a pathway for DNA catabolism. *Proc. Natl Acad. Sci. USA*, **108**, 4858–4863.
 57. Vartanian, J.P., Guetard, D., Henry, M. and Wain-Hobson, S. (2008) Evidence for editing of human papillomavirus DNA by APOBEC3 in benign and precancerous lesions. *Science*, **320**, 230–233.
 58. Suspene, R., Aynaud, M.M., Koch, S., Padeloup, D., Labetoulle, M., Gaertner, B., Vartanian, J.P., Meyerhans, A. and Wain-Hobson, S. (2011) Genetic editing of herpes simplex virus 1 and Epstein-Barr herpesvirus genomes by human APOBEC3 cytidine deaminases in culture and *in vivo*. *J. Virol.*, **85**, 7594–7602.
 59. Khatua, A.K., Taylor, H.E., Hildreth, J.E. and Popik, W. (2010) Inhibition of LINE-1 and Alu retrotransposition by exosomes encapsidating APOBEC3G and APOBEC3F. *Virology*, **400**, 68–75.
 60. Kinomoto, M., Kanno, T., Shimura, M., Ishizaka, Y., Kojima, A., Kurata, T., Sata, T. and Tokunaga, K. (2007) All APOBEC3 family proteins differentially inhibit LINE-1 retrotransposition. *Nucleic Acids Res.*, **35**, 2955–2964.
 61. Kimberland, M.L., Divoky, V., Prchal, J., Schwahn, U., Berger, W. and Kazazian, H.H. Jr (1999) Full-length human L1 insertions retain the capacity for high frequency retrotransposition in cultured cells. *Hum. Mol. Genet.*, **8**, 1557–1560.
 62. Kulpa, D.A. and Moran, J.V. (2005) Ribonucleoprotein particle formation is necessary but not sufficient for LINE-1 retrotransposition. *Hum. Mol. Genet.*, **14**, 3237–3248.
 63. Stauch, B., Hofmann, H., Perkovic, M., Weisel, M., Kopietz, F., Cichutek, K., Münk, C. and Schneider, G. (2009) Model structure of APOBEC3C reveals a binding pocket modulating ribonucleic acid interaction required for encapsidation. *Proc. Natl Acad. Sci. USA*, **106**, 12079–12084.
 64. Hulme, A.E., Bogerd, H.P., Cullen, B.R. and Moran, J.V. (2007) Selective inhibition of Alu retrotransposition by APOBEC3G. *Gene*, **390**, 199–205.
 65. Wei, W., Morrish, T.A., Alisch, R.S. and Moran, J.V. (2000) A transient assay reveals that cultured human cells can accommodate multiple LINE-1 retrotransposition events. *Anal. Biochem.*, **284**, 435–438.
 66. Ostertag, E.M., Prak, E.T., DeBerardinis, R.J., Moran, J.V. and Kazazian, H.H. Jr (2000) Determination of L1 retrotransposition kinetics in cultured cells. *Nucleic Acids Res.*, **28**, 1418–1423.
 67. Wei, W., Gilbert, N., Ooi, S.L., Lawler, J.F., Ostertag, E.M., Kazazian, H.H. Jr, Boeke, J.D. and Moran, J.V. (2001) Human L1 retrotransposition: cis preference versus trans complementation. *Mol. Cell. Biol.*, **21**, 1429–1439.
 68. Raiz, J., Damert, A., Chira, S., Held, U., Klawitter, S., Hamdorf, M., Löwer, J., Stratling, W.H., Löwer, R. and Schumann, G.G. (2012) The non-autonomous retrotransposon SVA is trans-mobilized by the human LINE-1 protein machinery. *Nucleic Acids Res.*, **40**, 1666–1683.
 69. Kamentsky, L., Jones, T.R., Fraser, A., Bray, M.A., Logan, D.J., Madden, K.L., Ljosa, V., Rueden, C., Eliceiri, K.W. and Carpenter, A.E. (2011) Improved structure, function and compatibility for CellProfiler: modular high-throughput image analysis software. *Bioinformatics*, **27**, 1179–1180.
 70. Huthoff, H., Autore, F., Gallois-Montbrun, S., Fraternali, F. and Malim, M.H. (2009) RNA-dependent oligomerization of APOBEC3G is required for restriction of HIV-1. *PLoS Pathog.*, **5**, e1000330.
 71. Kulpa, D.A. and Moran, J.V. (2006) Cis-preferential LINE-1 reverse transcriptase activity in ribonucleoprotein particles. *Nat. Struct. Mol. Biol.*, **13**, 655–660.
 72. Navarro, F., Bollman, B., Chen, H., König, R., Yu, Q., Chiles, K. and Landau, N.R. (2005) Complementary function of the two catalytic domains of APOBEC3G. *Virology*, **333**, 374–386.
 73. Newnan, E.N., Holmes, R.K., Craig, H.M., Klein, K.C., Lingappa, J.R., Malim, M.H. and Sheehy, A.M. (2005) Antiviral function of APOBEC3G can be dissociated from cytidine deaminase activity. *Curr. Biol.*, **15**, 166–170.
 74. Wissing, S., Montano, M., Garcia-Perez, J.L., Moran, J.V. and Greene, W.C. (2011) Endogenous APOBEC3B restricts LINE-1 retrotransposition in transformed cells and human embryonic stem cells. *J. Biol. Chem.*, **286**, 36427–36437.
 75. Moran, J.V., Holmes, S.E., Naas, T.P., DeBerardinis, R.J., Boeke, J.D. and Kazazian, H.H. Jr (1996) High frequency retrotransposition in cultured mammalian cells. *Cell*, **87**, 917–927.
 76. Brouha, B., Schustak, J., Badge, R.M., Lutz-Prigge, S., Farley, A.H., Moran, J.V. and Kazazian, H.H. Jr (2003) Hot L1s account for the bulk of retrotransposition in the human population. *Proc. Natl Acad. Sci. USA*, **100**, 5280–5285.
 77. Goodier, J.L., Ostertag, E.M., Engleka, K.A., Seleme, M.C. and Kazazian, H.H. Jr (2004) A potential role for the nucleolus in L1 retrotransposition. *Hum. Mol. Genet.*, **13**, 1041–1048.
 78. Goodier, J.L., Zhang, L., Vetter, M.R. and Kazazian, H.H. Jr (2007) LINE-1 ORF1 protein localizes in stress granules with other RNA-binding proteins, including components of RNA interference RNA-induced silencing complex. *Mol. Cell. Biol.*, **27**, 6469–6483.
 79. Goodier, J.L., Mandal, P.K., Zhang, L. and Kazazian, H.H. Jr (2010) Discrete subcellular partitioning of human retrotransposon RNAs despite a common mechanism of genome insertion. *Hum. Mol. Genet.*, **19**, 1712–1725.
 80. Lackey, L., Law, E.K., Brown, W.L. and Harris, R.S. (2013) Subcellular localization of the APOBEC3 proteins during mitosis

- and implications for genomic DNA deamination. *Cell Cycle*, **12**, 762–772.
81. Goodier, J.L., Cheung, L.E. and Kazazian, H.H. Jr (2012) MOV10 RNA helicase is a potent inhibitor of retrotransposition in cells. *PLoS Genet.*, **8**, e1002941.
 82. Eulalio, A., Behm-Ansmant, I. and Izaurralde, E. (2007) P bodies: at the crossroads of post-transcriptional pathways. *Nat. Rev. Mol. Cell Biol.*, **8**, 9–22.
 83. Wang, T., Tian, C., Zhang, W., Luo, K., Sarkis, P.T., Yu, L., Liu, B., Yu, Y. and Yu, X.F. (2007) 7SL RNA mediates virion packaging of the antiviral cytidine deaminase APOBEC3G. *J. Virol.*, **81**, 13112–13124.
 84. Guo, F., Cen, S., Niu, M., Saadatmand, J. and Kleiman, L. (2006) Inhibition of formula-primed reverse transcription by human APOBEC3G during human immunodeficiency virus type 1 replication. *J. Virol.*, **80**, 11710–11722.
 85. Luo, K., Wang, T., Liu, B., Tian, C., Xiao, Z., Kappes, J. and Yu, X.F. (2007) Cytidine deaminases APOBEC3G and APOBEC3F interact with human immunodeficiency virus type 1 integrase and inhibit proviral DNA formation. *J. Virol.*, **81**, 7238–7248.
 86. Wang, X., Ao, Z., Chen, L., Kobinger, G., Peng, J. and Yao, X. (2012) The cellular antiviral protein APOBEC3G interacts with HIV-1 reverse transcriptase and inhibits its function during viral replication. *J. Virol.*, **86**, 3777–3786.
 87. Doucet, A.J., Hulme, A.E., Sahinovic, E., Kulpa, D.A., Moldovan, J.B., Kopera, H.C., Athanikar, J.N., Hasnaoui, M., Bucheton, A., Moran, J.V. *et al.* (2010) Characterization of LINE-1 ribonucleoprotein particles. *PLoS Genet.*, **6**, e1001150.
 88. Chiu, Y.L., Witkowska, H.E., Hall, S.C., Santiago, M., Soros, V.B., Esnault, C., Heidmann, T. and Greene, W.C. (2006) High-molecular-mass APOBEC3G complexes restrict Alu retrotransposition. *Proc. Natl Acad. Sci. USA*, **103**, 15588–15593.
 89. Shindo, K., Takaori-Kondo, A., Kobayashi, M., Abudu, A., Fukunaga, K. and Uchiyama, T. (2003) The enzymatic activity of CEM15/Apobec-3G is essential for the regulation of the infectivity of HIV-1 virion but not a sole determinant of its antiviral activity. *J. Biol. Chem.*, **278**, 44412–44416.
 90. Bulliard, Y., Turelli, P., Rohrig, U.F., Zoete, V., Mangeat, B., Michielin, O. and Trono, D. (2009) Functional analysis and structural modeling of human APOBEC3G reveal the role of evolutionarily conserved elements in the inhibition of human immunodeficiency virus type 1 infection and Alu transposition. *J. Virol.*, **83**, 12611–12621.
 91. Prochnow, C., Bransteitter, R., Klein, M.G., Goodman, M.F. and Chen, X.S. (2007) The APOBEC-2 crystal structure and functional implications for the deaminase AID. *Nature*, **445**, 447–451.
 92. Vasudevan, A.A., Smits, S.H., Hoppner, A., Haussinger, D., Koenig, B.W. and Münk, C. (2013) Structural features of antiviral DNA cytidine deaminases. *Biol. Chem.*, **394**, 1357–1370.
 93. Goodier, J.L., Cheung, L.E. and Kazazian, H.H. Jr (2013) Mapping the LINE1 ORF1 protein interactome reveals associated inhibitors of human retrotransposition. *Nucleic Acids Res.*, **41**, 7401–7419.
 94. Strub, K. and Walter, P. (1990) Assembly of the Alu domain of the signal recognition particle (SRP): dimerization of the two protein components is required for efficient binding to SRP RNA. *Mol. Cell. Biol.*, **10**, 777–784.
 95. Chiu, Y.L., Soros, V.B., Kreisberg, J.F., Stopak, K., Yonemoto, W. and Greene, W.C. (2005) Cellular APOBEC3G restricts HIV-1 infection in resting CD4+ T cells. *Nature*, **435**, 108–114.
 96. Wang, T., Zhang, W., Tian, C., Liu, B., Yu, Y., Ding, L., Spearman, P. and Yu, X.F. (2008) Distinct viral determinants for the packaging of human cytidine deaminases APOBEC3G and APOBEC3C. *Virology*, **377**, 71–79.
 97. Hohjoh, H. and Singer, M.F. (1997) Sequence-specific single-strand RNA binding protein encoded by the human LINE-1 retrotransposon. *EMBO J.*, **16**, 6034–6043.
 98. Kolosha, V.O. and Martin, S.L. (1997) *In vitro* properties of the first ORF protein from mouse LINE-1 support its role in ribonucleoprotein particle formation during retrotransposition. *Proc. Natl Acad. Sci. USA*, **94**, 10155–10160.
 99. Lovsin, N. and Peterlin, B.M. (2009) APOBEC3 proteins inhibit LINE-1 retrotransposition in the absence of ORF1p binding. *Ann. N Y Acad. Sci.*, **1178**, 268–275.
 100. Kozak, S.L., Marin, M., Rose, K.M., Bystrom, C. and Kabat, D. (2006) The anti-HIV-1 editing enzyme APOBEC3G binds HIV-1 RNA and messenger RNAs that shuttle between polysomes and stress granules. *J. Biol. Chem.*, **281**, 29105–29119.
 101. Wichroski, M.J., Robb, G.B. and Rana, T.M. (2006) Human retroviral host restriction factors APOBEC3G and APOBEC3F localize to mRNA processing bodies. *PLoS Pathog.*, **2**, e41.
 102. Gallois-Montbrun, S., Kramer, B., Swanson, C.M., Byers, H., Lynham, S., Ward, M. and Malim, M.H. (2007) Antiviral protein APOBEC3G localizes to ribonucleoprotein complexes found in P bodies and stress granules. *J. Virol.*, **81**, 2165–2178.
 103. Bishop, K.N., Holmes, R.K. and Malim, M.H. (2006) Antiviral potency of APOBEC proteins does not correlate with cytidine deamination. *J. Virol.*, **80**, 8450–8458.
 104. Carmi, S., Church, G.M. and Levanon, E.Y. (2011) Large-scale DNA editing of retrotransposons accelerates mammalian genome evolution. *Nat. Commun.*, **2**, 519.
 105. Khan, H., Smit, A. and Boissinot, S. (2006) Molecular evolution and tempo of amplification of human LINE-1 retrotransposons since the origin of primates. *Genome Res.*, **16**, 78–87.

Supplementary Data

Human LINE-1 restriction by APOBEC3C is deaminase independent and mediated by an ORF1p interaction that affects LINE reverse transcriptase activity

Axel V. Horn, Sabine Klawitter, Ulrike Held, André Berger, Ananda Ayyapan Jaguva Vasudevan, Anja Bock, Henning Hofmann, Kay-Martin O. Hanschmann, Jan-Hendrik Trösemeier, Egbert Flory, Robert A. Jabulowsky, Jeffrey S. Han, Johannes Löwer, Roswitha Löwer, Carsten Münk and Gerald G. Schumann

Supplementary Methods

Coimmunoprecipitation and Immunoblot analysis to characterize A3C dimerization

2×10^5 293T cells were cotransfected with 1 μ g of a plasmid expressing V5-tagged A3C-WT and 1 μ g expression construct encoding HA-tagged A3C-WT, F55A or W74A, respectively, using Lipofectamine LTX (Invitrogen). Two days after cotransfection, cells were harvested and lysed in ice-cold lysis buffer [25mM Tris (pH 8.0), 137 mM NaCl, 1 % glycerol, 0.1 % SDS, 0.5 % Na-deoxycholate, 1 % Nonidet P-40, 2 mM EDTA, and complete protease inhibitor mixture (Roche)]. Small aliquots of the cleared lysates were subjected to SDS-PAGE followed by transfer to a PVDF membrane. The remaining cleared lysates were incubated with 30 μ l α -HA Affinity Matrix Beads (Roche) for 60 min at 4°C. The samples were washed 5 times with ice-cold lysis buffer. Bound proteins were eluted by boiling the beads for 5 min at 95°C in SDS loading buffer.

A3C-HA proteins were detected using an α -HA antibody (1:10⁴ dilution; Covance) and α -mouse horseradish peroxidase (1:7500 dilution; Amersham Biosciences). For detection of A3C-V5, an α -V5 antibody (1: 4000 dilution; Serotec) was applied. Alpha-tubulin was detected using an α -tubulin antibody (1:10⁴ dilution; Sigma). Signals were visualized by ECL plus (Amersham Biosciences).

Analysis of A3C–RNA interaction

To demonstrate protein–RNA interaction, plasmids expressing A3C-WT or R122A were transfected to 293T cells as described above. Cells were lysed in ice-cold lysis buffer

[PBS with 1% Triton X-100, 16 U/mL RiboLock RNase Inhibitor (Fermentas), and complete protease inhibitor mixture (Roche)]. The cleared lysates were incubated with 50 μ l-HA Affinity Matrix Beads (Roche) for 60 min at 4°C. The samples were washed 5 times with ice-cold lysis buffer. RNA bound to immobilized proteins was extracted from HA beads using TRIzol reagent (Invitrogen), according to the manufacturer's instructions. RNAs coprecipitated with A3C proteins were dissolved in diethyl pyrocarbonate-treated H₂O. Specific RT-PCR on A3C-bound RNAs was performed using Revert Aid First Strand cDNA synthesis kit (Fermentas) and random hexamer primers.

Supplementary Tables

Supplementary Table S1: L1 retrotransposition rates in the presence of overexpressed WT and mutant A3A and A3C proteins. WT, pJM101/L1_{RP}; RT-, negative control construct pJM105/L1_{RP}; N, number of individual cotransfection experiments;

	APOBEC Construct	LINE-1 Status	N	Retrotransposition frequency (2×10^5 transfected)	Experimental range (2×10^5 transfected)	Wild-type activity (%) \pm s.e.m.	p-value (1) (relative to mock)		p-value (2) (relative to A3C-WT)	
Comparison of A3A/A3C CDA Mutants	mock	WT	6	136.8	121-158	100.0 \pm 7.7	/	/	/	/
	A3A-WT	WT	6	8.7	6-14	6.3 \pm 1.6	<0.0001	***	/	/
	A3A-E72A	WT	6	136.5	116-156	99.8 \pm 8.4	1.0000		<0.0001	***
	A3A-C101A/C106A	WT	6	217.7	161-245	159.1 \pm 15.4	0.0014	**	<0.0001	***
	A3C-WT	WT	6	40.2	32-44	29.4 \pm 3.3	<0.0001	***		
	A3C-E68Q	WT	6	85.8	54-119	62.7 \pm 11.1	0.0063	**	0.0054	**
	A3C-C97S/C100S	WT	6	46.8	40-54	34.2 \pm 2.6	<0.0001	***	0.3282	
	A3C-WT	RT-	6	1.2	0-4	0.9 \pm 0.9	/	/	/	/
A3C CDA Mutants	mock	WT	3	202	177-218	100.0 \pm 8.3	/	/	/	/
	A3C-WT	WT	3	91.7	87-100	45.4 \pm 2.8	0.0093	**	/	/
	A3C-C97S	WT	3	25.3	18-30	12.5 \pm 2.4	0.0014	**	0.0023	**
	A3C-C100S	WT	3	58.7	51-63	29.0 \pm 2.5	0.0033	**	0.0349	*
	A3C-H66R	WT	3	102	93-114	50.5 \pm 4.0	0.0168	*	1.0	
	A3C-WT	RT-	3	0	0-0	0 \pm 0				

A3C Dimerization Mutants	mock	WT	6	136.8	121-158	100.0 ± 7.7	/	/	/	/
	A3C-WT	WT	6	40.2	32-44	29.4 ± 3.3	<0.0001	***	/	/
	A3C-F55A	WT	6	144.2	115-161	105.4 ± 11.3	1.0000		<0.0001	***
	A3C-W74A	WT	6	135.5	112-148	99.0 ± 6.8	1.0000		<0.0001	***
	A3C-WT	RT-	6	1.2	0-4	0.9 ± 0.9				
A3C RNA Binding Pocket Mutants	mock	WT	6	222.3	179-269	100.0 ± 9.6	/	/	/	/
	A3C-WT	WT	6	83.7	60-103	37.6 ± 5.4	<0.0001	***	/	/
	A3C-K22A	WT	6	158	115-196	71.1 ± 9.2	0.0236	*	0.0015	**
	A3C-N177A	WT	6	103.8	38-121	46.7 ± 6.2	0.0002	***	1.0	
	A3C-R122A	WT	6	361.4	231-440	162.6 ± 21.6	0.0328	*	0.0001	***
	A3C-WT	RT-	6	0	0-0	0 ± 0				
Titration of A3C-WT and A3C RNA Binding Pocket Mutant R122A	mock	WT	3	147.3	138-157	100.0 ± 6.5	/	/	/	/
	0.25µg A3C-R122A	WT	3	137	120-153	93.0 ± 11.2	1.0000		/	/
	0.5µg A3C-R122A	WT	3	289.7	241-327	196.6 ± 29.9	0.0546		/	/
	0.75µg A3C-R122A	WT	3	270.3	241-290	183.5 ± 17.6	0.0151	*	0.0008 (3)	***
	1.5µg A3C-R122A	WT	3	256.7	230-303	174.2 ± 27.3	0.1022		0.0086 (4)	**
	0.25µg A3C-WT	WT	3	22.3	18-25	15.2 ± 2.6	0.0003	***	/	/
	0.5µg A3C-WT	WT	3	35.7	20-48	24.2 ± 9.7	0.0035	**	/	/
	1.0µg A3C-WT	WT	3	34.3	22-44	23.3 ± 7.6	0.0018	**	/	/
	1.5µg A3C-WT	WT	3	32	25-41	21.7 ± 5.6	0.0009	***	/	/
	0.5µg A3C-WT	RT-	3	0	0-0	0 ± 0	/	/	/	/

p-values adjusted from t-test according to Bonferroni multiple comparisons

(1) p-values resulting from comparison with retrotransposition rates in mock-transfected cells

(2) p-values resulting from comparison with retrotransposition rates in A3C-WT-transfected cells

(3) p-value resulting from comparison of retrotransposition rates: 0.75 µg A3C-R122A vs. 0.25 µg A3C-WT

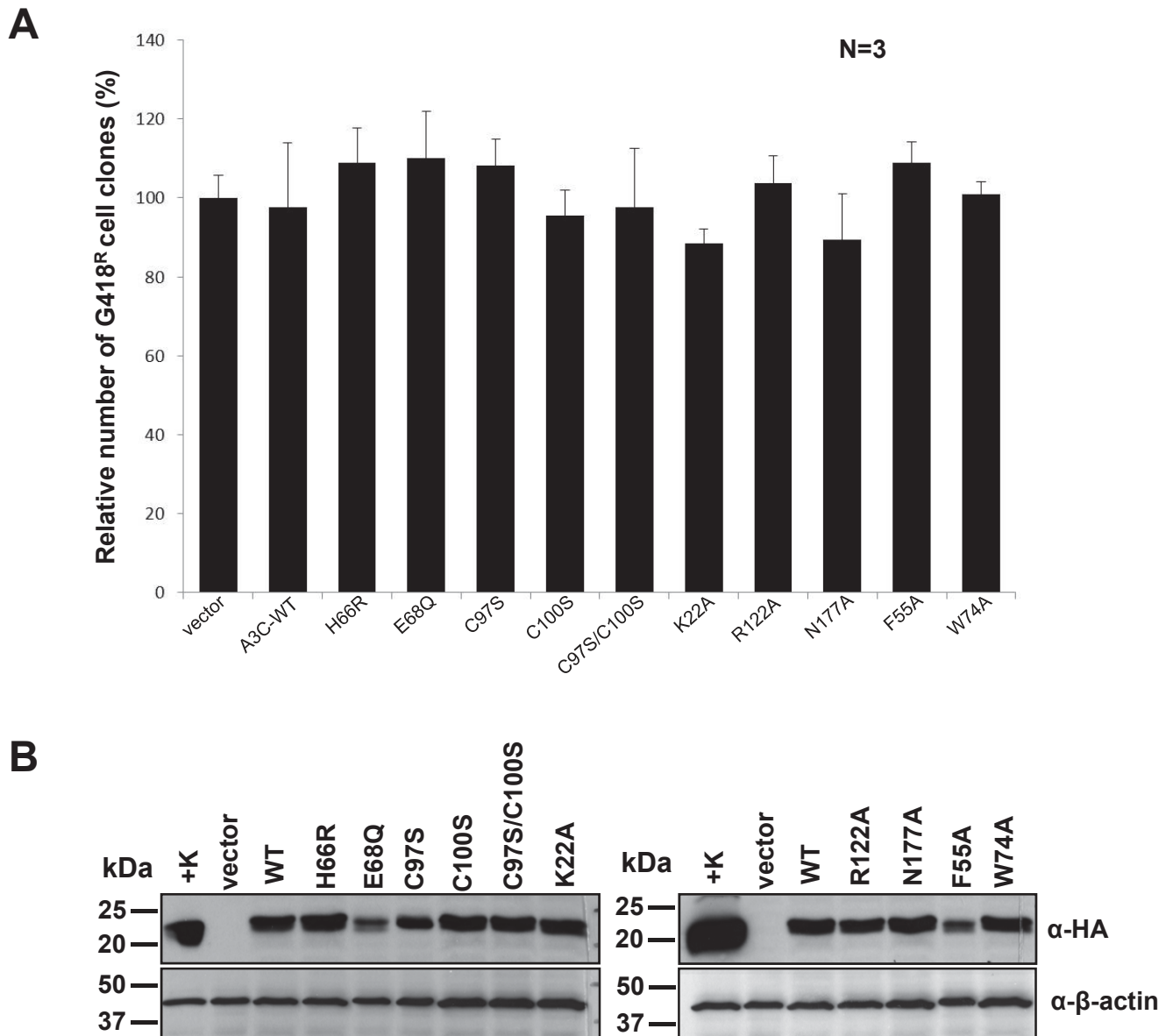
(4) p-value resulting from comparison of retrotransposition rates: 1.5 µg A3C-R122A vs. 0.5 µg A3C-WT

Supplementary Table S2: Percentage of L1 ORF1p foci in HA-HeLa and 143 BTK- cells colocalizing with A3C-WT or mutant protein.

Cell type	Mutan	N ¹	Median [%]	Min [%]	LQ [%] ²	UQ [%] ²	Max [%]
HA HeLa	A3C wildtype	125	33.8	3.8	26.8	42.1	68.2
	R122A	75	5.6	0.4	4.0	7.5	16.1
	N177A	75	15.9	7.9	12.5	21.4	32.2
	W74A	75	7.4	0.4	4.7	10.8	23.3
	C975/C100S	50	11.5	4.1	9.3	14.6	22.8
	pcDNA	75	0.3	0.0	0.0	0.8	17.4
143 BTK-	A3C wildtype	125	20.5	6.5	15.2	28.1	67.3

1 – Number of percentages (25 images per plate evaluated); 2 – Lower and Upper Quartile

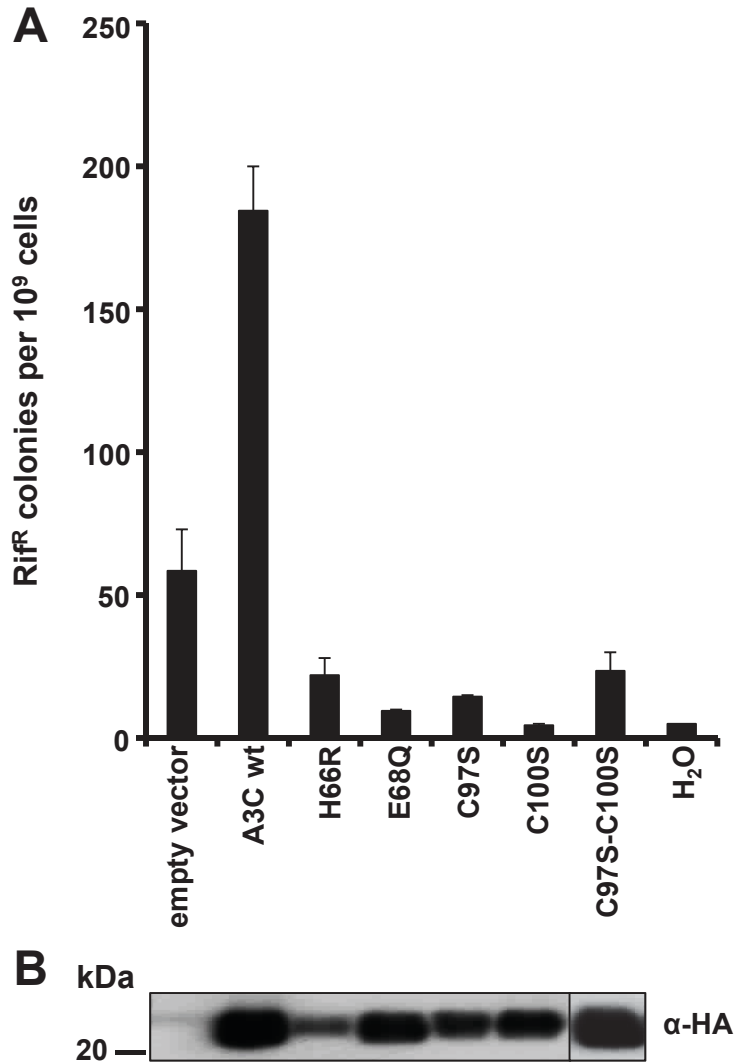
Supplementary Figures



Supplementary Figure S1: Evaluation of potential cytotoxic effects of APOBEC3C and its mutant proteins.

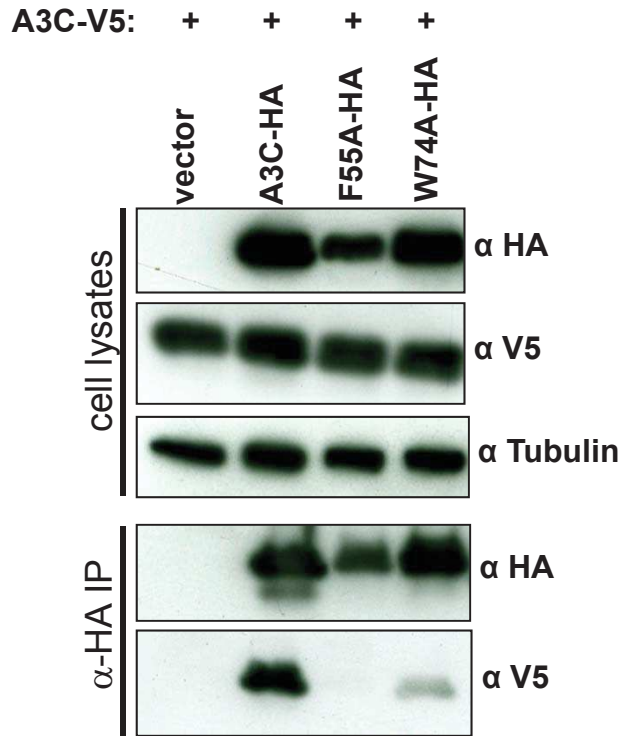
A) Overexpression of WT or mutant A3C proteins has no considerable effect on cell viability. HeLa cells were cotransfected with 0.5 μ g of pcDNA3.1(+) and 0.5 μ g of each A3C-WT or mutant expression plasmid or parental plasmid pcDNA3.1/Zeo(+) (vector). In the case of the A3C mutant R122A, it was necessary to cotransfect 1.5 μ g expression plasmid with 0.5 μ g of pcDNA3.1(+) to ensure that the cellular R122A expression level was comparable to the remaining A3C mutant and WT proteins (see B). The number of G418^R cell colonies in the absence of any overexpressed A3C-WT or mutant protein was set as 100% (vector). Bars represent arithmetic means \pm SD of three independent cotransfection experiments.

B) Immunoblot analysis of the expression levels of HA-tagged WT and mutant A3C proteins that were existent during the toxicity assay using an anti-HA antibody. β -actin expression served as loading control.



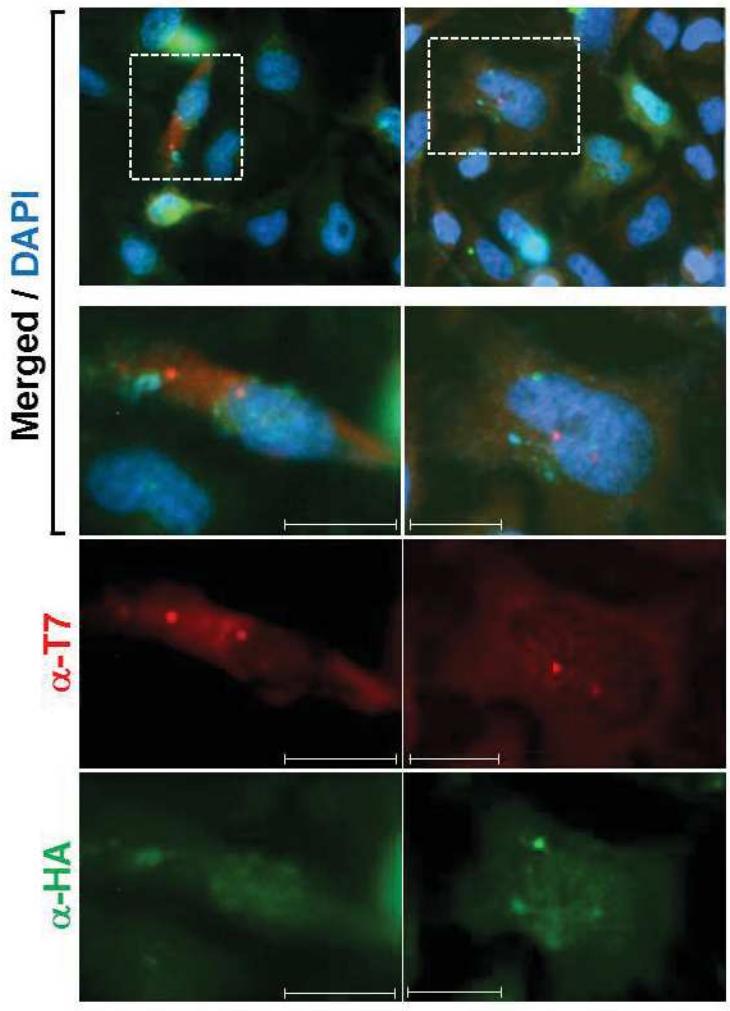
Supplementary Figure S2:

A) Editing activity of A3C-WT and A3C CDA mutant proteins measured as Rif-resistant (Rif^R) colonies. B) Immunoblot analysis to demonstrate expression levels of A3C-WT and mutant proteins in *E. coli*. Cell extract of C97S/C100S double mutant expressing cells was blotted on the same membrane as the remaining samples, but was originally separated from the samples by several lanes.

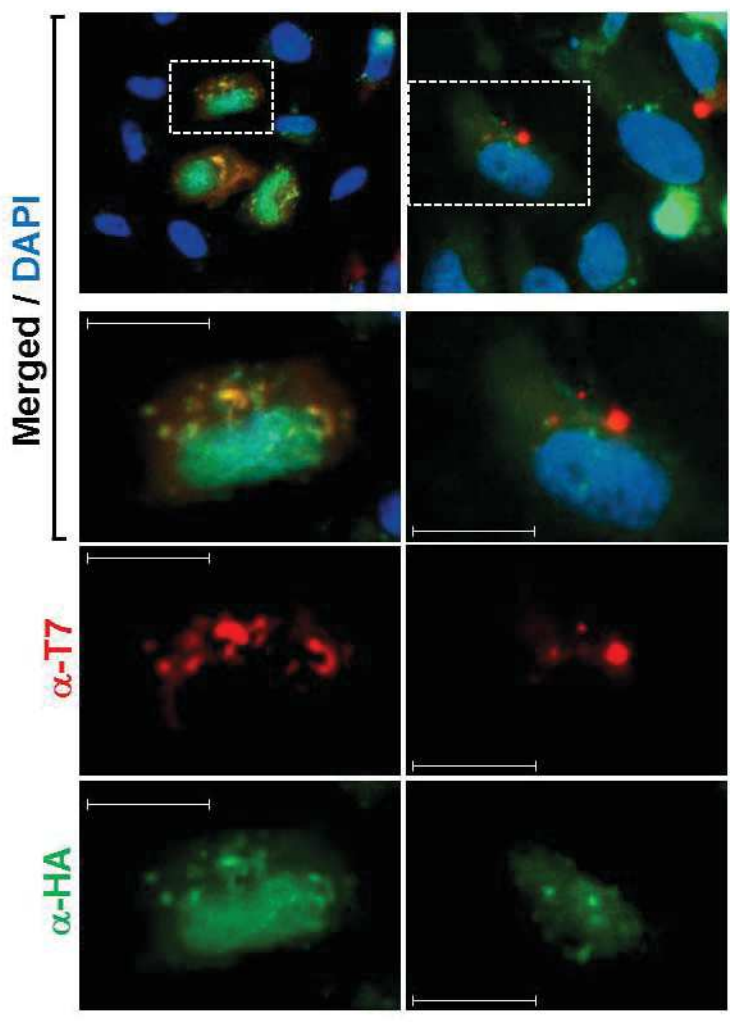


Supplementary Figure S3: Immunoblot analysis of A3C dimerization: F55 and W74 residues participate in the dimerization of A3C. 293T cells were cotransfected with the respective HA-tagged A3C-WT or mutant (F55A and W74A) expression construct and the V5-tagged A3C-WT expression plasmid. Cell lysates and immune precipitates (IP) were subjected to immunoblot analysis using anti-HA- and anti-V5-antibodies, respectively. W74A-HA coprecipitated only negligible amounts of V5-tagged A3C-WT, while F55A-HA was not able to bind any detectable V5-tagged A3C-WT. Tubulin expression served as loading control.

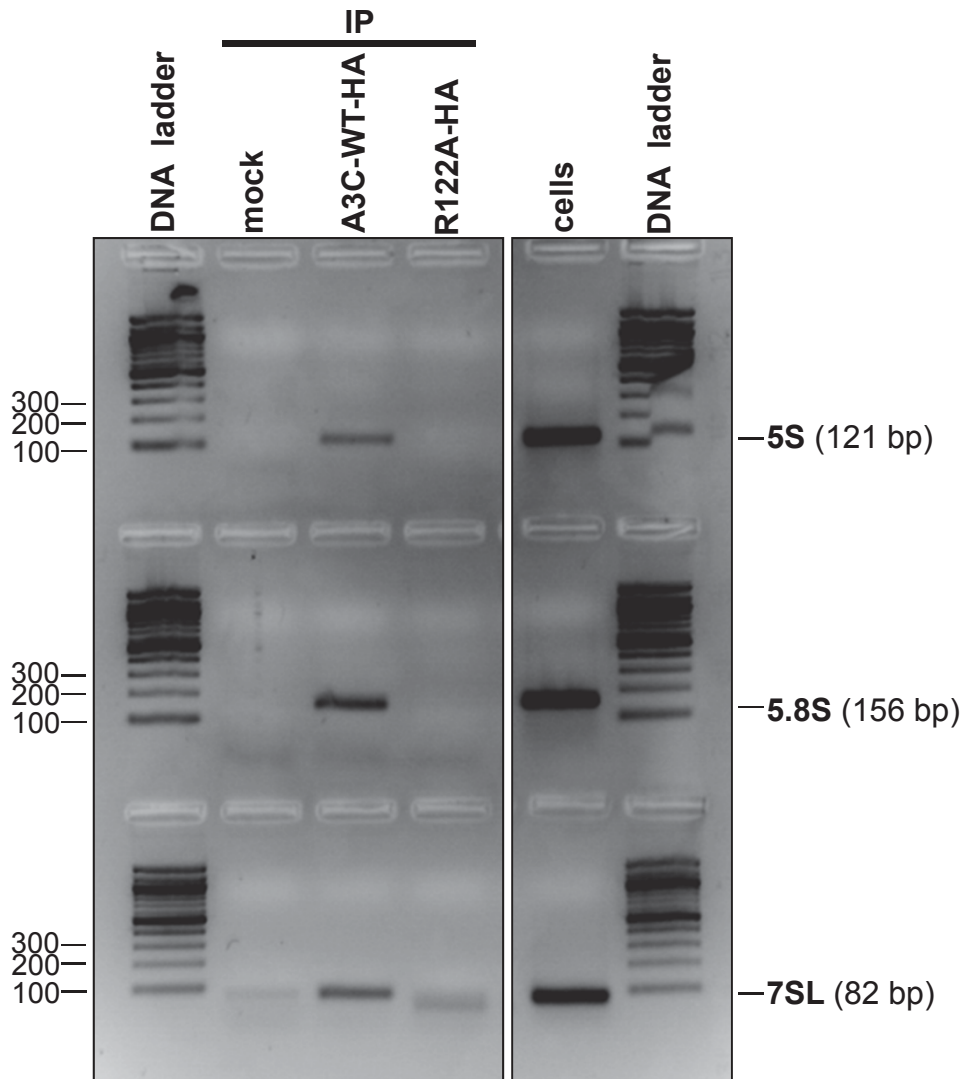
C.
R122A-HA
ORF1p-T7



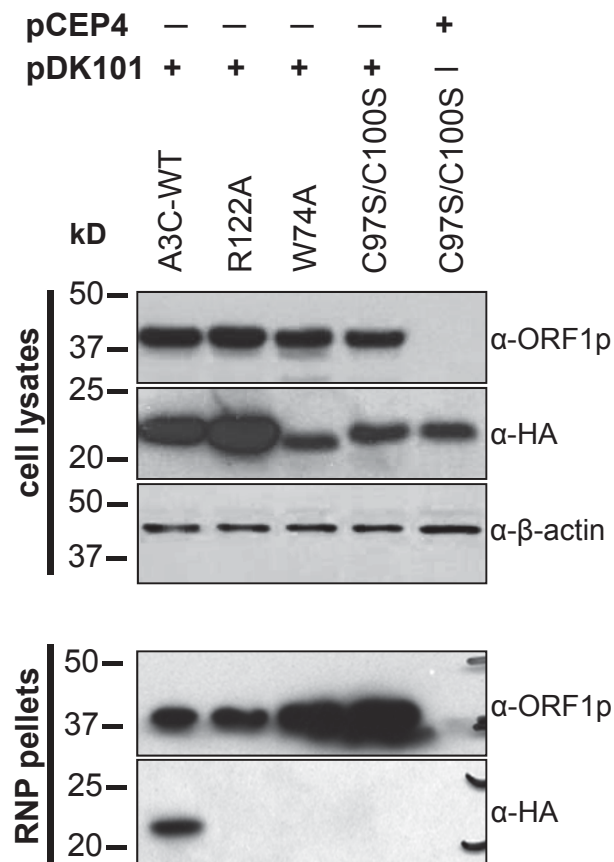
D.
N177A-HA
ORF1p-T7



Supplementary Figure S4: Subcellular localization of coexpressed T7-tagged L1 ORF1p and HA-tagged A3C mutant proteins W74A (A), C97S/C100S (B), R122A (C), and N177A (D) in HeLa cells. Immunofluorescence staining was performed using α -T7 (red) and α -HA-tag (green) antibodies. Two (W47A, R122A, N177A) or three (C97S/C100S) representative images of stained, cotransfected cells are presented. A3C mutations negatively affect the formation of A3C foci and their frequency of colocalization with ORF1p granules by varying degrees. The quantification of colocalization frequencies is illustrated in Figure 6C.



Supplementary Figure S5: RT-PCR on RNA interacting with A3C proteins. Isolated and A3C-bound RNA (IP) was reverse-transcribed and amplified using specific primers for 5S, 5.8S and 7 SL RNA. Background signal was determined with RNA from untransfected cells (mock). Availability of the tested RNAs in the cells was confirmed for each sample through RT-PCR on RNA isolated from cells before immunoprecipitation (IP) was performed (cells). DNA size standard, GeneRuler™ 100-bp Plus DNA Ladder (Fermentas).



Supplementary Figure S6: Mutant A3C proteins are not associated with L1 RNP fractions.

Immunoblot analysis of cell lysates and RNP pellets isolated from HeLa cells overexpressing the L1 protein machinery and HA-tagged A3C-mutants R122A, W74A or C97S/C100S or A3C-WT. β -actin expression served as loading control. Cell lysates and RNP pellets isolated from HeLa cells that were cotransfected with pCEP4 and the C97S/ C100S expression construct, served as negative control for RNP formation. α -HA antibody was used to detect expression of HA-tagged wildtype and mutant A3C proteins.

Data show the expression of large amounts of the L1 protein machinery and A3C-WT and mutant A3C proteins in cotransfected HeLa cells. RNPs isolated from these cells did not include any A3C mutant proteins, although A3C-WT was efficiently incorporated in the RNP fraction (RNP pellets).

While the absence of mutants R122A and W74A from the RNPs is consistent with their inability to interact with L1 ORF1p (Figure 7C), the C97S/C100S double mutant was expected to be part of the RNPs because it was shown to interact with ORF1p (Figure 7C). However, the absence of the C97S/C100S mutant protein from L1 RNPs could be explained by the fact that salt/buffer conditions L1 RNPs are exposed to during the RNP isolation procedure, are not concordant with conditions used for immunoprecipitation experiments presented in Figure 7.

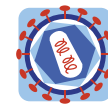
Chapter XI

A functional conserved intronic G run in HIV-1 intron 3 is critical to counteract APOBEC3G-mediated host restriction

Journal : **Retrovirology** (published in 2014)

Own contribution to this work:

- Cloned mutant Vif expression plasmids, assessed Vif counteraction activity towards A3G by HIV-1 infectivity assay and immunoblotting (presented in Figures 6B and 6C)



RESEARCH

Open Access

A functional conserved intronic G run in HIV-1 intron 3 is critical to counteract APOBEC3G-mediated host restriction

Marek Widera^{1,3}, Frank Hillebrand¹, Steffen Erkelenz¹, Ananda Ayyappan Jaguva Vasudevan², Carsten Münk² and Heiner Schaal^{1*}

Abstract

Background: The HIV-1 accessory proteins, Viral Infectivity Factor (Vif) and the pleiotropic Viral Protein R (Vpr) are important for efficient virus replication. While in non-permissive cells an appropriate amount of Vif is critical to counteract APOBEC3G-mediated host restriction, the Vpr-induced G2 arrest sets the stage for highest transcriptional activity of the HIV-1 long terminal repeat.

Both *vif* and *vpr* mRNAs harbor their translational start codons within the intron bordering the non-coding leader exons 2 and 3, respectively. Intron retention relies on functional cross-exon interactions between splice sites A1 and D2 (for *vif* mRNA) and A2 and D3 (for *vpr* mRNA). More precisely, prior to the catalytic step of splicing, which would lead to inclusion of the non-coding leader exons, binding of U1 snRNP to the 5' splice site (5'ss) facilitates recognition of the 3'ss by U2 snRNP and also supports formation of *vif* and *vpr* mRNA.

Results: We identified a G run localized deep in the *vpr* AUG containing intron 3 (G₁₃₋₂), which was critical for balanced splicing of both *vif* and *vpr* non-coding leader exons. Inactivation of G₁₃₋₂ resulted in excessive exon 3 splicing as well as exon-definition mediated *vpr* mRNA formation. However, in an apparently mutually exclusive manner this was incompatible with recognition of upstream exon 2 and *vif* mRNA processing. As a consequence, inactivation of G₁₃₋₂ led to accumulation of Vpr protein with a concomitant reduction in Vif protein. We further demonstrate that preventing hnRNP binding to intron 3 by G₁₃₋₂ mutation diminished levels of *vif* mRNA. In APOBEC3G-expressing but not in APOBEC3G-deficient T cell lines, mutation of G₁₃₋₂ led to a considerable replication defect. Moreover, in HIV-1 isolates carrying an inactivating mutation in G₁₃₋₂, we identified an adjacent G-rich sequence (G₁₃₋₁), which was able to substitute for the inactivated G₁₃₋₂.

Conclusions: The functionally conserved intronic G run in HIV-1 intron 3 plays a major role in the apparently mutually exclusive exon selection of *vif* and *vpr* leader exons and hence in *vif* and *vpr* mRNA formation. The competition between these exons determines the ability to evade APOBEC3G-mediated antiviral effects due to optimal *vif* expression.

Keywords: HIV-1 infection, Host restriction, Cytidine deaminase, APOBEC3G, Viral infectivity factor (Vif), Viral protein R (Vpr), Alternative pre-mRNA splicing, G run, hnRNP F/H, Locked nucleic acids (LNAs)

* Correspondence: schaal@uni-duesseldorf.de

¹Institute for Virology, Medical Faculty, Heinrich-Heine-University Düsseldorf, Universitätsstraße 1, Düsseldorf 40225, Germany

Full list of author information is available at the end of the article



Background

The *Human immunodeficiency virus type 1* (HIV-1) exploits cellular components of the host cell for efficient replication, while being counteracted by so called host restriction factors, which have antiviral properties and negatively affect viral replication.

Currently known host restriction factors consist of five major classes that are the DNA deaminase subfamily APOBEC3 (apolipoprotein B mRNA-editing enzyme, catalytic polypeptide-like) [1-3], the Ubl conjugation ligase TRIM5 α (Tripartite motif-containing protein 5 alpha) [4-6], the integral membrane protein BST-2 (bone stromal tumor protein 2)/tetherin [7,8], the dNTP hydrolase and RNase SAMHD1 (SAM domain and HD domain-containing protein 1) [9-13], and the tRNA binding protein SLFN11 (Schlafen 11) [14-16]. The APOBEC3 (A3) family includes seven members (A3A to A3D and A3F to A3H) that are located in a gene cluster on chromosome 22 [17-19], from which A3D, A3F, A3G and A3H have HIV-1 restrictive capacities [20-22]. They are encapsidated in newly assembled virions, and following the subsequent infection of a host cell, introduce C-to-U substitutions during minus-strand synthesis. This results in G-to-A hypermutations in the HIV-1 genome, which negatively impact viral replication. Hereby, A3G causes GG to AG transitions, whereas A3D, A3F, and A3H lead to an overrepresentation of GA to AA hypermutations [20,21,23-26]. However, the HIV-1 encoded accessory protein Vif counteracts the four A3 proteins by binding CBF β and recruiting an E3 ubiquitin ligase complex, thus inducing their polyubiquitination and proteasomal degradation [20,27].

Since all early HIV-1 proteins are expressed from spliced intronless viral mRNAs, splicing factors and splicing regulatory proteins are particularly involved in viral infection. Moreover, CAP-dependent translation is initiated by binding of the 40S ribosomal subunit at the mRNAs' 5' end and by ribosomal scanning for an efficient AUG. By using at least four 5' splice sites (5'ss) and eight 3' splice sites (3'ss), the HIV-1 9 kb pre-mRNA is processed into more than 40 alternatively spliced mRNA isoforms [28] encoding at least 18 HIV-1 proteins, most of them interacting with a wide variety of host cell components [29]. Thus, HIV-1 relies on massive alternative splicing to bring each of its eight translational start codons (*gag-pol*, *vif*, *vpr*, *tat*, *rev*, *nef*, *vpu*, and *env*) into close proximity of the 5' cap of the respective alternatively spliced mRNA. The only exception to this rule is the *env* ORF, which is translated from the bicistronic *vpu/env* mRNA. Here, a minimal upstream ORF upstream of the *vpu* ORF allows efficient translation initiation at the downstream *env* AUG [30,31].

Within the 4 kb class of mRNAs (Figure 1A-B), downstream of 5'ss D2-D4 translational start codons are

localized, which can only be recognized by the 40S ribosomal subunit if the respective introns are retained. In particular, *vif* mRNA is formed when the intron upstream of exon 2 is spliced out, while its downstream intron is retained. In a similar way, *vpr* mRNA is formed by removing upstream introns carrying translational inhibitory AUGs but repressing D3 and thus retaining intron 3. Both mRNAs rely on functional cross-exon interactions between the 5'ss and the corresponding upstream 3'ss [32-34]. Thus, formation of unproductive spliceosomal complexes at the 5'ss is essential for 3'ss activation and exon definition as well as for splicing-repression at the 5'ss [35]. Hence, the expression levels of *vif* and *vpr* mRNAs are dependent on U1 bound, but splicing repressed 5'ss [32,33].

Notably, excessive splicing at A2 was shown to result in detrimental impairment of the balanced ratio of spliced to unspliced viral mRNAs and loss of the viral unspliced genomic 9 kb mRNA, a phenotype referred to as oversplicing [36,37]. Since Gag and Pol are encoded by the unspliced 9 kb mRNA, oversplicing decreases the amounts of all Gag and Pol proteins including p55Gag and p24-CA resulting in massive inhibition of viral particle production and replication [36-39].

Moreover, transcripts containing either non-coding leader exon 2 or 3 as required for *vif* and *vpr* mRNAs, respectively, appear to be regulated in a similar way as 3'ss A1 and A2 recognition, which appears to underlie a mutually exclusive selection [33]. However, the molecular mechanism is still poorly understood.

Since 3'ss A2 was shown to be an intrinsically strong 3'ss [40], *trans*-acting elements are necessary to repress its usage. Indeed, the ESSV within the non-coding leader exon 3, which consists of three UAG motifs, has been reported to inhibit splicing at 3'ss A2 [41-43]. In addition, the Tra2-alpha and Tra2-beta-dependent splicing regulatory element ESE_{*vpr*} positively regulates balanced amounts of exon 3 recognition by acting positively on U1 snRNP recruitment to 5'ss D3, which in turn promotes recognition of the upstream 3'ss A2 via cross exon interaction [33]. Vpr formation was further proposed to be regulated by high-mobility group A protein 1a (HMGA1a), which binds immediately upstream of 5'ss D3 and acts to repress splicing at this position. Here, trapping of U1 snRNP might activate 3'ss A2 and repress splicing at 5'ss D3 [44].

Recently, we identified a G run with high affinity for hnRNP F/H and A2/B1 proteins localized within intron 2 (G₁₂-1), but upstream of the *vif* AUG, which represses usage of the alternative 5'ss D2b [34]. Mutations of G₁₂-1 led to considerable upregulation of *vif* mRNA expression [34]. Here, we analyzed whether regulation of exon 3 inclusion and processing of *vpr* mRNAs is regulated in an analogous manner by intronic G runs located in HIV-1 intron 3.

Results

The guanosine run element (G_{13-2}) localized deeply within HIV-1 intron 3 is critical for efficient replication in PBMCs

Previously we have shown that an intronic G run within HIV-1 intron 2 is critical for splicing regulation of *vif* mRNA [34]. To examine whether an intronic G run is likewise critical for regulation of *vpr* mRNA, whose processing similarly depends on intron retention, we inspected HIV-1 intron 3 for the occurrence of G runs. Since they are highly abundant in mammalian introns [45-47], it was not surprising that we found four G runs, which we termed G_{13-1} to G_{13-4} according to their 5' to 3' localization (Figure 1). However, only two of these, G_{13-2} and G_{13-3} , were found to match the consensus motif DGGGD (where D is G, A, or T) of the high affinity binding site for members of the hnRNP F/H family [48]. Moreover, since G_{13-2} and G_{13-3} were highly conserved in HIV-1 strains (Figure 1D), we analyzed whether one or even both had an impact on viral replication. To this end, we disrupted each of them in the molecular clone pNL4-3 by introducing single nucleotide substitutions (pNL4-3 G_{13-2} mut: AGGGA > AGAGA, pNL4-3 G_{13-3} mut: GGGGA > GGCGA). Since for G_{13-2} it was not possible to introduce a mutation without changing the coding sequence of the overlapping *vif* and *vpr* open reading frames (ORFs), we chose a nucleotide substitution, which was present in HIV-1 subtypes J, G, and AE (Figure 2A, C). This exchange, however, resulted in a single amino acid substitution within the C terminus of Vif (AGGGA > AGAGA, G185E). To be able to infect PBMCs with equal amounts of viral particles, we first transfected HEK 293 T cells with the proviral plasmid pNL4-3 or its mutant derivatives, pNL4-3 G_{13-2} mut or pNL4-3 G_{13-3} mut, and then harvested virus-containing supernatants 48 h post transfection. The TCID₅₀ were calculated by X-Gal staining of infected TZM-bl reporter cells. These cells carry a luciferase and β -galactosidase expression cassette under the control of the HIV-1 LTR and thus express both reporter genes in the presence of HIV-1 Tat [49]. With a multiplicity of infection (MOI) of each of 0.05 and 0.5, PBMCs from two healthy donors were then infected and p24-CA protein levels were determined at various time points. As shown in Figure 3, G_{13-3} , but not G_{13-2} mutated virus, was able to replicate in PBMCs indicating that specifically G_{13-2} was critical for efficient virus replication in primary T cells.

Mutating G_{13-2} results in an impaired ratio of spliced to unspliced mRNAs

In order to investigate the molecular cause for the replication defect of G_{13-2} mutant virus, we analyzed the splicing patterns of proviral DNA from pNL4-3 and G run mutant. To this end, total RNA of HEK 293 T cells transfected with each of the proviral DNAs was subjected to Northern

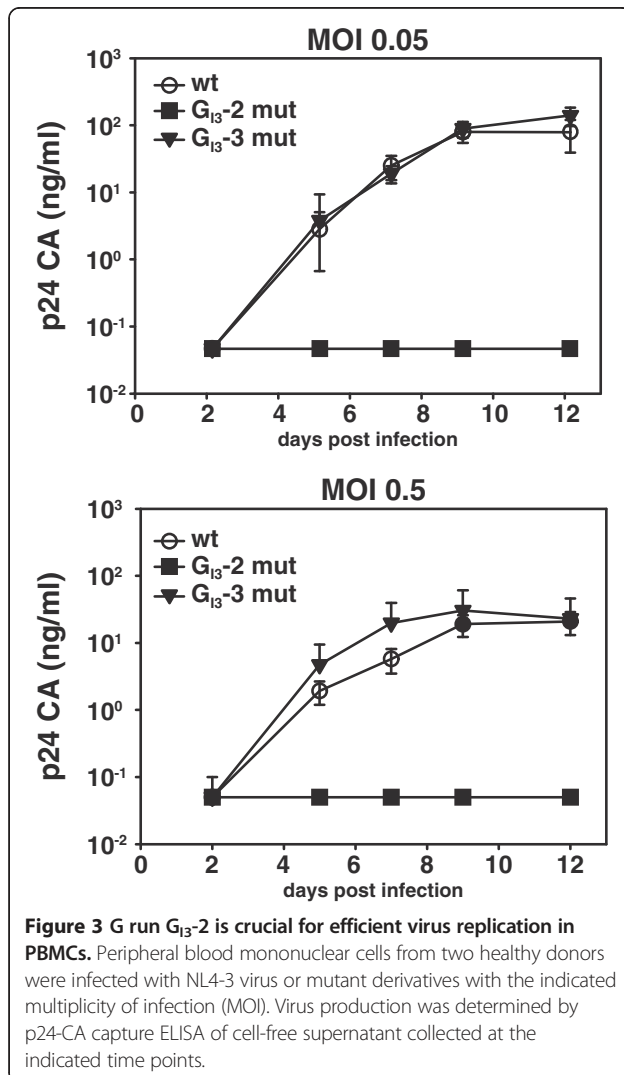
blot analysis and probed with a DIG-labeled HIV-1 exon 7 amplicon detecting all viral mRNA classes. While the overall splicing pattern was not changed for the G_{13-3} provirus (data not shown), inactivation of G_{13-2} caused massive disturbance of the balanced ratio of the three viral mRNA classes with the most obvious decrease in the amount of unspliced 9 kb mRNA (Figure 4A-B). Concomitantly, the ratio of 2 and 4 kb mRNA classes was increased indicating massive splicing defects (Figure 4B).

In order to quantify the amounts of the viral RNA classes, we performed quantitative RT-PCR analysis using primers (Additional file 1: Figure S1) binding in intron 1 (*gag-pol*) to detect unspliced 9 kb mRNA, as well as primers to quantify the relative amount of multiply spliced mRNAs (exon junction D4/A7). As shown in Figure 4C, the relative amount of unspliced, i.e. intron 1 containing mRNAs, was three-fold decreased compared to the amount from non-mutated virus. In parallel, the relative amount of multiply spliced mRNAs was three-fold increased. Thus, inactivation of G_{13-2} shifted the balance towards intronless viral mRNAs.

Since p24-CA protein is encoded by the unspliced 9 kb mRNA, the widening gap between unspliced and multiply spliced mRNAs that has been previously described and referred to as oversplicing or excessive splicing [36-39] might result in diminished viral p24-CA production. However, since unspliced 9 kb mRNA was still detectable in the Northern blot analysis of G_{13-2} mutant virus, a lower level of viral particle production was probably not the only cause of the totally abolished replication of G_{13-2} mutant virus in PBMCs.

G_{13-2} plays a major role in exon 2 vs. exon 3 selection and *vif* vs. *vpr* mRNA expression

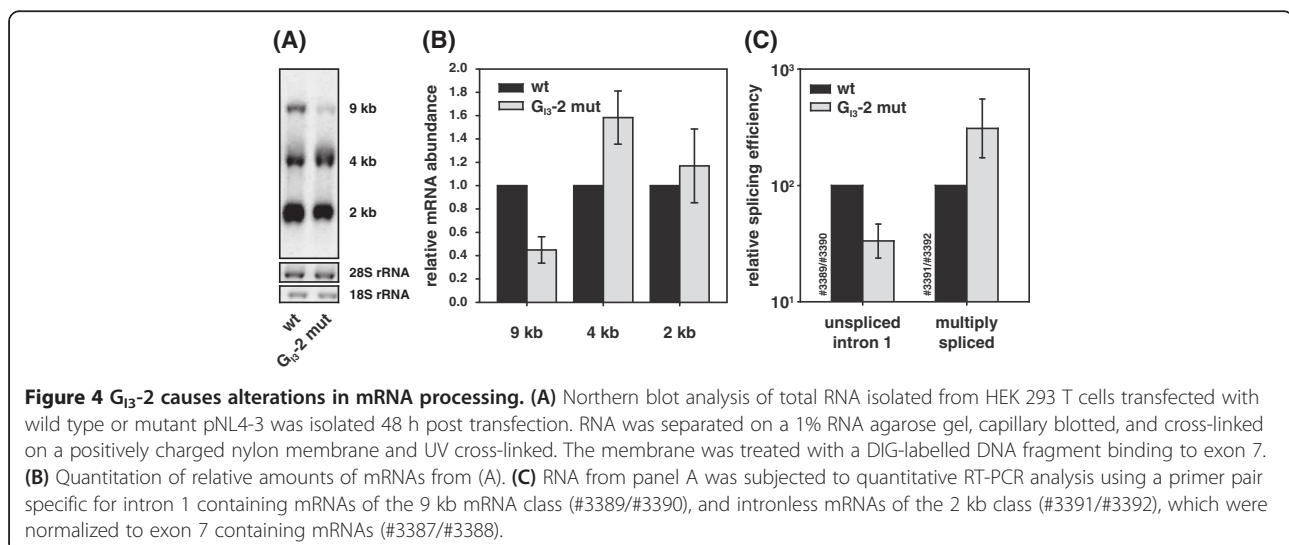
Since activated PBMCs exhibit high expression of the host restriction factor A3G [34,50], we were interested in whether the replication defect of G_{13-2} mutant virus might have originated from disturbed expression of the viral antagonist of A3G, which is the accessory protein Vif. For this purpose, we analyzed the impact of the G_{13-2} inactivating mutation on *vif* gene expression. HEK 293 T cells were transiently transfected with pNL4-3 or the G_{13-2} mutant proviral plasmid pNL4-3 G_{13-2} mut, and total RNA and proteins were harvested 48 h post transfection. As determined by semi-quantitative RT-PCR using primer pairs to specifically amplify intron-containing (4 kb) or intronless (2 kb) HIV-1 mRNAs (Additional file 1: Figure S1), inactivation of G_{13-2} resulted in excessive exon 3 splicing in the *tat*, *nef*, and *env* mRNAs (Tat3, Nef4, Env8), and concomitantly led to accumulation of *vpr* mRNA indicating that G_{13-2} represses exon 3 and 3' ss A2 recognition (Figure 5A). However, enhanced splicing of A2 was obviously incompatible with the recognition of the upstream exon 2 as observed by means of multiply



conclusion, the intronic G run G₁₃-2 acts to repress the activation of 3' ss A2 and plays a major role in the apparently mutually exclusive selection of exon 2 and exon 3, which in turn regulates the expression of Vpr and Vif protein.

G₁₃-2 is critical for viral replication in APOBEC3G-expressing but not -deficient cells

Since physiological levels of Vif are necessary to counteract A3G-mediated host restriction, we were interested in whether the diminished Vif protein levels of G₁₃-2 mutated virus were the underlying cause of the replication incompetence in PBMCs. In order to prove this hypothesis, we aimed to analyze the replication kinetics of mutant and non-mutant virus in A3G low expressing CEM-SS [2,51-53] and high expressing CEM-A [54] cell lines, whose expression we previously confirmed by A3G immunoblot analysis [34]. As a control, the *vif* deficient NL4-3 Δvif virus was included in this analysis [55]. CEM cells were infected with an MOI of 0.01, cell free supernatants were harvested at frequent intervals, and p24 capsid protein production (CA) was monitored by capture ELISA to quantify viral replication (Figure 6A). As anticipated, in A3G low expressing CEM-SS cells, *vif* deficient virus was able to produce viral particles with comparable efficiency as non-mutant NL4-3 virus. However, the replication curve of G₁₃-2 mutant virus flattened out at a tenfold lower p24-CA amount compared to non-mutant and *vif* deficient virus, confirming that inactivating G₁₃-2 not exclusively alters *vif* mRNA processing but generally disturbs the balanced ratio of all classes of RNA impairing viral replication. On the contrary, *vif* deficient as well as G₁₃-2 inactivated viruses were replication incompetent in A3G high expressing CEM-A cells and thus ended up in an abortive infection. These results indicate that the replication incompetence was the net



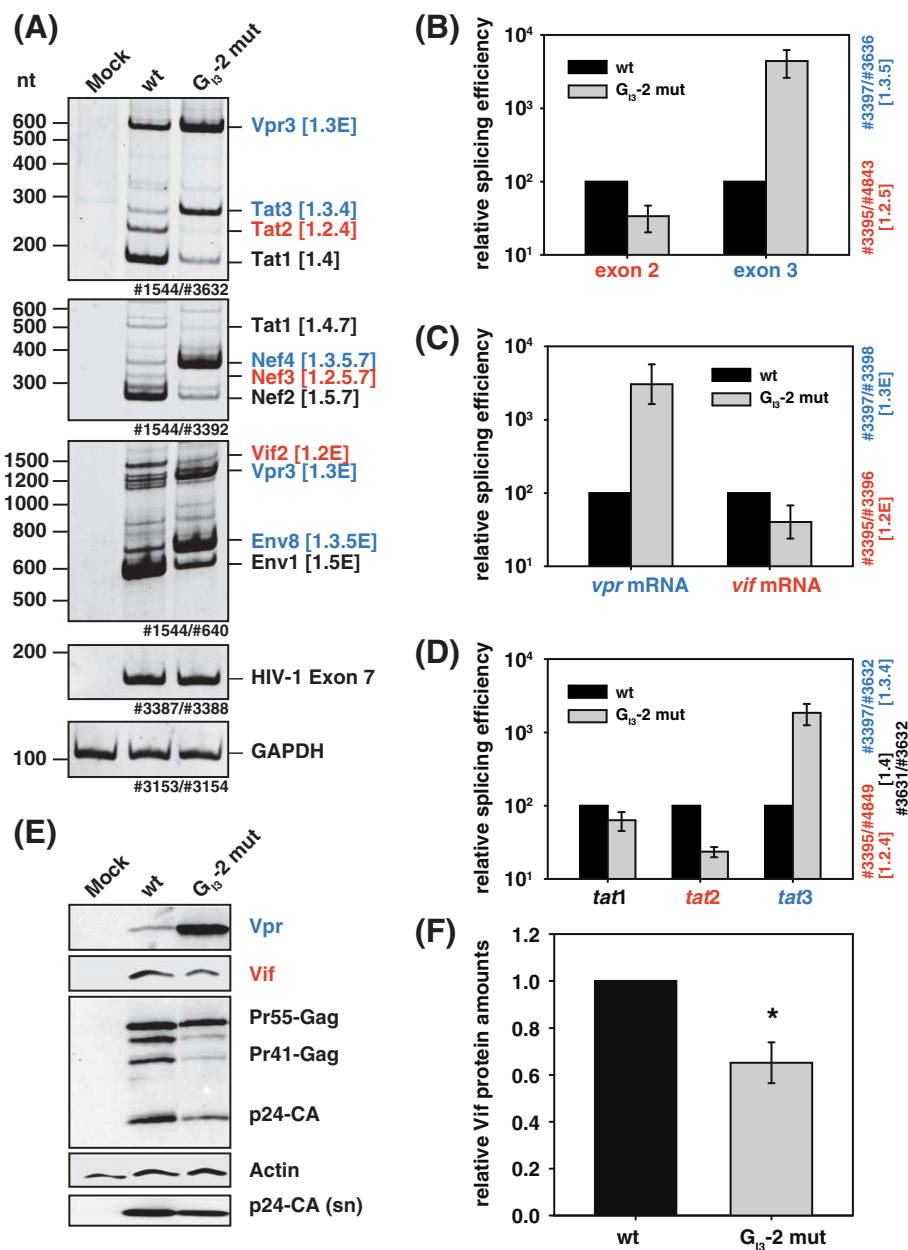


Figure 5 Mutation G_{13-2} increases *vpr*, but decreases *vif* mRNA and Vif protein levels. (A) RT-PCR analysis of RNA from HEK 293 T cells transiently transfected with pNL4-3 or its G_{13-2} mutant derivative. Compare with Additional file 1: Figure S1 for specific primer binding sites. RNA was isolated 48 h post transfection. Primer pairs are indicated at the bottom of each panel, transcript isoforms on the right. To compare total RNA amounts, separate RT-PCRs were performed by using primer pairs amplifying HIV-1 exon 7 and cellular GAPDH sequence. PCR amplicons were separated on a non-denaturing polyacrylamide gel (10%) and stained with ethidium bromide. **(B-D)** Quantitative RT-PCR of total RNA from (A) using primers indicated in Additional file 1: Figure S1. The NL4-3 splicing pattern (wt) was set to 100% and the relative splice site usage was normalized to exon 7 containing HIV-1 transcripts. **(E)** Immunoblot analysis of the indicated proteins employing lysates or pelleted virions from supernatant (sn) obtained from HEK 293 T cells that were transiently transfected with wild type or G_{13-2} mutant proviral DNA. Transfected cells were lysed in RIPA buffer and the lysates were collected 48 h post transfection. Cell-free supernatant was concentrated by sucrose centrifugation. **(F)** Quantification of Vif protein amounts from (E).

result of diminished Vif protein levels as well as reduced virus production caused by the G run mutation. These results also demonstrate that G_{13-2} was critical for efficient virus replication in A3G expressing cells and that

the threshold of Vif required for optimal viral replication was in a narrow range.

To determine the viral rescuing activity of Vif and Vif point mutant G185E we used two different constructs

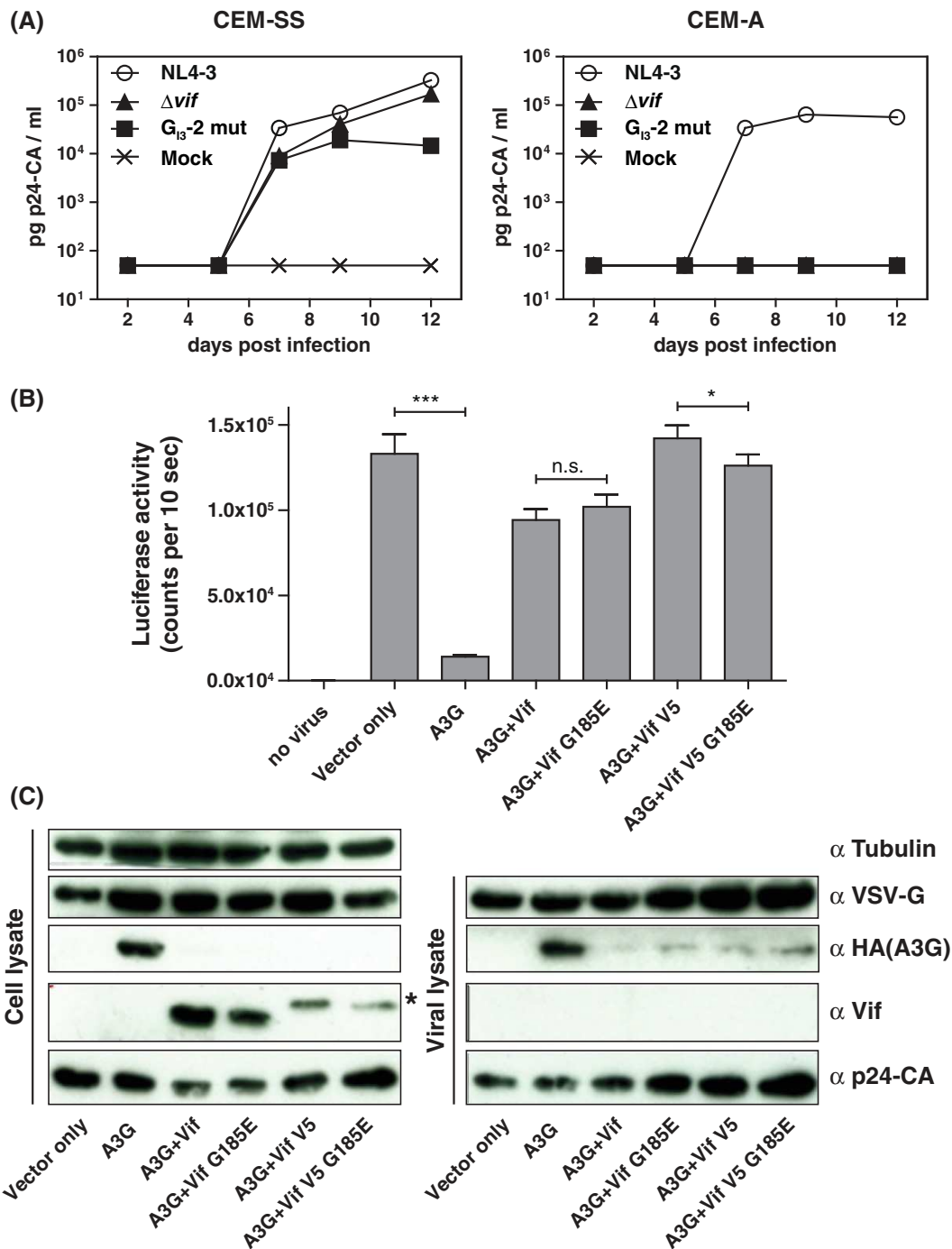


Figure 6 G₁₃-2 is critical for efficient virus replication in A3G expressing cells. **(A)** CEM-SS and CEM-A cells were infected with wild type or G₁₃-2 mutant NL4-3 virus and virus production was determined by p24 CA capture ELISA of cell-free supernatant collected at the indicated time points. **(B)** Vif G185E mutant counteracts A3G with comparable efficiency as wild type Vif. Viral rescuing activity of Vif and Vif G185E mutant against A3G compared to vector only control (no A3G). HIV-1 Δvif .luc reporter viruses were generated in the presence of A3G and absence of A3G (vector control), and A3G in combination with Vif, Vif G185E, Vif-V5, and Vif-V5 G185E plasmids. Virions were normalized by RT activity. Luciferase activity was measured 48 hours post infection. Unpaired *t* tests were computed to determine the differences between the group of samples reached the level of statistical significance (ns, not significant; *, *P* 0.05 and ***, *P* 0.0001). **(C)** Viral supernatants were concentrated through a 20% sucrose cushion by ultracentrifugation. Immunoblot analysis of the expression and encapsidation of A3G in the presence and absence of Vif, Vif G185E, Vif-V5, and Vif-V5 G185E: A3G was detected by an anti (α)-HA antibody. Vif, VSV-G, and p24-CA were detected by their respective monoclonal antibodies. Tubulin served as loading control for cell lysates and p24-CA and VSV-G for viral lysates. Asterisk in the Vif blot indicates the shift in the molecular weight of V5-tagged Vif.

that have Vif without a tag and Vif with a C-terminal V5 tag. The point mutation yielding to the amino acid substitution G185E was introduced in both plasmids by site directed mutagenesis and used to produce viral particles by transfection of HEK 293 T cells. Normalized amounts of particles were used to transduce HEK 293 T cells and the intracellular luciferase activity was quantified two days post transduction. A3G reduced the infectivity of HIV-1 luc reporter vectors about 10-fold, and the presence of Vif and Vif G185E (both versions) rescued the reporter virus infectivity to above 70% attained by HIV-1 vectors generated without A3G (Figure 6B). Immunoblot analysis of cellular and viral lysates confirmed wild type Vif- and G185E mutant Vif-triggered proteosomal degradation of A3G in the viral producer cells (Figure 6C). In the absence of Vif or Vif G185E, A3G was efficiently incorporated in the viral particles. However, in the presence of Vif or Vif G185E only traces of A3G were detectable in encapsidated viruses. The amount of Vif and Vif G185E within the viral particles was under the detection limit.

In conclusion, G_{13-2} is critical for efficient virus replication in A3G expressing cells while G185E mutation does not alter the Vif protein's counteracting function.

Inhibition of hnRNP protein binding to the intronic G run G_{13-2} restricts viral particle production

Since G runs were demonstrated to act as high affinity binding sites for members of the hnRNP F/H and A2/B1 protein families [34,48], RNA affinity precipitation assays were performed to screen for potential interaction also with the viral G run G_{13-2} . Therefore, short RNA oligonucleotides containing an MS2 coat protein RNA stem loop (Figure 7A), and either the wild type or mutant G_{13-2} sequence, were transcribed *in vitro*. The RNAs were then covalently immobilized on agarose beads and incubated in HeLa cell nuclear extract supplemented with recombinant MS2 coat protein to allow monitoring RNA pull-down efficiency. Subsequently, the associated proteins were eluted and separated on SDS-PAGE and subjected to immunoblot analysis (Figure 7B). As expected, we could detect high levels of hnRNP F/H and A2/B1 proteins on RNAs containing the wild type G_{13-2} sequence, while these were markedly reduced for the mutated RNA substrate (Figure 7B, upper and middle panel, lanes 3 and 4). Noticeably, equal levels of MS2 protein detected on wild type and mutated RNAs indicated comparable precipitation efficiencies for both RNAs (Figure 7B, lower panel, lanes 3 and 4) and therefore suggested that hnRNP F/H and/or A2/B1 may act through the G_{13-2} sequence to contribute to splicing regulation of *vif* and *vpr* mRNAs.

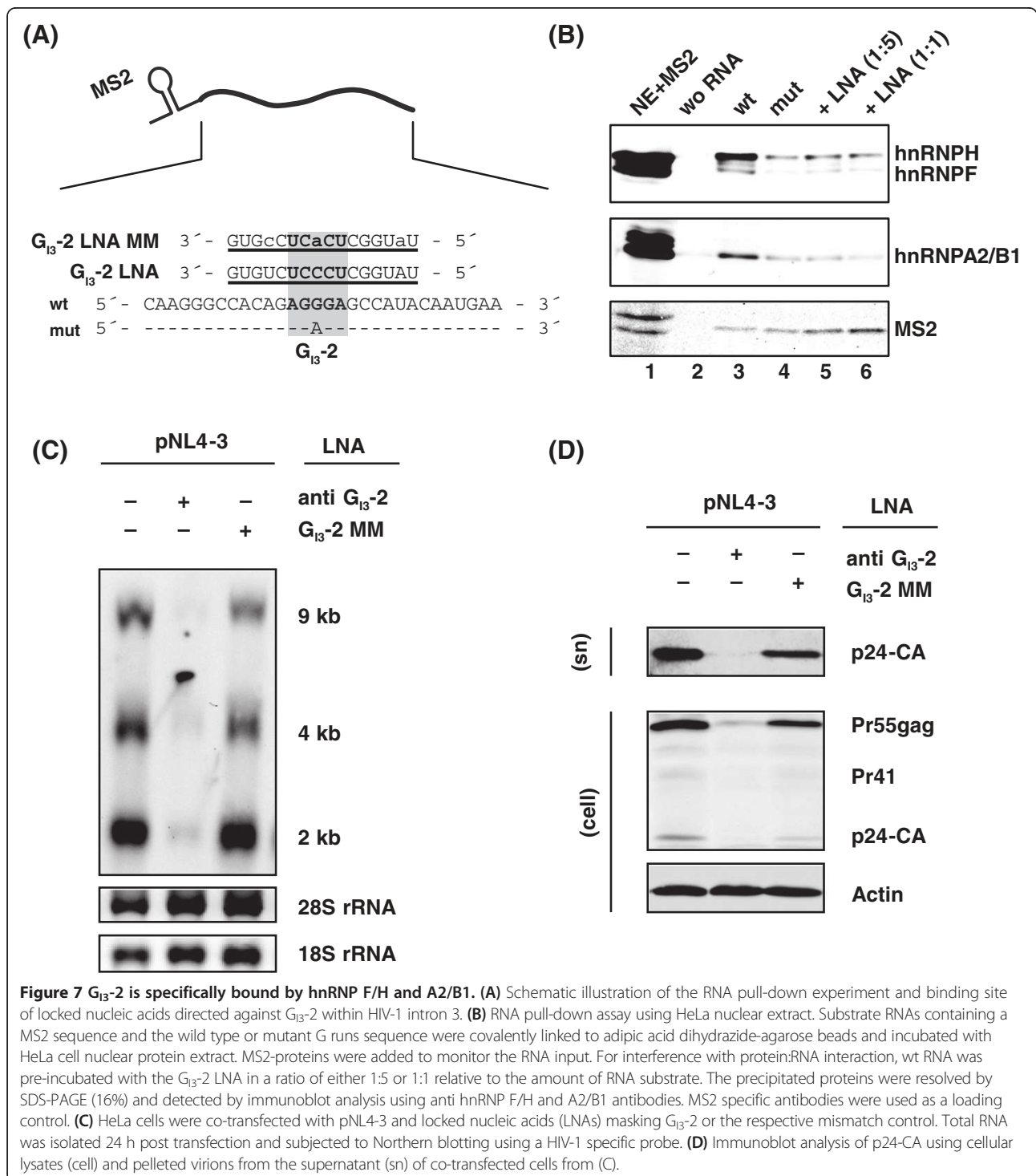
To test whether hnRNP binding can be prevented by masking G_{13-2} sequence using an RNA-based antisense approach, we also determined the precipitated levels of

hnRNP F/H and A2/B1 proteins together with wild type RNAs in presence of a locked nucleic acid (LNA) specifically targeting the G_{13-2} sequence (G_{13-2} LNA). Herein, decreased levels of hnRNP F/H and A2/B1 proteins were detected on wild type RNA to which the G_{13-2} LNA had been added (Figure 7B, cf. lanes 3 and 5). Moreover, upon increasing the concentration of the G_{13-2} LNA, hnRNP F/H and A2/B1 precipitation efficiency could be further slightly reduced (Figure 7B, cf. lanes 3, 5 and 6). Altogether, these results demonstrate that this LNA rendered G_{13-2} inaccessible for hnRNP F/H and A2/B1 binding.

Next, we were interested in whether the G_{13-2} LNA might be suitable to impair viral particle production. Following co-transfection of HeLa cells with pNL4-3 and either the G_{13-2} LNA or a control LNA (G_{13-2} MM LNA) that contained three mismatches, total RNA was harvested and analyzed by Northern blotting using a HIV-1 exon 7 specific probe. Co-transfection of the G_{13-2} LNA resulted in a considerable reduction in viral RNAs compared to pNL4-3 alone or pNL4-3 co-transfected with the mismatch control LNA, G_{13-2} MM (Figure 7C). To further determine whether viral particle production and Gag protein expression were also affected, total proteins of the transfected cells and the virus containing supernatant were subjected to immunoblot analysis and detected with a p24-CA specific antibody. In line with the above findings, Gag precursor (Pr55gag) as well as Gag processing intermediate (Pr41) and product (p24-CA) were significantly reduced in the presence of the G_{13-2} LNA (Figure 7D). There was little effect on the Gag protein expression and virus production when co-transfecting the G_{13-2} MM LNA emphasizing the specificity of the G_{13-2} LNA and the impact of G_{13-2} on viral particle production.

The G_{13-2} binding site is functionally conserved in HIV-1

To assess whether G_{13-2} might be a valuable target for LNA-mediated antiviral therapy, we were interested in whether G_{13-2} is conserved in all HIV-1 subtypes. Indeed, an alignment of all HIV-1 consensus sequences showed that 9 out of 12 consensus sequences encode a conserved G run at the designated position (Figure 2A). The remaining three subtypes lacking a G run at this particular position contain a G run only 6 nucleotides upstream due to a compensatory nucleotide substitution in position 2 of G_{13-1} restoring the protein binding consensus sequence DGGGD. The A > G substitution in G_{13-1} likely converts a low affinity (AAGGGC) into a high affinity binding site (AGGGGC). To demonstrate that the compensatory G_{13-1} mutation could functionally substitute for an inactivated downstream G_{13-2} binding site we inserted the corresponding mutations into pNL4-3 and pNL4-3 G_{13-2} mut (Figure 2C) and determined their splicing outcomes. Total RNA was isolated 24 h following transient transfection of HEK 293 T cells, and splicing patterns were analyzed



by qualitative (Figure 8A) and quantitative RT-PCR (Figure 8B). Introducing an A > G mutation in position 2 of G_{13-1} while G_{13-2} was inactivated by the G > A mutation, we could compensate the excessive exon 3 and *vpr* mRNA splicing phenotype described above and restored the amounts of exon 2 containing transcripts (Figure 8A, lane 3) as well as *vif* mRNA (Figure 8B). These results

demonstrate that the A > G nucleotide change in position 2 of G_{13-1} (cf. Figure 2C; J, G, AE) is a compensatory mutation. The introduction of this substitution without inactivating downstream G_{13-2} had no effect on *vif* and *vpr* mRNA amounts (Figure 8A-B, cf. lanes 1 and 5) suggesting that there is no evolutionary pressure on two functional binding sites. To determine whether the

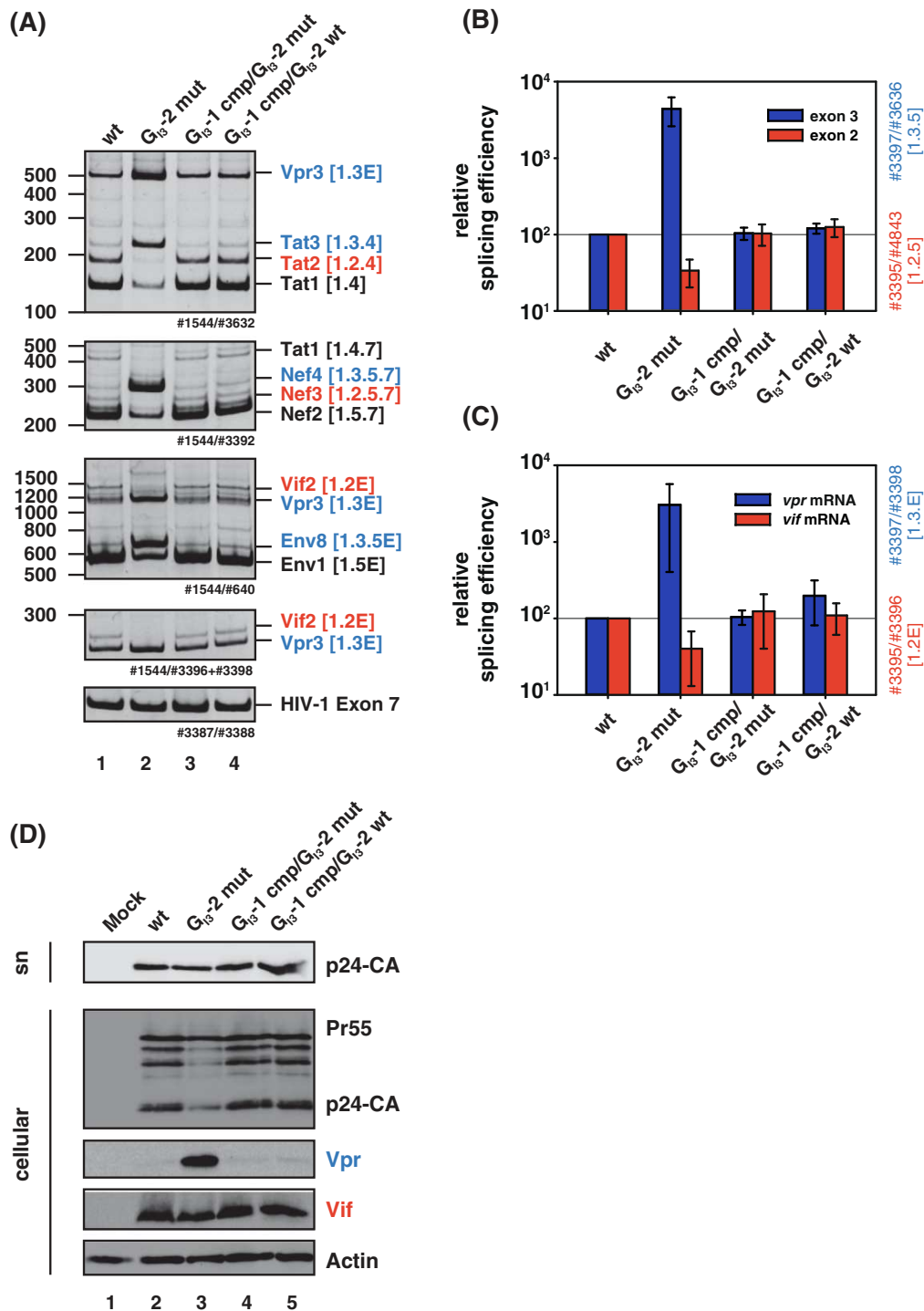


Figure 8 A single G run is sufficient to maintain the HIV-1 splicing pattern. (A) RT-PCR analysis of RNA isolated from HEK 293 T cells transiently transfected with pNL4-3 or its mutant derivatives 48 h post transfection. The used primer pairs are illustrated in Additional file 1: Figure S1. Transcript isoforms are indicated on the right. Separate RT-PCRs were performed by using primer pairs amplifying HIV-1 exon 7 to compare total RNA amounts. PCR amplicons were separated on a non-denaturing polyacrylamide gel (10%) and stained with ethidium bromide. **(B-C)** Quantitative RT-PCR of total RNA obtained from panel (A). The NL4-3 splicing pattern (wt) was set to 100% and the relative splice site usage was normalized to exon 7 containing HIV-1 transcripts. Compare with Additional file 1: Figure S1 for specific primer binding sites. **(D)** Immunoblot analysis of the indicated proteins employing lysates from HEK 293 T cells (cellular) and their supernatants (sn) transiently transfected with the indicated proviral DNAs. Transfected cells were lysed in RIPA buffer and lysates were collected 48 h post transfection. Virions were pelleted by sucrose centrifugation.

compensatory mutant was also capable of restoring and rescuing Vif and Vpr protein levels, we isolated total cellular proteins and subjected them to immunoblot analysis. Consistent with the findings above, the compensatory A > G mutation reduced Vpr amounts and restored Vif protein levels to those levels obtained with wild type pNL4-3 (Figure 8D, Vpr, Vif). In addition, the reduced amount in Gag precursor as well as viral particle production could be rescued (Figure 8D, p24-CA). The data obtained in these experiments highlights a functional conservation of the G run in all HIV-1 subtypes supporting an indispensable role for G_{I3-2} in HIV-1 replication.

Discussion

Within HIV-1 NL4-3 intron 3 we identified a high affinity binding site for members of the hnRNP F/H family, termed G_{I3-2}. Binding of hnRNP F/H and A2/B1 proteins to G_{I3-2} was confirmed by RNA pull-down experiments and could be efficiently prevented either by point mutation or upon co-transfection with an LNA specifically targeting G_{I3-2}. Inactivation of G_{I3-2} led to aberrant alternative splicing and to a replication defective phenotype in PBMCs and A3G expressing CEM-A cells.

The G_{I3-2} inactivating mutation resulted at the same time in an amino acid (aa) substitution at position 185 (G185E) in the Vif protein, which is localized in the Gag, p7-NC, and membrane binding domain [27]. Residues 172 to 192 were shown to be involved in membrane association [56], and mutating aa positions 179 to 184 (KTKGHR > ATAGHA) resulted in 25% loss of membrane binding and decreased Pr55Gag binding [57]. However, a T > A substitution at aa position 188 of Vif had no effect on the ability to decrease A3G levels [58]. Moreover, since the G185E substitution in Vif is also present in three (G, J and AE) of twelve HIV-1 consensus sequences, we assumed that it is highly unlikely that it affects Vif's A3G counteracting activity. However, to experimentally rule out that the Vif G185E substitution indeed did not impact Vif's functionality we confirmed it by using an HIV-1 Vif deficient luciferase reporter, which was supplemented with expression vectors coding for either wild type or G185E Vif protein.

At the RNA level, in parallel to an increase in exon 3 recognition, mutating G_{I3-2} also decreased levels of exon 2 containing transcripts as well as *vif* mRNA, demonstrating that recognition of either exon strongly influences the other. Indeed, we have shown recently that excessive splicing of exon 3 and *vpr* mRNA processing concomitantly resulted in considerable decrease of exon 2 and *vif* mRNA splicing, indicating an apparently mutually exclusive exon selection of exon 2 and exon 3 [33]. In this work we demonstrated that this competition, which is regulated by G_{I3-2}, determines the ability to evade A3G-mediated antiviral effects due to *vif* expression.

Hence, an insufficient level of Vif is unable to maintain viral replication due to insufficient A3G-counteraction.

All HIV-1 intron-containing mRNAs that harbor translational start codons in their introns immediately downstream of their leader exon (avoiding translational inhibitory AUGs) depend on the recognition of the leader exons' 3'ss. However, their corresponding 5'ss must be rendered splicing incompetent in order to include the start codons into the nascent transcript. For instance, the intron-containing *env* mRNAs, which belong to the class of HIV-1 4 kb mRNAs, are formed by using a splice acceptor that is derived from either one of the 3'ss central cluster (A4c, a, b and A5), and splicing repression at D4. Hereby, U1 bound to D4 and U2 snRNPs bound to 3'ss A4cab or A5 pair with each other via cross-exon interactions [35] and facilitate exon definition [59,60]. In addition, these interactions are supported by the strong guanosine-adenosine-rich enhancer GAR ESE, which is localized immediately downstream of 3'ss A5 [35,61]. Importantly, the binding of a splicing incompetent U1 snRNA was sufficient to promote exon definition and 3'ss activation indicating that exon definition but not splicing at D4 is crucial to activate upstream splice acceptor usage in order to gain *env/vpu* mRNAs [35]. In a similar way, *vif* and *vpr* mRNAs seem to rely on comparable functional cross-exon interactions, in these cases between splice sites A1 and D2 (exon 2) as well as A2 and D3 (exon 3), respectively, which determined the splicing efficiency of *vif* and *vpr* mRNA. In agreement with the formation of *env/vpu* mRNAs, exon 3 inclusion and *vpr* mRNA expression can be modulated by up and down mutations of 5'ss D3 as well as by co-transfection of modified U1 snRNAs with perfect complementarity to the 5'ss D3 [33,37]. Hereby, binding of U1 snRNP to a non-functional 5'ss was shown to be already sufficient to enhance splicing at the upstream 3'ss A2 indicating that *vpr* encoding mRNAs are dependent on the relative occurrence of U1-bound, but splicing-repressed 5'ss [33]. Correspondingly, the co-expression of a U1 snRNA that was fully complementary to a splicing deficient HIV-1 D2 mutant was sufficient to maintain *vif* mRNA formation [32]. Since both D3 up [33] as well as G_{I3-2} mutations increased exon 3 inclusion as well as *vpr* formation, it seems plausible that G_{I3-2} might play a role in the inhibition of U1 snRNP recruitment to D3.

So far *vif* mRNA formation has been known to be maintained by the two SRSF1 dependent heptameric exonic splicing enhancers ESEM1 and ESEM2 [40], the SRSF4 dependent ESE Vif [32], as well by the intronic G rich silencer elements G4 overlapping with the intronic nucleotides of 5'ss D2 and thus likely competing with U1 snRNP binding [32]. In addition, we recently identified the intronic G run G_{I2-1}, which impairs usage of the HIV-1 alternative 5'ss D2b as well as exon definition of

exon 2b, and thus inhibits splicing at 3' splice site A1 [34]. Here, we show that *vif* mRNA is not only regulated by exon 2 and exon 2b associated SREs [32,34,40], but in addition is also controlled by the balanced exon recognition and splicing of exon 2 and exon 3. In contrast to G_{12-1} , G_{13-2} is entitled as a "deep intronic" splicing regulatory element. The mechanism, although not yet known, seems likely to be different to that described for G_{12-1} . Whereas any splicing regulatory element immediately upstream or downstream of a 5' splice site exerts a clear positional splicing regulatory effect [62] this is unpredictable for deeper intronic ones. Thus, the intronic G runs, G_{13-1} and G_{13-2} , extend the repertoire of SREs, acting on *vif* and *vpr* mRNA splicing regulation.

Conserved non-coding sequences often harbor *cis*-regulatory elements that can vary in their sequence. However, since G_{13-1} and G_{13-2} are localized in both *vif* and *vpr* ORFs, there is little room left to maintain proper protein affinity forming a compromise between splicing efficiency on the one hand and protein function on the other hand. Comparing HIV-1 consensus sequences (Los Alamos HIV database) it turned out that G_{13-2} matches the consensus sequences of HIV-1 strains A2, B and D. In addition, the three consensus sequences of strains J, G and AE were equivalent to the inactivating G_{13-2} mutation but contained a high affinity hnRNP F/H binding site in position of G_{13-1} (comparable to G_{13-1} cmp/ G_{13-2} mut). However, most of the consensus sequences contain both G runs, G_{13-1} and G_{13-2} , as high affinity binding sites. Thus, removal of only a single G run preserves phenotypic functioning indicating that a single protein binding site irrespective of the exact nucleotide sequence is sufficient to maintain proper splicing. Since viral replication of G_{13-2} mutant NL4-3 virus was considerably impaired in A3G-expressing, but not in A3G-deficient cells, we propose that at least one functional high affinity binding site for hnRNP F/H and A2/B1, either G_{13-1} or G_{13-2} , is critical to maintain an optimal Vif to A3G ratio. Further support for this model comes from previous studies showing that siRNA-directed down-regulation of hnRNP A2/B1 proteins within pNL4-3-transfected HEK 293 T cells leads to a viral oversplicing phenotype of exon 3 containing and *vpr* coding mRNAs reminiscent to that seen for the G_{13-2} mutant [63,64]. In addition, the redundancy of these G runs could represent a viral backup mechanism to easily re-substitute defect binding sites by an exchange of a single nucleotide.

Targeting Vif gene expression represents an attractive therapeutic strategy as it supports infected cells to defend themselves in an APOBEC3-dependent manner. Since viral replication of G_{13-2} mutant NL4-3 virus was strongly impaired in human primary T-lymphocytes, G runs G_{13-1} and G_{13-2} may represent suitable therapeutic targets. Therefore we tested the effect of an LNA specifically designed to target G_{13-2} on viral particle production.

Surprisingly, we found that targeting G_{13-2} had an even more dramatic effect on the viral particle production than inactivating G_{13-2} upon mutation. This apparent stronger effect might to some extent result from an yet unknown degradation mechanism of the viral target RNAs. Since we used mixmer LNAs (combination of LNA and DNA residues) it is highly unlikely that they recruit RNaseH, which has been shown to need at least a gap of 6 neighbouring deoxynucleotides for noteworthy RNase H activity [65,66]. Although the mechanism of action is not yet fully understood, viral particle production seems to be specific as the control mismatch LNA did not cause any harm.

Since sublethal levels are proposed to contribute to viral genetic diversity, suboptimal Vif inactivation might give rise to the emergence of viral quasi-species and drug resistant HIV-1 strains [1,67,68]. Hence, there is a need for multiple therapeutic approaches to inactivate Vif in parallel. Potentially, this can be achieved by masking numerous SREs that facilitate *vif* expression. Furthermore, this strategy could minimize the risk of second site mutations that may potentially substitute therapeutically induced aberrant splicing. Moreover, it will be interesting to analyze the effect of G_{13-2} -mutation derived increase of Vpr protein levels, which are important for HIV-1 replication in macrophages.

Conclusions

Our data suggest that the intronic G runs G_{13-1} and G_{13-2} , which are functionally conserved in most HIV-1 strains, are critical for efficient viral replication in A3G-expressing but not in A3G-deficient T cell lines. Hereby, inactivation of G_{13-2} results in increased levels of both mRNA and protein levels of Vpr, but concomitantly in decreased amounts of Vif mRNA and protein levels. G_{13-2} , which is bound by hnRNP F/H and A2/B1 proteins, plays a major role in the apparent mutually exclusive exon selection of *vif* and *vpr* leader exon selection. Furthermore, mutating G_{13-2} decreased viral mRNA levels, altered the ratio of unspliced 9 kb mRNA and thus reduced viral production. Since competition between these exons determines the ability to evade A3G-mediated antiviral effects due to *vif* expression, we propose that G_{13-2} is critical for viral replication in non-permissive cells due to an optimal Vif-to-A3G ratio as well as for maintenance of efficient virus production.

Methods

Plasmids

Proviral DNA pNL4-3 G_{13-2} mut was generated by replacing the AflII/NarI fragment of pNL4-3 [GenBank: M19921] [69] by the PCR-amplicon obtained by using primer pair #2339/#3896 (for all sequences see Table 1). Proviral plasmid pNL4-3 G_{13-3} mut was generated by substitution of the EcoRI/NdeI fragment of pNL4-3 with

Table 1 DNA oligonucleotides used in this work

Primer	Primer sequence
#0640	5'- CAATACTACT TCTGTGGGT TGG
#1544	5'- CTTGAAAGCG AAAGTAAAGC
#2330	5'- TCTGGATCCA CCACCACCAC CGTAGAT
#2339	5'- TGGGAGCTCT CTGGCTAAGT AGG GAACCCACTGCTTAAGC
#3153	5'- CCACTCTCC ACCTTTGAC
#3154	5'- ACCCTGTTGC TGTAGCCA
#3387	5'- TTGCTCAATG CCACAGCCAT
#3388	5'- TTTGACCACT TGCCACCCAT
#3389	5'- TTCTCAGAG CAGACCAGAG C
#3390	5'- GCTGCCAAG AGTGATCTGA
#3391	5'- TCTATCAAAG CAACCCACCTC
#3392	5'- CGTCCCAGAT AAGTGCTAAGG
#3395	5'- GCGCACTGGG ACAGCA
#3396	5'- CCTGTCTACT TGCCACAC
#3397	5'- CGGCGACTGA ATCTGCTAT
#3398	5'- CCTAACACTA GGCAAAGGTG
#3631	5'- CGGCGACTGA ATTGGGTGT
#3632	5'- TGGATGCTC CAGGGCTC
#3633	5'- CGACACCAA TTCTGTATG GTC
#3636	5'- CCGCTTCTC CTGTATTATG C
#3896	5'- TTCACTCTTA AGTTCCTCTA AAAGCTCTAG TGCCATTCA TTGTATGGCT CTCTCTGTGG C CCTTGGTCT TCTG
#3897	5'- GTTGCAGAAT TCTTATTATG GCTTCCACTC CTGCCAAGT ATCGCCGTAA GTTTCATAGA T ATGTTGTCC TAAGTTATG
#4324	5'- TAATACGACT CACTATAGG
#4355	5'- TTCATCGAAT TCAGTGCCAA GAAGAAAAGC AAAGATCA
#4614	5'- TTCATTGTAT GGCTCCCTCT GTGGCCCTTG ACAT GGGTGA TCCTCATGTC CTATAGTGAG TCGTATTA
#4615	5'- TTCATTGTAT GGCTCTCTCT GTGGCCCTTG ACA TGGGTGA TCCTCATGTC CTATAGTGAG TCGTATTA
#4718	5'- TAGTGTCCAT TCATTGTATG GCTCCCTCTG TGGCC CCTGG T
#4720	5'- TAGTGTCCAT TCATTGTATG GCTCTCTCTG TGGCC CCTGG T
#4843	5'- CCGCTTCTC CTTTCCAGAG G
#4849	5'- CCTCTGAAA GAATTGGGT
vifmut-forward	5'- AGGGCCACAG AGAGAGCCAT ACAATG
vifmut-reverse	5'- CATTGTATGG CTCTCTCTGT GGCCCT

a PCR product containing equal restriction sites by using primer pair #2330/#3897. The respective PCR products for pNL4-3 G₁₃-1 cmp (#4355/#4718) and pNL4-3 G₁₃-1 cmp/G₁₃-2 mut (#4355/#4720) containing PflMI and XcmI restriction sites were cloned into pNL4-3 by

substitution of the PflMI/XcmI fragment. Due to the overlapping *vif* and *vpr* open reading frames (ORFs), mutations resulted in single amino acid substitutions (K181R G₁₃-1 cmp; G185E G₁₃-2 mut) within the Vif protein (Figure 8D). pXGH5 [70] was co-transfected to monitor transfection efficiency in quantitative and semi-quantitative RT-PCR analyses. pcDNA3.1 Vif and pcDNA Vif-V5 plasmids [71] were used to introduce point mutation G185E by site directed mutagenesis using PCR primers (vifmut-forward/vifmut-reverse). PCR products were treated for 1 h at 37°C with 10 units of DpnI restriction enzyme to digest the parental methylated plasmids and transformed into *E. coli*. All PCR-amplified sequences of the plasmids were validated by DNA-sequencing.

Oligonucleotides

All DNA oligonucleotides (Table 1) were obtained from Metabion (Germany), those used for real time PCR analysis were HPLC purified. RNase-Free HPLC purified LNAs (G₁₃-2: TATGGCTCCCTCTGTG; G₁₃-2 mismatch control: TTTGGCTCACTCCGTG) were purchased from Exiqon (Denmark).

Cell culture, transfection conditions and preparation of virus stocks

HEK 293 T and HeLa cells were maintained in Dulbecco's high glucose modified Eagle's medium (Invitrogen) supplemented with 10% (v/v) heat-inactivated fetal calf serum (FCS) and 50 µg/ml of penicillin and streptomycin (P/S) each (Invitrogen). Transient transfection experiments were performed in six-well plates (2.5 × 10⁵ cells per well) using TransIT[®]-LT1 transfection reagent (Mirus Bio LLC) according to the manufacturer's instructions. For LNA co-transfection experiments, 2.5 × 10⁵ HeLa cells per well (six-well plate) were cultured in Opti-MEM reduced serum medium (Invitrogen) with 5% FCS. The next day, medium was replaced with Opti-MEM reduced serum medium without FCS. For LNA transfection 4 µl of Lipofectamine 2000 (Invitrogen) was added to 250 µl Opti-MEM reduced serum medium. Separately, proviral plasmid pNL4-3 (0.7 µg), plasmid pXGH5 (0.7 µg) and the respective LNAs (80 nM) were added to 250 µl Opti-MEM reduced serum medium. After 5 min the LNA/DNA mixtures were added to the Lipofectamine 2000 containing medium, incubated for 20 min and subsequently added to the cells. After 4 hours, medium was removed and cells were washed twice with PBS and cultured with Opti-MEM reduced serum medium with 5% FCS for 24 hours.

For preparation of virus stocks 6.5 × 10⁶ HEK 293 T cells were cultured in T175 flasks that were previously coated with 0.1% gelatine solution. Cells were transiently transfected with 9 µg of pNL4-3 or mutant proviral DNA using polyethylenimine (Sigma-Aldrich). Following overnight incubation, cells were supplemented with fresh

IMDM cell culture medium containing 10% FCS and 1% P/S. 48 hours post transfection, virus containing supernatant was purified by centrifugation, aliquoted and stored at -80°C . Transfection efficiency was monitored by using pNL4-3 GFP [72].

CEM-A and CEM-SS cells were maintained in RPMI 1640 medium (Invitrogen) supplemented with 10% FCS and P/S (50 $\mu\text{g}/\text{ml}$ each, Invitrogen). Peripheral blood mononuclear cells (PBMCs) were isolated from 15 ml whole blood from two healthy donors by ficoll gradient centrifugation. PBMCs were maintained in RPMI 1640 GlutaMax medium containing 10% FCS and 1% P/S and activated with phytohemagglutinin PHA (5 $\mu\text{g}/\text{ml}$). 48 hours post isolation cells were treated with IL-2 (30 mg/ml).

RNA-isolation, quantitative and semi-quantitative RT-PCR

Total RNA was isolated by using acid guanidinium thiocyanate-phenol-chloroform as described previously [73]. RNA concentration and quality was analyzed by photometric measurement using Nano-Drop 1000 spectrophotometer, ND-1000 version 3.7.0 (Thermo Scientific). Reverse transcription of 5 μg of total RNA was performed as described previously [34]. For quantitative and qualitative analysis of HIV-1 mRNAs the indicated primers (Table 1) were used to amplify the cDNA-template. As a loading control, a separate PCR detecting GAPDH was performed with primers #3153 and #3154. PCR products were separated on non-denaturing polyacrylamide gels (10%), stained with ethidium bromide and visualized with the Intas Gel iX Darkbox II (Intas, Germany). Quantitative RT-PCR analysis was performed by using Precision 2 \times real-time PCR MasterMix with SYBR green (Primerdesign, UK) using LightCycler 1.5 (Roche). Primers used for qualitative and quantitative RT-PCR are listed in Table 1.

Protein isolation and Western blotting

For protein isolation cells were lysed using RIPA lysis buffer (25 mM Tris HCl [pH 7.6], 150 mM NaCl, 1% NP-40, 1% sodium deoxycholate, 0.1% SDS, protease inhibitor cocktail [Roche]). Subsequently, the lysates were subjected to SDS-PAGE under denaturing conditions [74] in 8-12% polyacrylamide gels (Rotiphorese Gel 30, Roth) as described before [34]. The following primary antibodies were used for immunoblot analysis: Sheep antibody against HIV-1 p24 CA from Aalto (Ireland); mouse monoclonal antibodies specific for HIV-1 Vif (ab66643) and hnRNP F + H proteins (ab10689) from Abcam (United Kingdom); hnRNPA2/B1 (DP3B3): sc-32316 from Santa Cruz; rabbit anti-HIV-1-Vpr (51143-1-AP) polyclonal antibody from Proteintech Group (United Kingdom); rabbit polyclonal antibody against MS2 (TC-7004) from Tetracore (Rockwill, USA); mouse anti β -actin monoclonal antibody (A5316) from Sigma-Aldrich. The following horseradish peroxidase (HRP) conjugated secondary antibodies were

used: anti-rabbit HRP conjugate (A6154) from Sigma-Aldrich; anti-mouse antibody (NA931) from GE Healthcare (Germany), and anti-sheep HRP from Jackson ImmunoResearch Laboratories Inc. (West Grove, PA). Blots were visualized by an ECL chemiluminescence detection system (Amersham) and Intas ChemoCam imager (Intas, Germany).

For analysis of expression of viral structural proteins, Vif and A3G transfected cells were harvested, washed with PBS and lysed using RIPA assay buffer for 20 min on ice [25 mM Tris (pH 8.0), 137 mM NaCl, 1% glycerol, 0.1% SDS, 0.5% Na-deoxycholate, 1% Nonidet P-40, 2 mM EDTA, and complete protease inhibitor mixture (Roche)]. Soluble lysates were clarified by centrifugation and subjected to SDS-PAGE followed by transfer to a PVDF membrane (Millipore). Viral particles were concentrated by ultracentrifugation over 20% sucrose cushion (in PBS) in ultra-clear centrifuge tubes (13 \times 51 mm, Beckman Coulter) and centrifuged at 37,000 rpm for 2 h at 4°C in an MLS-50 rotor (Beckman Coulter). Pelleted particles were lysed by RIPA assay buffer and directly subjected to immunoblotting. Membranes were probed with mouse anti-HA antibody to detect A3G (1:10⁴ dilution; Covance, Munich, Germany), mouse anti-Vif antibody (1:10³) [75] p24 was detected using mouse p24/p27 monoclonal antibody AG3.0 (1:250) [76]. Mouse anti-VSV-G (1:2 \times 10⁴ dilutions; Sigma-Aldrich), anti-mouse horseradish peroxidase (1:10⁴ dilution; GE Healthcare, Munich, Germany). Alpha-tubulin was detected using an anti-tubulin antibody (1:10⁴ dilution; Sigma-Aldrich). Signals were visualized by ECL prime reagent (GE Healthcare).

Northern blotting

For Northern blotting of HIV-1 mRNAs 3 μg of total RNA were separated on denaturing 1% agarose gel and capillary blotted onto positively charged nylon membrane and hybridized with an digoxigenin (DIG)-labeled HIV-1 exon 7 PCR-amplicon (#3387/#3388) as previously described [34].

Measurement of HIV-1 replication kinetics

Virus containing supernatants, which were generated by transient transfection of HEK 293 T cells (see above), were assayed for p24-CA via p24-CA ELISA or alternatively for TCID₅₀ as determined by calculation of X-Gal stained TZM-bl cells. 4 \times 10⁵ CEM-SS or CEM-A cells were infected with 1.6 ng of p24-CA of WT and mutant viruses in serum-free RPMI medium at 37°C for 6 hrs. Infected cells were washed in PBS (Invitrogen) and re-suspended in RPMI media (Invitrogen) containing 10% FCS and 1% P/S (Invitrogen). Aliquots of cell-free media were harvested at intervals and subjected to p24-CA ELISA (see below). 8 \times 10⁵ PBMCs were infected with the indicated MOI as determined by TCID₅₀ calculation.

p24-CA ELISA

For HIV-1 p24-CA quantification using twin-site sandwich ELISA [77,78] Nunc-Immuno 96 MicroWell solid plates (Nunc) were coated with anti p24 polyclonal antibody (7.5 µg/ml of D7320, Aalto) in bicarbonate coating buffer (100 mM NaHCO₃ pH 8.5) and incubated overnight at room temperature. Subsequently, the plates were washed with TBS (144 mM NaCl, 25 mM Tris pH 7.5). HIV in the cell culture supernatant was inactivated by adding Empigen zwitterionic detergent (Sigma, 45165) followed by incubation at 56°C for 30 min. After p24 capturing and subsequent TBS-washing, sample specific p24 was quantified by using an alkaline phosphatase-conjugated anti-p24 monoclonal antibody raised against conserved regions of p24 (BC 1071 AP, Aalto) using the AMPAK detection system, (K6200, Oxoid (Ely) Ltd). For a p24 calibration curve, recombinant p24 was treated as described above.

Infectivity assay

Transfections of HEK 293 T cells were performed using Lipofectamine LTX reagent (Invitrogen, Karlsruhe, Germany). HIV-1 luc reporter vectors were produced in the presence and absence of A3G, wild type (wt) Vif, wt Vif-V5, Vif G185E and Vif-V5 G185E or empty vector (pcDNA3.1) by transient transfection of 600 ng of pMDLg/pRRE, 250 ng of pRSV-Rev, 150 ng of pMD.G (VSV-G) and 600 ng of reporter vector pSIN.PPT.CMV.Luc.IRES-GFP. The HIV-1 packaging plasmid pMDLg/pRRE encodes *gag-pol* and the pRSV-Rev HIV-1 *rev* [79]. The HIV-1 derived vector pSIN.PPT.CMV.Luc.IRES.GFP expresses the firefly luciferase and GFP. The luciferase cDNA (luc 3) was cloned into NheI and BamHI restriction sites of pSIN.PPT.CMV.mcsIRES.GFP [80], a gift of Neeltje Kootsta. A3G and Vif expression plasmids were kept in a ratio of 1:1 (600 ng each). 48 h post transfection, viral particles containing supernatants were collected and stored at -80°C until they were used. RT activity was quantified using the Lenti-RT Activity Assay (Cavidi Tech, Uppsala, Sweden).

To determine virus rescuing activity of wt Vif and Vif G185E (and the V5 tagged version) HEK 293 T cells were transduced in the presence or absence of A3G with normalized amounts of viral like particles (determined by RT activity). Two days after transduction, intracellular luciferase activity was quantified using Steady Lite HTS (Perkin-Elmer). Data were presented as the average of actual luciferase activity per ten seconds of the quadruplicate (with mean and standard deviations). Statistically significant differences between two groups were analyzed using unpaired Student's *t* test in GraphPad Prism, version 5 (GraphPad Software, San Diego, CA). A minimum *P* value of 0.05 was considered statistically significant.

HIV-sequence alignments and sequence logos

HIV-1 sequences were downloaded from the Los Alamos HIV-1 Sequence Compendium 2012 (<http://www.hiv.lanl.gov/>). The subtype sequences were analysed with the RIP 3.0 software (<http://www.hiv.lanl.gov/content/sequence/RIP/RIP.html>). Sequence logos were generated by using R Statistical Computing (<http://www.r-project.org>) and R package seqLogo version 1.28.0 [81].

RNA pull-down

Pre-annealed DNA oligonucleotides containing G₁₃-2 wt and mutant sequences as well as a single copy of the MS2 binding site and T7 sequences (Table 1) were subjected to *in vitro* transcription using RiboMAX™ Large Scale RNA Production Systems (Promega) according to the manufactures instructions (T7 Primer: #4324; G₁₃-2 wt: #4614; G₁₃-2 mut: #4615). Following a phenol-chloroform extraction, the RNAs were covalently immobilized on adipic acid dihydrazide-agarose beads (Sigma) and incubated in 60% HeLa cell nuclear extract (Cilbiotech) in buffer D (20 mM HEPES-KOH [pH 7.9], 5% [vol/vol] glycerol, 0.1 M KCl, 0.2 mM EDTA, 0.5 mM dithiothreitol). Recombinant MS2 protein (1 µg) was added to compare the input of each sample. Unspecific bound proteins were removed by repetitive washing with buffer D containing 4 mM magnesium chloride. The associated proteins were eluted by heating at 95°C for 10 min, separated via SDS-PAGE (16%) and subjected to immunoblot analysis. For interference with protein:RNA interaction, wt RNA substrate was pre-incubated with the G₁₃-2 LNA in a ratio of either 1:5 or 1:1 relative to the amount of RNA substrate (1000 pmol).

Additional file

Additional file 1: Figure S1. Binding sites of RT-PCR primers used in this work. Schematic illustration of the positions of all NL4-3 related PCR primers used in quantitative and qualitative RT-PCR assays. Locations of 5' and 3' splice sites (ss), exons and introns are indicated. Vif and Vpr exons are highlighted in red and blue. The positions of relevant PCR forward and reverse primers are indicated by black triangles. Primer pairs were used as follows: unspliced 9 kb mRNAs (#3389/#3390), intronless 2 kb mRNAs (#3391/#3392), exon 2 containing viral mRNAs (#3395/#4843), exon 3 containing viral mRNAs (#3397/#3636), *vif* mRNA (#3395/#3396), *vpr* mRNA (#3397/#3398), *tat1* mRNA (#3631/#3632), *tat2* mRNA (#3395/#4849), *tat3* mRNA (#3397/#3632), and all viral mRNAs containing exon 7 (#3387/#3388).

Abbreviations

SRE: Splicing regulatory element; hnRNP: Heterogeneous ribonucleoprotein particle; HIV: Human immunodeficiency virus; SRSF: SR splicing factor; APOBEC: Apolipoprotein B mRNA-editing enzyme, catalytic polypeptide-like; ORF: Open reading frame; PBMC: Peripheral blood mononuclear cell; ELISA: Enzyme-linked immunosorbent assay; LNA: Locked nucleic acid; snRNP: Small nuclear ribonucleic particle; aa: Amino acid; HBS: HBond score.

Competing interests

The authors declare that they have no competing interests.

Authors' contributions

MW performed the cloning work, conceived, designed, and performed HIV-related infection and readout experiments, performed RNA-pull-down analysis, sequence alignments, and wrote the manuscript. FH performed LNA-related transfection and readout experiments, AAVJ cloned mutant Vif expression plasmids, tested for A3G counteraction and performed anti A3G Western blotting. SE performed RNA-LNA-pull-down analysis. CM planned experiments and analyzed data. HS conceived the study, supervised its design and its coordination, and wrote the manuscript. All authors read and approved the final manuscript.

Acknowledgements

We thank Björn Wefers for excellent technical assistance. We thank Stephan Theiss for critical reading of the manuscript. These studies were funded by the DFG (SCHA 909/3-1), the Stiftung für AIDS-Forschung, Düsseldorf (H.S. and C.M.), Jürgen-Manchot-Stiftung (M.W., H.S.), and the Forschungskommission of the Heinrich-Heine-University, Düsseldorf (S.E. and H.S.). The following reagents were obtained through the AIDS Research and Reference Reagent Program, Division of AIDS, NIAID, NIH: CEM-SS from Peter L. Nara, and CEM-A cells from Mark Wainberg and James McMahon, HIV-1 Vif Monoclonal Antibody (#319) from Michael H. Malim, and Monoclonal Antibody to HIV-1 p24 (AG3.0) from Jonathan Allan. We are grateful to Nathaniel Landau and Neeltje Kootsta for providing pNL4-3 Δ vif and pSIN.PPT.CMVmcsIRES.GFP. We thank Dieter Häussinger for constant support.

Author details

¹Institute for Virology, Medical Faculty, Heinrich-Heine-University Düsseldorf, Universitätsstraße 1, Düsseldorf 40225, Germany. ²Clinic for Gastroenterology, Hepatology, and Infectiology, Medical Faculty, Heinrich-Heine-University Düsseldorf, Moorenstr. 5, Düsseldorf 40225, Germany. ³Current address: Institute of Virology, University Hospital of Essen, University Duisburg-Essen, Virchowstr. 179, Essen 45147, Germany.

Received: 30 April 2014 Accepted: 8 August 2014

Published: 29 August 2014

References

- Münk C, Jensen BE, Zielonka J, Häussinger D, Kamp C: **Running loose or getting lost: how HIV-1 counters and capitalizes on APOBEC3-induced mutagenesis through its Vif protein.** *Viruses* 2012, **4**:3132–3161.
- Sheehy AM, Gaddis NC, Choi JD, Malim MH: **Isolation of a human gene that inhibits HIV-1 infection and is suppressed by the viral Vif protein.** *Nature* 2002, **418**:646–650.
- Vasudevan AA, Smits SH, Hoppner A, Häussinger D, König BW, Münk C: **Structural features of antiviral DNA cytidine deaminases.** *Biol Chem* 2013, **394**:1357–1370.
- Rahm N, Telenti A: **The role of tripartite motif family members in mediating susceptibility to HIV-1 infection.** *Curr Opin HIV AIDS* 2012, **7**:180–186.
- Keckesova Z, Ylinen LM, Towers GJ: **The human and African green monkey TRIM5alpha genes encode Ref1 and Lv1 retroviral restriction factor activities.** *Proc Natl Acad Sci U S A* 2004, **101**:10780–10785.
- Uchil PD, Quinlan BD, Chan WT, Luna JM, Mothes W: **TRIM E3 ligases interfere with early and late stages of the retroviral life cycle.** *PLoS Pathog* 2008, **4**:e16.
- Van Damme N, Goff D, Katsura C, Jorgenson RL, Mitchell R, Johnson MC, Stephens EB, Guatelli J: **The interferon-induced protein BST-2 restricts HIV-1 release and is downregulated from the cell surface by the viral Vpu protein.** *Cell Host Microbe* 2008, **3**:245–252.
- Neil SJ, Zang T, Bieniasz PD: **Tetherin inhibits retrovirus release and is antagonized by HIV-1 Vpu.** *Nature* 2008, **451**:425–430.
- Hrecka K, Hao C, Gierszewska M, Swanson SK, Kesik-Brodacka M, Srivastava S, Florens L, Washburn MP, Skowronski J: **Vpx relieves inhibition of HIV-1 infection of macrophages mediated by the SAMHD1 protein.** *Nature* 2011, **474**:658–661.
- Laguette N, Sobhian B, Casartelli N, Ringeard M, Chable-Bessia C, Segal E, Yatim A, Emiliani S, Schwartz O, Benkirane M: **SAMHD1 is the dendritic- and myeloid-cell-specific HIV-1 restriction factor counteracted by Vpx.** *Nature* 2011, **474**:654–657.
- Berger A, Sommer AF, Zwarg J, Hamdorf M, Welzel K, Esly N, Panitz S, Reuter A, Ramos I, Jatiani A, Mulder LC, Fernandez-Sesma A, Rutsch F, Simon V, König R, Flory E: **SAMHD1-deficient CD14+ cells from individuals with Aicardi-Goutieres syndrome are highly susceptible to HIV-1 infection.** *PLoS Pathog* 2011, **7**:e1002425.
- Ryoo J, Choi J, Oh C, Kim S, Seo M, Kim SY, Seo D, Kim J, White TE, Brandariz-Nunez A, Diaz-Griffero F, Yun CH, Hollenbaugh JA, Kim B, Baek D, Ahn K: **The ribonuclease activity of SAMHD1 is required for HIV-1 restriction.** *Nat Med* 2014, **20**:936–941.
- Beloglazova N, Flick R, Tchigvintsev A, Brown G, Popovic A, Nocek B, Yakunin AF: **Nuclease activity of the human SAMHD1 protein implicated in the Aicardi-Goutieres syndrome and HIV-1 restriction.** *J Biol Chem* 2013, **288**:8101–8110.
- Jakobsen MR, Mogensen TH, Paludan SR: **Caught in translation: innate restriction of HIV mRNA translation by a schlafen family protein.** *Cell Res* 2013, **23**:320–322.
- Li M, Kao E, Gao X, Sandig H, Limmer K, Pavon-Eterod M, Jones TE, Landry S, Pan T, Weitzman MD, David M: **Codon-usage-based inhibition of HIV protein synthesis by human schlafen 11.** *Nature* 2012, **491**:125–128.
- Razzak M: **Genetics: Schlafen 11 naturally blocks HIV.** *Nat Rev Urol* 2012, **9**:605.
- Coticello SG, Thomas CJ, Petersen-Mahrt SK, Neuberger MS: **Evolution of the AID/APOBEC family of polynucleotide (deoxy)cytidine deaminases.** *Mol Biol Evol* 2005, **22**:367–377.
- Jamuz A, Chester A, Bayliss J, Gisbourne J, Dunham I, Scott J, Navaratnam N: **An anthropoid-specific locus of orphan C to U RNA-editing enzymes on chromosome 22.** *Genomics* 2002, **79**:285–296.
- Münk C, Willemsen A, Bravo IG: **An ancient history of gene duplications, fusions and losses in the evolution of APOBEC3 mutators in mammals.** *BMC Evol Biol* 2012, **12**:71.
- Harris RS, Hultquist JF, Evans DT: **The restriction factors of human immunodeficiency virus.** *J Biol Chem* 2012, **287**:40875–40883.
- Refsland EW, Hultquist JF, Harris RS: **Endogenous origins of HIV-1 G-to-A hypermutation and restriction in the nonpermissive T cell line CEM2n.** *PLoS Pathog* 2012, **8**:e1002800.
- Hultquist JF, Lengyel JA, Refsland EW, LaRue RS, Lackey L, Brown WL, Harris RS: **Human and rhesus APOBEC3D, APOBEC3F, APOBEC3G, and APOBEC3H demonstrate a conserved capacity to restrict Vif-deficient HIV-1.** *J Virol* 2011, **85**:11220–11234.
- Miyagi E, Opi S, Takeuchi H, Khan M, Goila-Gaur R, Kao S, Strebel K: **Enzymatically active APOBEC3G is required for efficient inhibition of human immunodeficiency virus type 1.** *J Virol* 2007, **81**:13346–13353.
- Mangeat B, Turelli P, Caron G, Friedli M, Perrin L, Trono D: **Broad antiretroviral defence by human APOBEC3G through lethal editing of nascent reverse transcripts.** *Nature* 2003, **424**:99–103.
- Harris RS, Bishop KN, Sheehy AM, Craig HM, Petersen-Mahrt SK, Watt IN, Neuberger MS, Malim MH: **DNA deamination mediates innate immunity to retroviral infection.** *Cell* 2003, **113**:803–809.
- Zhang H, Yang B, Pomerantz RJ, Zhang C, Arunachalam SC, Gao L: **The cytidine deaminase CEM15 induces hypermutation in newly synthesized HIV-1 DNA.** *Nature* 2003, **424**:94–98.
- Wissing S, Galloway NL, Greene WC: **HIV-1 Vif versus the APOBEC3 cytidine deaminases: an intracellular duel between pathogen and host restriction factors.** *Mol Asp Med* 2010, **31**:383–397.
- Purcell DF, Martin MA: **Alternative splicing of human immunodeficiency virus type 1 mRNA modulates viral protein expression, replication, and infectivity.** *J Virol* 1993, **67**:6365–6378.
- Jager S, Cimermancic P, Gulbahce N, Johnson JR, McGovern KE, Clarke SC, Shales M, Mercenne G, Pache L, Li K, Hernandez H, Jang GM, Roth SL, Akiva E, Marlett J, Stephens M, D'Orso I, Fernandes J, Fahey M, Mahon C, O'Donoghue AJ, Todorovic A, Morris JH, Maltby DA, Alber T, Cagney G, Bushman FD, Young JA, Chanda SK, Sundquist WI, et al: **Global landscape of HIV-human protein complexes.** *Nature* 2012, **481**:365–370.
- Krummheuer J, Johnson AT, Hauber J, Kammler S, Anderson JL, Hauber J, Purcell DF, Schaal H: **A minimal uORF within the HIV-1 vpu leader allows efficient translation initiation at the downstream env AUG.** *Virology* 2007, **363**:261–271.
- Anderson JL, Johnson AT, Howard JL, Purcell DF: **Both linear and discontinuous ribosome scanning are used for translation initiation from bicistronic human immunodeficiency virus type 1 env mRNAs.** *J Virol* 2007, **81**:4664–4676.
- Exline CM, Feng Z, Stoltzfus CM: **Negative and positive mRNA splicing elements act competitively to regulate human immunodeficiency virus type 1 vif gene expression.** *J Virol* 2008, **82**:3921–3931.

33. Erkelenz S, Poschmann G, Theiss S, Stefanski A, Hillebrand F, Otte M, Stuhler K, Schaal H: **Tra2-mediated recognition of HIV-1 5' splice site D3 as a key factor in the processing of vpr mRNA.** *J Virol* 2013, **87**:2721–2734.
34. Widera M, Erkelenz S, Hillebrand F, Krikoni A, Widera D, Kaisers W, Deenen R, Gombert M, Dellen R, Pfeiffer T, Kaltschmidt B, Münk C, Bosch V, Köhrer K, Schaal H: **An Intronic G Run within HIV-1 Intron 2 Is Critical for Splicing Regulation of vif mRNA.** *J Virol* 2013, **87**:2707–2720.
35. Asang C, Hauber I, Schaal H: **Insights into the selective activation of alternatively used splice acceptors by the human immunodeficiency virus type-1 bidirectional splicing enhancer.** *Nucleic Acids Res* 2008, **36**:1450–1463.
36. Madsen JM, Stoltzfus CM: **A suboptimal 5' splice site downstream of HIV-1 splice site A1 is required for unspliced viral mRNA accumulation and efficient virus replication.** *Retrovirology* 2006, **3**:10.
37. Mandal D, Feng Z, Stoltzfus CM: **Excessive RNA splicing and inhibition of HIV-1 replication induced by modified U1 small nuclear RNAs.** *J Virol* 2010, **84**:12790–12800.
38. Stoltzfus CM: **Chapter 1. Regulation of HIV-1 alternative RNA splicing and its role in virus replication.** *Adv Virus Res* 2009, **74**:1–40.
39. Mandal D, Feng Z, Stoltzfus CM: **Gag-processing defect of human immunodeficiency virus type 1 integrase E246 and G247 mutants is caused by activation of an overlapping 5' splice site.** *J Virol* 2008, **82**:1600–1604.
40. Kammler S, Otte M, Hauber I, Kjems J, Hauber J, Schaal H: **The strength of the HIV-1 3' splice sites affects Rev function.** *Retrovirology* 2006, **3**:89.
41. Domsic JK, Wang Y, Mayeda A, Krainer AR, Stoltzfus CM: **Human immunodeficiency virus type 1 hnRNP A/B-dependent exonic splicing silencer ESSV antagonizes binding of U2AF65 to viral polypyrimidine tracts.** *Mol Cell Biol* 2003, **23**:8762–8772.
42. Bilodeau PS, Domsic JK, Mayeda A, Krainer AR, Stoltzfus CM: **RNA splicing at human immunodeficiency virus type 1 3' splice site A2 is regulated by binding of hnRNP A/B proteins to an exonic splicing silencer element.** *J Virol* 2001, **75**:8487–8497.
43. Madsen JM, Stoltzfus CM: **An exonic splicing silencer downstream of the 3' splice site A2 is required for efficient human immunodeficiency virus type 1 replication.** *J Virol* 2005, **79**:10478–10486.
44. Tsuruno C, Ohe K, Kuramitsu M, Kohma T, Takahama Y, Hamaguchi Y, Hamaguchi I, Okuma K: **HMGAT1a is involved in specific splice site regulation of human immunodeficiency virus type 1.** *Biochem Biophys Res Commun* 2011, **406**:512–517.
45. Xiao X, Wang Z, Jang M, Nutiu R, Wang ET, Burge CB: **Splice site strength-dependent activity and genetic buffering by poly-G runs.** *Nat Struct Mol Biol* 2009, **16**:1094–1100.
46. Yeo G, Hoon S, Venkatesh B, Burge CB: **Variation in sequence and organization of splicing regulatory elements in vertebrate genes.** *Proc Natl Acad Sci U S A* 2004, **101**:15700–15705.
47. Zhang XH, Leslie CS, Chasin LA: **Dichotomous splicing signals in exon flanks.** *Genome Res* 2005, **15**:768–779.
48. Schaub MC, Lopez SR, Caputi M: **Members of the heterogeneous nuclear ribonucleoprotein H family activate splicing of an HIV-1 splicing substrate by promoting formation of ATP-dependent spliceosomal complexes.** *J Biol Chem* 2007, **282**:13617–13626.
49. Wei X, Decker JM, Liu H, Zhang Z, Arani RB, Kilby JM, Saag MS, Wu X, Shaw GM, Kappes JC: **Emergence of resistant human immunodeficiency virus type 1 in patients receiving fusion inhibitor (T-20) monotherapy.** *Antimicrob Agents Chemother* 2002, **46**:1896–1905.
50. Raposo RA, Abdel-Mohsen M, Biliska M, Montefiori DC, Nixon DF, Pillai SK: **Effects of cellular activation on Anti-HIV-1 restriction factor expression profile in primary cells.** *J Virol* 2013, **87**:11924–11929.
51. Foley GE, Lazarus H, Farber S, Uzman BG, Boone BA, McCarthy RE: **Continuous Culture of Human Lymphoblasts from Peripheral Blood of a Child with Acute Leukemia.** *Cancer* 1965, **18**:522–529.
52. Nara PL, Fischinger PJ: **Quantitative infectivity assay for HIV-1 and-2.** *Nature* 1988, **332**:469–470.
53. Nara PL, Hatch WC, Dunlop NM, Robey WG, Arthur LO, Gonda MA, Fischinger PJ: **Simple, rapid, quantitative, syncytium-forming microassay for the detection of human immunodeficiency virus neutralizing antibody.** *AIDS Res Hum Retrovir* 1987, **3**:283–302.
54. Tremblay M, Sullivan AK, Rooke R, Gelezianus R, Tsoukas C, Shematek G, Gilmore N, Wainberg MA: **New CD4(+) cell line susceptible to infection by HIV-1.** *J Med Virol* 1989, **28**:243–249.
55. Mariani R, Chen D, Schrofelbauer B, Navarro F, König R, Bollman B, Münk C, Nymark-McMahon H, Landau NR: **Species-specific exclusion of APOBEC3G from HIV-1 virions by Vif.** *Cell* 2003, **114**:21–31.
56. Goncalves J, Jallepalli P, Gabuzda DH: **Subcellular localization of the Vif protein of human immunodeficiency virus type 1.** *J Virol* 1994, **68**:704–712.
57. Goncalves J, Shi B, Yang X, Gabuzda D: **Biological activity of human immunodeficiency virus type 1 Vif requires membrane targeting by C-terminal basic domains.** *J Virol* 1995, **69**:7196–7204.
58. Mehle A, Strack B, Ancuta P, Zhang C, McPike M, Gabuzda D: **Vif overcomes the innate antiviral activity of APOBEC3G by promoting its degradation in the ubiquitin-proteasome pathway.** *J Biol Chem* 2004, **279**:7792–7798.
59. Hoffman BE, Grabowski PJ: **U1 snRNP targets an essential splicing factor, U2AF65, to the 3' splice site by a network of interactions spanning the exon.** *Genes Dev* 1992, **6**:2554–2568.
60. Robberson BL, Cote GJ, Berget SM: **Exon definition may facilitate splice site selection in RNAs with multiple exons.** *Mol Cell Biol* 1990, **10**:84–94.
61. Kammler S, Leurs C, Freund M, Krummheuer J, Seidel K, Tange TO, Lund MK, Kjems J, Scheid A, Schaal H: **The sequence complementarity between HIV-1 5' splice site SD4 and U1 snRNA determines the steady-state level of an unstable env pre-mRNA.** *RNA* 2001, **7**:421–434.
62. Erkelenz S, Mueller WF, Evans MS, Busch A, Schoneweis K, Hertel KJ, Schaal H: **Position-dependent splicing activation and repression by SR and hnRNP proteins rely on common mechanisms.** *RNA* 2013, **19**:96–102.
63. Jablonski JA, Caputi M: **Role of cellular RNA processing factors in human immunodeficiency virus type 1 mRNA metabolism, replication, and infectivity.** *J Virol* 2009, **83**:981–992.
64. Lund N, Milev MP, Wong R, Sanmuganatham T, Woolaway K, Chabot B, Abou Elela S, Moulard AJ, Cochrane A: **Differential effects of hnRNP D/AUF1 isoforms on HIV-1 gene expression.** *Nucleic Acids Res* 2012, **40**:3663–3675.
65. Kurreck J, Wyszko E, Gillen C, Erdmann VA: **Design of antisense oligonucleotides stabilized by locked nucleic acids.** *Nucleic Acids Res* 2002, **30**:1911–1918.
66. Elmen J, Zhang HY, Zuber B, Ljungberg K, Wahren B, Wahlestedt C, Liang Z: **Locked nucleic acid containing antisense oligonucleotides enhance inhibition of HIV-1 genome dimerization and inhibit virus replication.** *FEBS Lett* 2004, **578**:285–290.
67. Strebler K: **HIV accessory proteins versus host restriction factors.** *Curr Opin Virol* 2013, **3**:692–699.
68. Pillai SK, Wong JK, Barbour JD: **Turning up the volume on mutational pressure: is more of a good thing always better? (A case study of HIV-1 Vif and APOBEC3).** *Retrovirology* 2008, **5**:26.
69. Adachi A, Gendelman HE, Koenig S, Folks T, Willey R, Rabson A, Martin MA: **Production of acquired immunodeficiency syndrome-associated retrovirus in human and nonhuman cells transfected with an infectious molecular clone.** *J Virol* 1986, **59**:284–291.
70. Selden RF, Howie KB, Rowe ME, Goodman HM, Moore DD: **Human growth hormone as a reporter gene in regulation studies employing transient gene expression.** *Mol Cell Biol* 1986, **6**:3173–3179.
71. Jaguva Vasudevan AA, Perkovic M, Bulliard Y, Cichutek K, Trono D, Häussinger D, Münk C: **Prototypic foamy virus bet impairs the dimerization and cytosolic solubility of human APOBEC3G.** *J Virol* 2013, **87**:9030–9040.
72. Widera M, Klein AN, Cinar Y, Funke SA, Willbold D, Schaal H: **The D-amino acid peptide D3 reduces amyloid fibril boosted HIV-1 infectivity.** *AIDS Res Ther* 2014, **11**:1.
73. Chomczynski P, Sacchi N: **Single-step method of RNA isolation by acid guanidinium thiocyanate-phenol-chloroform extraction.** *Anal Biochem* 1987, **162**:156–159.
74. Laemmli UK: **Cleavage of structural proteins during the assembly of the head of bacteriophage T4.** *Nature* 1970, **227**:680–685.
75. Simon JH, Southerling TE, Peterson JC, Meyer BE, Malim MH: **Complementation of vif-defective human immunodeficiency virus type 1 by primate, but not nonprimate, lentivirus vif genes.** *J Virol* 1995, **69**:4166–4172.
76. Simm M, Shahabuddin M, Chao W, Allan JS, Volsky DJ: **Aberrant Gag protein composition of a human immunodeficiency virus type 1 vif mutant produced in primary lymphocytes.** *J Virol* 1995, **69**:4582–4586.
77. McKeating JA, McKnight A, Moore JP: **Differential loss of envelope glycoprotein gp120 from virions of human immunodeficiency virus type 1 isolates: effects on infectivity and neutralization.** *J Virol* 1991, **65**:852–860.
78. Moore JP, McKeating JA, Weiss RA, Sattentau QJ: **Dissociation of gp120 from HIV-1 virions induced by soluble CD4.** *Science* 1990, **250**:1139–1142.

79. Dull T, Zufferey R, Kelly M, Mandel RJ, Nguyen M, Trono D, Naldini L: **A third-generation lentivirus vector with a conditional packaging system.** *J Virol* 1998, **72**:8463–8471.
80. Kootstra NA, Münk C, Tonnu N, Landau NR, Verma IM: **Abrogation of postentry restriction of HIV-1-based lentiviral vector transduction in simian cells.** *Proc Natl Acad Sci USA* 2003, **100**:1298–1303.
81. Bembom O: **seqLogo: Sequence Logos for DNA Sequence Alignments.** In *Book seqLogo: Sequence Logos for DNA Sequence Alignments (Editor ed.^eds.)*. vol. R package version 1.280, 1.280th edition; 1990. pp. seqLogo takes the position weight matrix of a DNA sequence motif and plots the corresponding sequence logo as introduced by Schneider and Stephens. City; 2014:seqLogo takes the position weight matrix of a DNA sequence motif and plots the corresponding sequence logo as introduced by Schneider and Stephens (1990).

doi:10.1186/s12977-014-0072-1

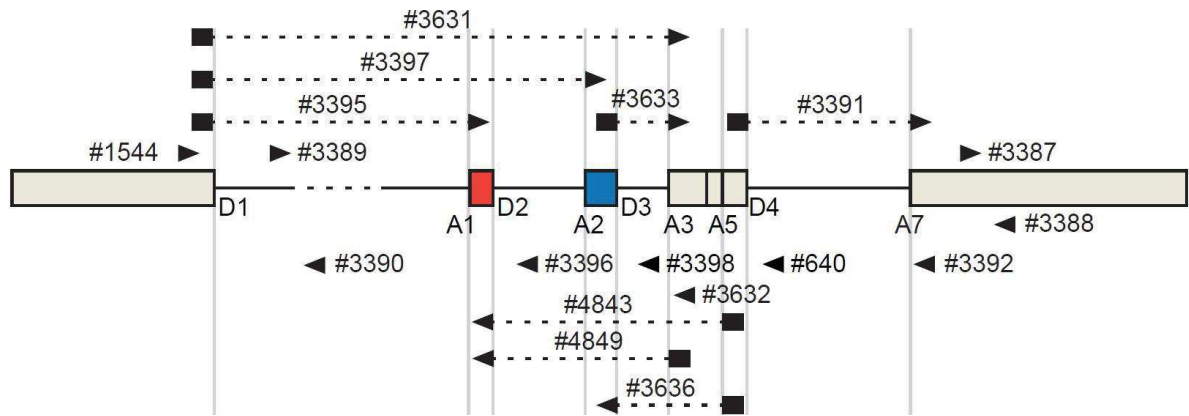
Cite this article as: Widera *et al.*: A functional conserved intronic G run in HIV-1 intron 3 is critical to counteract APOBEC3G-mediated host restriction. *Retrovirology* 2014 **11**:72.

**Submit your next manuscript to BioMed Central
and take full advantage of:**

- Convenient online submission
- Thorough peer review
- No space constraints or color figure charges
- Immediate publication on acceptance
- Inclusion in PubMed, CAS, Scopus and Google Scholar
- Research which is freely available for redistribution

Submit your manuscript at
www.biomedcentral.com/submit





Additional file 1: Figure S1.: Binding sites of RT-PCR primers used in this work. Schematic illustration of the positions of all NL4-3 related PCR primers used in quantitative and qualitative RT-PCR assays. Locations of 5' and 3' splice sites (ss), exons and introns are indicated. *Vif* and *Vpr* exons are highlighted in red and blue. The positions of relevant PCR forward and reverse primers are indicated by black triangles. Primer pairs were used as follows: unspliced 9 kb mRNAs (#3389/#3390), intronless 2 kb mRNAs (#3391/#3392), exon 2 containing viral mRNAs (#3395/#4843), exon 3 containing viral mRNAs (#3397/#3636), *vif* mRNA (#3395/#3396), *vpr* mRNA (#3397/#3398), *tat1* mRNA (#3631/#3632), *tat2* mRNA (#3395/#4849), *tat3* mRNA (#3397/#3632), and all viral mRNAs containing exon 7 (#3387/#3388). (PDF 264 KB)

Summary

The APOBEC3 (A3) family of cytidine deaminases plays a vital role for innate defence against retroviruses, retroelements and other viral pathogens. They act as restriction factors that catalyze the hydrolytic deamination of deoxycytidine to deoxyuridine on single-stranded viral DNA (ssDNA), leading to coding changes and premature stop codons that abrogate virus replication. Viral infectivity factor (Vif) of Human immunodeficiency virus-1 (HIV-1) binds to intracellular A3s and depletes them by inducing polyubiquitination and proteosomal degradation. The key objective of this thesis is to characterize A3 enzyme family activity against diverse retroviruses and retroelements, with a focus on molecular interaction between certain A3s and their viral counterparts.

Among the seven human A3s, A3G and A3F are the best-studied. The work in this thesis shows for the first time that a point mutant of A3C, A3C.S61P, enhances enzymatic activity and efficiently inhibits retroviruses, likely by local structural changes induced by the serine-to-proline substitution. A3C.S61P had markedly increased antiviral activity against simian immunodeficiency virus lacking Vif (SIV Δ vif) and murine leukemia virus (MLV), but was only marginally active against HIV-1 Δ vif. A3C.S61P hypermutated the genomes of SIV Δ vif and MLV, but not HIV Δ vif, suggesting an unknown escape mechanism of HIV-1.

Moreover, the investigation of A3C orthologues from various primates revealed that A3C from sooty mangabey (smmA3C) potentially restricts HIV-1 in a deamination-dependent manner and resists HIV-1 Vif-mediated degradation. Taken together, these results confirm that the catalytic activity of A3C is important for antiviral function. It also highlights the robust antiviral activity of smmA3C, which is an interesting candidate for structural investigations.

Anti-MLV activity of A3A is another focus of this thesis, as findings on A3A-mediated MLV inhibition described in the literature are contradictory. The effect of producer cell and target cell A3A was tested against MLV. Producer cell A3A was encapsidated by MLV into the viral core, triggered hypermutations in MLV genome and inhibited the virus. However, strikingly MLV-glycosylated Gag (glycogag) counteracted the encapsidation of producer cell A3A whereas, target cell A3A was not affected by glycogag. Future research should elucidate the mechanism of the anti-A3 activity of glycogag.

Whereas HIV-1 Vif opposes A3G by triggering its degradation, this thesis demonstrates a novel mechanism whereby prototype foamy virus Bet counteracts A3G by impairing its cytosolic solubility and consequently prevents its virion packaging. Bet binds A3G presumably through a direct interaction, but does not affect its catalytic activity. It would be exciting to explore how Bet acts on other A3s, especially A3A and A3B, as these A3s likely drive cancer mutations. In that respect, a method to detect and characterize the specific A3s expressed in cancer cells is described in this thesis.

Finally, this thesis reports the possible function of APOBEC4 (A4), a very distant relative of A3, on HIV-1 replication. A4 did not exhibit detectable cytidine deamination activity *in vitro* and weakly interacted with single-stranded DNA. In contrast to A3, A4 enhanced the production of HIV-1.

Taken together, these findings show that A3 interactions with different retroviruses are complex and often virus-specific. Further studies may help to develop new antiretroviral therapeutics that target viral interaction with cellular A3s.

Summary in German (Zusammenfassung)

Die Cytidin-Desaminasen der APOBEC3 (A3) Familie haben eine wichtige Funktion in der intrinsischen angeborenen Abwehr gegen Retroviren, Retroelemente und andere Viren. Diese Enzyme wirken als Restriktionsfaktoren, die eine hydrolytische Deaminierung von dCTP zu dUTP in Einzelstrang DNA (ssDNA) bewirken. Durch diese Deaminierungen entstehen Veränderungen in der Aminosäurekodierung und Stoppcodons im viralen Genom. Das humane Immundefizienzvirus 1 (HIV-1) exprimiert das Vif Protein („viral infectivity factor“). Vif bindet an die A3 Proteine und induziert deren Polyubiquitinierung und damit ihren proteosomalen Abbau. Ziel dieser Arbeit war die Charakterisierung der Aktivität von verschiedenen A3s gegen diverse Retroviren und Retroelemente. Der Fokus lag dabei auf der molekularen Interaktion zwischen bestimmten A3 Proteinen und den viralen Gegenproteinen.

Von den sieben humanen A3 Proteinen sind A3F und A3G am besten untersucht. Diese Arbeit beschreibt zum ersten Mal die Relevanz der Mutation S61P in A3C, die die antivirale Aktivität von A3C signifikant beeinflusst. Die Ergebnisse unterstützen ein Modell, wodurch der Einbau von Prolin anstelle von Serin eine Strukturänderung verursacht, die die enzymatische Aktivität von A3C steigert. A3C.S61P zeigte deutlich höhere antivirale Aktivität gegen simianes Immundefizienz Virus mit *vif* Deletion (*SIV Δ vif*) und murines Leukämievirus (*MLV*). Im Gegensatz dazu war die Infektiosität von *HIV-1 Δ vif* weder durch A3C noch durch A3C.S61P besonders stark reduziert. A3C.S61P war in der Lage die Genome von *SIV Δ vif* und von *MLV* zu hypermutieren, zeigte aber keine Hypermutationsaktivität gegen *HIV Δ vif*. Diese Daten deuten auf einen noch unbekanntem Resistenzmechanismus gegen A3C in *HIV-1 Δ vif*.

In weiteren Untersuchungen von A3C Orthologen aus anderen Primaten konnte die Cytidineaminase A3C aus der Rußmangabe (*smmA3C*) als starker HIV-1 Inhibitor mit Desaminaseaktivität identifiziert werden. *A3Csmm* war im Gegensatz zu humanem A3C auch resistent gegen das Vif Protein von HIV-1. Insgesamt zeigen die Daten, dass *smmA3C* nur antiviral wirkt, wenn es katalytisch aktiv ist. Die mechanistischen Ursachen für die verstärkte anti-HIV Aktivität von *smmA3C* sind noch unklar; Strukturvergleiche mit humanem A3C bieten einen Ansatz den Mechanismus besser zu verstehen.

Diese Arbeit hatte auch das Ziel, wegen vieler kontroverser Literaturdaten die anti-*MLV* Aktivität von A3A zu klären. Die Wirkung von A3A wurde analysiert, wenn A3A in der *MLV*

Produzentenzelle oder wenn es in der Zielzelle exprimiert wurde. Die Ergebnisse belegen, dass A3A aus der Virus produzierenden Zelle in MLV Cores verpackt wurde und die Virusinfektion der nächsten Zelle durch Hypermutation des viralen Genoms hemmte. Das neben dem normalen Gag protein exprimierte glykosylierte Gag Protein (glycogag) von MLV verminderte jedoch die Verpackung des A3A deutlich. Im Gegensatz dazu wurde A3A, das nur in der Virus-Zielzelle exprimiert wurde, nicht durch virales glycogag gehemmt. Zukünftige Forschungsarbeiten sollten den genauen Mechanismus der anti-A3 Aktivität von glycogag genauer ausarbeiten.

Ein weiterer viraler A3 Gegenspieler ist das Foamyvirus Protein Bet. Bet hemmt die Verpackung von A3 Proteinen in Retroviruspartikel durch einen neuen Mechanismus, unabhängig von einer Degradierung, aber eine Veränderung der zytoplasmatischen Löslichkeit von A3G beinhaltet. Bet bindet an A3G, vermutlich durch eine direkte Interaktion, aber hemmt nicht seine enzymatische Aktivität. In der Zukunft wäre zu untersuchen, wie Bet andere A3 Proteine inhibiert, besonders solche wie A3B, die für Krebs-assoziierte Mutationen verantwortlich gemacht werden. In diesem Zusammenhang wird in der Arbeit auch die Methodik zur Detektion und Analyse von spezifischen A3-Enzymen in Krebszellen beschrieben.

In weiteren Experimenten wurde die mögliche Funktion von APOBEC4 (A4) , das entfernt mit den A3-Proteinen verwandt ist, im Kontext der HIV-1-Replikation analysiert. A4 zeigte in keinem Testansatz eine enzymatische Desaminierungsaktivität an Einzelstrang-DNA und band auch nur schwach an Einzelstrang-DNA. Im Vergleich zu A3-Proteinen erhöhte die Expression von A4 die Virusmenge.

Zusammenfassend belegen die Ergebnisse dieser Arbeit, dass die Wechselwirkungen von A3-Enzymen mit unterschiedlichen Retroviren komplex und im Detail oft Virus-spezifisch sind. Weitere Arbeiten in diesem Bereich könnten „Grundlage“ für neue therapeutische Ansätze gegen HIV-1 bilden.

(The translation of summary in German was done by my supervisor Prof. Münk and other German colleagues.)

Acknowledgements

Thank you all!

Firstly, dear Carsten, my mentor- for everything from picking me up at airport in 2010 to translating my thesis summary, it has been a long journey. For his expertise, guidance, providing excellent work environment, his open-door and open-mind for new ideas, stimulating suggestions, the motivation, scientific freedom and the trust shown on-my favourite quote from him, “do what you want” (that make sense).

Our clinic, and the director, Prof. Dr. Dieter Häussinger for the great support and research facilities.

Dear Dieter (forschungszentrum Jülich), my co-supervisor, for a thorough support; dear Lutz (Biochemistry I, HHU), for the inspiration and timely help, for allowing me to perform some part of my study in your respective labs and learn a number of different things pertaining to multidisciplinary research.

Sander (Biochemistry) and Bernd (Jülich) for the collaboration, incredible discussions, all the moral support and encouragements.

Apart from the financial support from Biostruct School, it also granted outstanding opportunities to enhance my research and soft skills. Scholar meetings, conferences, iGrad courses were all very helpful. Dear Cordula for writing a number of letters for me in German and organize my research contract and dear Christian for assistance.

Lab1- Virus team!

1st Generation—I had a great time at the beginning of the study, the 2010 winter-carnival is a memorable event☺...Henning, the APO-BECKs master, for all A3C stuffs!

Mario-for helping in Bet project, Dani-teaching cell culture, and delicious tiramisu cakes, also Jörg, Katerina,. Best wishes to you

Wio-for all your technical assistance, guidance and personal support and care.

Christian, Ute, Boris, for various help.

2nd generation--Anika, Augustin, Edmund, Qin, Zeli and number of guest students Anna, André, Anne, Ariane, Benny, Marion, Shabnam, Sebastian, Kannan, Kristina—All the very best to you.

Lab2-Biochmistry team!

Britta-showed how to purify proteins, Jan for answering all my questions, till now..., Philipp, André, Christian, Mero, Martina and many more.. for various help!

The time spent there was very nice, informative and celebrations were awesome. :0 – Greetings to you!

Lab3-NMR/SPR!

Sven for introducing ^{15}N -labelling and some NMR spectra, Julian-more than those critical SPR measurements, I enjoyed those rides with immortal beats on! and Melanie-for kind help with SPR.

Lab4-Cancer team!

Wolfgang and Günter for scientific and moral support at the final stage, Johanna and Maggie for kindly giving me access to gel-doc all the time, Nicki for brilliant proof-reading of the thesis summary and suggestions, and Alex, Alessandro, Amp, Christiane, David, Marija and Michèle, you guys are cool! My best wishes.

..Indian gang: Prashant D for backing me, all those times spent together watching BBT, and fun, Sathish, Prashant S, Bala for various help and fun,Badri, Jag, Mamta, Rohit, Prakash, and many others. It was pleasant.

For motivation, training, education, back from home: All my teachers, dear Mr. S. Ramanathan (former UN advisor), dear Mr. V. Parthasarathy (Vivekananda college), dear Dr. Mayilraj (IMTECH), for, "showing me the door", credits go to you! I will never forget some Rotarians from Madurai for their support and invigoration.

My family members, especially parents, the late uncle, and my wife for letting me complete my journey, and little Aadi!- I love you!

My lovely friends from Madurai, IMTECH mates (Jay, Fazal, Suru, Neera) and who are in other part of the world for all appreciation, inspiration and fun.

Biographical Sketch

Ananda Ayyappan Jaguva Vasudevan was born in 1986 at Madurai (a temple city), India. He attended Sourashtra college (affiliated to Madurai Kamaraj University) from 2003-2008 and acquired B. Sc., (Biochemistry) and M. Sc., (Biotechnology) with Gold Medal for Excellence in both degrees. His craving towards research was boosted when he worked in the late Jain lab, at Institute of Microbial Technology (Nov 2008-Dec 2009). He began graduate studies at the Heinrich-Heine-University, Düsseldorf in summer of 2010 with a stipend awarded by NRW research school, "Biostruct" (2010-2013). Under the supervision of Carsten Münk PhD, he studied the molecular interaction between certain APOBEC3s and their viral counterparts. He attended various workshops, training programs, and conferences (presented a paper in Virology meeting, Alpbach, Austria, 2014 and a poster in Cold spring harbor meeting, USA, 2014). The following publications were as a result of work conducted during doctoral study.

1. Jaguva Vasudevan, A. A., Hofmann, H., Willbold, D., Häussinger, D., Koenig, B. W., and Münk, C. (2017) Enhancing the Catalytic Deamination Activity of APOBEC3C Is Insufficient to Inhibit Vif-Deficient HIV-1. *J Mol Biol* **429**, 1171-1191
2. Jaguva Vasudevan, A. A., Smits, S. H., Hoppner, A., Häussinger, D., Koenig, B. W., and Münk, C. (2013) Structural features of antiviral DNA cytidine deaminases. *Biol Chem* **394**, 1357-1370
3. Jaguva Vasudevan, A. A., Krikoni, A., Franken, A., Marino, D., König, R., Schumann, G. G., Häussinger, D., and Münk, C. Glycosylated gag protects murine leukemia virus from producer cell-derived but not from target cell APOBEC3A. Manuscript under preparation
4. Jaguva Vasudevan, A. A., Zhang, Z., Häussinger, D., and Münk, C. A Naturally Occurring APOBEC3C from Sooty Mangabey Potently Inhibits Human Immunodeficiency Virus Replication. Manuscript under preparation
5. Jaguva Vasudevan, A. A.*, Perkovic, M*, Bulliard, Y., Cichutek, K., Trono, D., Häussinger, D., and Münk, C. (2013) Prototype foamy virus Bet impairs the dimerization and cytosolic solubility of human APOBEC3G. *J Virol* **87**, 9030-9040
6. Jaguva Vasudevan, A. A., Göring, W., Häussinger, D., and Münk, C. Detection of APOBEC3 proteins and catalytic activity in urothelial carcinoma. (Accepted for a book chapter on "Urothelial Carcinoma", to be published in the lab protocol series, *Methods in Molecular Biology*, by Springer in press (Chief editor: W. A. Schulz)
7. Marino, D*, Perkovic, M*, Hain, A*, Jaguva Vasudevan, A. A.*, Hofmann, H., Hanschmann, K. M., Muhlebach, M. D., Schumann, G. G., König, R., Cichutek, K., Häussinger, D., and Münk, C. (2016) APOBEC4 Enhances the Replication of HIV-1. *PLoS One* **11**, e0155422
8. Horn, A. V., Klawitter, S., Held, U., Berger, A., Jaguva Vasudevan, A. A., Bock, A., Hofmann, H., Hanschmann, K. M., Troschmeier, J. H., Flory, E., Jabulowsky, R. A., Han, J. S., Lower, J., Lower, R., Münk, C., and Schumann, G. G. (2014) Human LINE-1 restriction by APOBEC3C is deaminase independent and mediated by an ORF1p interaction that affects LINE reverse transcriptase activity. *Nucleic Acids Res* **42**, 396-416

9. Kopietz, F., Jaguva Vasudevan, A. A., Kramer, M., Muckenfuss, H., Sanzenbacher, R., Cichutek, K., Flory, E., and Münk, C. (2012) Interaction of human immunodeficiency virus type 1 Vif with APOBEC3G is not dependent on serine/threonine phosphorylation status. *J Gen Virol* **93**, 2425-2430
10. Zhang, Z., Gu, Q., Jaguva Vasudevan, A. A., Hain, A., Kloke, B. P., Hasheminasab, S., Mulnaes, D., Sato, K., Cichutek, K., Haussinger, D., Bravo, I. G., Smits, S. H., Gohlke, H., and Münk, C. (2016) Determinants of FIV and HIV Vif sensitivity of feline APOBEC3 restriction factors. *Retrovirology* **13**, 46
11. Zhang, Z., Gu, Q., Jaguva Vasudevan, A. A., Jeyaraj, M., Schmidt, S., Zielonka, J., Perkovic, M., Heckel, J. O., Cichutek, K., Häussinger, D., Smits, S. H., and Münk, C. (2016) Vif Proteins from Diverse Human Immunodeficiency Virus/Simian Immunodeficiency Virus Lineages Have Distinct Binding Sites in A3C. *J Virol* **90**, 10193-10208
12. Bähr, A., Singer, A., Hain, A., Jaguva Vasudevan, A. A., Schilling, M., Reh, J., Riess, M., Panitz, S., Serrano, V., Schweizer, M., Konig, R., Chanda, S., Haussinger, D., Kochs, G., Lindemann, D., and Munk, C. (2016) Interferon but not MxB inhibits foamy retroviruses. *Virology* **488**, 51-60
13. Maney, S. K., McIlwain, D. R., Polz, R., Pandyra, A. A., Sundaram, B., Wolff, D., Ohishi, K., Marezky, T., Brooke, M. A., Evers, A., Jaguva Vasudevan, A. A., Aghaeepour, N., Scheller, J., Munk, C., Haussinger, D., Mak, T. W., Nolan, G. P., Kelsell, D. P., Blobel, C. P., Lang, K. S., and Lang, P. A. (2015) Deletions in the cytoplasmic domain of iRhom1 and iRhom2 promote shedding of the TNF receptor by the protease ADAM17. *Sci Signal* **8**, ra109
14. Widera, M., Hillebrand, F., Erkelenz, S., Jaguva Vasudevan, A. A., Münk, C., and Schaal, H. (2014) A functional conserved intronic G run in HIV-1 intron 3 is critical to counteract APOBEC3G-mediated host restriction. *Retrovirology* **11**, 72

* equally contributed to the work

Declaration

I hereby declare that this thesis is an original work and has not been submitted in whole, or in part, for a degree at this or any other university. Nor does it contain, to the best of my knowledge and belief, any material published or written by any other person, except as acknowledged in the text. Figures, facts from other works were duly cited and the permission from the journal publishers was obtained. I have not made any unsuccessful promotions.

Düsseldorf

Date:

Ananda Ayyappan Jaguva Vasudevan